METABOLITE AND NUTRIENT TRANSPORTERS IN CANCER-CELL METABOLISM: ROLE IN CANCER PROGRESSION AND METASTASIS

EDITED BY: Vadivel Ganapathy, Maria E. Mycielska, Eric Kenneth Parkinson and Sebastian Haferkamp

PUBLISHED IN: Frontiers in Cell and Developmental Biology

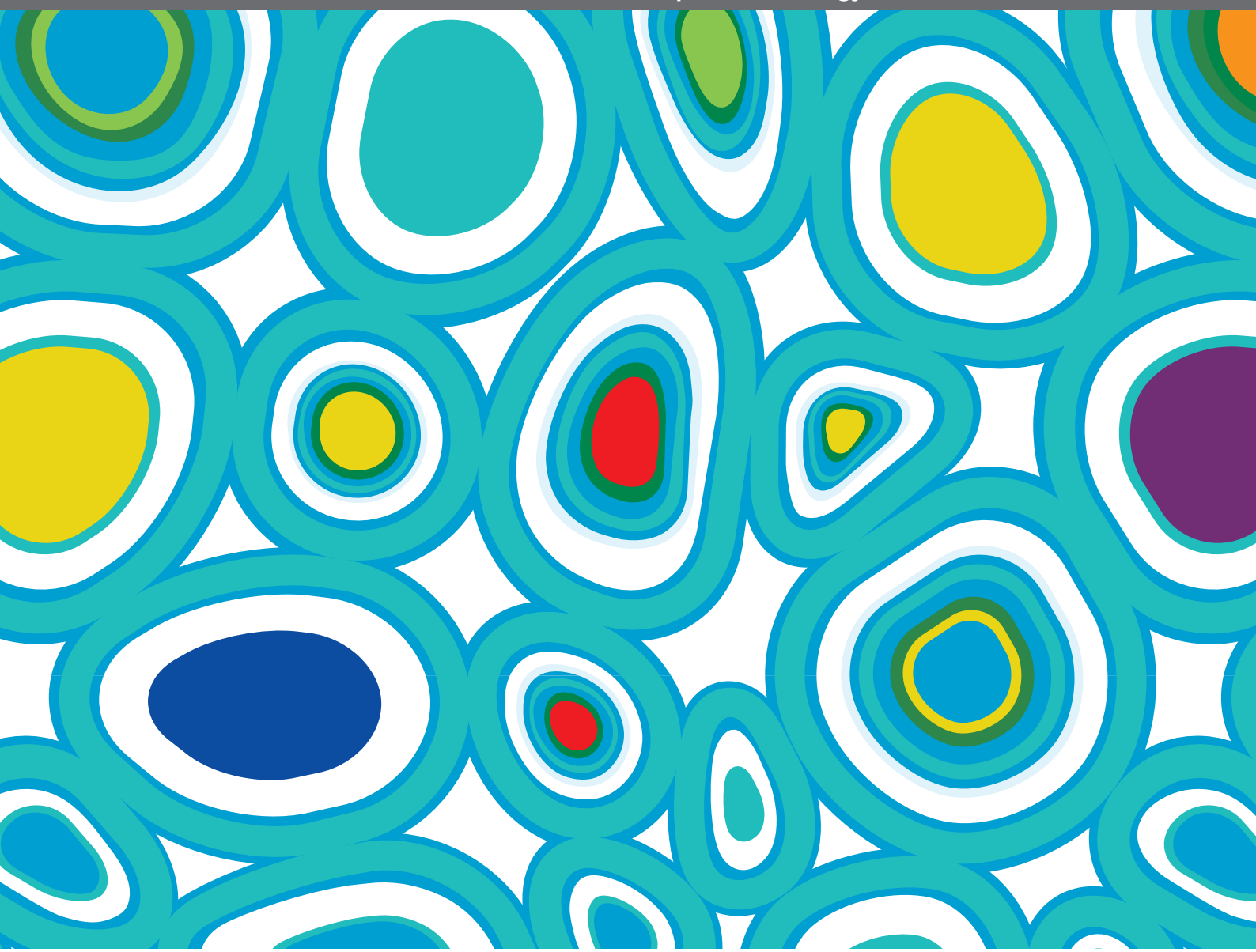

frontiers Research Topics

frontiers

ISSN 1664-8714
ISBN 978-2-88976-768-7
DOI 10.3389/978-2-88976-768-7

About Frontiers

Frontiers is more than just an open-access publisher of scholarly articles: it is a pioneering approach to the world of academia, radically improving the way scholarly research is managed. The grand vision of Frontiers is a world where all people have an equal opportunity to seek, share and generate knowledge. Frontiers provides immediate and permanent online open access to all its publications, but this alone is not enough to realize our grand goals.

Frontiers Journal Series

The Frontiers Journal Series is a multi-tier and interdisciplinary set of open-access, online journals, promising a paradigm shift from the current review, selection and dissemination processes in academic publishing. All Frontiers journals are driven by researchers for researchers; therefore, they constitute a service to the scholarly community. At the same time, the Frontiers Journal Series operates on a revolutionary invention, the tiered publishing system, initially addressing specific communities of scholars, and gradually climbing up to broader public understanding, thus serving the interests of the lay society, too.

Dedication to Quality

Each Frontiers article is a landmark of the highest quality, thanks to genuinely collaborative interactions between authors and review editors, who include some of the world's best academicians. Research must be certified by peers before entering a stream of knowledge that may eventually reach the public - and shape society; therefore, Frontiers only applies the most rigorous and unbiased reviews.
Frontiers revolutionizes research publishing by freely delivering the most outstanding research, evaluated with no bias from both the academic and social point of view. By applying the most advanced information technologies, Frontiers is catapulting scholarly publishing into a new generation.

What are Frontiers Research Topics?

Frontiers Research Topics are very popular trademarks of the Frontiers Journals Series: they are collections of at least ten articles, all centered on a particular subject. With their unique mix of varied contributions from Original Research to Review Articles, Frontiers Research Topics unify the most influential researchers, the latest key findings and historical advances in a hot research area! Find out more on how to host your own Frontiers Research Topic or contribute to one as an author by contacting the Frontiers Editorial Office: frontiersin.org/about/contact

METABOLITE AND NUTRIENT TRANSPORTERS IN CANCER-CELL METABOLISM: ROLE IN CANCER PROGRESSION AND METASTASIS

Topic Editors:
Vadivel Ganapathy, Texas Tech University Health Sciences Center, United States
Maria E. Mycielska, University of Regensburg, Germany
Eric Kenneth Parkinson, Queen Mary University of London, United Kingdom
Sebastian Haferkamp, University of Regensburg, Germany

Citation: Ganapathy, V., Mycielska, M. E., Parkinson, E. K., Haferkamp, S., eds. (2022). Metabolite and Nutrient Transporters in Cancer-Cell Metabolism: Role in Cancer Progression and Metastasis. Lausanne: Frontiers Media SA.
doi: 10.3389/978-2-88976-768-7

Table of Contents

frontiers | Frontiers in Cell and Developmental Biology

EDITORIAL
published: 25 April 2022
doi: 10.3389/fcell.2022.885717

Editorial: Metabolite and Nutrient Transporters in Cancer-Cell Metabolism: Role in Cancer Progression and Metastasis

Vadivel Ganapathy[1]*, *Sebastian Haferkamp*[2]*, *Eric K. Parkinson*[3]* and *Maria E. Mycielska*[4]*

[1]Department of Cell Biology and Biochemistry, Texas Tech University Health Sciences Center, Lubbock, TX, United States, [2]Department of Dermatology, University Hospital Regensburg, Regensburg, Germany, [3]Centre for Immunobiology and Regenerative Medicine, Queen Mary University of London, London, United Kingdom, [4]Department of Structural Biology, Institute of Biophysics and Physical Biochemistry, University of Regensburg, Regensburg, Germany

Keywords: cancer-cell metabolism, nutrient/acid/base transporters, Warburg effect, metabolomics, citrate, carnitine, amino acids, glucose

OPEN ACCESS

Edited by:
Shyamala Maheswaran, Harvard Medical School, United States

Reviewed by:
Yohei Miyagi, Kanagawa Cancer Center, Japan

***Correspondence:**
Vadivel Ganapathy
Vadivel.ganapathy@ttuhsc.edu
Sebastian Haferkamp
sabastian.haferkamp@klinik.uni-regensberg.de
Eric K. Parkinson
e.k.parkinson@qmul.ac.uk
Maria E. Mycielska
Maria.Mycielska@biologie.uni-regensburg.de

Specialty section:
This article was submitted to Cancer Cell Biology, a section of the journal Frontiers in Cell and Developmental Biology

Received: *28 February 2022*
Accepted: *07 April 2022*
Published: *25 April 2022*

Citation:
Ganapathy V, Haferkamp S, Parkinson EK and Mycielska ME (2022) Editorial: Metabolite and Nutrient Transporters in Cancer-Cell Metabolism: Role in Cancer Progression and Metastasis. Front. Cell Dev. Biol. 10:885717. doi: 10.3389/fcell.2022.885717

Editorial on the Research Topic

Metabolite and Nutrient Transporters in Cancer-Cell Metabolism: Role in Cancer Progression and Metastasis

INTRODUCTION

There has been a noticeable surge of interest in cancer-cell metabolism. In order to support their specific metabolic needs and rapid proliferation, cancer cells not only enhance the rates of normal metabolic pathways but also short-circuit and/or substantially modify other metabolic pathways (Ganapathy-Kanniappan, 2018; Kubicka et al., 2021; Vaupel and Multhoff, 2021; Pavlova et al., 2022). These changes are carried out through induction or suppression of specific enzymes and also through mutations in particular enzymes. As a result, terms such as Warburg effect, aerobic glycolysis, glutamine addiction, glutaminolysis, reductive carboxylation, oncometabolites, methionine-serine-one-carbon pathway, and ferroptosis have become routine in the vocabulary related to cancer biology. The relatively recent identification of cell-surface G-protein-coupled receptors for metabolites such as lactate and the ketone body β-hydroxybutyrate also tie into cancer-cell metabolism (Ristic et al., 2017; Brown and Ganapathy, 2020). These new developments in the cancer field are likely to result in identification of novel, hitherto unrecognized, drug targets for cancer treatment. Surprisingly however, as exciting as these new discoveries are in cancer-cell metabolism, the fact that enhanced entry of selective nutrients and metabolites into cancer cells is the first upstream event in driving these metabolic pathways has not received its due recognition and attention. This was the impetus for the Special Issue in Frontiers in Cell and Developmental Biology to focus on metabolite and nutrient transporters in cancer-cell metabolism.

Contributions to the Research Topic

The key metabolites/nutrients that are central to the above-mentioned cancer-cell-specific metabolic pathways are glucose, amino acids, fatty acids, lactate, citrate, cholesterol, carnitine, and iron. Metabolism of glucose in cancer cells is related to Warburg effect, aerobic glycolysis, endogenous synthesis of serine for the one-carbon pathway, and provision of the starting substrate (glucose-6-phosphate) for the pentose-phosphate pathway. The article by Shin and Koo focuses on the role of

the facilitative glucose transporter GLUT1 (SLC2A1) in breast cancer how this transporter and glycolysis-associated enzymes are upregulated in cancer cells, and how the resultant enhanced glucose delivery into cells feeds into specific pathways to generate lactate, serine, and NADPH. When the rate of glycolysis is enhanced in cancer cells, the intermediates in the pathway are present at higher than normal levels. The first intermediate is glucose-6-phosphate that can be siphoned off into the pentose-phosphate pathway to generate NADPH, a critical component of the anti-oxidant machinery essential for cancer-cell survival. 3-Phosphoglycerate, another intermediate, is used to synthesize serine, the major carbon source for the one-carbon metabolism that is essential for purine/pyrimidine synthesis, methionine-homocysteine cycle, and maintenance of epigenetic landscape. Recent studies have however shown that the increased glucose entry into cancer cells might not be solely due to the upregulation of GLUTs; Na^+-coupled glucose transporters SGLT1 and SGLT2 are also expressed at increased levels in certain cancers and aid in the successful use of PET scan-dependent diagnosis of cancers (Sala-Rabanal et al., 2016). The review by Nałęcz is related to the amino acid transporter SLC6A14, which is upregulated in several cancers such as pancreatic cancer, breast cancer, colon cancer, and ER-positive breast cancer (Sniegowski et al., 2021). This transporter is broad-specific with ability to transport 18 of the 20 proteinogenic amino acids coupled to multiple driving forces (Sikder et al., 2017). This article details the trafficking pathway for the newly synthesized SLC6A14 protein across the Golgi and the relevance of cancer-related signaling pathways to the increased cell-surface expression of the transporter in cancer cells. The article by Nunes et al. is on cysteine. Generally, this amino acid is discussed in the cancer field primarily in relation to its role in glutathione synthesis and the resultant protection against oxidative stress and ferroptosis (Koppula et al., 2021). But, Nunes et al. focus on the role of cysteine as an energy substrate for cancer cells. In this article, they outline not only the transport pathway for acquisition of extracellular cystine via the transporter xCT (SLC7A11) as a source of cellular cysteine but also the endogenous synthetic pathway via cystathionine.

Fatty acids are energy-rich nutrients with the highest caloric value among the major nutrients. Normoxic cancer cells with capacity for oxidative metabolism use fatty acids via mitochondrial fatty acid oxidation to generate energy. This is the topic for the article by Console et al. The delivery of fatty acids from the cytoplasm into mitochondria across the inner mitochondrial membrane is obligatorily dependent on the metabolite/nutrient carnitine. The review by Console *et al* details the various transporters for carnitine in terms of their expression and function in cancer cells.

Most cancer cells function as if they are under hypoxic conditions even when they are not. Hypoxic environment is common for cancer cells that grow far away from blood vessels. But, even in those cells that are present close to blood vessels, metabolites such as lactate, succinate, and fumarate stabilize the hypoxia-inducible factor-1α by inhibiting prolyl hydroxylases to facilitate hypoxic metabolism. The result is the generation of lactate as the end product of glycolysis and the process is called aerobic glycolysis. The article by Sun et al. describes the monocarboxylate transporters MCT1 (SLC16A1) and MCT4 (SLC16A3) in the handling of lactate in cancer cells. Interestingly, even though it is easy to explain Warburg hypothesis by assuming all cancer cells behave as if they are in a hypoxic environment, it has become clear that cancer cells in solid tumors are heterogeneous, some clearly in hypoxic mode, but others in normoxic mode with ability for oxidative metabolism. This highlights the differential roles of MCT1 versus MCT4 in the handling of lactate. MCT4 seems to play a major role in the release of lactate from hypoxic cancer cells whereas MCT1 facilitates the uptake of lactate into oxidative cancer cells, thus providing a metabolic link and crosstalk between cancer cells in different microenvironment. This crosstalk might also extend to cancer-associated stromal cells.

Citrate is at the intersection of multiple biochemical pathways. It is a carbon source for endogenous synthesis of fatty acids and cholesterol, both occurring in the cytoplasm, and also a substrate for the Kreb's cycle to generate ATP within the mitochondria. The article by Haferkamp et al. highlights the function of two different transporters for citrate, NaCT/SLC13A5 and pmCiC (an isoform of SLC25A1), both functioning in the plasma membrane, and their relevance to cancer. NaCT/SLC13A5 mediates the uptake of citrate from extracellular milieu into cancer cells (Jaramillo-Martinez et al., 2021) whereas pmCiC secretes citrate into the extracellular milieu from cancer-associated stromal cells (Drexler et al., 2021) but changes to a citrate importer in many cancer cell types (Mycielska et al., 2018), again underlining the metabolic crosstalk between different types of cells in solid tumors. Coleman and Parlo focus on cholesterol as an important metabolite for cancer-cell proliferation and describe the metabolic pathways for its endogenous synthesis using citrate as the carbon source. They also highlight the synthesis of citrate from glutamine via the cancer cell-specific pathway known as reductive carboxylation within mitochondria in which the reaction catalyzed by isocitrate dehydrogenase (isocitrate → α-ketoglutarate) is facilitated in the reverse direction in cancer cells by IDH2, an isoform of the enzyme that uses $NADP^+$/NADPH instead of NAD^+/NADH as the coenzyme.

Since cancer cells generate lactic acid and CO_2 (i.e., H_2CO_3) in large quantities in metabolism, the cells have to find ways to eliminate the acid load and maintain intracellular pH. This is the topic of the review by Venkateswaran and Dedhar, primarily focusing on the CAIX isoform of carbonic anhydrase, a membrane-bound protein with its catalytic site located externally. This enzyme catalyzes the following reaction: $CO_2 + H_2O \rightarrow H_2CO_3 \rightarrow H^+ + HCO_3^-$. The Na^+/bicarbonate transporter NBCn1 (SLC4A7) then transports HCO_3^- into cells, leaving H^+ outside. CAIX and NBCn1 form a complex to carry out these functions efficiently.

We have seen in recent years an explosion of structural studies on membrane transport proteins aided by x-ray crystallography and cryogenic-electron microscopy. Many of these transporters are closely related to cancer-cell metabolism. Examples include SLC7A5, SLC1A5, SLC6A14, and SLC7A11. The article by Carusela and Rubi provides insights into the computational modeling of the structures of membrane transporters

belonging to the ABC (ATP-Binding Cassette) family and the SLC (SoLute Carrier) family. With the ABC transporters, the authors highlight the structural changes that follow in connection with ATP hydrolysis. With SLC transporters, the focus is on the structural changes that follow the binding of substrates to the substrate-binding site.

It is well recognized that we need less-invasive biomarkers to diagnose different cancers and to monitor therapeutic efficacy, but success in this area still remains elusive. Two articles in this Special Issue (Du et al.; Ge et al.) use metabolomic profiles in serum as biomarkers for papillary thyroid cancer and intravenous leiomyomatosis, which pinpoint altered metabolism of aspartate and glutamate as well as the Kreb's cycle and urea cycle in the former and the utility of hypoxanthine, acetylcarnitine, and glycerophosphocholine in the diagnosis of the latter.

Synopsis

The articles assembled in the Special Issue collectively provide valuable insight into the cancer cell-specific reprogramming of metabolic pathways and the mechanisms by which the cancer cells acquire key nutrients to support their energy needs and promote their growth, proliferation, invasion and migration. These aspects of cancer-cell biology are fundamental for cancer progression and metastasis, thus fulfilling the primary goal of the Special Issue.

AUTHOR CONTRIBUTIONS

All authors listed have made a substantial, direct, and intellectual contribution to the work and approved it for publication.

FUNDING

This work was supported by the Welch Endowed Chair in Biochemistry to TTUHSC (BI-0028). Maria Mycielska was supported by DFG (Deutsche Forschungsgemeinschaft; grant GE1188/5-1).

REFERENCES

Brown, T. P., and Ganapathy, V. (2020). Lactate/GPR81 Signaling and Proton Motive Force in Cancer: Role in Angiogenesis, Immune Escape, Nutrition, and Warburg Phenomenon. *Pharmacol. Ther.* 206, 107451. doi:10.1016/j.pharmthera.2019.107451

Drexler, K., Schmidt, K. M., Jordan, K., Federlin, M., Milenkovic, V. M., Liebisch, G., et al. (2021). Cancer-associated Cells Release Citrate to Support Tumour Metastatic Progression. *Life Sci. Alliance* 4, e202000903. doi:10.26508/lsa.202000903

Ganapathy-Kanniappan, S. (2018). Molecular Intricacies of Aerobic Glycolysis in Cancer: Current Insights into the Classic Metabolic Phenotype. *Crit. Rev. Biochem. Mol. Biol.* 53, 667–682. doi:10.1080/10409238.2018.1556578

Jaramillo-Martinez, V., Urbatsch, I. L., and Ganapathy, V. (2021). Functional Distinction between Human and Mouse Sodium-Coupled Citrate Transporters and its Biologic Significance: An Attempt for Structural Basis Using a Homology Modeling Approach. *Chem. Rev.* 121, 5359–5377. doi:10.1021/acs.chemrev.0c00529

Koppula, P., Zhuang, L., and Gan, B. (2021). Cystine Transporter SLC7A11/xCT in Cancer: Ferroptosis, Nutrient Dependency, and Cancer Therapy. *Protein Cell* 12, 599–620. doi:10.1007/s13238-020-00789-5

Kubicka, A., Matczak, K., and Łabieniec-Watała, M. (2021). More Than Meets the Eye Regarding Cancer Metabolism. *Ijms* 22, 9507. doi:10.3390/ijms22179507

Mycielska, M. E., Dettmer, K., Rümmele, P., Schmidt, K., Prehn, C., Milenkovic, V. M., et al. (2018). Extracellular Citrate Affects Critical Elements of Cancer Cell Metabolism and Supports Cancer Development *In Vivo*. *Cancer Res.* 78, 2513–2523. doi:10.1158/0008-5472.can-17-2959

Pavlova, N. N., Zhu, J., and Thompson, C. B. (2022). The Hallmarks of Cancer Metabolism: Still Emerging. *Cell Metab* S1550-4131 (22), 00022–00025. doi:10.1016/j.cmet.2022.01.007

Ristic, B., Bhutia, Y. D., and Ganapathy, V. (2017). Cell-surface G-Protein-Coupled Receptors for Tumor-Associated Metabolites: A Direct Link to Mitochondrial Dysfunction in Cancer. *Biochim. Biophys. Acta (Bba) - Rev. Cancer* 1868, 246–257. doi:10.1016/j.bbcan.2017.05.003

Sala-Rabanal, M., Hirayama, B. A., Ghezzi, C., Liu, J., Huang, S.-C., Kepe, V., et al. (2016). Revisiting the Physiological Roles of SGLTs and GLUTs Using Positron Emission Tomography in Mice. *J. Physiol.* 594, 4425–4438. doi:10.1113/jp271904

Sikder, M. O. F., Yang, S., Ganapathy, V., and Bhutia, Y. D. (2017). The Na+/Cl−-Coupled, Broad-specific, Amino Acid Transporter SLC6A14 (ATB0,+): Emerging Roles in Multiple Diseases and Therapeutic Potential for Treatment and Diagnosis. *AAPS J.* 20, 12. doi:10.1208/s12248-017-0164-7

Sniegowski, T., Korac, K., Bhutia, Y. D., and Ganapathy, V. (2021). SLC6A14 and SLC38A5 Drive the Glutaminolysis and Serine-Glycine-One-Carbon Pathways in Cancer. *Pharmaceuticals* 14, 216. doi:10.3390/ph14030216

Vaupel, P., and Multhoff, G. (2021). Revisiting the Warburg Effect: Historical Dogma versus Current Understanding. *J. Physiol.* 599, 1745–1757. doi:10.1113/jp278810

Conflict of Interest: The authors declare that the research was conducted in the absence of any commercial or financial relationships that could be construed as a potential conflict of interest.

Publisher's Note: All claims expressed in this article are solely those of the authors and do not necessarily represent those of their affiliated organizations, or those of the publisher, the editors and the reviewers. Any product that may be evaluated in this article, or claim that may be made by its manufacturer, is not guaranteed or endorsed by the publisher.

frontiers in Cell and Developmental Biology

MINI REVIEW
published: 17 July 2020
doi: 10.3389/fcell.2020.00651

Role of Proton-Coupled Monocarboxylate Transporters in Cancer: From Metabolic Crosstalk to Therapeutic Potential

Xiangyu Sun[1], Mozhi Wang[1], Mengshen Wang[1], Litong Yao[1], Xinyan Li[1], Haoran Dong[1], Meng Li[1], Tie Sun[1], Xing Liu[1], Yang Liu[2] and Yingying Xu[1]**

[1] Department of Breast Surgery, The First Affiliated Hospital of China Medical University, Shenyang, China, [2] The Second Affiliated Hospital of China Medical University, Shenyang, China

Proton-coupled monocarboxylate transporters (MCTs), representing the first four isoforms of the *SLC16A* gene family, mainly participate in the transport of lactate, pyruvate, and other monocarboxylates. Cancer cells exhibit a metabolic shift from oxidative metabolism to an enhanced glycolytic phenotype, leading to a higher production of lactate in the cytoplasm. Excessive accumulation of lactate threatens the survival of cancer cells, and the overexpression of proton-coupled MCTs observed in multiple types of cancer facilitates enhanced export of lactate from highly glycolytic cancer cells. Proton-coupled MCTs not only play critical roles in the metabolic symbiosis between hypoxic and normoxic cancer cells within tumors but also mediate metabolic interaction between cancer cells and cancer-associated stromal cells. Of the four proton-coupled MCTs, MCT1 and MCT4 are the predominantly expressed isoforms in cancer and have been identified as potential therapeutic targets in cancer. Therefore, in this review, we primarily focus on the roles of MCT1 and MCT4 in the metabolic reprogramming of cancer cells under hypoxic and nutrient-deprived conditions. Additionally, we discuss how MCT1 and MCT4 serve as metabolic links between cancer cells and cancer-associated stromal cells via transport of crucial monocarboxylates, as well as present emerging opportunities and challenges in targeting MCT1 and MCT4 for cancer treatment.

Keywords: tumor microenvironment, metabolic networks and pathways, monocarboxylic acid transporters, lactic acid, glycolysis

OPEN ACCESS

Edited by:
Vadivel Ganapathy, Texas Tech University Health Sciences Center, United States

Reviewed by:
Marilyn Morris, University at Buffalo, United States
Lester R. Drewes, University of Minnesota Duluth, United States

****Correspondence:***
Yang Liu
yliuq@dicp.ac.cn
Yingying Xu
xuyingying@cmu.edu.cn

Specialty section:
This article was submitted to Molecular and Cellular Oncology, a section of the journal Frontiers in Cell and Developmental Biology

Received: *17 May 2020*
Accepted: *01 July 2020*
Published: *17 July 2020*

Citation:
Sun X, Wang M, Wang M, Yao L, Li X, Dong H, Li M, Sun T, Liu X, Liu Y and Xu Y (2020) Role of Proton-Coupled Monocarboxylate Transporters in Cancer: From Metabolic Crosstalk to Therapeutic Potential. Front. Cell Dev. Biol. 8:651. doi: 10.3389/fcell.2020.00651

INTRODUCTION

Monocarboxylate transporters (MCTs) belong to the *SLC16A* gene family and comprise 14 members. Of these identified 14 members, the proton-coupled isoforms MCT1–4 are critical in the metabolic process due to their roles in the transport of monocarboxylates such as lactate, pyruvate, and ketoacids (Halestrap and Price, 1999; Halestrap and Meredith, 2004). The function of proton-coupled MCTs as transporters of monocarboxylates is crucial for the metabolic rewiring of tumor cells and stromal cells (Martinez-Outschoorn U. et al., 2014; Pucino et al., 2018). Cancer cells display a metabolic shift from oxidative metabolism to glycolysis to rapidly produce ATP and lactate

in the cytoplasm (Koppenol et al., 2011). The lactate export mediated by proton-coupled MCTs is essential for the survival of cancer cells (Ganapathy et al., 2009; Draoui and Feron, 2011). Moreover, cancer cells exist within a complex microenvironment, surrounded by stromal cells primarily including immune cells, endothelial cells, and fibroblasts. The metabolic interplay between tumor cells and these stromal cells provides advantages for tumor proliferation and progression. MCT1 and MCT4 play the most dominant role in the transport of monocarboxylates, and they have been found to be significantly upregulated and associated with poor prognosis in multiple malignant tumors including peritoneal carcinomatosis, prostate cancer, lymphoma, and oral cavity cancer (Pértega-Gomes et al., 2011; Simões-Sousa et al., 2016; Kim et al., 2018; Afonso et al., 2019). Compared to MCT1 and MCT4, MCT2 and MCT3 have been less studied in cancer. Therefore, this review explores the metabolic crosstalk and therapeutic implications of proton-coupled MCTs with a primary focus on the current roles of MCT1 and MCT4 as targets in cancer.

THE METABOLIC ROLES OF MCT1 AND MCT4 IN CANCER CELLS

MCT1 and MCT4 are crucial players in the process of lactate exchange within tumors. The two isoforms differ in multiple aspects including biochemical properties and tissue distribution (Halestrap and Meredith, 2004; Pérez-Escuredo et al., 2016). MCT1, which exhibits a high affinity for lactate, preferentially facilitates lactate uptake to fuel oxidative phosphorylation (OXPHOS) and is also involved in lactate efflux from cancer cells. MCT4 is a low-affinity, lactate-preferring transporter, adapted to export lactate from glycolytic cancer cells (Dimmer et al., 2000; Halestrap and Meredith, 2004). It should be noted that both normoxic and hypoxic cancer cells co-exist within the tumors, with a lactate shuttling commonly observed between hypoxic and normoxic sites. Hypoxic tumor cells depend on glucose as the main fuel source to satisfy their energy demand, and the high levels of lactate produced are subsequently transported out of the cytoplasm primarily via MCT4. Concurrently, tumor cell-derived lactate can enter the neighboring normoxic cancer cells via MCT1 for OXPHOS, thus sparing glucose for glycolytic cancer cells (Sonveaux et al., 2008; Doherty and Cleveland, 2013). This form of metabolic symbiosis illustrates how the apparent waste product from hypoxic tumor cells may be exploited by oxidative tumor cells to sustain their energy production under nutrient-deprived condition. The relative contributions of glucose and lactate to the tricarboxylic acid (TCA) cycle of non-small cell lung carcinoma cells have been compared. Infusing tumors with 13C-labeled lactate resulted in higher amounts of labeled metabolites TCA cycle metabolites compared to infusion with 13C-labeled glucose (Faubert et al., 2017). These findings highlight that the lactate transport between hypoxic and normoxic tumor cells mediated by MCT1/4 may be crucial for energy production, tumor proliferation and invasion.

An additional role of MCTs is their capability to transport pyruvate across the plasma membrane. Pyruvate is the end-product of glycolysis and a turning point for production of glucose, lactate, fatty acids, and amino acids. As a significant substrate for the TCA cycle, cytoplasmic pyruvate can be transported into the mitochondria to further undergo oxidative metabolism to produce ATP and provide important intermediates. MCT4 shows a high affinity for pyruvate, which may prevent pyruvate efflux that is essential for maintaining of a high glycolytic flux (Halestrap, 2013). MCT1, with a lower affinity for pyruvate, is responsible for the bidirectional transport of pyruvate (Halestrap, 2013). Hong et al. (2016) proposed that MCT1 expression is elevated in glycolytic cancers to enhance pyruvate export to impair mitochondrial OXPHOS. MCT1 inhibition blocks pyruvate export without glycolysis impairment in glycolytic breast tumor cells co-expressing MCT1 and MCT4, which promotes mitochondrial oxidative metabolism and suspends tumor growth (Hong et al., 2016). However, Diers et al. (2012) found that MCT1 upregulation may enhance pyruvate uptake in breast cancer cells, fueling OXPHOS and proliferative potential. MCT inhibition impaired mitochondrial respiration and decreased cell growth through inhibition of cellular pyruvate uptake (Diers et al., 2012). Although the precise roles of MCT1/4 in the pyruvate transport of cancer cells need further investigation, these conflicting results proposed alternative molecular mechanisms for the action of MCT inhibitors in addition to their effects on lactate transport.

HOW MCT1 AND MCT4 LINK CANCER CELLS AND THE TUMOR MICROENVIRONMENT

MCT1 and MCT4 are not only essential for metabolic symbiosis between glycolytic and oxidative cancer cells; they also mediate metabolic rewiring within the tumor microenvironment (TME). MCT1/4-mediated metabolic interplay between cancer cells and stromal cells may be critical for tumor immune response, angiogenesis, and therapy resistance (**Figure 1**). Thus, targeting the metabolic interplay within the TME is indispensable for developing new interventions for cancer management.

Immune Cells

Cancer cells display metabolic crosstalk with immune cells using a variety of mechanisms. Studies have shown that high levels of lactate produced by glycolytic tumor cells can lead to immune evasion (Bohn et al., 2018; Sekine et al., 2018). Macrophages, a key representative of myeloid lineages possess two polarized types of the classically activated (M1) macrophage phenotype and the alternatively activated (M2) macrophage phenotype (Biswas and Mantovani, 2010). MCT1/4-mediated lactate secretion from cancer cells plays an important role in mediating macrophage polarization to the M2-like state, which presents with immunosuppressive properties (Colegio et al., 2014; Ohashi et al., 2017; Mu et al., 2018; Liu et al., 2019; Stone et al., 2019). In gastric cancer, the lactate-MCT-hypoxic inducible factor-1α (HIF-1α) axis has been identified as a crucial signaling axis that connects metabolic rewiring and immune evasion. MCT1 inhibition or knockdown of HIF-1α can remarkably

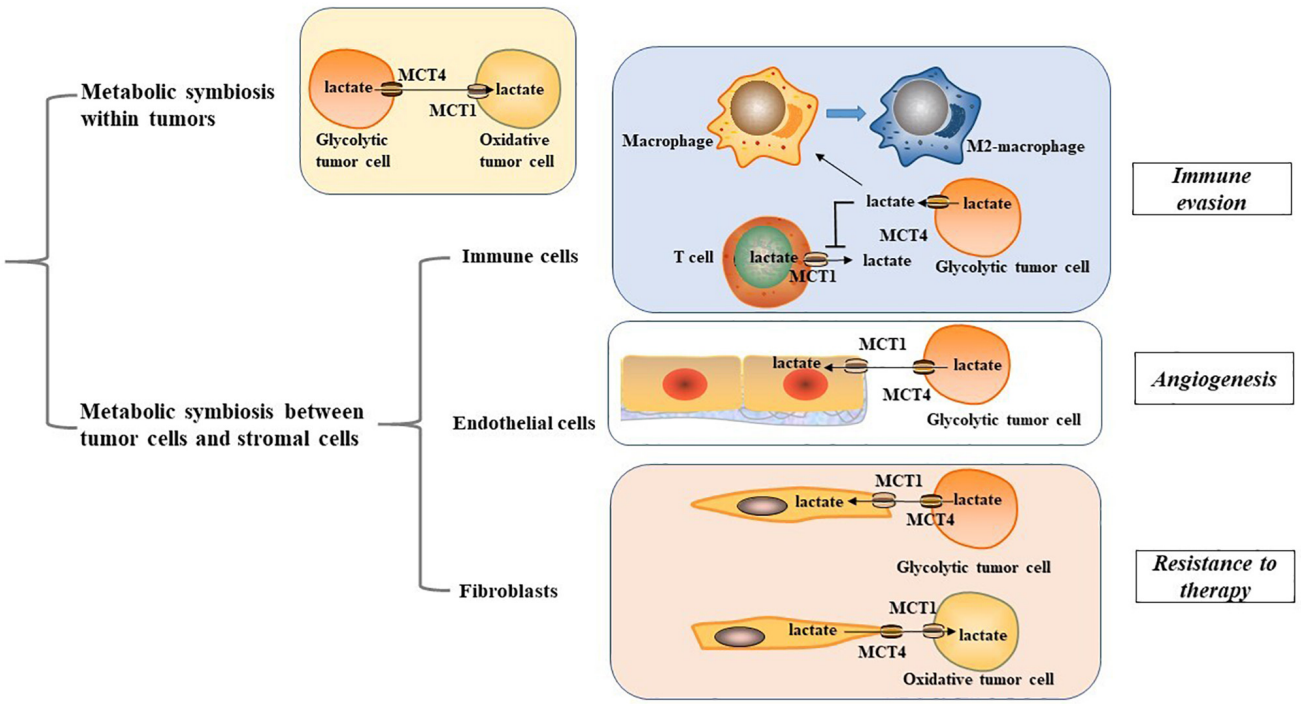

FIGURE 1 | Metabolic symbiosis within tumor microenvironment. MCT1, monocarboxylate transporter 1; MCT4, monocarboxylate transporter 4; M2 macrophage, alternatively activated macrophage.

abrogate the expression of key M2 marker CD163 and arginase 1 in macrophages (Zhang and Li, 2020). Activation of nuclear factor E2-related factor-2, a transcription factor for regulating oxidative stress response, can induce MCT1 upregulation, fuel lactate uptake of premalignant colonic epithelial cells exposed to inflammatory M1 macrophages and shift colonic epithelial cells toward a reversed Warburg metabolism, favoring malignant transformation of the colonic epithelium (Diehl et al., 2018). This adds new insights for the impact of MCT1/4-mediated lactate transport on macrophage functionality. Nevertheless, the carcinogenic role on MCT 1/4 in macrophages may not be restricted to their effect on lactate transport. In glioblastoma, transport of branched-chain ketoacids (BCKAs), metabolites of branched-chain amino acid catabolism, is also mediated by MCT1. Tumor-excreted BCKAs can be taken up and re-aminated to branched-chain amino acids in macrophages. Exposure to BCKAs abrogates the phagocytic activity of macrophages, and the anti-proliferative effects of MCT1 silencing may also be involved with impaired excretion of BCKAs (Silva et al., 2017). These findings imply a significant role of MCT1/4 in mediating the metabolic crosstalk between tumor cells and macrophages to provide potential metabolic vulnerabilities for cancer management.

T cells have a decisive protective role in host defenses against cancer, and therapeutic strategies targeting T cell immunometabolism have developed quickly in the past years (Jiang and Yan, 2016; Kishton et al., 2017). It is well established that T cells undergo metabolic adaption for the bioenergetic needs of their immune response. During activation, T cells rely on their enhanced glycolytic phenotype to support their growth and effector functions (Thommen and Schumacher, 2018). However, high lactate concentration in the TME blocks lactate export from T cells, thereby disturbing their metabolism and function (Brand et al., 2016). For instance, cytolytic CD8+ T lymphocytes have been found to rely on MCT1-mediated lactate export to sustain their cytokine production and cytotoxic activity (Fischer et al., 2007). Thus, targeting this metabolic pathway in tumors is a promising strategy to enhance tumor immunogenicity. It has been found that silencing MCT1 and MCT4 can suppress lactate secretion, restore T cell-induced immune function, and boost response to immune checkpoint inhibitors in melanoma patients (Renner et al., 2019). Given that immune checkpoint inhibitors function to activate the effective immune response of T cells, MCT1/4 provide new insights for cancer immunotherapy.

Endothelial Cells

The Warburg effect, accompanied with high MCT1/4 expression in the tumor-endothelial cells (EC) micro-environment contributes significantly to angiogenic capacity and cancer progression (Rohlenova et al., 2018; Guo et al., 2019). Glycolytic cancer cells primarily depend on MCT4 to release lactate into the TME, ECs take up lactate in a MCT1-mediated manner, similar to oxidative cancer cells. MCT1/4-mediated lactate transport has been shown to serve as a crucial pro-angiogenic factor to mediate tumor-EC metabolic rewiring, angiogenic activity, and tumor progression in multiple cancers, including glioblastoma,

renal cancer, colorectal, and breast cancer, which may rely on activation of oncogenic signaling including nuclear factor-κB (NF-κB) and HIF-1α (Miranda-Gonçalves et al., 2017; Rohlenova et al., 2018; Guo et al., 2019). In tumor ECs, lactate activates the vascular endothelial growth factor signaling pathway to promote lactate-mediated proangiogenic activity, which may act through a poly-ADP ribosylation-dependent mechanism (Kumar et al., 2007). Upon entry into the ECs, lactate can be oxidized by lactate dehydrogenase to produce pyruvate that can subsequently interact with prolylhydroxylases and inhibit prolylhydroxylases activity. This promotes an autocrine NF-κB/IL-8 pathway to drive angiogenic activity and tumor progression (Vegran et al., 2011). The pro-angiogenic properties of the tumor-EC network suggest that MCT1/4 have valuable implications for new therapeutic concepts targeting tumor angiogenesis.

Fibroblasts

In tumor-stroma contact models, a symbiotic relationship termed as the reverse Warburg effect has been established in which stromal cells are induced by oxidative cancer cells to undergo a glycolytic switch and MCT4 upregulation, and metabolites including lactate and pyruvate are imported into the cancer cells for OXPHOS in a MCT1-dependent manner. This metabolic compartmentalization creates a nutrient-rich microenvironment to produce mitochondrial fuels and enables oxidative cancer cells to satisfy their metabolic demand (Koukourakis et al., 2006; Martinez-Outschoorn U.E. et al., 2014; Whitaker-Menezes et al., 2014; Sakamoto et al., 2019). The catabolic phenotypes observed in cancer-associated fibroblasts (CAFs) are driven by multiple cell signaling pathways including loss of caveolin-1 and the activation of HIF-1α and NF-κB signaling, which may serve as metabolic vulnerabilities in the metabolic rewiring of the tumor-CAF network (Pavlides et al., 2009; Bonuccelli et al., 2010; Wilde et al., 2017). In a prostate cancer cell model, tumor-CAF contact triggers a sirtuin 3 -mediated regulation of HIF1 stabilization and glycolytic phenotype to upregulate MCT4 and enhance lactate secretion from CAFs, while prostate cancer cells increase lactate uptake mediated by MCT1 (Fiaschi et al., 2012). Consistently, prostate cancer cells have been shown to undergo sirtuin 1-dependent PGC-1α activation to enhance mitochondrial OXPHOS (Ippolito et al., 2019). Therefore, the reverse Warburg effect mediated by MCT1/4 leads to an enhanced malignant phenotype, making it a crucial therapeutic target.

However, opposite situation exist wherein stromal cells metabolically use lactate and other monocarboxylates exported by highly glycolytic cancer cells for their own energetic requirements. This metabolic interplay not only spares glucose for adjacent glycolytic tumor cells, but it also enables CAFs to provide metabolites of lactate oxidation, such as pyruvate, to meet the energy needs of tumor cells (Koukourakis et al., 2006, 2017; Patel et al., 2017). It has been shown that tyrosine kinase inhibitors-resistant cancer cells exhibit an enhanced glycolytic phenotype and lactate production, while CAFs increase their lactate uptake via MCT1. This further induces upregulation of HGF transcriptional level in CAFs through an NF-kB-dependent manner, which leads to drug resistance to tyrosine kinase inhibitors (Apicella et al., 2018). These emerging opposite situations indicate the existence of tumor metabolic heterogeneity, highlighting the need for further investigations into the metabolic interplay between tumor cells and CAFs.

IMPLICATIONS FOR CANCER TREATMENT

Based on its role in facilitating tumor progression, blocking MCT1/4-mediated monocarboxylate transport may provide novel insights for cancer therapy. Several MCT1 inhibitors have been described, especially AZD3965 and its analog AR-C155858. AZD3965 is a specific MCT1/2 inhibitor that is currently being evaluated in a phase 1 clinical trial[1] in solid tumors (NCT01791595). AZD3965 has shown promising anti-tumor effects in treating MCT1-overexpressing models of diverse malignancies including Burkitt lymphoma, diffuse large B-cell lymphoma, gastric cancer, and small cell lung cancer (Bola et al., 2014; Polanski et al., 2014; Noble et al., 2017). Evidence indicates that AZD3965 and its analog AR-C155858 may not be effective. *In vivo* AR-C155858 treatment was shown to be ineffective in the murine 4T1 xenograft breast tumor model, which may relate to the immune status of the preclinical xenograft model (Guan et al., 2018). Another disadvantage of MCT1-selective inhibition is that it is ineffective when MCT4 is expressed due to the compensatory effect of MCT4 for MCT1 activity (Fiaschi et al., 2012). However, MCT4 inhibitors are still in the discovery phase. Developing drugs that co-inhibit MCT1 and MCT4 may be more effective in blocking lactate secretion and tumor growth. However, inhibition of lactate uptake via MCT1/4 inhibitor may drive glucose influx to mitochondrial metabolism to maintain tumor cell survival (Beloueche-Babari et al., 2017; Corbet et al., 2018). Therefore, co-administration of MCT1/4 inhibitors and mitochondrial-targeted therapy, such as the mitochondrial complex I inhibitor metformin or mitochondrial pyruvate carrier inhibitors, may counteract the elevated mitochondrial metabolism (Beloueche-Babari et al., 2017; Benjamin et al., 2018). It is noteworthy that MCT1 may mediate tumor progression beyond its role as a lactate transporter. For instance, MCT1 has been found to activate the transcription factor NF-κB to facilitate tumor cell migration independently of its transporter activity (Payen et al., 2017). This suggests that coordination of MCT1 inhibitors and other therapeutic agents to block tumor development may be a key point for future pharmacological strategies.

CD147 is a transmembrane glycoprotein that whose overexpression significantly correlates with poor prognosis in multiple malignancies (Nabeshima et al., 2006; Iacono et al., 2007; Pinheiro et al., 2009; Zhong et al., 2012; Huang et al., 2018; Landras et al., 2019). Importantly, CD147 forms complex with MCT1/4, which is necessary for maintaining MCT1/4 cell surface expression and activity (Kirk et al., 2000; Gallagher et al., 2007; Eichner et al., 2016). Therefore, the major pro-tumoral action of CD147 was shown to involve a metabolic modification of the TME through its interaction with MCT1 and MCT4 (Le Floch et al., 2011; Marchiq et al., 2015; Updegraff et al., 2018). Currently, potential CD147 inhibitors

[1] www.clinicaltrials.gov

including p-chloromercuribenzene sulfonate, which disrupts CD147-MCT1/4 interaction, and AC-73, which targets CD147 dimeric interface, have been proposed (Wilson et al., 2005; Spinello et al., 2019). These studies illustrate that CD147 has therapeutic implications for cancer treatment in addition to directly target proton-coupled MCTs.

CONCLUSION

Proton-coupled MCTs, especially MCT1 and MCT4, are emerging as promising therapeutic targets for cancer treatment. Indeed, MCT1/4-mediated transport of metabolites such as lactate and pyruvate not only plays a decisive role in metabolic symbiosis between hypoxic and normoxic cancer cells within tumors and also links crosstalk between cancer cells and stromal cells including immune cells, endothelial cells and fibroblasts. These metabolic interplays mediated by MCT1 and MCT4 necessitate further exploration in the clinical settings. MCT1 inhibitors are currently being tested in the clinical trial, and potential combination with other agents may provide new prospects for cancer management. CD147, which is necessary for MCT1 and MCT4 activity, also serves as a therapeutic target to block MCT1/4-mediated transport of crucial metabolites to impair cancer progression. Unfortunately, our understanding of the effects of MCT1/4 are still limited and most studies are based on *in vitro* and preclinical data. Thus, a better understanding of the role of MCT1 and MCT4 in metabolic reprogramming and cancer development is required for novel therapeutic strategies.

AUTHOR CONTRIBUTIONS

XS wrote and elaborated the figures. MoW, MeW, LY, XLi, HD, ML, TS, and XLiu wrote and reviewed the manuscript. YL and YX wrote and reviewed the final version. All authors contributed to the article and approved the submitted version.

FUNDING

This work was supported by the National Natural Science Foundation of China (81773083), Scientific and Technological Innovation Leading Talent Project of Liaoning Province (XLYC1802108), and Support Project for Young and Technological Innovation Talents of Shenyang (RC190393).

REFERENCES

Afonso, J., Pinto, T., Simões-Sousa, S., Schmitt, F., Longatto-Filho, A., Pinheiro, C., et al. (2019). Clinical significance of metabolism-related biomarkers in non-Hodgkin lymphoma – MCT1 as potential target in diffuse large B cell lymphoma. *Cell Oncol.* 42, 303–318. doi: 10.1007/s13402-019-00426-2

Apicella, M., Giannoni, E., Fiore, S., Ferrari, K. J., Fernández-Pérez, D., Isella, C., et al. (2018). Increased lactate secretion by cancer cells sustains non-cell-autonomous adaptive resistance to MET and EGFR targeted therapies. *Cell Metab.* 28, 848.e6–865.e6. doi: 10.1016/j.cmet.2018.08.006

Beloueche-Babari, M., Wantuch, S., Casals Galobart, T., Koniordou, M., Parkes, H. G., Arunan, V., et al. (2017). MCT1 inhibitor AZD3965 increases mitochondrial metabolism, facilitating combination therapy and noninvasive magnetic resonance spectroscopy. *Cancer Res.* 77, 5913–5924. doi: 10.1158/0008-5472.CAN-16-2686

Benjamin, D., Robay, D., Hindupur, S. K., Pohlmann, J., Colombi, M., El-Shemerly, M. Y., et al. (2018). Dual inhibition of the lactate transporters MCT1 and mct4 is synthetic lethal with metformin due to NAD+ depletion in cancer cells. *Cell Rep.* 25, 3047.e4–3058.e4. doi: 10.1016/j.celrep.2018.11.043

Biswas, S. K., and Mantovani, A. (2010). Macrophage plasticity and interaction with lymphocyte subsets: cancer as a paradigm. *Nat. Immunol.* 11, 889–896. doi: 10.1038/ni.1937

Bohn, T., Rapp, S., Luther, N., Klein, M., Bruehl, T., Kojima, N., et al. (2018). Tumor immunoevasion via acidosis-dependent induction of regulatory tumor-associated macrophages. *Nat. Immunol.* 19, 1319–1329. doi: 10.1038/s41590-018-0226-8

Bola, B. M., Chadwick, A. L., Michopoulos, F., Blount, K. G., Telfer, B. A., Williams, K. J., et al. (2014). Inhibition of monocarboxylate transporter-1 (MCT1) by AZD3965 enhances radiosensitivity by reducing lactate transport. *Mol. Cancer Ther.* 13, 2805–2816. doi: 10.1158/1535-7163.MCT-13-1091

Bonuccelli, G., Whitaker-Menezes, D., Castello-Cros, R., Pavlides, S., Pestell, R. G., Fatatis, A., et al. (2010). The reverse Warburg effect Glycolysis inhibitors prevent the tumor promoting effects of caveolin-1 deficient cancer associated fibroblasts. *Cell Cycle* 9, 1960–1971. doi: 10.4161/cc.9.10.11601

Brand, A., Singer, K., Koehl, G. E., Kolitzus, M., Schoenhammer, G., Thiel, A., et al. (2016). LDHA-associated lactic acid production blunts tumor immunosurveillance by T and NK Cells. *Cell Metab.* 24, 657–671. doi: 10.1016/j.cmet.2016.08.011

Colegio, O. R., Chu, N., Szabo, A. L., Chu, T., Rhebergen, A. M., Jairam, V., et al. (2014). Functional polarization of tumour-associated macrophages by tumour-derived lactic acid. *Nature* 513, 559–563. doi: 10.1038/nature13490

Corbet, C., Bastien, E., Draoui, N., Doix, B., Mignion, L., Jordan, B. F., et al. (2018). Interruption of lactate uptake by inhibiting mitochondrial pyruvate transport unravels direct antitumor and radiosensitizing effects. *Nat. Commun.* 9:1208. doi: 10.1038/s41467-018-03525-0

Diehl, K., Dinges, L., Helm, O., Ammar, N., Plundrich, D., Arlt, A., et al. (2018). Nuclear factor E2-related factor-2 has a differential impact on MCT1 and MCT4 lactate carrier expression in colonic epithelial cells: a condition favoring metabolic symbiosis between colorectal cancer and stromal cells. *Oncogene* 37, 39–51. doi: 10.1038/onc.2017.299

Diers, A. R., Broniowska, K. A., Chang, C., and Hogg, N. (2012). Pyruvate fuels mitochondrial respiration and proliferation of breast cancer cells: effect of monocarboxylate transporter inhibition. *Biochem. J.* 444, 561–571. doi: 10.1042/BJ20120294

Dimmer, S., Friedrich, B., Lang, F., Deitmer, J. W., and Bröer, S. (2000). The low-affinity monocarboxylate transporter MCT4 is adapted to the export of lactate in highly glycolytic cells. *Biochem. J.* 350, 219–227. doi: 10.1042/bj3500219

Doherty, J. R., and Cleveland, J. L. (2013). Targeting lactate metabolism for cancer therapeutics. *J. Clin. Invest.* 123, 3685–3692. doi: 10.1172/JCI69741

Draoui, N., and Feron, O. (2011). Lactate shuttles at a glance: from physiological paradigms to anti-cancer treatments. *Dis. Model Mech.* 2011, 727–732. doi: 10.1242/dmm.007724

Eichner, R., Heider, M., Fernández-Sáiz, V., van Bebber, F., Garz, A., Lemeer, S., et al. (2016). Immunomodulatory drugs disrupt the cereblon–CD147–MCT1 axis to exert antitumor activity and teratogenicity. *Nat. Med.* 22, 735–743. doi: 10.1038/nm.4128

Faubert, B., Li, K. Y., Cai, L., Hensley, C. T., Kim, J., Zacharias, L. G., et al. (2017). Lactate metabolism in human lung tumors. *Cell* 171, 358.e9–371.e9. doi: 10.1016/j.cell.2017.09.019

Fiaschi, T., Marini, A., Giannoni, E., Taddei, M. L., Gandellini, P., Donatis, A. D., et al. (2012). Reciprocal metabolic reprogramming through lactate shuttle coordinately influences tumor-stroma interplay. *Cancer Res.* 72, 5130–5140. doi: 10.1158/0008-5472.CAN-12-1949

Fischer, K., Hoffmann, P., Voelkl, S., Meidenbauer, N., Ammer, J., Edinger, M., et al. (2007). Inhibitory effect of tumor cell–derived lactic acid on human T cells. *Blood* 109, 3812–3819. doi: 10.1182/blood-2006-07-035972

Gallagher, S. M., Castorino, J. J., Wang, D., and Philp, N. J. (2007). Monocarboxylate transporter 4 regulates maturation and trafficking of CD147 to the plasma membrane in the metastatic breast cancer cell line MDA-MB-231. *Cancer Res.* 67, 4182–4189. doi: 10.1158/0008-5472.CAN-06-3184

Ganapathy, V., Thangaraju, M., and Prasad, P. D. (2009). Nutrient transporters in cancer: relevance to Warburg hypothesis and beyond. *Pharmacol. Therapeut.* 121, 29–40. doi: 10.1016/j.pharmthera.2008.09.005

Guan, X. W., Bryniarski, M. A., and Morris, M. E. (2018). In vitro and in vivo efficacy of the monocarboxylate transporter 1 inhibitor AR-C155858 in the murine 4T1 breast cancer tumor model. *AAPS J.* 21:3. doi: 10.1208/s12248-018-0261-2

Guo, C., Huang, T., Wang, Q., Li, H., Khanal, A., Kang, E., et al. (2019). Monocarboxylate transporter 1 and monocarboxylate transporter 4 in cancer-endothelial co-culturing microenvironments promote proliferation, migration, and invasion of renal cancer cells. *Cancer Cell Int.* 19:170. doi: 10.1186/s12935-019-0889-8

Halestrap, A. P. (2013). Monocarboxylic acid transport. *Compr. Physiol.* 3, 1611–1643. doi: 10.1002/cphy.c130008

Halestrap, A. P., and Meredith, D. (2004). The SLC16 gene family-from monocarboxylate transporters (MCTs) to aromatic amino acid transporters and beyond. *Pflugers Arch.* 447, 619–628. doi: 10.1007/s00424-003-1067-2

Halestrap, A. P., and Price, N. T. (1999). The proton-linked monocarboxylate transporter (MCT) family: structure, function and regulation. *Biochem. J.* 343(Pt 2), 281–299. doi: 10.1042/bj3430281

Hong, C. S., Graham, N. A., Gu, W., Espindola Camacho, C., Mah, V., Maresh, E. L., et al. (2016). MCT1 modulates cancer cell pyruvate export and growth of tumors that Co-express MCT1 and MCT4. *Cell Rep.* 14, 1590–1601. doi: 10.1016/j.celrep.2016.01.057

Huang, P., Mao, L., Zhang, Z., Lv, W., Feng, X., Liao, H., et al. (2018). Down-regulated miR-125a-5p promotes the reprogramming of glucose metabolism and cell malignancy by increasing levels of CD147 in thyroid cancer. *Thyroid* 28, 613–623. doi: 10.1089/thy.2017.0401

Iacono, K. T., Brown, A. L., Greene, M. I., and Saouaf, S. J. (2007). CD147 immunoglobulin superfamily receptor function and role in pathology. *Exp. Mol. Pathol.* 83, 283–295. doi: 10.1016/j.yexmp.2007.08.014

Ippolito, L., Morandi, A., Taddei, M. L., Parri, M., Comito, G., Iscaro, A., et al. (2019). Cancer-associated fibroblasts promote prostate cancer malignancy via metabolic rewiring and mitochondrial transfer. *Oncogene* 38, 5339–5355. doi: 10.1038/s41388-019-0805-7

Jiang, S., and Yan, W. (2016). T-cell immunometabolism against cancer. *Cancer Lett.* 382, 255–258. doi: 10.1016/j.canlet.2016.09.003

Kim, H. K., Lee, I., Bang, H., Kim, H. C., Lee, W. Y., Yun, S. H., et al. (2018). MCT4 expression is a potential therapeutic target in colorectal cancer with peritoneal carcinomatosis. *Mol. Cancer Ther.* 17, 838–848. doi: 10.1158/1535-7163.MCT-17-0535

Kirk, P., Wilson, M. C., Heddle, C., Brown, M. H., Barclay, A. N., and Halestrap, A. P. (2000). CD147 is tightly associated with lactate transporters MCT1 and MCT4 and facilitates their cell surface expression. *EMBO J.* 19, 3896–3904. doi: 10.1093/emboj/19.15.3896

Kishton, R. J., Sukumar, M., and Restifo, N. P. (2017). Metabolic regulation of T Cell longevity and function in tumor immunotherapy. *Cell Metab.* 26, 94–109. doi: 10.1016/j.cmet.2017.06.016

Koppenol, W. H., Bounds, P. L., and Dang, C. V. (2011). Otto Warburg's contributions to current concepts of cancer metabolism. *Nat. Rev. Cancer* 11, 325–337. doi: 10.1038/nrc3038

Koukourakis, M. I., Giatromanolaki, A., Harris, A. L., and Sivridis, E. (2006). Comparison of metabolic pathways between cancer cells and stromal cells in colorectal carcinomas: a metabolic survival role for tumor-associated stroma. *Cancer Res.* 66, 632–637. doi: 10.1158/0008-5472.CAN-05-3260

Koukourakis, M. I., Kalamida, D., Mitrakas, A. G., Liousia, M., Pouliliou, S., Sivridis, E., et al. (2017). Metabolic cooperation between co-cultured lung cancer cells and lung fibroblasts. *Lab Invest.* 97, 1321–1331. doi: 10.1038/labinvest.2017.79

Kumar, V. B. S., Viji, R. I., Kiran, M. S., and Sudhakaran, P. R. (2007). Endothelial cell response to lactate: Implication of PAR modification of VEGF. *J. Cell Physiol.* 211, 477–485. doi: 10.1002/jcp.20955

Landras, A., de Moura, C. R., Jouenne, F., Lebbe, C., Menashi, S., and Mourah, S. (2019). CD147 is a promising target of tumor progression and a prognostic biomarker. *Cancers* 11:1803. doi: 10.3390/cancers11111803

Le Floch, R., Chiche, J., Marchiq, I., Naiken, T., Ilc, K., Murray, C. M., et al. (2011). CD147 subunit of lactate/H+ symporters MCT1 and hypoxia-inducible MCT4 is critical for energetics and growth of glycolytic tumors. *Proc. Natl. Acad. Sci. U.S.A.* 108, 16663–16668. doi: 10.1073/pnas.1106123108

Liu, N., Luo, J., Kuang, D., Xu, S., Duan, Y., Xia, Y., et al. (2019). Lactate inhibits ATP6V0d2 expression in tumor-associated macrophages to promote HIF-2α–mediated tumor progression. *J. Clin. Invest.* 129, 631–646. doi: 10.1172/JCI123027

Marchiq, I., Le Floch, R., Roux, D., Simon, M., and Pouyssegur, J. (2015). Genetic disruption of lactate/H+ Symporters (MCTs) and their subunit CD147/BASIGIN sensitizes glycolytic tumor cells to phenformin. *Cancer Res.* 75, 171–180. doi: 10.1158/0008-5472.CAN-14-2260

Martinez-Outschoorn, U., Sotgia, F., and Lisanti, M. P. (2014). Tumor microenvironment and metabolic synergy in breast cancers: critical importance of mitochondrial fuels and function. *Semin. Oncol.* 41, 195–216. doi: 10.1053/j.seminoncol.2014.03.002

Martinez-Outschoorn, U. E., Lisanti, M. P., and Sotgia, F. (2014). Catabolic cancer-associated fibroblasts transfer energy and biomass to anabolic cancer cells, fueling tumor growth. *Semin. Cancer Biol.* 25, 47–60. doi: 10.1016/j.semcancer.2014.01.005

Miranda-Gonçalves, V., Bezerra, F., Costa-Almeida, R., Freitas-Cunha, M., Soares, R., Martinho, O., et al. (2017). Monocarboxylate transporter 1 is a key player in glioma-endothelial cell crosstalk. *Mol. Carcinogen.* 56, 2630–2642. doi: 10.1002/mc.22707

Mu, X., Shi, W., Xu, Y., Xu, C., Zhao, T., Geng, B., et al. (2018). Tumor-derived lactate induces M2 macrophage polarization via the activation of the ERK/STAT3 signaling pathway in breast cancer. *Cell Cycle* 17, 428–438. doi: 10.1080/15384101.2018.1444305

Nabeshima, K., Iwasaki, H., Koga, K., Hojo, H., Suzumiya, J., and Kikuchi, M. (2006). Emmprin (basigin/CD147): matrix metalloproteinase modulator and multifunctional cell recognition molecule that plays a critical role in cancer progression. *Pathol. Int.* 56, 359–367. doi: 10.1111/j.1440-1827.2006.01972.x

Noble, R. A., Bell, N., Blair, H., Sikka, A., Thomas, H., Phillips, N., et al. (2017). Inhibition of monocarboxyate transporter 1 by AZD3965 as a novel therapeutic approach for diffuse large B-cell lymphoma and Burkitt lymphoma. *Haematologica* 102, 1247–1257. doi: 10.3324/haematol.2016.163030

Ohashi, T., Aoki, M., Tomita, H., Akazawa, T., Sato, K., Kuze, B., et al. (2017). M2-like macrophage polarization in high lactic acid-producing head and neck cancer. *Cancer Sci.* 108, 1128–1134. doi: 10.1111/cas.13244

Patel, B. B., Ackerstaff, E., Serganova, I. S., Kerrigan, J. E., Blasberg, R. G., Koutcher, J. A., et al. (2017). Tumor stroma interaction is mediated by monocarboxylate metabolism. *Exp. Cell Res.* 352, 20–33. doi: 10.1016/j.yexcr.2017.01.013

Pavlides, S., Whitaker-Menezes, D., Castello-Cros, R., Flomenberg, N., Witkiewicz, A. K., Frank, P. G., et al. (2009). The reverse Warburg effect: aerobic glycolysis in cancer associated fibroblasts and the tumor stroma. *Cell Cycle* 8, 3984–4001. doi: 10.4161/cc.8.23.10238

Payen, V. L., Hsu, M. Y., Rädecke, K. S., Wyart, E., Vazeille, T., Bouzin, C., et al. (2017). Monocarboxylate transporter MCT1 Promotes tumor metastasis independently of its activity as a lactate transporter. *Cancer Res.* 77, 5591–5601. doi: 10.1158/0008-5472.CAN-17-0764

Pérez-Escuredo, J., Van Hée, V. F., Sboarina, M., Falces, J., Payen, V. L., Pellerin, L., et al. (2016). Monocarboxylate transporters in the brain and in cancer. *Biochim. Biophys. Acta* 863, 2481–2497. doi: 10.1016/j.bbamcr.2016.03.013

Pértega-Gomes, N., Vizcaíno, J. R., Miranda-Gonçalves, V., Pinheiro, C., Silva, J., Pereira, H., et al. (2011). Monocarboxylate transporter 4 (MCT4) and CD147 overexpression is associated with poor prognosis in prostate cancer. *BMC Cancer* 11:312. doi: 10.1186/1471-2407-11-312

Pinheiro, C., Longatto-Filho, A., Simões, K., Jacob, C. E., Bresciani, C. J. C., Zilberstein, B., et al. (2009). The prognostic value of CD147/EMMPRIN is associated with monocarboxylate transporter 1 co-expression in gastric cancer. *Eur. J. Cancer* 45, 2418–2424. doi: 10.1016/j.ejca.2009.06.018

Polanski, R., Hodgkinson, C. L., Fusi, A., Nonaka, D., Priest, L., Kelly, P., et al. (2014). Activity of the monocarboxylate transporter 1 Inhibitor AZD3965 in small cell lung cancer. *Clin. Cancer Res.* 20, 926–937. doi: 10.1158/1078-0432.CCR-13-2270

Pucino, V., Cucchi, D., and Mauro, C. (2018). Lactate transporters as therapeutic targets in cancer and inflammatory diseases. *Expert Opin. Ther. Targets* 22, 735–743. doi: 10.1080/14728222.2018.1511706

Renner, K., Bruss, C., Schnell, A., Koehl, G., Becker, H. M., Fante, M., et al. (2019). Restricting glycolysis preserves T cell effector functions and augments checkpoint therapy. *Cell Rep.* 29, 135.e9–150.e9. doi: 10.1016/j.celrep.2019.08.068

Rohlenova, K., Veys, K., Miranda-Santos, I., De Bock, K., and Carmeliet, P. (2018). Endothelial cell metabolism in health and disease. *Trends Cell Biol.* 28, 224–236. doi: 10.1016/j.tcb.2017.10.010

Sakamoto, A., Kunou, S., Shimada, K., Tsunoda, M., Aoki, T., Iriyama, C., et al. (2019). Pyruvate secreted from patient-derived cancer-associated fibroblasts supports survival of primary lymphoma cells. *Cancer Sci.* 110, 269–278. doi: 10.1111/cas.13873

Sekine, H., Yamamoto, M., and Motohashi, H. (2018). Tumors sweeten macrophages with acids. *Nat. Immunol.* 19, 1281–1283. doi: 10.1038/s41590-018-0258-0

Silva, L. S., Poschet, G., Nonnenmacher, Y., Becker, H. M., Sapcariu, S., Gaupel, A. C., et al. (2017). Branched-chain ketoacids secreted by glioblastoma cells via MCT1 modulate macrophage phenotype. *EMBO Rep.* 18, 2172–2185. doi: 10.15252/embr.201744154

Simões-Sousa, S., Granja, S., Pinheiro, C., Fernandes, D., Longatto-Filho, A., Laus, A. C., et al. (2016). Prognostic significance of monocarboxylate transporter expression in oral cavity tumors. *Cell Cycle* 15, 1865–1873. doi: 10.1080/15384101.2016.1188239

Sonveaux, P., Végran, F., Schroeder, T., Wergin, M. C., Verrax, J., Rabbani, Z. N., et al. (2008). Targeting lactate-fueled respiration selectively kills hypoxic tumor cells in mice. *J. Clin. Invest.* 118, 3930–3942. doi: 10.1172/JCI36843

Spinello, I., Saulle, E., Quaranta, M. T., Pasquini, L., Pelosi, E., Castelli, G., et al. (2019). The small-molecule compound AC-73 targeting CD147 inhibits leukemic cell proliferation, induces autophagy and increases the chemotherapeutic sensitivity of acute myeloid leukemia cells. *Haematologica* 104, 973–985. doi: 10.3324/haematol.2018.199661

Stone, S. C., Rossetti, R. A. M., Alvarez, K. L. F., Carvalho, J. P., Margarido, P. F. R., Baracat, E. C., et al. (2019). Lactate secreted by cervical cancer cells modulates macrophage phenotype. *J. Leukocyte Biol.* 105, 1041–1054. doi: 10.1002/JLB.3A0718-274RR

Thommen, D. S., and Schumacher, T. N. (2018). T cell dysfunction in cancer. *Cancer Cell* 33, 547–562. doi: 10.1016/j.ccell.2018.03.012

Updegraff, B. L., Zhou, X., Guo, Y., Padanad, M. S., Chen, P., Yang, C., et al. (2018). Transmembrane protease TMPRSS11B promotes lung cancer growth by enhancing lactate export and glycolytic metabolism. *Cell Rep.* 25, 2223.e6–2233.e6. doi: 10.1016/j.celrep.2018.10.100

Vegran, F., Boidot, R., Michiels, C., Sonveaux, P., and Feron, O. (2011). Lactate influx through the endothelial cell monocarboxylate transporter MCT1 Supports an NF-κB/IL-8 pathway that drives tumor angiogenesis. *Cancer Res.* 71, 2550–2560. doi: 10.1158/0008-5472.CAN-10-2828

Whitaker-Menezes, D., Martinez-Outschoorn, U. E., Lin, Z., Ertel, A., Flomenberg, N., Witkiewicz, A. K., et al. (2014). Evidence for a stromal-epithelial "lactate shuttle" in human tumors. *Cell Cycle* 10, 1772–1783. doi: 10.4161/cc.10.11.15659

Wilde, L., Roche, M., Domingo-Vidal, M., Tanson, K., Philp, N., Curry, J., et al. (2017). Metabolic coupling and the reverse warburg effect in cancer: implications for novel biomarker and anticancer agent development. *Semin. Oncol.* 44, 198–203. doi: 10.1053/j.seminoncol.2017.10.004

Wilson, M. C., Meredith, D., Manning Fox, J. E., Manoharan, C., Davies, A. J., and Halestrap, A. P. (2005). Basigin (CD147) is the target for organomercurial inhibition of monocarboxylate transporter isoforms 1 and 4: the ancillary protein for the insensitive MCT2 Is EMBIGIN (gp70). *J. Biol. Chem.* 280, 27213–27221. doi: 10.1074/jbc.M411950200

Zhang, L., and Li, S. (2020). Lactic acid promotes macrophage polarization through MCT-HIF1α signaling in gastric cancer. *Exp. Cell Res.* 388:111846. doi: 10.1016/j.yexcr.2020.111846

Zhong, W., Liang, Y., Lin, S. X., Li, L., He, H., Bi, X., et al. (2012). Expression of CD147 is associated with prostate cancer progression. *Int. J. Cancer* 130, 300–308. doi: 10.1002/ijc.25982

Conflict of Interest: The authors declare that the research was conducted in the absence of any commercial or financial relationships that could be construed as a potential conflict of interest.

frontiers in Cell and Developmental Biology

REVIEW
published: 18 September 2020
doi: 10.3389/fcell.2020.583850

Carnitine Traffic in Cells. Link With Cancer

*Lara Console[1], Mariafrancesca Scalise[1], Tiziano Mazza[1], Lorena Pochini[1], Michele Galluccio[1], Nicola Giangregorio[2], Annamaria Tonazzi[2] and Cesare Indiveri[1,2]**

[1] Unit of Biochemistry and Molecular Biotechnology, Department DiBEST (Biologia, Ecologia, Scienze della Terra), University of Calabria, Arcavacata di Rende, Italy, [2] Institute of Biomembranes, Bioenergetics and Molecular Biotechnologies (IBIOM), National Research Council, Bari, Italy

Metabolic flexibility is a peculiar hallmark of cancer cells. A growing number of observations reveal that tumors can utilize a wide range of substrates to sustain cell survival and proliferation. The diversity of carbon sources is indicative of metabolic heterogeneity not only across different types of cancer but also within those sharing a common origin. Apart from the well-assessed alteration in glucose and amino acid metabolisms, there are pieces of evidence that cancer cells display alterations of lipid metabolism as well; indeed, some tumors use fatty acid oxidation (FAO) as the main source of energy and express high levels of FAO enzymes. In this metabolic pathway, the cofactor carnitine is crucial since it serves as a "shuttle-molecule" to allow fatty acid acyl moieties entering the mitochondrial matrix where these molecules are oxidized via the β-oxidation pathway. This role, together with others played by carnitine in cell metabolism, underlies the fine regulation of carnitine traffic among different tissues and, within a cell, among different subcellular compartments. Specific membrane transporters mediate carnitine and carnitine derivatives flux across the cell membranes. Among the SLCs, the plasma membrane transporters OCTN2 (Organic cation transport novel 2 or SLC22A5), CT2 (Carnitine transporter 2 or SLC22A16), MCT9 (Monocarboxylate transporter 9 or SLC16A9) and $ATB^{0,+}$ [Sodium- and chloride-dependent neutral and basic amino acid transporter B(0+) or SLC6A14] together with the mitochondrial membrane transporter CAC (Mitochondrial carnitine/acylcarnitine carrier or SLC25A20) are the most acknowledged to mediate the flux of carnitine. The concerted action of these proteins creates a carnitine network that becomes relevant in the context of cancer metabolic rewiring. Therefore, molecular mechanisms underlying modulation of function and expression of carnitine transporters are dealt with furnishing some perspective for cancer treatment.

Keywords: transporters, SLC, mitochondria, β-oxidation, carnitine, cancer, drugs

OPEN ACCESS

Edited by:
Vadivel Ganapathy, Texas Tech University Health Sciences Center, United States

Reviewed by:
David Thwaites, Newcastle University, United Kingdom
Ikumi Tamai, Kanazawa University, Japan

***Correspondence:**
Cesare Indiveri
cesare.indiveri@unical.it

Specialty section:
This article was submitted to Molecular and Cellular Oncology, a section of the journal Frontiers in Cell and Developmental Biology

Received: *15 July 2020*
Accepted: *31 August 2020*
Published: *18 September 2020*

Citation:
Console L, Scalise M, Mazza T, Pochini L, Galluccio M, Giangregorio N, Tonazzi A and Indiveri C (2020) Carnitine Traffic in Cells. Link With Cancer. Front. Cell Dev. Biol. 8:583850. doi: 10.3389/fcell.2020.583850

Abbreviations: ER, endoplasmic reticulum; PDH, pyruvate dehydrogenase; TCA, tricarboxylic acid; CPT1, carnitine palmitoyltransferase 1; TMAO, trimethylamine N-oxide; OCTN2, organic cation transporter novel 2; BBB, blood-brain barrier; PCD, primary carnitine deficiency; FAO, fatty acid oxidation; CPT2, carnitine palmitoyltransferase 2; CAT, carnitine acetyltransferase; INF-γ, interferon γ; TNF-α, tumor necrosis factor-α; IDH1, isocitrate dehydrogenase 1; ROS, reactive oxygen species; PPARα, peroxisome proliferator-activated receptor α; PPAR γ, peroxisome proliferator-activated receptor γ; GBM, glioblastoma; ER+, estrogen receptor positive; CRC, colorectal cancer; OCT, organic cation transporter; IngMeb, ingenol mebutate.

INTRODUCTION

Carnitine is a crucial cofactor given its pleiotropic role in human metabolism (**Figure 1**). The endogenous biosynthesis which mainly takes place in the liver, kidney, and to some extent in the brain, meets only 25% of the carnitine required by the human body, while the remaining 75% is obtained from the diet under regular diet regimen, i.e., consuming either meat, fish, dairy product, and vegetables (Longo et al., 2006; Almannai et al., 2019). Therefore, carnitine homeostasis is maintained by the balance between intestinal absorption, endogenous synthesis, and renal reabsorption (Pochini et al., 2013; Almannai et al., 2019). In particular, the kidney needs to be very efficient in regulating urinary carnitine excretion; in case of a strict vegetarian diet, the renal reabsorption, together with an increase of biosynthesis, compensate, at least partially, for inadequate carnitine intake (Lombard et al., 1989; Vaz and Wanders, 2002; Rebouche, 2004). Carnitine homeostasis does not consist of the simple maintenance of constant carnitine concentration. Cells from various tissues require different amounts of carnitine to ensure their survival; as an example, the highest carnitine level in the human body is reached in testis where carnitine is necessary for sperm maturation (Bresolin et al., 1982; Rebouche and Seim, 1998; Pochini et al., 2019). A proof of the dynamic balancing of carnitine homeostasis derives from the observation that, under regular diet, patients carrying defects of the carnitine biosynthesis enzymes, do not apparently display carnitine deficiency, because the reduced synthesis is compensated by carnitine dietary intake and increased renal reabsorption (El-Hattab and Scaglia, 2015). On the contrary, defects of the transport protein that mainly mediated the absorption and renal reabsorption of carnitine, lead to a syndrome called primary carnitine deficiency (PCD – OMIM 212140; Stanley et al., 1992; Magoulas and El-Hattab, 2012; Rose et al., 2012). The maintenance of carnitine homeostasis is crucial in cell metabolism due to the major role of carnitine as a shuttle of acyl groups for fatty acid oxidation (FAO). Indeed, carnitine can be converted into acylcarnitine by acyltransferase isoenzymes present in various subcellular compartments. As an example, in the heart acylcarnitine may act as a reservoir of activated acyl groups that can be transferred to CoA to provide an immediate source of energy through FAO. It has to be stressed that several features make carnitine an optimal vehicle for moving acyl groups: at first, the carnitine derivatives are more stable and less reactive with respect to the acyl-CoA (Ramsay and Arduini, 1993); moreover, acylcarnitine can be moved across plasma as well as intracellular membranes by specific transporters, shuttling the acyl groups among the different subcellular compartments to meet the metabolic needs (Indiveri et al., 2010). For instance, the mitochondrial "shuttle-system" allows the transport of fatty acids, as acylcarnitines, from the cytosol into the mitochondrial matrix where these nutrients are oxidized for ATP production. Similar shuttles have been proposed in peroxisomes or the endoplasmic reticulum (ER), but definitive demonstrations of their existence are still lacking (Tonazzi et al., 2006; Pochini et al., 2013; Demarquoy and Le Borgne, 2015; Juraszek and Nalecz, 2019). Carnitine is then involved in the regulation of the acyl-CoA/CoA balance that has important consequences in the modulation of carbohydrate metabolism, lipid biosynthesis and degradation, and gene expression (**Figure 1**; Pietrocola et al., 2015). For instance, a high acetyl-CoA/CoA ratio in the mitochondrial matrix inhibits pyruvate dehydrogenase (PDH) that catalyzes the oxidative decarboxylation of pyruvate to acetyl-CoA (Pietrocola et al., 2015). Noteworthy, PDH represents a connection between glycolysis and the tricarboxylic acid (TCA) cycle; then, a decrease of acetyl-CoA/CoA ratio can relieve the inhibition of PDH thus affecting glucose oxidation. On the contrary, Acetyl-CoA is an activator of pyruvate carboxylase, thus promoting the TCA flux or the gluconeogenesis (Pietrocola et al., 2015). These allosteric effects can be modulated through the action of carnitine acetyltransferase (CAT), a mitochondrial isoenzyme that transfers the acetyl groups from acetyl-CoA to carnitine, forming acetylcarnitine. In good agreement with the above-described processes, carnitine seems to be involved also in insulin sensitivity (**Figure 1**): it was observed that the muscle accumulation of fatty acyl-CoA derivatives or acyl metabolites inhibits both insulin signaling and glucose oxidation (Pietrocola et al., 2015; Console et al., 2018). Another metabolically relevant compound that links carnitine and CoA derivatives is the malonyl-CoA that is required for fatty acid biosynthesis but acts as a potent inhibitor of the carnitine acyltransferases using cytoplasmic substrates, such as carnitine palmitoyltransferase 1 (CPT1), which is the first component of the mitochondrial carnitine shuttle (Ramsay and Arduini, 1993). Thus, when the malonyl-CoA concentration rises, the fatty acid synthesis increases but the flow of acylcarnitine into the mitochondrial matrix and, in turn, into the β-oxidation pathway decreases. Furthermore, the acetyl-CoA derived from carnitine has been also reported to regulate gene expression by influencing histone acetylation (Madiraju et al., 2009). A novel role for carnitine was recently discovered as potentially relevant to human health; it was reported that carnitine is a dietary precursor from which gut microbiota releases trimethylamine (TMA) which is then subjected to human cell metabolism and converted to trimethylamine N-oxide (TMAO) by hepatic flavin monooxygenase (FMO; Phillips and Shephard, 2020). In terms of relevance to human health, carnitine shows anti-inflammatory, and anti-oxidant properties (Bene et al., 2018; Wang et al., 2020; **Figure 1**). In the brain, acetylcarnitine supports the synthesis of neurotransmitters (Pochini et al., 2019; **Figure 1**). Finally, carnitine is also used to reduce the toxicity of compounds deriving from partially metabolized acyl groups and breakdown of xenobiotics by facilitating their excretion in carnitine ester form (Duran et al., 1990; Bene et al., 2018; **Figure 1**). The wide collection of functions above described, could not be met without a proper interconnection across the tissues and the cell sub-compartments provided by dedicated membrane transporters that regulate the carnitine traffic in the human body. In this respect, it is not surprising that under pathological conditions such as cancer, this traffic is altered. An overview of the relationships among alterations of carnitine traffic and the metabolic switch typical of cancer cells will be the object of the present review.

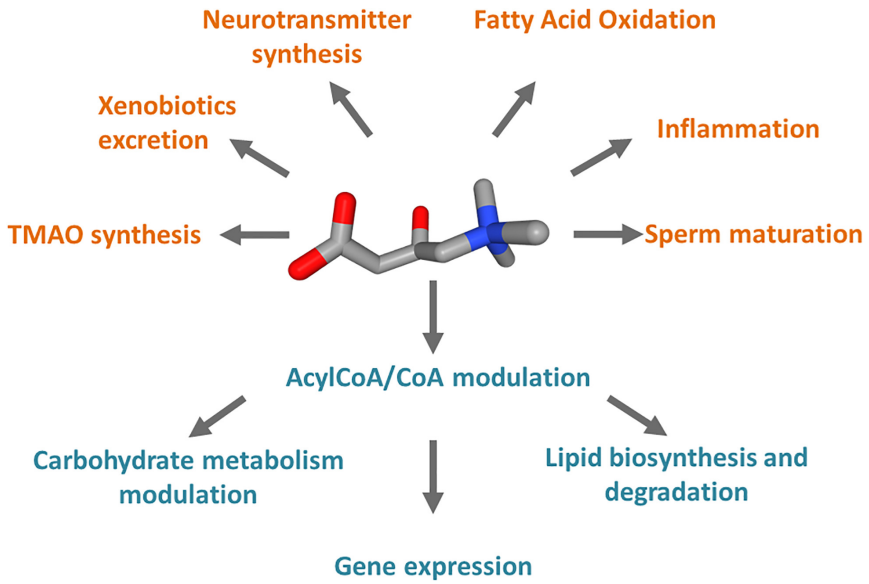

FIGURE 1 | Schematic representation of the cell processes linked to carnitine. Carnitine is represented as 3D conformer with oxygen atoms in red and ammonium atom in blue. In orange, pathways in which carnitine is involved and compounds synthesized from carnitine metabolism. In teal, processes regulated by the Acyl-CoA/CoA ratio derived from carnitine function in mitochondria.

CARNITINE TRAFFIC

The carnitine traffic in the body is regulated by a dedicated network of membrane transport proteins showing different tissue and subcellular localization (**Figure 2**). The intestinal absorption of carnitine, as well as its renal reabsorption, is primarily mediated by the plasma membrane organic cation transporter novel 2 (OCTN2 – SLC22A5) that, among the carnitine-handling transporters, shows the highest affinity toward carnitine. OCTN2 plays a major role also in the distribution of carnitine to the various tissues (**Figure 2**). Besides intestine and kidney, OCTN2 is expressed in several tissues such as placenta, mammary gland, liver, heart, testis, skeletal muscle, and brain, where it is also expressed at the level of the blood-brain barrier (BBB; Koepsell, 2013; Pochini et al., 2019; Koepsell, 2020). In good agreement with the localization of OCTN2 in the brain, the administration of carnitine-derivatives may sustain neuroprotection (Juraszek and Nalecz, 2019; Pochini et al., 2019). The carnitine transport mediated by OCTN2 is Na^+-dependent. This feature allows for carnitine accumulation in cells giving rise to a concentration gradient between intracellular space and blood. The intracellular concentration of carnitine ranges from 1 to 5 mM, while the concentration in the plasma ranges from 25 to 50 μM (Bene et al., 2018). The major role of OCTN2 in carnitine absorption and tissue distribution is demonstrated by the existence of a human disease caused by inborn defects of the OCTN2 gene, namely PCD (Magoulas and El-Hattab, 2012). The disease is characterized by general metabolic derangement, cardiomyopathy, hyperammonemia, hypoglycemia, muscle weakness, and myopathy, in line with the crucial role of carnitine in FAO (Nezu et al., 1999). Interestingly, the clinical manifestations of the disorder can be improved by supplementation of high doses of carnitine. The partial rescue of the above-described symptomatology can be ascribed to the activity of other transporters such as $ATB^{0,+}$(SLC6A14), MCT9, and probably, OCTN1 (SLC22A4) that accept carnitine with a much lower affinity if compared to OCTN2. In particular, the relevance of the $ATB^{0,+}$-mediated carnitine transport, in patients with PCD, may be explained considering that this protein is highly expressed in the intestine (**Figure 2**). $ATB^{0,+}$ is also expressed in the lung (Sloan et al., 2003), eye (Ganapathy and Ganapathy, 2005), and mammary gland (Nakanishi et al., 2001) allowing for carnitine distribution in these tissues. Concerning the plasma membrane transporter MCT9, its transport features are still poorly characterized. MCT9 is ubiquitous with the highest expression level in the kidney and adrenal gland; then, its involvement in managing carnitine traffic is plausible (**Figure 2**; Halestrap and Wilson, 2012; Halestrap, 2013). Indeed, MCT9 in the basolateral membrane of enterocytes might ensure the passage of carnitine into the blood. However, no conclusive data are available on its involvement in carnitine traffic under physiological conditions. MCT9 is also expressed in human umbilical vein endothelial cells where it may have a role in the pro-inflammatory response linked to carnitine (**Figure 1**). Indeed, the MCT9 expression is increased by the pro-inflammatory tumor necrosis factor-α (TNF-α); this, as a consequence, induces a carnitine accumulation in endothelial cells contributing to energy production via FAO for sustaining the inflammatory response (Knyazev et al., 2018). Even more controversial is the role played by OCTN1 that is ubiquitously expressed even if its actual physiological role in carnitine homeostasis is uncertain. There is evidence on its ability to mediate carnitine and acetylcarnitine transport albeit with a very low affinity (Pochini et al., 2011, 2016) since carnitine

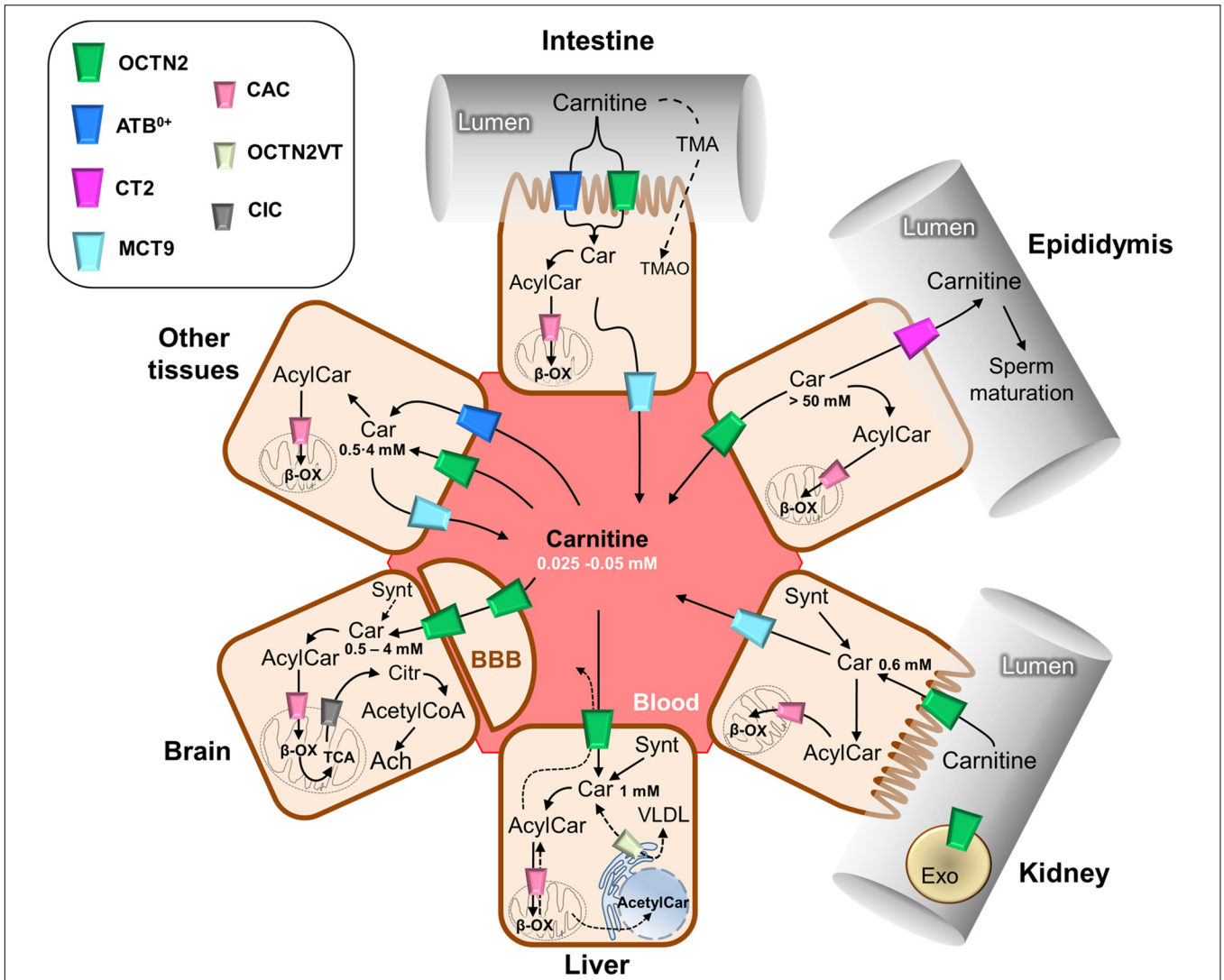

FIGURE 2 | Schematic representation of carnitine traffic. Carnitine (Car) traffic is described by continuous arrows; dotted arrows refer to the transport of some other substrates such as carnitine derivatives and trimethylamine (TMA) that are indirectly involved in carnitine traffic. The organic cation transporter novel 2 (OCTN2) mediates carnitine transport by a sodium dependent mechanism, which is not reported for the sake of clarity. $ATB^{0,+}$ mediates a sodium and chloride dependent transport, which is not reported for the sake of clarity. Carnitine/acylcarnitine carrier (CAC), the mitochondrial carnitine transporter, allows for the completion of β-oxidation (β-ox) and mediates acylcarnitine/carnitine antiport in mitochondria which is reported in details in **Figure 3**. The longest isoform of OCTN2, named OCTN2VT, is depicted in the endoplasmic reticulum (ER). The other transporters are depicted in the cell types in which they are expressed. The role of carnitine in the synthesis of the neurotransmitter acetylcholine (Ach) is reported in the sketch representing the brain tissue; the blood-brain barrier is indicated as BBB. Carnitine concentrations in the different tissues are reported. Synt, carnitine synthesis; CIC, citrate transporter; Citr, citrate; Exo, exosomes; VLDL, very low density lipoprotein; BBB, blood-brain barrier.

is not its main substrate. One of the physiological substrates of this transporter is acetylcholine, underlying a key role in the non-neuronal cholinergic system in both physiological and pathological conditions, as testified by the occurrence of a natural mutation of OCTN1 in inflammatory conditions such as Crohn's Disease (Pochini et al., 2019). An intriguing history is related to another member of the OCTN family, namely OCTN3 (SLC22A21). It is a carnitine specific transporter that disappeared during evolution: it is present in mouse, but not in chimpanzee or humans (Pochini et al., 2013). As stated in the introduction, carnitine homeostasis is also gender-specific, being crucial for sperm maturation (**Figures 1, 2**). In testis and the epididymis, carnitine concentration reaches the highest level of the body, up to 60 mM in the epididymal lumen. The terrific carnitine concentration gradient between epididymal lumen and plasma is allowed by the presence of OCTN2 at the blood side and by the presence of another carnitine specific transporter, namely CT2 (SLC22A16) on the lumen side of epithelia (Gong et al., 2002). The functional characterization of CT2 is still at its infancy, but its peculiar tissue distribution suggests that this transporter is involved in maintaining the epididymal gradient of carnitine that plays as osmolyte and

FAO cofactor. Surprisingly, CT2 becomes almost ubiquitous in human cancers with a dramatic broadening of its function (Koepsell, 2013). Another tissue with high content of carnitine is placenta. In the mouse placenta carnitine concentration is up to 10-fold compared with heart. Also in this tissue, the transport of carnitine is mediated by OCTN2 (Shekhawat et al., 2004). The placenta has to provide the fetus with the nutrients and to serve to eliminate waste products of fetal metabolism. To perform these unique roles placenta requires energy. At first it was established that glucose was the major source of energy for the placenta-fetus unit, but more recent studies demonstrated that FAO play an important role for placental and fetus growth (Shekhawat et al., 2004). Moreover, carnitine seems to be critical in fetal maturation, and fetal gene regulation. Studies also have showed a correlation between the intrauterine growth retardation due to hypoglycemia and to hypoxia-ischemia in the newborn with decreased plasma free carnitine concentration and impaired FAO (Xi et al., 2008). After entering the cell, carnitine traffic among the cytosol and the intracellular compartments is needed. Therefore, transporters located in organelle membranes must operate to fulfill the intracellular traffic of carnitine and its derivatives. The most well-studied transporter of the endocellular membranes is the mitochondrial carnitine/acylcarnitine carrier (CAC; SLC25A20) that is the central component of the mitochondrial carnitine shuttle (**Figure 3**). This system includes the CPT1 which grapples on the mitochondrial outer membrane and converts acyl-CoAs into acylcarnitines. These cross the inner mitochondrial membrane through the CAC. Once in the mitochondrial matrix, carnitine palmitoyltransferase 2 (CPT2) converts acylcarnitines back into acyl-CoAs for oxidation and energy production (**Figure 3**; Indiveri et al., 2011). The essential link between the mitochondrial carnitine transport and FAO is demonstrated by the life-threatening inherited carnitine/acylcarnitine translocase deficiency (OMIM 613698) that, in contrast to the PCD caused by OCTN2 defects, cannot be compensated by the administration of carnitine (Indiveri et al., 2011). Less information is available on carnitine transporters of other subcellular compartments such as the ER. The longest splicing variant of the SLC22A5 gene codes for an OCTN2 variant called OCTN2VT containing an insertion of 24 amino acids in the first extracellular loop, that seems to be localized in the ER (**Figure 2**; Maekawa et al., 2007; Pochini et al., 2013). A still unsolved issue, connected with the role of carnitine in modulating gene expression (**Figure 1**) is the link between mitochondria and nucleus: acetylcarnitine produced in mitochondria would reach the nucleus providing acetyl units (**Figure 2**). This further step in carnitine traffic can be possible if a nuclear isoform of CAT exists for regenerating acetyl-CoA from acetylcarnitine. This aspect is, indeed still mysterious even if a protein with CAT feature has been described in the nuclear extract from HEK293 cells (Madiraju et al., 2009). Furthermore, the role of carnitine in mediating TMAO synthesis has relevance to human health. Indeed, TMAO was suggested as one of the factors promoting atherosclerosis and increased cardiovascular risk (Koeth et al., 2013; Gao et al., 2017; Roncal et al., 2019). Later on, it has been shown that more than 200 variants exist in the coding region of TMAO producing enzyme, with different outcomes on the cardiovascular risk (Phillips and Shephard, 2020). The actual interest around TMAO and, hence, carnitine contribution to its synthesis, is the association with

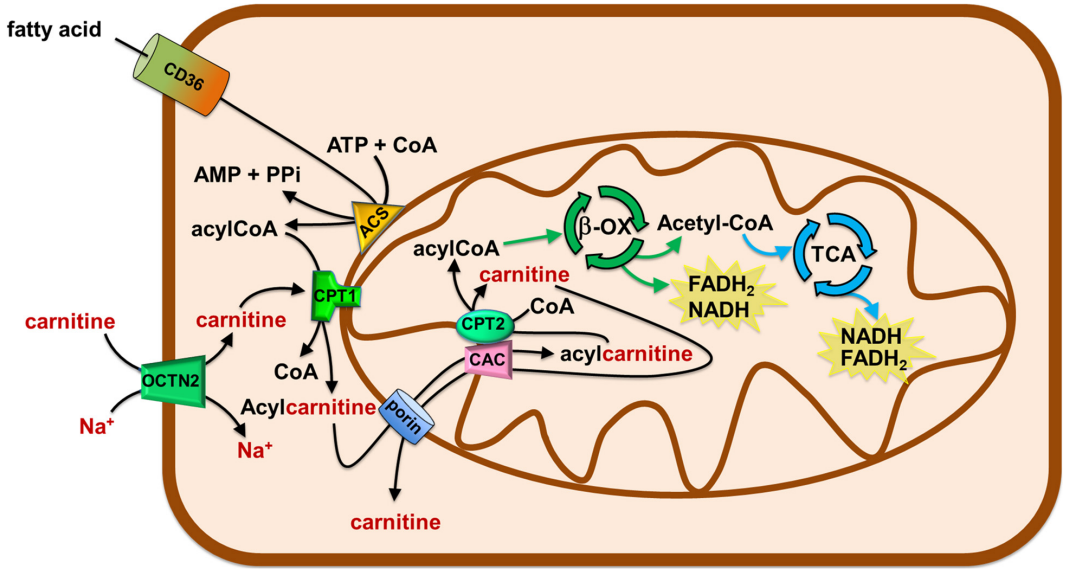

FIGURE 3 | Role of Carnitine in the mitochondrial β-oxidation pathway. The organic cation transporter novel 2 (OCTN2) mediates the uptake of carnitine in cells. Fatty acids (FA) crosses the plasma membrane via CD36. In the cytosol, FA are converted in acyl-CoA by acetyl-CoA synthetase (ACS) and then are translocated in the mitochondrial matrix by the carnitine shuttle. The shuttle is constituted by carnitine palmitoyltransferase 1 (CPT1), carnitine/acylcarnitine carrier (CAC), and carnitine palmitoyltransferase 2 (CPT2). Once in the matrix, acyl-CoA undergoes β-oxidation (β-ox) with the production of acetyl-CoA that enters the tricarboxylic acid cycle (TCA). NADH and $FADH_2$ are generated by β-oxidation and TCA.

increased risk of colorectal and gastrointestinal cancers; however, given that TMAO levels are also greatly influenced by diet-microbiota interactions that are subjected to great variability, the link between TMAO and some human cancers cannot be easily defined (Oellgaard et al., 2017). Finally, a novel branch in the carnitine traffic has been suggested which is linked to vesicles of endocellular origin, namely exosomes. In this respect, exosomes loaded with the plasma membrane transporter OCTN2 can transfer from one cell to another, the capacity of absorbing carnitine. In particular, exosomes derived from HEK293 cells treated with interferon-γ (INF-γ) carry a higher amount of OCTN2 with respect to exosomes derived from untreated cells. This correlates well with the suggestion that carnitine is involved in the inflammatory response and that the expression of OCTN2 in epithelia can be modulated by inflammatory cytokines such as INF-γ and TNF-α (Console et al., 2018; Juraszek and Nalecz, 2019; Pochini et al., 2019).

FATTY ACID METABOLISM, CARNITINE AND CANCER

The carnitine supply is *conditio sine qua non* to carry out the β-oxidation of fatty acids by mitochondria. This is one of the most efficient energy-producing pathways in cells, therefore, high energy demanding tissues, such as heart and kidney, mainly rely on fatty acids utilization (Console et al., 2020). If we consider human diseases, a pathological condition characterized by a high energy request is cancer. Cancer cells need the energy to sustain the high rate of proliferation and the energy need further increases with the grade of malignancy (Hanahan and Weinberg, 2011). The association of FAO derangements with cancer has been studied since 1952 (Waterman et al., 1952). However, the current largest body of evidence, in the field of metabolic adaptation of cancer cells, deals with the flexible utilization of glutamine and glucose as the main sources of energy. Glucose and glutamine as energetic substrates are considered a hallmark of cancer cells and the metabolic switch that allow their utilization under virtually anaerobic conditions is known as the Warburg effect (Warburg et al., 1927). The canonical interpretation of the Warburg effect implies that cells bypass the mitochondrial respiratory chain for the synthesis of ATP even in the presence of adequate oxygen supply (Ganapathy et al., 2009). However, it is nowadays evident that the Warburg effect needs to be considered in a more general metabolic context that includes also the utilization of fatty acids in line with the efficiency of these substrates in terms of ATP yield. In this view, the mitochondrial function in cancer is not totally impaired and the TCA, as well as the oxidative phosphorylation pathway, are working (Currie et al., 2013). In agreement, it is more and more evident that some cancers with dual capacity for glycolytic and oxygen-consuming metabolism exist. The described metabolic flexibility is a relevant phenomenon observed in different types of cancers, and, within the same cancer type, at different stages of progression. Concerning the lipid metabolism, there is compelling evidence showing that in some cancer types the fatty acid utilization is increased, while in others this pathway is down-regulated. Noteworthy, in all the mentioned cases, an appropriate intervention in regulating the carnitine level and/or traffic is required, given its role in FAO. The alterations of FAO can affect the availability of membrane structural lipids, the abundance of lipids with signaling functions, the synthesis and degradation of lipids for energy production and utilization (Carracedo et al., 2013; Currie et al., 2013; Rohrig and Schulze, 2016; Koundouros and Poulogiannis, 2020). As an example, prostate cancer and diffuse large B-cell lymphoma, use FAO as the main source of energy and express FAO enzymes at high levels (Liu, 2006; Svensson et al., 2016; Yamamoto et al., 2020). FAO substrates are derived from the external environment via specific transporters able to mediate fatty acid uptake, such as CD36 (**Figure 3**). This is a membrane transporter allowing for fatty acids storage in adipose tissues and for the uptake of fatty acids in cells to produce ATP. CD36 is a heavy glycosylated protein with a hairpin conformation. Indeed it consists of two transmembrane domains, a large extracellular domain, and two short intracellular domains that are required for CD36 function after substrate binding (Su and Abumrad, 2009). In those cancers relying on lipid metabolism, CD36 and other fatty acid binding proteins (FABP) are over-expressed to catch fatty acids stored in surrounding adipocytes (Koundouros and Poulogiannis, 2020). CD36 is distinct from the transporters regulating the traffic of carnitine and acylcarnitines, since it handles the hydrophobic fatty acid molecules as such, thus not directly participating to the carnitine network. Another source of lipid for FAO is the lipid droplets, which are commonly formed in cancer cells. Besides the direct advantage in terms of ATP synthesized from fatty acids, FAO is also relevant in managing oxidative stress derived from the electron transport chain activity. Indeed, the end-product of FAO, acetyl-CoA enters TCA and can leave the cycle as isocitrate. This is, then, oxidized by cytosolic isocitrate dehydrogenase 1 (IDH1) to α-ketoglutarate with the production of NADPH required for the detoxification from reactive oxygen species (ROS; Jeon et al., 2012; Qu et al., 2016). Then, α-ketoglutarate can enter back into the TCA for completing the cycle. The strong requirement for NADPH is testified by the presence of diverse pathways, which are activated in cancer cells to fulfill their need. NADPH can derive also from the activity of the malic enzyme and the pentose phosphate pathway. The genes encoding for these enzymes are positively regulated by the oncogene AKT which acts upstream the transcription factor Nrf2. Furthermore, AKT may directly activate the nicotinamide adenine nucleotide kinase (NADK) responsible for the phosphorylation of NADH forming NADPH (Jeon et al., 2012; Currie et al., 2013; Koundouros and Poulogiannis, 2020). However, the involvement of lipid metabolism in cancer is not only linked to the oxidative route; indeed, cancer cells are greatly committed in anabolic metabolism required for generating new building blocks that sustain cell growth and proliferation. In this frame, lipids are in the list of molecules required by proliferating cells being components of cell membranes. Therefore, cancer cells not only use FAO to oxidize fatty acids and to derive energy by mitochondria but they also use acetyl-CoA to endogenously synthesize fatty acids in the cytosol using NADPH as key cofactor for anabolic enzymes

(Currie et al., 2013). This is a typical example of a futile cycle activated by cancer cells that is forbidden in the "canonical" biochemistry. Such a condition is centered on the removal of inhibition of the carnitine handling enzyme CPT1 via the specific down-regulation of acetyl-CoA carboxylase 2 (ACC2), with a strong reduction of the malonyl-CoA pool responsible for CPT1 inhibition (Koundouros and Poulogiannis, 2020). In this complex network of metabolic alterations promoting FAO in cancer, the traffic of carnitine can be considered the start-up process. Indeed, FAO cannot occur without a proper carnitine traffic interplay (**Figure 2**; Melone et al., 2018).

ROLE OF CARNITINE TRANSPORTERS IN CANCERS

Changes in expression and/or activity of carnitine transporters in plasma or intracellular membranes are expected, especially in those cancers characterized by either an increased or a decreased utilization of fatty acids. The *status artis* of the link of altered carnitine transporter expression with cancer will be depicted in this section. Each transporter will be dealt with and described in terms of its role in the derangements occurring in cancer cells.

General Features of OCTN2 (SLC22A5)

The membrane transporter OCTN2 is one of the upstream players of the carnitine network (**Figure 2**). It is one of the 13 members of the SLC22 family that includes organic cation transporters (OCTs), organic zwitterion/cation transporters novel (OCTNs), and organic anion transporters (OATs). The gene encoding the human isoform of OCTN2 has been annotated and cloned in 1998, in parallel to the murine one (Tamai et al., 1998, 2000; Wu et al., 1998, 1999). It maps in the chromosome 5 in the "inflammatory bowel diseases 5 (IBD)" risk region and is formed by 11 exons giving rise to two variants of different lengths, which have different subcellular localization (**Figure 2**). Over the years, the function of OCTN2 has been characterized, employing intact cell systems as well as proteoliposomes harboring the native rat and human protein (Tamai et al., 1998, 2000; Lahjouji et al., 2002; Ohashi et al., 2002; Pochini et al., 2004; Console et al., 2018). The main substrates of OCTN2 are carnitine and its acyl derivatives and their transport is coupled to Na^+ co-transport (**Figure 3** and **Table 1**; Pochini et al., 2013). OCTN2 mediates also the transport of organic cations such as TEA in Na^+-independent manner. Data from studies using cross species chimeric OCTN2 and mutagenesis demonstrated that the active site for carnitine and that for organic cations overlap but are not identical. Indeed, the mutation P478L of OCTN2, abolished only the carnitine transport activity (Seth et al., 1999). This mutation causes the PCD (Seth et al., 1999). An important model to study the consequences of systemic carnitine deficiency is the homozygous OCTN2 null mouse, in which OCTN2 function is abolished by the missense mutation L352R. In contrast with P478L, this second mutation abrogates both carnitine and organic cations transport. Homozygous OCTN2 null mice showed liver fatty infiltration and hypoglycemia. In absence of carnitine administration these mice die within 3–4 weeks after birth with dilated cardiomyopathy, which is also seen in children with PCD (Seth et al., 1999; Shekhawat et al., 2004). Intriguingly, different transport modes have been described for OCTN2, either murine or human, namely a Na^+-carnitine symport and a Na^+-dependent carnitine/acylcarnitine antiport (Ohashi et al., 2001; Ohnishi et al., 2003; Pochini et al., 2013). This protein also mediates the efflux of carnitine derivatives

TABLE 1 | Carnitine transporters involved in cancer.

	Alias	Substrates	Expression in Cancers
SLC22A5	OCTN2	- Carnitine - Carnitine derivatives - Drugs among which anti-cancer drugs such as: Imatinib, oxaliplatin, and paclitaxel	- Glioblastoma multiforme - Ovarian carcinoma - ER+ breast cancer - Colorectal cancer - Epithelial HPV-mediated-carcinoma
SLC22A4	OCTN1	- TEA - Acetylcholine - Ergothioneine - Acetylcarnitine - Choline - Drugs among which anti-cancer drugs such as: imatinib, cytarabine, camptothecin, oxaliplatin, mitoxantrone, and doxorubicin	- Several NCI-60 cancer cell lines - Sporadic colorectal cancer and malignant progression of inflammatory bowel diseases (IBDs)
SLC22A16	CT2	- Carnitine - Drugs among which anti-cancer drugs such as: doxorubicin, bleomycin, and cisplatin	- Breast cancer - Ovarian cancer - Leukemia - Lung cancer - Gut cancer - Nasopharyngeal cancer - Diffuse large cell lymphoma - HCT116 cell line
SLC6A14	$ATB^{0,+}$	- Amino acids - Carnitine - Propionylcarnitine - L-carnitine conjugated nanoparticles (LC-PLGANPS)	- Colorectal cancer - ER+ breast cancer - Pancreatic cancer - Cervical cancer
SLC16A9	MCT9	- Carnitine - Creatine	- Adrenocortical tumors - Diffuse large B-cell lymphoma
SLC25A20	CAC	- Carnitine - Acylcarnitine	- Prostate cancer - Non-muscle invasive bladder cancer

OCTN2, organic cation transporter novel 2; CAC, carnitine/acylcarnitine carrier.

favored by their outwardly directed concentration gradient (**Figure 2** and **Table 1**; Xiang et al., 2017). Therefore, the actual transport mechanism, i.e., symport and/or antiport is a still an open question: it can be speculated that OCTN2 may show different transport features according to isoforms and to the tissue in which it is expressed (Ohashi et al., 1999; Pochini et al., 2013); such a regulation could be ascribed also to post-translational modifications. In this respect, the N-glycosylation pathway (Filippo et al., 2011), as well as a more complicated process involving a multiprotein complex that traffics OCTN2 to the definitive location, have been described (Jurkiewicz et al., 2017). Interestingly, the interactions with the scaffold proteins PDZK1 and PDZK2 have been described as begin responsible for the regulation of both rat and human OCTN2 transport function (Kato et al., 2005; Juraszek and Nalecz, 2019). The possible transport mechanisms together with the wide tissue distribution underlie the role of OCTN2 as the major transporter responsible for the traffic of carnitine and carnitine derivatives in the intestine, distribution to several body districts and reabsorption/excretion in the kidney (**Figure 2**). Even though the 3D structure of OCTN2 is still not known, the molecular determinants for substrate specificity have been revealed: one ammonium and one carboxylate groups are strictly required for transport, while the distance between them is not important (Ohashi et al., 2002; Pochini et al., 2013). The esterification of the carnitine hydroxyl group is well tolerated. The wide specificity toward carnitine derivatives is very important in the regulation of their traffic and is in line with the detection of more than 100 different types of acylcarnitines in plasma and urine (Xiang et al., 2017). The extracellular Km toward carnitine, measured in different experimental systems, ranges from 8 to 80 μM depending on different species and/or tissues. This range falls within the average carnitine concentration in plasma (Indiveri et al., 2010; Pochini et al., 2013; **Figure 2**). The intracellular Km for carnitine, which is also important for understanding the mechanism of carnitine traffic has been measured only in proteoliposomes, an experimental system which gives access to the internal face of a transporter (Scalise et al., 2013). The internal Km value is in the millimolar range, i.e., in the average intracellular carnitine concentrations (Pochini et al., 2004). In line with the link with FAO, the regulation of OCTN2 occurs via some transcription factors which also govern other proteins connected with lipid metabolism. As an example, the peroxisome proliferator-activated receptor α (PPARα) can activate OCTN2 expression as well as the FAO (Maeda et al., 2008). Moreover, the peroxisome proliferator-activated receptor γ (PPARγ) regulates OCTN2 expression by binding to the PPAR-response element within the first intron (Qu et al., 2014). Moreover, an estrogen hormonal regulation has been reported. Indeed, a responsive element for estrogen is located in the second intron of OCTN2 (Wang et al., 2012). Finally, insulin-dependent hormonal regulation has also been reported (Stephens et al., 2006). As stated above, the key role of OCTN2 in fatty acid metabolism is testified by human pathologies caused by alterations of the transporter function (Magoulas and El-Hattab, 2012). Some of the symptoms which characterize the inherited disease are mimicked by the administration of drugs interacting with OCTN2 as off-target or by some diet regimens (Pochini et al., 2009, 2019; El-Hattab and Scaglia, 2015). It has to be stressed that chronic inflammatory conditions may be the basis for the insurgence of other pathological states, including cancer, broadening the role of OCTN2 and its main substrate, carnitine, in human pathology. In the next section, the connections between OCTN2 expression/function and lipid metabolism in cancer will be dealt with.

Implications of OCTN2 in Cancer

To date, several studies reported a link between the altered expression of OCTN2 and cancer development and progression (Lu et al., 2008; Scalise et al., 2012; Wang et al., 2012; Elsnerova et al., 2016; Lee et al., 2016; Fink et al., 2019; Juraszek and Nalecz, 2019; **Table 1**). Interestingly, its expression is found up or down-regulated depending on the carbon source that the tumors use to produce energy. Lipid utilization is increased in those cancers surrounded by a lipid-rich or lipid-enriched environment (Quail and Joyce, 2013; Koundouros and Poulogiannis, 2020). As recently reviewed, OCTN2 is overexpressed in endometrial, ovarian, renal, pancreatic cancers and also in glioblastoma (GBM) even if neurons do not normally use fatty acids to derive energy (Juraszek and Nalecz, 2019). It can be speculated that, in a condition of high aggressiveness, typical of GBM, an increase of carnitine cell content is required to sustain the high energy demand of cell proliferation. The high OCTN2 expression is associated with poor overall patient survival and a siRNA-mediated OCTN2 silencing in GBM led to a loss of tumor cell viability (Fink et al., 2019). Data were confirmed by the use of an orthotopic mouse model of GBM, in which OCTN2 was inhibited by meldonium and a reduction of tumor growth was observed (Fink et al., 2019). In metastatic breast cancer ER+ (estrogen receptor positive), OCTN2 is overexpressed due to the control exerted by the estrogen signaling. This has been experimentally demonstrated by silencing the estrogen receptor in breast cancer (ER+) with consequent decrease of OCTN2 expression (Wang et al., 2012). The link with lipid metabolism has been provided by employing a siRNA for OCTN2, which lowered carnitine uptake triggering an increased formation of lipid droplets and a decreased cell proliferation. These results suggested OCTN2 as a potential therapeutic target for breast cancer ER+. However, as recently reviewed, the role of OCTN2 in breast cancer, either ER+ or ER-, is not straightforward when considering prognosis and patient survival after cancer treatment; upon a deep analysis of breast cancer data set, the existence of a threshold level of OCTN2 expression that may affect the different prognosis has been proposed (Juraszek and Nalecz, 2019). In contrast, colorectal cancer (CRC) is characterized by decreased OCTN2 expression (Juraszek and Nalecz, 2019). In good agreement, the association between an OCTN2 SNP (rs27437), down-regulating the OCTN2 expression and the CRC risk has been identified (Zou et al., 2018). The expression of OCTN2 is decreased also in epithelial HPV-mediated carcinoma. Indeed, both mRNA and protein levels were reduced in keratinocytes retrotransduced with the high-risk HPV16E6 compared to the control (Scalise et al., 2012). A similar result was also observed in CaSki, a cervical carcinoma

cell line naturally infected by HPV16. In this case, the mechanism of down-regulation is linked to promoter methylation (Scalise et al., 2012; Qu et al., 2013). As other members of the SLC22 family, OCTN2 can mediate cellular uptake of oxaliplatin and other chemotherapeutic agents (Jong et al., 2011; Pochini et al., 2019; Koepsell, 2020; Kou et al., 2020). Therefore, the epigenetic modulation of OCTN2 in cancer may by exploited to increase the efficacy of anti-cancer drugs. It is reported that treatment of CRC cells with luteolin, a naturally occurring flavonoid which is an agonist of PPARγ, increased mRNA and protein expression of OCTN2 in a time- and dose-dependent manner, enhancing the intracellular accumulation of oxaliplatin (Qu et al., 2014). In this respect, OCTN2 targeted nanoparticles have been exploited for improving paclitaxel delivery (Kou et al., 2018). Furthermore, imatinib that is the first-line treatment of patients with chronic myeloid leukemia seems to be transported in cells by OCTN2 and OCTN1 (Hu et al., 2008 and **Table 1**). Accordingly, an association between the SNP rs2631365-TC located in the promotor region of OCTN2 and failure of imatinib treatment has been described (Jaruskova et al., 2017). Imatinib is also used in the treatment of the gastrointestinal stromal tumor. In this cancer, the failure of imatinib mainly depends on mutations of the tyrosine-protein kinase KIT and the platelet-derived growth factor receptor α (PDGFRα). Nevertheless, some patients with responsive genotype develop resistance. After analyzing 31 polymorphisms in 11 genes, it has been discovered that in presence of the C allele in SLC22A4 (OCTN1 rs1050152), and the two minor alleles (G) in SLC22A5 (OCTN2 rs2631367 and rs2631372) the time to progression was significantly improved (Angelini et al., 2013). These studies are essential to develop personalize therapy.

General Features of OCTN1 (SLC22A4) and Implications in Cancer

Organic cation transporter OCTN1 is another member of the SLC22 family. Its gene, named SLC22A4, counts 11 exons and encodes for a protein of 551 amino acids. This transporter is strongly expressed in the kidneys and, at a lower level, in trachea, bone marrow, liver, skeletal muscle, prostate, lung, pancreas, intestine, placenta, heart, uterus, spleen, spinal cord, and neurons (Pochini et al., 2013). The functional properties of OCTN1 have been investigated using several experimental models such as intact cells, membrane vesicles, proteoliposomes and oocyte from xenopus laevis. However, the physiological substrates of OCTN1 are still matter of discussion (Pochini et al., 2019 and **Table 1**). In term of transport efficiency the best substrate is the synthetic compound TEA, whereas carnitine is a poor substrate (Yabuuchi et al., 1999; Tamai et al., 2004; Pochini et al., 2019). Some studies suggest that OCTN1 mediate the uptake of a mushroom metabolite named ergothioneine, which probably exerts an anti-oxidant function in tissues exposed to ROS (Gründemann et al., 2005; Halliwell et al., 2016). Other studies demonstrated that this transporter mediates a sodium-regulated acetylcholine export suggesting a role of OCTN1 in the non-neuronal cholinergic system (Pochini et al., 2012, 2016), a ubiquitous pathway that modulates several cell functions, among which inflammation (Grando et al., 2015). Choline and acetylcarnitine have been identified as additional substrates using intact cells and proteoliposome transport assays (Pochini et al., 2015, 2016). OCTN1 is expressed in different cancer cell lines (Okabe et al., 2008). It is associated with sporadic CRC in early age, and its polymorphisms, such as L503F, may help to predict malignant progression of the disease in IBD patients (Martini et al., 2012). The involvement of OCTN1 in cancer metabolism, is probably unrelated to the poor ability of this transporter to mediate carnitine transport, however, it is interesting to know that OCTN1 is involved in the uptake of anti-cancer drugs (**Table 1**) such as Cytarabine (Drenberg et al., 2017), Camptothecin (Zheng et al., 2016), mitoxantrone and doxorubicin (Okabe et al., 2008).

General Features of CT2 (SLC22A16)

The plasma membrane carnitine transporter CT2 belongs to the SLC22 family as OCTN2. The gene, mapping on chromosome 6, has been identified in 2002 in two parallel studies that classified CT2 as the sixth member of the OCT subfamily (Enomoto et al., 2002; Gong et al., 2002). One of the two reports has been conducted using healthy tissues highlighting the very narrow CT2 expression that is present almost exclusively in the plasma membrane of Sertoli cells of the testis and in the luminal membrane of epididymal cells (Koepsell, 2013). On the contrary, the other work has been performed using leukemia cells showing that CT2 is indeed expressed in cancers. In terms of functional characterization, human CT2 can transport L-carnitine with a Km of 20.3 μM. The CT2-mediated transport is partially sodium-dependent and shows a preference for basic pH (Enomoto et al., 2002 and **Table 1**). Apart from this preliminary characterization, no other information is available and its physiological role remains uncertain. Given its peculiar tissue distribution, a role in the sperm maturation occurring in epididymal lumen has been proposed. The sperm maturation requires a high amount of carnitine that is accumulated in epididymal cells from blood, thanks to OCTN2 (**Figure 2**). Then, carnitine is released in the epididymal lumen via CT2 (Jeulin and Lewin, 1996; Enomoto et al., 2002; Cotton et al., 2010) where its measured concentration reaches 50–100 mM (**Figure 2**). In good agreement with this role, carnitine supply to patients with asthenozoospermia results in an increase of sperm motility. Concerning the regulation, CT2 seems to respond to progesterone stimuli (Sato et al., 2007); in line with this, CT2 is expressed at a higher level during the decidualization of the endometrium that is characterized by high progesterone levels (Sato et al., 2007; Tsai et al., 2014; Liang et al., 2018).

Implications of CT2 in Cancer

Unlike the restricted expression in healthy tissue, CT2 is largely expressed in several cancer types also originating from tissues that normally do not express this protein (Lal et al., 2007; Ota et al., 2007; Bray et al., 2010; Sagwal et al., 2018; Zhang et al., 2019 and **Table 1**). This denotes a profound rewiring of cancer cells concerning the carnitine linked metabolism. As an example, it is reported that the acute myeloid leukemia (AML) is strictly

dependent on FAO. Knocking-down CT2 reduces the viability of tumors (Wu et al., 2015). Moreover, a recent study conducted using data of over 300 patients in 10 years, linked the up-regulation of CT2 with poor survival of gut cancer patients (Zhao et al., 2018). For the above-mentioned reasons, CT2 is considered a druggable target and has also been exploited for drug delivery. Many authors report this capacity to recognize and transport several types of anti-cancer drugs such as doxorubicin with high affinity (Okabe et al., 2005). In line with this, by using whole-exome sequencing on diffuse large B-cell lymphoma patients, a loss of the chromosomic region including CT2 gene in half of the patients has been shown. These patients experienced a lack of remission or early relapse at 24 months after diagnosis; this phenomenon has been linked with the increased resistance at doxorubicin treatment due to the lack of CT2 in the cell membrane that, in turn, impairs drug entry into cancer cells (Novak et al., 2015). The doxorubicin accumulation seems to be at the basis of the positive effects of the innovative anti-neoplastic treatment known as cold physical plasma used on different melanoma cell lines. This therapeutic approach is based on a gas treatment that induces the production of ROS/RNS able to specifically target cancer cells; interestingly, upon cold physical plasma treatment, the expression of CT2 is augmented explaining the parallel increase in doxorubicin accumulation (Sagwal et al., 2018). CT2 is also involved in the intracellular accumulation of bleomycin in human testicular cancer cells, which are sensitive to this drug (**Table 1**). In the same study, the human colon carcinoma cell line HCT116 was revealed to be less sensitive to the bleomycin treatment, in line with the very low expression of CT2 and with the metabolism based on glycolysis rather than on FAO (Aouida et al., 2010). Finally, cisplatin is also recognized as substrate by CT2: higher levels of CT2 expression in lung cancer was correlated to increased cellular uptake of cisplatin (**Table 1**). While, down-regulation of the transporter directly confers resistance against the drug, via decreasing the intracellular platinum concentration (Kunii et al., 2015).

General Features of $ATB^{0,+}$ (SLC6A14)

$ATB^{0,+}$ is a plasma membrane transporter belonging to the SLC6 family that includes amino acid transporters, neurotransmitter transporters, and osmolyte transporters (Pramod et al., 2013). The gene has been annotated in the human genome on the chromosome X, it is composed of 13 exons encoding only one splice variant, and has been cloned in 1999 (Sloan and Mager, 1999). $ATB^{0,+}$ mediates the transport of all proteogenic amino acids except for aspartate and glutamate. Intriguingly, $ATB^{0,+}$ also recognizes carnitine as a substrate, even though with a lower affinity (Km in the millimolar range) with respect to the amino acid substrates (Sloan and Mager, 1999; Bode, 2001) and to OCTN2 (**Table 1**). The transport reaction catalyzed by $ATB^{0,+}$ occurs as a co-transport of $2Na^+$ and $1Cl^-$ being highly concentrative and sensitive to membrane potential (Nakanishi et al., 2001). In contrast with OCTN2, $ATB^{0,+}$ does not transport carnitine derivatives except for propionylcarnitine (Nakanishi et al., 2001). The subcellular localization of $ATB^{0,+}$ is in the apical side of lung and intestine epithelia (**Figure 2**). In this location, the transporter is exposed to the external environment, and then, to bacteria (Rotoli et al., 2020). In agreement with this, $ATB^{0,+}$ is up-regulated in inflammatory states, such as ulcerative colitis and Crohn's disease (Broer and Fairweather, 2018). The interplay of $ATB^{0,+}$ with lung bacteria has been suggested as responsible for modulating *Pseudomonas aeruginosa* attachment to human bronchial epithelial cells with consequent effects on lung disease severity in cystic fibrosis (Di Paola et al., 2017).

Implications of $ATB^{0,+}$ in Cancer

In the last decade, the over-expression of $ATB^{0,+}$ in several human cancers became a hallmark of this pathology similar to what it is described for other plasma membrane transporters (Bhutia and Ganapathy, 2016 and **Table 1**). This has been linked particularly with the ability of $ATB^{0,+}$ to mediate high capacity transport of amino acids (Gupta et al., 2006; Ruffin et al., 2020) making this transporter a druggable target (Karunakaran et al., 2011). However, in light of its ability to mediate uptake of carnitine, it cannot be excluded that the over-expression of $ATB^{0,+}$ is also responsible for providing this essential co-factor to those cells in which FAO is responsible for deriving energy required for cell growth and progression. $ATB^{0,+}$ represents also a way to deliver drugs; in this respect, studies conducted employing fluorescently labeled nanoparticles, showed the co-localization of OCTN2 and $ATB^{0,+}$ which are responsible for mediating the cellular uptake of L-carnitine conjugated nanoparticles (LC-PLGANPs) loaded with 5-fluorouracil (**Table 1**). As the expression levels of OCTN2 and $ATB^{0,+}$ are higher in colon cancer cells than in normal colon cells, LC-PLGA NPs can be used to deliver chemotherapeutic drugs selectively to cancer cells for colon cancer therapy. These findings indicate a great potential of the dual-targeting strategy (Kou et al., 2017).

General Features of MCT9 (SLC16A9) and Implications in Cancer

MCT9 is a plasma membrane transporter belonging to the monocarboxylic acid transporter family SLC16 that counts 14 members. The gene has been identified in 1999 and annotated on chromosome 10 (Halestrap and Price, 1999). The majority of SLC16 proteins usually catalyze proton-linked transport of monocarboxylate substrates like lactic acid and pyruvic acid, while some members recognize aromatic amino acids and thyroid hormone (Halestrap and Wilson, 2012; Halestrap, 2013). In contrast with the other members of SLC16 family, MCT9 is responsible for carnitine, but also creatine, transport presumably at the basolateral membrane of enterocytes (**Figure 2** and **Table 1**). In good agreement with this role, genome-wide association studies correlated SNPs occurring at the level of SLC16A9 gene, with carnitine, propionylcarnitine and urate levels in serum (Kolz et al., 2009; Demirkan et al., 2015). The transport mechanism of MCT9, described in *Xenopus* oocytes, revealed to be Na^+ and pH-independent (Futagi et al., 2020). An important link with carnitine derives from chronic hepatitis B patients. HBsAg loss in this patient, which is the most important step forward to the recovery from disease, is strictly related

to polymorphisms of SLC16A9 gene and, consequently to the carnitine levels (Jansen et al., 2014). A possible implication of MCT9 in some cancer types was reported: the transporter seems to be a good diagnostic target to distinguish benign from malignant adrenocortical tumors (Fernandez-Ranvier et al., 2008). Moreover, SLC16A9 is highly expressed in diffuse large B-cell lymphoma (Lim et al., 2015; **Table 1**).

General Features of CAC (SLC25A20)

Carnitine/acylcarnitine carrier belongs to the SLC25 family also called mitochondrial carrier family; its gene maps on chromosome 3 (Palmieri, 2013). It is well assessed that the CAC catalyzes the entry of acylcarnitines into the mitochondrial matrix in exchange for free carnitine (**Figure 3** and **Table 1**). In mammals, CAC can accept acylcarnitines with acyl chains of various lengths from 2 to 18 carbon atoms as substrates, but it showed a higher affinity for acylcarnitines with longer carbon chains (Indiveri et al., 2011). CAC is crucial in the control of the influx of acyl units into mitochondria and hence of FAO (**Figures 2, 3**). CAC transport activity is finely regulated by post-translational modifications. It has been demonstrated that acetylation of some lysine of CAC inhibits the uptake of carnitine into mitochondria and hence negatively affect FAO (Giangregorio et al., 2017). Interestingly, the citrate carrier (SLC25A1), involved in fatty acid synthesis (**Figure 2**), is activated by acetylation (Palmieri et al., 2015). CAC is extremely sensitive to the redox state of the cell. In particular, the oxidation state of two out of six cysteines controls the CAC via the formation of a disulfide bridge that switches off the transporter activity. In this respect, it is interesting that gasotransmitters, such as NO or H_2S, can act on the same two cysteine residues modulating the CAC function (Giangregorio et al., 2016; Tonazzi et al., 2017). It is reported that the expression of CAC is up-regulated by statins, fibrates and retinoic acid. As for OCTN2 and several other enzymes involved in FAO, also the expression of CAC is regulated by PPAR-α. While other reports exclude that CAC could be regulated by PPAR factors (Indiveri et al., 2011).

Implications of CAC in Cancer

To date, the correlation between CAC and cancer has received little attention, and only a few studies have reported a link between the altered expression of CAC and cancer (**Table 1**). As previously described, prostate cancer cells are more prone to FA utilization than normal prostate cells. A great contribution to FAO deregulation is due to the down-regulation of the same microRNAs that target CPT1A, CAC, and CAT. In particular, miR-129-5p, which shows an aberrant expression level in prostate cancer, seems to regulate the CAC expression. Forced expression of these miRNAs in prostate cancer cells, PC3 and LNCaP, results in reduced expression of CPT1A, CAC, and CAT, and hence, negatively affects FAO. This has, as a consequence, the interference with the adaptive metabolic reprogramming in prostate cancer cells (Valentino et al., 2017). Moreover, another microRNA, that is miR-212, has an aberrant expression in prostate cancer and has been shown to directly target CAC (Soni et al., 2014). These observations suggested the mitochondrial carnitine system as a potentially druggable pathway for prevention and treatment of prostate cancer (Valentino et al., 2017). Furthermore, significant alterations in the carnitine/acylcarnitine pathway were detected in bladder cancer patients. In patients with non-muscle invasive bladder cancer, the expression of CAC was significantly down-regulated compared to normal bladder tissues. A similar result was achieved also for CPT1B, CPT1C, and CAT (Kim et al., 2016). CAC seems to be a target of a first-in-class treatment for the precancerous skin condition actinic keratosis. The diterpenoid ester ingenol mebutate (IngMeb) induces cell death causing mitochondrial dysfunction and local inflammatory response. A photoreactive analog of IngMeb together with quantitative proteomic experiments were used to discover targets of IngMeb in human cancer cell lines and primary human keratinocytes. Among others, CAC results as the most prominent target of IngMeb. This drug impairs FAO through the inhibition of CAC transport activity and this can explain, at least in part, the IngMeb pharmacological mechanism of action (Parker et al., 2017). Another intriguing observation is that a relationship between the composition of the cardiolipin, the most abundant phospholipid of the inner mitochondrial membrane, and cancer cell proliferation has been found. Cardiolipin is made of a central glycerol backbone carrying four acyl groups. The nature of these acyl groups seems to be difference between cancer and normal cells (Kiebish et al., 2008). The link between the acyl composition of cardiolipin and CAC lies in the fact that this special lipid is essential for the transport activity of CAC (Tonazzi et al., 2015). If the up- or down-regulation of CAC causes an increase or decrease of mitochondrial carnitine remains to be established. It is plausible that the CAC mostly influences the rate of translocation of acyl moiety to the mitochondrial matrix. Indeed, a direct link between the activity of the CAC and the β-oxidation rate has been proposed (Indiveri et al., 2011; Tonazzi et al., 2015).

CONCLUSION

The maintenance of carnitine homeostasis is crucial for cell life in physiological and pathological conditions in which FAO occurs at a high rate. Carnitine, indeed, plays the key role of shuttling acyl groups through intracellular membranes for FAO. Several human cancers rely on FAO for their development and progression to malignancy. Furthermore, carnitine is crucial in the regulation of the acyl-CoA/CoA balance, which in turn, modulates the carbohydrate and the lipid metabolisms. The carnitine and acylcarnitine traffic could not occur without the concerted activity of dedicated membrane transporters localized at the cell surface and in intracellular organelles. In line with the depicted scenario, derangements of the transporters regulating carnitine traffic and hence, carnitine homeostasis was found in several human cancers. For this reason, these proteins represent potential targets for anti-cancer therapy and should be added to the existing list, including sugar and amino acid transporters, which are already considered druggable targets. In particular,

changes in the expression/function of OCTN2 and CT2 have been observed in human cancers indicating that cell supply of carnitine is strictly regulated during cancer development and that chemical KO of these proteins may serve as a strategy to impair energy production from FAO. Curiously, CT2 that, in normal conditions, has a very narrow and specific tissue distribution, becomes widely expressed in cancers even originating from tissues in which CT2 is normally not present, further highlighting the carnitine role in human cancers. The appearance of CT2 in cancers is shared with another plasma membrane transporter responsible for regulating the traffic of essential amino acids, that is LAT1 (SLC7A5; Scalise et al., 2018). Noteworthy, these two membrane transporters are also responsible for drug uptake in the cell, further highlighting their role in developing novel anti-cancer approaches and/or improving those already existing. Indeed, CT2 and OCTN2 mediate the uptake of several anti-cancer drugs such as doxorubicin and oxaliplatin, respectively. Then, changes in their expression or activity may explain the ineffectiveness of some treatments and it may be exploited to improve the delivery of drugs also in the form of carnitine-derivatives.

AUTHOR CONTRIBUTIONS

LC contributed in collecting bibliography, in writing the manuscript, and in conceiving and creating the figures. MS contributed in writing the manuscript and in conceiving and creating the figures. TM contributed in collecting bibliography and in writing the manuscript. AT contributed in creating the figures and in the critical revision of the manuscript. NG, MG, and LP were involved in the critical revision and writing of the manuscript. CI supervised the work and wrote and revised the manuscript. All authors contributed to the article and approved the submitted version.

FUNDING

This work was in part supported by "Fondi di Ateneo" from the Università della Calabria (to CI, MS, MG, and LP) and in part by PON (Programma Operativo Nazionale) Project No. 01_00937 granted by MIUR (Ministry of Education, University and Research) Italy to CI.

REFERENCES

Almannai, M., Alfadhel, M., and El-Hattab, A. W. (2019). Carnitine inborn errors of metabolism. *Molecules* 24:3251. doi: 10.3390/molecules24183251

Angelini, S., Pantaleo, M. A., Ravegnini, G., Zenesini, C., Cavrini, G., Nannini, M., et al. (2013). Polymorphisms in OCTN1 and OCTN2 transporters genes are associated with prolonged time to progression in unresectable gastrointestinal stromal tumours treated with imatinib therapy. *Pharmacol. Res.* 68, 1–6. doi: 10.1016/j.phrs.2012.10.015

Aouida, M., Poulin, R., and Ramotar, D. (2010). The human carnitine transporter SLC22A16 mediates high affinity uptake of the anticancer polyamine analogue bleomycin-A5. *J. Biol. Chem.* 285, 6275–6284. doi: 10.1074/jbc.m109.046151

Bene, J., Hadzsiev, K., and Melegh, B. (2018). Role of carnitine and its derivatives in the development and management of type 2 diabetes. *Nutr. Diabetes* 8:8.

Bhutia, Y. D., and Ganapathy, V. (2016). Glutamine transporters in mammalian cells and their functions in physiology and cancer. *Biochim. Biophys. Acta* 1863, 2531–2539. doi: 10.1016/j.bbamcr.2015.12.017

Bode, B. P. (2001). Recent molecular advances in mammalian glutamine transport. *J. Nutr.* 131(Suppl. 9), 2475S–2485S.

Bray, J., Sludden, J., Griffin, M. J., Cole, M., Verrill, M., Jamieson, D., et al. (2010). Influence of pharmacogenetics on response and toxicity in breast cancer patients treated with doxorubicin and cyclophosphamide. *Br. J. Cancer* 102, 1003–1009. doi: 10.1038/sj.bjc.6605587

Bresolin, N., Freddo, L., Vergani, L., and Angelini, C. (1982). Carnitine, carnitine acyltransferases, and rat brain function. *Exp. Neurol.* 78, 285–292. doi: 10.1016/0014-4886(82)90047-4

Broer, S., and Fairweather, S. J. (2018). Amino acid transport across the mammalian intestine. *Compr. Physiol.* 9, 343–373. doi: 10.1002/cphy.c170041

Carracedo, A., Cantley, L. C., and Pandolfi, P. P. (2013). Cancer metabolism: fatty acid oxidation in the limelight. *Nat. Rev. Cancer* 13, 227–232. doi: 10.1038/nrc3483

Console, L., Scalise, M., Giangregorio, N., Tonazzi, A., Barile, M., and Indiveri, C. (2020). The link between the mitochondrial fatty acid oxidation derangement and kidney injury. *Front. Physiol.* 11:794. doi: 10.3389/fphys.2020.00794

Console, L., Scalise, M., Tonazzi, A., Giangregorio, N., and Indiveri, C. (2018). Characterization of Exosomal SLC22A5 (OCTN2) carnitine transporter. *Sci. Rep.* 8:3758.

Cotton, L. M., Rodriguez, C. M., Suzuki, K., Orgebin-Crist, M. C., and Hinton, B. T. (2010). Organic cation/carnitine transporter, OCTN2, transcriptional activity is regulated by osmotic stress in epididymal cells. *Mol. Reprod. Dev.* 77, 114–125. doi: 10.1002/mrd.21122

Currie, E., Schulze, A., Zechner, R., Walther, T. C., and Farese, R. V. Jr. (2013). Cellular fatty acid metabolism and cancer. *Cell Metab.* 18, 153–161. doi: 10.1016/j.cmet.2013.05.017

Demarquoy, J., and Le Borgne, F. (2015). Crosstalk between mitochondria and peroxisomes. *World J. Biol. Chem.* 6, 301–309. doi: 10.4331/wjbc.v6.i4.301

Demirkan, A., Henneman, P., Verhoeven, A., Dharuri, H., Amin, N., van Klinken, J. B., et al. (2015). Insight in genome-wide association of metabolite quantitative traits by exome sequence analyses. *PLoS Genet.* 11:e1004835. doi: 10.1371/journal.pgen.1004835

Di Paola, M., Park, A. J., Ahmadi, S., Roach, E. J., Wu, Y. S., Struder-Kypke, M., et al. (2017). SLC6A14 is a genetic modifier of cystic fibrosis that regulates *Pseudomonas aeruginosa* attachment to human bronchial epithelial cells. *mBio* 8:e02073-17. doi: 10.1128/mBio.02073-17

Drenberg, C. D., Gibson, A. A., Pounds, S. B., Shi, L., Rhinehart, D. P., Li, L., et al. (2017). OCTN1 is a high-affinity carrier of nucleoside analogues. *Cancer Res.* 77, 2102–2111. doi: 10.1158/0008-5472.can-16-2548

Duran, M., Loof, N. E., Ketting, D., and Dorland, L. (1990). Secondary carnitine deficiency. *J. Clin. Chem. Clin. Biochem.* 28, 359–363.

El-Hattab, A. W., and Scaglia, F. (2015). Disorders of carnitine biosynthesis and transport. *Mol. Genet. Metab.* 116, 107–112. doi: 10.1016/j.ymgme.2015.09.004

Elsnerova, K., Mohelnikova-Duchonova, B., Cerovska, E., Ehrlichova, M., Gut, I., Rob, L., et al. (2016). Gene expression of membrane transporters: importance for prognosis and progression of ovarian carcinoma. *Oncol. Rep.* 35, 2159–2170. doi: 10.3892/or.2016.4599

Enomoto, A., Wempe, M. F., Tsuchida, H., Shin, H. J., Cha, S. H., Anzai, N., et al. (2002). Molecular identification of a novel carnitine transporter specific to human testis. Insights into the mechanism of carnitine recognition. *J. Biol. Chem.* 277, 36262–36271. doi: 10.1074/jbc.m203883200

Fernandez-Ranvier, G. G., Weng, J., Yeh, R. F., Khanafshar, E., Suh, I., Barker, C., et al. (2008). Identification of biomarkers of adrenocortical carcinoma using genomewide gene expression profiling. *Arch. Surg.* 143, 841–846; discussion 846.

Filippo, C. A., Ardon, O., and Longo, N. (2011). Glycosylation of the OCTN2 carnitine transporter: study of natural mutations identified in patients with primary carnitine deficiency. *Biochim. Biophys. Acta* 1812, 312–320. doi: 10.1016/j.bbadis.2010.11.007

Fink, M. A., Paland, H., Herzog, S., Grube, M., Vogelgesang, S., Weitmann, K., et al. (2019). L-carnitine-mediated tumor cell protection and poor patient survival associated with OCTN2 overexpression in glioblastoma multiforme. *Clin. Cancer Res.* 25, 2874–2886. doi: 10.1158/1078-0432.ccr-18-2380

Futagi, Y., Narumi, K., Furugen, A., Kobayashi, M., and Iseki, K. (2020). Molecular characterization of the orphan transporter SLC16A9, an extracellular pH- and Na(+)-sensitive creatine transporter. *Biochem. Biophys. Res. Commun.* 522, 539–544. doi: 10.1016/j.bbrc.2019.11.137

Ganapathy, M. E., and Ganapathy, V. (2005). Amino acid transporter ATB0,+ as a delivery system for drugs and prodrugs. *Curr. Drug Targets Immune Endocr. Metabol. Disord.* 5, 357–364. doi: 10.2174/156800805774912953

Ganapathy, V., Thangaraju, M., and Prasad, P. D. (2009). Nutrient transporters in cancer: relevance to Warburg hypothesis and beyond. *Pharmacol. Ther.* 121, 29–40. doi: 10.1016/j.pharmthera.2008.09.005

Gao, C., Catucci, G., Castrignano, S., Gilardi, G., and Sadeghi, S. J. (2017). Inactivation mechanism of N61S mutant of human FMO3 towards trimethylamine. *Sci. Rep.* 7:14668.

Giangregorio, N., Tonazzi, A., Console, L., and Indiveri, C. (2017). Post-translational modification by acetylation regulates the mitochondrial carnitine/acylcarnitine transport protein. *Mol. Cell Biochem.* 426, 65–73. doi: 10.1007/s11010-016-2881-0

Giangregorio, N., Tonazzi, A., Console, L., Lorusso, I., De Palma, A., and Indiveri, C. (2016). The mitochondrial carnitine/acylcarnitine carrier is regulated by hydrogen sulfide via interaction with C136 and C155. *Biochim. Biophys. Acta* 1860, 20–27. doi: 10.1016/j.bbagen.2015.10.005

Gong, S., Lu, X., Xu, Y., Swiderski, C. F., Jordan, C. T., and Moscow, J. A. (2002). Identification of OCT6 as a novel organic cation transporter preferentially expressed in hematopoietic cells and leukemias. *Exp. Hematol.* 30, 1162–1169. doi: 10.1016/s0301-472x(02)00901-3

Grando, S. A., Kawashima, K., Kirkpatrick, C. J., Kummer, W., and Wessler, I. (2015). Recent progress in revealing the biological and medical significance of the non-neuronal cholinergic system. *Int. Immunopharmacol.* 29, 1–7. doi: 10.1016/j.intimp.2015.08.023

Gründemann, D., Harlfinger, S., Golz, S., Geerts, A., Lazar, A., Berkels, R., et al. (2005). Discovery of the ergothioneine transporter. *Proc. Natl. Acad. Sci. U.S.A.* 102, 5256–5261. doi: 10.1073/pnas.0408624102

Gupta, N., Prasad, P. D., Ghamande, S., Moore-Martin, P., Herdman, A. V., Martindale, R. G., et al. (2006). Up-regulation of the amino acid transporter ATB(0,+) (SLC6A14) in carcinoma of the cervix. *Gynecol. Oncol.* 100, 8–13. doi: 10.1016/j.ygyno.2005.08.016

Halestrap, A. P. (2013). The SLC16 gene family – structure, role and regulation in health and disease. *Mol. Aspects Med.* 34, 337–349. doi: 10.1016/j.mam.2012.05.003

Halestrap, A. P., and Price, N. T. (1999). The proton-linked monocarboxylate transporter (MCT) family: structure, function and regulation. *Biochem. J.* 343(Pt 2), 281–299. doi: 10.1042/0264-6021:3430281

Halestrap, A. P., and Wilson, M. C. (2012). The monocarboxylate transporter family–role and regulation. *IUBMB Life* 64, 109–119. doi: 10.1002/iub.572

Halliwell, B., Cheah, I. K., and Drum, C. L. (2016). Ergothioneine, an adaptive antioxidant for the protection of injured tissues? A hypothesis. *Biochem. Biophys. Res. Commun.* 470, 245–250. doi: 10.1016/j.bbrc.2015.12.124

Hanahan, D., and Weinberg, R. A. (2011). Hallmarks of cancer: the next generation. *Cell* 144, 646–674. doi: 10.1016/j.cell.2011.02.013

Hu, S., Franke, R. M., Filipski, K. K., Hu, C., Orwick, S. J., de Bruijn, E. A., et al. (2008). Interaction of imatinib with human organic ion carriers. *Clin. Cancer Res.* 14, 3141–3148. doi: 10.1158/1078-0432.ccr-07-4913

Indiveri, C., Iacobazzi, V., Tonazzi, A., Giangregorio, N., Infantino, V., Convertini, P., et al. (2011). The mitochondrial carnitine/acylcarnitine carrier: function, structure and physiopathology. *Mol. Aspects Med.* 32, 223–233. doi: 10.1016/j.mam.2011.10.008

Indiveri, C., Pochini, L., Oppedisano, F., and Tonazzi, A. (2010). The carnitine transporter network: interactions with drugs. *Curr. Chem. Biol.* 4, 108–123. doi: 10.2174/187231310791170748

Jansen, L., de Niet, A., Stelma, F., van Iperen, E. P., van Dort, K. A., Plat-Sinnige, M. J., et al. (2014). HBsAg loss in patients treated with peginterferon alfa-2a and adefovir is associated with SLC16A9 gene variation and lower plasma carnitine levels. *J. Hepatol.* 61, 730–737. doi: 10.1016/j.jhep.2014.05.004

Jaruskova, M., Curik, N., Hercog, R., Polivkova, V., Motlova, E., Benes, V., et al. (2017). Genotypes of SLC22A4 and SLC22A5 regulatory loci are predictive of the response of chronic myeloid leukemia patients to imatinib treatment. *J. Exp. Clin. Cancer Res.* 36:55.

Jeon, S. M., Chandel, N. S., and Hay, N. (2012). AMPK regulates NADPH homeostasis to promote tumour cell survival during energy stress. *Nature* 485, 661–665. doi: 10.1038/nature11066

Jeulin, C., and Lewin, L. M. (1996). Role of free L-carnitine and acetyl-L-carnitine in post-gonadal maturation of mammalian spermatozoa. *Hum. Reprod. Update* 2, 87–102. doi: 10.1093/humupd/2.2.87

Jong, N. N., Nakanishi, T., Liu, J. J., Tamai, I., and McKeage, M. J. (2011). Oxaliplatin transport mediated by organic cation/carnitine transporters OCTN1 and OCTN2 in overexpressing human embryonic kidney 293 cells and rat dorsal root ganglion neurons. *J. Pharmacol. Exp. Ther.* 338, 537–547. doi: 10.1124/jpet.111.181297

Juraszek, B., and Nalecz, K. A. (2019). SLC22A5 (OCTN2) carnitine transporter-indispensable for cell metabolism, a Jekyll and Hyde of human cancer. *Molecules* 25:14. doi: 10.3390/molecules25010014

Jurkiewicz, D., Michalec, K., Skowronek, K., and Nalecz, K. A. (2017). Tight junction protein ZO-1 controls organic cation/carnitine transporter OCTN2 (SLC22A5) in a protein kinase C-dependent way. *Biochim. Biophys. Acta Mol. Cell Res.* 1864, 797–805. doi: 10.1016/j.bbamcr.2017.02.014

Karunakaran, S., Ramachandran, S., Coothankandaswamy, V., Elangovan, S., Babu, E., Periyasamy-Thandavan, S., et al. (2011). SLC6A14 (ATB0,+) protein, a highly concentrative and broad specific amino acid transporter, is a novel and effective drug target for treatment of estrogen receptor-positive breast cancer. *J. Biol. Chem.* 286, 31830–31838. doi: 10.1074/jbc.m111.229518

Kato, Y., Sai, Y., Yoshida, K., Watanabe, C., Hirata, T., and Tsuji, A. (2005). PDZK1 directly regulates the function of organic cation/carnitine transporter OCTN2. *Mol. Pharmacol.* 67, 734–743. doi: 10.1124/mol.104.002212

Kiebish, M. A., Han, X., Cheng, H., Chuang, J. H., and Seyfried, T. N. (2008). Cardiolipin and electron transport chain abnormalities in mouse brain tumor mitochondria: lipidomic evidence supporting the Warburg theory of cancer. *J. Lipid Res.* 49, 2545–2556. doi: 10.1194/jlr.m800319-jlr200

Kim, W. T., Yun, S. J., Yan, C., Jeong, P., Kim, Y. H., Lee, I. S., et al. (2016). Metabolic pathway signatures associated with urinary metabolite biomarkers differentiate bladder cancer patients from healthy controls. *Yonsei Med. J.* 57, 865–871. doi: 10.3349/ymj.2016.57.4.865

Knyazev, E. N., Mal'tseva, D. V., Zacharyants, A. A., Zakharova, G. S., Zhidkova, O. V., and Poloznikov, A. A. (2018). TNFalpha-induced expression of transport protein genes in HUVEC cells is associated with enhanced expression of transcription factor genes RELB and NFKB2 of the non-canonical NF-kappaB Pathway. *Bull. Exp. Biol. Med.* 164, 757–761. doi: 10.1007/s10517-018-4074-1

Koepsell, H. (2013). The SLC22 family with transporters of organic cations, anions and zwitterions. *Mol. Aspects Med.* 34, 413–435. doi: 10.1016/j.mam.2012.10.010

Koepsell, H. (2020). Organic cation transporters in health and disease. *Pharmacol. Rev.* 72, 253–319. doi: 10.1124/pr.118.015578

Koeth, R. A., Wang, Z., Levison, B. S., Buffa, J. A., Org, E., Sheehy, B. T., et al. (2013). Intestinal microbiota metabolism of L-carnitine, a nutrient in red meat, promotes atherosclerosis. *Nat. Med.* 19, 576–585. doi: 10.1038/nm.3145

Kolz, M., Johnson, T., Sanna, S., Teumer, A., Vitart, V., Perola, M., et al. (2009). Meta-analysis of 28,141 individuals identifies common variants within five new loci that influence uric acid concentrations. *PLoS Genet.* 5:e1000504. doi: 10.1371/journal.pgen.1000504

Kou, L., Hou, Y., Yao, Q., Guo, W., Wang, G., Wang, M., et al. (2018). L-Carnitine-conjugated nanoparticles to promote permeation across blood-brain barrier and to target glioma cells for drug delivery via the novel organic cation/carnitine transporter OCTN2. *Artif. Cells Nanomed. Biotechnol.* 46, 1605–1616.

Kou, L., Sun, R., Xiao, S., Cui, X., Sun, J., Ganapathy, V., et al. (2020). OCTN2-targeted nanoparticles for oral delivery of paclitaxel: differential impact of the polyethylene glycol linker size on drug delivery in vitro, in situ, and in vivo. *Drug Deliv.* 27, 170–179. doi: 10.1080/10717544.2019.1710623

Kou, L., Yao, Q., Sivaprakasam, S., Luo, Q., Sun, Y., Fu, Q., et al. (2017). Dual targeting of l-carnitine-conjugated nanoparticles to OCTN2 and ATB(0,+) to deliver chemotherapeutic agents for colon cancer therapy. *Drug Deliv.* 24, 1338–1349. doi: 10.1080/10717544.2017.1377316

Koundouros, N., and Poulogiannis, G. (2020). Reprogramming of fatty acid metabolism in cancer. *Br. J. Cancer* 122, 4–22. doi: 10.1038/s41416-019-0650-z

Kunii, E., Oguri, T., Kasai, D., Ozasa, H., Uemura, T., Takakuwa, O., et al. (2015). Organic cation transporter OCT6 mediates cisplatin uptake and resistance to

cisplatin in lung cancer. *Cancer Chemother. Pharmacol.* 75, 985–991. doi: 10.1007/s00280-015-2723-x

Lahjouji, K., Malo, C., Mitchell, G. A., and Qureshi, I. A. (2002). L-Carnitine transport in mouse renal and intestinal brush-border and basolateral membrane vesicles. *Biochim. Biophys. Acta* 1558, 82–93. doi: 10.1016/s0005-2736(01)00433-3

Lal, S., Wong, Z. W., Jada, S. R., Xiang, X., Chen Shu, X., Ang, P. C., et al. (2007). Novel SLC22A16 polymorphisms and influence on doxorubicin pharmacokinetics in Asian breast cancer patients. *Pharmacogenomics* 8, 567–575. doi: 10.2217/14622416.8.6.567

Lee, J. H., Zhao, X. M., Yoon, I., Lee, J. Y., Kwon, N. H., Wang, Y. Y., et al. (2016). Integrative analysis of mutational and transcriptional profiles reveals driver mutations of metastatic breast cancers. *Cell Discov.* 2:16025.

Liang, Y. X., Liu, L., Jin, Z. Y., Liang, X. H., Fu, Y. S., Gu, X. W., et al. (2018). The high concentration of progesterone is harmful for endometrial receptivity and decidualization. *Sci. Rep.* 8:712.

Lim, D. H., Kim, W. S., Kim, S. J., Yoo, H. Y., and Ko, Y. H. (2015). Microarray gene-expression profiling analysis comparing PCNSL and non-CNS diffuse large B-cell lymphoma. *Anticancer Res.* 35, 3333–3340.

Liu, Y. (2006). Fatty acid oxidation is a dominant bioenergetic pathway in prostate cancer. *Prostate Cancer Prostatic. Dis.* 9, 230–234. doi: 10.1038/sj.pcan.4500879

Lombard, K. A., Olson, A. L., Nelson, S. E., and Rebouche, C. J. (1989). Carnitine status of lactoovovegetarians and strict vegetarian adults and children. *Am. J. Clin. Nutr.* 50, 301–306. doi: 10.1093/ajcn/50.2.301

Longo, N., Amat di San Filippo, C., and Pasquali, M. (2006). Disorders of carnitine transport and the carnitine cycle. *Am. J. Med. Genet. C Semin. Med. Genet.* 142C, 77–85. doi: 10.1002/ajmg.c.30087

Lu, X., Wang, Z. C., Iglehart, J. D., Zhang, X., and Richardson, A. L. (2008). Predicting features of breast cancer with gene expression patterns. *Breast Cancer Res. Treat.* 108, 191–201. doi: 10.1007/s10549-007-9596-6

Madiraju, P., Pande, S. V., Prentki, M., and Madiraju, S. R. (2009). Mitochondrial acetylcarnitine provides acetyl groups for nuclear histone acetylation. *Epigenetics* 4, 399–403. doi: 10.4161/epi.4.6.9767

Maeda, T., Wakasawa, T., Funabashi, M., Fukushi, A., Fujita, M., Motojima, K., et al. (2008). Regulation of OCTN2 transporter (SLC22A5) by peroxisome proliferator activated receptor alpha. *Biol. Pharm. Bull.* 31, 1230–1236. doi: 10.1248/bpb.31.1230

Maekawa, S., Mori, D., Nishiya, T., Takikawa, O., Horinouchi, T., Nishimoto, A., et al. (2007). OCTN2VT, a splice variant of OCTN2, does not transport carnitine because of the retention in the endoplasmic reticulum caused by insertion of 24 amino acids in the first extracellular loop of OCTN2. *Biochim. Biophys. Acta* 1773, 1000–1006. doi: 10.1016/j.bbamcr.2007.04.005

Magoulas, P. L., and El-Hattab, A. W. (2012). Systemic primary carnitine deficiency: an overview of clinical manifestations, diagnosis, and management. *Orphanet. J. Rare Dis.* 7:68. doi: 10.1186/1750-1172-7-68

Martini, M., Ferrara, A. M., Giachelia, M., Panieri, E., Siminovitch, K., Galeotti, T., et al. (2012). Association of the OCTN1/1672T variant with increased risk for colorectal cancer in young individuals and ulcerative colitis patients. *Inflamm. Bowel Dis.* 18, 439–448. doi: 10.1002/ibd.21814

Melone, M. A. B., Valentino, A., Margarucci, S., Galderisi, U., Giordano, A., and Peluso, G. (2018). The carnitine system and cancer metabolic plasticity. *Cell Death Dis.* 9:228.

Nakanishi, T., Hatanaka, T., Huang, W., Prasad, P. D., Leibach, F. H., Ganapathy, M. E., et al. (2001). Na+- and Cl–coupled active transport of carnitine by the amino acid transporter ATB(0,+) from mouse colon expressed in HRPE cells and Xenopus oocytes. *J. Physiol.* 532(Pt 2), 297–304. doi: 10.1111/j.1469-7793.2001.0297f.x

Nezu, J., Tamai, I., Oku, A., Ohashi, R., Yabuuchi, H., Hashimoto, N., et al. (1999). Primary systemic carnitine deficiency is caused by mutations in a gene encoding sodium ion-dependent carnitine transporter. *Nat. Genet.* 21, 91–94. doi: 10.1038/5030

Novak, A. J., Asmann, Y. W., Maurer, M. J., Wang, C., Slager, S. L., Hodge, L. S., et al. (2015). Whole-exome analysis reveals novel somatic genomic alterations associated with outcome in immunochemotherapy-treated diffuse large B-cell lymphoma. *Blood Cancer J.* 5:e346. doi: 10.1038/bcj.2015.69

Oellgaard, J., Winther, S. A., Hansen, T. S., Rossing, P., and von Scholten, B. J. (2017). Trimethylamine N-oxide (TMAO) as a new potential therapeutic target for insulin resistance and cancer. *Curr. Pharm. Des.* 23, 3699–3712.

Ohashi, R., Tamai, I., Inano, A., Katsura, M., Sai, Y., Nezu, J., et al. (2002). Studies on functional sites of organic cation/carnitine transporter OCTN2 (SLC22A5) using a Ser467Cys mutant protein. *J. Pharmacol. Exp. Ther.* 302, 1286–1294. doi: 10.1124/jpet.102.036004

Ohashi, R., Tamai, I., Nezu, Ji J, Nikaido, H., Hashimoto, N., Oku, A., et al. (2001). Molecular and physiological evidence for multifunctionality of carnitine/organic cation transporter OCTN2. *Mol. Pharmacol.* 59, 358–366. doi: 10.1124/mol.59.2.358

Ohashi, R., Tamai, I., Yabuuchi, H., Nezu, J. I., Oku, A., Sai, Y., et al. (1999). Na(+)-dependent carnitine transport by organic cation transporter (OCTN2): its pharmacological and toxicological relevance. *J. Pharmacol. Exp. Ther.* 291, 778–784.

Ohnishi, S., Saito, H., Fukada, A., and Inui, K. (2003). Distinct transport activity of tetraethylammonium from L-carnitine in rat renal brush-border membranes. *Biochim. Biophys. Acta* 1609, 218–224. doi: 10.1016/s0005-2736(02)00703-4

Okabe, M., Szakács, G., Reimers, M. A., Suzuki, T., Hall, M. D., Abe, T., et al. (2008). Profiling SLCO and SLC22 genes in the NCI-60 cancer cell lines to identify drug uptake transporters. *Mol. Cancer Ther.* 7, 3081–3091. doi: 10.1158/1535-7163.mct-08-0539

Okabe, M., Unno, M., Harigae, H., Kaku, M., Okitsu, Y., Sasaki, T., et al. (2005). Characterization of the organic cation transporter SLC22A16: a doxorubicin importer. *Biochem. Biophys. Res. Commun.* 333, 754–762. doi: 10.1016/j.bbrc.2005.05.174

Ota, K., Ito, K., Akahira, J., Sato, N., Onogawa, T., Moriya, T., et al. (2007). Expression of organic cation transporter SLC22A16 in human epithelial ovarian cancer: a possible role of the adriamycin importer. *Int. J. Gynecol. Pathol.* 26, 334–340. doi: 10.1097/01.pgp.0000236951.33914.1b

Palmieri, E. M., Spera, I., Menga, A., Infantino, V., Porcelli, V., Iacobazzi, V., et al. (2015). Acetylation of human mitochondrial citrate carrier modulates mitochondrial citrate/malate exchange activity to sustain NADPH production during macrophage activation. *Biochim. Biophys. Acta* 1847, 729–738. doi: 10.1016/j.bbabio.2015.04.009

Palmieri, F. (2013). The mitochondrial transporter family SLC25: identification, properties and physiopathology. *Mol. Aspects Med.* 34, 465–484. doi: 10.1016/j.mam.2012.05.005

Parker, C. G., Kuttruff, C. A., Galmozzi, A., Jorgensen, L., Yeh, C. H., Hermanson, D. J., et al. (2017). Chemical proteomics identifies SLC25A20 as a functional target of the ingenol class of actinic keratosis drugs. *ACS Cent Sci.* 3, 1276–1285. doi: 10.1021/acscentsci.7b00420

Phillips, I. R., and Shephard, E. A. (2020). Flavin-containing monooxygenase 3 (FMO3): genetic variants and their consequences for drug metabolism and disease. *Xenobiotica* 50, 19–33. doi: 10.1080/00498254.2019.1643515

Pietrocola, F., Galluzzi, L., Bravo-San Pedro, J. M., Madeo, F., and Kroemer, G. (2015). Acetyl coenzyme A: a central metabolite and second messenger. *Cell Metab.* 21, 805–821. doi: 10.1016/j.cmet.2015.05.014

Pochini, L., Galluccio, M., Scalise, M., Console, L., and Indiveri, C. (2019). OCTN: a small transporter subfamily with great relevance to human pathophysiology, drug discovery, and diagnostics. *SLAS Discov.* 24, 89–110. doi: 10.1177/2472555218812821

Pochini, L., Oppedisano, F., and Indiveri, C. (2004). Reconstitution into liposomes and functional characterization of the carnitine transporter from renal cell plasma membrane. *Biochim. Biophys. Acta* 1661, 78–86. doi: 10.1016/j.bbamem.2003.12.001

Pochini, L., Scalise, M., Di Silvestre, S., Belviso, S., Pandolfi, A., Arduini, A., et al. (2016). Acetylcholine and acetylcarnitine transport in peritoneum: role of the SLC22A4 (OCTN1) transporter. *Biochim. Biophys. Acta* 1858, 653–660. doi: 10.1016/j.bbamem.2015.12.026

Pochini, L., Scalise, M., Galluccio, M., Amelio, L., and Indiveri, C. (2011). Reconstitution in liposomes of the functionally active human OCTN1 (SLC22A4) transporter overexpressed in *Escherichia coli*. *Biochem. J.* 439, 227–233. doi: 10.1042/bj20110544

Pochini, L., Scalise, M., Galluccio, M., and Indiveri, C. (2013). OCTN cation transporters in health and disease: role as drug targets and assay development. *J. Biomol. Screen* 18, 851–867. doi: 10.1177/1087057113493006

Pochini, L., Scalise, M., Galluccio, M., Pani, G., Siminovitch, K. A., and Indiveri, C. (2012). The human OCTN1 (SLC22A4) reconstituted in liposomes catalyzes acetylcholine transport which is defective in the mutant L503F associated to the

Crohn's disease. *Biochim. Biophys. Acta* 1818, 559–565. doi: 10.1016/j.bbamem.2011.12.014

Pochini, L., Scalise, M., and Indiveri, C. (2009). Inactivation by omeprazole of the carnitine transporter (OCTN2) reconstituted in liposomes. *Chem. Biol. Interact.* 179, 394–401. doi: 10.1016/j.cbi.2008.10.052

Pochini, L., Scalise, M., and Indiveri, C. (2015). Immuno-detection of OCTN1 (SLC22A4) in HeLa cells and characterization of transport function. *Int. Immunopharmacol.* 29, 21–26. doi: 10.1016/j.intimp.2015.04.040

Pramod, A. B., Foster, J., Carvelli, L., and Henry, L. K. (2013). SLC6 transporters: structure, function, regulation, disease association and therapeutics. *Mol Aspects Med.* 34, 197–219. doi: 10.1016/j.mam.2012.07.002

Qu, Q., Qu, J., Guo, Y., Zhou, B. T., and Zhou, H. H. (2014). Luteolin potentiates the sensitivity of colorectal cancer cell lines to oxaliplatin through the PPARgamma/OCTN2 pathway. *Anticancer Drugs* 25, 1016–1027. doi: 10.1097/cad.0000000000000125

Qu, Q., Qu, J., Zhan, M., Wu, L. X., Zhang, Y. W., Lou, X. Y., et al. (2013). Different involvement of promoter methylation in the expression of organic cation/carnitine transporter 2 (OCTN2) in cancer cell lines. *PLoS One* 8:e76474. doi: 10.1371/journal.pone.0076474

Qu, Q., Zeng, F., Liu, X., Wang, Q. J., and Deng, F. (2016). Fatty acid oxidation and carnitine palmitoyltransferase I: emerging therapeutic targets in cancer. *Cell Death Dis.* 7:e2226. doi: 10.1038/cddis.2016.132

Quail, D. F., and Joyce, J. A. (2013). Microenvironmental regulation of tumor progression and metastasis. *Nat. Med.* 19, 1423–1437. doi: 10.1038/nm.3394

Ramsay, R. R., and Arduini, A. (1993). The carnitine acyltransferases and their role in modulating acyl-CoA pools. *Arch. Biochem. Biophys.* 302, 307–314. doi: 10.1006/abbi.1993.1216

Rebouche, C. J. (2004). Kinetics, pharmacokinetics, and regulation of L-carnitine and acetyl-L-carnitine metabolism. *Ann. N. Y. Acad. Sci.* 1033, 30–41. doi: 10.1196/annals.1320.003

Rebouche, C. J., and Seim, H. (1998). Carnitine metabolism and its regulation in microorganisms and mammals. *Annu. Rev. Nutr.* 18, 39–61. doi: 10.1146/annurev.nutr.18.1.39

Rohrig, F., and Schulze, A. (2016). The multifaceted roles of fatty acid synthesis in cancer. *Nat. Rev. Cancer* 16, 732–749. doi: 10.1038/nrc.2016.89

Roncal, C., Martinez-Aguilar, E., Orbe, J., Ravassa, S., Fernandez-Montero, A., Saenz-Pipaon, G., et al. (2019). Trimethylamine-N-Oxide (TMAO) predicts cardiovascular mortality in peripheral artery disease. *Sci. Rep.* 9:15580.

Rose, E. C., di San Filippo, C. A., Ndukwe Erlingsson, U. C., Ardon, O., Pasquali, M., and Longo, N. (2012). Genotype-phenotype correlation in primary carnitine deficiency. *Hum. Mutat.* 33, 118–123. doi: 10.1002/humu.21607

Rotoli, B. M., Visigalli, R., Barilli, A., Ferrari, F., Bianchi, M. G., Di Lascia, M., et al. (2020). Functional analysis of OCTN2 and ATB0,+ in normal human airway epithelial cells. *PLoS One* 15:e0228568. doi: 10.1371/journal.pone.0228568

Ruffin, M., Mercier, J., Calmel, C., Mesinele, J., Bigot, J., Sutanto, E. N., et al. (2020). Update on SLC6A14 in lung and gastrointestinal physiology and physiopathology: focus on cystic fibrosis. *Cell Mol. Life Sci.* 77, 3311–3323. doi: 10.1007/s00018-020-03487-x

Sagwal, S. K., Pasqual-Melo, G., Bodnar, Y., Gandhirajan, R. K., and Bekeschus, S. (2018). Combination of chemotherapy and physical plasma elicits melanoma cell death via upregulation of SLC22A16. *Cell Death Dis.* 9:1179.

Sato, N., Ito, K., Onogawa, T., Akahira, J., Unno, M., Abe, T., et al. (2007). Expression of organic cation transporter SLC22A16 in human endometria. *Int. J. Gynecol. Pathol.* 26, 53–60. doi: 10.1097/01.pgp.0000225845.67245.b3

Scalise, M., Galluccio, M., Accardi, R., Cornet, I., Tommasino, M., and Indiveri, C. (2012). Human OCTN2 (SLC22A5) is down-regulated in virus- and nonvirus-mediated cancer. *Cell Biochem. Funct.* 30, 419–425. doi: 10.1002/cbf.2816

Scalise, M., Galluccio, M., Console, L., Pochini, L., and Indiveri, C. (2018). The human SLC7A5 (LAT1): the intriguing histidine/large neutral amino acid transporter and its relevance to human health. *Front. Chem.* 6:243. doi: 10.3389/fchem.2018.00243

Scalise, M., Pochini, L., Giangregorio, N., Tonazzi, A., and Indiveri, C. (2013). Proteoliposomes as tool for assaying membrane transporter functions and interactions with xenobiotics. *Pharmaceutics* 5, 472–497. doi: 10.3390/pharmaceutics5030472

Seth, P., Wu, X., Huang, W., Leibach, F. H., and Ganapathy, V. (1999). Mutations in novel organic cation transporter (OCTN2), an organic cation/carnitine transporter, with differential effects on the organic cation transport function and the carnitine transport function. *J. Biol. Chem.* 274, 33388–33392. doi: 10.1074/jbc.274.47.33388

Shekhawat, P. S., Yang, H. S., Bennett, M. J., Carter, A. L., Matern, D., Tamai, I., et al. (2004). Carnitine content and expression of mitochondrial beta-oxidation enzymes in placentas of wild-type (OCTN2(+/+)) and OCTN2 Null (OCTN2(−/−)) Mice. *Pediatr. Res.* 56, 323–328. doi: 10.1203/01.pdr.0000134252.02876.55

Sloan, J. L., Grubb, B. R., and Mager, S. (2003). Expression of the amino acid transporter ATB 0+ in lung: possible role in luminal protein removal. *Am J. Physiol. Lung. Cell Mol. Physiol.* 284, L39–L49.

Sloan, J. L., and Mager, S. (1999). Cloning and functional expression of a human Na(+) and Cl(-)-dependent neutral and cationic amino acid transporter B(0+). *J. Biol. Chem.* 274, 23740–23745. doi: 10.1074/jbc.274.34.23740

Soni, M. S., Rabaglia, M. E., Bhatnagar, S., Shang, J., Ilkayeva, O., Mynatt, R., et al. (2014). Downregulation of carnitine acyl-carnitine translocase by miRNAs 132 and 212 amplifies glucose-stimulated insulin secretion. *Diabetes.* 63, 3805–3814. doi: 10.2337/db13-1677

Stanley, C. A., Hale, D. E., Berry, G. T., Deleeuw, S., Boxer, J., and Bonnefont, J. P. (1992). Brief report: a deficiency of carnitine-acylcarnitine translocase in the inner mitochondrial membrane. *N. Engl. J. Med.* 327, 19–23. doi: 10.1056/nejm199207023270104

Stephens, F. B., Constantin-Teodosiu, D., Laithwaite, D., Simpson, E. J., and Greenhaff, P. L. (2006). Insulin stimulates L-carnitine accumulation in human skeletal muscle. *FASEB J.* 20, 377–379. doi: 10.1096/fj.05-4985fje

Su, X., and Abumrad, N. A. (2009). Cellular fatty acid uptake: a pathway under construction. *Trends Endocrinol. Metab.* 20, 72–77. doi: 10.1016/j.tem.2008.11.001

Svensson, R. U., Parker, S. J., Eichner, L. J., Kolar, M. J., Wallace, M., Brun, S. N., et al. (2016). Inhibition of acetyl-CoA carboxylase suppresses fatty acid synthesis and tumor growth of non-small-cell lung cancer in preclinical models. *Nat. Med.* 22, 1108–1119. doi: 10.1038/nm.4181

Tamai, I., Nakanishi, T., Kobayashi, D., China, K., Kosugi, Y., Nezu, J., et al. (2004). Involvement of OCTN1 (SLC22A4) in pH-dependent transport of organic cations. *Mol. Pharm.* 1, 57–66. doi: 10.1021/mp0340082

Tamai, I., Ohashi, R., Nezu, J., Yabuuchi, H., Oku, A., Shimane, M., et al. (1998). Molecular and functional identification of sodium ion-dependent, high affinity human carnitine transporter OCTN2. *J. Biol. Chem.* 273, 20378–20382. doi: 10.1074/jbc.273.32.20378

Tamai, I., Ohashi, R., Nezu, J. I., Sai, Y., Kobayashi, D., Oku, A., et al. (2000). Molecular and functional characterization of organic cation/carnitine transporter family in mice. *J. Biol. Chem.* 275, 40064–40072. doi: 10.1074/jbc.m005340200

Tonazzi, A., Galluccio, M., Oppedisano, F., and Indiveri, C. (2006). Functional reconstitution into liposomes and characterization of the carnitine transporter from rat liver microsomes. *Biochim. Biophys. Acta* 1758, 124–131. doi: 10.1016/j.bbamem.2006.01.004

Tonazzi, A., Giangregorio, N., Console, L., De Palma, A., and Indiveri, C. (2017). Nitric oxide inhibits the mitochondrial carnitine/acylcarnitine carrier through reversible S-nitrosylation of cysteine 136. *Biochim. Biophys. Acta Bioenerg.* 1858, 475–482. doi: 10.1016/j.bbabio.2017.04.002

Tonazzi, A., Giangregorio, N., Console, L., and Indiveri, C. (2015). Mitochondrial carnitine/acylcarnitine translocase: insights in structure/ function relationships. Basis for drug therapy and side effects prediction. *Mini Rev. Med. Chem.* 15, 396–405. doi: 10.2174/1389557515051504081420 32

Tsai, J. H., Chi, M. M., Schulte, M. B., and Moley, K. H. (2014). The fatty acid beta-oxidation pathway is important for decidualization of endometrial stromal cells in both humans and mice. *Biol. Reprod.* 90:34.

Valentino, A., Calarco, A., Di Salle, A., Finicelli, M., Crispi, S., Calogero, R. A., et al. (2017). Deregulation of MicroRNAs mediated control of carnitine cycle in prostate cancer: molecular basis and pathophysiological consequences. *Oncogene* 36, 6030–6040. doi: 10.1038/onc.2017.216

Vaz, F. M., and Wanders, R. J. (2002). Carnitine biosynthesis in mammals. *Biochem. J.* 361(Pt 3), 417–429. doi: 10.1042/0264-6021:3610417

Wang, C., Uray, I. P., Mazumdar, A., Mayer, J. A., and Brown, P. H. (2012). SLC22A5/OCTN2 expression in breast cancer is induced by estrogen via a novel intronic estrogen-response element (ERE). *Breast Cancer Res. Treat.* 134, 101–115. doi: 10.1007/s10549-011-1925-0

Wang, S., Xu, J., Zheng, J., Zhang, X., Shao, J., Zhao, L., et al. (2020). Anti-inflammatory and antioxidant effects of Acetyl-L-Carnitine on atherosclerotic rats. *Med. Sci. Monit.* 26:e920250.

Warburg, O., Wind, F., and Negelein, E. (1927). The metabolism of tumors in the body. *J. Gen. Physiol.* 8, 519–530. doi: 10.1085/jgp.8.6.519

Waterman, N., Bos, C. J., and Barendregt, T. J. (1952). On fatty acid oxidation in malignant and normal livers. *Enzymologia* 15, 307–312.

Wu, X., Huang, W., Prasad, P. D., Seth, P., Rajan, D. P., Leibach, F. H., et al. (1999). Functional characteristics and tissue distribution pattern of organic cation transporter 2 (OCTN2), an organic cation/carnitine transporter. *J. Pharmacol. Exp. Ther.* 290, 1482–1492.

Wu, X., Prasad, P. D., Leibach, F. H., and Ganapathy, V. (1998). cDNA sequence, transport function, and genomic organization of human OCTN2, a new member of the organic cation transporter family. *Biochem. Biophys. Res. Commun.* 246, 589–595. doi: 10.1006/bbrc.1998.8669

Wu, Y., Hurren, R., MacLean, N., Gronda, M., Jitkova, Y., Sukhai, M. A., et al. (2015). Carnitine transporter CT2 (SLC22A16) is over-expressed in acute myeloid leukemia (AML) and target knockdown reduces growth and viability of AML cells. *Apoptosis* 20, 1099–1108. doi: 10.1007/s10495-015-1137-x

Xi, L., Brown, K., Woodworth, J., Shim, K., Johnson, B., and Odle, J. (2008). Maternal dietary L-carnitine supplementation influences fetal carnitine status and stimulates carnitine palmitoyltransferase and pyruvate dehydrogenase complex activities in swine. *J. Nutr.* 138, 2356–2362. doi: 10.3945/jn.108.095638

Xiang, L., Wei, J., Tian, X. Y., Wang, B., Chan, W., Li, S., et al. (2017). Comprehensive analysis of *Acylcarnitine* species in db/db mouse using a novel method of high-resolution parallel reaction monitoring reveals widespread metabolic dysfunction induced by diabetes. *Anal. Chem.* 89, 10368–10375. doi: 10.1021/acs.analchem.7b02283

Yabuuchi, H., Tamai, I., Nezu, J., Sakamoto, K., Oku, A., Shimane, M., et al. (1999). Novel membrane transporter OCTN1 mediates multispecific, bidirectional, and pH-dependent transport of organic cations. *J. Pharmacol. Exp. Ther.* 289, 768–773.

Yamamoto, K., Abe, S., Honda, A., Hashimoto, J., Aizawa, Y., Ishibashi, S., et al. (2020). Fatty acid beta oxidation enzyme HADHA is a novel potential therapeutic target in malignant lymphoma. *Lab. Invest.* 100, 353–362. doi: 10.1038/s41374-019-0318-6

Zhang, J. Z., Wu, Z. H., and Cheng, Q. (2019). Screening and identification of key biomarkers in nasopharyngeal carcinoma: evidence from bioinformatic analysis. *Medicine (Baltimore).* 98:e17997. doi: 10.1097/md.0000000000017997

Zhao, W., Wang, Y., and Yue, X. (2018). SLC22A16 upregulation is an independent unfavorable prognostic indicator in gastric cancer. *Future Oncol.* 14, 2139–2148. doi: 10.2217/fon-2018-0207

Zheng, J., Chan, T., Zhu, L., Yan, X., Cao, Z., Wang, Y., et al. (2016). The inhibitory effects of camptothecin (CPT) and its derivatives on the substrate uptakes mediated by human solute carrier transporters (SLCs). *Xenobiotica* 46, 831–840. doi: 10.3109/00498254.2015.1129080

Zou, D., Lou, J., Ke, J., Mei, S., Li, J., Gong, Y., et al. (2018). Integrative expression quantitative trait locus-based analysis of colorectal cancer identified a functional polymorphism regulating SLC22A5 expression. *Eur. J. Cancer* 93, 1–9. doi: 10.1016/j.ejca.2018.01.065

Conflict of Interest: The authors declare that the research was conducted in the absence of any commercial or financial relationships that could be construed as a potential conflict of interest.

The reviewer DT declared a past collaboration with one of the authors CI to the handling Editor.

frontiers in Cell and Developmental Biology

REVIEW
published: 21 October 2020
doi: 10.3389/fcell.2020.594464

Amino Acid Transporter SLC6A14 ($ATB^{0,+}$) – A Target in Combined Anti-cancer Therapy

*Katarzyna A. Nałęcz**

Laboratory of Transport Through Biomembranes, Nencki Institute of Experimental Biology, Warsaw, Poland

Cancer cells are characterized by quick growth and proliferation, demanding constant supply of various nutrients. Several plasma membrane transporters delivering such compounds are upregulated in cancer. Solute carrier family 6 member 14 (SLC6A14), known as amino acid transporter $B^{0,+}$ ($ATB^{0,+}$) transports all amino acids with exception of the acidic ones: aspartate and glutamate. Its malfunctioning is correlated with several pathological states and it is upregulated in solid tumors. The high expression of *SLC6A14* is prognostic and unfavorable in pancreatic cancer, while in breast cancer it is expressed in estrogen receptor positive cells. As many plasma membrane transporters it resides in endoplasmic reticulum (ER) membrane after translation before further trafficking through Golgi to the cell surface. Transporter exit from ER is strictly controlled. The proper folding of SLC6A14 was shown to be controlled from the cytoplasmic side by heat shock proteins, further exit from ER and formation of coatomer II (COPII) coated vesicles depends on specific interaction with COPII cargo-recognizing subunit SEC24C, phosphorylated by kinase AKT. Inhibition of heat shock proteins, known to be upregulated in cancer, directs SLC6A14 to degradation. Targeting proteins regulating SLC6A14 trafficking is proposed as an additional pharmacological treatment of cancer.

Keywords: amino acid transporter, cancer, SLC6A14, estrogen receptor, trafficking, heat shock proteins, AKT 3

OPEN ACCESS

Edited by:
Vadivel Ganapathy, Texas Tech University Health Sciences Center, United States

Reviewed by:
Cesare Indiveri, University of Calabria, Italy
Stefan Broer, Australian National University, Australia

***Correspondence:**
Katarzyna A. Nałęcz
k.nalecz@nencki.edu.pl

Specialty section:
This article was submitted to Molecular and Cellular Oncology, a section of the journal Frontiers in Cell and Developmental Biology

Received: *13 August 2020*
Accepted: *30 September 2020*
Published: *21 October 2020*

Citation:
Nałęcz KA (2020) Amino Acid Transporter SLC6A14 ($ATB^{0,+}$) – A Target in Combined Anti-cancer Therapy. Front. Cell Dev. Biol. 8:594464. doi: 10.3389/fcell.2020.594464

INTRODUCTION

All cells need a constant supply of necessary nutrients for their proper functioning, as well as removal of metabolic products. The polar and ionized small molecular weight compounds are capable to cross the lipid bilayer of the plasma membrane due to functioning of transporting proteins - solute carriers (SLC), coded in humans by more than 400 genes. Based on their homology and similarity, the *SLC* genes are divided into 65 families[1] according to the following convention: *SLCnXm*, where *n* is the number of the family, *X*-the letter indicating a subfamily, *m*-the member of the family. Currently, the traditional names indicating the transporter function and specificity have been replaced by the SLCnXm names also for the proteins.

Among the hallmarks of cancer cells is their ability for quick growth and proliferation (Hanahan and Weinberg, 2011), what relies on energy delivery and on anabolic processes. Several SLCs have been reported to be upregulated in cancer. Among them there is a glucose transporter GLUT1 – SLC2A1 (Yamamoto et al., 1990; Yu et al., 2017), delivering glucose for aerobic glycolysis (so-called Warburg effect), but as well for synthesis of ribose, serine and protein glycosylation. The

[1]http://slc.bioparadigms.org/

nucleoside transporters from SLC28 and SLC29 families, found in most, possibly all, cell types, not only deliver substrates for nucleotide synthesis [for review, see Young (2016)], but have become targets for nucleoside-derived drugs used, among others, in the treatment of solid tumors (Pastor-Anglada and Perez-Torras, 2015).

Quickly proliferating cancer cells demand also a supply of amino acids, not only the essential ones. Amino acids are necessary for protein synthesis but also for some other processes, as *de novo* biosynthesis of nucleotides, indispensable in energy metabolism and nucleic acids synthesis, as well as in signal transduction. Glutamine and aspartate are the substrates for *de novo* 6-steps synthesis of pyrimidine nucleotide uridine 5′-monophosphate (UMP) and, after formation of UTP, glutamine is an amino group donor for formation cytidine nucleotide by CTP synthase. A 10-steps buildup of purine nucleotide ring demands glutamine, glycine and aspartate, as carbon donors, beside ATP and N^{10}-formyl H_4-folate (tetrahydrofolate). This leads to formation of inosine 5′-monophoshate, a precursor of GMP and ATP, whose formation demands presence of glutamine and aspartate, respectively. Amino acids are also necessary for tetrahydrofolate metabolism as C1 unit donors: serine and histidine are necessary to form methylene tetrahydrofolate or methenyl tetrahydropholate, respectively. Last, but not least, glutamine, after conversion to glutamic acid is a precursor of non-essential amino acids [for review, see Wise and Thompson (2010)]. Studies with use of ^{13}C NMR spectroscopy demonstrated another role of glutamine, namely its high rate metabolism in transformed cells. It has been observed that glutamine contributes to ATP production through conversion to glutamate and α-ketoglutarate (Scalise et al., 2017). Since glutamine uptake in cancer cells exceeds its incorporation to proteins in cancer, its metabolism has been studied in more detail. The tracer studies with [U-^{13}C, U-^{15}N] L-glutamine showed that it is metabolized in mitochondria and through glutamate and α-ketoglutarate forms fumarate and malate. A part of malate is converted to oxaloacetate and citrate in the TCA reactions. Another part of malate is exported to cytoplasm and is converted to pyruvate by malic enzyme 1 (Murai et al., 2017). This reaction generates NADPH, pyruvate and CO_2. Citrate exported from mitochondria is a donor of acetyl moiety due to citrate lyase reaction, which produces malate as well [for review, see Wise and Thompson (2010)]. Since both NADPH and citrate formed in the tricarboxylic acid cycle, as a donor of acetyl moiety, are necessary for fatty acid synthesis, glutamine metabolism could lead to augmented membrane synthesis, necessary for cell growth and proliferation. Moreover, it should be added, that another amino acid – serine is a precursor of ethanolamine and choline necessary for the synthesis of phospholipids.

The augmented anabolic processes and the important function of abovementioned amino acids in growth and proliferation result in up-regulation of several amino acid transporters in cancer. They comprise exchangers SLC7A5 (LAT1), SLC7A11 (xCT), SLC1A5 (ASCT2) and a protein catalyzing a net amino acid uptake SLC6A14 ($ATB^{0,+}$) [for review, see Bhutia et al. (2015)].

SLC7A5 (LAT1), highly expressed in many, although not all, cancers (Fuchs and Bode, 2005; Kaira et al., 2008) transports mainly essential amino acids, is specific toward branched-chain- and bulky amino acids and the influx of one substrate is coupled with removal of another amino acid from the cell. SLC1A5, whose historic name ASCT2 comes from alanine, serine and cysteine catalyzes an inward transport of Ala, Val, Met and bidirectional transport of Ser, Thr, Asn, and Gln, while Cys was shown to trigger the efflux reaction, without being transported itself (Scalise et al., 2015). Although the transport is electroneutral, it is coupled with Na^+ in both directions. It was proposed that the activities of both transporters are coupled: SLC1A5 transports glutamine to the cell in an exchange reaction, while efflux of glutamine is catalyzed by SLC7A5 in an exchange with leucine entering the cell (Scalise et al., 2016). However, the measurements of [^{3}H]His transport by LAT1 reconstituted in proteoliposomes showed almost complete inhibition by hydrophobic amino acids Ile, Val, Leu, Cys, Met, while Phe and Ala inhibited His transport to much lower extent. Inhibition by Gln was below 50%, pointing to much lower affinity of SLC7A5 for glutamine (Napolitano et al., 2015). Amino acids, including leucine and glutamine, are necessary for cell growth and proliferation, processes augmented in cancer cells and controlled by mechanistic target of rapamycin (mTOR) regulating cell growth, what leads to protein translation and macrophagy inhibition (Nicklin et al., 2009; Efeyan et al., 2015; Duval et al., 2018). SLC7A11 (xCT) catalyzes uptake of cystine in an exchange with glutamate and, through formation of cysteine, increases the level of glutathione in the cell, protecting the cell from oxidative stress (Lewerenz et al., 2013).

What is interesting, the expression of genes coding these three transporters is regulated by oncogenic transcription factor c-Myc (Hayashi et al., 2012; Bhutia et al., 2015; Wang and Holst, 2015; Grzes et al., 2017; White et al., 2017; Zhao et al., 2019).

SLC6A14 – A Transporter With Broad Substrate Specificity

SLC6A14 is coding a plasma membrane transporter called system $B^{0,+}$ (amino acid transporter $ATB^{0,+}$) specific toward neutral (index "0") and basic (index "+") amino acids. On the contrary to the amino acid exchangers mentioned above, it transports one molecule of amino acid in a symport with 2 Na^+ and 1 Cl^-, using as well the transmembrane potential (Sloan and Mager, 1999).

As presented in **Table 1**, $ATB^{0,+}$ is a member of SLC6 family of neurotransmitter, osmolyte and amino acid transporters, comprising 4 subfamilies: (i) osmolyte, creatine, GABA transporters, (ii) monoamine neurotransmitter transporters, (iii) amino acid transporters (I), and (iv) amino acid transporters (II) [for review, see Broer and Gether (2012)]. The majority of these transporters were cloned at early 90-ties, especially neurotransmitter transporters. All of them demand Na^+ and, with the exception of SLC6A15 and SLC6A19, also Cl^-.

Additionally, the SLC6A4 after translocation of serotonin, Na^+ and Cl^- to the cell, translocates K^+ outside (Gu et al., 1994).

SLC6A14 was cloned in 1999 from human mammary gland cDNA (Sloan and Mager, 1999). Its gene is located at chromosome X (Xq23) with the current location

TABLE 1 | Transporters from SLC6 family.

Transporter	Main substrate(s)	Cotransported ions	References
GABA, osmolyte, creatine transporters:			
SLC6A1/GAT1	GABA	$2Na^+$, 1C1-	Nelson et al., 1990; Pantanowitz et al., 1993
SLC6A6/TauT	taurine, p-alanine	$2Na^+$, 1C1-	Liu et al., 1992a; Ramamoorthy et al., 1994
SLC6A8/CTI/CreaTI	creatine	$2Na^+$, 1C1-	Dai et al., 1999; Nash et al., 1994
SLC6A10/CT2/CreaT2	creatine	$2Na^+$, 1C1-*	Iyer et al., 1996; Xu et al., 1997
SLC6A11/GAT3	GABA	$2Na^+$, 1C1-	Borden et al., 1994; Clark and Amara, 1994; Karakossian et al., 2005; Liu et al., 1993b
SLC6A12/BGT1	betaine/GABA	$3Na^+$, 1C1-	Lopez-Corcuera et al., 1992; Yamauchi et al., 1992
SLC6A13/GAT2	GABA	$2Na^+$, 1C1-	Borden et al., 1994; Liu et al., 1993b
Monoamine neurotransmitter transporters:			
SLC6A2/NET	norepinephrine, dopamine	INa^+, 1C1-	Gu et al., 1994; Gu et al., 1996; Pacholczyk et al., 1991
SLC6A3/DAT	dopamine	$2Na^+$, 1C1-	Gu et al., 1994; Shimada et al., 1991
SLC6A4/SERT	serotonin	$1Na^+$, $1Cl^-$, $1K^+$	Gu et al., 1994; Hoffman et al., 1991
Amino acid transporters (I):			
SLC6A5/GlyT2	glycine	$3Na^+$, 1C1-	Liu et al., 1993a; Roux and Supplisson, 2000
SLC6A7/PROT	proline	$2Na^+$, 1C1-	Fremeau et al., 1992; Galli et al., 1999
SLC6A9/GlyTI	glycine	$2Na^+$, 1C1-	Liu et al., 1992b; Roux and Supplisson, 2000
SLC6A14/$ATB^{0,+}$	neutral, cationic amino acids	$2Na^+$, 1C1-	Nakanishi et al., 2001; Sloan and Mager, 1999
Amino acid/nutrient transporters (II):			
SLC6A15/B°AT2	large, neutral amino acids	INa^+	Broer et al., 2006
SLC6A16/NTT5	unknown orphan		
SLC6A17/NTT4	neutral amino acids	INa^+	Parra et al., 2008; Zaia and Reimer, 2009
SLC6A18/B°AT3	neutral amino acids	$2Na^+$, 1C1-	
SLC6A19/B°AT1	neutral amino acids	INa^+	Broer et al., 2004
SLC6A20/SIT1/ system IMINO	proline, pipecolate, sarcosine	$2Na^+$, 1 Cl^-	Kowalczuk et al., 2005; Takanaga et al., 2005

*GABA, γ-aminobutyric acid; *, stoichiometry not determined.*

116436606.116461458 (NC_000023.11). It contains 14 exons (each about 100–200 base pairs in length), coding a 642 amino acid protein. Hydrophobicity prediction of this protein suggested 12 putative transmembrane domains with both N- and C-termini localized intracellularly. Such topology, at least with the C-terminus localized at the cytoplasmic side was confirmed with the overexpressed transporter with a C-terminally added tag (3xFLAG), since the transporter was not detected in non-permeabilized cells, while the immunofluorescence signal of anti-FLAG antibody was detected after permeabilization (Samluk et al., 2012). SLC6A14 was not crystallized, anyhow, it has been predicted to have a core structure of the bacterial LeuT transporter (Yamashita et al., 2005). Recently, however, the structural model was proposed using a chimeric model based on the crystal structure of *Drosophila* DAT and the structure of phosphofructokinase from *S. cerevisiae*, as a model for the second extracellular loop (Palazzolo et al., 2019). Using the molecular dynamics simulation and a molecular docking procedure with SLC6A14 substrates, the authors presented a model with 2 binding sites for substrates/inhibitor (S1 and S2) and co-transported ions (Na1 and Na2). They defined several amino acid residues in binding of particular amino acids with Try52, Gly57, Val 128, Ser322 composing an ensemble orienting the substrates. They also proposed Tyr321 at the bottom of S2 site to be involved in gating, while Arg104 and Asp479 define the S1 binding site.

Possibility of several post-translational modifications was predicted from amino acid sequence (Sloan and Mager, 1999).

Phosphorylation by protein kinase C (PKC) has been proven experimentally, moreover, activation of this kinase with phorbol ester augmented level of phosphoserine in $ATB^{0,+}$, a process reversed by PKC inhibitor bis-indolylmaleimide (Samluk et al., 2010, 2012). Phorbol ester treatment resulted as well in a shift of pI of $ATB^{0,+}$ in 2-D electrophoresis (Czeredys et al., 2013). It should be noted that, as demonstrated in experiments using biotinylation of surface proteins, activation of PKC was correlated with an increase of the transporter in the plasma membrane and with the increase of leucine uptake (Samluk et al., 2010, 2012). The observed sensitivity of $ATB^{0,+}$, to phorbol ester treatment suggested an involvement of classical and/or novel isoform of PKC (Newton, 1995) and co-precipitation experiments and immunofluorescence analysis demonstrated an interaction of $ATB^{0,+}$ with the isoform α of PKC (Samluk et al., 2012). Sloan and Mager (1999) predicted also seven possible glycosylation

sites on the second putative extracellular loop and one on the third putative extracellular loop. In a model structure of LeuT bacterial transporter glycosylation sites were found at the second extracellular loop, a localization confirmed by crystallization of SERT in which N-acetylglucoseamine electron density were found to be linked to Asn moieties of the second extracellular loop (Coleman et al., 2016). As shown by Kovalchuk et al. (2019), $ATB^{0,+}$ overexpressed in HEK293 cells was sensitive to deglycosylating enzymes: peptide-N^4-(acetyl-β-glucosaminyl)-asparagine amidase (PNGase F, EC 3.5.1.52) and endoglycosidase (Endo H, EC 3.2.1.96), confirming the presence of glycosylated form of the transporter in the plasma membrane.

SLC6A14 was shown to be expressed in lung, trachea, salivary gland and also in stomach, mammary gland and in hippocampus (Sloan and Mager, 1999). At the protein level SLC6A14 was detected in colonic epithelium apical membrane (Ahmadi et al., 2018), at the apical membrane of brain capillary endothelial cells forming the blood-brain barrier (Michalec et al., 2014) and in cultured astrocytes (Samluk et al., 2010). It was also detected in rabbit corneal epithelium (Jain-Vakkalagadda et al., 2004).

SLC6A14 with its broad substrate specificity has the highest affinity (K_m below 50 μM) for non-polar amino acids Ileu, Leu, Met, Val, and for Ser (Sloan and Mager, 1999). It was as well shown to transport several D-amino acids, such as D-Ser, D-Ala, D-Met, D-Leu and D-Trp (Hatanaka et al., 2002). This can explain the important physiological role of this transporter present in the colon in absorption of amino acids (Ugawa et al., 2001), including the bacteria-derived D-amino acids, in particular D-Ser, known to be an important modulator of N-methyl-D-aspartate (NMDA) receptors in the brain (Matsui et al., 1995). Although D-Ser is synthesized by glial cells (Wolosker et al., 1999), an additional transport of this amino acid by SLC6A14 present in the blood-brain barrier (Michalec et al., 2014) can lead to its increased level in the brain. SLC6A14 was also shown to transport non-proteinogenic amino acids. In the ileum and colon it transports β-alanine (Anderson et al., 2008), a component of the dipeptide carnosine (β-alanine-L-histidine) found in skeletal muscles (Harris et al., 2006). It transports as well L-carnitine (Nakanishi et al., 2001), a compound necessary for transfer of fatty acid acyl moieties to mitochondria, where they undergo β-oxidation [for reviews, see Kerner and Hoppel (2000), Juraszek and Nalecz (2020)]. Although SLC6A14 transports carnitine with a very low affinity in comparison with an ubiquitously expressed high affinity carnitine transporter SLC22A5 (OCTN2), it can partially rescue carnitine supply in case of *SLC22A5* mutations. Such a case was observed in not changed carnitine accumulation in the brain in a mouse strain with functionally defective OCTN2 (Kido et al., 2001). SLC6A14 was also proposed to take over the defective OCTN2 and to mediate transport of butyryl-L carnitine, a compound used for treatment of ulcerative colitis (Srinivas et al., 2007).

Although acidic amino acids are not the substrates of SLC6A14, the β-carboxyl derivatives of aspartate and γ-carboxyl derivatives of glutamate were shown by electrophysiological methods to be transported (Hatanaka et al., 2004). Also the valyl esters of acyclovir and ganciclovir were shown to be transported by overexpressed SLC6A14 (Hatanaka et al., 2004; Umapathy et al., 2004), what indicates a potential role of this transporter as a target for delivery of amino acid-based drugs and prodrugs [for review, see Ganapathy and Ganapathy (2005)]. Moreover, SLC6A14 transports as well the side chain hydroxyl group esters of Ser and Thr (Ganapathy and Ganapathy, 2005) and it was shown to transport zwitterionic or cationic inhibitors of nitric oxide synthase (Hatanaka et al., 2001).

Physiological Consequences of SLC6A14 Malfunction

As mentioned above, SLC6A14 ($ATB^{0,+}$) is expressed in colon, where it can absorb amino acids from intestinal content, including the D-isomers (Ugawa et al., 2001). The levels of *SLC6A14* mRNA are higher in colonal mucosal specimens from patients with Crohn's disease, when compared to control samples (Eriksson et al., 2008).

SLC6A14 ($ATB^{0,+}$) is expressed in mammalian blastocysts in species (mouse, rat, human) in which blastocysts undergo the implantation stage with the penetration to uterine epithelium (Schlafke and Enders, 1975), a process regulated by 4-hydroxy-17β-estradiol and $β_1$ integrins (Schultz et al., 1997; Paria et al., 1998). It was shown that trophoblast motility was triggered by uptake of leucine through mTOR and polyamine signaling about 20 h before implantation and that activity of $ATB^{0,+}$ was suppressed by uterine environment 12–25 h after estrogen administration (Van Winkle et al., 2006). Therefore, SLC6A14 was proposed to regulate trophoblast motility and to protect blastocysts from immunological rejection and, through supply of amino acids, to influence embryo nutrition and birth weight (Van Winkle et al., 2006). Of note, undernutrition of embryo is correlated with an increased risk of developing obesity. Interestingly, single nucleotide polymorphism (SNP) in the 3′-untranslated region of *SLC6A14* gene was associated with obesity of Finnish population (Suviolahti et al., 2003; Tiwari and Allison, 2003). SNPs in *SLC6A14* were also detected in obese French Caucasians (Durand et al., 2004). It was proposed that this association with obesity resulted from availability of a SLC6A14 substrate – Trp, a precursor of serotonin, which controls appetite (Suviolahti et al., 2003). Another study correlated SNPs in *SLC6A14* gene with susceptibility to male infertility/subfertility in Macedonian/and Slovenian populations (Noveski et al., 2014), a phenomenon proposed to depend as well on availability of Trp and serotonin, associated with testosterone synthesis (Tinajero et al., 1993).

SLC6A14 has been also proposed (Ruffin et al., 2020) to modify the phenotype of cystic fibrosis (CF) – a fatal genetic disorder caused by mutations in the Cystic Fibrosis Transmembrane Conductance Regulator (*CFTR*) gene (Riordan et al., 1989; Rommens et al., 1989). Genome-wide analysis of CF patients from France and North America associated SNPs in *SLC6A14* and *SLC26A9* genes (Sun et al., 2012), the latter one coding the Cl^-/CO_3^{2-} exchanger. The authors proposed that variations in these transporters under conditions of loss of CFTR function can be associated with meconium ileus – a severe intestine obstruction at birth, which occurs in 15% of CF patients. Ahmadi et al. (2018) showed in CF-mice model that

disruption of *Slc6a14* inhibited by 75% transport of arginine, what worsened fluid secretion in colonic epithelium and affected nitric oxide →cGMP → protein kinase G (PKG) - mediated regulation of CFTR.

SLC6A14 and Cancer

Expression of *SLC6A14* gene is significantly increased in several human cancer cell lines as well as in patients samples, in particular from solid tumors. The analysis of Cancer Genome Atlas (ACGA) database shows its upregulation in 12 different tumors with the greatest upregulation in pancreatic, cervical and colorectal cancer (Sikder et al., 2017).

RNA sequencing applied to examine expression of genes in the paraffin-embedded tissues of patients with low– and high-grade squamous intraepithelial lesions and compared with the normal cervical epithelium detected *SLC6A14* among differentially expressed and upregulated genes (Royse et al., 2014). Use of commercial array of cDNA from squamous cell carcinoma patients and control normal tissues, as well as the fluorescence studies of cancer specimens demonstrated almost 6-fold upregulation of SLC6A14 at mRNA and protein level in cancer samples (Gupta et al., 2006). Of note, the transporter was observed to co-localize with inducible nitric oxide synthase (iNOS), also upregulated in cervix cancer. Since high levels of nitric oxide (NO) lead to apoptosis and have been associated with protumorigenic effects, SLC6A14 capable of transporting NOS inhibitors could become a therapeutic target through decreasing NO formation. Interestingly, an increase of iNOS was also detected in colorectal cancer samples (Gupta et al., 2005). Semi-quantitative RT-PCR analysis demonstrated about 20-fold increase of $ATB^{0,+}$ mRNA in surgical specimen of patients with colorectal cancer, as well as in metastases in liver and lymph node. Moreover, both transcripts resulting from alternative splicing increased in cancer cells. The increase of SLC6A14 was also detected at protein level what suggests a pathogenic role of the transporter in colorectal cancer (Gupta et al., 2005). Recently, the upregulation of SLC6A14 was reported in most human colon cancer cell lines and in a majority of patient-derived xenografts (Sikder et al., 2020). The deletion of Slc6a14 protected mice from colon cancer, while it's silencing or blocking with its specific blocker - α-methyltryptophan (α-MT) (Karunakaran et al., 2008) led to a reduced tumor growth and suppressed proliferation due to autophagy and apoptosis. Wnt signaling was reported to be involved in cancer progression, since SLC6A14 expression was shown to be reduced by silencing of β-catenin with shRNA and incubation of cancer cells with Wnt antagonist, while an opposite effect was observed after Wnt agonist treatment and β - catenin overexpression (Sikder et al., 2020). Transcription factor TCF4 (T-cell factor 4) is known to be indispensable for tumor initiation (Hrckulak et al., 2018) and TCF4/β-catenin transcriptional activity mediated by Wnt signaling was proposed to control upregulation of SLC6A14 in colon cancer. This was confirmed by binding of TCF4/β-catenin to promoter of *SLC6A14*, in which four TCF4 binding motifs were found by nucleotide blast (Sikder et al., 2020).

SLC6A14 was also detected by next generation sequencing in a lymph-node negative subtype of prostate cancer, in one of the most widely represented subtype with the expression of the fusion transcript *TMPRSS2-ERG*, associated with unfavorable survival prognosis (Pudova et al., 2019).

On the contrary to the above-mentioned cancers the transcriptome profiling of biopsies from patients with ulcerative colitis showed that SLC6A14 was among the top 10 downregulated genes (Low et al., 2019).

Karunakaran et al. (2011) showed upregulation of SLC6A14 in estrogen receptor–positive breast cancer tissues and breast cancer cell lines. They found several putative estrogen receptor-binding sites in the *SLC6A14* promoter and confirmed the promoter activity after estradiol treatment with luciferase as reporter. Estradiol treatment increased *SLC6A14* expression in estrogen receptor-positive cell line, while anti-estrogens treatment with tamoxifen reversed this effect (Karunakaran et al., 2011). Treatment of MCF7 - an estrogen receptor-positive cell line with α-MT - a selective blocker of the transporter (Karunakaran et al., 2008) led to amino acid deprivation and induced autophagy, while co-treatment with autophagy inhibitor led to apoptosis and cell death. These phenomena were not detected in SLC6A14 negative cells and the involvement of SLC6A14 was further confirmed by silencing its gene. Moreover, in the mouse xenograft studies administration of *a*-MT reduced tumor volume in case of estrogen receptor-positive cancer cells (Karunakaran et al., 2011). When the *Slc6a14* KO mice were crossed with model mouse lines developing a spontaneous breast cancer, the development of tumor was significantly delayed and its growth was decreased on $Slc6a15^{-}/^{-}$ background. Deletion of *Slc6a14* resulted in amino acid deficiency what led to a decrease in mTOR phosphorylation and attenuated expression of genes controlled by HIF1α signaling (Babu et al., 2015). It should be noted, however, that although the majority of breast tumors are estrogen receptor α positive, about 40% of patients acquire resistance to endocrine therapy, affecting either the estrogen receptor itself or the conversion of androgens to estrogens. A global transcription analysis reveals downregulation of *SLC6A14* and an enhanced expression of miR-23b-3p in endocrine therapy resistant breast cancers, what correlates with a prosurvival autophagy and a selective upregulation of *SLC1A2* and results in an increased uptake of Glu and Asp (Bacci et al., 2019). It should be added that miR-23b-3p expression is upregulated by a transcription factor GATA2, reported to promote progression of breast cancer (Wang et al., 2012). Also 4 other miRNA were predicted to regulate SLC6A14 in cancer, their role, however, has to be investigated (Sikder et al., 2017).

Gene expression omnibus database analysis showed 13- to 163-fold increase of *SLC6A14* expression in pancreatic tumors, when compared with normal pancreatic tissue, an increase much higher than the increase of expression of other amino acid transporters: *SLC1A5, SLC7A5, SLC7A11* (Coothankandaswamy et al., 2016). Moreover this upregulation was also confirmed at protein level in a tissue microarray and immunofluorescence quantification (Coothankandaswamy et al., 2016). Many tumors can be detected by imaging techniques such as magnetic resonance imaging or computer tomography, the techniques not sensitive enough to detect the early stages of pancreatic ductal adenocarcinoma, in particular in diffusely infiltrating

subgroup of tumors, so finding the diagnostic markers is of high importance. Taking into account the previous reports on functional imaging of sodium iodine symporter in thyroid cancer as well as use of ^{18}FDG PET (^{18}Fdeoxyglucose positron tomography) imaging to trace the SLC2A1 (GLUT) level known to be upregulated in many cancers, (Penheiter et al., 2015) performed a transcriptomic analysis of in human pancreatic ductal adenocarcinoma samples obtained by laser capture microdissection. The microarray and RNAseq showed 15 SLC transporters being overexpressed when compared with the normal tissue; among them (apart from glucose transporter SLC2A1) lactate transporter SLC16A3 and SLC6A14, which was overexpressed at least 2-fold in cancer patients. This increase in mRNA was further confirmed at protein level and more than 75% of tumor cells were stained with anti-SLC6A14 antibody (Penheiter et al., 2015). Interestingly, the transporter was predominantly detected in the cytoplasm. Based on the data from Protein Atlas[2] survival prognosis at either low or high *SLC6A14* expression level was found prognostic for pancreatic cancer, being unfavorable at high SLC6A14 expression (**Table 2**), although the cohorts were relatively small. Another study using an integrated microarray analysis of differentially expressed genes detected 596 upregulated and 540 downregulated genes in pancreatic cancer, when compared with non-tumor control (Yang et al., 2020). *SLC6A14* was found among possible diagnostic and prognostic genes, together with *AHNAK2, CDH3, IFI27, ITGA2, LAMB3*, *and TMPRSS4*. The upregulated genes were annotated to such processes as cell proliferation, apotosis, protein binding and the analysis of enriched genes showed involvement in pancreatic secretion and p53 signaling, MAPK signaling and insulin signaling pathways (Yang et al., 2020).

Another study (Cheng et al., 2019) analyzing differentially expressed genes in pancreatic cancer also detected *SLC6A14* among the top ten upregulated genes and survival analysis of seven of these genes (*TMPRSS4, SERPINB5, SCEL SCL6A14, TMC7, SLC2A1, CENPF*) is associated with patient poor prognosis. The higher expression of these genes was confirmed at protein level with tissue microarray chips and detection with the corresponding antibodies. The retrospective clinical study showed that patients with high level of these genes had significantly shorter survival time. Further experiments with pancreatic cancer cell lines treated with shRNA showed that *SLC6A14* knock-down decreased the invasion of cancer cells, as measured in the transwell assay (Cheng et al., 2019).

This upregulation of *SLC6A14* in pancreatic cancer makes it not only a good candidate as a marker but may make it a drugable target. Experiments performed with pancreatic cancer cells characterized by various *SLC6A14* expression level showed that treatment with α - MT - SLC6A14 blocker, led to amino acid starvation of cells with high SLC6A14. This was not observed in normal pancreatic cell lines. Moreover, blocking of the transporter in the cells with its high expression promoted formation of autophagosomes, suppression of mechanistic target of rapamycin complex 1 (mTORC1) signaling and reduction of migration and invasive properties. α-MT treatment also reduced hypoxia-inducible factor 1α (HIF-1α), usually overexpressed under hypoxic condition of a tumor. Silencing of SLC6A14 with shRNA led also to a decrease in transport of glycine, one of the SLC6A14 substrates. The same authors verified the effect of α-MT treatment in pancreatic cancer cells in mouse xenographs. A marked reduction of tumor growth was observed when α-MT was administered before injection of tumor cells and the treatment was continued, while tumors stopped growing, when α-MT was administered after tumor had grown. A reduction of tumor growth was also observed in xenographs obtained with cancer cells, in which SLC6A14 was knocked-down (Coothankandaswamy et al., 2016). These experiments demonstrated in an elegant way that α-MT can be a pharmacological tool used in tumors with a high SLC6A14 level.

It has to be added that α-MT is a blocker of SLC6A14, while 1-methyltryptophan is a transportable substrate (Karunakaran et al., 2008). 1-Methyltryptophan is used as a pharmacological inhibitor of indoleamine 2,3-dioxygenase (Cady and Sono, 1991), a cytosolic enzyme, whose inhibition activates immune system leading to killing of cancer cells (Hou et al., 2007). So SLC6A14 can be a target in cancer treatment, either by blocking the transporter with α-MT, what results in an arrest of cells at G_1/G_0 stage, amino acid deprivation and autophagy, or by affecting tumor-associated immune cells (Karunakaran et al., 2008, 2011).

SLC6A14 can be used as a target for prodrugs, since it accepts esters of hydroxyl group of serine, threonine and tyrosine (Bhutia et al., 2014), as well as drugs conjugated with glutamate and aspartate, such as valacyclovir and valganciclovir (Hatanaka et al., 2004; Umapathy et al., 2004). Beside the abovementioned compounds, the conjugates of acyclovir, ganciclovir irinotecan have been proposed as prodrugs in anti-cancer therapy (Scalise et al., 2020), while butyryl-L-carnitine was proposed for treatment of gut inflammation (Srinivas et al., 2007).

SLC6A14 can be also used as a target for liposomal drug delivery. Aspartate polyoxyethylene stearate conjugate covered liposomes targeting SLC6A14 transporter were shown to increase efficiency of encapsulated docetaxel delivery to human lung cells (Luo et al., 2017). Another study showed that binding of lysine conjugated liposomes to breast cancer MCF7 cells was higher than that of bare liposomes, a process inhibited by α-MT. The further internalization by endocytosis allowed delivery of gemcitabine (chemotherapeutic used in pancreatic cancer treatment) leading to cytotoxicity and, although the transporter is partly degraded, it recovers after some time (Kou et al., 2020). This may lead to novel strategy in nanodelivery of drugs to cancer cells.

It is worth noting that SLC6A14 activity can be detected by a non-invasive method using the cationic amino acid O-2(2-[^{18}F]fluoroethyl)methyl-amino)ethyltyrosine in PET (Muller et al., 2014).

Regulation of SLC6A14

Presence of any plasma membrane transporter at the cell surface, a *sine qua non-condition* of its function, can be regulated at several steps, as transcription of its gene, regulation of translation and trafficking in vesicles to the plasma membrane. Moreover, localization and activity can be regulated by post-translational

[2]https://www.proteinatlas.org/ENSG00000268104-SLC6A14/pathology

TABLE 2 | Analysis of cancer patient survival correlated to *SLC6A14* expression.

Cancer Type	Prognosis	p Value	% 5-year survival		n		FPKM Best cut off	Median Expression
			High	Low	High	Low		
Glioma	Not prognostic	0.0017	0*	11*	33	120	0.01	0
Thyroid	Not prognostic	0.17	92	93	159	342	0.53	0.17
Lung	Not prognostic	0.037	37	50	431	563	7.39	5.56
Colorectal	Not prognostic	0.085	81	57	128	469	5.2	1.71
Head and Neck	Not prognostic	0.015	48	38	398	101	0.4	2.46
Stomach	Not prognostic	0.039	35	34	270	84	1.11	4.57
Liver	Not prognostic	0.0074	42	50	93	272	0.02	0
Pancreatic	Prognostic, high expression							
	Unfavorable	0.00097	16	45	107	69	6.08	8.92
Urothelial	Not prognostic	0.16	38	43	126	280	0.65	0.23
Prostate	Not prognostic	0.013	100	96	233	261	1.27	1.12
Testis	Not prognostic	0.021	100	94	77	57	0.02	0.03
Breast	Not prognostic	0.031	83	80	508	567	0.29	0.26
Cervical	Not prognostic	0.036	61	72	178	113	2.17	4.08
Endometrial	Not prognostic	0.0010	81	63	392	144	0.07	0.38
Ovarian	Not prognostic	0.018	35	22	291	82	0.01	0.03
Melanoma	Not prognostic	0.27	36*	26*	28	74	0.56	0.04

*The data from Protein Atlas (https://www.proteinatlas.org/ENSG00000268104-SLC6A14/pathology). FPKM, Fragments per Kilobase of exon per Million reads. * 3-year survival.*

modifications. As mentioned above, transcription of *SLC6A14* can be regulated by estrogen receptor (Karunakaran et al., 2011) and by TCF4 transcription factor (Sikder et al., 2020). It has to be, however, emphasized, that the prognosis in various types of cancer was based on the mRNA level, what does not fully correlate with the amount of protein, in particular presence in the plasma membrane what is necessary for transporter function.

As any hydrophobic plasma membrane protein, SLC6A14 is inserted to the membrane of endoplasmic reticulum (ER) co-translationally. On the contrary to secreted proteins, it does not have a signal sequence, cleaved later-on[3]. The first transmembrane domain of α-helical structure, formed already within the ribosomal tunnel (Martinez-Gil et al., 2011; Park and Rapoport, 2012; Gogala et al., 2014), is inserted to the ER membrane bilayer by a lateral movement from a proteinaceous channel (Martinez-Gil et al., 2011; Park and Rapoport, 2012), followed by insertion of the other transmembrane helices. The proper folding of any transmembrane protein is strictly controlled. The first steps of glycosylation, so called core-glycosylation, take place in the ER lumen: The initial N-glycan: $Glc_3Man_9GlcNAc_2$ (Glc – glucose, Man – mannose, GlcNAc – N-acetylglucosamine) is transferred to a nascent polypeptide from dolichol phosphate linked precursor and, after trimming two glucose residues (Moremen et al., 2012) undergoes a quality check, by two lectin chaperons acting in the ER lumen: soluble calretinin and membrane bound calnexin (Lederkremer, 2009; Chevet et al., 2010). As shown by Kovalchuk et al. (2019), SLC6A14 co-localizes with calnexin, moreover, the core-glycosylated species of the transporter, characterized by lower M_r than the fully glycosylated one can be detected by Western blot. Inhibition of SLC6A14 exit from ER results in accumulation of core-glycosylated transporter and directs the protein to ER-associated protein degradation (ERAD) (Kovalchuk et al., 2019). The further glycosylation steps take place in Golgi apparatus and lead to fully glycosylated protein (Moremen et al., 2012) which from *trans*-Golgi is trafficked in the vesicles to the plasma membrane.

Apart from the folding control on the luminal side, more and more information is emerging about control of transmembrane proteins at the cytoplasmic side of the ER membrane. As shown previously for adenosine receptor (Keuerleber et al., 2011; Bergmayr et al., 2013) and serotonin transporter (El-Kasaby et al., 2014), the heat shock proteins (HSPs) are involved in the proper folding of the cytoplasmic domain of several plasma membrane proteins. HSPs are highly expressed in various cancers promoting cell survival [for reviews, see Murphy (2013), Lianos et al. (2015)]. HSP70 (HSPA14) and HSP90beta were detected in SLC6A14 proteome and their inhibition with VER155008 and radicicol, respectively led to decreased level of the transporter in the plasma membrane, as assayed by cell surface biotinylation (Rogala-Koziarska et al., 2019; **Figure 1**). Treatment with HSPs inhibitors attenuated their interaction with SLC6A14 and directed the transporter to endoplasmic reticulum associated degradation (ERAD), a process reversed by proteasome inhibitor bortezomib. Inhibition of HSP70 and HSP90 decreased the amount of SLC6A14 not only after its overexpression, but

[3]http://sigpep.services.came.sbg.ac.at/results/tempxUDJjT/signalblast.html

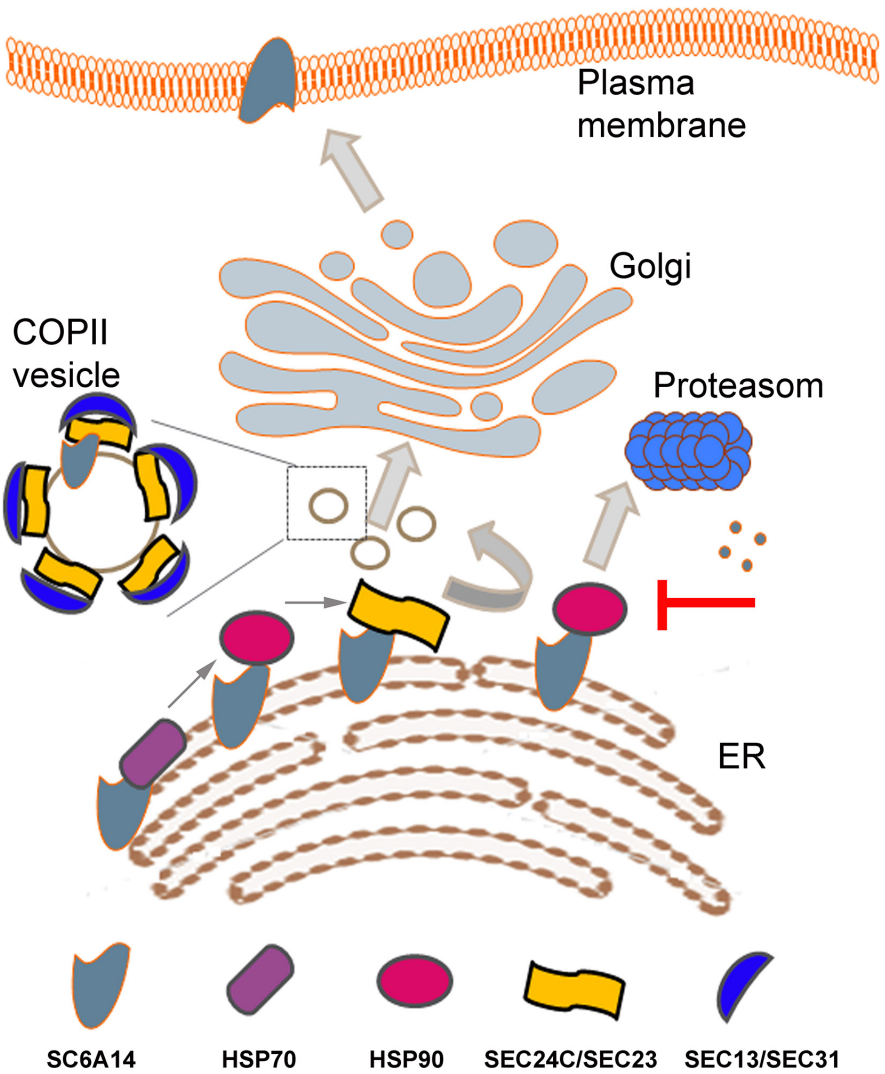

FIGURE 1 | Schematic presentation of SLC6A14 trafficking from endoplasmic reticulum (ER) to plasma membrane. Sequential binding of HSP70, HSP90 and Sec24C in a SEC24/SEC23 dimer is shown in the left bottom part. Inhibition of HSP90 leads to SLC6A14 proteosomal degradation (right, middle part). Coatomer II (COPII) vesicle is shown as a magnified image when vesicles are trafficking between ER and *cis*-Golgi. Details are described in the text.

also in MCF7 estrogen receptor positive breast cancer cell line (Rogala-Koziarska et al., 2019).

The family of HSP70 proteins prevent aggregation of unfolded or misfolded proteins by binding to stretches of exposed hydrophobic residues and the process of unfolding demands both, ATP and co-chaperons [for review, see Murphy (2013)]. Interestingly, several co-chaperons, such as Q8WXX5 (*DNAJC9*) and P31689 (*DNAJA1*) were detected in proteome of SLC6A14 overexpressed in HEK293 cells (Rogala-Koziarska et al., 2019). HSP70 is known to be overexpressed in cancer and its high expression is correlated with increased tumor grade and poor prognosis, in particular in colon cancer, breast cancer, melanoma and bladder cancer (Lianos et al., 2015). Moreover HSP70 overexpression was shown to be a marker of lymph node metastasis in some cancers, including breast cancer (Lazaris et al., 1997). These effects result from HSP70 inhibition of apoptosis, control of cell senescence and autophagy impairment (Murphy, 2013). HSP70 proteins deliver their client protein to HSP90 and it is worth mentioning that the level of HSP90 is elevated in aggressive breast cancers, what makes it a target, at least for diagnostics (Osada et al., 2017). The level of HSP90 is augmented in several cancers (pancreatic, ovarian, breast, lung, endometrial, oropharyngeal, squamous cell and multiple myeloma), what correlates with decreased apoptosis and promotes tumor cell adhesion, motility metastasis and angiogenesis (Wu et al., 2017), therefore it has become a target in cancer treatment [for review, see Wu et al. (2017)]. Out of HSP90 inhibitors, ganetespib seems to be a promising compound as a therapeutic agent (Jhaveri and Modi, 2015). HSP90 forms dimers through its C-terminal domains, while ATPase domain and client protein binding domain are at N-terminus and middle domain, respectively

(Wu et al., 2017). We were able to demonstrate a direct interaction between SLC6A14 and both HSPs: HSP90beta and HSP70 (HSPA14). Moreover, we measured the HSP90beta ATPase activity and we detected inhibition of this activity by a peptide QRIIKCCRPASNWGPYLEKH from the C-terminus of SLC6A14, what further confirms the involvement of HSP90beta in the control of SLC6A14 conformation and folding (Rogala-Koziarska et al., 2019). These observations led to a conclusion that inhibition of HSPs can diminish the amount of SLC6A14 in the plasma membrane.

Any plasma membrane protein has to leave ER to reach *cis*-Golgi in the vesicles coated by coatomer II (COPII). Formation of COPII starts from converting Sar1 in a GTP-bound form by Sec12, what recruits a heterodimer Sec24/Sec23 and formation of COPII is completed by binding Sec13/Sec31. Sec24 is a cargo recognizing subunit and in humans there are 4 isomers of this protein, named SEC24A-D [for review, see Miller and Schekman (2013)]. Experiments with over-expressed SLC6A14 showed that this transporter interacts exclusively with the SEC24C isoform and co-expression with SEC24C dominant negative mutant resulted in diminution of the transporter level in the plasma membrane (Kovalchuk et al., 2019). It was proposed that, similarly to other members of SLC6 family (Sucic et al., 2013), motif RIIK within SLC6A14 C-terminal part is responsible for interaction with SEC24C (Rogala-Koziarska et al., 2019). Of note, this motif is within the sequence interacting with HSP90 (Rogala-Koziarska et al., 2019). A relay HSP70/HSP90/SEC24 was proposed as a sequence of binding to A(2A)-adenosine receptor (Keuerleber et al., 2011). These observations lead to the conclusion that inhibition of either HSP70 or HSP90 should prevent binding of SLC6A14 to SEC24C, resulting in directing the transporter to proteasomal degradation (Rogala-Koziarska et al., 2019) and, as a consequence, lowering the amount of SLC6A14 in plasma membrane.

Interestingly, the recombinant Sec24C was shown *in vitro* to be phosphorylated by recombinant kinase Akt (Sharpe et al., 2011), moreover, using the antibodies directed against phosphorylated Akt substrates, the same authors showed phosphorylation of overexpressed Sec24C, when the cells were treated with insulin-growth factor, an up-stream AKT activator. They also detected binding of Sec23 to phosphorylated Sec24C. These observations could suggest a facilitated formation of COPII upon AKT activation.

AKT (protein kinase B) is a serine/threonine protein kinase, known to be activated by an up-stream pathway from activated tyrosine kinase receptors, G-protein-coupled receptors, or integrins, what is followed by activation of phosphatidylinositol 3-kinase (PI3K) and phosphorylation of AKT at T^{308} by phosphoinositide-dependent kinase (PDK-1) [for review, see Nicholson and Anderson (2002)]. This activates AKT and leads to phosphorylation of SIN1, a component of the serine/threonine kinase - mammalian target of rapamycin complex 2 (mTOR2), what is followed by phosphorylation of AKT at S^{473}. It should be added that the cell surface receptors are either constitutively active or overexpressed in many human cancers (Harari and Yarden, 2000). Moreover, also the *PKB/AKT* gene was observed to be amplified in several human cancers [see, Nicholson and Anderson (2002)] and AKT pathway is known to be hyperactivated in many types of cancer and dominantly inherited cancer syndromes [for review, see Altomare and Testa (2005)]. It is worth to add that Akt1 deficiency in a mouse model delayed mammary tumor growth and reduced lung metastases (Ju et al., 2007). Active AKT promotes cell survival by phosphorylating proteins regulating apoptotic cascade, just to mention phosphorylation of BAD. AKT is as well involved in the progression of cell cycle, what results in cell proliferation. It phosphorylates complex I of mTOR (mTORC1), thus controlling translation machinery (Broer and Broer, 2017; Thoreen, 2017). Therefore, the cell has a high demand for amino acids, when AKT is active. Although mTORC1 is controlled by a lysosomal amino acid transporter SLC38A9 (Rebsamen et al., 2015; Wang et al., 2015), mTORC2 – a kinase activating AKT (Riaz et al., 2012), conveys the nutrient information from the environment (for review, see Harachi et al., 2018). This suggests that AKT through influence on COPII formation could control transporter exit from ER and its presence in plasma membrane.

CONCLUSION AND FUTURE PERSPECTIVES

Cancer cells are characterized by quick growth and proliferation, demanding a constant supply of nutrients. SLC6A14, being upregulated in many cancers catalyzes a net uptake of all basic and neutral amino acids. In order to fulfill this role, it has to reach the plasma membrane and the first step of trafficking to the cell surface is SLC6A14 exit from ER. This process is promoted by active heat shock proteins HSP70 (HSPA14) and HSP90beta, rescuing the transporter from proteolytic degradation. ER exit of SLC6A14 demands interaction with a component of coatomer II (COPII) – SEC24C, a protein phosphorylated by kinase AKT, known to be hyperactivated in many cancers. Therefore, inhibition of SLC6A14 trafficking before AKT action by inhibition of HSPs seems to be a promising strategy, especially that HSP90 inhibitor – ganetespib has been subjected to phase II clinical trials (Jhaveri and Modi, 2015) in combination with chemotherapeutics used in treatment of several types of cancer. This should lead to a new approach of cancer treatment, for example by inhibiting SLC6A14 with αMT, HSP90 with ganetespib and estrogen receptor with tamoxifen in case of breast cancer.

AUTHOR CONTRIBUTIONS

KN was responsible for conception and writing of this manuscript.

FUNDING

This work was funded with National Science Centre in Poland grant 2018/31/B/NZ3/00669 (KN).

REFERENCES

Ahmadi, S., Xia, S., Wu, Y. S., Di Paola, M., Kissoon, R., Luk, C., et al. (2018). SLC6A14, an amino acid transporter, modifies the primary CF defect in fluid secretion. *eLife* 7:e37963. doi: 10.7554/eLife.37963

Altomare, D. A., and Testa, J. R. (2005). Perturbations of the AKT signaling pathway in human cancer. *Oncogene* 24, 7455–7464. doi: 10.1038/sj.onc.1209085

Anderson, C. M., Ganapathy, V., and Thwaites, D. T. (2008). Human solute carrier SLC6A14 is the beta-alanine carrier. *J. Physiol.* 586, 4061–4067. doi: 10.1113/jphysiol.2008.154500

Babu, E., Bhutia, Y. D., Ramachandran, S., Gnanaprakasam, J. P., Prasad, P. D., Thangaraju, M., et al. (2015). Deletion of the amino acid transporter Slc6a14 suppresses tumour growth in spontaneous mouse models of breast cancer. *Biochem. J.* 469, 17–23. doi: 10.1042/BJ20150437

Bacci, M., Lorito, N., Ippolito, L., Ramazzotti, M., Luti, S., Romagnoli, S., et al. (2019). Reprogramming of amino acid transporters to support aspartate and glutamate dependency sustains endocrine resistance in Breast Cancer. *Cell Rep.* 28, 104.e8–118.e8. doi: 10.1016/j.celrep.2019.06.010

Bergmayr, C., Thurner, P., Keuerleber, S., Kudlacek, O., Nanoff, C., Freissmuth, M., et al. (2013). Recruitment of a cytoplasmic chaperone relay by the A2A adenosine receptor. *J. Biol. Chem.* 288, 28831–28844. doi: 10.1074/jbc.M113.464776

Bhutia, Y. D., Babu, E., Prasad, P. D., and Ganapathy, V. (2014). The amino acid transporter SLC6A14 in cancer and its potential use in chemotherapy. *Asian J. Pharm. Sci.* 9, 293–303. doi: 10.1016/j.ajps.2014.04.004

Bhutia, Y. D., Babu, E., Ramachandran, S., and Ganapathy, V. (2015). Amino Acid transporters in cancer and their relevance to "glutamine addiction": novel targets for the design of a new class of anticancer drugs. *Cancer Res.* 75, 1782–1788. doi: 10.1158/0008-5472.CAN-14-3745

Borden, L. A., Dhar, T. G., Smith, K. E., Branchek, T. A., Gluchowski, C., and Weinshank, R. L. (1994). Cloning of the human homologue of the GABA transporter GAT-3 and identification of a novel inhibitor with selectivity for this site. *Receptors Channels* 2, 207–213.

Broer, A., Klingel, K., Kowalczuk, S., Rasko, J. E., Cavanaugh, J., and Broer, S. (2004). Molecular cloning of mouse amino acid transport system B0, a neutral amino acid transporter related to Hartnup disorder. *J. Biol. Chem.* 279, 24467–24476. doi: 10.1074/jbc.M400904200

Broer, A., Tietze, N., Kowalczuk, S., Chubb, S., Munzinger, M., Bak, L. K., et al. (2006). The orphan transporter v7-3 (slc6a15) is a Na+-dependent neutral amino acid transporter (B0AT2). *Biochem. J.* 393, 421–430. doi: 10.1042/BJ20051273

Broer, S., and Broer, A. (2017). Amino acid homeostasis and signalling in mammalian cells and organisms. *Biochem. J.* 474, 1935–1963. doi: 10.1042/BCJ20160822

Broer, S., and Gether, U. (2012). The solute carrier 6 family of transporters. *Brit. J. Pharmacol.* 167, 256–278. doi: 10.1111/j.1476-5381.2012.01975.x

Cady, S. G., and Sono, M. (1991). 1-Methyl-DL-tryptophan, beta-(3-benzofuranyl)-DL-alanine (the oxygen analog of tryptophan), and beta-[3-benzo(b)thienyl]-DL-alanine (the sulfur analog of tryptophan) are competitive inhibitors for indoleamine 2,3-dioxygenase. *Arch. Biochem. Biophys.* 291, 326–333. doi: 10.1016/0003-9861(91)90142-6

Cheng, Y., Wang, K., Geng, L., Sun, J., Xu, W., Liu, D., et al. (2019). Identification of candidate diagnostic and prognostic biomarkers for pancreatic carcinoma. *EBioMedicine* 40, 382–393. doi: 10.1016/j.ebiom.2019.01.003

Chevet, E., Smirle, J., Cameron, P. H., Thomas, D. Y., and Bergeron, J. J. (2010). Calnexin phosphorylation: linking cytoplasmic signalling to endoplasmic reticulum lumenal functions. *Semin. Cell Dev. Biol.* 21, 486–490. doi: 10.1016/j.semcdb.2009.12.005

Clark, J. A., and Amara, S. G. (1994). Stable expression of a neuronal gamma-aminobutyric acid transporter, GAT-3, in mammalian cells demonstrates unique pharmacological properties and ion dependence. *Mol. Pharmacol.* 46, 550–557.

Coleman, J. A., Green, E. M., and Gouaux, E. (2016). X-ray structures and mechanism of the human serotonin transporter. *Nature* 532, 334–339. doi: 10.1038/nature17629

Coothankandaswamy, V., Cao, S., Xu, Y., Prasad, P. D., Singh, P. K., Reynolds, C. P., et al. (2016). Amino acid transporter SLC6A14 is a novel and effective drug target for pancreatic cancer. *Brit. J. Pharmacol.* 173, 3292–3306. doi: 10.1111/bph.13616

Czeredys, M., Samluk, L., Michalec, K., Tulodziecka, K., Skowronek, K., and Nalecz, K. A. (2013). Caveolin-1 - a novel interacting partner of organic cation/carnitine transporter (octn2): effect of protein kinase C on this interaction in rat astrocytes. *PLoS One* 8:e82105. doi: 10.1371/journal.pone.0082105

Dai, W., Vinnakota, S., Qian, X., Kunze, D. L., and Sarkar, H. K. (1999). Molecular characterization of the human CRT-1 creatine transporter expressed in Xenopus oocytes. *Arch. Biochem. Biophys.* 361, 75–84. doi: 10.1006/abbi.1998.0959

Durand, E., Boutin, P., Meyre, D., Charles, M. A., Clement, K., Dina, C., et al. (2004). Polymorphisms in the amino acid transporter solute carrier family 6 (neurotransmitter transporter) member 14 gene contribute to polygenic obesity in French Caucasians. *Diabetes Metab. Res. Rev.* 53, 2483–2486. doi: 10.2337/diabetes.53.9.2483

Duval, A. P., Jeanneret, C., Santoro, T., and Dormond, O. (2018). mTOR and tumor cachexia. *Int. J. Mol. Sci.* 19:2225. doi: 10.3390/ijms19082225

Efeyan, A., Comb, W. C., and Sabatini, D. M. (2015). Nutrient-sensing mechanisms and pathways. *Nature* 517, 302–310. doi: 10.1038/nature14190

El-Kasaby, A., Koban, F., Sitte, H. H., Freissmuth, M., and Sucic, S. (2014). A cytosolic relay of heat shock proteins HSP70-1A and HSP90beta monitors the folding trajectory of the serotonin transporter. *J. Biol. Chem.* 289, 28987–29000. doi: 10.1074/jbc.M114.595090

Eriksson, A., Jennische, E., Flach, C. F., Jorge, A., and Lange, S. (2008). Real-time PCR quantification analysis of five mucosal transcripts in patients with Crohn's disease. *Eur. J. Gastroenterol. Hepatol.* 20, 290–296. doi: 10.1097/MEG.0b013e3282f3557c

Fremeau, R. T. Jr., Caron, M. G., and Blakely, R. D. (1992). Molecular cloning and expression of a high affinity L-proline transporter expressed in putative glutamatergic pathways of rat brain. *Neuron* 8, 915–926. doi: 10.1016/0896-6273(92)90206-S

Fuchs, B. C., and Bode, B. P. (2005). Amino acid transporters ASCT2 and LAT1 in cancer: partners in crime? *Semin. Cancer Biol.* 15, 254–266. doi: 10.1016/j.semcancer.2005.04.005

Galli, A., Jayanthi, L. D., Ramsey, I. S., Miller, J. W., Fremeau, R. T. Jr., DeFelice, L. J., et al. (1999). L-proline and L-pipecolate induce enkephalin-sensitive currents in human embryonic kidney 293 cells transfected with the high-affinity mammalian brain L-proline transporter. *J. Neurosci.* 19, 6290–6297. doi: 10.1523/JNEUROSCI.19-15-06290.1999

Ganapathy, M. E., and Ganapathy, V. (2005). Amino acid transporter ATB0,+ as a delivery system for drugs and prodrugs. *Curr. Drug Targets Immune. Endocr. Metabol. Disord.* 5, 357–364. doi: 10.2174/156800805774912953

Gogala, M., Becker, T., Beatrix, B., Armache, J. P., Barrio-Garcia, C., Berninghausen, O., et al. (2014). Structures of the Sec61 complex engaged in nascent peptide translocation or membrane insertion. *Nature* 506, 107–110. doi: 10.1038/nature12950

Grzes, K. M., Swamy, M., Hukelmann, J. L., Emslie, E., Sinclair, L. V., and Cantrell, D. A. (2017). Control of amino acid transport coordinates metabolic reprogramming in T-cell malignancy. *Leukemia* 31, 2771–2779. doi: 10.1038/leu.2017.160

Gu, H., Wall, S. C., and Rudnick, G. (1994). Stable expression of biogenic amine transporters reveals differences in inhibitor sensitivity, kinetics, and ion dependence. *J. Biol. Chem.* 269, 7124–7130.

Gu, H. H., Wall, S., and Rudnick, G. (1996). Ion coupling stoichiometry for the norepinephrine transporter in membrane vesicles from stably transfected cells. *J. Biol. Chem.* 271, 6911–6916. doi: 10.1074/jbc.271.12.6911

Gupta, N., Miyauchi, S., Martindale, R. G., Herdman, A. V., Podolsky, R., Miyake, K., et al. (2005). Upregulation of the amino acid transporter ATB0,+ (SLC6A14) in colorectal cancer and metastasis in humans. *Biochim. Biophys. Acta* 1741, 215–223. doi: 10.1016/j.bbadis.2005.04.002

Gupta, N., Prasad, P. D., Ghamande, S., Moore-Martin, P., Herdman, A. V., Martindale, R. G., et al. (2006). Up-regulation of the amino acid transporter ATB(0,+) (SLC6A14) in carcinoma of the cervix. *Gynecol. Oncol.* 100, 8–13.

Hanahan, D., and Weinberg, R. A. (2011). Hallmarks of cancer: the next generation. *Cell* 144, 646–674.

Harachi, M., Masui, K., Okamura, Y., Tsukui, R., Mischel, P. S., and Shibata, N. (2018). mTOR complexes as a nutrient sensor for driving cancer progression. *Int .J. Mol. Sci.* 19:3267.

Harari, D., and Yarden, Y. (2000). Molecular mechanisms underlying ErbB2/HER2 action in breast cancer. *Oncogene* 19, 6102–6114.

Harris, R. C., Tallon, M. J., Dunnett, M., Boobis, L., Coakley, J., Kim, H. J., et al. (2006). The absorption of orally supplied beta-alanine and its effect on muscle carnosine synthesis in human vastus lateralis. *Amino Acids* 30, 279–289.

Hatanaka, T., Haramura, M., Fei, Y. J., Miyauchi, S., Bridges, C. C., Ganapathy, P. S., et al. (2004). Transport of amino acid-based prodrugs by the Na+- and Cl(-) -coupled amino acid transporter ATB0,+ and expression of the transporter in tissues amenable for drug delivery. *J. Pharmacol. Exp. Ther.* 308, 1138–1147.

Hatanaka, T., Huang, W., Nakanishi, T., Bridges, C. C., Smith, S. B., Prasad, P. D., et al. (2002). Transport of D-serine via the amino acid transporter ATB(0,+) expressed in the colon. *Biochem. Biophys. Res. Commun.* 291, 291–295.

Hatanaka, T., Nakanishi, T., Huang, W., Leibach, F. H., Prasad, P. D., Ganapathy, V., et al. (2001). Na+ - and Cl- -coupled active transport of nitric oxide synthase inhibitors via amino acid transport system B(0,+). *J. Clin. Invest.* 107, 1035–1043.

Hayashi, K., Jutabha, P., Endou, H., and Anzai, N. (2012). c-Myc is crucial for the expression of LAT1 in MIA Paca-2 human pancreatic cancer cells. *Oncol. Rep.* 28, 862–866.

Hoffman, B. J., Mezey, E., and Brownstein, M. J. (1991). Cloning of a serotonin transporter affected by antidepressants. *Science* 254, 579–580.

Hou, D. Y., Muller, A. J., Sharma, M. D., DuHadaway, J., Banerjee, T., Johnson, M., et al. (2007). Inhibition of indoleamine 2,3-dioxygenase in dendritic cells by stereoisomers of 1-methyl-tryptophan correlates with antitumor responses. *Cancer Res.* 67, 792–801.

Hrckulak, D., Janeckova, L., Lanikova, L., Kriz, V., Horazna, M., Babosova, O., et al. (2018). Wnt effector TCF4 is dispensable for Wnt signaling in human cancer cells. *Genes* 9:431. doi: 10.3390/genes9090439

Iyer, G. S., Krahe, R., Goodwin, L. A., Doggett, N. A., Siciliano, M. J., Funanage, V. L., et al. (1996). Identification of a testis-expressed creatine transporter gene at 16p11.2 and confirmation of the X-linked locus to Xq28. *Genomics* 34, 143–146. doi: 10.1006/geno.1996.0254

Jain-Vakkalagadda, B., Pal, D., Gunda, S., Nashed, Y., Ganapathy, V., and Mitra, A. K. (2004). Identification of a Na+-dependent cationic and neutral amino acid transporter. B(0,+), in human and rabbit cornea. *Mol. Pharm.* 1, 338–346. doi: 10.1021/mp0499499

Jhaveri, K., and Modi, S. (2015). Ganetespib: research and clinical development. *Onco Targets Ther.* 8, 1849–1858. doi: 10.2147/OTT.S65804

Ju, X., Katiyar, S., Wang, C., Liu, M., Jiao, X., Li, S., et al. (2007). Akt1 governs breast cancer progression in vivo. *Proc. Natl. Acad. Sci. U.S.A.* 104, 7438–7443. doi: 10.1073/pnas.0605874104

Juraszek, B., and Nalecz, K. A. (2020). SLC22A5 (OCTN2) carnitine transporter-indispensable for cell metabolism, a jekyll and hyde of Human Cancer. *Molecules* 25:14. doi: 10.3390/molecules25010014

Kaira, K., Oriuchi, N., Imai, H., Shimizu, K., Yanagitani, N., Sunaga, N., et al. (2008). l-type amino acid transporter 1 and CD98 expression in primary and metastatic sites of human neoplasms. *Cancer Sci.* 99, 2380–2386. doi: 10.1111/j.1349-7006.2008.00969.x

Karakossian, M. H., Spencer, S. R., Gomez, A. Q., Padilla, O. R., Sacher, A., Loo, D. D., et al. (2005). Novel properties of a mouse gamma-aminobutyric acid transporter (GAT4). *J. Membr. Biol.* 203, 65–82. doi: 10.1007/s00232-004-0732-5

Karunakaran, S., Ramachandran, S., Coothankandaswamy, V., Elangovan, S., Babu, E., Periyasamy-Thandavan, S., et al. (2011). SLC6A14 (ATB0,+) protein, a highly concentrative and broad specific amino acid transporter, is a novel and effective drug target for treatment of estrogen receptor-positive breast cancer. *J. Biol. Chem.* 286, 31830–31838. doi: 10.1074/jbc.M111.229518

Karunakaran, S., Umapathy, N. S., Thangaraju, M., Hatanaka, T., Itagaki, S., Munn, D. H., et al. (2008). Interaction of tryptophan derivatives with SLC6A14 (ATB0,+) reveals the potential of the transporter as a drug target for cancer chemotherapy. *Biochem. J.* 414, 343–355. doi: 10.1042/BJ20080622

Kerner, J., and Hoppel, C. (2000). Fatty acid import into mitochondria. *Biochim. Biophys. Acta* 1486, 1–17. doi: 10.1016/S1388-1981(00)00044-5

Keuerleber, S., Gsandtner, I., and Freissmuth, M. (2011). From cradle to twilight: the carboxyl terminus directs the fate of the A(2A)-adenosine receptor. *Biochim. Biophys. Acta* 1808, 1350–1357. doi: 10.1016/j.bbamem.2010.05.009

Kido, Y., Tamai, I., Ohnari, A., Sai, Y., Kagami, T., Nezu, J., et al. (2001). Functional relevance of carnitine transporter OCTN2 to brain distribution of L-carnitine and acetyl-L-carnitine across the blood- brain barrier. *J. Neurochem.* 79, 959–969. doi: 10.1046/j.1471-4159.2001.00621.x

Kou, L., Huang, H., Lin, X., Jiang, X., Wang, Y., Luo, Q., et al. (2020). Endocytosis of ATB(0,+)(SLC6A14)-targeted liposomes for drug delivery and its therapeutic application for pancreatic cancer. *Expert Opin. Drug Deliv.* 17, 395–405. doi: 10.1080/17425247.2020.1723544

Kovalchuk, V., Samluk, L., Juraszek, B., Jurkiewicz-Trzaska, D., Sucic, S., Freissmuth, M., et al. (2019). Trafficking of the amino acid transporter B(0,+) (SLC6A14) to the plasma membrane involves an exclusive interaction with SEC24C for its exit from the endoplasmic reticulum. *Biochim. Biophys. Acta Mol. Cell Res.* 1866, 252–263. doi: 10.1016/j.bbamcr.2018.11.005

Kowalczuk, S., Broer, A., Munzinger, M., Tietze, N., Klingel, K., and Broer, S. (2005). Molecular cloning of the mouse IMINO system: an Na+- and Cl–dependent proline transporter. *Biochem. J.* 386, 417–422. doi: 10.1042/BJ20050100

Lazaris, A., Chatzigianni, E. B., Panoussopoulos, D., Tzimas, G. N., Davaris, P. S., and Golematis, B. (1997). Proliferating cell nuclear antigen and heat shock protein 70 immunolocalization in invasive ductal breast cancer not otherwise specified. *Breast Cancer Res. Treat.* 43, 43–51. doi: 10.1023/A:1005706110275

Lederkremer, G. Z. (2009). Glycoprotein folding, quality control and ER-associated degradation. *Curr. Opin. Struct. Biol.* 19, 515–523. doi: 10.1016/j.sbi.2009.06.004

Lewerenz, J., Hewett, S. J., Huang, Y., Lambros, M., Gout, P. W., Kalivas, P. W., et al. (2013). The cystine/glutamate antiporter system x(c)(-) in health and disease: from molecular mechanisms to novel therapeutic opportunities. *Antioxid. Redox Signal.* 18, 522–555. doi: 10.1089/ars.2011.4391

Lianos, G. D., Alexiou, G. A., Mangano, A., Mangano, A., Rausei, S., Boni, L., et al. (2015). The role of heat shock proteins in cancer. *Cancer Lett.* 360, 114–118. doi: 10.1016/j.canlet.2015.02.026

Liu, Q. R., Lopez-Corcuera, B., Mandiyan, S., Nelson, H., and Nelson, N. (1993a). Cloning and expression of a spinal cord- and brain-specific glycine transporter with novel structural features. *J. Biol. Chem.* 268, 22802–22808.

Liu, Q. R., Lopez-Corcuera, B., Mandiyan, S., Nelson, H., and Nelson, N. (1993b). Molecular characterization of four pharmacologically distinct gamma-aminobutyric acid transporters in mouse brain. *J. Biol. Chem.* 268, 2106–2112.

Liu, Q. R., Lopez-Corcuera, B., Nelson, H., Mandiyan, S., and Nelson, N. (1992a). Cloning and expression of a cDNA encoding the transporter of taurine and beta-alanine in mouse brain. *Proc. Natl. Acad. Sci. U.S.A.* 89, 12145–12149. doi: 10.1073/pnas.89.24.12145

Liu, Q. R., Nelson, H., Mandiyan, S., Lopez-Corcuera, B., and Nelson, N. (1992b). Cloning and expression of a glycine transporter from mouse brain. *FEBS Lett.* 305, 110–114. doi: 10.1016/0014-5793(92)80875-H

Lopez-Corcuera, B., Liu, Q. R., Mandiyan, S., Nelson, H., and Nelson, N. (1992). Expression of a mouse brain cDNA encoding novel gamma-aminobutyric acid transporter. *J. Biol. Chem.* 267, 17491–17493.

Low, E. N. D., Mokhtar, N. M., Wong, Z., and Raja Ali, R. A. (2019). Colonic mucosal transcriptomic changes in patients with long-duration ulcerative colitis revealed colitis-associated cancer pathways. *J. Crohns Colitis* 13, 755–763. doi: 10.1093/ecco-jcc/jjz002

Luo, Q., Yang, B., Tao, W., Li, J., Kou, L., Lian, H., et al. (2017). ATB(0,+) transporter-mediated targeting delivery to human lung cancer cells via aspartate-modified docetaxel-loading stealth liposomes. *Biomater. Sci.* 5, 295–304. doi: 10.1039/C6BM00788K

Martinez-Gil, L., Sauri, A., Marti-Renom, M. A., and Mingarro, I. (2011). Membrane protein integration into the endoplasmic reticulum. *FEBS J.* 278, 3846–3858. doi: 10.1111/j.1742-4658.2011.08185.x

Matsui, T., Sekiguchi, M., Hashimoto, A., Tomita, U., Nishikawa, T., and Wada, K. (1995). Functional comparison of D-serine and glycine in rodents: the effect on cloned NMDA receptors and the extracellular concentration. *J. Neurochem.* 65, 454–458. doi: 10.1046/j.1471-4159.1995.65010454.x

Michalec, K., Mysiorek, C., Kuntz, M., Berezowski, V., Szczepankiewicz, A. A., Wilczynski, G. M., et al. (2014). Protein kinase C restricts transport of carnitine

by amino acid transporter ATB(0,+) apically localized in the blood-brain barrier. *Arch. Biochem. Biophys.* 554, 28–35. doi: 10.1016/j.abb.2014.05.006

Miller, E. A., and Schekman, R. (2013). COPII - a flexible vesicle formation system. *Curr. Opin. Cell Biol.* 25, 420–427. doi: 10.1016/j.ceb.2013.04.005

Moremen, K. W., Tiemeyer, M., and Nairn, A. V. (2012). Vertebrate protein glycosylation: diversity, synthesis and function. *Nat. Rev. Mol. Cell Biol.* 13, 448–462. doi: 10.1038/nrm3383

Muller, A., Chiotellis, A., Keller, C., Ametamey, S. M., Schibli, R., Mu, L., et al. (2014). Imaging tumour ATB0,+ transport activity by PET with the cationic amino acid O-2((2-[18F]fluoroethyl)methyl-amino)ethyltyrosine. *Mol. Imaging Biol.* 16, 412–420. doi: 10.1007/s11307-013-0711-2

Murai, S., Ando, A., Ebara, S., Hirayama, M., Satomi, Y., and Hara, T. (2017). Inhibition of malic enzyme 1 disrupts cellular metabolism and leads to vulnerability in cancer cells in glucose-restricted conditions. *Oncogenesis* 6:e329. doi: 10.1038/oncsis.2017.34

Murphy, M. E. (2013). The HSP70 family and cancer. *Carcinogenesis* 34, 1181–1188. doi: 10.1093/carcin/bgt111

Nakanishi, T., Hatanaka, T., Huang, W., Prasad, P. D., Leibach, F. H., Ganapathy, M. E., et al. (2001). Na+- and Cl–coupled active transport of carnitine by the amino acid transporter ATB(0,+) from mouse colon expressed in HRPE cells and Xenopus oocytes. *J. Physiol.* 532, 297–304. doi: 10.1111/j.1469-7793.2001.0297f.x

Napolitano, L., Scalise, M., Galluccio, M., Pochini, L., Albanese, L. M., and Indiveri, C. (2015). LAT1 is the transport competent unit of the LAT1/CD98 heterodimeric amino acid transporter. *Int. J. Biochem. Cell Biol.* 67, 25–33. doi: 10.1016/j.biocel.2015.08.004

Nash, S. R., Giros, B., Kingsmore, S. F., Rochelle, J., Suter, S. T., Gregor, P., et al. (1994). Cloning, pharmacological characterization, and genomic localization of the human creatine transporter. *Receptors Channels* 2, 165–174.

Nelson, H., Mandiyan, S., and Nelson, N. (1990). Cloning of the human brain GABA transporter. *FEBS Lett.* 269, 181–184. doi: 10.1016/0014-5793(90)81149-I

Newton, A. C. (1995). Protein kinase C: structure, function, and regulation. *J. Biol. Chem.* 270, 28495–28498. doi: 10.1074/jbc.270.48.28495

Nicholson, K. M., and Anderson, N. G. (2002). The protein kinase B/Akt signalling pathway in human malignancy. *Cell Signal.* 14, 381–395. doi: 10.1016/S0898-6568(01)00271-6

Nicklin, P., Bergman, P., Zhang, B., Triantafellow, E., Wang, H., Nyfeler, B., et al. (2009). Bidirectional transport of amino acids regulates mTOR and autophagy. *Cell* 136, 521–534. doi: 10.1016/j.cell.2008.11.044

Noveski, P., Mircevska, M., Plaseski, T., Peterlin, B., and Plaseska-Karanfilska, D. (2014). Study of Three Single Nucleotide Polymorphisms in the SLC6A14 Gene in Association with Male Infertility. *Balkan J. Med. Genet.* 17, 61–66. doi: 10.2478/bjmg-2014-0075

Osada, T., Kaneko, K., Gwin, W. R., Morse, M. A., Hobeika, A., Pogue, B. W., et al. (2017). In vivo detection of hsp90 identifies breast cancers with aggressive behavior. *Clin. Cancer Res.* 23, 7531–7542. doi: 10.1158/1078-0432.CCR-17-1453

Pacholczyk, T., Blakely, R. D., and Amara, S. G. (1991). Expression cloning of a cocaine- and antidepressant-sensitive human noradrenaline transporter. *Nature* 350, 350–354. doi: 10.1038/350350a0

Palazzolo, L., Paravicini, C., Laurenzi, T., Adobati, S., Saporiti, S., Guerrini, U., et al. (2019). SLC6A14, a pivotal actor on cancer stage: when function meets structure. *SLAS Discov.* 24, 928–938. doi: 10.1177/2472555219867317

Pantanowitz, S., Bendahan, A., and Kanner, B. I. (1993). Only one of the charged amino acids located in the transmembrane alpha-helices of the gamma-aminobutyric acid transporter (subtype A) is essential for its activity. *J. Biol. Chem.* 268, 3222–3225.

Paria, B. C., Lim, H., Wang, X. N., Liehr, J., Das, S. K., and Dey, S. K. (1998). Coordination of differential effects of primary estrogen and catecholestrogen on two distinct targets mediates embryo implantation in the mouse. *Endocrinology* 139, 5235–5246. doi: 10.1210/endo.139.12.6386

Park, E., and Rapoport, T. A. (2012). Mechanisms of Sec61/SecY-mediated protein translocation across membranes. *Annu. Rev. Biophys.* 41, 21–40. doi: 10.1146/annurev-biophys-050511-102312

Parra, L. A., Baust, T., El Mestikawy, S., Quiroz, M., Hoffman, B., Haflett, J. M., et al. (2008). The orphan transporter Rxt1/NTT4 (SLC6A17) functions as a synaptic vesicle amino acid transporter selective for proline, glycine, leucine, and alanine. *Mol. Pharmacol.* 74, 1521–1532. doi: 10.1124/mol.108.050005

Pastor-Anglada, M., and Perez-Torras, S. (2015). Nucleoside transporter proteins as biomarkers of drug responsiveness and drug targets. *Front. Pharmacol.* 6:13. doi: 10.3389/fphar.2015.00013

Penheiter, A. R., Erdogan, S., Murphy, S. J., Hart, S. N., Felipe Lima, J., Rakhshan Rohakhtar, F., et al. (2015). Transcriptomic and immunohistochemical profiling of SLC6A14 in pancreatic ductal adenocarcinoma. *Biomed. Res. Int.* 2015:593572. doi: 10.1155/2015/593572

Pudova, E. A., Lukyanova, E. N., Nyushko, K. M., Mikhaylenko, D. S., Zaretsky, A. R., Snezhkina, A. V., et al. (2019). differentially expressed genes associated with prognosis in locally advanced lymph node-negative Prostate Cancer. *Front. Genet.* 10:730. doi: 10.3389/fgene.2019.00730

Ramamoorthy, S., Leibach, F. H., Mahesh, V. B., Han, H., Yang-Feng, T., Blakely, R. D., et al. (1994). Functional characterization and chromosomal localization of a cloned taurine transporter from human placenta. *Biochem. J.* 300, 893–900. doi: 10.1042/bj3000893

Rebsamen, M., Pochini, L., Stasyk, T., de Araujo, M. E., Galluccio, M., Kandasamy, R. K., et al. (2015). SLC38A9 is a component of the lysosomal amino acid sensing machinery that controls mTORC1. *Nature* 519, 477–481. doi: 10.1038/nature14107

Riaz, A., Zeller, K. S., and Johansson, S. (2012). Receptor-specific mechanisms regulate phosphorylation of AKT at Ser473: role of RICTOR in beta1 integrin-mediated cell survival. *PLoS One* 7:e32081. doi: 10.1371/journal.pone.0032081

Riordan, J. R., Rommens, J. M., Kerem, B., Alon, N., Rozmahel, R., Grzelczak, Z., et al. (1989). Identification of the cystic fibrosis gene: cloning and characterization of complementary DNA. *Science* 245, 1066–1073. doi: 10.1126/science.2475911

Rogala-Koziarska, K., Samluk, L., and Nalecz, K. A. (2019). Amino acid transporter SLC6A14 depends on heat shock protein HSP90 in trafficking to the cell surface. *Biochim. Biophys. Acta Mol. Cell Res.* 1866, 1544–1555. doi: 10.1016/j.bbamcr.2019.07.009

Rommens, J. M., Iannuzzi, M. C., Kerem, B., Drumm, M. L., Melmer, G., Dean, M., et al. (1989). Identification of the cystic fibrosis gene: chromosome walking and jumping. *Science* 245, 1059–1065. doi: 10.1126/science.2772657

Roux, M. J., and Supplisson, S. (2000). Neuronal and glial glycine transporters have different stoichiometries. *Neuron* 25, 373–383. doi: 10.1016/S0896-6273(00)80901-0

Royse, K. E., Zhi, D., Conner, M. G., Clodfelder-Miller, B., Srinivasasainagendra, V., Vaughan, L. K., et al. (2014). Differential gene expression landscape of co-existing cervical pre-cancer lesions using RNA-seq. *Front. Oncol.* 4:339. doi: 10.3389/fonc.2014.00339

Ruffin, M., Mercier, J., Calmel, C., Mesinele, J., Bigot, J., Sutanto, E. N., et al. (2020). Update on SLC6A14 in lung and gastrointestinal physiology and physiopathology: focus on cystic fibrosis. *Cell Mol. Life. Sci.* 77, 3311–3323. doi: 10.1007/s00018-020-03487-x

Samluk, L., Czeredys, M., and Nalecz, K. A. (2010). Regulation of amino acid/carnitine transporter B 0,+ (ATB 0,+) in astrocytes by protein kinase C: independent effects on raft and non-raft transporter subpopulations. *J. Neurochem.* 115, 1386–1397. doi: 10.1111/j.1471-4159.2010.07040.x

Samluk, L., Czeredys, M., Skowronek, K., and Nalecz, K. A. (2012). Protein kinase C regulates amino acid transporter ATB(0,+). *Biochem. Biophys. Res.Commun.* 422, 64–69. doi: 10.1016/j.bbrc.2012.04.106

Scalise, M., Pochini, L., Galluccio, M., Console, L., and Indiveri, C. (2020). Glutamine transporters as pharmacological targets: From function to drug design. *Asian J. Pharm. Sci.* 15, 207–219. doi: 10.1016/j.ajps.2020.02.005

Scalise, M., Pochini, L., Galluccio, M., and Indiveri, C. (2016). Glutamine transport. From energy supply to sensing and beyond. *Biochim. Biophys. Acta* 1857, 1147–1157. doi: 10.1016/j.bbabio.2016.03.006

Scalise, M., Pochini, L., Gallucio, M., Console, L., and Indiveri, C. (2017). Glutamine transport and mitochondrial metabolism in cancer cell growth. *Front. Oncol.* 7:306. doi: 10.3389/fonc.2017.00306

Scalise, M., Pochini, L., Pingitore, P., Hedfalk, K., and Indiveri, C. (2015). Cysteine is not a substrate but a specific modulator of human ASCT2 (SLC1A5) transporter. *FEBS Lett.* 589, 3617–3623. doi: 10.1016/j.febslet.2015.10.011

Schlafke, S., and Enders, A. C. (1975). Cellular basis of interaction between trophoblast and uterus at implantation. *Biol. Reprod.* 12, 41–65. doi: 10.1095/biolreprod12.1.41

Schultz, J. F., Mayernik, L., Rout, U. K., and Armant, D. R. (1997). Integrin trafficking regulates adhesion to fibronectin during differentiation of mouse peri-implantation blastocysts. *Dev. Genet.* 21, 31–43. doi: 10.1002/(SICI)1520-6408(1997)21:1<31::AID-DVG4>3.0.CO;2-9

Sharpe, L. J., Luu, W., and Brown, A. J. (2011). Akt phosphorylates Sec24: new clues into the regulation of ER-to-Golgi trafficking. *Traffic* 12, 19–27. doi: 10.1111/j.1600-0854.2010.01133.x

Shimada, S., Kitayama, S., Lin, C. L., Patel, A., Nanthakumar, E., Gregor, P., et al. (1991). Cloning and expression of a cocaine-sensitive dopamine transporter complementary DNA. *Science* 254, 576–578. doi: 10.1126/science.1948034

Sikder, M. O. F., Sivaprakasam, S., Brown, T. P., Thangaraju, M., Bhutia, Y. D., and Ganapathy, V. (2020). SLC6A14, a Na+/Cl–coupled amino acid transporter, functions as a tumor promoter in colon and is a target for Wnt signaling. *Biochem. J.* 477, 1409–1425. doi: 10.1042/BCJ20200099

Sikder, M. O. F., Yang, S., Ganapathy, V., and Bhutia, Y. D. (2017). The Na(+)/Cl(-)-Coupled, broad-specific, amino acid transporter SLC6A14 (ATB(0,+)): emerging roles in multiple diseases and therapeutic potential for treatment and diagnosis. *AAPS J.* 20:12. doi: 10.1208/s12248-017-0164-7

Sloan, J. L., and Mager, S. (1999). Cloning and functional expression of a human Na(+) and Cl(-)-dependent neutral and cationic amino acid transporter B(0+). *J. Biol. Chem.* 274, 23740–23745. doi: 10.1074/jbc.274.34.23740

Srinivas, S. R., Prasad, P. D., Umapathy, N. S., Ganapathy, V., and Shekhawat, P. S. (2007). Transport of butyryl-L-carnitine, a potential prodrug, via the carnitine transporter OCTN2 and the amino acid transporter ATB0,+. *Am. J. Physiol. Gastrointest. Liver Physiol.* 293, G1046–G1053. doi: 10.1152/ajpgi.00233.2007

Sucic, S., Koban, F., El-Kasaby, A., Kudlacek, O., Stockner, T., Sitte, H. H., et al. (2013). Switching the clientele: a lysine residing in the C terminus of the serotonin transporter specifies its preference for the coat protein complex II component SEC24C. *J. Biol. Chem* 288:53305341. doi: 10.1074/jbc.M112.408237

Sun, L., Rommens, J. M., Corvol, H., Li, W., Li, X., Chiang, T. A., et al. (2012). Multiple apical plasma membrane constituents are associated with susceptibility to meconium ileus in individuals with cystic fibrosis. *Nat. Genet.* 44:562569.

Suviolahti, E., Oksanen, L. J., Ohman, M., Cantor, R. M., Ridderstrale, M., Tuomi, T., et al. (2003). The SLC6A14 gene shows evidence of association with obesity. *J. Clin. Invest.* 112, 1762–1772. doi: 10.1172/JCI200317491

Takanaga, H., Mackenzie, B., Suzuki, Y., and Hediger, M. A. (2005). Identification of mammalian proline transporter SIT1 (SLC6A20) with characteristics of classical system imino. *J. Biol. Chem.* 280, 8974–8984. doi: 10.1074/jbc.M413027200

Thoreen, C. C. (2017). The molecular basis of mTORC1-regulated translation. *Biochem. Soc. Trans.* 45, 213–221. doi: 10.1042/BST20160072

Tinajero, J. C., Fabbri, A., Ciocca, D. R., and Dufau, M. L. (1993). Serotonin secretion from rat Leydig cells. *Endocrinology* 133, 3026–3029. doi: 10.1210/endo.133.6.8243331

Tiwari, H. K., and Allison, D. B. (2003). Do allelic variants of SLC6A14 predispose to obesity? *J. Clin. Invest.* 112:16331636. doi: 10.1172/JCI200320448

Ugawa, S., Sunouchi, Y., Ueda, T., Takahashi, E., Saishin, Y., and Shimada, S. (2001). Characterization of a mouse colonic system B(0+) amino acid transporter related to amino acid absorption in colon. *Am. J. Physiol. Gastrointest. Liver Physiol.* 281, G365–G370. doi: 10.1152/ajpgi.2001.281.2.G365

Umapathy, N. S., Ganapathy, V., and Ganapathy, M. E. (2004). Transport of amino acid esters and the amino-acid-based prodrug valganciclovir by the amino acid transporter ATB(0,+). *Pharm. Res.* 21, 1303–1310. doi: 10.1023/B:PHAM.0000033019.49737.28

Van Winkle, L. J., Tesch, J. K., Shah, A., and Campione, A. L. (2006). System B0,+ amino acid transport regulates the penetration stage of blastocyst implantation with possible long-term developmental consequences through adulthood. *Hum. Reprod. Update* 12, 145–157. doi: 10.1093/humupd/dmi044

Wang, Q., and Holst, J. (2015). L-type amino acid transport and cancer: targeting the mTORC1 pathway to inhibit neoplasia. *Am. J. Cancer Res.* 5, 1281–1294.

Wang, S., Tsun, Z. Y., Wolfson, R. L., Shen, K., Wyant, G. A., Plovanich, M. E., et al. (2015). Metabolism. Lysosomal amino acid transporter SLC38A9 signals arginine sufficiency to mTORC1. *Science* 347, 188–194. doi: 10.1126/science.1257132

Wang, Y., He, X., Ngeow, J., and Eng, C. (2012). GATA2 negatively regulates PTEN by preventing nuclear translocation of androgen receptor and by androgen-independent suppression of PTEN transcription in breast cancer. *Hum. Mol. Genet.* 21, 569–576. doi: 10.1093/hmg/ddr491

White, M. A., Lin, C., Rajapakshe, K., Dong, J., Shi, Y., Tsouko, E., et al. (2017). Glutamine transporters are targets of multiple oncogenic signaling pathways in Prostate Cancer. *Mol Cancer Res.* 15, 1017–1028. doi: 10.1158/1541-7786.MCR-16-0480

Wise, D. R., and Thompson, C. B. (2010). Glutamine addiction: a new therapeutic target in cancer. *Trends Biochem. Sci.* 35, 427–433. doi: 10.1016/j.tibs.2010.05.003

Wolosker, H., Blackshaw, S., and Snyder, S. H. (1999). Serine racemase: a glial enzyme synthesizing D-serine to regulate glutamate-N-methyl-D-aspartate neurotransmission. *Proc. Natl. Acad. Sci. U.S.A.* 96, 13409–13414. doi: 10.1073/pnas.96.23.13409

Wu, J., Liu, T., Rios, Z., Mei, Q., Lin, X., and Cao, S. (2017). Heat Shock Proteins and Cancer. *Trends Pharmacol. Sci.* 38, 226–256. doi: 10.1016/j.tips.2016.11.009

Xu, W., Liu, L., Gorman, P. A., Sheer, D., and Emson, P. C. (1997). Assignment of the human creatine transporter type 2 (SLC6A10) to chromosome band 16p11.2 by in situ hybridization. *Cytogenet. Cell Genet.* 76:19. doi: 10.1159/000134503

Yamamoto, T., Seino, Y., Fukumoto, H., Koh, G., Yano, H., Inagaki, N., et al. (1990). Over-expression of facilitative glucose transporter genes in human cancer. *Biochem. Biophys. Res. Commun.* 170, 223–230. doi: 10.1016/0006-291X(90)91263-R

Yamashita, A., Singh, S. K., Kawate, T., Jin, Y., and Gouaux, E. (2005). Crystal structure of a bacterial homologue of Na+/Cl–dependent neurotransmitter transporters. *Nature* 437, 215–223. doi: 10.1038/nature03978

Yamauchi, A., Uchida, S., Kwon, H. M., Preston, A. S., Robey, R. B., Garcia-Perez, A., et al. (1992). Cloning of a Na(+)- and Cl(-)-dependent betaine transporter that is regulated by hypertonicity. *J. Biol. Chem.* 267, 649–652.

Yang, Z. Q., Liu, Y. J., and Zhou, X. L. (2020). An integrated microarray analysis reveals significant diagnostic and prognostic biomarkers in Pancreatic Cancer. *Med. Sci. Monit.* 26:e921769. doi: 10.12659/MSM.921769

Young, J. D. (2016). The SLC28 (CNT) and SLC29 (ENT) nucleoside transporter families: a 30-year collaborative odyssey. *Biochem. Soc. Trans.* 44, 869–876. doi: 10.1042/BST20160038

Yu, M., Yongzhi, H., Chen, S., Luo, X., Lin, Y., Zhou, Y., et al. (2017). The prognostic value of GLUT1 in cancers: a systematic review and meta-analysis. *Oncotarget* 8, 43356–43367. doi: 10.18632/oncotarget.17445

Zaia, K. A., and Reimer, R. J. (2009). Synaptic VESICLE PROTEIN NTT4/XT1 (SLC6A17) Catalyzes Na+-coupled neutral amino acid transport. *J. Biol. Chem.* 284, 8439–8448. doi: 10.1074/jbc.M806407200

Zhao, X., Petrashen, A. P., Sanders, J. A., Peterson, A. L., and Sedivy, J. M. (2019). SLC1A5 glutamine transporter is a target of MYC and mediates reduced mTORC1 signaling and increased fatty acid oxidation in long-lived Myc hypomorphic mice. *Aging Cell* 18:e12947. doi: 10.1111/acel.12947

Conflict of Interest: The author declares that the research was conducted in the absence of any commercial or financial relationships that could be construed as a potential conflict of interest.

frontiers in Cell and Developmental Biology

MINI REVIEW
published: 09 November 2020
doi: 10.3389/fcell.2020.602668

Interplay of Carbonic Anhydrase IX With Amino Acid and Acid/Base Transporters in the Hypoxic Tumor Microenvironment

Geetha Venkateswaran[1,2] *and Shoukat Dedhar*[1,2,3]*

[1] Department of Integrative Oncology, British Columbia Cancer Research Centre, Vancouver, BC, Canada, [2] Interdisciplinary Oncology Program, The University of British Columbia, Vancouver, BC, Canada, [3] Department of Biochemistry and Molecular Biology, The University of British Columbia, Vancouver, BC, Canada

Solid tumors are challenged with a hypoxic and nutrient-deprived microenvironment. Hence, hypoxic tumor cells coordinatively increase the expression of nutrient transporters and pH regulators to adapt and meet their bioenergetic and biosynthetic demands. Carbonic Anhydrase IX (CAIX) is a membrane-bound enzyme that plays a vital role in pH regulation in the tumor microenvironment (TME). Numerous studies have established the importance of CAIX in mediating tumor progression and metastasis. To understand the mechanism of CAIX in mediating tumor progression, we performed an unbiased proteomic screen to identify the potential interactors of CAIX in the TME using the proximity-dependent biotin identification (BioID) technique. In this review, we focus on the interactors from this BioID screen that are crucial for nutrient and metabolite transport in the TME. We discuss the role of transport metabolon comprising CAIX and bicarbonate transporters in regulating intra- and extracellular pH of the tumor. We also discuss the role of amino acid transporters that are high confidence interactors of CAIX, in optimizing favorable metabolic state for tumor progression, and give our perspective on the coordinative interplay of CAIX with the amino acid transporters in the hypoxic TME.

Keywords: tumor microenvironment, hypoxia, carbonic anhydrase IX, amino acid transport, tumor metabolism

OPEN ACCESS

Edited by:
Eric Kenneth Parkinson, Queen Mary University of London, United Kingdom

Reviewed by:
Johanna Chiche, INSERM U1065 Centre Mediterraneien de Medecine Moleiculaire, France
Eliska Svastova, Slovak Academy of Sciences, Slovakia

***Correspondence:**
Shoukat Dedhar
sdedhar@bccrc.ca

Specialty section:
This article was submitted to Molecular and Cellular Oncology, a section of the journal Frontiers in Cell and Developmental Biology

Received: *04 September 2020*
Accepted: *09 October 2020*
Published: *09 November 2020*

Citation:
Venkateswaran G and Dedhar S (2020) Interplay of Carbonic Anhydrase IX With Amino Acid and Acid/Base Transporters in the Hypoxic Tumor Microenvironment. Front. Cell Dev. Biol. 8:602668. doi: 10.3389/fcell.2020.602668

INTRODUCTION

Tumor cells metabolize nutrients in an anabolic or catabolic mode to maintain their biosynthetic and bioenergetic demands, respectively. In a catabolic pathway, nutrients are broken down to generate energy for maintaining cellular integrity. Whereas, in an anabolic pathway, they are utilized to build new macromolecules such as nucleotides and amino acids that support cell growth and proliferation. Tumor cells can alter their metabolism in favor of either of these pathways based on their requirements, which is called metabolic reprogramming/rewiring (Ward and Thompson, 2012). Besides, tumor cells can utilize a diverse array of nutrients such as glucose, glutamine (Gln), essential amino acids, and fatty acids, thus offering them metabolic flexibility (DeNicola and Cantley, 2015). Both, metabolic reprogramming and flexibility give tumor cells the plasticity to adapt to any metabolic shifts and survive. Several cell-intrinsic and extrinsic factors influence metabolic reprogramming and flexibility in tumor cells (DeNicola and Cantley, 2015). One of the most important extrinsic factors is oxygen availability in the tumor microenvironment (TME)

(Nakazawa et al., 2016). Solid tumors are characterized by chaotic, immature vasculature that causes zones of varying oxygen tensions within the tumor. Depending on the proximity to blood vessels, tumors are comprised of poorly perfused, chronic hypoxic zones, and intermittently perfused, cycling hypoxic zones (Michiels et al., 2016). To survive the nutrient and oxygen deprivation caused by insufficient perfusion, tumor cells trigger hypoxia-inducible factor (HIF) signaling, which culminates in the stabilization and activation of the transcription factor, HIF1α or HIF2α, and alters the expression of several downstream targets to promote survival, tumor growth and progression (Xie and Simon, 2017). One of the HIF1α regulated proteins that play an important role in the hypoxic TME is the Carbonic Anhydrase IX (CAIX) (Wykoff et al., 2000; McDonald and Dedhar, 2014).

CAIX – FUNCTION AND ROLE IN CANCER

Carbonic anhydrase IX is a dimeric, membrane-bound metabolic enzyme that belongs to the carbonic anhydrase (CA) family (Alterio et al., 2012). It plays a crucial role in pH regulation through the reversible hydration of carbon dioxide into bicarbonate and proton. CAIX comprises of extracellular facing proteoglycan (PG) and catalytic (CA) domains, a transmembrane (TM) domain, and an intracytoplasmic (IC) domain (Opavský et al., 1996). The presence of the PG domain is a unique feature of CAIX and is absent in other isozymes of the CA family. The dimerization of CAIX is mediated by the formation of a disulfide bond between the Cys-41 residue located on the CA domain (Alterio et al., 2009). Although CAIX expression is primarily driven under hypoxia through the HIF1α stabilization, the presence of extracellular lactate (Panisova et al., 2017) and glutamate (Glu) (Briggs et al., 2016) have also been shown to stabilize HIF1α and promote CAIX expression under normoxia. CAIX is predominantly expressed in solid tumors, with restricted expression in normal tissues (McDonald et al., 2012; Mboge et al., 2018) and, its expression can be correlated with poor prognosis (Chia et al., 2001; Loncaster et al., 2001; Klatte et al., 2009; Korkeila et al., 2009; Ilie et al., 2010) and response to therapy in solid tumors (Koukourakis et al., 2001; Generali et al., 2006; Tan et al., 2009; McIntyre et al., 2012). The role of CAIX in various steps of tumor progression and metastasis is well established in the past decade. Targeting CAIX, both, by genetic depletion and using small molecule inhibitors, has elucidated the importance of CAIX in tumor growth *in vivo* (Lou et al., 2011). In addition to its role in tumor growth, CAIX plays a crucial role in metastasis (Lou et al., 2011; Gieling et al., 2012; Chafe et al., 2015). Before the cancer cells metastasize to a distant site, they establish a conducive microenvironment for their survival, called the pre-metastatic niche. CAIX promotes granulocyte colony-stimulating factor (G-CSF) production by hypoxic breast cancer cells, which helps in the mobilization of granulocytic myeloid-derived suppressor cells to lung metastatic niche and primes for metastasis (Chafe et al., 2015). Furthermore, CAIX helps in the maintenance of stemness in cancer stem cells and favor metastasis (Lock et al., 2013; Gibadulinova et al., 2020; Peppicelli et al., 2020). While it is evident that CAIX is important in mediating various steps in tumor progression, the underlying mechanisms remain unclear. Considering the importance of CAIX in the hypoxic microenvironment, it is plausible that CAIX interacts with other proteins in tumor cells to mediate various functions. Hence, we recently conducted a comprehensive, unbiased study to identify the protein interactome of CAIX using the proximity-dependent biotinylation labeling technique called the BioID method (Roux et al., 2012). This study identified over 140 high confidence protein interactors of CAIX (Swayampakula et al., 2017). In this mini review, we will focus on the amino acid transporters (AATs) and acid/base transporters that were identified as high confidence interactors.

CAIX AND PH REGULATION

Active metabolism within tumor cells leads to the accumulation of acidic metabolic by-products, which, if unbuffered, will be lethal to the tumor cells. Therefore, tumor cells deploy several membrane acid/base transporters (pH regulators) to establish a favorable pH within the tumor cells (Neri and Supuran, 2011). Two major acidic metabolic by-products that are produced by tumor cells are CO_2 and lactic acid (Corbet and Feron, 2017). While CO_2 is predominantly produced as a by-product of aerobic respiration, lactic acid production is a result of anaerobic respiration or aerobic glycolysis in tumor cells. The CO_2 generated by tumor cells acts as a substrate for CAs, to produce bicarbonate and protons. Lactic acid, on the other hand, is extruded out of the cells by monocarboxylate transporters (MCT) as lactate and protons, or buffered intracellular by bicarbonate ions to produce CO_2 (Sun et al., 2020). The contribution of CO_2 and lactic acid in defining the intratumoral pH will depend on factors such as oxygenation and mitochondrial respiration in tumor cells. In deep hypoxic zones of a tumor, the mitochondrial respiration is impeded, and therefore, glycolysis becomes the primary state of metabolism (Corbet and Feron, 2017). Conversely, in moderately hypoxic zones of the tumor, the lactate that is released by surrounding anaerobic cells or Gln imported into cells can feed the TCA cycle and drive oxidative phosphorylation (Corbet and Feron, 2017; Faubert et al., 2017). Using tumor spheroids, Swietach et al. (2009, 2010) demonstrated that in spheroids of up to 300 um in size, CO_2 released by the mitochondria acts as a major substrate for CAIX activity rather than lactic acid accumulation. The source of CO_2 can either be from the tumor cells or can be provided to anaerobic regions by surrounding aerobic cells.

Carbonic anhydrase IX establishes a pH gradient of alkaline intracellular pH and acidic extracellular pH in tumor cells that helps in survival and tumor growth (Chiche et al., 2009). Maintenance of intracellular pH by CAIX is critical to support glycolysis and help cancer cells to adapt under hypoxia (Benej et al., 2020). Numerous studies have shown that CAs associate with acid/base transporters to form a temporary complex called transport metabolon (Deitmer and Becker, 2013). CAs form a transport metabolon with MCTs to effectively shuttle the protons from and to MCT, and enhance its activity (Klier et al.,

2014). In CAIX, the 18 Glu and 8 Asp residues in the PG domain have been proposed to act as proton antenna or proton collectors (Ames et al., 2018), whereas the His200 in the catalytic domain facilitates the proton shuttle from the catalytic center into surrounding space, and support MCT activity (Jamali et al., 2015). Another important transport metabolon in the context of CAIX is the bicarbonate metabolon that involves the association of CAIX with bicarbonate transporters. CAIX co-localizes and functionally cooperates with the bicarbonate transporter, NbCe1 (SLC4A4), in the invadopodia to achieve an alkaline pH that promotes invadopodia formation (Debreova et al., 2019). Additionally, CAIX interacts with matrix metalloproteinase 14 (MMP14) in invadopodia. MMP14 is a proteolytic enzyme that degrades the extracellular matrix (ECM) and its activation is important for invadopodial function. The association of CAIX with MMP14 provides protons for MMP14 activation and therefore helps in the invadopodial function (Swayampakula et al., 2017). The increased MMP14 activity, coupled with the intracellular alkalinization within the invadopodia, aids in invadopodia elongation and therefore in tumor cell invasion.

The sodium-bicarbonate transporter, NBCn1 (also known as SLC4A7) is a high confidence interactor of CAIX that emerged in the BioID study. Genome-wide association studies have shown NBCn1 to be a causative gene in breast cancer (Ahmed et al., 2009). NBCn1 functions as an acid extruder and creates a favorable pH gradient in tumors (Boedtkjer et al., 2013; Lee et al., 2016). Furthermore, loss of function studies by the genetic depletion of NBCn1 has elucidated its role in tumor growth (Lee et al., 2016) and cell cycle progression (Flinck et al., 2018). Considering the importance of this bicarbonate transporter in regulating pH in tumor cells, it may mediate an important function by forming a bicarbonate metabolon with CAIX. However, to this date, the role of this interaction remains uninvestigated.

CAIX AND AMINO ACID TRANSPORT

Hypoxic zones in the tumor have a restricted supply of nutrients and therefore continually adapt to metabolize various nutrients to maintain their biologic functions (Samanta and Semenza, 2018). Amino acids are a major source of carbon and nitrogen for the biosynthesis of various macromolecules (**Figure 1**). In this section, we will discuss three AATs that were identified as potential interactors of CAIX from the BioID screen (**Table 1**). We will describe the role and regulation of these transporters in cancer, and then discuss how these transporters may work coordinatively with CAIX in the hypoxic TME.

ASCT2

The Alanine Serine Cysteine Transporter 2 (ASCT2) aka SLC1A5, is a plasma membrane amino acid transporter that mediates sodium-dependent antiport of neutral amino acids. Despite what the name suggests, ASCT2 preferentially transports glutamine, while cysteine acts as a modulator of the transport (Utsunomiya-Tate et al., 1996; Scalise et al., 2018). ASCT2 is a trimeric protein comprising a scaffold domain that enables the interaction between protomers, and a transport domain that helps in the amino acid transport (Garaeva et al., 2018). As one of the major glutamine transporters in cells, ASCT2 is ubiquitously expressed across various tissues in the body and plays a crucial role in mediating cellular functions such as hematopoietic stem cell differentiation (Oburoglu et al., 2014) and T-cell activation (Nakaya et al., 2014; Poffenberger et al., 2014). Increased expression of ASCT2 is observed in several cancer types and is associated with poor prognosis (Witte et al., 2002; Shimizu et al., 2014; Kaira et al., 2015b; Liu et al., 2015; Sun et al., 2016; Bernhardt et al., 2017). The upregulated cellular expression of ASCT2 in cancer is mediated by oncogenic signals such as Kirsten rat sarcoma (K-Ras) (Toda et al., 2017) and myelocytomatosis (N-Myc) (Ren et al., 2015). K-Ras plays an important role in mediating various growth signaling pathways in cells. Mutation in K-Ras is shown to upregulate the expression of ASCT2 and promote cell proliferation in colorectal cancer (Toda et al., 2017). N-Myc, on the other hand, is a transcription factor that drives the expression of genes involved in cell proliferation. Ren et al. (2015) showed N-Myc to upregulate ASCT2 expression by directly binding to its promoter region. In addition to oncogenic signals, cellular stress such as amino acid starvation can also upregulate ASCT2 expression. Under amino acid deprivation, a stress response transcription factor called activating transcription factor 4 (ATF4) binds to ASCT2 promoter and increases ASCT2 expression (Ren et al., 2015). Functional studies using *in vitro* and *in vivo* models have shown ASCT2 inhibition to effectively reduce tumor growth in various types of cancer (van Geldermalsen et al., 2016; Marshall et al., 2017; Ye et al., 2018) by attenuating the mechanistic Target of Raptor (mTOR) signaling pathway (**Figure 1**; Wang et al., 2014, 2015). Furthermore, ASCT2 has been shown to facilitate Gln uptake in cancer stem cells and promote tumor growth in pancreatic ductal adenocarcinoma (PDAC) (Wang V.M. et al., 2019). Based on this evidence, it can be concluded that ASCT2 plays an important role in tumorigenesis and is an attractive candidate to target cancer. Over the years, several drug candidates to target ASCT2 have been discovered. However, identifying drugs that selectively target ASCT2 has been a challenge due to limited structural studies until recently (Jiang et al., 2020). The recent development of an antagonist, V9302 by Schulte et al. (2018) has shown promise in targeting ASCT2 (Scopelliti et al., 2018).

SNAT2

Sodium coupled neutral amino acid transporter 2 (SNAT2) aka SLC38A2, mediates uniport of neutral amino acids including glutamine in a sodium-dependent manner (Mackenzie and Erickson, 2004). It comprises of 11 hydrophobic membrane-spanning domains with an extracellular C-terminus and an intracellular N-terminus (Ge et al., 2018). SNAT2 expression is regulated by extracellular amino acid. Under amino acid deprivation, the global translation is halted, with a concomitant increase in the ATF4 translation. The binding of ATF4 to the amino acid response element (AARE) on the SNAT2 promoter increases SNAT2 expression (Palii et al., 2006). Conversely, SNAT2 can sense the presence of amino acids such as Tyr and Gln, and inhibit its expression (Hyde et al., 2007; Hundal

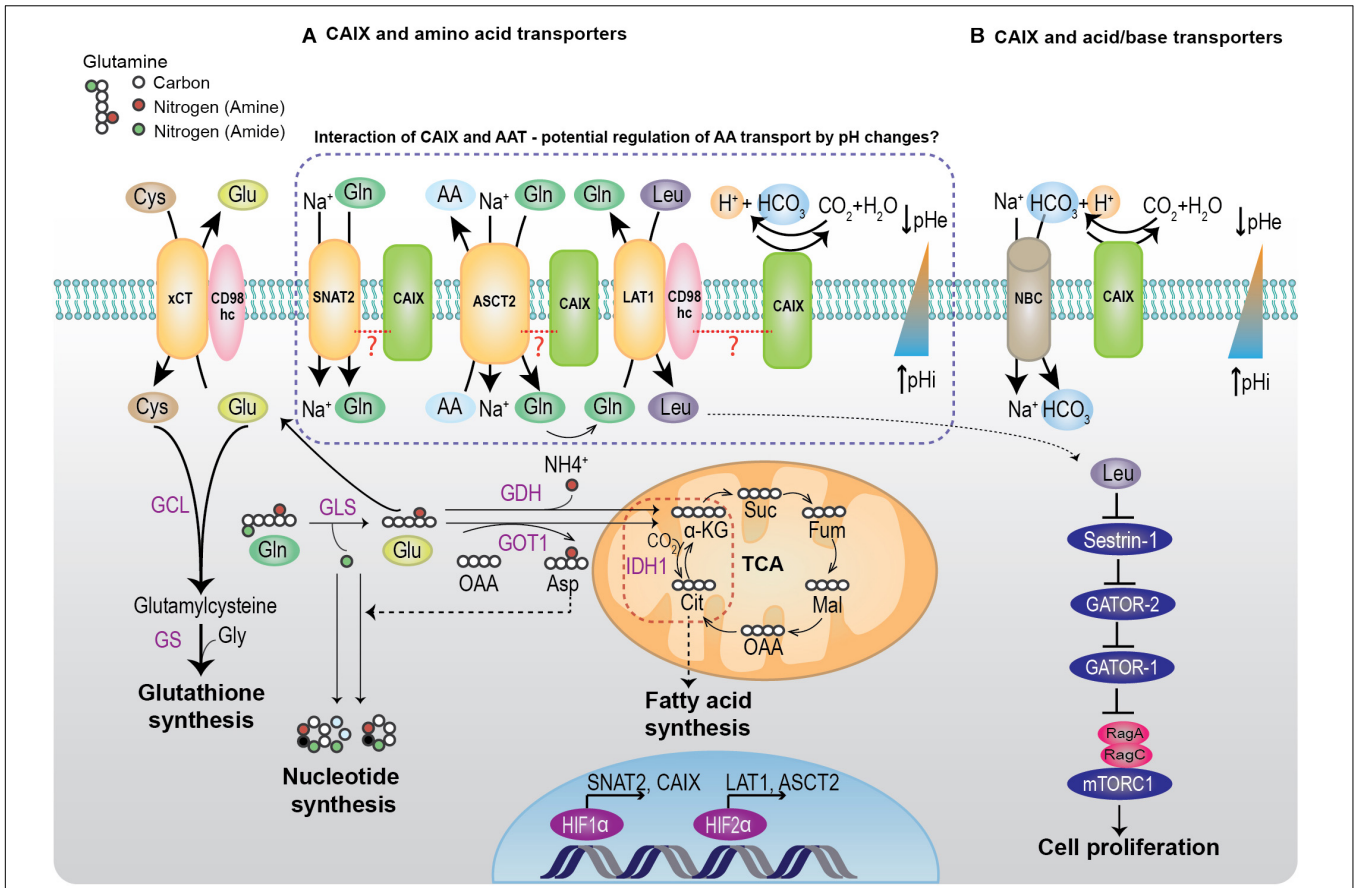

FIGURE 1 | Interaction of CAIX with amino acid transporters and acid/base regulators from BioID. **(A)** Under hypoxia or low amino acid conditions, cells upregulate the expression of SNAT2 and ASCT2 to increase Gln uptake. Normally, Gln can be utilized for biosynthetic reactions such as nucleotide synthesis, bioenergetic reactions by entering the TCA, or for REDOX reactions by glutathione synthesis. Under hypoxia, Gln is utilized for fatty acid synthesis by the reductive carboxylation of α-KG to citrate by IDH1. Alternatively, the intracellular glutamine can be utilized for importing essential amino acids such as leucine, by coupling the transport activity of ASCT2 with LAT1. The imported leucine can bind to a leucine sensor, Sestrin2, removing its inhibitory effect on the RagA/B and activate mTORC1 (Wolfson et al., 2016). The activated mTORC1 promotes protein translation and cell proliferation. **(B)** Hypoxic cells upregulate CAs, MCTs, and acid/base transporters to buffer the intracellular pH changes that occur due to the accumulation of metabolic acids such as CO_2 and lactic acid (see text). CAIX mediates the reversible conversion of CO_2 to proton and bicarbonate. This reaction is coupled with the bicarbonate import through NBC, thereby creating a pH gradient of alkaline intracellular pH and acidic extracellular pH that is favorable for cell survival and growth. xCT, cysteine/glutamate transporter; SNAT2, sodium coupled neutral amino acid transporter; ASCT2, alanine serine cysteine transporter 2; LAT1, L-type amino acid transporter; CAIX, carbonic anhydrase IX; NBC, sodium coupled bicarbonate transporter; GLS, glutaminase; GDH, glutamate dehydrogenase; GOT, glutamic oxaloacetic transaminase; GCL, glutamate-cysteine ligase; GS, glutathione synthase; IDH1, Isocitrate dehydrogenase 1.

TABLE 1 | List of potential CAIX interactors with role in nutrient or metabolite transport function from the BioID.

Functional class	Gene symbol	Gene name	Biological role
Amino acid transporters	SLC3A2 or CD98hc	Solute carrier family 3 member 2 or Cluster differentiation 98 heavy chain	Amino acid transport heavy chain subunit. Forms a complex with light chain subunit to create functional heteromeric amino acid transporter
	SLC7A5 or LAT1	Solute carrier family 7 member 5 or L-type amino acid transporter 1	Sodium independent transport of large neutral amino acids such as Leu, Ile, Val, His, Met, Trp, and Phe Tyr (Kanai et al., 1998)
	SLC1A5 or ASCT2	Solute carrier family 1 member 5, ASCT2 or Alanine Serine Cysteine transporter 2	Sodium-dependent transport of neutral amino acids such as Glu, Gln, Ala, Ser, Thr, Val, and Gly (Utsunomiya-Tate et al., 1996)
	SLC38A2 or SNAT2	Solute carrier family 38 member 2 or Sodium coupled neutral amino acid transporter 2	Sodium-dependent transport of neutral amino acids such as Ala, Gln, Ser, Met, Asn, Cys, Gly, His, and Pro (Mackenzie and Erickson, 2004)
Acid/base transporter	SLC4A7 or NBCn1	Solute carrier family 4 member 7 or Sodium bicarbonate cotransporter 3	Sodium bicarbonate cotransport

and Taylor, 2009). Besides extracellular amino acid, SNAT2 expression is regulated by endoplasmic reticulum stress (ERS). In breast cancer cells, paclitaxel-induced ERS causes a ubiquitin ligase, RNFα to associate with SNAT2 and ASCT2, and cause their degradation. This leads to decreased Gln uptake, decreased proliferation, and increased cell death in the tumor cells (Jeon et al., 2015; Moses and Neckers, 2015). Studies from Broer's group have elucidated that SNAT2 expression increases upon the disruption of ASCT2 transporter activity (Broer et al., 2016, 2019), thereby classifying SNAT2 as a rescue transporter. In addition to its role as a Gln transporter, SNAT2 has shown to play an important role in transporting Ala into PDAC cells from the surrounding pancreatic stellate cells (Parker et al., 2020). Furthermore, genetic depletion of SNAT2 in PDAC cells decreases the Ala uptake and reduce tumor growth *in vivo* (Parker et al., 2020). These studies highlight the importance of SNAT2 in cancer, however, the clinical relevance of this transporter in cancers remains unexplored.

LAT1

The L-type amino acid transporter (LAT1) aka SLC7A5, is a heterodimeric amino acid transporter that mediates a sodium independent antiport of neutral essential amino acids (Kanai et al., 1998; Wagner et al., 2001). It comprises a heavy chain subunit called cluster differentiation 98 (CD98hc) that associates with a light chain subunit such as LAT1. The heavy chain consists of an extracellular C-terminus, a transmembrane helix, and an intracellular NH2 terminus. The light chain, on the other hand, has 12 transmembrane domains with both COOH and the NH2 termini facing the intracellular space (Yan et al., 2019). While LAT1 is expressed across various tissues, it is highly expressed at the blood-brain barrier and functions in amino acid transport to the brain (Boado et al., 1999). The importance of LAT1 in tumor growth was elucidated by Cormerais et al., using knock out models for LAT1 and CD98hc. This study showed the genetic disruption of LAT1 to decrease leucine uptake and inhibit mTORC1, causing decreased tumor growth *in vivo*. N-Myc upregulates LAT1 expression by directly binding to the promoter region of LAT1. The resulting amino acid uptake promotes the sustained translation of Myc, thereby working in a feed-forward loop that helps in tumorigenesis (Yue et al., 2017). LAT1 expression is associated with poor prognosis (Kaira et al., 2015a; Shimizu et al., 2015) and resistance to chemotherapy in solid tumors (Altan et al., 2018). Downregulation of LAT1 has been shown to decrease cell growth (Marshall et al., 2016) invasion, and migration (Janpipatkul et al., 2014). Targeting LAT1 using a small molecule inhibitor, JPH203 has shown success in pre-clinical trials and was recently evaluated in clinical phase trial 1. Although the sample size was low in this clinical trial, the drug was well tolerated and showed promise in targeting LAT1 in patients with advanced solid tumors (Okano et al., 2018).

Potential Role of CAIX in Amino Acid Transport Regulation

As discussed above, AATs play important roles in promoting tumor progression, and their interaction with CAIX suggests an important mode of functional regulation that requires further investigation.

It is well-known that Gln is an important amino acid in cancer metabolism and several cancer types rely on Gln, which is called Gln addiction (Wise and Thompson, 2010). In hypoxic tumor cells, Gln is channeled for lipid biosynthesis to support cell proliferation (**Figure 1**). This process is mediated by the reductive carboxylation of α-ketoglutarate (α-KG) to citrate, and the subsequent entry of citrate into lipogenesis (Metallo et al., 2011). Furthermore, it is shown that Gln carbon and nitrogen are efficiently metabolized to support lipid biosynthesis under hypoxia (Wang Y. et al., 2019). The glutamine transporter SNAT2 is upregulated under hypoxia (Morotti et al., 2019) and support glutamine uptake in cancer cells. Interestingly, studies have shown that SNAT2 compensates for the loss of function of ASCT2 (Broer et al., 2019). Moreover, ASCT2 and LAT1 function as obligatory transporters, in which, the influx through one transporter is coupled to the efflux through the second transporter (Nicklin et al., 2009). These data suggest that these three AATs work cooperatively in the TME to promote cancer progression (**Figure 1**). To our knowledge, there is no existing evidence in the literature on the functional role of CAIX in AA transport, although the identification of potential interactions between CAIX and these AATs suggests that reciprocal functional regulations may be important hallmarks for tumor progression. Considering the pivotal role of CAIX in pH regulation, it is probable that the pH gradient mediated by CAIX in the tumor could influence the function of these AATs. In fact, the transport function of these AATs are influenced by pH, however, the effects are different. The amino acid transport by SNAT2 is sensitive to extracellular pH, where increased extracellular protons compete with sodium ions and impede the SNAT2 activity. This pH sensitivity of SNAT2 is shown to be mediated by the presence of His residues at the C-terminus (Baird et al., 2006). In contrast, glutamine transport by ASCT2 is not hugely influenced by pH (Utsunomiya-Tate et al., 1996). However, ASCT2 also mediates Glu antiport, and this is highly pH-dependent (Utsunomiya-Tate et al., 1996). At a pH gradient of low extracellular pH (6.0) and high intracellular pH (7.0), the Glu influx increased in proteoliposomes containing ASCT2 (Scalise et al., 2020). In addition to altering the transport by ASCT2, changes in pH has shown to impact the expression of ASCT2. Under chronic acidosis, ASCT2 is upregulated by HIF2α and cause a shift in the cancer cell metabolism to favor reductive glutamine metabolism (Corbet et al., 2014). These studies suggest that the pH gradient across the tumor could influence the function of AATs, however, whether CAIX's pH regulatory role influences the coordinative interplay of these AATs remains a topic of future investigation. Investigating the effect of loss of function of CAIX on amino acid transport and metabolism could reveal the importance of CAIX's interaction with the AATs. Such studies could be of importance in highly aggressive cancers like pancreatic cancer that have complex metabolic network (Sperb et al., 2020) and are difficult to treat. CAIX expression (Strapcova et al., 2020) and its function in altering tumoral pH (Cruz-Monserrate et al., 2014) are shown to be important in the early events of pancreatic carcinogenesis. Furthermore, ASCT2 and SNAT2 play an important role in

importing AA in pancreatic cancer, as described earlier in this section. Therefore, it is plausible that CAIX and AATs coordinate their functions to support tumor metabolism and promote pancreatic cancer progression.

One of the interesting findings of the BioID CAIX interactome (Swayampakula et al., 2017) was the potential interaction of LAT1 and CD98hc with CAIX. Modulation of LAT1 function and transport of neutral amino acids by CAIX, perhaps in the context of complexes with integrins, which also associate with CD98hc (Fenczik et al., 2001; Feral et al., 2005), may have significant effects on cellular growth through the regulation of protein translation by mTORC1. While this possibility needs to be investigated in further detail, it is interesting that inhibition of CAIX modulates mTORC1 signaling in breast cancer cells grown in 3D cultures (Lock et al., 2013).

CONCLUSION

Since the seminal findings of Otto Warburg on altered metabolism in cancer, the concept of metabolic reprogramming in cancer has evolved and led to a better understanding of the complex nature of cancer metabolism (Martinez-Outschoorn et al., 2017). Research on the role of metabolite transport has progressed tremendously and unraveled the importance of numerous nutrient and acid/base transporters in the TME (Ganapathy et al., 2009; Bhutia et al., 2015; Becker and Deitmer, 2020). Understanding the interaction of these metabolic proteins in the TME would be beneficial in identifying novel targets for effective therapy. Based on our interactome study, we identified the potential interaction of nutrient transporters and acid/base transporters with CAIX in the hypoxic TME. CAIX is an important pH regulatory protein in the TME that mediates tumor progression in several solid tumors. The CAIX/CAXII specific small-molecule inhibitor, SLC-0111 (Pacchiano et al., 2011; Supuran, 2018) has shown promising effect on suppressing tumor growth and metastasis by itself and in combination with conventional chemotherapeutic drugs (Boyd et al., 2017; McDonald et al., 2019) or immune checkpoint inhibitors (Chafe et al., 2019). Currently, SLC-0111 has completed the Phase-I clinical trial and progressed into a Phase-Ib trial (ClinicalTrials.gov Identifier: NCT03450018) in combination with gemcitabine in CAIX-positive pancreatic cancer patients (McDonald et al., 2020).Furthermore, recent studies have shown that the metabolic plasticity in solid tumors offers adaptation and resistance to single therapy strategies by initiating compensatory mechanisms, however, this is effectively overcome by combinatorial therapy (Biancur et al., 2017; Momcilovic et al., 2018). Therefore, investigating the interaction of CAIX with these nutrient transporters might open new avenues of co-targeting strategies for the treatment of solid tumors.

AUTHOR CONTRIBUTIONS

GV and SD conceived and designed the manuscript and revised and approved the final manuscript. GV drafted the manuscript. Both authors contributed to the article and approved the submitted version.

FUNDING

This work was supported by grants to SD from the Canadian Cancer Society Research Institute (CCSRI Grant # 703191), the Canadian Institutes of Health Research (CIHR Grant # FDN-143318) as well as funding from Pancreas Centre BC and the BC Cancer Foundation.

REFERENCES

Ahmed, S., Thomas, G., Ghoussaini, M., Healey, C. S., Humphreys, M. K., Platte, R., et al. (2009). Newly discovered breast cancer susceptibility loci on 3p24 and 17q23.2. *Nat. Genet.* 41, 585–590. doi: 10.1038/ng.354

Altan, B., Kaira, K., Watanabe, A., Kubo, N., Bao, P., Dolgormaa, G., et al. (2018). Relationship between LAT1 expression and resistance to chemotherapy in pancreatic ductal adenocarcinoma. *Cancer Chemother. Pharmacol.* 81, 141–153. doi: 10.1007/s00280-017-3477-4

Alterio, V., Di Fiore, A., D'Ambrosio, K., Supuran, C. T., and De Simone, G. (2012). Multiple binding modes of inhibitors to carbonic anhydrases: how to design specific drugs targeting 15 different isoforms? *Chem. Rev.* 112, 4421–4468. doi: 10.1021/cr200176r

Alterio, V., Hilvo, M., Di Fiore, A., Supuran, C. T., Pan, P., Parkkila, S., et al. (2009). Crystal structure of the catalytic domain of the tumor-associated human carbonic anhydrase IX. *Proc. Natl. Acad. Sci.* 106:16233. doi: 10.1073/pnas.0908301106

Ames, S., Pastorekova, S., and Becker, H. M. (2018). The proteoglycan-like domain of carbonic anhydrase IX mediates non-catalytic facilitation of lactate transport in cancer cells. *Oncotarget* 9, 27940–27957. doi: 10.18632/oncotarget.25371

Baird, F. E., Pinilla-Tenas, J. J., Ogilvie, W. L. J., Ganapathy, V., Hundal, H. S., and Taylor, P. M. (2006). Evidence for allosteric regulation of pH-sensitive System A (SNAT2) and System N (SNAT5) amino acid transporter activity involving a conserved histidine residue. *Biochem. J.* 397, 369–375. doi: 10.1042/BJ20060026

Becker, H. M., and Deitmer, J. W. (2020). Transport Metabolons and Acid/Base Balance in Tumor Cells. *Cancers* 12:899. doi: 10.3390/cancers12040899

Benej, M., Svastova, E., Banova, R., Kopacek, J., Gibadulinova, A., Kery, M., et al. (2020). CA IX Stabilizes Intracellular pH to Maintain Metabolic Reprogramming and Proliferation in Hypoxia. *Front. Oncol.* 10:1462. doi: 10.3389/fonc.2020.01462

Bernhardt, S., Bayerlova, M., Vetter, M., Wachter, A., Mitra, D., Hanf, V., et al. (2017). Proteomic profiling of breast cancer metabolism identifies SHMT2 and ASCT2 as prognostic factors. *Breast Cancer Res.* 19:112. doi: 10.1186/s13058-017-0905-7

Bhutia, Y. D., Babu, E., Ramachandran, S., and Ganapathy, V. (2015). Amino Acid transporters in cancer and their relevance to "glutamine addiction": novel targets for the design of a new class of anticancer drugs. *Cancer Res.* 75, 1782–1788. doi: 10.1158/0008-5472.Can-14-3745

Biancur, D. E., Paulo, J. A., Malachowska, B., Quiles Del, Rey, M., Sousa, C. M., et al. (2017). Compensatory metabolic networks in pancreatic cancers upon perturbation of glutamine metabolism. *Nat. Commun.* 8:15965. doi: 10.1038/ncomms15965

Boado, R. J., Li, J. Y., Nagaya, M., Zhang, C., and Pardridge, W. M. (1999). Selective expression of the large neutral amino acid transporter at the blood-brain barrier. *Proc. Natl. Acad. Sci. U S A* 96, 12079–12084. doi: 10.1073/pnas.96.21.12079

Boedtkjer, E., Moreira, J. M., Mele, M., Vahl, P., Wielenga, V. T., Christiansen, P. M., et al. (2013). Contribution of Na+,HCO3(-)-cotransport to cellular pH

control in human breast cancer: a role for the breast cancer susceptibility locus NBCn1 (SLC4A7). *Int. J. Cancer* 132, 1288–1299. doi: 10.1002/ijc.27782

Boyd, N. H., Walker, K., Fried, J., Hackney, J. R., McDonald, P. C., Benavides, G. A., et al. (2017). Addition of carbonic anhydrase 9 inhibitor SLC-0111 to temozolomide treatment delays glioblastoma growth in vivo. *JCI Insight* 2:e92928. doi: 10.1172/jci.insight.92928

Briggs, K. J., Koivunen, P., Cao, S., Backus, K. M., Olenchock, B. A., Patel, H., et al. (2016). Paracrine Induction of HIF by Glutamate in Breast Cancer: EglN1 Senses Cysteine. *Cell* 166, 126–139. doi: 10.1016/j.cell.2016.05.042

Broer, A., Gauthier-Coles, G., Rahimi, F., van Geldermalsen, M., Dorsch, D., Wegener, A., et al. (2019). Ablation of the ASCT2 (SLC1A5) gene encoding a neutral amino acid transporter reveals transporter plasticity and redundancy in cancer cells. *J. Biol. Chem.* 294, 4012–4026. doi: 10.1074/jbc.RA118.006378

Broer, A., Rahimi, F., and Broer, S. (2016). Deletion of Amino Acid Transporter ASCT2 (SLC1A5) Reveals an Essential Role for Transporters SNAT1 (SLC38A1) and SNAT2 (SLC38A2) to Sustain Glutaminolysis in Cancer Cells. *J. Biol. Chem.* 291, 13194–13205. doi: 10.1074/jbc.M115.700534

Chafe, S. C., Lou, Y., Sceneay, J., Vallejo, M., Hamilton, M. J., McDonald, P. C., et al. (2015). Carbonic anhydrase IX promotes myeloid-derived suppressor cell mobilization and establishment of a metastatic niche by stimulating G-CSF production. *Cancer Res.* 75, 996–1008. doi: 10.1158/0008-5472.can-14-3000

Chafe, S. C., McDonald, P. C., Saberi, S., Nemirovsky, O., Venkateswaran, G., Burugu, S., et al. (2019). Targeting Hypoxia-Induced Carbonic Anhydrase IX Enhances Immune-Checkpoint Blockade Locally and Systemically. *Cancer Immunol. Res.* 7, 1064–1078. doi: 10.1158/2326-6066.Cir-18-0657

Chia, S. K., Wykoff, C. C., Watson, P. H., Han, C., Leek, R. D., Pastorek, J., et al. (2001). Prognostic significance of a novel hypoxia-regulated marker, carbonic anhydrase IX, in invasive breast carcinoma. *J. Clin. Oncol.* 19, 3660–3668. doi: 10.1200/jco.2001.19.16.3660

Chiche, J., Ilc, K., Laferriere, J., Trottier, E., Dayan, F., Mazure, N. M., et al. (2009). Hypoxia-inducible carbonic anhydrase IX and XII promote tumor cell growth by counteracting acidosis through the regulation of the intracellular pH. *Cancer Res.* 69, 358–368. doi: 10.1158/0008-5472.Can-08-2470

Corbet, C., Draoui, N., Polet, F., Pinto, A., Drozak, X., Riant, O., et al. (2014). The SIRT1/HIF2alpha axis drives reductive glutamine metabolism under chronic acidosis and alters tumor response to therapy. *Cancer Res.* 74, 5507–5519. doi: 10.1158/0008-5472.can-14-0705

Corbet, C., and Feron, O. (2017). Tumour acidosis: from the passenger to the driver's seat. *Nat. Rev. Cancer* 17, 577–593. doi: 10.1038/nrc.2017.77

Cruz-Monserrate, Z., Roland, C. L., Deng, D., Arumugam, T., Moshnikova, A., Andreev, O. A., et al. (2014). Targeting pancreatic ductal adenocarcinoma acidic microenvironment. *Sci. Rep.* 4:4410. doi: 10.1038/srep04410

Debreova, M., Csaderova, L., Burikova, M., Lukacikova, L., Kajanova, I., Sedlakova, O., et al. (2019). CAIX Regulates Invadopodia Formation through Both a pH-Dependent Mechanism and Interplay with Actin Regulatory Proteins. *Int. J. Mol. Sci.* 20:2745 doi: 10.3390/ijms20112745

Deitmer, J., and Becker, H. (2013). Transport metabolons with carbonic anhydrases. *Front. Physiol.* 4:291 doi: 10.3389/fphys.2013.00291

DeNicola, G. M., and Cantley, L. C. (2015). Cancer's Fuel Choice: New Flavors for a Picky Eater. *Mol. Cell* 60, 514–523. doi: 10.1016/j.molcel.2015.10.018

Faubert, B., Li, K. Y., Cai, L., Hensley, C. T., Kim, J., Zacharias, L. G., et al. (2017). Lactate Metabolism in Human Lung Tumors. *Cell* 171:358.e–371.e. doi: 10.1016/j.cell.2017.09.019

Fenczik, C. A., Zent, R., Dellos, M., Calderwood, D. A., Satriano, J., Kelly, C., et al. (2001). Distinct domains of CD98hc regulate integrins and amino acid transport. *J. Biol. Chem.* 276, 8746–8752. doi: 10.1074/jbc.M011239200

Feral, C. C., Nishiya, N., Fenczik, C. A., Stuhlmann, H., Slepak, M., and Ginsberg, M. H. (2005). CD98hc (SLC3A2) mediates integrin signaling. *Proc. Natl. Acad. Sci. U S A* 102, 355–360. doi: 10.1073/pnas.0404852102

Flinck, M., Kramer, S. H., Schnipper, J., Andersen, A. P., and Pedersen, S. F. (2018). The acid-base transport proteins NHE1 and NBCn1 regulate cell cycle progression in human breast cancer cells. *Cell Cycle* 17, 1056–1067. doi: 10.1080/15384101.2018.1464850

Ganapathy, V., Thangaraju, M., and Prasad, P. D. (2009). Nutrient transporters in cancer: relevance to Warburg hypothesis and beyond. *Pharmacol. Ther.* 121, 29–40. doi: 10.1016/j.pharmthera.2008.09.005

Garaeva, A. A., Oostergetel, G. T., Gati, C., Guskov, A., Paulino, C., and Slotboom, D. J. (2018). Cryo-EM structure of the human neutral amino acid transporter ASCT2. *Nat. Struct. Mol. Biol.* 25, 515–521. doi: 10.1038/s41594-018-0076-y

Ge, Y., Gu, Y., Wang, J., and Zhang, Z. (2018). Membrane topology of rat sodium-coupled neutral amino acid transporter 2 (SNAT2). *Biochim. Biophy. Acta Biomembr.*1860, 1460–1469. doi: 10.1016/j.bbamem.2018.04.005

Generali, D., Fox, S. B., Berruti, A., Brizzi, M. P., Campo, L., Bonardi, S., et al. (2006). Role of carbonic anhydrase IX expression in prediction of the efficacy and outcome of primary epirubicin/tamoxifen therapy for breast cancer. *Endocr. Relat. Cancer* 13, 921–930. doi: 10.1677/erc.1.01216

Gibadulinova, A., Bullova, P., Strnad, H., Pohlodek, K., Jurkovicova, D., Takacova, M., et al. (2020). CAIX-Mediated Control of LIN28/let-7 Axis Contributes to Metabolic Adaptation of Breast Cancer Cells to Hypoxia. *Int. J. Mol. Sci.* 21:4299. doi: 10.3390/ijms21124299

Gieling, R. G., Babur, M., Mamnani, L., Burrows, N., Telfer, B. A., Carta, F., et al. (2012). Antimetastatic effect of sulfamate carbonic anhydrase IX inhibitors in breast carcinoma xenografts. *J. Med. Chem.* 55, 5591–5600. doi: 10.1021/jm300529u

Hundal, H. S., and Taylor, P. M. (2009). Amino acid transceptors: gate keepers of nutrient exchange and regulators of nutrient signaling. *Am. J. Physiol. Endocrinol. Metab.* 296, E603–E613. doi: 10.1152/ajpendo.91002.2008

Hyde, R., Cwiklinski, E. L., MacAulay, K., Taylor, P. M., and Hundal, H. S. (2007). Distinct sensor pathways in the hierarchical control of SNAT2, a putative amino acid transceptor, by amino acid availability. *J. Biol. Chem.* 282, 19788–19798. doi: 10.1074/jbc.M611520200

Ilie, M., Mazure, N. M., Hofman, V., Ammadi, R. E., Ortholan, C., Bonnetaud, C., et al. (2010). High levels of carbonic anhydrase IX in tumour tissue and plasma are biomarkers of poor prognostic in patients with non-small cell lung cancer. *Br. J. Cancer* 102, 1627–1635. doi: 10.1038/sj.bjc.6605690

Jamali, S., Klier, M., Ames, S., Felipe Barros, L., McKenna, R., Deitmer, J. W., et al. (2015). Hypoxia-induced carbonic anhydrase IX facilitates lactate flux in human breast cancer cells by non-catalytic function. *Sci. Rep.* 5:13605. doi: 10.1038/srep13605

Janpipatkul, K., Suksen, K., Borwornpinyo, S., Jearawiriyapaisarn, N., Hongeng, S., Piyachaturawat, P., et al. (2014). Downregulation of LAT1 expression suppresses cholangiocarcinoma cell invasion and migration. *Cell Signal* 26, 1668–1679. doi: 10.1016/j.cellsig.2014.04.002

Jeon, Y. J., Khelifa, S., Ratnikov, B., Scott, D. A., Feng, Y., Parisi, F., et al. (2015). Regulation of glutamine carrier proteins by RNF5 determines breast cancer response to ER stress-inducing chemotherapies. *Cancer Cell* 27, 354–369. doi: 10.1016/j.ccell.2015.02.006

Jiang, H., Zhang, N., Tang, T., Feng, F., Sun, H., and Qu, W. (2020). Target the human Alanine/Serine/Cysteine Transporter 2(ASCT2): Achievement and Future for Novel Cancer Therapy. *Pharmacol. Res.*158:104844. doi: 10.1016/j.phrs.2020.104844

Kaira, K., Nakamura, K., Hirakawa, T., Imai, H., Tominaga, H., Oriuchi, N., et al. (2015a). Prognostic significance of L-type amino acid transporter 1 (LAT1) expression in patients with ovarian tumors. *Am. J. Transl. Res.* 7, 1161–1171.

Kaira, K., Sunose, Y., Arakawa, K., Sunaga, N., Shimizu, K., Tominaga, H., et al. (2015b). Clinicopathological significance of ASC amino acid transporter-2 expression in pancreatic ductal carcinoma. *Histopathology* 66, 234–243. doi: 10.1111/his.12464

Kanai, Y., Segawa, H., Miyamoto, K., Uchino, H., Takeda, E., and Endou, H. (1998). Expression cloning and characterization of a transporter for large neutral amino acids activated by the heavy chain of 4F2 antigen (CD98). *J. Biol. Chem.* 273, 23629–23632. doi: 10.1074/jbc.273.37.23629

Klatte, T., Seligson, D. B., Rao, J. Y., Yu, H., de Martino, M., Kawaoka, K., et al. (2009). Carbonic anhydrase IX in bladder cancer: a diagnostic, prognostic, and therapeutic molecular marker. *Cancer* 115, 1448–1458. doi: 10.1002/cncr.24163

Klier, M., Andes, F. T., Deitmer, J. W., and Becker, H. M. (2014). Intracellular and extracellular carbonic anhydrases cooperate non-enzymatically to enhance activity of monocarboxylate transporters. *J. Biol. Chem.* 289, 2765–2775. doi: 10.1074/jbc.M113.537043

Korkeila, E., Talvinen, K., Jaakkola, P. M., Minn, H., Syrjanen, K., Sundstrom, J., et al. (2009). Expression of carbonic anhydrase IX suggests poor outcome in rectal cancer. *Br. J. Cancer* 100, 874–880. doi: 10.1038/sj.bjc.6604949

Koukourakis, M. I., Giatromanolaki, A., Sivridis, E., Simopoulos, K., Pastorek, J., Wykoff, C. C., et al. (2001). Hypoxia-regulated carbonic anhydrase-9 (CA9)

relates to poor vascularization and resistance of squamous cell head and neck cancer to chemoradiotherapy. *Clin Cancer Res.* 7, 3399–3403.

Lee, S., Axelsen, T. V., Andersen, A. P., Vahl, P., Pedersen, S. F., and Boedtkjer, E. (2016). Disrupting Na(+), HCO(3)(-)-cotransporter NBCn1 (Slc4a7) delays murine breast cancer development. *Oncogene* 35, 2112–2122. doi: 10.1038/onc.2015.273

Liu, Y., Yang, L., An, H., Chang, Y., Zhang, W., Zhu, Y., et al. (2015). High expression of Solute Carrier Family 1, member 5 (SLC1A5) is associated with poor prognosis in clear-cell renal cell carcinoma. *Sci. Rep.* 5:16954. doi: 10.1038/srep16954

Lock, F. E., McDonald, P. C., Lou, Y., Serrano, I., Chafe, S. C., Ostlund, C., et al. (2013). Targeting carbonic anhydrase IX depletes breast cancer stem cells within the hypoxic niche. *Oncogene* 32, 5210–5219. doi: 10.1038/onc.2012.550

Loncaster, J. A., Harris, A. L., Davidson, S. E., Logue, J. P., Hunter, R. D., Wycoff, C. C., et al. (2001). Carbonic anhydrase (CA IX) expression, a potential new intrinsic marker of hypoxia: correlations with tumor oxygen measurements and prognosis in locally advanced carcinoma of the cervix. *Cancer Res.* 61, 6394–6399.

Lou, Y., McDonald, P. C., Oloumi, A., Chia, S., Ostlund, C., Ahmadi, A., et al. (2011). Targeting tumor hypoxia: suppression of breast tumor growth and metastasis by novel carbonic anhydrase IX inhibitors. *Cancer Res.* 71, 3364–3376. doi: 10.1158/0008-5472.can-10-4261

Mackenzie, B., and Erickson, J. D. (2004). Sodium-coupled neutral amino acid (System N/A) transporters of the SLC38 gene family. *Pflugers Arch.* 447, 784–795. doi: 10.1007/s00424-003-1117-9

Marshall, A. D., van Geldermalsen, M., Otte, N. J., Anderson, L. A., Lum, T., Vellozzi, M. A., et al. (2016). LAT1 is a putative therapeutic target in endometrioid endometrial carcinoma. *Int. J. Cancer* 139, 2529–2539. doi: 10.1002/ijc.30371

Marshall, A. D., van Geldermalsen, M., Otte, N. J., Lum, T., Vellozzi, M., Thoeng, A., et al. (2017). ASCT2 regulates glutamine uptake and cell growth in endometrial carcinoma. *Oncogenesis* 6:e367. doi: 10.1038/oncsis.2017.70

Martinez-Outschoorn, U. E., Peiris-Pages, M., Pestell, R. G., Sotgia, F., and Lisanti, M. P. (2017). Cancer metabolism: a therapeutic perspective. *Nat. Rev. Clin. Oncol.* 14, 11–31. doi: 10.1038/nrclinonc.2016.60

Mboge, M. Y., Mahon, B. P., McKenna, R., and Frost, S. C. (2018). Carbonic Anhydrases: Role in pH Control and Cancer. *Metabolites* 8:19 doi: 10.3390/metabo8010019

McDonald, P. C., Chafe, S. C., Brown, W. S., Saberi, S., Swayampakula, M., Venkateswaran, G., et al. (2019). Regulation of pH by Carbonic Anhydrase 9 Mediates Survival of Pancreatic Cancer Cells With Activated KRAS in Response to Hypoxia. *Gastroenterology* 157, 823-837 doi: 10.1053/j.gastro.2019.05.004

McDonald, P. C., Chia, S., Bedard, P. L., Chu, Q., Lyle, M., Tang, L., et al. (2020). A Phase 1 Study of SLC-0111, a Novel Inhibitor of Carbonic Anhydrase IX, in Patients With Advanced Solid Tumors. *Am. J. Clin. Oncol.* 43, 484–490. doi: 10.1097/coc.0000000000000691

McDonald, P. C., and Dedhar, S. (2014). Carbonic anhydrase IX (CAIX) as a mediator of hypoxia-induced stress response in cancer cells. *Subcell. Biochem.* 75, 255–269. doi: 10.1007/978-94-007-7359-2_13

McDonald, P. C., Winum, J. Y., Supuran, C. T., and Dedhar, S. (2012). Recent developments in targeting carbonic anhydrase IX for cancer therapeutics. *Oncotarget* 3, 84–97. doi: 10.18632/oncotarget.422

McIntyre, A., Patiar, S., Wigfield, S., Li, J. L., Ledaki, I., Turley, H., et al. (2012). Carbonic anhydrase IX promotes tumor growth and necrosis in vivo and inhibition enhances anti-VEGF therapy. *Clin. Cancer Res.* 18, 3100–3111. doi: 10.1158/1078-0432.Ccr-11-1877

Metallo, C. M., Gameiro, P. A., Bell, E. L., Mattaini, K. R., Yang, J., Hiller, K., et al. (2011). Reductive glutamine metabolism by IDH1 mediates lipogenesis under hypoxia. *Nature* 481, 380–384. doi: 10.1038/nature10602

Michiels, C., Tellier, C., and Feron, O. (2016). Cycling hypoxia: A key feature of the tumor microenvironment. *Biochim. Biophys. Acta* 1866, 76–86. doi: 10.1016/j.bbcan.2016.06.004

Momcilovic, M., Bailey, S. T., Lee, J. T., Fishbein, M. C., Braas, D., Go, J., et al. (2018). The GSK3 Signaling Axis Regulates Adaptive Glutamine Metabolism in Lung Squamous Cell Carcinoma. *Cancer Cell* 33:905.e–921.e. doi: 10.1016/j.ccell.2018.04.002

Morotti, M., Bridges, E., Valli, A., Choudhry, H., Sheldon, H., Wigfield, S., et al. (2019). Hypoxia-induced switch in SNAT2/SLC38A2 regulation generates endocrine resistance in breast cancer. *Proc. Natl. Acad. Sci. U S A* 116, 12452–12461. doi: 10.1073/pnas.1818521116

Moses, M. A., and Neckers, L. (2015). The GLU that holds cancer together: targeting GLUtamine transporters in breast cancer. *Cancer Cell* 27, 317–319. doi: 10.1016/j.ccell.2015.02.010

Nakaya, M., Xiao, Y., Zhou, X., Chang, J.-H., Chang, M., Cheng, X., et al. (2014). Inflammatory T Cell Responses Rely on Amino Acid Transporter ASCT2 Facilitation of Glutamine Uptake and mTORC1 Kinase Activation. *Immunity* 40, 692–705. doi: 10.1016/j.immuni.2014.04.007

Nakazawa, M. S., Keith, B., and Simon, M. C. (2016). Oxygen availability and metabolic adaptations. *Nat. Rev. Cancer* 16, 663–673. doi: 10.1038/nrc.2016.84

Neri, D., and Supuran, C. T. (2011). Interfering with pH regulation in tumours as a therapeutic strategy. *Nat. Rev. Drug Discov.* 10, 767–777. doi: 10.1038/nrd3554

Nicklin, P., Bergman, P., Zhang, B., Triantafellow, E., Wang, H., Nyfeler, B., et al. (2009). Bidirectional transport of amino acids regulates mTOR and autophagy. *Cell* 136, 521–534. doi: 10.1016/j.cell.2008.11.044

Oburoglu, L., Tardito, S., Fritz, V., de Barros, S. C., Merida, P., Craveiro, M., et al. (2014). Glucose and glutamine metabolism regulate human hematopoietic stem cell lineage specification. *Cell Stem Cell* 15, 169–184. doi: 10.1016/j.stem.2014.06.002

Okano, N., Kawai, K., Yamauchi, Y., Kobayashi, T., Naruge, D., Nagashima, F., et al. (2018). First-in-human phase I study of JPH203 in patients with advanced solid tumors. *Journal of Clinical Oncology* 36, 419–419. doi: 10.1200/JCO.2018.36.4_suppl.419

Opavský, R., Pastoreková, S., Zelnìk, V. R., Gibadulinová, A., Stanbridge, E. J., Závada, J., et al. (1996). HumanMN/CA9Gene, a Novel Member of the Carbonic Anhydrase Family: Structure and Exon to Protein Domain Relationships. *Genomics* 33, 480–487. doi: 10.1006/geno.1996.0223

Pacchiano, F., Carta, F., McDonald, P. C., Lou, Y., Vullo, D., Scozzafava, A., et al. (2011). Ureido-substituted benzenesulfonamides potently inhibit carbonic anhydrase IX and show antimetastatic activity in a model of breast cancer metastasis. *J. Med. Chem.* 54, 1896–1902. doi: 10.1021/jm101541x

Palii, S. S., Thiaville, M. M., Pan, Y. X., Zhong, C., and Kilberg, M. S. (2006). Characterization of the amino acid response element within the human sodium-coupled neutral amino acid transporter 2 (SNAT2) System A transporter gene. *Biochem. J.* 395, 517–527. doi: 10.1042/bj20051867

Panisova, E., Kery, M., Sedlakova, O., Brisson, L., Debreova, M., Sboarina, M., et al. (2017). Lactate stimulates CA IX expression in normoxic cancer cells. *Oncotarget* 8, 77819–77835. doi: 10.18632/oncotarget.20836

Parker, S. J., Amendola, C. R., Hollinshead, K. E. R., Yu, Q., Yamamoto, K., Encarnación-Rosado, J., et al. (2020). Selective Alanine Transporter Utilization Creates a Targetable Metabolic Niche in Pancreatic Cancer. *Cancer Discov.* 10, 1018–1037. doi: 10.1158/2159-8290.Cd-19-0959

Peppicelli, S., Andreucci, E., Ruzzolini, J., Bianchini, F., Nediani, C., Supuran, C. T., et al. (2020). The Carbonic Anhydrase IX inhibitor SLC-0111 as emerging agent against the mesenchymal stem cell-derived pro-survival effects on melanoma cells. *J. Enzyme Inhib. Med. Chem.* 35, 1185–1193. doi: 10.1080/14756366.2020.1764549

Poffenberger, Maya, C., Jones, and Russell, G. (2014). Amino Acids Fuel T Cell-Mediated Inflammation. *Immunity* 40, 635–637. doi: 10.1016/j.immuni.2014.04.017

Ren, P., Yue, M., Xiao, D., Xiu, R., Gan, L., Liu, H., et al. (2015). ATF4 and N-Myc coordinate glutamine metabolism in MYCN-amplified neuroblastoma cells through ASCT2 activation. *J. Pathol.* 235, 90–100. doi: 10.1002/path.4429

Roux, K. J., Kim, D. I., Raida, M., and Burke, B. (2012). A promiscuous biotin ligase fusion protein identifies proximal and interacting proteins in mammalian cells. *J. Cell Biol.* 196, 801–810. doi: 10.1083/jcb.201112098

Samanta, D., and Semenza, G. L. (2018). Metabolic adaptation of cancer and immune cells mediated by hypoxia-inducible factors. *Biochim. Biophy. Acta Rev. Cancer* 1870, 15–22. doi: 10.1016/j.bbcan.2018.07.002

Scalise, M., Mazza, T., Pappacoda, G., Pochini, L., Cosco, J., Rovella, F., et al. (2020). The Human SLC1A5 Neutral Amino Acid Transporter Catalyzes a pH-Dependent Glutamate/Glutamine Antiport, as Well. *Front. Cell Dev. Biol.* 8:603 doi: 10.3389/fcell.2020.00603

Scalise, M., Pochini, L., Console, L., Losso, M. A., and Indiveri, C. (2018). The Human SLC1A5 (ASCT2) Amino Acid Transporter: From Function to Structure and Role in Cell Biology. *Front. Cell Dev. Biol.* 6, 96–96. doi: 10.3389/fcell.2018.00096

Schulte, M. L., Fu, A., Zhao, P., Li, J., Geng, L., Smith, S. T., et al. (2018). Pharmacological blockade of ASCT2-dependent glutamine transport leads to antitumor efficacy in preclinical models. *Nat. Med.* 24, 194–202. doi: 10.1038/nm.4464

Scopelliti, A. J., Font, J., Vandenberg, R. J., Boudker, O., and Ryan, R. M. (2018). Structural characterisation reveals insights into substrate recognition by the glutamine transporter ASCT2/SLC1A5. *Nat. Commun.* 9:38. doi: 10.1038/s41467-017-02444-w

Shimizu, A., Kaira, K., Kato, M., Yasuda, M., Takahashi, A., Tominaga, H., et al. (2015). Prognostic significance of L-type amino acid transporter 1 (LAT1) expression in cutaneous melanoma. *Melanoma Res.* 25, 399–405. doi: 10.1097/cmr.0000000000000181

Shimizu, K., Kaira, K., Tomizawa, Y., Sunaga, N., Kawashima, O., Oriuchi, N., et al. (2014). ASC amino-acid transporter 2 (ASCT2) as a novel prognostic marker in non-small cell lung cancer. *Br. J. Cancer* 110, 2030–2039. doi: 10.1038/bjc.2014.88

Sperb, N., Tsesmelis, M., and Wirth, T. (2020). Crosstalk between Tumor and Stromal Cells in Pancreatic Ductal Adenocarcinoma. *Int. J. Mol. Sci.* 21:5486 doi: 10.3390/ijms21155486

Strapcova, S., Takacova, M., Csaderova, L., Martinelli, P., Lukacikova, L., Gal, V., et al. (2020). Clinical and Pre-Clinical Evidence of Carbonic Anhydrase IX in Pancreatic Cancer and Its High Expression in Pre-Cancerous Lesions. *Cancers* 12:2005 doi: 10.3390/cancers12082005

Sun, H. W., Yu, X. J., Wu, W. C., Chen, J., Shi, M., Zheng, L., et al. (2016). GLUT1 and ASCT2 as Predictors for Prognosis of Hepatocellular Carcinoma. *PLoS One* 11:e0168907. doi: 10.1371/journal.pone.0168907

Sun, X., Wang, M., Wang, M., Yao, L., Li, X., Dong, H., et al. (2020). Role of Proton-Coupled Monocarboxylate Transporters in Cancer: From Metabolic Crosstalk to Therapeutic Potential. *Front. Cell Dev. Biol.* 8:651 doi: 10.3389/fcell.2020.00651

Supuran, C. T. (2018). Carbonic anhydrase inhibitors as emerging agents for the treatment and imaging of hypoxic tumors. *Expert Opin. Investig. Drugs* 27, 963–970. doi: 10.1080/13543784.2018.1548608

Swayampakula, M., McDonald, P. C., Vallejo, M., Coyaud, E., Chafe, S. C., Westerback, A., et al. (2017). The interactome of metabolic enzyme carbonic anhydrase IX reveals novel roles in tumor cell migration and invadopodia/MMP14-mediated invasion. *Oncogene* 36, 6244–6261. doi: 10.1038/onc.2017.219

Swietach, P., Hulikova, A., Vaughan-Jones, R. D., and Harris, A. L. (2010). New insights into the physiological role of carbonic anhydrase IX in tumour pH regulation. *Oncogene* 29, 6509–6521. doi: 10.1038/onc.2010.455

Swietach, P., Patiar, S., Supuran, C. T., Harris, A. L., and Vaughan-Jones, R. D. (2009). The role of carbonic anhydrase 9 in regulating extracellular and intracellular ph in three-dimensional tumor cell growths. *J. Biol. Chem.* 284, 20299–20310. doi: 10.1074/jbc.M109.006478

Tan, E. Y., Yan, M., Campo, L., Han, C., Takano, E., Turley, H., et al. (2009). The key hypoxia regulated gene CAIX is upregulated in basal-like breast tumours and is associated with resistance to chemotherapy. *Br. J. Cancer* 100, 405–411. doi: 10.1038/sj.bjc.6604844

Toda, K., Nishikawa, G., Iwamoto, M., Itatani, Y., Takahashi, R., Sakai, Y., et al. (2017). Clinical Role of ASCT2 (SLC1A5) in KRAS-Mutated Colorectal Cancer. *Int. J. Mol. Sci.* 18:1632. doi: 10.3390/ijms18081632

Utsunomiya-Tate, N., Endou, H., and Kanai, Y. (1996). Cloning and functional characterization of a system ASC-like Na+-dependent neutral amino acid transporter. *J. Biol. Chem.* 271, 14883–14890.

van Geldermalsen, M., Wang, Q., Nagarajah, R., Marshall, A. D., Thoeng, A., Gao, D., et al. (2016). ASCT2/SLC1A5 controls glutamine uptake and tumour growth in triple-negative basal-like breast cancer. *Oncogene* 35, 3201–3208. doi: 10.1038/onc.2015.381

Wagner, C. A., Lang, F., and Broer, S. (2001). Function and structure of heterodimeric amino acid transporters. *Am. J. Physiol. Cell Physiol.* 281, C1077–C1093.

Wang, Q., Beaumont, K. A., Otte, N. J., Font, J., Bailey, C. G., van Geldermalsen, M., et al. (2014). Targeting glutamine transport to suppress melanoma cell growth. *Int. J. Cancer* 135, 1060–1071. doi: 10.1002/ijc.28749

Wang, Q., Hardie, R. A., Hoy, A. J., van Geldermalsen, M., Gao, D., Fazli, L., et al. (2015). Targeting ASCT2-mediated glutamine uptake blocks prostate cancer growth and tumour development. *J. Pathol.* 236, 278–289. doi: 10.1002/path.4518

Wang, V. M., Ferreira, R. M. M., Almagro, J., Evan, T., Legrave, N., Zaw Thin, M., et al. (2019). CD9 identifies pancreatic cancer stem cells and modulates glutamine metabolism to fuel tumour growth. *Nat. Cell Biol.* 21, 1425–1435. doi: 10.1038/s41556-019-0407-1

Wang, Y., Bai, C., Ruan, Y., Liu, M., Chu, Q., Qiu, L., et al. (2019). Coordinative metabolism of glutamine carbon and nitrogen in proliferating cancer cells under hypoxia. *Nat. Commun.* 10:201. doi: 10.1038/s41467-018-08033-9

Ward, P. S., and Thompson, C. B. (2012). Metabolic reprogramming: a cancer hallmark even warburg did not anticipate. *Cancer Cell* 21, 297–308. doi: 10.1016/j.ccr.2012.02.014

Wise, D. R., and Thompson, C. B. (2010). Glutamine addiction: a new therapeutic target in cancer. *Trends Biochem. Sci.* 35, 427–433. doi: 10.1016/j.tibs.2010.05.003

Witte, D., Ali, N., Carlson, N., and Younes, M. (2002). Overexpression of the neutral amino acid transporter ASCT2 in human colorectal adenocarcinoma. *Anticancer Res.* 22, 2555–2557.

Wolfson, R. L., Chantranupong, L., Saxton, R. A., Shen, K., Scaria, S. M., Cantor, J. R., et al. (2016). Sestrin2 is a leucine sensor for the mTORC1 pathway. *Science* 351, 43–48. doi: 10.1126/science.aab2674

Wykoff, C. C., Beasley, N. J., Watson, P. H., Turner, K. J., Pastorek, J., Sibtain, A., et al. (2000). Hypoxia-inducible expression of tumor-associated carbonic anhydrases. *Cancer Res.* 60, 7075–7083.

Xie, H., and Simon, M. C. (2017). Oxygen availability and metabolic reprogramming in cancer. *J. Biol. Chem.* 292, 16825–16832. doi: 10.1074/jbc.R117.799973

Yan, R., Zhao, X., Lei, J., and Zhou, Q. (2019). Structure of the human LAT1-4F2hc heteromeric amino acid transporter complex. *Nature* 568, 127–130. doi: 10.1038/s41586-019-1011-z

Ye, J., Huang, Q., Xu, J., Huang, J., Wang, J., Zhong, W., et al. (2018). Targeting of glutamine transporter ASCT2 and glutamine synthetase suppresses gastric cancer cell growth. *J. Cancer Res. Clin. Oncol.* 144, 821–833. doi: 10.1007/s00432-018-2605-9

Yue, M., Jiang, J., Gao, P., Liu, H., and Qing, G. (2017). Oncogenic MYC Activates a Feedforward Regulatory Loop Promoting Essential Amino Acid Metabolism and Tumorigenesis. *Cell Rep.* 21, 3819–3832. doi: 10.1016/j.celrep.2017.12.002

Conflict of Interest: The authors declare that the research was conducted in the absence of any commercial or financial relationships that could be construed as a potential conflict of interest.

frontiers in Cell and Developmental Biology

REVIEW
published: 04 December 2020
doi: 10.3389/fcell.2020.602476

Extracellular Citrate Fuels Cancer Cell Metabolism and Growth

Sebastian Haferkamp[1], Konstantin Drexler[1], Marianne Federlin[2], Hans J. Schlitt[3], Mark Berneburg[1], Jerzy Adamski[4,5,6], Andreas Gaumann[7], Edward K. Geissler[3], Vadivel Ganapathy[8], E. Kenneth Parkinson[9†] and Maria E. Mycielska[3*†]*

[1] Department of Dermatology, University Medical Center, Regensburg, Germany, [2] Department of Conservative Dentistry and Periodontology, University Medical Center, Regensburg, Germany, [3] Department of Surgery, University Medical Center Regensburg, Regensburg, Germany, [4] Research Unit Molecular Endocrinology and Metabolism, Helmholtz Zentrum München, German Research Center for Environmental Health, Neuherberg, Germany, [5] Lehrstuhl für Experimentelle Genetik, Technische Universität München, Munich, Germany, [6] Department of Biochemistry, Yong Loo Lin School of Medicine, National University of Singapore, Singapore, Singapore, [7] Institute of Pathology, Kaufbeuren-Ravensburg, Kaufbeuren, Germany, [8] Department of Cell Biology and Biochemistry, Texas Tech University Health Sciences Center, Lubbock, TX, United States, [9] Center for Immunobiology and Regenerative Medicine, Barts and The London School of Medicine and Dentistry, Blizard Institute, London, United Kingdom

OPEN ACCESS

Edited by:
Alison Colquhoun, University of São Paulo, Brazil

Reviewed by:
Anna Maria Giudetti, University of Salento, Italy
Bèla Ózsvàri, University of Salford, United Kingdom

***Correspondence:**
Maria E. Mycielska
maria.mycielska@ukr.de
E. Kenneth Parkinson
e.k.parkinson@qmul.ac.uk

† These authors have contributed equally to this work

Specialty section:
This article was submitted to Molecular and Cellular Oncology, a section of the journal Frontiers in Cell and Developmental Biology

Received: *03 September 2020*
Accepted: *16 November 2020*
Published: *04 December 2020*

Citation:
Haferkamp S, Drexler K, Federlin M, Schlitt HJ, Berneburg M, Adamski J, Gaumann A, Geissler EK, Ganapathy V, Parkinson EK and Mycielska ME (2020) Extracellular Citrate Fuels Cancer Cell Metabolism and Growth. Front. Cell Dev. Biol. 8:602476. doi: 10.3389/fcell.2020.602476

Cancer cells need excess energy and essential nutrients/metabolites not only to divide and proliferate but also to migrate and invade distant organs for metastasis. Fatty acid and cholesterol synthesis, considered a hallmark of cancer for anabolism and membrane biogenesis, requires citrate. We review here potential pathways in which citrate is synthesized and/or supplied to cancer cells and the impact of extracellular citrate on cancer cell metabolism and growth. Cancer cells employ different mechanisms to support mitochondrial activity and citrate synthesis when some of the necessary substrates are missing in the extracellular space. We also discuss the different transport mechanisms available for the entry of extracellular citrate into cancer cells and how citrate as a master metabolite enhances ATP production and fuels anabolic pathways. The available literature suggests that cancer cells show an increased metabolic flexibility with which they tackle changing environmental conditions, a phenomenon crucial for cancer cell proliferation and metastasis.

Keywords: cancer, metabolism, transporter, cancer associated fibroblast (CAF), senescent fibroblasts

INTRODUCTION

To successfully grow and metastasise, cancer cells need to adjust their metabolism to fulfill high-energy requirements. The essential metabolites necessary for this process can be obtained from blood, synthesized *de novo*, or supplied by cancer-associated stromal cells. Uptake or release of different substrates from and to the extracellular space can occur through specific transporters expressed in the plasma membrane. The same holds true for the transport across the mitochondrial inner membrane where several transporters are present. Control of transporter expression is one of the ways by which metabolite uptake and release can be regulated. Differences in expression of the plasma membrane and mitochondrial transporters take part in the regulation of various metabolic pathways in the cytoplasm and mitochondria. Several transporters for specific nutrients and metabolites have been shown to be upregulated in cancer cells such as glucose, lactate or amino acids transporters (Ganapathy et al., 2009; Bhutia et al., 2015; El Ansari et al., 2018; Ma et al., 2018; Brown and Ganapathy, 2020; Brown et al., 2020b; Zhang and Li, 2020).

Synthesis of the building blocks necessary for the process of proliferation and membrane biogenesis requires increased production of fatty acids and cholesterol, considered a hallmark of cancer. Cytoplasmic citrate is the primary substrate in this process (**Table 1**). Until recently, it was believed that cancer cells cannot obtain citrate from the extracellular space and that the entire pool of cellular citrate arises from intracellular synthesis, mainly in the reverse Krebs cycle through reductive carboxylation from glutamine (Metallo et al., 2011), and to a much lesser extent, from glucose-derived pyruvate. Indeed, increased glutamine uptake has been associated with cancer growth (Bhutia and Ganapathy, 2016). However, some recent studies have shown that cancer cells are glutamine-dependent *in vitro*, whilst glutamine uptake rate is similar to normal cells when the same cancer cells are grown *in vivo* (Davidson et al., 2016). Moreover, radiotracer studies of glutamine uptake in mouse brain implanted with primary human tumors have shown that increased glutamine uptake occurs in the tissue surrounding the cancer but not in the cancer itself (Marin-Valencia et al., 2012). Therefore, the way citrate is synthesized in cancer cells might depend on the surrounding metabolic conditions.

We have recently discovered that cancer cells are able to take up citrate through the plasma membrane variant (pmCiC) of the mitochondrial (mCiC) citrate carrier (SLC25A1) belonging to the *SLC25* gene family (Mazurek et al., 2010). Our studies have also shown that uptake of extracellular citrate supports cancer metabolism, proliferation, fatty acid and protein synthesis (Mycielska et al., 2018). There is also another citrate transporter in the plasma membrane (SLC13A5) belonging to the *SLC13* gene family (Willmes et al., 2018; Jaramillo-Martinez et al., 2020). Here, we will discuss the transporters and the metabolic pathways that are involved in the uptake and utilization of extracellular citrate in cancer cells and the impact of extracellular citrate on cancer cell metabolism and growth.

TABLE 1 | Reactions involved in the conversion of citrate into fatty acids and cholesterol in the cytoplasm.

Reaction	Enzyme(s)
Citrate + ATP + CoA → Acetyl-CoA + Oxaloacetate + ADP + Pi	ATP-Citrate lyase
Acetyl-CoA + CO_2 + ATP → Malonyl-CoA + ADP + Pi	Acetyl-CoA carboxylase
Malonyl-CoA →→→ Fatty acyl-CoA	Fatty acid synthase
Citrate + ATP + CoA → Acetyl-CoA + Oxaloacetate + ADP + Pi	ATP-Citrate lyase
3 Acetyl-CoA → HMG-CoA + 2 CoA	Thiolase and HMG-CoA synthase 1
HMG-CoA + 2 NADPH + 2 H^+ → Mevalonate + CoA + 2 $NADP^+$	HMG-CoA reductase
Mevalonate →→→ Cholesterol	Several enzymes

THE PATHWAYS SUPPORTING MITOCHONDRIAL ACTIVITY IN CANCER

Mitochondria consist of two membranes, an inner membrane that is impermeable to small molecules and an outer membrane that is permeable to small molecules. The impermeable nature of the inner membrane necessitates the presence of specific transporters to facilitate exchange of metabolites and nutrients between mitochondrial matrix and cytoplasm. As such, the inner membrane is rich in transporters, all of which belong to the SLC25 gene family; these transporters mediate the movement of a wide variety of metabolites in and out of the mitochondrial matrix (Gutiérrez-Aguilar and Baines, 2013). Abundance of these transporters in the mitochondrial membrane regulates the exchange rate of the substrates with cytoplasm and in consequence respective cytosolic and matrix metabolic pathways.

Fatty acid synthesis occurs in the cytoplasm, for which citrate is the primary substrate; this pathway is activated in cancer and it is a metabolic hallmark of cancer cells (Wang et al., 2015). Citrate is produced in the Krebs cycle within the mitochondrial matrix from the condensation of acetyl-CoA and oxaloacetate. In most cells, citrate is further metabolized into isocitrate through the action of mitochondrial aconitase (m-ACN/ACO2), which then goes through the rest of the reactions in the Krebs cycle. One notable exception is the prostate epithelial cell. The Krebs cycle is truncated in this cell type where citrate generated in the matrix fails to go through the next step mediated by m-ACN because of markedly reduced activity of this enzyme. This unique metabolic phenotype renders prostate epithelial cells net citrate producers. Citrate thus generated is then secreted into the prostatic fluid to facilitate the maturation and motility of spermatozoa. The reduced activity of m-ACN in these cells is due to Zn^{2+}-mediated inhibition, and prostate epithelial cells exhibit a robust capacity to accumulate this metal. This allows the ratio of citrate to isocitrate to increase to 30–40:1 in these cells (Costello et al., 1976). As citrate fails to go through the Krebs cycle within the matrix in these cells, it accumulates and gets transported out of the matrix into the cytoplasm via the citrate transporter SLC25A1 in the inner membrane, which occurs in exchange for malate (i.e., citrate enters the cytoplasm and malate enters the matrix). Once in the cytoplasm, citrate is released into the luminal space via pmCiC, an alternative splice variant of SLC25A1 (Mycielska et al., 2009; Mazurek et al., 2010) and most likely also via the recently described citrate exporter ANKH (SLC62A1) (Szeri et al., 2020). The metabolic phenotype of the normal prostate epithelium as a citrate producer is reversed upon transformation into cancer cells. As a consequence, normal prostate has high concentrations of citrate whereas prostate cancer has low concentrations of citrate, a metabolic distinction that is exploited in the clinics for differential and minimally invasive diagnosis of prostate cancer (Banerjee et al., 2017; Braadland et al., 2017). This switch is facilitated by the loss of ability to accumulate Zn^{2+} during oncogenic transformation, which relieves m-ACN from the Zn^{2+}-mediated inhibition (Costello and Franklin, 2006). The net outcome is the reduced levels of citrate inside the cancer cells. This ability of prostate cancer cells to oxidize citrate is surprising, as this process would lead to reduced net citrate accumulation whilst cancer cells need excess citrate level to support fatty acid synthesis in cytoplasm. How, therefore, do cancer cells manage to supply cytoplasm with the necessary amount of citrate?

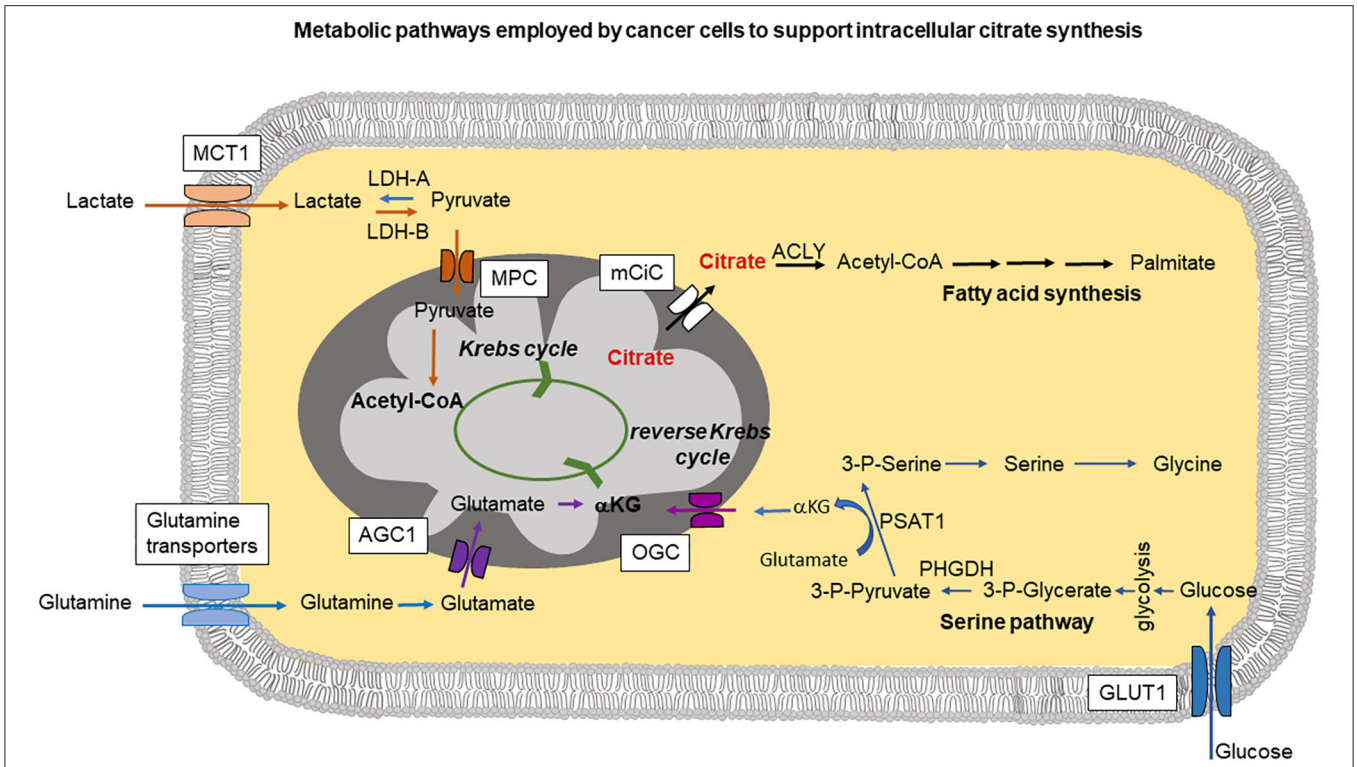

FIGURE 1 | The cartoon summarizes intracellular pathways used by cancer cells to support increased citrate synthesis in mitochondria. This can occur through a serine pathway, where increased expression of phosphoglycerate dehydrogenase (PHGDH) creates a diversion from glycolysis. PSAT1 (phosphoserine aminotransferase) reaction requires conversion of glutamate into αKG (α-ketoglutarate) which can be then transported into mitochondria by oxoglutarate carrier (OGC) and support mitochondrial citrate synthesis through the reverse Krebs cycle. Lactate taken up through MCT1 (monocarboxylate transporter 1) is metabolized by lactate dehydrogenase-A (LDH-A) into pyruvate imported into mitochondria through MPC (mitochondrial pyruvate carrier) followed by Acetyl-CoA synthesis which can then join the Krebs cycle. Part of glutamine pool can be metabolized into glutamate and transported into mitochondria through AGC1 (aspartate-glutamate carrier isoform 1) followed by conversion into αKG. Released into the cytoplasm citrate is metabolized by ATP-citrate lyase (ACLY) and plays a central role in fatty acid synthesis.

It was widely believed that cancer cells did not take up citrate from the circulation (blood levels of citrate, ∼200 μM) and that they met their increased demands for this metabolite via de no synthesis from glutamine (Metallo et al., 2011). This requires a novel reprogramming of the metabolism involving the reversal of the Krebs cycle in which α-ketoglutarate arising from glutamine gets converted into citrate by a process known as "reductive carboxylation." Indeed, uptake of glutamine resulting from increased expression of multiple glutamine transporters has been associated with cancer cells (Bhutia and Ganapathy, 2016; Wang et al., 2020; **Figure 1**). Further studies indicated that glutamine addiction of cancer cells might depend on the metabolic environment. In particular, it has been determined that whilst there is a clear dependence on glutamine of human lung cancer cells *in vitro*, the same cells when injected in mice, synthesize citrate from glucose rather than glutamine (Davidson et al., 2016). Therefore, the metabolic environment of the cancer cells dictates the choice of extracellular metabolites and biochemical pathways used for satisfying the increased demands for citrate. A similar phenomenon of glutamine independence of cancer cells *in vivo* has been shown using primary cultures of human glioblastoma. In line with the previous report, when injected into mice, human glioblastoma cells did not show any increase in the uptake of glutamine. Interestingly, increased uptake of glutamine was observed in the stromal cells present in the tumor environment (Marin-Valencia et al., 2012). This increase in glutamine uptake would be consistent with cancer-associated stroma synthesizing metabolic substrates to support cancer cells; this could potentially include citrate.

Citrate synthesis in mitochondria from glutamine through a truncated (and reverse) Krebs cycle as postulated by several research groups (Metallo et al., 2011; Mullen et al., 2014) requires increased efforts to supply mitochondria with sufficient amounts of intermediates. Therefore, some additional pathways in cancer cells have been identified that could be used to fulfill the increased mitochondrial needs. A serine pathway has been recently postulated to be an alternative means to produce α-ketoglutarate (Locasale et al., 2011; Possemato et al., 2011). According to these studies, increased expression of phosphoglycerate dehydrogenase (PHGDH) siphons the glycolytic intermediate 3-phosphoglycerate for increased synthesis of serine and glycine (**Figure 1**). Serine and glycine are abundant in the plasma, and depletion of PHGDH could not decrease intracellular levels of

these metabolites, suggesting that uptake of extracellular serine and glycine is also a likely contributor to these two amino acids in cancer cells. Suppression of PHGDH resulted, however, in decreased α-ketoglutarate levels which can be used to support Krebs cycle activity. This additional α -ketoglutarate synthesis could be potentially the main reason for cancer cells to use serine pathway (Possemato et al., 2011; **Figure 1**). In addition to the widely recognized role of serine and glycine in one-carbon metabolism, an obligatory pathway for any highly proliferating cell, including cancer cells, these amino acids also participate in the synthesis of α-ketoglutarate for use in the Krebs cycle in the forward direction to generate NADH and $FADH_2$ for subsequent ATP production and also in the Krebs cycle in the reverse direction for reductive carboxylation for subsequent citrate production.

Another metabolite that has been implicated in support of cancer cell mitochondrial metabolism and in consequence in citrate synthesis, is lactate (**Figure 1**). Lactate can be imported into the cell through monocarboxylate transporter MCT1, heavily overexpressed in majority of aggressive tumors (Park et al., 2018; Tasdogan et al., 2020). Intracellularly, lactate can be converted into pyruvate and then into acetyl-CoA to feed into the Krebs cycle. Moreover, the conversion of lactate to pyruvate is accompanied by reduction of NAD^+ into NADH, which suppresses the activity of glyceraldehyde-3-phosphate dehydrogenase in the direction of glucose breakdown but reverses the reaction to go in the opposite direction, thus sparing glucose 6 phosphate to feed into the pentose-phosphate pathway (Tasdogan et al., 2020). The pentose phosphate pathway is a major mechanism for production of NADPH, a reducing equivalent obligatory for anabolic pathways that are essential for cancer cells. Increased MCT1 expression and excess pentose-phosphate pathway activity have been shown to be necessary for metastasising human melanoma cells in mice (Tasdogan et al., 2020).

Most of the mechanisms described above are designed to supply cancer cell mitochondria with glutamate/α-ketoglutarate to sustain reverse Krebs cycle activity leading to excess citrate synthesis. In this case, glutamate needs to be transported through the inner mitochondrial membrane at a higher rate (**Figure 1**). Mitochondrial glutamate transporters GC1 (SLC25A22) and GC2 (SLC25A18) are the members of the *SLC25* gene family of mitochondrial carriers. Import of glutamate into mitochondria is dependent on H^+. Under normal conditions, there exists a H^+ gradient across the inner mitochondrial membrane in the cytoplasm-to-matrix direction, which provides energy for the activity of GC1 and GC2. High expression of GC1 is associated with organs such as brain, pancreas and the fatty acid synthesizing liver (Monné et al., 2019). GC2 is ubiquitously expressed in most tissues. Another mitochondrial carrier involved in the transport of glutamate into mitochondria is the aspartate-glutamate carrier isoform 1 (AGC1), encoded by *SLC25A12* gene. In this case, glutamate is transported into the mitochondria in exchange for aspartate (Infantino et al., 2019). Because of this exchange phenomenon, the transport function of AGC1 is electroneutral and there is no energy involvement in the process.

Recent studies showed that AGC1 is crucial for different cancer cell types deprived of extracellular glutamine to sustain intracellular aspartate level, cell proliferation and survival (Profilo et al., 2017; Alkan et al., 2018). Intracellular aspartate normally produced in the process of glutamine anaplerosis can be rescued by mitochondrial aspartate synthesis and release through AGC1 into the cytoplasm in case of extracellular glutamine deficiency.

Altogether, based on the published data, it can be concluded that cancer cells engage several different pathways to produce Krebs cycle intermediates. Their import into mitochondria can sustain increased synthesis of citrate using the reductive carboxylation pathway.

Once produced within the mitochondrial matrix, citrate normally enters the Krebs cycle. However, if the cells are energy sufficient, Krebs cycle is suppressed and citrate now is exported into cytoplasm through the mitochondrial citrate carrier mCiC (SLC25A1) in exchange for malate (Iacobazzi et al., 1996). Consistent with the notion of cancer cells producing citrate intracellularly, mCiC expression was found to be increased in different tumor types (Catalina-Rodriguez et al., 2012; Kolukula et al., 2014) and in pathophysiological conditions such as hypoxia. Blocking of the citrate transport from mitochondria into the cytoplasm with an SLC25A1 inhibitor, benzenetricarboxylate (BTA), had several effects on cancer cells including increased glycolysis, ROS synthesis, mitophagy and disrupted mitochondrial homeostasis (Catalina-Rodriguez et al., 2012; Kolukula et al., 2014; Fernandez et al., 2018). Moreover, *in vivo* treatment with BTA resulted in a decreased subcutaneous tumor growth of human breast cancer cell line MDA-MB-231, lung cancer cell line H1299 and bladder cancer line xenografts (Catalina-Rodriguez et al., 2012; Kolukula et al., 2014). Due to its ability to regulate ROS synthesis, mCiC was found to play a major role in acquiring resistance to anti-cancer treatments (Fernandez et al., 2018). Consistently, blocking of SLC25A1 with BTA sensitized the cells to ionizing radiation through increased ROS synthesis. Moreover, citrate carrier expression was found to be increased under hypoxic conditions. Expression of SLC25A1 in patients with non-small cell lung carcinoma has been correlated with decreased survival (Hlouschek et al., 2018).

The results described above highlighting the role of mCiC in the regulation of glycolysis, mitochondrial activity and metabolism under hypoxia contain some controversies. Increased expression of mCiC under hypoxic conditions should not be able to effectively rescue mitochondrial citrate synthesis when no oxygen is present. Moreover, blocking of mCiC with BTA should decrease ROS synthesis due to the decreased mitochondrial activity rather than increase it (Fernandez et al., 2018). Most of these discrepancies could be potentially explained by our recent data showing that cancer cells of different origin can take up extracellular citrate through the plasma membrane citrate transporter pmCiC (Mycielska and Geissler, 2018; Mycielska et al., 2018, 2019), which is a variant of the mitochondrial SLC25A1 (mCiC). pmCiC has a different start codon which is located in the intron preceding second exon of the mCiC (Mazurek et al., 2010). The two variants have different first exons with the remaining sequences

identical between the two variants. Therefore, both transporters should be sensitive to the same blockers. Moreover, the primers, siRNAs and antibodies used in these studies will likely not distinguish between the two variants. This would indicate that BTA or siRNAs used are likely to affect both transporters and therefore produce a rather complex effect. Lack of the import of extracellular citrate by cancer cells subjected to such blockers or siRNAs would explain some of the described above results. First, blocking of extracellular citrate uptake could explain increased need of citrate synthesis in mitochondria consistent with increased glycolysis rate and ROS synthesis. In fact, we have shown already that mCiC expression is upregulated in cancer cells in the absence of extracellular citrate and the same holds true for the increased ROS synthesis (Mycielska et al., 2018). Second, increased expression of mCiC alone in hypoxia would not make much sense, as there is little oxygen available thus reducing mitochondrial activity. However, increased citrate import through pmCiC could explain the overall increase in the expression of mCiC/pmCiC as observed in different studies. Increased uptake of extracellular citrate under hypoxic conditions could rescue the overall cancer cell metabolism and sustain fatty acid synthesis. Finally, it will also be important to check the differential expression of mCiC and pmCiC in patient samples and study the correlation between the expression level of each of the variant and the overall survival.

SLC13A5 as another contributor to cytoplasmic citrate detected in cancer cells. SLC13A5 is a Na^+-coupled citrate transporter (also called NaCT) expressed in the plasma membrane of certain cell types (Inoue et al., 2002a,b, 2004; Gopal et al., 2015). It is expressed predominantly in liver, brain, and testes, with liver being the tissue of the most abundant expression. The location of the transporter in hepatocytes is restricted to the blood-facing sinusoidal membrane, indicating that the physiologic role of this transporter is to deliver citrate from the circulation into the cells (Gopal et al., 2007). Loss-of-function mutations in SLC13A5 cause a severe disease, known as Early Infantile Epileptic Encephalopathy-25 (EIEE-25) (Bhutia et al., 2017; Jaramillo-Martinez et al., 2020), which highlights the biologic role of the transporter that is obligatory for brain function. Surprisingly, *Slc13a5*-null mice are phenotypically normal with no evidence of brain dysfunction (Birkenfeld et al., 2011), underlining potential differences between mice and humans in terms of the involvement of the transporter in brain function. However, the *Slc13a5*-null mice are resistant to diet-induced obesity, insulin resistance and metabolic syndrome (Birkenfeld et al., 2011; Bhutia et al., 2017; Willmes et al., 2018; Jaramillo-Martinez et al., 2020), which is obviously related to the role of the transporter in the liver. We have shown that SLC13A5 delivers extracellular citrate into the liver carcinoma cell line HepG2 for subsequent lipid synthesis (Inoue et al., 2003). Therefore, SLC13A5 ought to play a critical role as a determinant of cytoplasmic citrate at least in the liver, brain and testes. Given that citrate in the cytoplasm is obligatory for fatty acid and cholesterol synthesis and for promotion of cancer cell growth and proliferation, SLC13A5 must have relevance to cancer, at least in the liver where its expression is the most abundant. This is supported by a recent study in which SLC13A5 was shown to be a tumor promoter in hepatocellular carcinoma (Li et al., 2017; Peters, 2017). Silencing the transporter in the liver cancer cells led to decreased ATP, increased AMP-dependent kinase activity, and decreased mTORC1 signaling, consequently resulting in decreased growth of HepG2 cells into tumor in mouse xenografts.

CITRATE METABOLISM IN CYTOPLASM

We have shown recently that cancer cells take up extracellular citrate through the pmCiC (Mycielska et al., 2015, 2018; Mycielska and Geissler, 2018), and others have shown a similar role for the Na^+-coupled citrate transporter NaCT (SLC13A5) (Inoue et al., 2003; Li et al., 2017; Kopel et al., 2020). Expression of pmCiC was found to correlate with the aggressiveness of cancer in human tissues and to be increased at the invasion front and at the sites of metastasis. *In vitro*, cancer cells incubated with extracellular citrate required less glucose, produced less ROS and decreased their mitochondrial activity (Mycielska et al., 2018). The presence of extracellular citrate reduced expression of mCiC in mitochondria consistent with the reduced release of this metabolite into the cytoplasm and increased uptake of citrate from the extracellular space. Extracellular citrate could directly supply cytosolic pathways and/or be incorporated into the Krebs cycle. However, reduced mCiC expression contradicts the latter possibility. The role of NaCT (SLC13A5) in supplying extracellular citrate has been documented at least in hepatocellular carcinoma and liver cancer cells (Inoue et al., 2003; Li et al., 2017; Kopel et al., 2020); this process is essential for the growth and proliferation of liver cancer cells *in vitro* and *in vivo*.

As in normal cells, cytoplasmic citrate could feed into several metabolic pathways and facilitate overall cancer cell metabolism. Citrate is the primary substrate for fatty acid and cholesterol synthesis; both of these two pathways occur in the cytoplasm. Therefore, citrate entering the cytoplasm via either pmCiC or NaCT could feed into these biosynthetic pathways directly. Citrate in the cytoplasm is metabolized by ATP-citrate lyase to acetyl-CoA and oxaloacetate (**Table 1**). Acetyl-CoA is then converted into malonyl CoA by acetyl-CoA carboxylase whilst oxaloacetate either enters into gluconeogenesis or gets metabolized to malate (malate dehydrogenase) and transported back to mitochondria through mCiC (Iacobazzi et al., 1996). For the entry of oxaloacetate into gluconeogenesis, the cytoplasmic enzyme phosphoenolpyruvate carboxykinase (PEPCK-C) is needed. It is an GTP-requiring enzyme. Oxaloacetate generated within the mitochondrial matrix via carboxylation of pyruvate by pyruvate carboxylase or via the TCA cycle using the various intermediates in the pathway (α-ketoglutarate, succinyl-CoA, and fumarate) could also enter gluconeogenesis via the mitochondrial PEPCK (PEPCK-M), and the resultant phosphoenolpyruvate is transported out of the mitochondria to feed into the gluconeogenic pathway in the cytoplasm. Interestingly, under glucose deprivation, cancer cells use mitochondrial PEPCK to support cell proliferation. In this case, glutamine is used as the primary substrate to produce phosphoenolpyruvate via oxaloacetate (glutamine → glutamate → α-ketoglutarate → succinyl-CoA → succinate → fumarate

→ malate → oxaloacetate) in the TCA cycle to supply the carbon skeleton for gluconeogenesis in the cytoplasm (Vincent et al., 2015). Similarly, cytosolic PEPCK has been determined to account for the switch from glutaminolysis to increased glucose consumption in case of glutamine restriction. Under the conditions of limited glucose supply, cancer cells also use glutamine to generate oxaloacetate, which enters the gluconeogenesis pathway in the cytoplasm to synthesize glucose-6-phosphate, which then feeds into the pentose-phosphate pathway to generate NADPH as a means to support the antioxidant machinery (Montal et al., 2015). Acetyl-CoA is used as the building block for the synthesis of fatty acids as well as cholesterol. Similar to fatty acids which are needed for the synthesis of phospholipids necessary for membrane biogenesis, cholesterol also serves an essential function in biomembranes, both being crucial for cancer cells (Coleman, 1986; Rao and Coleman, 1989). Accumulation of cholesterol in the mitochondrial membrane is responsible for its decreased permeability resulting in a tighter regulation of metabolite exchange with the cytoplasm (Baulies et al., 2018). Cholesterol plays a similar role in the control of permeability in the plasma membrane. Cytoplasmic citrate does not function simply as a precursor of acetyl-CoA to serve as the substrate for acetyl-CoA carboxylase; it is also a potent allosteric activator of this enzyme, thus promoting the synthesis of malonyl CoA. Interestingly, malonyl CoA feeds into fatty acid synthesis and at the same time blocks the entry of fatty acids into mitochondria by inhibiting the carnitine palmitoyl transferase 1. As such, malonyl CoA promotes fatty acid synthesis in the cytoplasm and simultaneously blocks breakdown of fatty acids inside the mitochondria. Thus, ATP-citrate lyase is obligatory for most of the anabolic pathways in the cytoplasm involving citrate. As such, this enzyme plays an essential role in cancer cells. Consequently, ATP-citrate lyase has been suggested as an anti-cancer drug target (Hatzivassiliou et al., 2005). Another function of acetyl-CoA in the cytoplasm is in the post-translational modification of enzymes via acetylation, which could impact on their biological function. Acetyl-CoA can also enter the nucleus to modify histones with acetylation, which plays an important role in epigenetic control of transcription (Wellen et al., 2009).

To enhance fatty acid synthesis, cancer cells not only need increased citrate supply in the cytoplasm but also increased supply of NADPH as the reducing equivalent as synthesis of one palmitate requires 14 NADPH molecules (Hochachka et al., 2002). The primary source of NADPH in mammalian cells is the pentose-phosphate pathway (PPP). This pathway is particularly pronounced in cancer cells, supplying pentose phosphates necessary for nucleic acids synthesis and NADPH necessary for anabolic pathways such as the fatty acid/cholesterol synthesis (Patra and Hay, 2014). The PPP consists of two arms: oxidative and non-oxidative. Diversion of PPP into oxidative arm occurs in cells which need to produce NADPH and maintain their redox balance while non-oxidative PPP is used to support nucleic acids synthesis and further proliferation. To support the increased demand for ribose-5-phosphate, cancer cells increase the non-oxidative arm of the PPP by regulating expression of specific target enzymes in the pathway (Langbein et al., 2006; Liu et al., 2010). Phosphoglycerate mutase (PGAM) is a dimeric enzyme comprising of two subunits PGAM1 and PGAM2. The tumor suppressor p53 elicits a negative effect on the oxidative arm of PPP by suppressing the glycolytic enzyme PGAM1 (phosphoglycerate mutase 1). As p53 gets mutated in a majority of cancers, this effect is reversed in cancer cells resulting in increased expression and activity of PGAM1. Since PGAM1 converts 3-phosphoglycerate into 2-phosphoglycerate in glycolysis, an increase in the activity of this enzyme in cancer cells causes a decrease in 3-phosphoglycerate. 6-Phosphogluconate dehydrogenase is an enzyme in the oxidative arm of PPP and this enzyme is inhibited by 3-phosphoglycerate. As such, the decrease in 3-phosphoglycerate in cancer cells relieves this inhibition and consequently potentiate the oxidative arm of PPP, thus resulting in increased generation of NADPH (Hitosugi et al., 2012).

NADPH can also be synthesized as a by-product in another cytosolic pathway involving citrate metabolism via cytosolic aconitase (c-ACN). c-ACN is an interesting protein known more commonly as Iron Regulatory Protein1 (IRP1). When intracellular Fe is low, IRP1 upregulates expression of proteins responsible for Fe uptake. In the presence of increased levels of intracellular Fe, IRP1 forms Fe-S clusters which prevent its binding to RNA; thus the protein loses its function as IRP1 but acquires activity of c-ACN (Bodiga and Krishnapillai, 2007; Wang et al., 2008). c-ACN metabolizes citrate into isocitrate which is then transformed into α-ketoglutarate with a concomitant synthesis of NADPH, the latter step mediated by cytosolic isocitrate dehydrogenases 1 and 2 (IDH1/2), which generate NADPH in contrast to the mitochondrial IDH (i.e., IDH3) which generates NADH. α-ketoglutarate is used in the Krebs cycle. Consistently, inhibition of c-ACN resulted in decreased NADPH:NADP ratio and decreased expression of genes associated with lipogenesis during differentiation of human adipocytes (Moreno et al., 2015). This would strongly suggest that increased synthesis of fatty acids requires activity of c-ACN.

The cytosolic c-ACN functioning as IRP1 as well as the enzyme in the conversion of citrate into isocitrate enables a cross-talk between cellular iron status and fatty acid synthesis. Cancer cells reprogram iron-regulatory pathways to increase iron uptake (Jung et al., 2019). Fe in blood is complexed with transferrin (Tf) and taken up by cells through TfR1 (Tf receptor 1). TfR1 expression has been found not only to be increased in cancer cells but also to correlate with increased motility, proliferation and adhesion, and also increased resistance to chemotherapy (Greene et al., 2017). Moreover, cancer cells express increased levels of DMT1 (divalent metal transporter 1; Xue et al., 2016) in endosomes facilitating Fe transport into the cytoplasm following TfR1-mediated endocytosis of transferrin-bound iron. Cancer cells also suppress the expression of the iron exporter ferroportin (SLC40A1), thus enhancing iron retention inside the cells (Kong et al., 2019). The expression of ferritin, responsible for iron storage inside the cells, is also expressed at higher levels in cancer cells (Wang et al., 2018). Increased intracellular Fe levels in cancer cells (Brown et al., 2020a) will facilitate the transition of c-ACN from IRP1 to the mediator of citrate-to-isocitrate conversion. With pmCiC and NaCT functioning to bring extracellular citrate into the cancer cells, excess iron

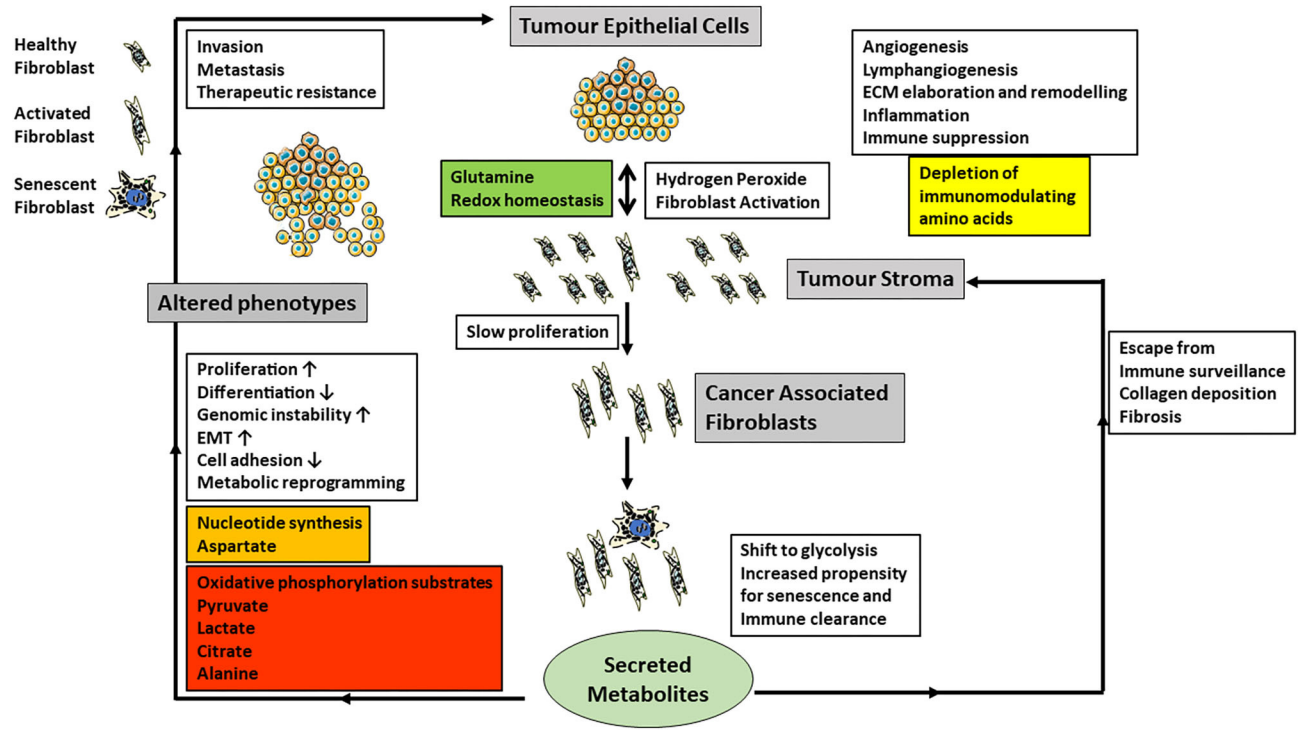

FIGURE 2 | The cartoon summarizes current data on the role of CAF-derived metabolites and the regulation of cancer phenotypes (gray boxes) and especially the influence CAFs have on epithelial-mesenchymal transition (EMT), invasion, metastasis and angiogenesis (white boxes). Carcinoma cells produce excess hydrogen peroxide and induce fibroblast activation in neighboring fibroblasts, which also have an increased propensity to undergo senescence. Senescent cells are normally cleared by the immune system. However, if they escape, they also produce tumor promoting stimuli, which are similar but not the same as those of CAFs. Metabolically CAFs and senescent fibroblasts modulate redox homeostasis and shift their metabolism toward glycolysis and the extracellular metabolites produced are summarized in the colored boxes. In particular, the secretion of energy metabolites to drive carcinoma cell energy and fatty acid metabolism as well as epigenetic regulation may be particularly important.

promotes the conversion of citrate into isocitrate in the cytoplasm via c-ACN with subsequent generation of NADPH. Therefore, this pathway could provide another way of supplying cancer cell cytoplasm with NADPH and help keeping redox balance. In this way, influx of extracellular citrate could release not only mitochondria from excess citrate synthesis, reduce ROS production (therefore increase resistance to chemotherapy) but also allow the use of other metabolic pathways like PPP in the most beneficial way for cancer cells. It is therefore not surprising that chronic exposure to excess iron as occurs in the genetic iron-overload disease hemochromatosis transforms normal cells into cells with a tumor phenotype (Gnanaprakasam et al., 2013; Bhutia et al., 2020) and also increases the risk of cancer, particularly liver cancer (Grosse et al., 2018) and colon cancer (Sivaprakasam et al., 2020).

METABOLIC CROSSTALK BETWEEN CANCER AND ITS ENVIRONMENT

Extracellular metabolic support is crucial for cancer cells, and cancer-associated stroma can potentially supply necessary metabolites. In recent years it has been realized that cancer operates as a dysfunctional and constantly evolving tissue rather than merely clonal evolution with the neoplastic cells themselves (Hanahan and Weinberg, 2000). The role and composition of the cancer microenvironment has been extensively reviewed in recent years (Sahai et al., 2020) and will only be summarized briefly here (**Figure 2**). The tumor microenvironment is composed of a distinctive microbiome, blood vessels, cells of the adaptive and innate immune systems and stromal cells which include cancer-associated fibroblasts (CAFs), which have been proposed as a novel cellular target for cancer therapy. The origin, defining features and properties of CAFs have been reviewed recently (Sahai et al., 2020). CAFs secrete a number of molecules that include transforming growth factor beta, vascular endothelial growth factor, platelet-derived growth factor, collagens, matrix metalloproteinases and cytokines. CAFs are also prone to undergo senescence albeit at a low frequency and exhibit a reduced replicative lifespan *in vitro* (Pitiyage et al., 2011; Costea et al., 2013; Hassona et al., 2013). The properties of CAFs and senescent fibroblasts overlap substantially (Lim et al., 2011; Faget et al., 2019; Sahai et al., 2020) but are not identical (Mellone et al., 2016). Fibroblast populations from pre-malignant (Pitiyage et al., 2011) and malignant (Mellone et al., 2016) lesions are composed of pro-fibrogenic and anti-fibrogenic cells.

The exchange of metabolites between cancer cells and CAFs has only been investigated relatively recently and has produced

a variety of observed relationships between CAFs and various types of cancer (Martinez-Outschoorn et al., 2014; Valencia et al., 2014; Bertero et al., 2019; Sanford-Crane et al., 2019; Sahai et al., 2020). However, one of the central observations is that CAFs shift their energy metabolism toward glycolysis (Kalluri, 2016) and advanced senescent fibroblasts likewise (James et al., 2015, 2018). In addition, senescent cells upregulate the PPP (James et al., 2015), NADPH (James et al., 2016), several lipids (James et al., 2016) and PGAM2 transcript (James et al., 2015) and so in these respects they resemble cancer cells but possess low chronic wild type p53 activity (Wiley and Campisi, 2016). The activation of fibroblasts into CAFs also promotes catabolism and autophagy (Kalluri, 2016). In prostate (Ippolito et al., 2019) and squamous cell carcinoma (Zhang et al., 2020), CAFs promote oxidative phosphorylation, epithelial-mesenchymal transition (Ippolito et al., 2019), tumorigenicity (Zhang et al., 2020), increased metastatic spread and drug resistance by secreting lactate (Ippolito et al., 2019; Zhang et al., 2020). There is a reciprocal relationship between CAFs and squamous cancer cells where glutamine provided by the cancer cells maintains redox homeostasis in the CAFs. The CAFs in turn release aspartate to promote nucleotide synthesis and a reduction in both amino acids in tumors reduces proliferation (Bertero et al., 2019). Pyruvate release by CAFs promotes lymphoma cell survival by upregulating the Krebs cycle (Sakamoto et al., 2019) and promotes extracellular matrix remodeling and breast cancer metastasis via α-ketoglutarate (Elia et al., 2019). Lactate is another tumor cell-derived metabolite that elicits a pivotal cross-talk with the tumor microenvironment. Extracellular lactate, generated and then released by cancer cells, acts as a signaling molecule via its receptor GPR81 expressed on immune cells present in the tumor microenvironment; this cross-talk facilitates immune evasion of the tumor cells (Brown et al., 2020). Lactate is not the only signaling molecule for the cross-talk between tumor cells and stromal cells. The ketone body β-hydroxybutryate also functions as a signaling molecule to facilitate communication between cancer cells and stromal cells (Ristic et al., 2017). Autophagy in stromal fibroblasts which is associated with both CAFs and senescence can generate alanine to fuel the Krebs cycle of pancreatic adenocarcinoma cells (Sousa et al., 2016; Sanford-Crane et al., 2019). Metabolic dysregulation of CAFs may also be coupled to altered immunoregulation, possibly through IL-6 production or depletion of immunomodulating amino acids (Valencia et al., 2014). Although many metabolites have now been implicated in the crosstalk between cancer cells and their environment, none of these studies as yet has focused on citrate which lies at the crossroads of energy and lipid metabolism as well as epigenetic regulation. With regard to citrate in the tumor microenvironment, two aspects seem very relevant. First, the acidic pH in the tumor microenvironment is important for the entry of extracellular citrate into cancer cells via pmCiC and NaCT. As citrate is a trivalent anion under physiological pH, its presence in the single-protonated divalent anionic form for transport via pmCiC is facilitated by the acidic tumor microenvironment. Similarly, even though NaCT is a Na^+-coupled transporter for citrate, its transport function is markedly stimulated by extracellular acidic pH because one of the Na^+-binding sites shows much higher affinity for H^+ than for Na^+ (Gopal et al., 2015). Second, citrate in the tumor microenvironment as a promoter of tumor cell growth becomes especially important metastatic tumors growing within the bone. Citrate is present at high concentrations in the bone matrix; in fact, ∼70% of citrate in the body resides within the bone. When metastatic tumors grow within the bone matrix, tumor cells secrete metalloproteinases to degrade bone matrix, thus essentially dissolving the bone mineral. This process releases citrate in the microenvironment. As such, tumor cells growing in bone are exposed to high levels of citrate in the microenvironment, which is available to support the tumor cell growth.

CONCLUSIONS

In the process of metastasis and distant organ colonization, cancer cells are faced with changing extracellular conditions including availability of different metabolites. Based on the available literature, we have shown here that cancer cells have a remarkable flexibility in using different pathways to overcome shortage in certain metabolites. This makes their metabolism adjustable and sustainable regardless of the extracellular conditions. Citrate supply and synthesis, discussed in this review, can be used as an example of how cancer cells account for the missing metabolites. In this case, several mechanisms are employed including serine/glycine pathway, truncated and reverse Krebs cycle or lactate uptake to boost mitochondrial citrate synthesis. Most of these reprogrammed metabolic pathways have been shown to function *in vitro*. It is however possible that *in vivo* where the surrounding conditions are less friendly, cancer cells must find a more stable way of getting the supply of the necessary metabolites, which could come from the stromal cells. It is important to fully understand the metabolic addictions of cancer cells and their reliance on the cancer-associated stroma to be able to devise novel and more efficient and selective strategies to combat cancer.

AUTHOR CONTRIBUTIONS

All authors listed have made a substantial, direct and intellectual contribution to the work, and approved it for publication.

FUNDING

This work was supported by the DFG grant (GE1188/5-1) and a DFG grant to SH (Research group FOR 2127, Selection and adaptation during metastatic cancer progression, DFG) and ReFoRmC to MM. KD is a fellow of the Else-Kröner-Fresenius-Stiftung.

REFERENCES

Alkan, H. F., Walter, K. E., Luengo, A., Madreiter-Sokolowski, C. T., Stryeck, S., Lau, A. N., et al. (2018). Cytosolic aspartate availability determines cell survival when glutamine is limiting. *Cell Metab*. 28, 706–720.e6. doi: 10.1016/j.cmet.2018.07.021

Banerjee, S., Zare, R. N., Tibshirani, R. J., Kunder, C. A., Nolley, R., Fan, R., et al. (2017). Diagnosis of prostate cancer by desorption electrospray ionization mass spectrometric imaging of small metabolites and lipids. *Proc. Natl. Acad. Sci. U. S. A*. 114, 3334–3339. doi: 10.1073/pnas.1700677114

Baulies, A., Montero, J., Matías, N., Insausti, N., Terrones, O., Basañez, G., et al. (2018). The 2-oxoglutarate carrier promotes liver cancer by sustaining mitochondrial GSH despite cholesterol loading. *Redox Biol*. 14, 164–177. doi: 10.1016/j.redox.2017.08.022

Bertero, T., Oldham, W. M., Grasset, E. M., Bourget, I., Boulter, E., Pisano, S., et al. (2019). Tumor-stroma mechanics coordinate amino acid availability to sustain tumor growth and malignancy. *Cell Metab*. 29, 124–140.e10. doi: 10.1016/j.cmet.2018.09.012

Bhutia, Y. D., Babu, E., Ramachandran, S., and Ganapathy, V. (2015). Amino acid transporters in cancer and their relevance to "glutamine addiction": novel targets for the design of a new class of anticancer drugs. *Cancer Res*. 75, 1782–1788. doi: 10.1158/0008-5472.CAN-14-3745

Bhutia, Y. D., and Ganapathy, V. (2016). Glutamine transporters in mammalian cells and their functions in physiology and cancer. *Biochim. Biophys. Acta* 1863, 2531–2539. doi: 10.1016/j.bbamcr.2015.12.017

Bhutia, Y. D., Kopel, J. J., Lawrence, J. J., Neugebauer, V., and Ganapathy, V. (2017). Plasma membrane Na?-coupled citrate transporter (SLC13A5) and neonatal epileptic encephalopathy. *Molecules* 22:378. doi: 10.3390/molecules22030378

Bhutia, Y. D., Ogura, J., Grippo, P. J., Torres, C., Sato, T., Wachtel, M., et al. (2020). Chronic exposure to excess iron promotes EMT and cancer via p53 loss in pancreatic cancer. *Asian J. Pharm. Sci*. 15, 237–252. doi: 10.1016/j.ajps.2020.02.003

Birkenfeld, A., Lee, H. Y., Guebre-Egziabher, F., Alves, T. C., Jurczak, M. J., Jornayvaz, F. R., et al. (2011). Deletion of the mammalian INDY homolog mimics aspects of dietary restriction and protects against adiposity and insulin resistance in mice. *Cell Metab*. 14, 184–195. doi: 10.1016/j.cmet.2011.06.009

Bodiga, S., and Krishnapillai, M. N. (2007). Concurrent repletion of iron and zinc reduces intestinal oxidative damage in iron- and zinc-deficient rats. *World J. Gastroenterol*. 13, 5707–5717. doi: 10.3748/wjg.v13.i43.5707

Braadland, P. R., Giskeødegård, G., Sandsmark, E., Bertilsson, H., Euceda, L. R., Hansen, A. F., et al. (2017). Br *ex vivo* metabolic fingerprinting identifies biomarkers predictive of prostate cancer recurrencefollowing radical prostatectomy. Mentions spermine but also citrate is high on the list. *J. Cancer* 117, 1656–1664. doi: 10.1038/bjc.2017.346

Brown, R. A. M., Richardson, K. L., Kabir, T. D., Trinder, D., Ganss, R., and Leedman, P. J. (2020a). Altered iron metabolism and impact in cancer biology, metastasis, and immunology. *Front. Oncol*. 10:476. doi: 10.3389/fonc.2020.00476

Brown, T. P., Bhattacharjee, P., Ramachandran, S., Sivaprakasam, S., Ristic, B., Sikder, M. O. F., et al. (2020b). The lactate receptor GPR81 promotes breast cancer growth via a paracrine mechanism involving antigen-presenting cells in the tumor microenvironment. *Oncogene* 39, 3292–3304. doi: 10.1038/s41388-020-1216-5

Brown, T. P., and Ganapathy, V. (2020). Lactate/GPR81 signaling and proton motive force in cancer: role in angiongenesis, immune escape, nutrition, and Warburg phenomenon. *Pharmacol Ther*. 206:107451. doi: 10.1016/j.pharmthera.2019.107451

Catalina-Rodriguez, O., Kolukula, V. K., Tomita, Y., Preet, A., Palmieri, F., Wellstein, A., et al. (2012). The mitochondrial citrate transporter, CIC, is essential for mitochondrial homeostasis. *Oncotarget* 3, 1220–1235. doi: 10.18632/oncotarget.714

Coleman, P. S. (1986). Membrane cholesterol and tumor bioenergetics. *Ann. N. Y. Acad Sci*. 488, 451–467. doi: 10.1111/j.1749-6632.1986.tb46578.x

Costea, D. E., Hills, A., Osman, A. H., Thurlow, J., Kalna, G., Huang, X., et al. (2013). Identification of two distinct carcinoma-associated fibroblast subtypes with differential tumor-promoting abilities in oral squamous cell carcinoma. *Cancer Res*. 73. 3888–3901. doi: 10.1158/0008-5472.CAN-12-4150

Costello, L. C., Franklin, R., and Stacey, R. (1976). Mitochondrial isocitrate dehydrogenase and isocitrate oxidation of rat ventral prostate. *Enzyme* 21, 495–506. doi: 10.1159/000458902

Costello, L. C., and Franklin, R. B. (2006). The clinical relevance of the metabolism of prostate cancer; zinc and tumor suppression: connecting the dots. *Mol. Cancer*. 5:17. doi: 10.1186/1476-4598-5-17

Davidson, S. M., Papagiannakopoulos, T., Olenchock, B. A., Heyman, J. E., Keibler, M. A., Luengo, A., et al. (2016). Environment impacts the metabolic dependencies of ras-driven non-small cell lung cancer. *Cell Metab*. 23, 517–528. doi: 10.1016/j.cmet.2016.01.007

El Ansari, R., Craze, M. L., Miligy, I., Diez-Rodriguez, M., Nolan, C. C., Ellis, I. O., et al. (2018). The amino acid transporter SLC7A5 confers a poor prognosis in the highly proliferative breast cancer subtypes and is a key therapeutic target in luminal B tumors. *Breast Cancer Res*. 20:21. doi: 10.1186/s13058-018-0946-6

Elia, I., Rossi, M., Stegen, S., Broekaert, D., Doglioni, G., van Gorsel, M., et al. (2019). Breast cancer cells rely on environmental pyruvate to shape the metastatic niche. *Nature* 568, 117–121. doi: 10.1038/s41586-019-0977-x

Faget, D. V., Ren, Q., and Stewart, S. A. (2019). Unmasking senescence: context-dependent effects of SASP in cancer. *Nat. Rev. Cancer* 19, 439–453. doi: 10.1038/s41568-019-0156-2

Fernandez, H. R., Gadre, S. M., Tan, M., Graham, G. T., Mosaoa, R., Ongkeko, M. S., et al. (2018). The mitochondrial citrate carrier, SLC25A1, drives stemness and therapy resistance in non-small cell lung cancer. *Cell Death Differ*. 25, 1239–1258. doi: 10.1038/s41418-018-0101-z

Ganapathy, V., Thangaraju, M., and Prasad, P. D. (2009). Nutrient transporters in cancer: relevance to Warburg hypothesis and beyond. *Pharmacol. Ther*. 121, 29–40. doi: 10.1016/j.pharmthera.2008.09.005

Gnanaprakasam, J. P., Veeranan-Karmegam, R., Coothankandaswamy, V., Reddy, S. K., Martin, P. M., Thangaraju, M., et al. (2013). Loss of Hfe leads to progression of tumor phenotype in primary retinal pigment epithelial cells. *Invest. Ophthalmol. Vis. Sci*. 54, 63–71. doi: 10.1167/iovs.12-10312

Gopal, E., Babu, E., Ramachandran, S., Bhutia, Y. D., Prasad, P. D., and Ganapathy, V. (2015). Species-specific influence of lithium on the activity of SLC13A5 (NaCT): lithium-induced activation is specific for the transporter in primates. *J. Pharmacol. Exp. Ther*. 353, 17–26. doi: 10.1124/jpet.114.221523

Gopal, E., Miyauchi, S., Martin, P. M., Ananth, S., Srinivas, S. R., Smith, S. B., et al. (2007). Expression and functional features of NaCT, a sodium-coupled citrate transporter, in human and rat livers and cell lines. *Am. J. Physiol. Gastrointest. Liver Physiol*. 292, G402–G408. doi: 10.1152/ajpgi.00371.2006

Greene, C. J., Attwood, K., Sharma, N. J., Gross, K. W., Smith, G. J., Xu, B., et al. (2017). Transferrin receptor 1 upregulation in primary tumor and downregulation in benign kidney is associated with progression and mortality in renal cell carcinoma patients. *Oncotarget* 8, 107052–107075. doi: 10.18632/oncotarget.22323

Grosse, S. D., Gurrin, L. C., Bertalli, N. A., and Allen, K. J. (2018). Clinical penetrance in hereditary hemochromatosis: estimates of the cumulative incidence of severe liver disease among HFE C282Y homozygotes. *Genet. Med*. 20, 383–389. doi: 10.1038/gim.2017.121

Gutiérrez-Aguilar, M., and Baines, C. P. (2013). Physiological and pathological roles of mitochondrial SLC25 carriers. *Biochem. J*. 454, 371–386. doi: 10.1042/BJ20121753

Hanahan, D., and Weinberg, R. A. (2000). The hallmarks of cancer. *Cell* 100, 57–70. doi: 10.1016/S0092-8674(00)81683-9

Hassona, Y., Cirillo, N., Lim, K. P., Herman, A., Mellone, M., Thomas, G. J., et al. (2013). Progression of genotype-specific oral cancer leads to senescence of cancer-associated fibroblasts and is mediated by oxidative stress and TGF-β. *Carcinogenesis* 34, 1286–1295. doi: 10.1093/carcin/bgt035

Hatzivassiliou, G., Zhao, F., Bauer, D. E., Andreadis, C., Shaw, A. N., Dhanak, D., et al. (2005). ATP citrate lyase inhibition can suppress tumor cell growth. *Cancer Cell* 8, 311–321. doi: 10.1016/j.ccr.2005.09.008

Hitosugi, T., Zhou, L., Elf, S., Fan, J., Kang, H. B., Seo, J. H., et al. (2012). Phosphoglycerate mutase 1 coordinates glycolysis and biosynthesis to promote tumro growth. *Cancer Cell* 22, 585–600. doi: 10.1016/j.ccr.2012.09.020

Hlouschek, J., Hansel, C., Jendrossek, V., and Matschke, J. (2018). The mitochondrial citrate carrier (SLC25A1) sustains Redox Homeostasis and mitochondrial metabolism supporting radioresistance of cancer cells with tolerance to cycling severe hypoxia. *Front. Oncol*. 8:170. doi: 10.3389/fonc.2018.00170

Hochachka, P. W., Rupert, J. L., Goldenberg, L., Gleave, M., and Kozlowski, P. (2002). Going malignant: the hypoxia-cancer connection in the prostate. *Bioessays* 24, 749–757. doi: 10.1002/bies.10131

Iacobazzi, V., De Palma, A., and Palmieri, F. (1996). Cloning and sequencing of the bovine cDNA encoding the mitochondrial tricarboxylate carrier protein. *Biochim. Biophys. Acta*. 1284, 9–12. doi: 10.1016/0005-2736(96)00115-0

Infantino, V., Dituri, F., Convertini, P., Santarsiero, A., Palmieri, F., Todisco, S., et al. (2019). Epigenetic upregulation and functional role of the mitochondrial aspartate/glutamate carrier isoform 1 in hepatocellular carcinoma. *Biochim. Biophys. Acta Mol. Basis Dis*. 1865, 38–47. doi: 10.1016/j.bbadis.2018.10.018

Inoue, K., Fei, Y. J., Zhuang, L., Gopal, E., Miyauchi, S., and Ganapathy, V. (2004). Functional features and genomic organization of mouse NaCT, a sodium-coupled transporter for tricarboxylic acid cycle intermediates. *Biochem. J*. 378, 949–957. doi: 10.1042/bj20031261

Inoue, K., Zhang, L., Maddox, D. M., Smith, S. B., and Ganapathy, V. (2002a). Structure, function, and expression pattern of a novel sodium-coupled citrate transporter (NaCT) cloned from mammalian brain. *J. Biol. Chem*. 277, 39469–39376. doi: 10.1074/jbc.M207072200

Inoue, K., Zhuang, L., and Ganapathy, V. (2002b). Human Na^+-coupled citrate transporter: primary structure, genomic organization, and transport function. *Biochem. Biophys. Res. Commun*. 299, 465–471. doi: 10.1016/S0006-291X(02)02669-4

Inoue, K., Zhuang, L., Maddox, D. M., Smith, S. B., and Ganapathy, V. (2003). Human sodium-coupled citrate transporter, the orthologue of Drosophila Indy, as a novel target for lithium action. *Biochem. J*. 374, 21–26. doi: 10.1042/bj20030827

Ippolito, L., Morandi, A., Taddei, M. L., Parri, M., Comito, G., Iscaro, A., et al. (2019). Cancer-associated fibroblasts promote prostate cancer malignancy via metabolic rewiring and mitochondrial transfer. *Oncogene* 38, 5339–5355. doi: 10.1038/s41388-019-0805-7

James, E. L., Lane, J. A., Michalek, R. D., Karoly, E. D., and Parkinson, E. K. (2016). Replicatively senescent human fibroblasts reveal a distinct intracellular metabolic profile with alterations in NAD+ and nicotinamide metabolism. *Sci. Rep*. 6:38489. doi: 10.1038/srep38489

James, E. L., Michalek, R. D., Pitiyage, G. N., de Castro, A. M., Vignola, K. S., Jones, J., et al. (2015). Senescent human fibroblasts show increased glycolysis and redox homeostasis with extracellular metabolomes that overlap with those of irreparable DNA damage, aging, and disease. *J. Proteome Res*. 14, 1854–1871. doi: 10.1021/pr501221g

James, E. N. L., Bennett, M. H., and Parkinson, E. K. (2018). The induction of the fibroblast extracellular senescence metabolome is a dynamic process. *Sci. Rep*. 8:12148. doi: 10.1038/s41598-018-29809-5

Jaramillo-Martinez, V., Urbatsch, I. L., and Ganapathy, V. (2020). Functional distinction between human and mouse sodium-coupled citrate transporters and its biologic significance: an attempt for structural basis using a homology modelling approach. *Chem. Rev*. doi: 10.1021/acs.chemrev.0c00529

Jung, M., Mertens, C., Tomat, E., and Brüne, B. (2019). Iron as a central player and promising target in cancer progression. *Int. J. Mol. Sci*. 20:273. doi: 10.3390/ijms20020273

Kalluri, R. (2016). The biology and function of fibroblasts in cancer. *Nat. Rev. Cancer*. 16, 582–598. doi: 10.1038/nrc.2016.73

Kolukula, V. K., Sahu, G., Wellstein, A., Rodriguez, O. C., Preet, A., Iacobazzi, V., et al. (2014). SLC25A1, or CIC, is a novel transcriptional target of mutant p53 and a negative tumor prognostic marker. *Oncotarget* 5, 1212–1225. doi: 10.18632/oncotarget.1831

Kong, Y., Hu, L., Lu, K., Wang, Y., Xie, Y., Gao, L., et al. (2019). Ferroportin downregulation promotes cell proliferation by modulating the Nrf2-miR-17-5p axis in multiple myeloma. *Cell Death Dis*. 10:624. doi: 10.1038/s41419-019-1854-0

Kopel, J., Higuchi, K., Ristic, B., Sato, T., Ramachandran, S., and Ganapathy, V. (2020). The hepatic plasma membrane citrate transporter NaCT (SLC13A5) as a molecular target for metformin. *Sci Rep*. 10:8536. doi: 10.1038/s41598-020-65621-w

Langbein, S., Zerilli, M., Zur Hausen, A., Staiger, W., Rensch-Boschert, K., Lukan, N., et al. (2006). Expression of transketolase TKTL1 predicts colon and urothelial cancer patient survival: Warburg effect reinterpreted. *Br. J. Cancer* 94, 578–585. doi: 10.1038/sj.bjc.6602962

Li, Z., Li, D., Choi, E. Y., Lapidus, R., Zhang, L., Huang, S. M., et al. (2017). Silencing of solute carrier family 13 member 5 disrupts energy homeostasis and inhibits proliferation of human hapatocarcinoma cells. *J. Biol. Chem*. 292, 13890–13901. doi: 10.1074/jbc.M117.783860

Lim, K. P., Cirillo, N., Hassona, Y., Wei, W., Thurlow, J. K., Cheong, S. C., et al. (2011). Fibroblast gene expression profile reflects the stage of tumor progression in oral squamous cell carcinoma. *J. Pathol*. 223, 459–469. doi: 10.1002/path.2841

Liu, H., Huang, D., McArthur, D. L., Boros, L. G., Nissen, N., and Heaney, A. P. (2010). Fructose induces transketolase flux to promote pancreatic cancer growth. *Cancer Res*. 70, 6368–6376. doi: 10.1158/0008-5472.CAN-09-4615

Locasale, J. W., Grassian, A. R., Melman, T., Lyssiotis, C. A., Mattaini, K. R., Bass, A. J., et al. (2011). Phosphoglycerate dehydrogenase diverts glycolytic flux and contributes to oncogenesis. *Nat. Genet*. 43, 869–874. doi: 10.1038/ng.890

Ma, Y., Wang, W., Idowu, M. O., Oh, U., Wang, X. Y., Temkin, S. M., et al. (2018). Ovarian cancer relies on glucose transporter 1 to fuel glycolysis and growth: anti-tumor activity of BAY-876. *Cancers*. 11:33. doi: 10.3390/cancers11010033

Marin-Valencia, I., Yang, C., Mashimo, T., Cho, S., Baek, H., Yang, X. L., et al. (2012). Analysis of tumor metabolism reveals mitochondrial glucose oxidation in genetically diverse human glioblastomas in the mouse brain *in vivo*. *Cell Metab*. 15, 827–837. doi: 10.1016/j.cmet.2012.05.001

Martinez-Outschoorn, U. E., Lisanti, M. P., and Sotgia, F. (2014). Catabolic cancer-associated fibroblasts transfer energy and biomass to anabolic cancer cells, fueling tumor growth. *Semin. Cancer Biol*. 25, 47–60. doi: 10.1016/j.semcancer.2014.01.005

Mazurek, M. P., Prasad, P. D., Gopal, E., Fraser, S. P., Bolt, L., Rizaner, N., et al. (2010). Molecular origin of plasma membrane citrate transporter in human prostate epithelial cells. *EMBO Rep*. 11, 431–437. doi: 10.1038/embor.2010.51

Mellone, M., Hanley, C. J., Thirdborough, S., Mellows, T., Garcia, E., Woo, J., et al. (2016). Induction of fibroblast senescence generates a non-fibrogenic myofibroblast phenotype that differentially impacts on cancer prognosis. *Aging*. 9, 114–132. doi: 10.18632/aging.101127

Metallo, C. M., Gameiro, P. A., Bell, E. L., Mattaini, K. R., Yang, J., Hiller, K., et al. (2011). Reductive glutamine metabolism by IDH1 mediates lipogenesis under hypoxia. *Nature* 481, 380–384. doi: 10.1038/nature10602

Monné, M., Vozza, A., Lasorsa, F. M., Porcelli, V., and Palmieri, F. (2019). Mitochondrial carriers for aspartate, glutamate and other amino acids: a review. *Int. J. Mol. Sci*. 20:4456. doi: 10.3390/ijms20184456

Montal, E. D., Dewi, R., Bhalla, K., Ou, L., Hwang, B. J., Ropell, A. E., et al. (2015). PEPCK coordinates the regulation of central carbon metabolism to promote cancer cell growth. *Mol. Cell*. 60, 571–583. doi: 10.1016/j.molcel.2015.09.025

Moreno, M., Ortega, F., Xifra, G., Ricart, W., Fernandez-Real, J. M., and Moreno-Navarrete, J. M. (2015). Cytosolic aconitase activity sustains adipogenic capacity of adipose tissue connecting iron metabolism and adipogenesis. *FASEB J*. 29, 1529–1539. doi: 10.1096/fj.14-258996

Mullen, A. R., Hu, Z., Shi, X., Jiang, L., Boroughs, L. K., Kovacs, Z., et al. (2014). Oxidation of alpha-ketoglutarate is required for reductive carboxylation in cancer cells with mitochondrial defects. *Cell Rep*. 7, 1679–1690. doi: 10.1016/j.celrep.2014.04.037

Mycielska, M. E., Dettmer, K., Rümmele, P., Schmidt, K., Prehn, C., Milenkovic, V. M., et al. (2018). Extracellular citrate affects critical elements of cancer cell metabolism and supports cancer development *in vivo*. *Cancer Res*. 78, 2513–2523. doi: 10.1158/0008-5472.CAN-17-2959

Mycielska, M. E., and Geissler, E. K. (2018). Extracellular citrate and cancer metabolism-response. *Cancer Res*. 78:5177. doi: 10.1158/0008-5472.CAN-18-1899

Mycielska, M. E., Milenkovic, V. M., Wetzel, C. H., Rümmele, P., and Geissler, E. K. (2015). Extracellular citrate in health and disease. *Curr. Mol. Med*. 15, 884–891. doi: 10.2174/1566524016666151123104855

Mycielska, M. E., Mohr, M. T. J., Schmidt, K., Drexler, K., Rümmele, P., Haferkamp, S., et al. (2019). Potential use of gluconate in cancer therapy. *Front. Oncol*. 9:522. doi: 10.3389/fonc.2019.00522

Mycielska, M. E., Patel, A., Rizaner, N., Mazurek, M. P., Keun, H., Patel, A., et al. (2009). Citrate transport and metabolism in mammalian cells: prostate epithelial cells and prostate cancer. *Bioessays* 31, 10–20. doi: 10.1002/bies.080137

Park, S. J., Smith, C. P., Wilbur, R. R., Cain, C. P., Kallu, S. R., Valasapalli, S., et al. (2018). An overview of MCT1 and MCT4 in GBM: small molecule transporters with large implications. *Am. J. Cancer Res.* 8, 1967–1976.

Patra, K. C., and Hay, N. (2014). The pentose phosphate pathway and cancer. *Trends Biochem. Sci.* 39, 347–354. doi: 10.1016/j.tibs.2014.06.005

Peters, J. M. (2017). Flipping a citrate switch on liver cancer cells. *J. Biol. Chem.* 292, 13902–13903. doi: 10.1074/jbc.H117.783860

Pitiyage, G. N., Slijepcevic, P., Gabrani, A., Chianea, Y. G., Lim, K. P., Prime, S. S., et al. (2011). Senescent mesenchymal cells accumulate in human fibrosis by a telomere-independent mechanism and ameliorate fibrosis through matrix metalloproteinases. *J. Pathol.* 223, 604–617. doi: 10.1002/path.2839

Possemato, R., Marks, K. M., Shaul, Y. D., Pacold, M. E., Kim, D., Birsoy, K., et al. (2011). Functional genomics reveal that the serine synthesis pathway is essential in breast cancer. *Nature* 476, 346–350. doi: 10.1038/nature10350

Profilo, E., Peña-Altamira, L. E., Corricelli, M., Castegna, A., Danese, A., Agrimi, G., et al. (2017). Down-regulation of the mitochondrial aspartate-glutamate carrier isoform 1 AGC1 inhibits proliferation and N-acetylaspartate synthesis in Neuro2A cells. *Biochim. Biophys. Acta Mol. Basis Dis.* 1863, 1422–1435. doi: 10.1016/j.bbadis.2017.02.022

Rao, S., and Coleman, P. S. (1989). Control of DNA replication and cell growth by inhibiting the export of mitochondrially derived citrate. *Exp. Cell Res.* 180, 341–352. doi: 10.1016/0014-4827(89)90062-1

Ristic, B., Bhutia, Y. D., and Ganapathy, V. (2017). Cell-surface G-protein-coupled receptors for tumor-associated metabolites: a direct link to mitochondrial dysfunction in cancer. *Biochim. Biophys. Acta* 1868, 246–257. doi: 10.1016/j.bbcan.2017.05.003

Sahai, E., Astsaturov, I., Cukierman, E., DeNardo, D. G., Egeblad, M., Evans, R. M., et al. (2020). A framework for advancing our understanding of cancer-associated fibroblasts. *Nat. Rev. Cancer* 20, 174–186. doi: 10.1038/s41568-019-0238-1

Sakamoto, A., Kunou, S., Shimada, K., Tsunoda, M., Aoki, T., Iriyama, C., et al. (2019). Pyruvate secreted from patient-derived cancer-associated fibroblasts supports survival of primary lymphoma cells. *Cancer Sci.* 110, 269–278. doi: 10.1111/cas.13873

Sanford-Crane, H., Abrego, J., and Sherman, M. H. (2019). Fibroblasts as modulators of local and systemic cancer metabolism. *Cancers.* 11:619. doi: 10.3390/cancers11050619

Sivaprakasam, S., Ristic, B., Mudaliar, N., Hamood, A. N., Colmer-Hamood, J., Wachtel, M. S., et al. (2020). Hereditary hemochromatosis promotes colitis and colon cancer and causes bacterial dysbiosis in mice. *Biochem. J.* 477:3867–3883. doi: 10.1042/BCJ20200392

Sousa, C. M., Biancur, D. E., Wang, X., Halbrook, C. J., Sherman, M. H., Zhang, L., et al. (2016). Pancreatic stellate cells support tumor metabolism through autophagic alanine secretion. *Nature* 536, 479–483. doi: 10.1038/nature19084

Szeri, F., Lundkvist, S., Donnelly, S., Engelke, U. F. H., Rhee, K., Williams, C. J., et al. (2020). The membrane protein ANKH is crucial for bone mechanical performance by mediating cellular export of citrate and ATP. *PLoS Genet.* 16:e1008884. doi: 10.1371/journal.pgen.1008884

Tasdogan, A., Faubert, B., Ramesh, V., Ubellacker, J. M., Shen, B., Solmonson, A., et al. (2020). Metabolic heterogeneity confers differences in melanoma metastatic potential. *Nature* 577, 115–120. doi: 10.1038/s41586-019-1847-2

Valencia, T., Kim, J. Y., Abu-Baker, S., Moscat-Pardos, J., Ahn, C. S., Reina-Campos, M., et al. (2014). Metabolic reprogramming of stromal fibroblasts through p62-mTORC1 signaling promotes inflammation and tumorigenesis. *Cancer Cell.* 26, 121–135. doi: 10.1016/j.ccr.2014.05.004

Vincent, E. E., Sergushichev, A., Griss, T., Gingras, M. C., Samborska, B., Ntimbane, T., et al. (2015). Mitochondrial phosphoenolpyruvate carboxykinase regulates metabolic adaptation and enables glucose-independent tumor growth. *Mol. Cell.* 60, 195–207. doi: 10.1016/j.molcel.2015.08.013

Wang, C., Ma, J., Zhang, N., Yang, Q., Jin, Y., and Wang, Y. (2015). The acetyl-CoA carboxylase enzyme: a target for cancer therapy? *Expert. Rev. Anticancer Ther.* 15, 667–676. doi: 10.1586/14737140.2015.1038246

Wang, J., Chen, G., Filebeen, C., and Pantopoulos, K. (2008). Insights on regulation and function of the iron regulatory protein 1 (IRP1). *Hemoglobin* 32, 109–115. doi: 10.1080/03630260701680326

Wang, R., Xiang, W., Xu, Y., Han, L., Li, Q., Dai, W., et al. (2020). Enhanced glutamine utilization mediated by SLC1A5 and GPT2 is an essential metabolic feature of colorectal signet ring cell carcinoma with therapeutic potential. *Ann. Transl. Med.* 8:302. doi: 10.21037/atm.2020.03.31

Wang, Y., Yu, L., Ding, J., and Chen, Y. (2018). Iron metabolism in cancer. *Int. J. Mol. Sci.* 20:95. doi: 10.3390/ijms20010095

Wellen, K. E., Hatzivassiliou, G., Sachdeva, U. M., Bui, T. V., Cross, J. R., and Thompson, C. B. (2009). ATP-citrate lyase links cellular metabolism to histone acetylation. *Science* 324, 1076–1080. doi: 10.1126/science.1164097

Wiley, C. D., and Campisi, J. (2016). From ancient pathways to aging cells-connecting metabolism and cellular senescence. *Cell Metab.* 23, 1013–1021. doi: 10.1016/j.cmet.2016.05.010

Willmes, D. M., Kurzbach, A., Henke, C., Schumann, T., Zahn, G., Heifetz, A., et al. (2018). The longevity gene INDY (I'm Not Dead Yet" in metabolic control: potential as a pharmacologic target. *Pharmacol. Ther.* 185, 1–11. doi: 10.1016/j.pharmthera.2017.10.003

Xue, X., Ramakrishnan, S. K., Weisz, K., Triner, D., Xie, L., Attili, D., et al. (2016). Iron uptake via DMT1 integrates cell cycle with JAK-STAT3 signaling to promote colorectal tumorigenesis. *Cell Metab.* 24, 447–461. doi: 10.1016/j.cmet.2016.07.015

Zhang, L., and Li, S. (2020). Lactic acid promotes macrophage polarization through MCT-HIF1α signaling in gastric cancer. *Exp. Cell Res.* 388:111846. doi: 10.1016/j.yexcr.2020.111846

Zhang, Z., Gao, Z., Rajthala, S., Sapkota, D., Dongre, H., Parajuli, H., et al. (2020). Metabolic reprogramming of normal oral fibroblasts correlated with increased glycolytic metabolism of oral squamous cell carcinoma and precedes their activation into carcinoma associated fibroblasts. *Cell Mol. Life Sci.* 77, 1115–1133. doi: 10.1007/s00018-019-03209-y

Conflict of Interest: The authors declare that the research was conducted in the absence of any commercial or financial relationships that could be construed as a potential conflict of interest.

frontiers in Cell and Developmental Biology

ORIGINAL RESEARCH
published: 01 February 2021
doi: 10.3389/fcell.2021.593510

Serum Metabolomics Study of Papillary Thyroid Carcinoma Based on HPLC-Q-TOF-MS/MS

Yang Du[1], Peizhi Fan[1], Lianhong Zou[2]*, Yu Jiang[2], Xiaowen Gu[1], Jie Yu[1] and Chaojie Zhang[1]*

[1] Department of Breast and Thyroid Surgery, Hunan Provincial People's Hospital/The First Affiliated Hospital of Hunan Normal University, Changsha, China, [2] Hunan Provincial Key Laboratory of Emergency and Critical Care Metabonomics, Institute of Emergency Medicine, Hunan Provincial People's Hospital/The First Affiliated Hospital of Hunan Normal University, Changsha, China

OPEN ACCESS

Edited by:
Maria E. Mycielska, University Medical Center Regensburg, Germany

Reviewed by:
Anna Artati, Helmholtz Zentrum München, Helmholtz-Gemeinschaft Deutscher Forschungszentren (HZ), Germany
Gisele Andre Baptista Canuto, Federal University of Bahia, Brazil
Marta Kordalewska, Medical University of Gdańsk, Poland

***Correspondence:**
Peizhi Fan
fanpzh64@163.com
Lianhong Zou
zoulh1986@hunnu.edu.cn

Specialty section:
This article was submitted to Molecular and Cellular Oncology, a section of the journal Frontiers in Cell and Developmental Biology

Received: *10 August 2020*
Accepted: *08 January 2021*
Published: *01 February 2021*

Citation:
Du Y, Fan P, Zou L, Jiang Y, Gu X, Yu J and Zhang C (2021) Serum Metabolomics Study of Papillary Thyroid Carcinoma Based on HPLC-Q-TOF-MS/MS. Front. Cell Dev. Biol. 9:593510. doi: 10.3389/fcell.2021.593510

This study examined metabolite profile differences between serum samples of thyroid papillary carcinoma (PTC) patients and healthy controls, aiming to identify candidate biomarkers and pathogenesis pathways in this cancer type. Serum samples were collected from PTC patients ($n = 80$) and healthy controls ($n = 80$). Using principal component analysis (PCA), partial least squares discrimination analysis(PLS-DA), orthogonal partial least square discriminant analysis (OPLS-DA), *t*-tests, and the volcano plot, a model of abnormal metabolic pathways in PTC was constructed. PCA, PLS-DA, and OPLS-DA analysis revealed differences in serum metabolic profiles between the PTC and control group. OPLS-Loading plot analysis, combined with Variable importance in the projection (VIP)>1, Fold change (FC) > 1.5, and $p < 0.05$ were used to screen 64 candidate metabolites. Among them, 22 metabolites, including proline betaine, taurocholic acid, L-phenylalanine, retinyl beta-glucuronide, alpha-tocotrienol, and threonine acid were upregulated in the PTC group; meanwhile, L-tyrosine, L-tryptophan, 2-arachidonylglycerol, citric acid, and other 42 metabolites were downregulated in this group. There were eight abnormal metabolic pathways related to the differential metabolites, which may be involved in the pathophysiology of PTC. Six metabolites yielded an area under the receiver operating curve of >0.75, specifically, 3-hydroxy-cis-5-tetradecenoylcarnitine, aspartylphenylalanine, l-kynurenine, methylmalonic acid, phenylalanylphenylalanine, and l-glutamic acid. The Warburg effect was observed in PTC. The levels of 3-hydroxy-cis-5-tetradecenoylcarnitine, aspartylphenylalanine, l-kynurenine, methylmalonic acid, phenylalanine, and L-glutamic acid may help distinguish PTC patients from healthy controls. Aspartic acid metabolism, glutamic acid metabolism, urea cycle, and tricarboxylic acid cycle are involved in the mechanism of PTC.

Keywords: thyroid papillary carcinoma, metabolite profile, serum samples, principal component analysis, orthogonal partial least square discriminant analysis

INTRODUCTION

Thyroid cancer is the most common type of endocrine tumor in clinical practice, accounting for 1.1% of all malignant tumors (Bray et al., 2018), while PTC is the most common type of thyroid cancer, accounting for ∼90% of all cases. It is more common in women aged 30–45 years. PTC has good differentiation and low malignancy; however, it is prone to early lymph node metastasis (Ferlay et al., 2013). Therefore, early diagnosis and treatment are paramount to patient survival. Ultrasound-guided fine needle aspiration cytology (FNAC) is a commonly used auxiliary examination for the diagnosis of thyroid cancer. Although imaging tests have high sensitivity in the diagnosis of thyroid cancer, their specificity is poor (Remonti et al., 2015). FNAC is currently the most accurate and cost-effective method for assessing benign and malignant thyroid nodules; however, ∼20–30% of cases cannot be confirmed as either benign or malignant by FNAC alone (Faquin, 2008; Fish, 2017). Because some papillary thyroid microcarcinomas have fewer abnormal cells, they may be missed or even misdiagnosed when only the FNAC method is performed (Kim et al., 2011). Therefore, several genetic tests have been proposed as useful in the diagnosis of thyroid cancer, including tests for *BRAF* and *NRAS* mutations, and *RET* translocation tests; in fact, *BRAF* mutations have been reported in 30–80% of PTC cases (Jin et al., 2006). However, samples from suspicious thyroid nodules that test negative for the *BRAF* gene mutation do not automatically exclude the possibility of PTC. In cases of inconclusive cytology findings, the detection of BRAF gene mutations can improve the rate of diagnosis of PTC (Johnson et al., 2014). Meanwhile, FNAC is an invasive examination, and the preoperative acceptance of patients is generally limited, but the clinical applicability of the latter is not very strong. Overall, this evidence indicates a need for a stable and reliable biomarker to assist in the diagnosis of thyroid cancer.

Metabolomics refers to a comprehensive analysis of the metabolome of biological systems under specific conditions. It is a type of high-throughput technology that plays an important role in systems biology research. The metabolome consists of thousands of complex molecular metabolites, whose relative molecular mass is $<1 \times 10^3$ (Barnes et al., 2016). High Performance Liquid Chromatography of Quadrupole Time of Flight Mass Spectrometry (HPLC-Q-TOF-MS/MS) combines liquid chromatography and mass spectrometry, thereby allowing to examine metabolites and perform stoichiometric analysis and improving the understanding of the molecular mechanisms of cancer development and associated biomarkers (Monteiro et al., 2013). The HPLC-Q-TOF-MS/MS platform allows for the separation and identification of complex mixtures, combining the compound separation capacity of the liquid chromatograph with the component identification ability of the mass spectrometer, resulting in high detection sensitivity and wide coverage of metabolite detection (Shepherd et al., 2011). Metabolomics is key to the understanding of the mechanisms of various cancers. For example, Yuan et al. (2018) used tandem mass spectrometry (UHPLC-MS/MS and FIA-MS/MS) to compare the types and levels of metabolites extracted from the plasma of patients with primary breast cancer with those of healthy controls, revealing that metabolites are mainly involved in amino acid metabolism and breast cancer cell growth pathways. Concurrently, Han et al. (2020) used UHPLC-MS/MS to show that retinol is a biomarker that distinguishes hepatocellular carcinoma (HCC) from adjacent tissues. The reported area under the curve associated with retinol (The area under curve, AUC = 0.991) suggests that it is important in HCC. Several previous studies have used metabolomics technology to distinguish PTC patients from healthy subjects; however, the studies had certain limitations. The advantages of the current study were as follows: (1). HPLC-Q-TOF-MS/MS is a novel method for identifying non-target metabolites, although it is less used in PTC research. (2). The sample size was sufficient. Using HPLC-Q-TOF-MS/MS to assess metabolic changes of PTC, we established a reliable statistical model that could distinguish and predict PTC patients and healthy controls. The main purpose of the study were as follows: (1). to identify metabolic markers that can distinguish PTC patients from healthy subjects using metabolomics; (2). to determine detailed metabolic changes and related metabolic pathways in PTC; and (3). to provide evidence for the diagnosis and treatment of PTC patients on the basis of science.

MATERIALS AND METHODS

Patients and Study Design

This study complied with the guidelines of the Declaration of Helsinki and the Conference for Coordination of Clinical Practice and was approved by the Ethics Committee of Hunan Provincial People's Hospital. Each participant signed an informed consent form. The seventh edition of the American Joint Committee on Cancer Tumor-Lymph Node Metastasis staging system was used to determine PTC stage (Edge and Compton, 2010). This case-control study involved obtaining a serum sample from PTC patients undergoing total thyroidectomy at the study site between October 2018 and February 2020. Patient eligibility was confirmed based on pathological findings after thyroidectomy; only patients diagnosed with PTC were included; in contrast, patients with micro-PTC were excluded from this study. None of the patients had a history of another cancer, normal levels of thyroid hormones (T3 and T4), thyroid-stimulating hormone (TSH), no thyroid hormone medications before surgery, no other forms of cancer, immune blood system diseases, or metabolic disorders (metabolic syndrome, diabetes, and insulin resistance). Healthy controls visited the hospital to draw blood voluntarily for regular physical examinations. Healthy controls were recruited from among the individuals referred to the Saeed Pathobiology and Genetics Laboratory for routine examinations. Laboratory examination results confirmed normal levels of T3, T4, and TSH, and the absence of hypothyroidism, hyperthyroidism, nodular goiter, or autoimmune thyroid inflammation.

Each PTC patient provided ∼5 ml of blood before the operation (patients were treatment-naïve at the time of sample collection); healthy controls provided blood samples after overnight fasting. Blood samples from both groups were

stored for 2 h at 4°C and were subsequently centrifuged for 10 min at 4°C and 3,000 rpm. The centrifuged serum samples were extracted into 1.5 ml Eppendorf (Eppendorf Corporation, Germany)microtubes and stored at −80°C for later use.

Serum Metabolite Extraction

Serum metabolites were extracted by adding 400 μl protein precipitant (MEthanol/ACN,v/v, 2:1) and 10 μl internal standard (L-2-chlorophenylalanine, 0.3 mg/ml, methanol preparation) to 100 μl of serum into 2 ml Eppendorf (Eppendorf Corporation, Germany)microtubes. The tube was vortexed for 30 s, ultrasonicated for 10 min (4°C water bath) and cooled at −20°C for 1 h. The tube was then centrifuged at 4°C at 13,000 rpm for 15 min to remove the precipitated protein.The supernatant of each sample was collected and stored in a refrigerator at −20°C.

Quality Control (QC) preparation: 10 μl was taken from each sample and added into 2 ml Eppendorf (Eppendorf Corporation, Germany)microtubes.Then vortex and divide into 200 μl for each tube.Quality control (QC) samples were pooled and pretreated using the same procedure to improve the data quality for metabolic profiling.

HPLC-Q-TOF-MS/MS Metabolomics Analysis

HPLC-Q-TOF-MS/MS (Bruker Corporation, USA) was used as a metabolite separation and detection platform to study the metabolite differences between the PTC and control groups. The data were collected under the positive and negative ion modes of mass spectrometry. HPLC-Q-TOF-MS/MS conditions were the following: ACCLAINMTMRSLC120-C18 column (100 × 2.1 mm,2.2 μm) (Thermo fisher scientific, USA) at 40°C with 3 μl sample injection; mobile phase A was 0.1% (volume fraction) formic acid/water, and mobile phase B was 0.1% (volume fraction) acetonitrile/water (containing 0.1% formic acid). The gradient was set as follows: 2% B for 0–2 min, 50% B for 2–12 min, 90% B for 10–30 min, and 98% B for 30–60 min. The flow rate was maintained at 400 μl/min. The mass spectrometry conditions were as follows: Electrospray ion source was detected using positive and negative ion mode; high purity N2-assisted spray ionization and solvent removal was used; the flow rate was 1.2 l/min, the mass scanning range was 20–1,000 m/z, and the drying temperature was 200°C. In ESI positive mode, the Spray voltage (ISVF) is 4,500 V, and the capillary voltage is 100 V; in ESI negative ion mode, the Spray voltage (ISVF) is −4,500 V, and the capillary voltage is −100 V, fragmentor voltage 70 V.Quality control samples (QC samples) were analyzed five times at the beginning of the run and injected once after every 20 injections of the random sequenced samples.

Raw HPLC-Q-TOF-MS/MS Data Processing

Metaboscape 3.0 (Bruker Corporation, USA) software was used to perform data cleaning, including peak extraction, noise reduction, standardization, and export, among others. Minimum Peak Length (3–5) spectrum; Recursive Feature Extraction/ Recursive Feature Extraction: Minimum Peak Length (Recursive) (5–7) spectrum. Minimum feature for extraction and presence of features in minimum of analyses will be selected according to the actual sample size. According to the 80% principle (Bijlsma et al., 2006), given 80 analyses, 64/80 analyses, retention time range [0, 30] min, and mass range [20, 1,000] M/Z. Ion Deconvolution/ Deconvolution inverse volume product EIC correlation ≥0.8. The ion fragments [such as [M+H]+, [M-H]–] were then recombined. Subsequently, the known false positive peaks, such as derivative chemical reagent peak, noise, and column loss peak, were removed from the data matrix; finally, the redundancy and peak combination procedures were performed. The data were uploaded to Annotate with Analyte List (HMDB database www.hmdb.ca), Annotate with Spectral Library [the standard product database created by Bruker [the most accurate]], and Annotate with Smartformula (online website database) database for matching and finally maintain the output A three-dimensional data matrix of time, mass response intensity, mass-to-nucleus ratio (M/Z), sample information, etc. This matrix was suitable for data analysis software such as SIMCAP, SPSS, and R language.

Statistical Analysis

The metabolic profiles of serum samples were compared between the PTC and control groups, using multivariate and univariate analyses. Variable distribution was normalized using Log transformation and Pareto scaling for all pre-processed data. The Mann-Whitney-Wilcoxon test with false discovery rate correction was used to measure the significance of each metabolite. The SIMCAP14.1 software (Umetrics, Umea, Sweden) was used to PCA, PLS-DA, and OPLS-DA to determine the differences in metabolic profiles between the groups. The quality of the model is determined by the values of R2Y and Q2. R2Y represents the explanatory rate model, Q2 represents the forecast rate. Higher values of R2Y and Q2 usually indicate that the model is more reliable.Benjamini-Hochberg false discovery rate (FDR) procedure was employed for the multiple test adjustments. Adjusted $p < 0.05$ were considered statistically significant. Two hundred Permutation test was used to test model reliability. R^2 and Q^2 are obtained through permutations test, and its function is to verify whether the model is overfitting. When $R^2 > 0$ and $Q^2 < 0$, it means that the model is not overfitting and the model is reliable.VIP index represents the importance of each variable to model performance and describes the overall contribution of each variable to the model. Variables with a VIP of >1 have greater significance than do their counterparts. These variables were obtained from the PLS-DA model and adjusted $p < 0.05$.One-way analysis of variance and volcano plot were used to identify which metabolites annotated in the HPLC-Q-TOF-MS/MS dataset were significantly affected by the factor assessed in the experiment. MetaboAnalyst 4.0 (https://www.metaboanalyst.ca/) drew a heatmap, which was based on the estimates derived from the Spearman rank correlation and cluster analysis. The receiver operating characteristic (ROC) curve analysis was performed using the survival analysis module to evaluate the area under the curve (AUC) and to compare the diagnostic ability of significant metabolites between the tested groups.

Metabolic Pathway Analysis

Use MetaboAnalyst 4.0 (https://www.metaboanalyst.ca/) on the difference of PTC patients serum and healthy subjects serum metabolites analysis of metabolic pathways, the purpose is to explain the biological correlation between PTC patients and healthy subjects. In this study, we referred to the Kyoto Encyclopedia of Gene and Genomes (KEGG, https://www.genome.jp/kegg) and the Human Metabolome Database (HMDB, https://hmdb.ca/) to elucidate any changes or interference patterns observed in the metabolic pathways in the study participants. KEGG is a knowledge base and is used for systematic analysis of metabolite function (Du et al., 2014). HMDB is a comprehensive database of metabolomics and metabolites biology (Wishart et al., 2013). MetaboAnalyst 4.0 combines enrichment and topology pathway analyses to identify relevant pathways. The module of pathway analysis was based on the KEGG database; the enrichment analysis was based on the Small Molecule Pathway Database (http://smpdb.ca/) (Jewison at al, 2014).

Ethics Statement

The study was conducted in accordance with the Helsinki Declaration and was approved by the Ethics Committee of Human Provincial People's Hospital in Changsha, Hunan Province, China. Patients/participants provided their written informed consent to participate in the study.

RESULTS

Clinical Characteristics of the Subjects

There were 80 PTC patients (18 men and 62 women; age range, 20–72 years), and 80 healthy controls (32 women and 48 men; age range, 30 and 67 years). The median age of the PTC and control groups was 41.63 ± 11.213 years and 43.44 ± 8.378 years, respectively; this difference was no statistically significant ($p > 0.05$) (**Table 1**).

Serum Metabolomics Profiles in the PTC and Control Groups

After Metaboscape 3.0 pretreatment, a series of metabonomic data was obtained. In positive ion patterns, there were 384 identifiable peaks (**Supplementary Figure 1**), representing 384 detected metabolites. **Supplementary Figure 1** shows the base peak chromatograms (BPC) of the PTC and control group serum samples. In negative ion patterns, there were 678 identifiable peaks (**Supplementary Figure 2**), representing 678 detected metabolites. **Supplementary Figure 2** shows the BPC of the PTC and control group serum samples. There were significant between-peak differences in intensity, indicating that in the positive and negative ion mode, there were significant between-group differences in the metabolic profiles.

Statistical tests commonly used to examine between-group differences in metabolite profiles include the *t*-test, FC analysis, and volcano plot. Univariate analysis can intuitively show the significance of different metabolites in two samples, and it is an essential statistical method in screening differential metabolites. A $p < 0.05$ was used to screen the different markers. Meanwhile, the volcano map (**Figures 1A,B**) was drawn based on the FC values and *t*-test findings (**Supplementary Tables 1, 2**). In the positive and negative ion mode, a total of 27 (**Supplementary Table 1**) and 73 different metabolites (**Supplementary Table 2**) were screened, respectively. Between-group differences in metabolites in the positive and negative ion modes were plotted as volcanic maps; red dots represent the differences in serum metabolites between the PTC and control groups. The volcanic map of metabolites given the positive and negative ion modes is shown in **Figures 1A,B**, respectively; there were 27 and 73 different metabolites, respectively. These findings indicated that amino acids, fatty acids and their derivatives, and nucleotides, among others, were the most important metabolites that differed between the groups. In particular, an increase in the levels of proline betaine, L-phenylalanine, threonic acid, isobutyryl-L-carnitine, and retinyl beta-glucuronide was observed in the PTC group, presenting candidate metabolic markers for differentiating PTC patients from healthy controls.

Hierarchical cluster analysis was used to cluster all metabolomic data with a $p < 0.05$ to examine the metabolites significantly changed between different groups. Within-group sample similarity was evaluated and presented as a heatmap obtained in positive and negative ion modes (**Figures 1C,D**, respectively). These data indicate specific patterns of differences in the metabolites between PTC and healthy controls.

TABLE 1 | Clinical and pathological characteristic of the participants.

Characteristic	PTC	Control (healthy subjects)
Patient number	80	80
Gender		
Male	18	48
Female	62	32
Age (Mean ± SD; year)	41.63 ± 11.213	43.44 ± 8.378
Clinical biochemistry tests (Mean ± SD)	-	
TSH (μIU/ml)		1.79 ± 0.81
T4T (nmol/l)		110.51 ± 12.35
T3T (nmol/l)		2 ± 0.54
Lymph node metastasis[a]		-
Negative	26	
Positive	54	
TNM stages[b]		-
I	20	
II	52	
III	5	
IVA	3	

PTC, papillary thyroid carcinoma. [a]Includes N1a and/or N1b. [b]American Joint Committee on Cancer (AJCC) Tumor-Node-Metastasis (TNM) staging system.

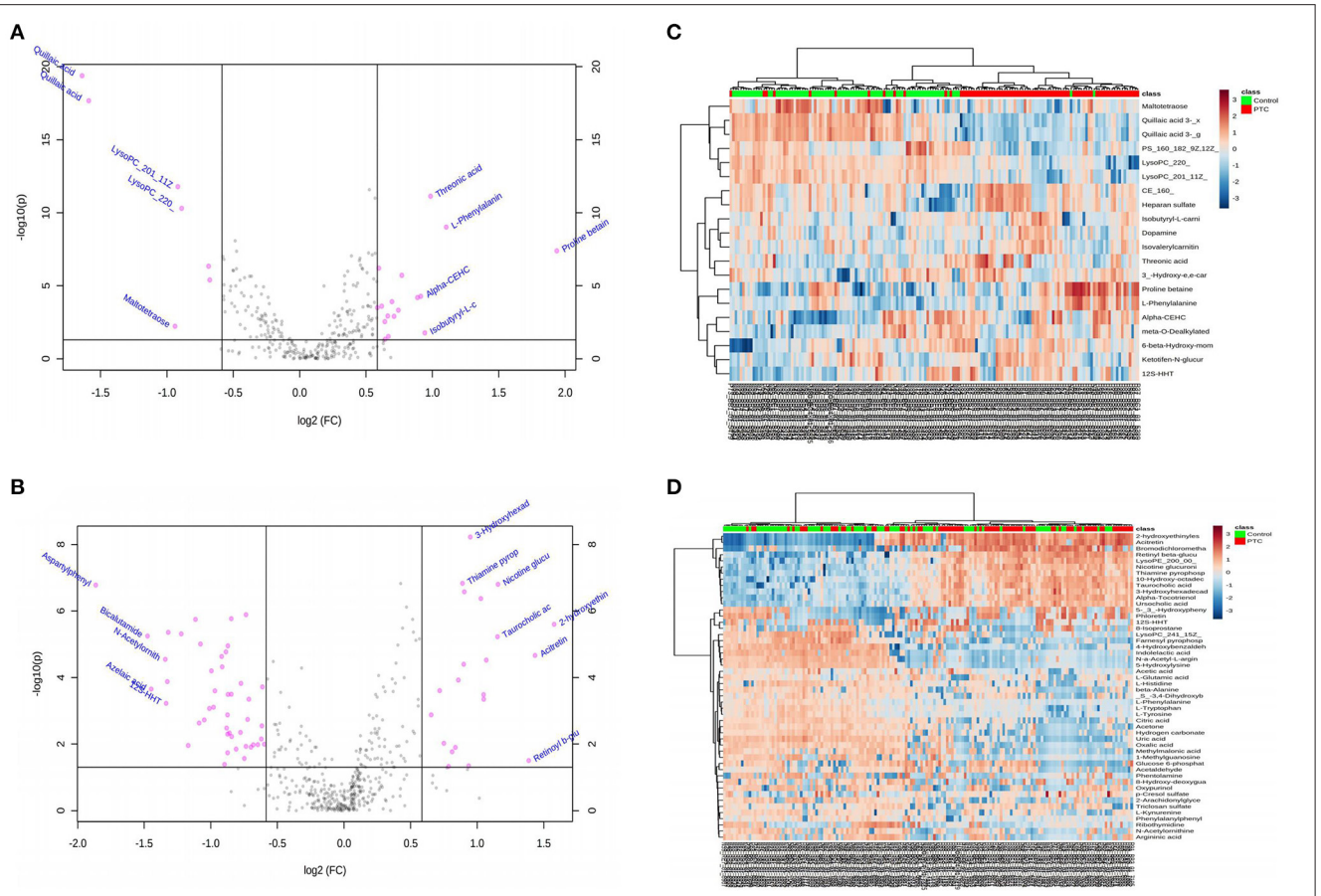

FIGURE 1 | (A,B) Volcano diagrams showing the changes in PTC and the most important metabolites of healthy subjects. **(A)** Represents the volcano map in positive ion mode, and **(B)** represents the volcano map in negative ion mode. The red dots in the figure represent differential metabolites, and the black dots represent no significant difference. The red dot on the right side of the figure represents the upregulated metabolite, and the red dot on the left side represents the downregulated metabolite. x-axis corresponds to $\log_2$ (fold change) and y-axis corresponds to $-\log_{10}$ (*p*-value). **(C,D)** Heatmap visualization of metabolomics data with hierarchical clustering analysis (HCA). **(C)** Represents the heatmap in positive ion mode, and **(D)** represents the heatmap in negative ion mode. The red color represents the peak value that is relatively large; the blue color represents the peak value that is relatively small; and the gray color represents the metabolite peak value of zero. The more similar the color, the more similar the peak value. The panel on the right represents the different metabolites. The upper dendritic structure is clustered according to the degree of metabolite similarity across samples. The red line below the dendritic structure represents the PTC group, and the green line represents the control group. PTC, papillary thyroid carcinoma; Control, healthy subject.

Screening of Differential Metabolites in Serum Samples Between the Two Groups

In the positive and negative ion mode, through the PCA model, we found that the clustering degree of the QC samples was good, indicating that the instrument was stable during this experiment. At the same time, we also found signs of separation between the PTC group and the Control group. The red triangle, green dot and blue square in the figure represent the QC group, the control group and the PTC group, respectively (**Figures 2A,B**).

Use the PLS-DA method to analyze the metabolite profile of the serum sample, as shown in **Figure 1C**: in the positive ion mode, the metabolomics data of serum samples were analyzed by PLS-DA, suggesting that there were significant differences between PTC and Control groups [R^2X (cum) = 0.497, R^2Y (cum) = 0.882, Q^2 (cum) = 0.735). In the PLS-DA model, after 200 permutations tests, the R^2 intercept of the substitution test in the positive ion mode was 0.505, and the intercept of Q^2 was −0.33 (**Figure 2E**), suggesting model reliability, given no evidence of over-fitting;As shown in **Figure 1D**: in the negative ion mode, the metabolomics data of the PTC and Control groups also have significant differences between groups [R^2X(cum) = 0.679, R^2Y(cum) = 0.916, Q^2(cum) = 0.634]. After 200 permutations tests, the R^2 intercept of the substitution test in the positive ion mode was 0.831, and the intercept of Q^2 was −0.0441 (**Figure 2F**), suggesting model reliability, given no evidence of over-fitting. These findings indicate that the PLS-DA model could be used to distinguish PTC patients from healthy controls; The parameters included in the model in both ion modes are shown in **Supplementary Tables 3, 4**.

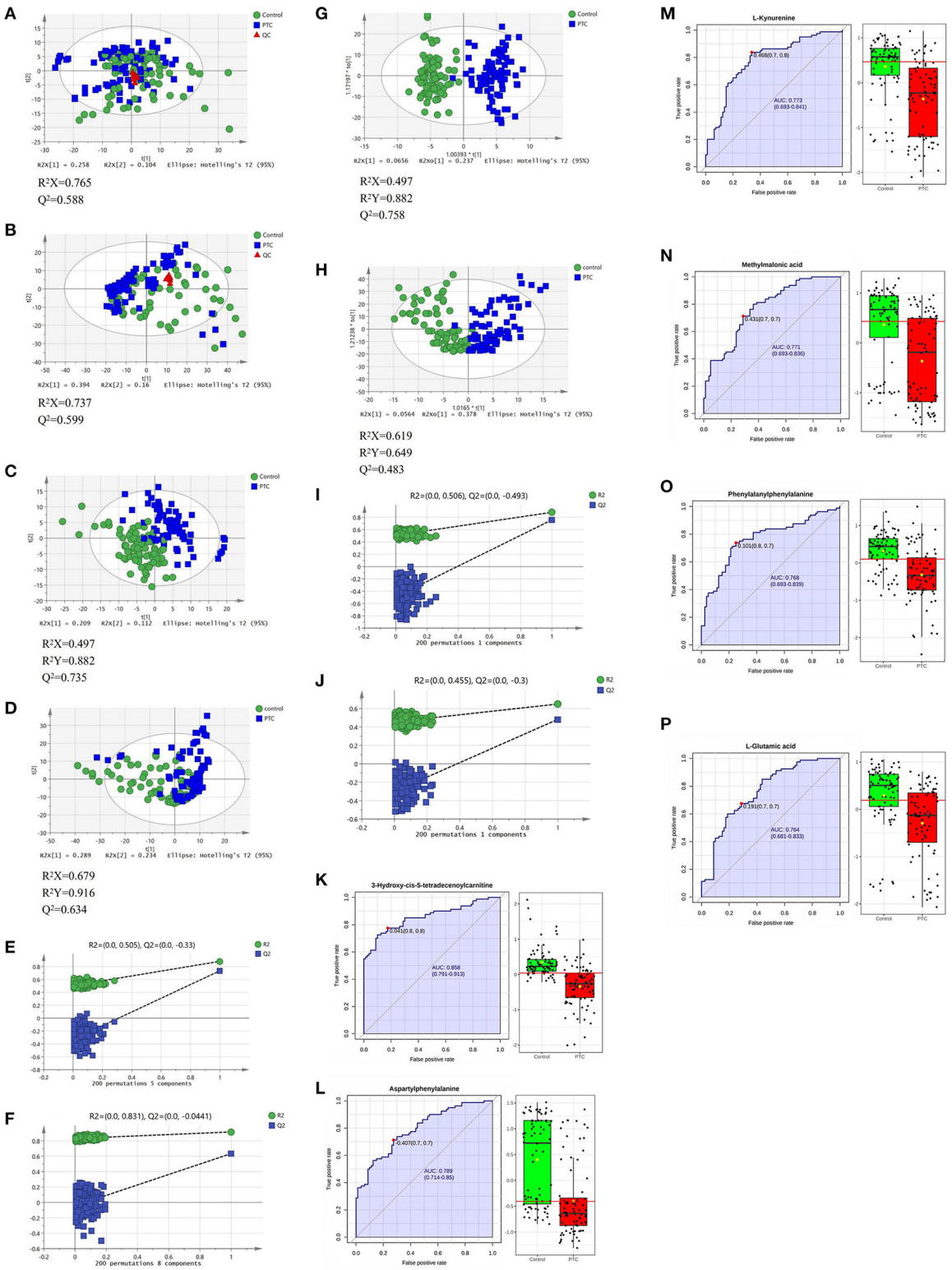

FIGURE 2 | PCA **(A,B)**, PLS-DA **(C,D)**, and OPLS-DA **(G,H)** analysis score scatter plots illustrating that the metabolic profiles of PTC are distinct from those of healthy subjects. PLS-DA and OPLS-DA analysis score scatter plots for metabolic profiles of healthy subjects (green dots) and PTC patients (blue squares) showing clear discrimination between the two groups. **(E,F,I,J)** Permutation test was used to assess the reliability of the models. ROC curve analyses of the ability of six metabolites to predict PTC patients and healthy subject **(K–P)**. PCA, principal component analysis; PLS-DA, partial least squares discrimination analysis; OPLS-DA, orthogonal partial least squares-discriminant analysis; QC, Quality Control; PTC, papillary thyroid carcinoma; Control, healthy subject. ROC, receiver operating characteristic.

To achieve the greatest separation of metabolites between the two sets of samples, OPLS-DA was performed (**Figures 2G,H**). In the positive and negative ion modes, there was a clear separation between the groups; concurrently, there were clear between-group differences in serum metabolic profiles. The samples from both groups tended to cluster in a concentrated manner, with a high degree of aggregation, without any obvious intragroup difference. In the OPLS-DA model, after 200 permutations tests, the R^2 intercept of the substitution test in the positive ion mode was 0.506, and the intercept of Q^2 was −0.493 (**Figure 2I**); the corresponding values in the negative ion mode were 0.455 and −0.3 (**Figure 2J**), suggesting model reliability, given no evidence of over-fitting. These findings indicate that the OPLS-DA model could be used to distinguish PTC patients from healthy controls; the model has a high discrimination and prediction rates ($P < 0.05$).

To distinguish the most important metabolites between the groups, FC, *p*-values, and VIP scores were used to screen for differential metabolites. In the positive and negative ion mode, the PCA-, PLS-DA-, and OPLS-DA-based models for distinguishing between the groups were constructed, and between-group metabolic differences were determined. Given VIP > 1.0, FC > 1.5, and $p < 0.05$, 64 metabolites were identified (**Table 2**). Among them, the levels of 22 metabolites showed a significant upward trend in the PTC group, including proline betaine, taurocholic acid, threonic acid, 3-hydroxyhexadecadienoylcarnitine, and dopamine. In contrast, the levels of 42 metabolites showed a significant downward trend in the PTC group, including L-tyrosine, 8-hydroxy-deoxyguanosine, 3-hydroxy-cis-5-tetradecenoylcarnitine, L-tryptophan, phenylalanylphenylalanine, argininic acid, beta-alanine, acetone, citric acid, and glucose 6-phosphate.

Finally, ROC curve analysis was used to evaluate the diagnostic ability of the differential metabolites for PTC screening (**Table 2**). False positive rate and True positive rate are presented along the x-axis and y-axis, respectively. The AUC values of 6 metabolites in the PTC and control groups were of >0.75 (**Figures 2K–P**).

Pathway Analysis

KEGG and HMDB (**Table 2**) were used to analyze 64 PTC-related metabolites, and the results were submitted to MetaboAnalyst to display the statistical analysis results of informatics analysis. The path analysis results are shown in **Supplementary Table 5** and **Figure 3A**. The most influenced metabolic pathway was considered a pathway influence cut-off value >0.1 to filter for less important pathways. The following eight important metabolic pathways were identified: phenylalanine, tyrosine and tryptophan biosynthesis; D-glutamine and D-glutamate metabolism; beta-alanine metabolism; phenylalanine metabolism; histidine metabolism; alanine, aspartate, and glutamate metabolism; citrate cycle (TCA cycle); and arginine biosynthesis.

DISCUSSION

With the rapid development of analysis technology, metabolomics has been applied in many fields such as cancer disease research (Tayanloo-Beik et al., 2020). At the molecular level, metabolomics uses novel biomarkers to explore the mechanism underlying disease development (Wang et al., 2011). To the best of our knowledge, this is the first study to use HPLC-Q-TOF-MS/MS to analyze metabolic pathways of a large number of serum samples from PTC patients and healthy subjects. In this study, based on PCA, PLS-DA, OPLS-DA model results (**Figures 2A–J**), and single-factor analysis results (**Figures 1A–D**), we first identified key metabolites related to PTC (**Table 2**). Based on these key metabolites, six metabolic markers, namely 3-hydroxy-cis-5-tetradecenoylcarnitine, aspartylphenylalanine, l-kynurenine, methylmalonic acid, phenylalanylphenylalanine, and l-glutamic acid, that could distinguish PTC patients from healthy subjects were further identified (**Figures 2K–P**). At the same time, we discovered eight important metabolic pathways related to PTC (**Figure 3A**), which were involved in PTC development; however, the detailed metabolic changes remain unknown. We also found the association among aspartate metabolism, glutamate metabolism, urea cycle, and tricarboxylic acid cycle in the PTC metabolic pathway, thereby explaining the pathogenesis of PTC (**Figure 3B**).

Warburg (Hsu and Sabatini, 2008) reported that a large amount of energy is being produced by glycolysis during the growth of cancer cells, which is distinct from the energy metabolism observed in normal cells, where it involves oxidative phosphorylation. This finding suggests that the different growth patterns of cancer and normal cells may be due to the different energy production pathways involved. The rates of glucose uptake, aerobic glycolysis, and metabolism are increased in cancer cells due to cell proliferation (Zhao et al., 2010). The energy in healthy cells comes from the mitochondria that oxidize sugar molecules; in contrast, tumor cells mainly rely on glycolysis for energy, which does not require the participation of oxygen atoms or mitochondria (Gioia et al., 2019). According to Abooshahab et al. (2020), sucrose levels can separate PTC from benign thyroid tumors (AUC = 0.92). Sucrose is converted into glucose and fructose through the hydrolysis process; subsequently, glucose enters the aerobic glycolysis pathway, where it is converted into two molecules of pyruvate. In this study, the level of glucose 6-phosphate in the serum of PTC patients was lower than that in the serum of healthy subjects, which may indicate that PTC tumor cells obtain energy through enhanced glycolysis, which accelerates the conversion of glucose 6-phosphate into pyruvate molecules, required for the TCA cycle. The citric acid levels in the PTC group were lower than those in the control group, indicating that thyroid cancer cells consume a significant amount of citric acid during the TCA cycle. The present findings are consistent with the Warburg effect.

Glycerol phospholipids are the most abundant type of phospholipid in eukaryotic cell membranes. Together, phosphatidylcholine (PC) and phosphatidylethanolamine(PE) account for ∼50% of the phospholipid components of cell membranes. In addition, glycerophospholipids are involved in protein recognition and signal transduction of cell membranes (Kuhajda, 2000). In malignant tumor tissues, as the rate of synthesis of glycerophospholipids is greater than that of their

TABLE 2 | Differential metabolites in the serum of papillary thyroid cancer patients and healthy subjects with positive and negative ion patterns.

Name	Retention time (min)	Mass-to charge ratio	Formula	VIP	FC	log_2(FC)	Adjusted *p* value	HMDB	ESI±
Quillaic acid 3-[galactosyl-(1->2)-glucuronide]	14.01	413.2084	C42H64O16	2.11539	0.33217	−1.59	<0.001	HMDB0033404	+
Quillaic acid 3-[xylosyl-(1->3)-[galactosyl-(1->2)]-glucuronide]	14.06	479.248	C47H72O20	2.06349	0.32061	−1.6411	<0.001	HMDB0033406	+
Aspartylphenylalanine	1.33	279.09845	C13H16N2O5	1.84875	0.27591	−1.8577	<0.001	HMDB0000706	-
L-Histidine	1.33	154.06227	C6H9N3O2	1.8051	0.4009	−1.3187	<0.001	HMDB0000177	-
Pyridinoline	1.32	427.21866	C18H28N4O8	1.7665	0.40468	−1.3051	<0.001	HMDB0000851	-
5-hydroxylysine	11.39	161.10051	C6H14N2O3	1.66697	0.47622	−1.0703	<0.001	HMDB0000450	-
L-glutamic acid	1.06	146.04601	C5H9NO4	1.64934	0.51228	−0.96499	<0.001	HMDB0000148	-
Hydrogen carbonate	1.44	60.9925	CH2O3	1.62898	0.58709	−0.76835	<0.001	HMDB0000595	-
L-phenylalanine	7.39	166.08415	C9H11NO2	1.62402	2.0901	1.0636	<0.001	HMDB0000159	+
Trans-trans-Muconic acid	1.45	140.97822	C6H6O4	1.59533	0.53257	−0.90896	<0.001	HMDB0002349	-
Taurocholic acid	20.77	514.26972	C26H45NO7S	1.5798	2.2144	1.1469	<0.001	HMDB0000036	-
Disulfiram	1.5	294.904	C10H20N2S4	1.56751	0.61107	−0.7106	<0.001	HMDB0014960	-
Citric acid	1.43	190.95495	C6H8O7	1.5526	0.54732	−0.86954	0.0049857	HMDB0000094	-
Dimercaprol	1.45	122.96761	C3H8OS2	1.54495	0.52417	−0.9319	<0.001	HMDB0015677	-
Argininic acid	1.15	174.0885	C6H13N3O3	1.53498	0.5726	−0.80439	0.014188	HMDB0003148	-
Ursocholic acid	22.41	407.24778	C24H40O5	1.53168	1.8474	0.88546	<0.001	HMDB0000917	-
Methylmalonic acid	1.18	117.01943	C4H6O4	1.52339	0.42889	−1.2213	<0.001	HMDB0000202	-
Nicotine glucuronide	16.8	337.14296	C16H22N2O6	1.50428	2.2215	1.1515	<0.001	HMDB0001272	-
L-Kynurenine	1.32	207.08727	C10H12N2O3	1.48824	0.46308	−1.1107	<0.001	HMDB0000684	-
2-hydroxyethinylestradiol	11.97	311.16896	C20H24O3	1.47693	2.9752	1.573	<0.001	HMDB0061027	-
Oleoylcarnitine	22.06	424.33074	C25H47NO4	1.45757	2.0335	1.024	<0.001	HMDB0005065	-
Retinyl beta-glucuronide	22.05	461.30177	C26H38O7	1.45534	2.0624	1.0443	<0.001	HMDB0010340	-
N-a-Acetyl-L-arginine	11.97	215.10839	C8H16N4O3	1.4469	0.53088	−0.91355	<0.001	HMDB0004620	-
Cyanate	1.3	44.0489	CHNO	1.43683	1.8665	0.90033	<0.001	HMDB0002078	+
10-Hydroxy-octadec-12Z-enoate-9-beta-D-glucuronide	20.76	489.24827	C24H42O10	1.43271	2.0631	1.0448	<0.001	HMDB0060120	-
Biotin	11.97	243.10362	C10H16N2O3S	1.42499	0.60751	−0.71902	0.0018047	HMDB0000030	-
2-arachidonylglycerol	19.72	377.27343	C23H38O4	1.41697	0.55461	−0.85046	0.0046278	HMDB0004666	-
Beta-Alanine	1.18	88.04025	C3H7NO2	1.41179	0.55975	−0.83715	0.0059028	HMDB0000056	-
Indolelactic acid	1.35	204.06539	C11H11NO3	1.39434	0.48593	−1.0412	0.0018691	HMDB0000671	-
Acitretin	12.45	325.18468	C21H26O3	1.39063	2.6931	1.4293	<0.001	HMDB0014602	-
Hippuric acid	1.32	178.0511	C9H9NO3	1.3891	0.55416	−0.85163	<0.001	HMDB0000714	-
L-Tryptophan	1.33	203.08273	C11H12N2O2	1.38814	0.61765	−0.69513	0.0050668	HMDB0000929	-
Ribothymidine	1.14	257.07558	C10H14N2O6	1.372	0.49838	−1.0047	<0.001	HMDB0000884	-
3-Hydroxy-cis-5-tetradecenoylcarnitine	10.26	386.27558	C21H39NO5	1.37183	0.61797	−0.6944	0.012251	HMDB0013330	+
N-Acetylornithine	1.28	173.09307	C7H14N2O3	1.36098	0.39628	−1.3354	<0.001	HMDB0003357	-
Threonic acid	1.3	159.02767	C4H8O5	1.35864	1.9251	0.94496	<0.001	HMDB0000943	+
Oxalic acid	1.2	88.98794	C2H2O4	1.32474	0.50332	−0.99047	<0.001	HMDB0002329	-
Alpha-Tocotrienol	0.09	423.32682	C29H44O2	1.3208	1.9807	0.98599	<0.001	HMDB0006327	-
Acetone	1.42	56.99484	C3H6O	1.31729	0.54805	−0.86763	<0.001	HMDB0001659	-
4′-O-Methylepicatechin 7-O-glucuronide	7.17	238.07747	C23H26O11	1.31537	1.6712	0.74089	<0.001	HMDB0029183	-
Glucosylgalactosyl hydroxylysine	22.13	485.32744	C18H34N2O13	1.29406	1.6334	0.7079	0.0012046	HMDB0000585	-
L-Tyrosine	1.95	180.06682	C9H11NO3	1.29302	0.65647	−0.60719	<0.001	HMDB0000158	-

(Continued)

TABLE 2 | Continued

Name	Retention time (min)	Mass-to charge ratio	Formula	VIP	FC	log_2(FC)	Adjusted *p* value	HMDB	ESI±
1-Methylguanosine	1.3	296.10035	C11H15N5O5	1.29055	0.60407	−0.72721	0.011676	HMDB0001563	-
Azelaic acid	1.34	187.09788	C9H16O4	1.29008	0.36788	−1.4427	<0.001	HMDB0000784	-
4-hydroxybenzaldehyde	1.34	121.02957	C7H6O2	1.2664	0.47227	−1.0823	0.0023175	HMDB0011718	-
(S)-3,4-Dihydroxybutyric acid	1.15	119.03508	C4H8O4	1.24485	0.6209	−0.68756	<0.001	HMDB0000337	-
Heparan sulfate	15.06	639.98222	C14H25NO21S3	1.22504	1.6421	0.71556	<0.001	HMDB0000693	+
4-glutathionyl cyclophosphamide	20.52	564.26422	C17H30Cl2N5O8PS	1.2227	0.6261	−0.67553	0.010508	HMDB0060387	-
Uric acid	1.29	167.02124	C5H4N4O3	1.19315	0.54884	−0.86554	<0.001	HMDB0000289	-
Thiamine pyrophosphate	17.05	424.07522	C12H19N4O7P2S	1.16992	1.8087	0.85496	<0.001	HMDB0001372	-
Phenylalanylphenylalanine	7.97	311.14035	C18H20N2O3	1.16405	0.60089	−0.73483	<0.001	HMDB0013302	-
Farnesyl pyrophosphate	1.14	381.10138	C15H28O7P2	1.16075	0.55865	−0.83999	<0.001	HMDB0000961	-
p-Cresol sulfate	1.33	187.00783	C7H8O4S	1.13682	0.44465	−1.1693	0.011129	HMDB0011635	-
3-hydroxyhexadecadienoylcarnitine	23.32	410.31521	C23H41NO5	1.11251	1.8723	0.90484	<0.001	HMDB0013335	-
Hesperetin 3′,7-O-diglucuronide	15.05	654.99189	C28H30O18	1.10556	1.6165	0.69291	<0.001	HMDB0041742	+
Glucose 6-phosphate	1.13	258.99652	C6H13O9P	1.08797	0.5463	−0.87223	0.0013207	HMDB0001401	-
Proline betaine	1.24	144.10164	C7H13NO2	1.08384	3.8372	1.9401	<0.001	HMDB0004827	+
Dopamine	1.29	154.08371	C8H11NO2	1.07989	0.66314	−0.59262	0.010018	HMDB0000073	+
3′-hydroxy-e,e-caroten-3-one	15.84	567.27116	C40H54O2	1.05843	1.5214	0.60537	<0.001	HMDB0002020	+
8-hydroxy-deoxyguanosine	1.24	282.08465	C10H13N5O5	1.05832	0.63158	−0.66296	0.0109	HMDB0003333	-
12(13)E*p*-9-KODE	11.93	309.1744	C18H30O4	1.04412	1.6818	0.75004	0.0092977	HMDB0013623	-
8-Isoprostane	19.38	279.44382	C20H40	1.03448	0.58342	−0.77739	0.00455	HMDB0004659	-
Maltotetraose	10.3	667.35056	C24H42O21	1.01631	0.52038	−0.94235	0.006033	HMDB0001296	+
Oxypurinol	1.32	151.02635	C5H4N4O2	1.00411	0.54446	−0.8771	0.003292	HMDB0000786	-

The metabolites were listed in a decreasing order based on variable importance in the projection values (VIP). p value adjusted by false discovery rate method across all the metabolites within the comparison.

decomposition, choline substances are expressed at high levels (Treede et al., 2007). As a result of the destruction of membrane structures associated with the development of a malignant tumor, choline levels tend to increase (Wu et al., 2016). According to Wojakowska et al. (2017), PC and glycerophosphocholine are expressed at high levels in PTC tissues, and choline, the end product of metabolism, can generate new PC again. This process demonstrates that PTC also decomposes phospholipids while synthesizing phospholipids, with the goal of meeting the needs of cancer cell proliferation. In the present study, serum levels of 3-hydroxy-cis-5-tetradecenoylcarnitine in the PTC group were lower than in the control group. In addition, the associated AUC value was >0.865, indicating that 3-this metabolite may help distinguish PTC patients from healthy controls. Moreover, 3-hydroxy-cis-5-tetradecenoylcarnitine belongs to the carnitine group; carnitine and its short-chain derivatives are necessary for fatty acids to enter the mitochondria for oxidation. Cheng et al. (2018) has shown that 3-hydroxy-cis-5-tetradecenoylcarnitine can be used as an important biomarker for the diagnosis of bladder cancer (AUC and sensitivity values of 0.899 and 0.881, respectively). Nevertheless, the diagnostic validity of 3-hydroxy-cis-5-tetradecenoylcarnitine in PTC requires further studies to confirm. Arachidonylglycerol (2-AG) is an important endogenous cannabinoid, associated with abnormal metabolism in pancreatic ductal adenocarcinoma (Qiu et al., 2019), prostate cancer (Endsley et al., 2008), and HCC (Yang et al., 2019). Serum levels of 2-AG in the PTC group were lower than those in the control group. This finding might be accounted for by the fact that PTC tends to be characterized by a lower degree of malignancy than does HCC. Moreover, 2-AG has strong anti-proliferative and pro-apoptotic properties in PTC patients. A large amount of 2-AG is consumed in anti-proliferation and pro-apoptosis processes, resulting in the rate of 2-AG degradation higher than that of its synthesis. Further studies are required to verify these observations.

Cancer cells maintain cell growth and proliferation through different metabolic pathways. New cancer cells require a large number of biomolecular components, including proteins, nucleic acids, lipids, and important cofactors to maintain the redox state of cells. Amino acids are used by tumors as a source of nutrition during development; they can also be used as the main carbon source by new cancer cells (Kuhajda, 2000; Voeller et al., 2004). In the present study, the OPLS-DA model was used to screen amino acid-related differential metabolites, showing that the levels of tyrosine, tryptophan, arginine, alanine,

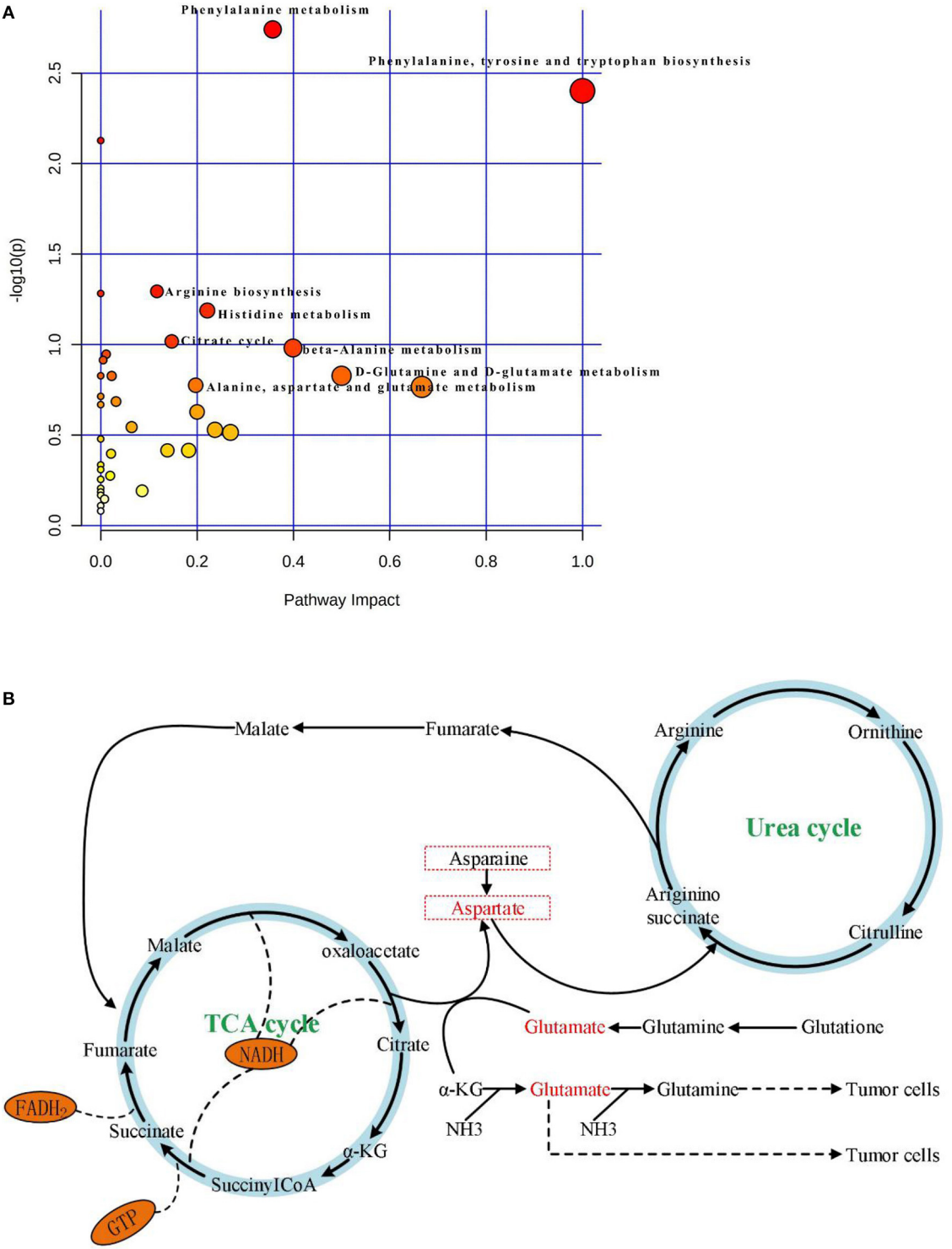

FIGURE 3 | (A) Results of pathway analysis of metabolomics data. Pathway analysis based on "Kyoto Encyclopedia of Genes and Genomes" (KEGG).The color and size of each circle is based on *p*-values (yellow: higher *p*-values and red: lower *p*-values) and pathway impact values (the larger the circle the higher the impact score) calculated from the topological analysis, respectively. Pathways were considered significantly enriched if $p < 0.05$, impact >0.1 and number of metabolite hits in the pathway >1. PTC, papillary thyroid carcinoma. **(B)** The significantly enriched pathways involved in the pathogenesis of papillary thyroid carcinoma, including Aspartate metabolism, Glutamate metabolism, Urea cycle, and TCA cycle.

glutamic acid, and histidine were lower in the PTC group than in the control group. Alanine is a glycogen amino acid that can be converted into an intermediate substrate in the tricarboxylic acid cycle, and then into glucose in the process of gluconeogenesis. Therefore, alanine can also be considered as an energy source for the rapid proliferation of PTC cells (Tian et al., 2015; Ryoo et al., 2016). In this study, serum levels of beta-alanine in the PTC group were lower than those in the control group. This finding might be accounted for by the fact that PTC cells use beta-alanine metabolism to convert large amounts of beta-alanine into raw materials for energy metabolism. Concurrently, this study examined amino acid metabolism in the context of energy metabolism. Aspartate and glutamate metabolism, and urea and TCA cycles emerged as important pathways in the development of PTC (**Figure 3B**). The metabolism of glutamate and aspartic acid is the most important participatory pathway in malignant thyroid tumors, linking the urea cycle with the TCA cycle. The urea cycle converts excess ammonia and aspartic acid into urea. Reduce the toxicity of its high ammonia content (Yekta et al., 2018). According to Nagamani and Erez (2016), in many malignant tumor tissues, the ASS1 enzyme is silenced in the urea cycle, which leads to the preferential synthesis of pyrimidine by aspartic acid to support cell proliferation, reducing the utilization of aspartic acid in pyrimidine synthesis, which limits the proliferation of cancer cells. Meanwhile, the silencing of the ASS1 enzyme in cancer cells supports their proliferation by activating carbamyl phosphate synthase-2, aspartate transcarbamylase, and the dihydrotransaminase complex, which promote pyrimidine synthesis (Rabinovich et al., 2015). This evidence suggests that silencing of the ASS1 enzyme is associated with poor prognosis in patients with malignant tumors. Ammonia plays an important role in the proliferation of PTC cells (**Figure 3B**). Glutamine provides ammonia and triggers autophagy in PTC cells. PTC cells generate glutamate through glutaminase and glutamate dehydrogenase, whereby glutamate further produces α-ketoglutarate, which provides sufficient energy for the survival of tumor cells. Glutamic acid and aspartic acid also undergo anaplerotic reactions, through which amino acids are oxidized and decomposed to generate intermediate metabolites of the TCA cycle, thereby supplying energy to tumor cells (Owen et al., 2002; Jones and Bianchi, 2015). A large number of studies has shown that in the proliferation of cancer cells, the metabolites of citric acid are transported out of the mitochondria, and used in lipid biosynthesis in the cytoplasm as a precursor of acetyl coenzyme-A to compensate for the continuous consumption of citric acid. Meanwhile, glutamine is the main anaplerotic precursor in cancer cells, compensating for the lack of citric acid, which is involved in energy generation (DeBerardinis et al., 2007). This study found that citric acid was significantly downregulated in PTC, as were glutamine and asparagine, reflecting the weakened replenishment response of glutamine in PTC. In addition, the levels of oxalic acid were lower in the PTC group than in the control group. The consumed oxalic acid was likely converted into an oxaloyl group, and the oxalic acid group was then converted into oxaloacetate. Oxalic acid is formed by combining an oxalyl group (after removing a hydroxyl group) and an acetic acid group. The acid cycle plays a catalyst-like role and determines the speed of the TCA cell cycle (Kuang et al., 2018). Oxaloacetic acid can also be transformed into non-essential amino acids such as asparate and asparagine, which are involved in nucleotide synthesis (Yang et al., 2017), suggesting that oxalic acid may be involved in PTC development.

In the present study, metabolomic and multivariate analyses were combined to distinguish PTC patients from healthy controls, aiming to determine the metabolic characteristics of PTC and improve the understanding of PTC development and associated prognosis. Future studies should include PTC tissue and lymph fluid analysis, and combine genomic and proteomic methods to yield further insights into PTC biomarkers and candidate treatment targets. Furthermore, future studies should involve accurate metabolomics analyses with a large number of specimens from PTC patients with lymph node metastasis, aiming to clarify the role of lymph node metastasis in PTC.

CONCLUSIONS

We found that metabolomics based on HPLC-Q-TOF-MS/MS can clearly distinguish PTC patients from healthy subjects. Lower levels of 3-hydroxy-cis-5-tetradecenoylcarnitine, aspartylphenylalanine, l-kynurenine, methylmalonic acid, phenylalanylphenylalanine, and l-glutamic acid were observed in the serum of PTC patients than in the serum of healthy subjects. These six metabolic markers can theoretically be used in combination with current PTC diagnostic methods to guide the clinical diagnosis of PTC. However, we the following issues need to be considered: (1). For future clinical studies of PTC, it is necessary to further analyze the serum of PTC patients of phase III and IV to further confirm and summarize the results of this study; (2). Tissue and urine samples of PTC patients should be combined. The metabolomics research of lymphatic fluid can be used as a plan for future metabolomics research. This multicenter research aims to improve the accuracy of prediction.

DATA AVAILABILITY STATEMENT

The raw data supporting the conclusions of this article will be made available by the authors, without undue reservation.

ETHICS STATEMENT

The studies involving human participants were reviewed and approved by Ethics Committee of Hunan Provincial People's Hospital. The patients/participants provided their written informed consent to participate in this study. Written informed consent was obtained from the individual(s) for the publication of any potentially identifiable images or data included in this article.

AUTHOR CONTRIBUTIONS

YD, LZ, and PF worked on the concept and design. XG, JY, and CZ have provided tools and patient specimens. YD, LZ, and YJ carried out experiments. YD and LZ analyzed and explained the results and edited the manuscript. YD organized the results and drafted the manuscript. LZ and PF approved the final version. All authors participated in the rigorous revision of manuscripts with important intellectual content.

FUNDING

The present study was supported by the Clinical Medical Technology Innovation and Guidance of Hunan Province (No. 2018SK50720), the Natural Science Foundation of Hunan Province (No. 2017JJ3171), the Key Project of Health Commission of Hunan Province (A2017003), and the Science and Technology Project of Changsha City (No. kq1701045). The funding bodies had no role in the design of the study or collection, analysis, and interpretation of data or in writing the manuscript.

ACKNOWLEDGMENTS

We would like to sincerely thank PF (the First Affiliated Hospital of Hunan Normal University) for his valuable suggestions. We would also like to thank LZ for his guidance in the experimental research process. This research was approved by the Clinical Experimental Research Institute of the First Affiliated Hospital of Hunan Normal University.

SUPPLEMENTARY MATERIAL

The Supplementary Material for this article can be found online at: https://www.frontiersin.org/articles/10.3389/fcell.2021.593510/full#supplementary-material

REFERENCES

Abooshahab, R., Hooshmand, K., Razavi, S. A., Gholami, M., and Hedayati, M. (2020). Plasma metabolic profiling of human thyroid nodules by gas chromatography-mass spectrometry (gc-ms)-based untargeted metabolomics. *Front. Cell Dev. Biol.* 8:385. doi: 10.3389/fcell.2020.00385

Barnes, S., Benton, H. P., Casazza, K., Cooper, S. J., and Tiwari, H. K. (2016). Training in metabolomics research. I. designing the experiment, collecting and extracting samples and generating metabolomics data. *J. Mass Spec.* 51, 461–475. doi: 10.1002/jms.3672

Bijlsma, S., Bobeldijk, I., Verheij, E. R., Ramaker, R., Kochhar, S., Macdonald, I. A., et al. (2006). Large-scale human metabolomics studies: a strategy for data (pre-) processing and validation. *Anal. Chem.* 78, 567–574. doi: 10.1021/ ac051495j

Bray, F., Ferlay, J., Soerjomataram, I., Siegel, R. L., Torre, L. A., and Jemal, A. (2018). Global cancer statistics 2018: GLOBOCAN estimates of incidence and mortality worldwide for 36 cancers in 185 countries. *CA Cancer J. Clin.* 68, 394–424. doi: 10.3322/caac.21492

Cheng, X., Liu, X., Guo, Z., Sun, H., Zhang, M., Zheng, J., et al. (2018). Metabolomics of non-muscle invasive bladder cancer: biomarkers for early detection of bladder cancer. *Front. Oncol.* 8:494. doi: 10.3389/fonc.2018.00494

DeBerardinis, R. J., Mancuso, A., Daikhin, E., Nissim, I., Yudkoff, M., Wehrli, S., et al. (2007). Beyond aerobic glycolysis: transformed cells can engage in glutamine metabolism that exceeds the requirement for protein and nucleotide synthesis. *Proc. Natl. Acad. Sci. U.S.A.* 104, 19345–19350. doi: 10.3389/fonc.2007.00067

Du, J., Yuan, Z., Ma, Z., Song, J., Xie, X., and Chen, Y. (2014). Kegg-path: kyoto encyclopedia of genes and genomes-based pathway analysis using a path analysis model. *Mol. Bio.* 10, 2441–2447. doi: 10.1039/c4mb0 0287c

Edge, S. B., and Compton, C. C. (2010). The American Joint Committee on Cancer: the 7th edition of the AJCC cancer staging manual and the future of TNM. *Ann. Surg. Oncol.* 17, 1471–1474. doi: 10.1245/s10434-010-0985-4

Endsley, M. P., Thill, R., Choudhry, I., Williams, C. L., Kajdacsy-Balla, A., Campbell, W. B., et al. (2008). Expression and function of fatty acid amide hydrolase in prostate cancer. *Int. J. Cancer* 123, 1318–1326. doi: 10.1002/ijc.23674

Faquin, W. C. (2008). The thyroid gland: recurring problems in histologic and cytologic evaluation. *Arch. Path. Lab. Med.* 132, 622–632. doi: 10.1043/1543-2165(2008)132[622:TTGRPI]2.0.CO;2

Ferlay, J., Steliarova-Foucher, E., Lortet-Tieulent, J., Rosso, S., Coebergh, J. W. W., Comber, H., et al. (2013). Cancer incidence and mortality patterns in Europe: estimates for 40 countries in 2012. *Eur. J. Cancer* 49, 1374–1403. doi: 10.1016/j.ejca.2012.12.027

Fish, S. A. (2017). Validation of american thyroid association ultrasound risk assessment of thyroid nodules selected for ultrasound fine-needle aspiration. *Thy.* 29, 411–414. doi: 10.1089/thy.2016.0555

Gioia, M. D., Spreafico, R., Springstead, J. R., Mendelson, M. M., Joehanes, R., Levy, D., et al. (2019). Endogenous oxidized phospholipids reprogram cellular metabolism and boost hyperinflammation. *Nat. Immunol.* 21, 42–53. doi: 10.1038/s415 90-019-0539-2

Han, J., Han, M.-L., Xing, H., Li, Z.-L., Yuan, D.-Y., Wu, H., et al. (2020). Tissue and serum metabolomic phenotyping for diagnosis and prognosis of hepatocellular carcinoma. *Int. J. Cancer* 146, 1741–1753. doi: 10.1002/ijc.32599

Hsu, P. P., and Sabatini, D. M. (2008). Cancer cell metabolism: warburg and beyond - sciencedirect. *Cell* 134, 703–707. doi: 10.1016/j.cell.2008.08.021

Jewison, T., Su, Y., Disfany, F., and Miril. (2014). SMPDB 2.0: big improvements to the small molecule pathway database. *Nucleic Acids Res.* 42, *D*478–84. doi: 10.3389/ fonc.2014.00085

Jin, L., Sebo, T. J., Nakamura, N., Qian, X., Oliveira, A., Majerus, J. A., et al. (2006). Braf mutation analysis in fine needle aspiration (fna) cytology of the thyroid. *Diag. Mole. Path. Ame. J. Sur. Path. Part B* 15, 136. doi: 10.1097/01. pdm.0000213461.53021.84

Johnson, S. J., Hardy, S. A., Roberts, C., Bourn, D., Mallick, U., and Perros, P. (2014). Pilot of braf mutation analysis in indeterminate, suspicious and malignant thyroid fna cytology. *Cytopath* 25, 146–154. doi: 10.1111/cyt.12125

Jones, W., and Bianchi, K. (2015). Aerobic glycolysis: beyond proliferation. *Front. Immunol.* 6:227. doi: 10.3389/fimmu.2015.00227

Kim, T., Oh, Y. L., Kim, K. M., and Shin, J. H. (2011). Diagnostic dilemmas of hyalinizing trabecular tumours on fine needle aspiration cytology: a study of seven cases with braf mutation analysis. *Cytopath* 22, 407–413. doi: 10.1111/j.13 65-2303.2011.00886.x

Kuang, Y., Han, X., Xu, M., and Yang, Q. (2018). Oxaloacetate induces apoptosis in hepg2 cells via inhibition of glycolysis. *Cancer Med.* 7,1416–1429. doi: 10.1002/cam4.1410

Kuhajda, F. P. (2000). Fatty-acid synthase and human cancer: new perspectives on its role in tumor biology. *Nutrition* 16, 202–208. doi: 10.1016/S0899-9007(99)00266-X

Monteiro, M. S., Carvalho, M., Bastos, M. L., and Guedes, d. P. P. (2013). Metabolomics analysis for biomarker discovery: advances and challenges. *Curr. Med. Chem.* 20, 257–271. doi: 10.2174/092986713804806621

Nagamani, S., and Erez, A. (2016). A metabolic link between the urea cycle and cancer cell proliferation. *Mol. Cell Oncol.* 3:e1127314. doi: 10.1080/23723556.2015. 1127314

Owen, O. E., Satish, K. C., and Richard, W. H. (2002). The key role of anaplerosis and cataplerosis for citric acid cycle function. *J. Biol. Chem.* 277, 30409–30412. doi: 10.1074/jbc.R200006200

Qiu, C., Yang, L., Wang, B., Cui, L., and Wang, X. (2019). The role of 2-arachidonoylglycerol in the regulation of the tumor-immune microenvironment in murine models of pancreatic cancer. *Bio. Pharm* 115:108952. doi: 10.1016/j.bio pha.2019.108952

Rabinovich, S., Adler, L., Yizhak, K., Sarver, A., Silberman, A., Agron, S., et al. (2015). Diversion of aspartate in ass1-deficient tumours fosters de novo pyrimidine synthesis. *Nature* 527, 379–383. doi: 10.1038/nature15529

Remonti, L. R., Kramer, C. K., Leit, O. C. B., Pinto, L. C. F., and Gross, J. L. (2015). Thyroid ultrasound features and risk of carcinoma: a systematic review and meta-analysis of observational studies. *Thy. Off J. Ame. Ass.* 25, 538–550. doi: 10.1 089/thy.2014.0353

Ryoo, I., Kwon, H., Kim, S. C., Jung, S. C., Yeom, J. A., Shin, H. S., et al. (2016). Metabolomic analysis of percutaneous fine-needle aspiration specimens of thyroid nodules: potential application for the preoperative diagnosis of thyroid cancer. *Sci. Rep.* 6:30075. doi: 10.1038/srep30075

Shepherd, L. V., Fraser, P., and Stewart, D. (2011). Metabolomics: a second-generation platform for crop and food analysis. *Bioa* 3, 1143–1159. doi: 10.4155/bio.11.61

Tayanloo-Beik, A., Sarvari, M., Payab, M., Gilany, K., and Arjmand, B. (2020). Omics insights into cancer histology; metabolomics and proteomics approach. *Clin. Biochem*. 84, 13–20. doi: 10.1016/j.clinbiochem.2020.06.008

Tian, Y., Nie, X., Xu, S., Li, Y., Huang, T., and Tang, H., et al. (2015). Integrative metabonomics as potential method for diagnosis of thyroid malignancy. *Sci. Rep*. 5:14869. doi: 10.1038/srep14869

Treede, I., Braun, A., Sparla, R., Mark, K., and Ehehalt, R. (2007). Anti-inflammatory effects of phosphatidylcholine. *J. Bio. Chem.* 282, 27155–27164. doi: 10.1074/jbc.M704408200

Voeller, D., Rahman, L., and Zajac-Kaye, M. (2004). Elevated levels of thymidylate synthase linked to neoplastic transformation of mammalian cells. *Cell Cycle* 3, 1003–1005. doi: 10.4161/cc.3.8.1064

Wang, T. J., Larson, M. G., Vasan, R. S., Cheng, S., Rhee, E. P., McCabe, E., et al. (2011). Metabolite profiles and the risk of developing diabetes. *Nat, Med.* 17, 448-453, 2011. doi: 10.1038/nm.2307

Wishart, D. S., Jewison, T., Guo, A. C., Wilson, M., Knox, C., Liu, Y., et al. (2013). HMDB 3.0 - the human metabolome database in 2013. *Nucleic Acids Res.* 41, D801–D807. doi: 10.1093/nar/gks1065

Wojakowska, A., Cole, L. M., Chekan, M., Bednarczyk, K., and Widlak, P. (2017). Discrimination of papillary thyroid cancer from non-cancerous thyroid tissue based on lipid profiling by mass spectrometry imaging. *Endo. Pol.* 69, 2–8. doi: 10.5603/EP.a2018.0003

Wu, X., Cao, H., Zhao, L., Song, J., She, Y., and Feng, Y. (2016). Metabolomic analysis of glycerophospholipid signatures of inflammation treated with non-steroidal anti-inflammatory drugs-induced-raw264.7 cells using 1h nmr and u-hplc/q-tof-ms. *J. Chrom. B* 1028, 199–215. doi: 10.1016/j.jchromb.2016.06.032

Yang, J., Tian, Y., Zheng, R., Li, L., and Qiu, F. (2019). Endocannabinoid system and the expression of endogenous ceramides in human hepatocellular carcinoma. *Oncol. Lett.* 18, 1530–1538. doi: 10.389 2/ol.2019.10399

Yang, L., Venneti, S., and Nagrath, D. (2017). Glutaminolysis: a hallmark of cancer metabolism. *Annu. Rev. Biomed. Eng.* 19:163. doi: 10.1146/annurev-bioeng-071516-044546

Yekta, R. F., Tavirani, M. R., Oskouie, A. A., Mohajeri-Tehrani, M. R., and Baghban, A. A. (2018). Serum-based metabolic alterations in patients with papillary thyroid carcinoma unveiled by non-targeted 1h-nmr metabolomics approach. *Iran. J. Basic Med. Sci.* 21, 1140–1147. doi: 10.22038/ijbms.2018.30375.7323

Yuan, B., Schafferer, S., and Tang, Q. (2018). A plasma metabolite panel as biomarkers for early primary breast cancer detection. *Int. J. Cancer* 144, 2833–2842. doi: 10.1002/ijc.31996

Zhao, Y., Liu, H., Riker, A. I., Fodstad, O., Ledoux, S. P., Wilson, G. L., et al. (2010). Emerging metabolic targets in cancer therapy. *Front. Biosci. A J. Virt. Library* 16:1844. doi: 10.2741/3826

Conflict of Interest: The authors declare that the research was conducted in the absence of any commercial or financial relationships that could be construed as a potential conflict of interest.

frontiers in Cell and Developmental Biology

ORIGINAL RESEARCH
published: 22 February 2021
doi: 10.3389/fcell.2021.642665

Computational Model for Membrane Transporters. Potential Implications for Cancer

María Florencia Carusela[1,2] *and J. Miguel Rubi*[3]*

[1] Instituto de Ciencias, Universidad Nacional de General Sarmiento, Buenos Aires, Argentina, [2] National Scientific and Technical Research Council, Buenos Aires, Argentina, [3] Departament de Física de la Matèria Condensada, Universitat de Barcelona, Barcelona, Spain

To explain the increased transport of nutrients and metabolites and to control the movement of drug molecules through the transporters to the cancer cells, it is important to understand the exact mechanism of their structure and activity, as well as their biological and physical characteristics. We propose a computational model that reproduces the functionality of membrane transporters by quantifying the flow of substrates through the cell membrane. The model identifies the force induced by conformational changes of the transporter due to hydrolysis of ATP, in ABC transporters, or by an electrochemical gradient of ions, in secondary transporters. The transport rate is computed by averaging the velocity generated by the force along the paths followed by the substrates. The results obtained are in accordance with the experiments. The model provides an overall framework for analyzing the membrane transport proteins that regulate the flows of ions, nutrients and other molecules across the cell membranes, and their activities.

Keywords: cancer transporters, membrane transport mechanisms, entropic forces, Langevin equation, cancer therapies

OPEN ACCESS

Edited by:
Maria E. Mycielska, University Medical Center Regensburg, Germany

Reviewed by:
Leonardo Dagdug, Metropolitan Autonomous University, Mexico
Stefano Pagliara, University of Exeter, United Kingdom

***Correspondence:**
J. Miguel Rubi
mrubi@ub.edu

Specialty section:
This article was submitted to Molecular and Cellular Oncology, a section of the journal Frontiers in Cell and Developmental Biology

Received: *16 December 2020*
Accepted: *04 February 2021*
Published: *22 February 2021*

Citation:
Carusela MF and Miguel Rubi J (2021) Computational Model for Membrane Transporters. Potential Implications for Cancer. Front. Cell Dev. Biol. 9:642665. doi: 10.3389/fcell.2021.642665

1. INTRODUCTION

Cancer cells synthesize increased amount of fatty acids and protein building blocks to successfully divide and metastasize. To support their metabolism cancer cells require increased supply of metabolic substrates and nutrients. Plasma membrane transporters secure import of a wide range of substrates into the cytoplasm. Consistently, increased expression of several transporting proteins has been correlated to the increased metabolic activity of cancer cells and poor disease prognosis (Natecz, 2020; Sampedro-Núñez et al., 2020; Xu et al., 2020; Yamada et al., 2020).

There are two types of transporters, ATP biding cassette (ABC) and secondary active transporters. Secondary active transporters carry substrates across the plasma membrane using electrochemical gradient of ions. They bind the substrate on one side of the membrane followed by a conformational change allowing to release the substrate on the other side of the membrane (Boudker and Verdon, 2010). Several of these transporters have been shown to play an important role in cancer cells by increasing uptake of such substrates as glucose, glutamine, lactate, etc., and supporting cancer cell metabolism (Payen et al., 2017; Reckzeh et al., 2019; Scalise et al., 2020).

ABC transporters belong to a large family of transporters carrying several different substrates across the plasma membrane. To translocate substrates ABC transporters use the energy from ATP hydrolysis. They play an important role in keeping cellular homeostasis by regulating the level of

several molecules including peptides, lipids, amino acids, or drugs (El-Awady et al., 2017; Neumann et al., 2017). Importantly, ABC transporters have also been shown to contribute to anti-cancer drug resistance presenting a major problem in finding an efficient anti-cancer therapy (Robey et al., 2018; Bock et al., 2019; Asif et al., 2020). These transporters carry out anti-cancer drugs efflux from cancer cells significantly decreasing the efficiency of anti-cancer therapies.

To be able to successfully overcome the problem of the increased transport of nutrients and metabolites and control drugs influx/efflux through transporters in cancer cells it is important to understand the exact mechanism of their structure and activity as well as their biological and physical features. This has been the objective of this article.

We have proposed a model that describes the trans-membrane transport and calculates the flow of substrates through the membrane. The model assumes that changes in transporter conformations induce forces that contribute to the translocation of substrates. Since entropy is a measure of conformations, the forces are referred to as entropic forces. These forces thus encode the information of the change in the available space of the substrates due to conformation changes (Zwanzig, 1992; Reguera and Rubí, 2001; Vazquez et al., 2008; Carusela and Rubi, 2017, 2018; Rubi, 2019). The computed translocation rates scale with the ratio between the time it takes for conformations to change and the time in which substrates diffuse through the transporter. This scaling behavior makes our model a general tool in the study of membrane transport.

2. THE MODEL

We model a transporter as a small funnel-shaped motor whose structure changes over time by alternately opening and closing to the intra/extracellular medium, as represented in **Figure 1**. This form has been observed for example in P-glycoprotein whose structure is narrow at the cytoplasmic side, of about 9–25 Å in the middle, and wider at the extracellular surface (Loo and Clarke, 2001). The conical form has also been observed in pumps (Rubi et al., 2017) by means of crystallization experiments (Olesen et al., 2007).

This periodic movement makes it possible for substrates, such as aminoacids, ions, neurotransmitters, nutrients and different drugs, to overcome the potential barriers generated by interactions allowing them to pass to the other side of the plasma membrane.

Alternating gating increases transport efficiency with respect to that of diffusion. Transport of substrates through the membrane is the result of changes in its conformation. Primary active transporters couple substrate movements to a source of chemical energy, such as ATP hydrolysis. Secondary active transporters are driven by electrochemical gradients of ions. Transporters differ from ion channels in that their turnover rate is much slower than that of channels which is typically of the order of $10^6 s^{-1}$. The rate of ABC transporters such as LeuT, MsbA, and of MFS secondary transporters frequently falls within the range $(10^{-1} - 10^3)s^{-1}$ (Ashcroft et al., 2009; Liu et al., 2018; Fitzgerald et al., 2019).

2.1. Force Induced by Transporter Conformation Changes

Our model considers that the changes in the conformation of both types of transporters that allow the passage of the substrates entail a variation in the space they have to move. This fact affects the entropy of the substrates as this quantity measures the degree of disorder of a system which in our case is less in the narrow area of the transporter, where the substrates have fewer positions to occupy, and more in the wider area where the space available is greater. This difference of entropies between the narrow and the wide part of the transporter gives rise to a gradient of free energy and consequently to a force on the substrates that we will call entropic force $\mathcal{F}_{ent}$ (see **Figure 2**).

The force arising from the uneven shape of the transporter must therefore be proportional to $\Delta A = A_2 - A_1$, with A_1 and A_2 the cross-sectional areas at the entrance and at the exit of the transporter (see **Figure 2**) which depend on time. Studies on ion translocation in Ca^{2+}-ATPase and in Na^+/K^+-ATPase have revealed that structural changes in a protein channel and their induced entropic forces contribute significantly to the transport of the ions (Rubi et al., 2017).

Changes in the concentration, or equivalently, in the chemical potential of the substrates on both sides of the plasma membrane generate a mass flow from high to low concentrations. The force associated with this effect, proportional to $\Delta c = c_2 - c_1$, with c_1 and c_2 the concentrations at the entrance and at the exit of the transporter (see **Figure 2**), is lower than the entropic force and is directed in the opposite direction, so the net effect is a flow of substrates against the gradient, an active transport due to the catalyst effect of the transporter.

Substrates are also affected by the thermal motion of the solvent which exert a random force $\mathcal{F}_r$ on them. The thermal energy is k_BT and the thermal random force is given by $\mathcal{F}_r = \sqrt{2k_BT\gamma}\eta(t)$, with $\eta(t)$ a Gaussian random quantity of mean zero and correlation $< \eta(t)\eta(t') >= \delta(t-t')$, T the temperature, k_B the Boltzmann constant and $\gamma = \frac{k_BT}{\mathcal{D}}$ the friction coefficient which is the inverse of the diffusion coefficient $\mathcal{D}$ in k_BT units (Gardiner, 2004).

The previous forces acting on the substrates capture the essential factors involved in the translocation process. In the model, we assume that the resulting velocity v is given through the Langevin equation (Gardiner, 2004)

$$\gamma v = \mathcal{F}_{ent} + \mathcal{F}_{\mu} + \mathcal{F}_r \tag{1}$$

It has been shown that entropic forces are given by $\mathcal{F}_{ent} = k_BT\frac{\nabla A(x,t)}{A(x,t)}$ (de Groot et al., 1963; Zwanzig, 1992; Reguera and Rubí, 2001; Kalinay and Percus, 2006; Vazquez et al., 2008; Rubi, 2019) and $\mathcal{F}_{\mu} = -k_BT\frac{\nabla c(x)}{c(x)}$. In Equation (1), these forces act on the substrates at their time-dependent positions. The entropic force depends on the local radius h(x,t) of the channel (Reguera and Rubí, 2001) and has the direction of the cross-sectional area gradient, i.e., it contributes to expel the substrates, whereas

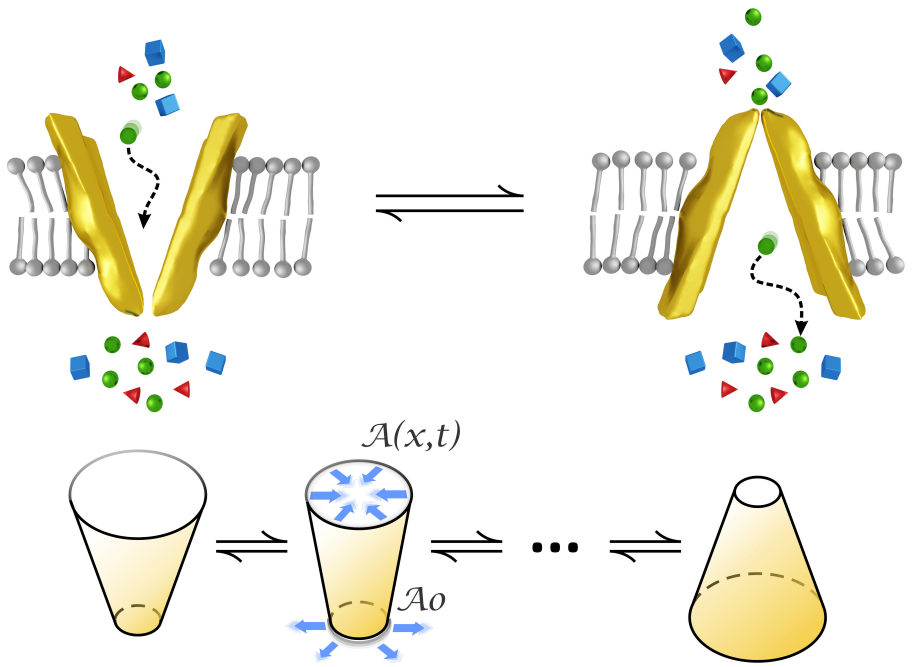

FIGURE 1 | Conformational changes of a transporter modeled by an oscillating conical-shaped channel which closes/opens to the intra/extra cellular medium. $\mathcal{A}_0$ stands for the cross-sectional area at the narrowest part whereas $\mathcal{A}(x,t)$ denotes that area at positions inside the transporter and time. Figures at the bottom represent the initial and final states and an intermediate state of the cone oscillations in the model.

the diffusive force has the opposite sign of the concentration gradient. A similar Langevin equation was proposed to model particle translocation through microfluidic channels promoted by an oscillating external potential (Tan et al., 2017).

To study how changes in conformation of the transporter affect the velocity of the substrate, we must model its geometry. A simple yet representative form is that of a conical shaped region of length L that oscillates periodically in time with a frequency ω (Carusela and Rubi, 2017, 2018), opening and closing to the intra/extra cellular environment, as sketched in **Figure 2**. The radius $h(x,t)$ of the channel changes from a maximum value h_{max} to a minimum value h_{min} evolving in time as

$$h(x,t) = (h_{max} - h_{min})(x/L - 1/2)\sin\omega t + (h_{max} + h_{min})/2 \quad (2)$$

The value $x = 0$ is located at one extreme of the transporter.

2.2. Computation Protocol

Measurements of translocation rates are performed over a time interval long enough to comprise many time periods $\bar{T}$ of the conformational change cycle of transporters of the same kind. To obtain a representative value of the velocity $\mathcal{V}$ of the substrates, we must thus average the instantaneous velocity $v(t)$, given in Equation (1), in time and over an ensemble of identical transporters. The average velocity is thus obtained as

$$\mathcal{V} = \frac{1}{\bar{T}} \int_{\bar{T}} < v(t) > \, dt \quad (3)$$

where $< \ldots >$ means average over an ensemble of realizations or initial states of the system.

To calculate $< v(t) >$, we integrate Equation (1) using a stochastic Velocity-Verlet algorithm (Gränbech-Jensen and Farago, 2013). The computation method runs as follows. We consider a particle at the entrance of the channel, on the extracellular environment, and set its initial velocity according to a Boltzmann distribution, at $T = 300K$. We then calculate its local velocity according to Equation (1). Once the particle reaches the exit of the transporter into the intracellular medium, we calculate the time average $\frac{1}{\bar{T}} \int_{\bar{T}} dt v(t)$, assuming that when the particle leaves the channel it cannot re-enter. This protocol is repeated for a large set of initial particle conditions at the transporter entrance. The average $(< \ldots >)$ of the obtained results gives us the value of $\mathcal{V}$. In the model, we have considered that the force due to the concentration gradient in Equation (1) is practically constant along the transporter which means that $\mathcal{F}_\mu \approx \frac{k_B T}{L} \frac{\Delta c}{\bar{c}} := \frac{k_B T}{L} f_\mu$. The ratio $\frac{\Delta c}{\bar{c}}$ and therefore f_μ typically takes values in the range $(10^{-1} - 1)$ (Sperelakis, 2000; Tashiro et al., 2005; Chu et al., 2013). The value of the entropic forces falls in the interval $(1 - 10^1)$, therefore $\mathcal{F}_\mu < \mathcal{F}_{ent}$ which means that changes in conformation is the main mechanism that regulates transport.

3. RESULTS

Following the protocol described in the previous section, we compute the transport rate $\Gamma = \mathcal{V}/L$ which is plotted in **Figure 3**

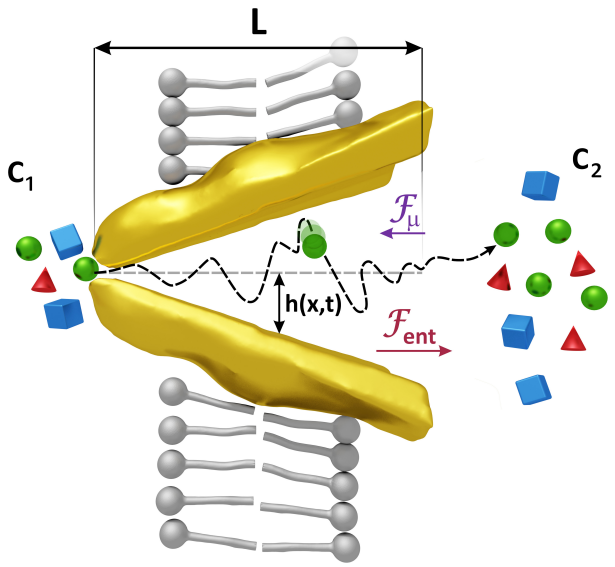

FIGURE 2 | Forces acting on the substrates. Changes in the shape of the transporter induce an entropic force F_{ent}, larger than the force F_μ generated by a difference of the concentrations c_1 and c_2, which helps to expel the substrates when the transporter is opened, and prevents the passage of them when it is closed. Substrates are also affected by the random motion of the molecules of the solvent whose average kinetic energy is proportional to k_BT. The associated force has been denoted by F_r in Equation (1). The radius of the transporter $h(x,t) = (h_{max} - h_{min})(x/L - 1/2)\sin\omega t + (h_{max} + h_{min})/2$ varies with position and time reaching maximum and minimum values, h_{max} and h_{min}, respectively. $x = 0$ is located at one extreme of the transporter.

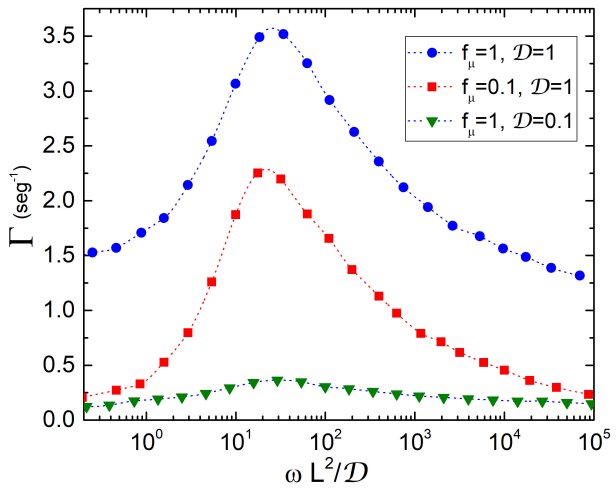

FIGURE 3 | Transport rate Γ vs. ratio between the time conformations take to change and the diffusion time: $\omega L^2/\mathcal{D}$. The quantities $\mathcal{D}$, f_μ, L, and ω which are defined in the text, have been measured in units of $\mathcal{D}_0 = 10^{-2}\mu m^2/seg$, k_BT/L_0 (T = 300 K), $L_0 = 10nm$ and $L_0^2/\mathcal{D}_0$, respectively. An enhancement of the velocity is observed at $\frac{\omega L^2}{D} \sim 30$ regardless of the values of f_μ, thus showing that transporters work in an optimal scenario dominated by entropic forces induced by conformational changes.

vs. $\omega L^2/\mathcal{D}$. This quantity represents the ratio between the time in which the conformation of the transporter changes and the time that substrates take to diffuse through the transporter. The presence of resonant peaks at $\frac{\omega L^2}{D} \sim 30$, practically independent of the values of f_μ, reveals the occurrence of an amplification of the velocity of the substrates at a certain value of the oscillation frequency and therefore shows that transporters work under optimal transport conditions. The peaks become more pronounced when f_μ increases or equivalently the rates are higher when the concentration of substrates increases, as observed for example in experiments for LeuT transporters (Fitzgerald et al., 2019). The existence of an optimal frequency for transport of particles in microfluidic devices subjected to an external oscillatory potential was also found in Tan et al. (2017).

Considering transporters with length of the order of $L_0 = 10nm$ and typical diffusion coefficients for membrane proteins of Eukaryotic cells, $\mathcal{D}_0 = (10^{-2} - 1)\mu m^2/seg$ (Kaňa, 2013), we obtain values for Γ in the range of $(10^{-1} - 10^3)seg^{-1}$. Our model also provides values of the rates in ion channels. In this case, one would expect that since particles are lighter they move faster. Typical values of $\mathcal{D}_0$ for ions are in the range $(10^3 - 10^4)\mu m^2/seg$, therefore Γ takes values between $(10^5 - 10^6)seg^{-1}$. These model predictions are in good agreement with data found in the literature for transport rates of slow and fast protein channels in membranes (Ashcroft et al., 2009). At the maximum opening configuration of the transporter, the entropic force changes from a value of the order of f_μ at the widest part, to about $20f_\mu$ at the narrowness. Our results then show that transporters work in a regime dominated by entropic forces induced by conformational changes.

4. CONCLUSIONS

Membrane proteins transporters regulate the efflux/influx of substrates across plasma membrane of cancer cells and play a paramount role in the efficiency of cancer therapies as they regulate the retention of anticancer drugs in the cells. It is believed that the effectiveness of chemotherapy may be largely dependent on the activity of transporters. Knowing which is the intimate mechanism that makes possible the passage of substrates through the cell membrane is therefore a matter of vital importance.

In this article, we have proposed a computational model that analyses the activity of transporters. The model shows that changes in the transport configuration produced by the energy of ATP hydrolysis (ABC transporters) or by a electrochemical gradient of ions (secondary transporters) give rise to a force that makes the substrates able to overcome the potential barrier generated by the constrictions in order to pass to the other side of the membrane. Such a force results from the variation of the space that the substrates have to move within the transporter when its configuration changes, which generates an entropy gradient.

Transport rates are computed by following a simulation protocol in which we first obtain the time average of the velocity of the substrates which is subsequently averaged over a set of initial conditions of the position of a substrate.

Our model reproduces experimental values of the rates for different ABC and secondary transporters and shows that they depend on substrate concentration, in accordance with data reported in recent experiments (Fitzgerald et al., 2019). It can also be used to compute translocation rates in ion channels showing that they are greater than for transporters, as observed in the experiments (Ashcroft et al., 2009). We have shown that the entropic force is greater than that produced by a mere concentration gradient and is directed in the opposite direction which shows that transport is active.

How readily substrates cross the membrane depends on the frequency of oscillation ω, which regulates the entropic force and therefore the changes in the conformation of the transporter, on the size of the substrates which is involved in $\mathcal{D}$ and on the size of the transporter L. The rates found scale with the combination of these quantities: $\omega L^2/\mathcal{D}$ which represents the ratio between the time in which conformations change and the time it takes for the substrates to diffuse. Our results could therefore be applied in general to membrane transport, to transport in microfluidic devices and peristaltic channels and to capture cellular heterogeneity beyond cancer cells (Pu et al., 2016; Łapińska et al., 2019; Rhia et al., 2020). Monitoring the entropic force by means of drugs could help to regulate transport activity leading to the design of better transport modulators that can be used in anti-cancer therapies.

DATA AVAILABILITY STATEMENT

The raw data supporting the conclusions of this article will be made available by the authors, without undue reservation.

AUTHOR CONTRIBUTIONS

All authors have made a substantial contribution to the work and approved it for publication.

FUNDING

MFC thanks PIO-CONICET and PICT 18/2036, JMR wants to thank financial support of MICIU of the Spanish Government, under Grant No. PGC2018-098373-B-I00.

REFERENCES

Ashcroft, F., Gadsby, D., and Miller, C. (2009). Introduction. The blurred boundary between channels and transporters. *Philos. Trans. R. Soc. Lond. B Biol. Sci*. 364, 145–147. doi: 10.1098/rstb.2008.0245

Asif, M., Usman, M., Ayub, S., Farhat, S., Huma, Z., Ahmed, J., et al. (2020). Role of ATP-binding cassette transporter proteins in CNS tumors: resistance-based perspectives and clinical updates. *Curr. Pharm. Design* 26, 4747–4763. doi: 10.2174/1381612826666200224112141

Bock, C., Zollmann, T., Lindt, K., Tampé, R., and Abele, R. (2019). Peptide translocation by the lysosomal abc transporter tapl is regulated by coupling efficiency and activation energy. *Sci. Rep*. 15:11884. doi: 10.1038/s41598-019-48343-6

Boudker, O., and Verdon, G. (2010). Structural perspectives on secondary active transporters. *Trends Pharm. Sci*. 31, 418–426. doi: 10.1016/j.tips.2010.06.004

Carusela, M. F., and Rubi, J. M. (2017). Entropic rectification and current inversion in a pulsating channel. *J. Chem. Phys*. 146:184901. doi: 10.1063/1.4982884

Carusela, M. F., and Rubi, J. M. (2018). Entropy production and rectification efficiency in colloid transport along a pulsating channel. *J. Phys. Cond. Matter* 30:244001. doi: 10.1088/1361-648X/aac0c0

Chu, X., Korzekwa, K., Elsby, R., Fenner, K., Galetin, A., Lai, Y., et al. (2013). Intracellular drug concentrations and transporters: measurement, modeling, and implications for the liver. *Clin. Pharmacol. Ther*. 94, 126–141. doi: 10.1038/clpt.2013.78

de Groot, S. R., Mazur, P., and King, A. L. (1963). Non-equilibrium thermodynamics. *Am. J. Phys*. 31, 558–559. doi: 10.1119/1.1969680

El-Awady, R., Saleh, E., Hashim, A., Soliman, N., Dallah, A., Elrasheed, A., et al. (2017). The role of eukaryotic and prokaryotic abc transporter family in failure of chemotherapy. *Front. Pharmacol*. 7:535. doi: 10.3389/fphar.2016.00535

Fitzgerald, G., Terry, D., Warren, A., Javitch, J. A., and Blanchard, S. C. (2019). Quantifying secondary transport at single-molecule resolution. *Nature* 575, 528–534. doi: 10.1038/s41586-019-1747-5

Gardiner, C. W. (2004). *Handbook of Stochastic Methods for Physics, Chemistry and the Natural Sciences, 3rd Edn*. Berlin: Springer-Verlag.

Gränbech-Jensen, N., and Farago, O. (2013). A simple and effective verlet-type algorithm for simulating langevin dynamics. *Mol. Phys*. 111, 983–991. doi: 10.1080/00268976.2012.760055

Kalinay, P., and Percus, J. K. (2006). Corrections to the Fick-Jacobs equation. *Phys. Rev. E* 74:041203. doi: 10.1103/PhysRevE.74.041203

Kaňa, R. (2013). Mobility of photosynthetic proteins. *Photosynth. Res*. 116, 465–479. doi: 10.1007/s11120-013-9898-y

Łapińska, U., Glover, G., Capilla-Lasheras, P., Young Andrew, J., and Pagliara, S. (2019). Bacterial ageing in the absence of external stressors. *Philos. Trans. R. Soc. B* 374:1786. doi: 10.1098/rstb.2018.0442

Liu, Y., Liu, Y., He, L., Zhao, Y., and Zhang, X. (2018). Single-molecule fluorescence studies on the conformational change of the abc transporter msba. *Biophys. Rep*. 4, 153–165. doi: 10.1007/s41048-018-0057-z

Loo, T. W., and Clarke, D. M. (2001). Determining the dimensions of the drug-binding domain of human p-glycoprotein using thiol cross-linking compounds as molecular rulers. *J. Biol. Chem*. 276:36877. doi: 10.1074/jbc.C100467200

Natecz, K. A. (2020). Amino acid transporter SLC6A14 ($ATB^{0,+}$) a target in combined anti-cancer therapy. *Front. Cell Dev. Biol*. 8:1178. doi: 10.3389/fcell.2020.594464

Neumann, J., Rose-Sperling, D., and Hellmich, U. A. (2017). Diverse relations between abc transporters and lipids: an overview. *Biochim. Biophys. Acta Biomemb*. 1859, 605–618. doi: 10.1016/j.bbamem.2016.09.023

Olesen, C., Picard, M., Winther, A.-M. L., Gyrup, C., Morth, J. P., Oxvig, C., et al. (2007). The structural basis of calcium transport by the calcium pump. *Nature* 450, 1036–42. doi: 10.1038/nature06418

Payen, V. L., Hsu, M. Y., Rädecke, K. S., Wyart, E., Vazeille, T., Bouzin, C., et al. (2017). Monocarboxylate transporter mct1 promotes tumor metastasis independently of its activity as a lactate transporter. *Cancer Res*. 77, 5591–5601. doi: 10.1158/0008-5472.CAN-17-0764

Pu, Y., Zhao, Z., Li, Y., Zou, J., Ma, Q., Zhao, Y., et al. (2016). Enhanced efflux activity facilitates drug tolerance in dormant bacterial cells. *Mol. Cell* 62, 284–294. doi: 10.1016/j.molcel.2016.03.035

Reckzeh, E. S., Karageorgis, G., Schwalfenberg, M., Ceballos, J., Nowacki, J., Stroet, M. C., et al. (2019). Inhibition of glucose transporters and glutaminase synergistically impairs tumor cell growth. *Cell Chem. Biol*. 26, 1214–1228.e25. doi: 10.1016/j.chembiol.2019.06.005

Reguera, D., and Rubi, J. M. (2001). Kinetic equations for diffusion in the presence of entropic barriers. *Phys. Rev. E* 64:061106. doi: 10.1103/PhysRevE.64.061106

Rhia, M., Stone, L., Łapińska, U., Pagliara, S., Masi, M., Blanchfield, J. T., et al. (2020). Fluorescent macrolide probes-synthesis and use in evaluation of bacterial resistance. *RSC Chem. Biol*. 1, 395–404. doi: 10.1039/D0CB00118J

Robey, R., Pluchino, K., Hall, M., Fojo, A., Bates, S., and Gottesman, M. (2018). Revisiting the role of abc transporters in multidrug-resistant cancer. *Nat. Rev. Cancer*. 7, 452–464. doi: 10.1038/s41568-018-0005-8

Rubi, J. M. (2019). Entropic diffusion in confined soft-matter and biological systems. *Europhys. Lett*. 127:10001. doi: 10.1209/0295-5075/127/10001

Rubi, J. M., Lervik, A., Bedeaux, D., and Kjelstrup, S. (2017). Entropy facilitated active transport. *J. Chem. Phys*. 146:185101. doi: 10.1063/1.4982799

Sampedro-Núñez, M., Bouthelier, A., Serrano-Somavilla, A., Martínez-Hernández, R., Adrados, M., Martín-Pérez, E., et al. (2020). LAT-1 and GLUT-1 carrier expression and its prognostic value in gastroenteropancreatic neuroendocrine tumors. *Cancers* 12, 1–17. doi: 10.3390/cancers12102968

Scalise, M., Pochini, L., Galluccio, M., Console, L., and Indiveri, C. (2020). Glutamine transporters as pharmacological targets: from function to drug design. *Asian J. Pharm. Sci*. 15, 207–219. doi: 10.1016/j.ajps.2020.02.005

Sperelakis, N. K. E. (2000). *Physiology and Pathophysiology of the Heart, 4th Edn*. Berlin: Springer.

Tan, Y., Gladrow, J., Keyser, U. F., Dagdug, L., and Pagliara, S. (2017). Particle transport across a channel via an oscillating potential. *Phys. Rev. E* 96:052401. doi: 10.1103/PhysRevE.96.052401

Tashiro, M., Tursun, P., and Konishi, M. (2005). Intracellular and extracellular concentrations of Na+ modulate Mg2+ transport in rat ventricular myocytes. *Biophys. J*. 89, 3235–3247. doi: 10.1529/biophysj.105.068890

Vazquez, M.-V., Berezhkovskii, A. M., and Dagdug, L. (2008). Diffusion in linear porous media with periodic entropy barriers: a tube formed by contacting spheres. *J. Chem. Phys*. 129:046101. doi: 10.1063/1.2955447

Xu, L., Chen, J., Jia, L., Chen, X., Awaleh Moumin, F., and Cai, J. (2020). SLC1A3 promotes gastric cancer progression via the PI3K/AKT signalling pathway. *J. Cell. Mol. Med*. 24, 14392–14404. doi: 10.1111/jcmm.16060

Yamada, Y., Yoshimatsu, K., Yokomizo, H., Okayama, S., and Shiozawa, S. (2020). Expression of ATP-binding cassette transporter 11 (ABCC11) protein in colon cancer. *Anticancer Res*. 40, 5405–5409. doi: 10.21873/anticanres.14549

Zwanzig, R. (1992). Diffusion past an entropy barrier. *J. Phys. Chem*. 96, 3926–3930. doi: 10.1021/j100189a004

Conflict of Interest: The authors declare that the research was conducted in the absence of any commercial or financial relationships that could be construed as a potential conflict of interest.

frontiers in Cell and Developmental Biology

REVIEW
published: 12 March 2021
doi: 10.3389/fcell.2021.626316

Warburg's Ghost—Cancer's Self-Sustaining Phenotype: The Aberrant Carbon Flux in Cholesterol-Enriched Tumor Mitochondria via Deregulated Cholesterogenesis

Peter S. Coleman[1]* *and Risa A. Parlo*[2]

[1] Independent (Retired) Academic, Beverly, MA, United States, [2] Kingsborough Community College, Brooklyn, NY, United States

OPEN ACCESS

Edited by:
Eric Kenneth Parkinson,
Queen Mary University of London,
United Kingdom

Reviewed by:
Ralph J. DeBerardinis,
University of Texas Southwestern Medical Center, United States
Li Zhang,
The University of Texas at Dallas, United States

***Correspondence:**
Peter S. Coleman
coleman@colemanps.com

Specialty section:
This article was submitted to Molecular and Cellular Oncology, a section of the journal Frontiers in Cell and Developmental Biology

Received: 04 December 2020
Accepted: 29 January 2021
Published: 12 March 2021

Citation:
Coleman PS and Parlo RA (2021) Warburg's Ghost—Cancer's Self-Sustaining Phenotype: The Aberrant Carbon Flux in Cholesterol-Enriched Tumor Mitochondria via Deregulated Cholesterogenesis. Front. Cell Dev. Biol. 9:626316. doi: 10.3389/fcell.2021.626316

Interpreting connections between the multiple networks of cell metabolism is indispensable for understanding how cells maintain homeostasis or transform into the decontrolled proliferation phenotype of cancer. Situated at a critical metabolic intersection, citrate, derived via glycolysis, serves as either a combustible fuel for aerobic mitochondrial bioenergetics or as a continuously replenished cytosolic carbon source for lipid biosynthesis, an essentially anaerobic process. Therein lies the paradox: under what conditions do cells control the metabolic route by which they process citrate? The Warburg effect exposes essentially the same dilemma—why do cancer cells, despite an abundance of oxygen needed for energy-generating mitochondrial respiration with citrate as fuel, avoid catabolizing mitochondrial citrate and instead rely upon accelerated glycolysis to support their energy requirements? This review details the genesis and consequences of the metabolic paradigm of a "truncated" Krebs/TCA cycle. Abundant data are presented for substrate utilization and membrane cholesterol enrichment in tumors that are consistent with criteria of the Warburg effect. From healthy cellular homeostasis to the uncontrolled proliferation of tumors, metabolic alterations center upon the loss of regulation of the cholesterol biosynthetic pathway. Deregulated tumor cholesterogenesis at the HMGR locus, generating enhanced carbon flux through the cholesterol synthesis pathway, is an absolute prerequisite for DNA synthesis and cell division. Therefore, expedited citrate efflux from cholesterol-enriched tumor mitochondria via the CTP/SLC25A1 citrate transporter is fundamental for sustaining the constant demand for cytosolic citrate that fuels the elevated flow of carbons from acetyl-CoA through the deregulated pathway of cholesterol biosynthesis.

Keywords: Warburg effect, tumor cholesterogenesis, mitochondrial citrate export, truncated Krebs/TCA cycle, tumor membrane cholesterol

INTRODUCTION

Since the 1970's, sophisticated biochemical research tools and techniques have yielded a cornucopia of new detail on the molecular mechanisms of mitochondrial cellular bioenergetics, the individual pathway steps of intermediary metabolism, and the metabolic regulation of cell proliferation. The amassment of enzymological data on metabolic pathways, detailing complex enzymatic controls, spotlighted one of the fundamental and persistent metabolic controversies in the field of cell growth and proliferation—particularly the most clinically intractable obstacle: cancer.

Thus, over 50 years ago the debate re-emerged over which metabolic profile initiates or dictates the cancer cell phenotype, known for nearly 100 years worldwide as the Warburg vs. the Crabtree effect (Warburg, 1925; Crabtree, 1929).

Warburg's original hypothesis, based on his careful tissue slice respiration measurements with the manometer apparatus he invented, posits that cancer cells, unlike normal tissue, derive the bulk of their ATP by means of glycolysis, a less efficient ATP-generating pathway, despite an abundance of systemic oxygen and the presumptive capacity for high yields of ATP via mitochondrial aerobic oxidative phosphorylation. Warburg's aerobic glycolysis concept for tumors proposed that the aberrant metabolic profile in tumor cells was based on malfunctioning mitochondria. Crabtree, offered a different interpretation of Warburg's theory of tumor metabolism. Based on similarly careful tissue slice respiration measurements in a variety of tumors, he proposed that in order to supply their ATP requirements, the high rate of metabolic flux through glycolysis actually depresses the tumor's capacity for normal mitochondrial oxidative respiration via feed-back regulatory processes. Crabtree wrote, "The tentative conclusion is that glycolytic activity exerts a significant checking effect on the capacity for respiration of tumour tissue."

It is remarkable that the Warburg-vs.-Crabtree-effect debate remains an open issue today. But, in Warburg's era it wasn't possible to detail any mitochondrial characteristics on a molecular level that might reveal their malfunction in cancer. And even with today's more sophisticated techniques, if differences on the molecular structure-function level between normal and tumor mitochondria were indisputably documented, how could we determine whether such differences were a cause or consequence of the cancer phenotype? (Koppenol et al., 2011; Senyilmaz and Teleman, 2015; Potter et al., 2016).

The resurgent and ongoing interest in the Warburg effect makes clear that it is not an artifact of experimental conditions or selection of unique tissue subjects chosen for study (Cassim et al., 2020; Pascale et al., 2020). Originally, Warburg emphasized aerobic glycolysis and malfunctioning mitochondria as a causal or initiating factor of cancer (Warburg, 1956), and although this belief remains current (Seyfried, 2015), consensus of opinion today considers the Warburg effect to arise as a result of primary genetic mutations (Carter et al., 2009; Vogelstein et al., 2013; Lu et al., 2015).

Yet, in our view, despite the almost logarithmic increase in research publications on the Warburg effect and cancer over the last two decades (see Figure 1 in Otto, 2016), one fundamental characteristic of the tumor's altered *overall* metabolic carbon flow pattern, involving cytosolic citrate, has not been addressed. While the cytoplasm's access to and acquisition of citrate is clearly recognized as a central metabolite required by the tumor's reorganized energy metabolomics and fatty acid synthesis, the mandatory role of citrate as precursor fuel for operation of the well-documented deregulated and enhanced carbon flux through the cholesterogenesis pathway in tumors has not been adequately recognized. This review hopes to emphasize a paramount link between mitochondrial bioenergetics in tumors and the select role(s) played by an increased membrane cholesterol content, which together help perpetuate the unrestrained cell proliferation phenotype of cancer.

PURPOSE OF THIS REVIEW

Tumorigenesis is a relatively long-term and steady pathological process, phenotypically characterized by uncontrolled cell proliferation. Within recent decades, advanced understanding of the molecular details on the "unrestrained" growth of cancers has revealed a chameleon-like propensity for their metabolic malleability. Such profound metabolic complexity arises as a function of the timeline of differentiation from normal to neoplastic, the cell type, tissue, and even location within the particular tissue (Faubert et al., 2020). With regard to classic Warburg effect descriptors, as has been noted (Abdel-Haleem et al., 2017), transient rapid cell division, such as T-cell activation and angiogenesis, is still "regulated," yet shares verifiable aerobic glycolysis features with "deregulated" tumor cell proliferation, and thus both display legitimate Warburg effect profiles. *No indisputably convincing argument has yet to identify, on a molecular level, first elements that become "deregulated" in the case of tumorigenesis, but remain "regulated" in transient cell proliferation.*

The purpose of this review is to reiterate our specifically focused perspective that:

(1) the Warburg effect's proposal of an aberrant respiratory pattern in tumors can be tightly linked with the long-held, well-documented, deregulated, and enhanced cholesterol synthesis (Siperstein and Fagan, 1964; Chen et al., 1978; Heiniger, 1981; Coleman et al., 1997);
(2) the tumor cell's membranes become enriched with cholesterol as a result of the well-evidenced enhanced rate of cholesterol biosynthesis in tumors;
(3) cholesterol enrichment of tumor mitochondrial membranes promotes and necessitates the continuous cytoplasmic supply of the precursor substrate (acetyl-CoA) for cholesterogenesis via the preferential export of citrate from mitochondria;
(4) implies, as others have, that communication or cross-talk between the plasma membrane Na^+-dependent citrate transporter (PMCT, encoded by *SLC13A5*) and the mitochondrial inner membrane citrate transport protein (CTP, encoded by *SLC25A1*) might be critical to the

proposed metabolic sequelae that largely define cell proliferation as the major phenotypic hallmark of cancer.

Mitochondrial Metabolism Is Anomalous in Tumors

More than 30 years ago, inspired by an increasing abundance of exciting research implicating the pivotal role assumed by altered enzyme regulation of the cholesterol synthesis pathway in tumor cell proliferation, many laboratories (including ours) began to focus on the affect such a change in cholesterol biosynthesis would have on mitochondria as the cell's main energy-generating machinery. As entry into the thrust of this review, the mitochondrial metabolomics involved in cholesterogenesis must be highlighted.

The Ins-and-Outs of Mitochondria: The Citrate Transporter (CTP/*SLC25A1*) Stands Out From the Crowd

The role of mitochondria is clearly of interest for two reasons. First, the stoichiometry of cholesterol biosynthesis requires 36 ATP per molecule, wherein mitochondrial oxidative phosphorylation would be the presumed major and most efficient ATP provider. Second, cytosolic acetyl-CoA is the initial precursor substrate of cholesterol (18 acetyl-CoA/cholesterol), whose multi-step synthesis is almost entirely localized on the endoplasmic reticulum (ER). In normal, oxygen-respiring cells amply supplied with glucose, the mitochondrion is a major cellular locus for glycolysis-derived acetyl-CoA, principally as a result of carbohydrate breakdown.

Canonically, the source of the cytosolic acetyl-CoA required by all lipid synthesis is the key cellular metabolite, citrate. Recognition of the centrality of citrate as a cytoplasmic source of carbons in tumors and other proliferating cells cannot be overstated (Icard et al., 2012; Iacobazzi and Infantino, 2014). Citrate, ultimately formed from the catabolism of glucose to acetyl-CoA and its subsequent combination with oxaloacetate via the first step of the Krebs/TCA cycle, may be transported out to the cytosol via the well-studied mitochondrial citrate transport protein (CTP, the product of the *SLC25A1* gene) in a 1:1 exchange for the electroneutral import of another TCA intermediate, malate (Hanse et al., 2017). Malate, formed from the cytosolic cleavage of citrate, will shuttle back into the mitochondria via the CTP, in exchange for another exiting citrate, and once again become a TCA cycle participant. This metabolic routing of citrate, from mitochondria to cytosol, is the classic pathway utilized to generate, via ATP-citrate lyase enzymatic activity, the acetyl-CoA required for lipid anabolism. It must be noted, however, that environmentally stressful circumstances (e.g., hypoxia) provide a platform for the tumor to demonstrate its creative metabolic flexibility. Since, as mentioned, tumors develop in diverse and heterogeneous environments *in vivo*, the citrate that ultimately feeds lipid synthesis may arise from glutamine/glutamate as the non-glycolytic (non-pyruvate) carbon source (DeBerardinis et al., 2007; Wise et al., 2011; Mullen et al., 2014; Yang et al., 2014). Thus, the reductive carboxylation of α-ketoglutarate (a "reversal" in direction of the more traditional Krebs/TCA cycle carbon flux) by mitochondrial isoforms of $NADP^+$/NADPH-requiring isocitrate dehydrogenase has also been shown to generate mitochondrial citrate, which then can become available to the cytosol. Human hepatomas, whose mitochondria are cholesterol enriched, have been shown to exhibit such an altered metabolite flow, through participation of the selective over-expression of the α-ketoglutarate transport protein (*SLC25A11*) (Baulies et al., 2018). Ultimately, it is recognized that by whatever metabolic manipulations the tumor's creativity elicits, supplying the cytosolic pool with citrate occupies the metabolic center of gravity for lipid biosynthesis (**Figure 1**).

But, wait! The operation of the conventional Krebs/TCA cycle (i.e., in normal, non-proliferating-cell mitochondria) is usually appreciated first, without considering the interplay of the numerous metabolite and ion transport proteins embedded in the mitochondrial inner membrane that allow communication with the cytosol (LaNoue and Schoolwerth, 1979; Palmieri, 2013). Participation of these membrane metabolite transport proteins simultaneous with the operation of the Krebs/TCA cycle, when comparing normal vs. pathological metabolism, complicates the metabolic reprogramming considerably!

For example, are we to believe that all (more than 50 in humans; Palmieri and Monné, 2016) inner mitochondrial membrane metabolite transporters operate independent of any sort of regulatory influence, oblivious to moment-to-moment cellular demands, such as the dividing cell's temporal position within the cell cycle? What metabolic environmental condition(s) in the cell could serve as signals that would control regulation of metabolite flux between mitochondrial matrix and cytosol?

Loss of Feed-Back Control of Cholesterogenesis in Tumors: Evidence and Some Consequences

By 1964 (Bloch, 1965) there was already reasonable suspicion that regulation of cholesterogenesis in animals centered on modulating the activity of the ER-bound enzyme 3-OH-3-CH_3-glutaryl-CoA-reductase (HMGR). Subsequent research leaves little doubt that inhibition of HMGR activity, and the resulting lack of cholesterol synthesis, suppresses cell division. Especially provocative are two findings (Chen et al., 1975; Brown and Goldstein, 1980; Heiniger, 1981; Doyle and Kandutsch, 1988).

First, the flow of anabolic carbons in the cholesterogenesis pathway, specifically the genesis of mevalonate, the product of the HMGR reaction, serves an indispensable role in initiating DNA synthesis and cell proliferation. In fact, the addition of mevalonate to circumvent a blocked HMGR activity re-establishes cell growth (Sinensky and Logel, 1985). Second, and even more relevant: the loss of feedback inhibition of HMGR, and a resulting increase in HMGR activity, is a fundamental metabolic defect of virtually all cancers (Siperstein and Fagan, 1964; Goldstein and Brown, 1990). The overwhelming conclusion of the collective data from diverse laboratories, beginning in the 1980's, reveals that cholesterogenesis in tumor cells not only lacks feedback regulation, but, depending on the rate of cell proliferation, can occur at very high, continuous rates. At first glance these findings would evince little surprise. After all, proliferating cells require newly replicated "everything"—the whole panoply of membrane lipids, including the membrane

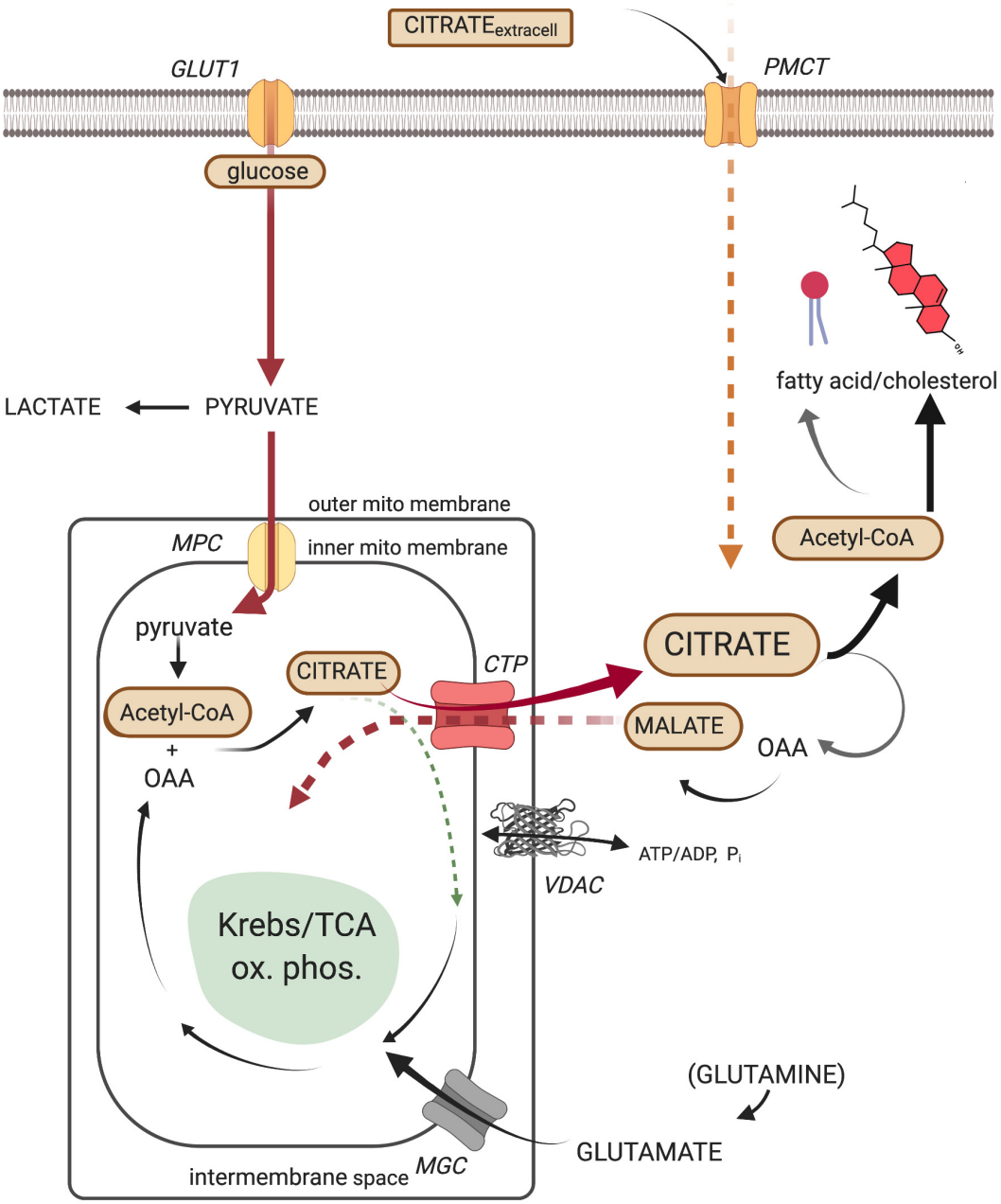

FIGURE 1 | The cellular metabolic origin and fate of citrate. GLUT1, facilitated mammalian glucose transporter (SLC2A1); PMCT, plasma membrane citrate transporter (SLC13A5); MPC, mitochondrial pyruvate carrier (SLC54A2); CTP, citrate transport protein (SLC25A1); MGC, mitochondrial glutamate carrier (SLC25A22); VDAC, mitochondrial outer membrane voltage-dependent anion-selective channel.

insertion of lipid bilayer fluidity-reducing cholesterol, the unique membrane-stabilizing sterol component in mammals (Demel and De Kruyff, 1976; Marquardt et al., 2016).

A penetrating question emerges. What global, as well as intracellularly specific, consequences can such abnormally high rates of cholesterogenesis reveal in proliferating tumors? Tumor cholesterol overproduction implies that the various cellular membrane categories (plasma, ER, etc.) might become differentially cholesterol-enriched, in some cases incorporating enlarged lipid-raft domains. Such enrichment might alter the phase-transition properties of membrane lipids, thereby modifying the functional characteristics of integrated

membrane-associated proteins (Siperstein, 1984; Liu et al., 2017). Would differential cholesterol enrichment of tumor membranes have meaningful consequences for the tumor's metabolomics and growth?

Siperstein's (1984) comprehensive review coincided with our own laboratory's ongoing investigations that sought correlations between the standard, respiration-linked oxidative phosphorylation patterns of normal liver, and those exhibited by the various cholesterol-enriched Morris hepatoma model systems. Specifically, we confirmed that the cholesterol content of isolated mitochondria generally parallels the growth rate of these hepatomas; faster growing tumors (e.g., Morris hepatoma 3924A) display substantially higher mitochondrial cholesterol than the mitochondria of slower growing tumors (e.g., Morris hepatoma 16), and both hepatomas possess higher membrane cholesterol than normal (or host rat) liver mitochondria. Indeed, the cholesterol enrichment of tumor mitochondrial membranes was then, and continues to remain, familiar to investigators (van Hoeven and Emmelot, 1972; Feo et al., 1975; Chan and Barbour, 1983; Epand, 2006).

The Road to Mitochondrial Membrane Cholesterol Enrichment

Metabolically speaking, the mitochondrial double membrane architecture gives rise to a division of labor. The matrix-facing inner membrane is responsible for a variety of mitochondrial functions including the entire O_2-requiring, Krebs/TCA cycle-linked bioenergetics enterprise, pregnenolone synthesis, and the operation of the more than 50 substrate transport protein complexes in at least 25 subfamilies embedded in the lipid bilayer, such as the CTP/*SLC25A1* transport protein (Palmieri, 2013; Palmieri and Monné, 2016). The outer mitochondrial membrane, the lipid bilayer barrier that separates the cytosol from the space between both mitochondrial membranes, contains the voltage-dependent anion channel (VDAC) as its most abundant protein (Colombini, 2004). Along with VDAC, other associated outer membrane protein moieties participate in regulating molecular traffic between cytosol and matrix (Campbell and Chan, 2008). VDAC is considered the fundamental control channel that regulates transport of ADP/ATP and other ions and metabolites through the outer membrane barrier into the inter-membrane space (Hiller et al., 2010; Shoshan-Barmatz et al., 2015). Within this inter-membrane space substrates are positioned proximal to the multiple transporters of the inner membrane which then transmit them to the enzymatic machinery of the matrix. VDAC's high-resolution structure has been established (Camara et al., 2017), and most compellingly, has been shown to bind cholesterol (Hulce et al., 2013).

Depending on the tissue in normal, non-proliferating cells, the cholesterol content of the inner mitochondrial membrane is poor compared with its outer, cytosol-facing membrane. Indeed, relative to other cell membranes, cholesterol is a minor lipid component of both mitochondrial membranes (Horvath and Daum, 2013). Nevertheless, there is general accord that cholesterol's presence in mitochondrial membranes influences mitochondrial metabolic function (Rostovtseva and Bezrukov, 2008; Martin et al., 2016). Despite the relatively modest cholesterol content of mitochondria compared with the plasma membrane, HeLa cell mitochondria have been shown to possess cholesterol/sphingolipid-rich (lipid raft) microdomains (Mollinedo et al., 2011). The well-established cholesterol enrichment of tumor mitochondria (Kaplan et al., 1982; Crain et al., 1983; Parlo and Coleman, 1984, 1986; Coleman et al., 1997) and its potential effect on the topology of lipid rafts and the fluidity of laterally surrounding phospholipids, might logically alter interactions between membrane-integral proteins, thereby yielding tumor-specific carbon flux patterns (Marquardt et al., 2016; Liu et al., 2017).

However, the intracellular route by which cholesterol reaches the CTP membrane environment may impact cholesterol's influence on the operation of the CTP. Cholesterol must be conveyed from its source of origin, then delivered from those intracellular membrane loci external to mitochondria, across the mitochondrial inter-membrane space, to the inner membrane (Liu et al., 2006; Flis and Daum, 2013). The vehicle primarily responsible for delivering cholesterol to the inner mitochondrial membrane is the steroidogenic acute regulatory protein (StAR/STARTD1), although its precise mechanism of cholesterol delivery to the inner membrane is not fully established (Martin et al., 2016; Elustondo et al., 2017). StAR/STARTD1-mediated cholesterol transport to the inner membrane is the rate-controlling step for all steroid hormone biosynthesis, and its over-expression has been proposed to correlate with enhanced delivery of cholesterol in breast cancer (Manna et al., 2019). Nevertheless, any potential effect on the activity of the CTP due to enhanced cholesterol delivery to the inner mitochondrial membrane by StAR/STARTD1 remains conjectural. Clinical evidence, however, indicates that mutations in the CTP gene can promote serious neuronal disfunction (Chaouch et al., 2014), so it is plausible that transmittal of excess cholesterol to the inner membrane by over-expressed StAR/STARTD1, and a resulting cholesterol-rich, laterally distorted lipid bilayer, could effect a significantly altered CTP activity (Demel and De Kruyff, 1976; Mollinedo et al., 2011; Marquardt et al., 2016).

In order to confront this possibility we reasoned that one of the most appropriate measurable functions to correlate with the extent of such mitochondrial cholesterol enrichment would concern the penultimate source of substrate for the tumor's deregulated cholesterogenesis: the citrate that shuttles between the mitochondrial matrix and the cytosol on the CTP (Gnoni et al., 2009). Indeed, contemporary data (Catalina-Rodriguez et al., 2012) indicate mitochondrial CTP levels are increased in several cancers, while oncogenic p53 mutants stimulate CTP expression and promote tumor cell proliferation (Kolukula et al., 2014).

Cholesterol-Enriched, Isolated Hepatoma Mitochondria Preferentially Export Citrate

As a reminder, the CTP in normal liver mitochondria catalyzes the electroneutral exchange across the mitochondrial inner membrane of citrate for either another tricarboxylate, a dicarboxylate (e.g., malate or succinate), or phosphoenolpyruvate (Palmieiri et al., 1972; LaNoue and Schoolwerth, 1979). Using the specific CTP inhibitor, 1,2,3-benzenetricarboxylate (BTC),

Kaplan et al. (1982) completed the first comprehensive study on the kinetic characteristics of CTP exchange transport in tumor vs. normal mitochondria, demonstrating that a highly probable positive correlation exists between cholesterol enrichment of tumor mitochondria and an increased V_{max} for citrate transport displayed by the CTP.

Corroborating evidence came from our laboratory's continuing experiments with the wider, more globally accessible metabolic respiratory profiles of normal liver, slow- and rapidly growing Morris hepatoma mitochondria. We documented the more than 4-fold faster pyruvate-supplied citrate efflux from the fast-growing, highly (>5-fold) cholesterol-enriched hepatoma 3924A mitochondria relative to their normal liver counterparts. Both intra-mitochondrial and external-milieu citrate levels were assayed periodically on aliquots of actively respiring mitochondria from the rapid (hepatoma 3924A) and slow (hepatoma 16) growing tumors vs. their control livers over an extended incubation time-course (**Figures 2A,B**). Strikingly, the accelerated, abbreviated carbon flux into and out of the tumor mitochondria (pyruvate$_{cyto}$— > pyruvate$_{mito}$— > acetyl-CoA$_{mito}$— > citrate$_{mito}$—> [CTP]— > citrate$_{cyto}$) was accompanied by a negligibly small ADP-initiated O_2 uptake (**Figure 3A**). These findings implied that the cholesterol-rich tumor mitochondria selectively ejected the Krebs/TCA cycle-generated citrate to the external milieu, rather than employing it to fuel respiration-linked oxidative phosphorylation. Slow-growing ("minimally deviated") Morris hepatoma 16 mitochondria elicited a similar, abbreviated citrate carbon efflux, albeit much reduced in proportion to their lower-level cholesterol enrichment (∼2-fold) compared with normal liver mitochondria (Parlo and Coleman, 1984).

Yet, this conspicuously aberrant tumor mitochondrial respiratory pattern that centered on the re-routing of citrate from the TCA cycle to the cytoplasm, was not detected when these cholesterol-rich mitochondria were fueled with substrates joining the TCA cycle beyond citrate (i.e., post the aconitate hydratase step). That is, although virtually no ADP-stimulated O_2 uptake occurred when supplied with either pyruvate or citrate, the cholesterol-rich tumor mitochondria respired almost indistinguishably as well as normal when fueled with substrates beyond citrate in the TCA cycle sequence: viz., isocitrate, α-ketoglutarate, succinate, and even with glutamate (**Figure 3A**; Parlo and Coleman, 1984; Kaplan et al., 1986).

Validation of this deviant mitochondrial respiratory carbon flux was further confirmed by blocking the hepatoma CTP with the selective inhibitor BTC, which remarkably (but expectedly) reversed the nearly absent respiration of pyruvate-fed O_2 uptake (**Figure 3B**). These results appeared to us as striking and far-reaching. Forcing citrate to remain in the TCA cycle by blocking its export to the cytosol allowed for the re-establishment of near-normal oxidative phosphorylation with cholesterol-enriched organelles from both fast and slow-growing tumors. The significance, here, establishes among other things, that the hepatoma mitochondria possess perfectly functional aconitate hydratase activity, and apart from their membranes being abnormally cholesterol-enriched, these tumor mitochondria proved eminently capable of performing the oxidative phosphorylation acrobatics of their normal

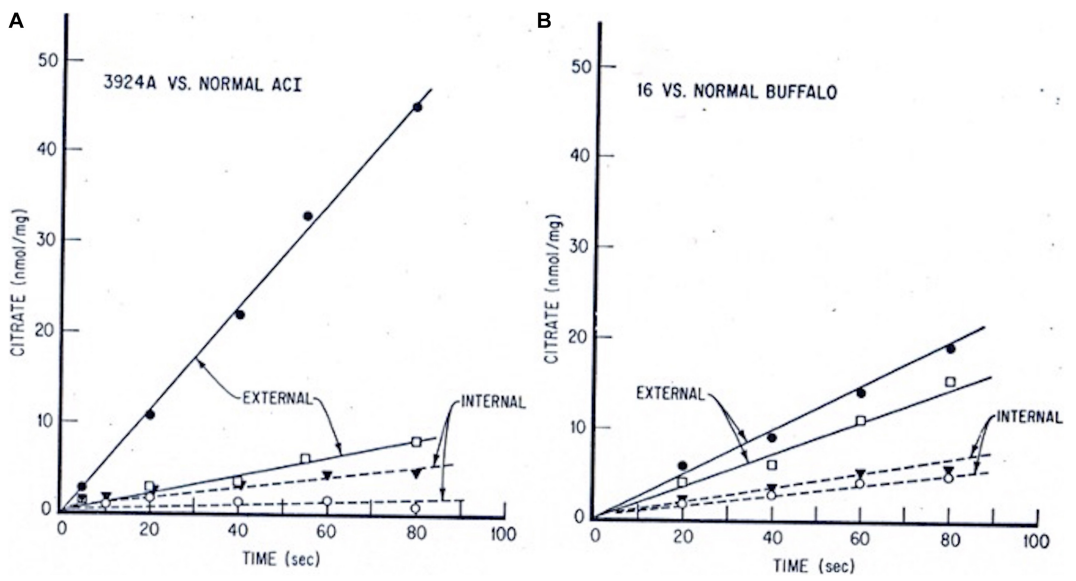

FIGURE 2 | Tumor vs. normal liver extra- and intra-mitochondrial citrate levels: time-course incubations fed pyruvate + malate. Mitochondria from each tissue source were incubated with 0.5 mM pyruvate/0.1 mM malate/15 mM ADP. At indicated time intervals, incubation aliquots were rapidly centrifuged through a silicone oil layer into perchloric acid. Extramitochondrial citrate was determined on the samples above, and intramitochondrial citrate was determined on samples below the silicone oil barrier. **(A)** Hepatoma 3924A, ● extramito; ○ intramito. Normal ACI rat liver, □ extramito; ▼ intramito. **(B)** Hepatoma 16, ● extramito; ○ intramito. Normal Buffalo rat liver, □ extramito, ▼ intramito (see: Parlo and Coleman, 1984, for details on methods).

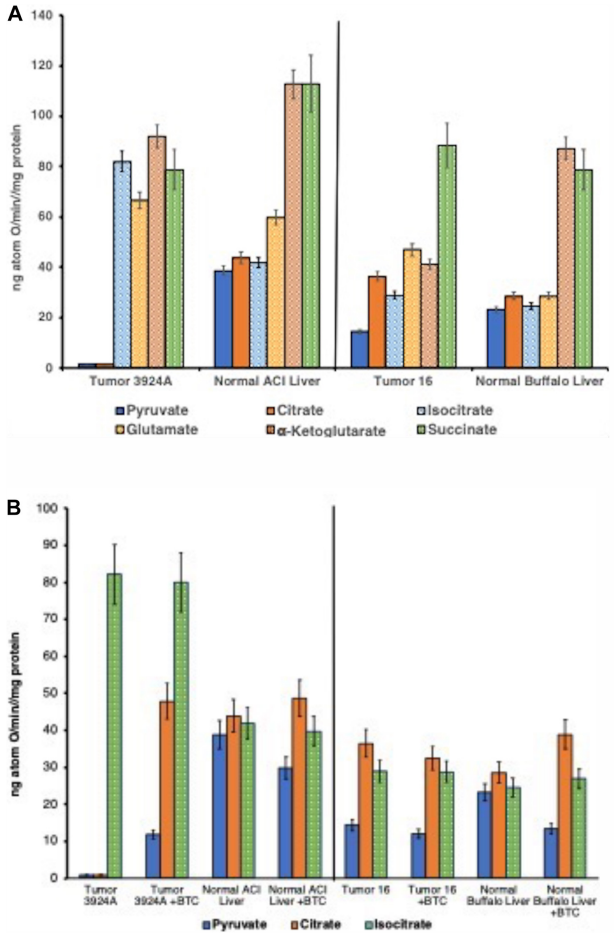

FIGURE 3 | (A) State 3 rates: O_2 consumption tumor vs. normal mitochondria. Duplicate incubations (30°C) contained 5 mM respiratory substrates *plus* 250 μM ADP addition aliquots. ADP/O ratios for all NAD^+-linked substrates averaged 2.63; for succinate, 1.77. ADP/O ratios were unmeasurable with mitochondria from Morris hepatoma 3924A when fueled by pyruvate or citrate since ADP-initiated O_2 uptake was negligible. Data error bars are means ± SD. **(B)** State 3 rates: O_2 consumption pre-/post-aconitate hydratase, tumor vs. normal mitochondria, ± BTC. Incubations were performed as described for **(A)**. 150 μM BTC additions to each incubation were made 30 s after substrate and 30 s prior to additions of 250 μM ADP. Data error bars are means ± SD.

counterparts, if matrix-generated citrate were prevented from exiting.

In this regard it is worth considering that early studies with isolated mitochondria from a variety of tumors (Aisenberg, 1961) displayed lower respiratory rates specifically fueled with pyruvate or citrate compared with corresponding normal mitochondria. Yet, because all tumor mitochondria tested since then have been shown to possess at least some capacity to respire with a number of alternative substrates (succinate, glutamate, even fatty acid derivatives like β-hydroxybutyrate—see for ex., Table 5, Aisenberg, 1961), the respiratory ability of tumor mitochondria in general was taken to be fundamentally normal, or at least functionally unexceptional, and allusion to Warburg's hypothesis unnecessary of discussion in this context.

Technical Controversies Regarding the Exogenous Enrichment of Normal Mitochondria With Cholesterol

Experimental approaches to the same or similar questions can often vary from one laboratory to another, especially as new technologies are applied. Explicitly presented methods, carefully followed and reproduced by different laboratories, become the "gold standard" by which the global veracity of experimental results are confirmed and established. However, deviation from one laboratory's carefully specified methods, regardless of how seemingly inconsequential, will often yield results by the second that differ from the first. Thus, contradictory conclusions about fundamental mechanisms based upon data derived by different methods, and/or relying on a single tumor system, can be misleading, at best!

Mindful of these considerations, the striking results seen on accelerated mitochondrial CTP-facilitated citrate transport in both slow- and rapidly growing rat hepatomas relative to normal liver organelles, encouraged consideration that there was a direct, positive correlation between the extent of mitochondrial cholesterol enrichment and citrate export, as described above. Would normal liver mitochondria, if purposefully enriched with cholesterol, mimic the behavior of tumor mitochondria with respect to their handling of citrate?

A variety of diverse methods have been employed over many years to alter the membrane cholesterol content of viable cells in experimental animals (Colell et al., 2003; Solsona-Vilarrasa et al., 2019) including relatively long-term dietary modification (Feo et al., 1975). Our laboratory had experimented with an early version of what we termed a solid-phase transfer method, described in detail, to covalently label the plasma membrane of viable human lymphocytes in suspension (Coleman et al., 1978a), employing Sephadex G-10 beads. After extensive further tests, we applied modifications of this solid-phase method that were able to successfully increase cholesterol levels in isolated normal mitochondria (see: Parlo and Coleman, 1984; **Supplementary Material**, for detailed methods; Coleman et al., 1978b; Coleman and Lavietes, 1981). This method reproducibly permitted the incremental titration of different amounts of cholesterol into the organelles. Yet, critically, such modified mitochondria were shown to retain full respiratory functional integrity.

The results obtained after exogenous cholesterol enrichment of normal mitochondria, titrated to three increasing levels of cholesterol relative to control, mimicked remarkably both the re-routing pattern of CTP-promoted citrate export, and, in like manner, altered respiratory-linked oxidative phosphorylation observed with naturally occurring cholesterol-rich hepatoma mitochondria (for details see: Parlo and Coleman, 1984). Correspondingly, the cholesterol-loaded normal liver mitochondria revealed a 2-fold increase in the rate of pyruvate-fed citrate efflux, and a lower intramitochondrial steady-state citrate level compared with control mitochondria, again corroborating the preferential export of citrate observed with the tumor mitochondria (**Figure 4**).

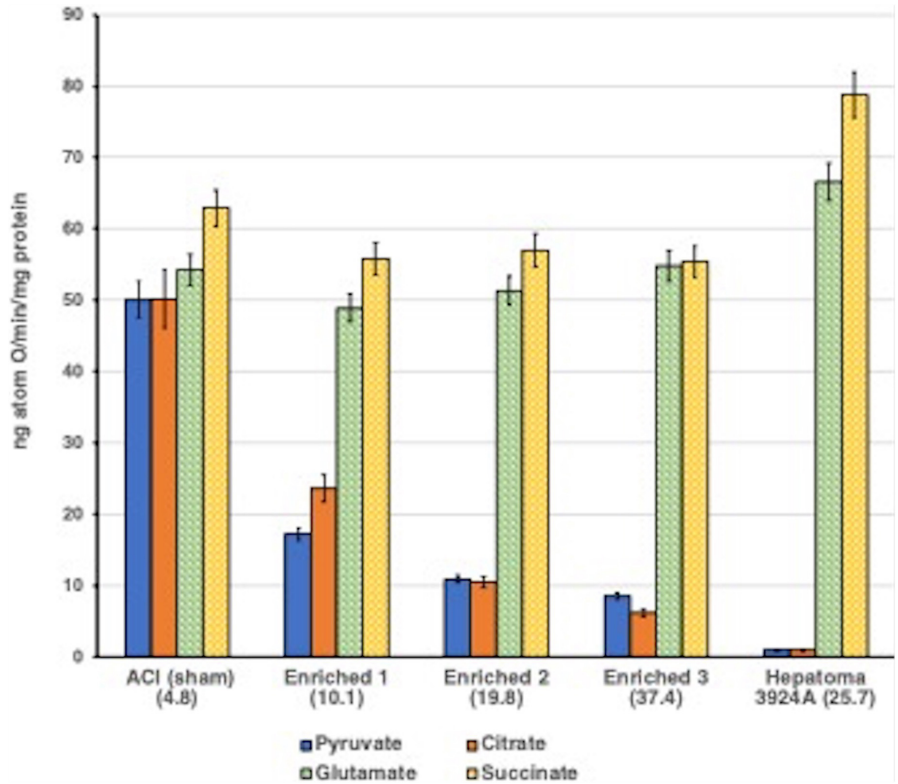

FIGURE 4 | Aberrant pyruvate- and citrate-fueled O_2 consumption by normal mitochondria exogenously enriched with cholesterol. Incubations were performed as described for **Figures 3A,B**. See text. For cholesterol-loading methodology with normal ACI liver mitochondria (see Parlo and Coleman, 1984). Data error bars are means ± SD. ACI (sham) indicates normal mitochondria treated by the cholesterol loading procedure, but without cholesterol. Normal mitochondria were enriched with three incremental cholesterol levels. The cholesterol content of each enrichment is shown as (μg total cholesterol/mg protein) in parentheses. Inverse correlation between the decrease in pyruvate- and citrate-fueled respiration as the cholesterol enrichment of normal mitochondria is exogenously increased is clear, dramatic and mirrors the respiratory pattern of tumor 3924A mitochondria. Note that respiration fueled by post-aconitate hydratase Krebs/TCA cycle substrates appears to be unaffected by the mitochondrial cholesterol content.

Studies from one other laboratory, limited to isolated AS-30D hepatoma mitochondria, yielded contrary results based either on flawed application of, or incompletely defined, experimental methodology and inadequate data interpretation (Dietzen and Davis, 1993, 1994). To date, these unique and contradictory reports have never been validated by other laboratories. There are overwhelming data from numerous laboratories acquired over many years that speak specifically to the functional effects of altered mitochondrial membrane cholesterol (Schneider et al., 1982; Weiser et al., 2014). A wealth of research clearly and repeatedly demonstrates that cholesterol levels in mitochondrial membranes contribute to that organelle's increasingly divergent metabolic function, by not only distorting cell maintenance mechanics, but also by affecting the process of cellular apoptosis (Colell et al., 2003; Tait and Green, 2012; Kennedy et al., 2014; Ribas et al., 2016).

Tracking Carbon Flux With Liver vs. Hepatoma Tissue *ex vivo*: What Happens to Pyruvate-Derived Citrate?

The well-established inability of tumors to demonstrate tight feedback control over cholesterogenesis suggests that the carbon flux through the multistep cholesterol biosynthesis pathway might operate continuously in tumors if amply supplied with acetyl CoA (Chen et al., 1978; Heiniger, 1981; Fairbanks et al., 1984; Mountford et al., 1984; Maltese and Sheridan, 1985; Erickson et al., 1988). Over a prolonged time-course therefore, buildup of cholesterol would be expected to be greater in tumors than in normal tissue, depending on the extent of the synthetic pathway's impairment of the HMGR rate-limiting step (Rostovtseva and Bezrukov, 2008; Marquardt et al., 2016).

Results outlined above with isolated tumor and cholesterol-loaded normal mitochondria (Parlo and Coleman, 1986) motivated further investigation of the preferential export of mitochondrially generated citrate, but under more biologically realistic, whole cell conditions, comparable to those employed by Warburg, viz., viable tissue slices from normal liver and Morris hepatoma 3924A.

The primary objective of these comparative *ex vivo* incubation studies was to track the fate of [U-^{14}C]-pyruvate carbons by following its metabolic conversion to both $^{14}CO_2$ and [^{14}C]-cholesterol. These data emerged, significantly, as two recognizably distinct carbon flux patterns. Normal and tumor systems were distinguishable by the preferential routes each tissue source used to metabolize the exogenous pyruvate; either

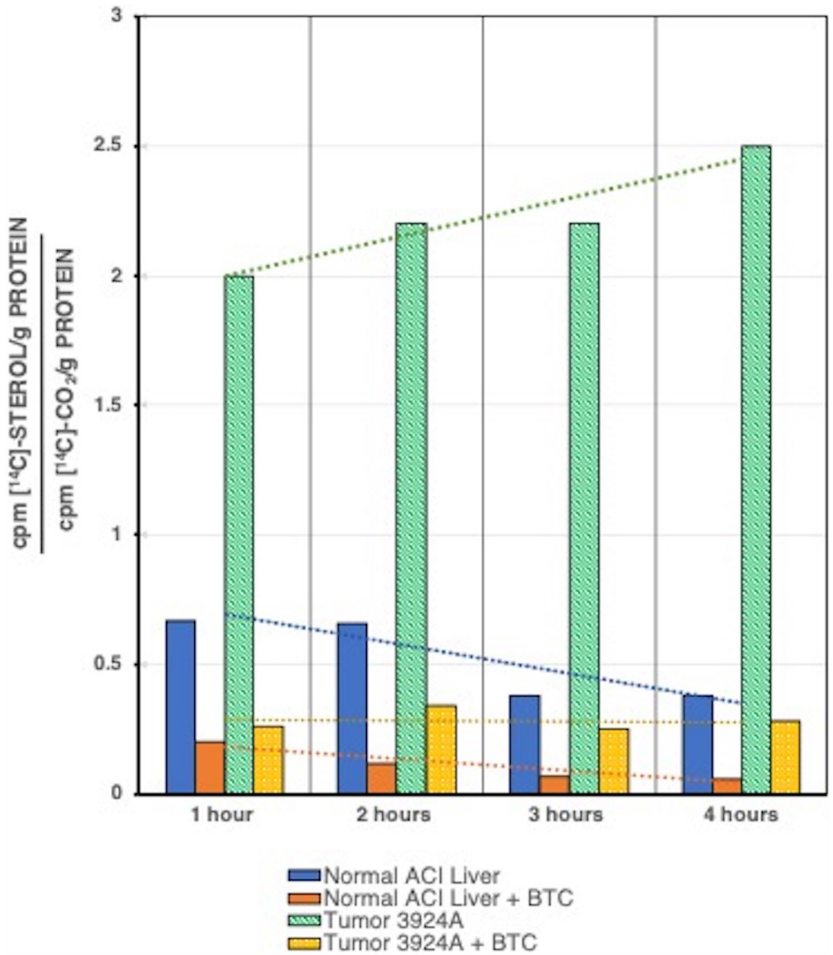

FIGURE 5 | [U-^{14}C]Pyruvate incorporation into [^{14}C]cholesterol or $^{14}CO_2$ for tumor 3924A vs. normal liver tissue slice incubations, ± BTC. Normal liver and tumor tissue slices were incubated with [U-^{14}C]pyruvate *plus* or *minus* 10 mM BTC, and assayed at each time interval shown. Data are given as ratios over time for ^{14}C incorporated into sterol vs. CO_2. In addition to the clearly enhanced rate of sterol synthesis in tumor 3924A, the trend lines over time indicate that in this rapidly growing hepatoma, whose mitochondria are highly enriched in membrane cholesterol, BTC dramatically reverses the pyruvate carbon flux from sterol incorporation to CO_2 formation (see: Parlo and Coleman, 1986 for details on methods).

via TCA cycle-linked oxidative decarboxylation or *via* anabolic cholesterogenesis (Parlo and Coleman, 1984).

Relative carbon flux ratios demonstrated clearly that after a 2-h incubation the hepatoma 3924A tissue slice system incorporated greater than 3-fold more [^{14}C] into cholesterol than into $^{14}CO_2$ compared with normal liver, and after a 4-hr incubation greater than 6-fold more [^{14}C] incorporation appeared in cholesterol than in $^{14}CO_2$, relative to normal liver. Most significantly, the specific mitochondrial CTP inhibitor, BTC, was capable of dramatically blocking [U-^{14}C]-pyruvate-to-[^{14}C]-cholesterol incorporation in the tumor tissue, effectively restoring a carbon flux pattern to one closely resembling the respiratory oxidative decarboxylation exhibited by normal liver tissue (**Figure 5**).

In later studies, described in section "Resurrecting the Truncated Krebs/TCA Cycle and the Warburg Effect." subsection "BTC Inhibition of CTP Arrests (Reversibly) Cholesterol Synthesis and DNA Replication in Synchronized Tumor Cells," below, the BTC uptake rate was directly measured and was confirmed to rapidly enter proliferating, cultured murine lymphoma cells during *in vitro* incubation.

Comprehensive evaluation of these metabolic patterns from normal and tumor sources, employing both isolated mitochondria and viable *ex vivo* tissue slices, supports the following general conclusions:

(1) When mitochondria of hepatomas become enriched with cholesterol by means of accelerated cholesterogenesis due to loss of feedback regulation of HMGR, they manifest an altered metabolic profile that exhibits a preferential export of citrate.
(2) Tumor mitochondria that are cholesterol enriched evince a significantly increased V_{max} for the mitochondrial membrane CTP.
(3) Preferential citrate efflux from the experimental tumor mitochondria deprives the conventional Krebs/TCA

cycle of this critical respiratory substrate for oxidative phosphorylation-linked ATP generation regardless of ambient oxygen levels.

(4) The specific CTP inhibitor, BTC, blocks the preferential efflux of citrate from cholesterol-rich tumor mitochondria, thereby restoring citrate-fueled respiration and re-establishing the Krebs/TCA cycle respiration-linked oxidative phosphorylation process of normal mitochondria.

(5) The ability to support respiration-linked oxidative phosphorylation fueled by alternative substrates joining the Krebs/TCA cycle beyond the formation of citrate appears unaffected by the enhanced rate of citrate export from cholesterol-rich tumor mitochondria.

(6) The ratio of mitochondrial citrate to cytosolic citrate in the cholesterol-rich tumor mitochondria may be a critical expression of cell proliferation in cancer.

Accelerated, De-Regulated Cholesterogenesis Is Reinforced by the Multifold Expression of HMGR in Tumors

Although the regulation of cholesterol biosynthesis in normal cells is effected by means of several highly complex mechanisms, including feedback inhibition of HMGR by mevalonate-fueled pathway intermediates, hydroxysterols and a diverse host of other cellular metabolites (Goldstein and Brown, 1990), one could question whether the same set of controls obtains in tumors (Erickson et al., 1988). On the basis of the cumulative results described above with normal liver vs. rapidly growing Morris hepatoma 3924A, and since HMGR is a membrane-integral protein of the ER, we questioned whether the significantly increased carbon flux from pyruvate to cholesterol in the tumor could be detected in a cell-free, post-mitochondrial supernatant system (PMS) incubation. Moreover, if detectable, would such cell-free, post-mitochondrial HMGR activity retain any capacity for regulation? Finally, we asked whether an enhanced carbon flux in the tumor PMS compared with that of normal liver depended on the expressed cellular amount of HMGR.

Our study (Azrolan and Coleman, 1989; Coleman and Sepp-Lorenzino, 1990) demonstrated the first, to our knowledge, mitochondria-free cell lysate (PMS) capable of lipid synthesis. In fact, the capacity of the PMS for cholesterol synthesis fueled by [^{14}C]-citrate over a 4-hr time course for both normal and hepatoma 3924A was clearly established. In addition to [^{14}C]-citrate, we also used [^{14}C]-acetate as substrate for the PMS, bypassing the ATP-citrate lyase conversion of citrate to acetyl-CoA, the immediate carbon source for cholesterogenesis. Both substrates yielded near identical results (**Figure 6A**). We noted, as well, that the tumor PMS exhibited a more than 9-fold greater ATP-citrate lyase activity than the normal system (Coleman and Sepp-Lorenzino, 1990), an observation later substantiated by others (Zaidi et al., 2012; Wang et al., 2017; **Figure 6B**).

Data reduction on a per-cell basis indicated that the tumor PMS had the capacity to synthesize cholesterol from either citrate or acetate more than 9-fold faster than did normal PMS. When normal liver PMS was supplied with [^{14}C]-mevalonate rather than [^{14}C]-acetate, the rate of cholesterol synthesis increased by 6-fold, confirming that the PMS from normal tissue retains

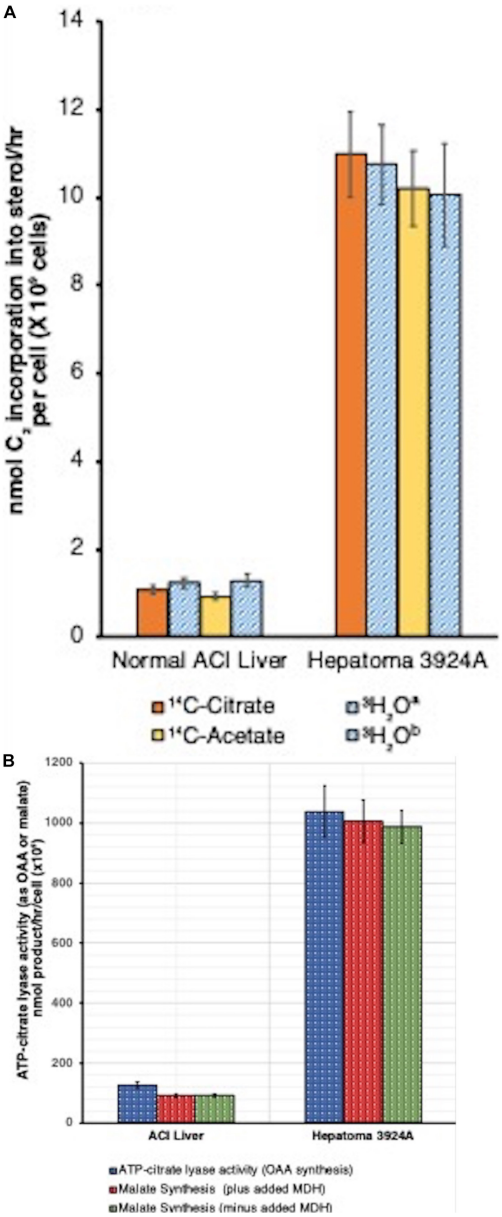

FIGURE 6 | (A) Cell-free (post-mitochondrial) sterol synthesis rates, tumor 3924A vs. normal liver. Post-mitochondrial system (PMS) incubations (4 h, 37°C) contained either [1,5-^{14}C]-citrate or [1-^{14}C]-acetate (1.5 μCi/ml, 10 mM), or 10 mM citrate[a] or acetate[b] in the presence of [^{3}H]-H_2O (5 mCi/ml). Data error bars are means ± SEM. A correction factor of 1.5 was required for calculation of C_2 incorporation into sterol from [1,5-^{14}C]-citrate or [1-^{14}C]-acetate because only 12 of the 18 C_2 units supplied are incorporated/mol cholesterol. With the [^{3}H]-H_2O incubations, a correction factor of 0.536 was used, equivalent to the (^{3}H/C) incorporation ratio into cholesterol (14-to-15 [^{3}H]/27 cholesterol carbons) (see: Azrolan and Coleman, 1989, for details on methods). **(B)** Cell-free (post-mitochondrial) ATP-citrate lyase activity, tumor 3924A vs. normal liver. Data from two complementary procedures on PMS incubation aliquots (4 h, 37°C) are shown **(1)**. Direct ATP-citrate lyase activity (measured as oxaloacetate, OAA formed), and **(2)** anion exchange-resolved malate generated (*plus* and *minus* added malate dehydrogenase, MDH, 2 units/ml, to assure reaction completion). Data error bars are means ± SEM (see: Azrolan and Coleman, 1989, for details on methods).

the rate-limiting site for cholesterogenesis (i.e., HMGR) between acetate and mevalonate. Alternatively, the tumor PMS showed no difference in the 9-fold accelerated rate of cholesterol synthesis when fueled by either acetate or mevalonate, indicating that with the tumor system, regardless of whether the initial cholesterol synthesis substrate was supplied before (acetate) or after (mevalonate) the HMGR rate-limiting step, carbon flux was unchanged.

These results support the carbon flux patterns obtained with both isolated mitochondria, as well as from tissue slice incubations, with normal vs. hepatoma preparations described in subsections "The Road to Mitochondrial Membrane Cholesterol Enrichment," "Cholesterol-Enriched, Isolated Hepatoma Mitochondria Preferentially Export Citrate," and " Tracking Carbon Flux With Liver vs. Hepatoma Tissue *ex vivo*: What Happens to Pyruvate-Derived Citrate?" above. Moreover, comparisons of steady-state concentrations of some early cholesterogenesis intermediates (e.g., acetate, acetoacetate, hydroxymethylglutarate, and mevalonate) dramatically mirrored the differences in carbon flux between normal and hepatoma 3924A PMS systems. Normal liver PMS displayed high steady-state levels of HMG-CoA and relatively low amounts of mevalonate. The tumor PMS, in contrast, revealed the reverse pattern (for details, see Azrolan and Coleman, 1989; Coleman and Sepp-Lorenzino, 1990).

HMGR immunopreciptation analyses on isolated microsomal fractions from the PMS of equivalent cell numbers of normal ACI rat liver and Morris hepatoma 3924A demonstrated an approximately 10-fold greater amount of HMGR protein in the microsomal fraction derived from the hepatoma vs. normal liver (Azrolan and Coleman, 1989).

Thus, for the first time, this result strongly suggested that the dramatically enhanced carbon flux from pre-mevalonate intermediates through the rate-controlling step of cholesterogenesis, may be mostly due to the considerably greater accumulation of HMGR in the hepatoma 3924A tumor cell. Of course, this could imply, minimally, that in the time-line of transformation from normal liver hepatocyte to hepatoma, a mutation affiliated with the regulation of either HMGR gene over-expression, or the enzyme's degradation, had occurred. With respect to cancer, overexpression of HMGR by activation of the gene for the sterol regulatory element binding protein (SREBP) is not fully understood (Brown and Goldstein, 1980; Porstmann et al., 2005; Goldstein et al., 2006), but a close interrelationship between SREBP and cancer's clinical hallmarks has been described (Bao et al., 2016). As well, ubiquitination and proteasome degradation has received serious attention as a mechanism of feedback regulation of the enzyme (Johnson and DeBose-Boyd, 2018).

Resurrecting the Truncated Krebs/TCA Cycle: Correlation With the Warburg Effect

Mitochondrial Carbon-Flux Traffic Detours in Tumors

Evidence, based on the long-established and repeatedly affirmed observation that tumor mitochondria possess higher membrane cholesterol levels, indicates that as a consequence of such altered membrane lipid composition, the functional behavior of tumor mitochondria can indeed be considered aberrant, as implied by Warburg. Moreover, the fundamental cause of tumor mitochondrial enrichment with cholesterol may be the concomitant loss of regulation of cholesterogenesis at the pathways's HMGR locus, together with the multifold increase in HMGR per cell, at least as observed with experimental hepatomas. The carbon flux "pull" toward cholesterogenesis may constitute a basis for correlating the re-programmed Krebs/TCA cycle pattern observed in tumors. Our laboratory's sequential studies on experimental animal hepatomas demonstrated, repeatedly, that a primary and critical metabolic response of cholesterol-enriched mitochondria—whether of tumor origin or artificially achieved via exogenous loading—is the dramatic preferential export of pyruvate-supplied, intramitochondrially generated citrate to the cytosol, where it serves to supply acetyl-CoA, the essential precursor substrate for cholesterol and lipid anabolism. Finally, and most significantly, the effect of depriving citrate from participating in the Krebs/TCA cycle can be definitively circumvented, or at least drastically diminished, by substituting alternative Krebs/TCA cycle intermediates (e.g., glutamate) to fuel respiration-linked oxidative phosphorylation. Such re-routing of citrate occurs independent of the presence of O_2. Collectively, these observations constitute a strong basis for the proposed continuously operating, "truncated" or abbreviated Krebs/TCA cycle, whereby faster-growing tumors export the bulk of the citrate from the mitochondria to the cytosol, thereby reinforcing Warburg's impaired mitochondrial respiratory profile. Moreover, as would be inferred as a consequence of the Warburg effect, enhanced glycolysis, in concert with deregulated cholesterogenesis, might realize both an overproduction of cholesterol and provide for ATP production, with the export of citrate featured as a key element of the tumorigenic process (**Figure 7**).

A striking manifestation of respiratory substrate re-routing that evolves from the proposed truncated Krebs/TCA cycle by preferential citrate export from tumor mitochondria, is the well-established elevation in mitochondrial glutaminolysis activity in cancer, and the correlative utilization of resulting glutamate as Krebs/TCA cycle participant upon its conversion to α-ketoglutarate by glutamate dehydrogenase or, as shown in **Figure 7**, aspartate aminotransferase (Reitzer et al., 1979; Frigerio et al., 2008; Erickson and Cerione, 2010; Wise et al., 2011; Matés et al., 2019). And, as **Figure 7** illustrates, glutamine is known to serve multiple key roles in cellular metabolomics, both in normal and pathologic tissues (Hensley et al., 2013; Cluntun et al., 2017). Such remodeling of the tumor's respiratory substrate utilization effectively *supplements* the tumor's enhanced glycolitic profile, rather than being supplanted by it (DeBerardinis and Chandel, 2016). It underscores the operational malleability of tumor bioenergetics (i.e., oxidative phosphorylation) concomitant with the anabolic diversion of citrate toward the latter's incorporation into the tumor's deregulated cholesterogenesis *de novo* as depicted in **Figure 7**, and documented in this Review (section "Mitochondrial Metabolism Is Anomalous in Tumors," subsection "Tracking Carbon Flux With Liver

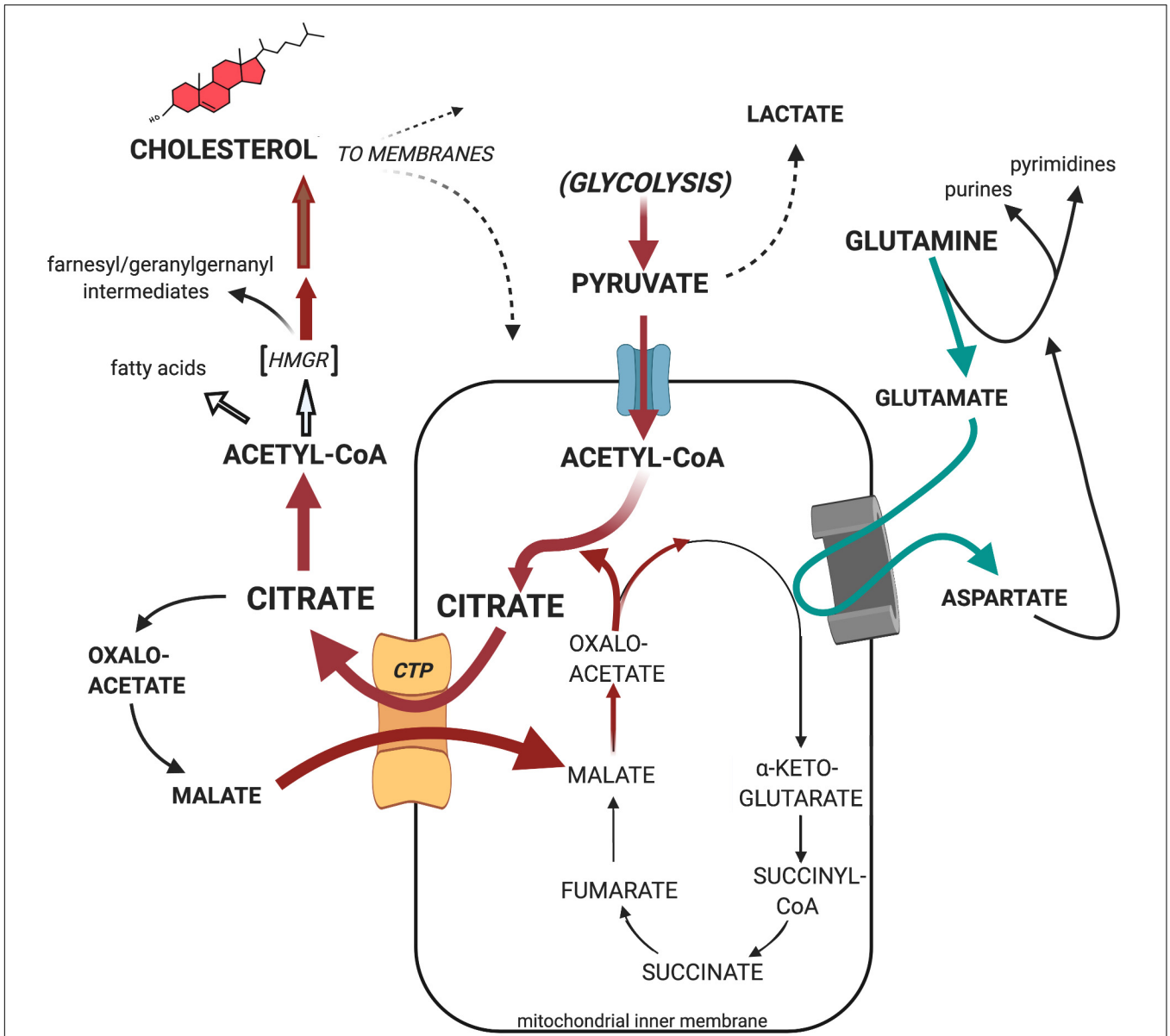

FIGURE 7 | Proposed substrate carbon flow through the truncated Krebs/TCA cycle of tumor mitochondria. Cholesterol-rich tumor mitochondria preferentially export pyruvate-generated citrate as the primary source of cytosolic acetyl-CoA to support the tumor's enhanced cholesterogenesis, rather than utilize it as substrate for oxidative phosphorylation. Nevertheless, cholesterol-rich tumor mitochondria efficiently engage mitochondrial respiration when fueled, for example, with glutamate together with the malate re-entering in exchange for exiting citrate on the CTP (see text for further details).

vs. Hepatoma Tissue *ex vivo*: What Happens to Pyruvate-Derived Citrate?").

SF188 glioblastoma cultures, exhibiting a pronounced Warburg effect, were examined in an elegant and comprehensive study by DeBerardinis et al. (2007). ^{13}C-NMR was employed with ^{13}C-labeled glucose, thus allowing for real-time, simultaneous analysis of multiple metabolic pathway carbon flux patterns in these cells. Their data dramatically revealed several important features of carbon flux in these gliomas. They found the major route of carbon entry into the Krebs/TCA cycle for ^{13}C-glucose-derived pyruvate-to-acetyl-CoA conversion is through mitochondrial pyruvate dehydrogenase. Further, they confirmed the anapleurotic utilization of glutamate in the Krebs/TCA cycle, and, most importantly, they substantiated that 60% of the ^{13}C-glucose tracer was incorporated into newly synthesized lipids, necessitating the efficient mitochondrial export of ^{13}C-citrate followed by cytosolic conversion to ^{13}C-acetyl-CoA. This study also confirmed, as had our own hepatoma work (Parlo and Coleman, 1986), that despite the tumor's distinct Warburg effect profile, the Krebs/TCA cycle performs unimpaired, although by way of an amended carbon flux.

With the preferential export of tumor mitochondrial citrate via the CTP resulting in a diminished availability of citrate to directly support TCA cycle-linked respiration, and the elevated conversion to cytosolic acetyl-CoA as precursor for deregulated cholesterogenesis, one begins to discern the outlines of a more general, over-arching metabolic pattern for tumor growth and proliferation.

To support the main tenet of the Warburg effect and the unrestrained cell proliferation of tumors—i.e., an increased dependence on aerobic glycolysis with diminished reliance on O_2-linked oxidative phosphorylation—we postulate an advantageous and, we emphasize, continually maintained carbon flux pattern; one that expands and supplements the metabolic focus of analysis beyond the prevalent mitochondria-centered considerations. Such a highlighted tumor-specific, more broadly viewed metabolic segment, would consist of the following sequence of events:

1. Cytosolic pyruvate enters mitochondria long enough to generate citrate, which no longer will become engaged in the TCA cycle;
2. but, upon accelerated exit to the cytosol, instead becomes the critical substrate pool precursor for de-regulated cholesterogenesis;
3. whose diverse mevalonate-derived isoprenyl intermediates serve as imperative triggers for DNA synthesis.

Glycolytic Response to Accelerated Cholesterogenesis in Tumors

Continuous, accelerated carbon flux from extramitochondrial pyruvate to cholesterol requires a coordinated and compensatory higher glycolytic activity. This reorganized carbon flow necessitates an escalated uptake of glucose into tumors, leading, ultimately, to an abnormal cholesterol enrichment of tumor cell membranes. The tumor's increased dependence on higher glycolytic carbon flux, corresponding with the Warburg effect requirements, takes advantage of many levels of metabolic signaling that shift emphasis toward anabolic profiles in the cytosol in order to prepare cells for impending proliferation. Here, the effect of enhanced mitochodrially exported cytosolic citrate is not to help regulate glycolysis by allosteric control of phosphofructokinase, as proposed in normal cells, but to serve as a constantly refreshed source of cytosolic precursor substrate for cholesterogenesis in tumors.

The classic regulation of glucose uptake and ensuing glycolysis has been reviewed in detail elsewhere (Cox and Nelson, 2005; Voet and Voet, 2011). However, select aspects of the exceedingly complicated and varied regulatory signals controlling glucose metabolism are abbreviated here to support peripheral evidence for the remodeling of glucose-fed tumor cell carbon flux. Generally speaking, considerable evidence indicates glycolysis enzymes are upregulated in tumors (Cairns et al., 2011).

Foremost among controlling elements is the dominant role in directing tumor cell glucose utilization via protein phosphorylations supervised by the phosphoinositide 3-kinase (PI3K)/serine-threonine-specific protein kinase (Akt) — PI3K/Akt cascade—along with another serine-threonine kinase called "mammalian-target-of-rapamycin" (mTor) (Vander Heiden et al., 2010; Hanahan and Weinberg, 2011; Fruman and Rommel, 2014). This family of signaling proteins has been shown to be constitutively amplified in tumors (Elstrom et al., 2004; Fruman and Rommel, 2014).

Upon activation of receptor tyrosine kinases on the plasma membrane cell surface, the PI3K/Akt pathway signals several glycolysis-linked components that stimulate glycolysis carbon flux. PI3K/Akt activity: (1) causes increased expression, and thus activity, of the cell's plasma membrane-embedded glucose transporter GLUT1, yielding increased glucose uptake; (2) promotes hexokinase (HK-II) mitochondrial-outer-membrane VDAC association, facilitating creation of glucose-6-phosphate; and (3) indirectly stimulates phosphofructokinase (PFK-I) activity to generate increased fructose 1,6,-fructose-*bis*-phosphate, the rate-limiting reaction of glycolysis. All of these effects act synergistically to stimulate enhanced glycolysis in tumors independent of the presence of O_2, consonant with the Warburg effect.

Insofar as regulation of glycolytic carbon flux, particularly with respect to tumors, cytosolic citrate is a commonly prescribed allosteric inhibitor of phosphofructokinase activity (Sola et al., 1994; Usenik and Legiša, 2010). But in the case of the tumor's deregulated and dramatically accelerated cholesterogenesis, where the steady-state pool of citrate is kept from accumulating as it continuously supplies the acetyl-CoA for lipid anabolism, it is doubtful if citrate plays a significant role in this regard.

When the glycolytic rate becomes excessive and less responsive to multi-levels of control, as in rapidly proliferating tumors, numerous metabolic ramifications become apparent which alter the cell's homeostasis. Thus, we can contemplate the fate of the end product of the pathway, pyruvate, positioned at a crossroad of further metabolism. While in the cytosol, pyruvate may be either reduced to lactate by lactate dehydrogenase (LDH), or become transported into mitochondria on the inner membrane pyruvate carrier (MPC) (Bender and Martinou, 2016; Rauckhorst and Taylor, 2016), where it will become engaged in TCA cycle mechanics. Not surprisingly, LDH over-expression also has been reported in tumors (Cui et al., 2014; Mishra and Banerjee, 2019). If the rate of glycolytic flux in tumors outpaces or overburdens the capacity of mitochondrial uptake of pyruvate, lactate production will predominate, allowing partial restoration of the cytosolic pool of NAD^+ that was required during operation of glycolysis.

On the other hand, cytosolic lactate accumulation can obtain when the tumor's environment compels its metabolic machinery to respond flexibly by means of divergent pathways. An example is the processing of malate either by the cytosolic $NADP^+$-requiring malic enzyme, which oxidatively decarboxylates malate to regenerate pyruvate, and concomitantly provides NADPH used in lipid biosynthesis, or by the NAD^+-requiring mitochondrial malic enzyme variant that participates in the alternative fueling of the truncated Krebs/TCA cycle by glutaminolysis (Vacanti et al., 2014; Yang et al., 2014).

Yet, tumor mitochondrial pyruvate dehydrogenase (PDH) is not only active, but can provide for substantial glucose carbon flux into lipogenic acetyl-CoA (Holleran et al., 1997). Such results

indicate that despite a seeming "competition" between cytosolic LDH and mitochondrial MPC for disposal of glycolysis-derived pyruvate carbons, a considerable flow of pyruvate carbons into the TCA-cycle to generate citrate via acetyl-CoA can and does occur. And, as was noted previously via the extensive ^{13}C-NMR analysis in glioblastoma cells (DeBerardinis et al., 2007; Yang et al., 2014), the carbon flux of ^{13}C-glucose-derived pyruvate-to-acetyl-CoA conversion not only confirmed unhindered participation of pyruvate dehydrogenase, but that respiratory-linked oxidation of the citrate generated by the TCA cycle in these tumors was limited by its efflux from mitochondria in order to support lipid synthesis. Such ^{13}C-flux routing of metabolism that demonstrated diminished mitochondrial citrate-fueled oxidation as a consequence of preferential lipid biosynthesis, both supports and confirms the data obtained with both cholesterol-enriched hepatoma mitochondria as well as with normal mitochondria exogenously enriched with cholesterol (Parlo and Coleman, 1984), described above (section "Mitochondrial Metabolism Is Anomalous in Tumors," subsection "Cholesterol-Enriched, Isolated Hepatoma Mitochondria Preferentially Export Citrate"). Moreover, experimentally manufactured CTP-deficient lung cancer cells were found to display dramatically re-programmed Krebs/TCA cycle metabolomics relative to their normal cell counterparts (Jiang et al., 2017), including enhanced glycolysis and lactate production, mirroring a principal Warburg effect motif.

Cell Cycle Consequences of Mitochondrially Effluxed Citrate—Cell Proliferation Requires Mevalonate-Derived Prenylated Protein Signaling and Adequate Membrane Cholesterol

Carbon flux through the cholesterogenesis pathway, long known as requisite for DNA synthesis and cell proliferation (Chen et al., 1975; Quesney-Huneeus et al., 1983; Fairbanks et al., 1984; Siperstein, 1984) is also recognized to be temporally coordinated with discrete intervals of the four sequential cell cycle phases that occur between successive mitoses (G_0, G_1, S, and G_2) (Sánchez-Martín et al., 2007). With synchronized cells in culture, carbon flux into *de novo* cholesterol is low during early G_1, increases rapidly to peak midway into G_1, and declines at the G_1/S interface. Abundant research data indicate that specific inhibition of cholesterogenesis at the HMGR locus prevents cells from progressing through the G_1/S boundary into DNA synthesis and cell division, a blockage that was repeatedly shown to be circumvented by addition of mevalonate, but not by the exogenous supplementation of cholesterol to the cultures (reviewed in Coleman et al., 1997). A more recent study, however, presented a unique case of contrasting results. Singh et al. (2013), observed that blocking HMGR activity in F111 fibroblast cultures with either a statin drug (which the authors termed a "proximal" pathway inhibitor), or by inhibiting the last-step conversion of desmosterol to cholesterol with triparanol (considered a "distal" pathway inhibitor) arrested the cell cycle in G_1, prior to S phase (DNA synthesis), stopping cell cycle progression and mitosis. However, supplying serum cholesterol to these cells appeared to be the *only* means of reversing the cell cycle blockage effected by either "proximal" or "distal" cholesterogenic inhibitors. Such disparate experimental outcomes highlight our insufficient molecular understanding about the consequences to cell proliferation by post-mevalonate intermediates, despite some of the more salient discoveries, briefly summarized here, on mevalonate-derived polyisoprenoids produced *en route* to the creation of cholesterol.

Undeniably, among the more exciting research discoveries relevant to cholesterogenesis was the discovery of mevalonate-derived, prenylated proteins. The lengthening isoprenoid intermediates generated by the mevalonate-to-cholesterol pathway features a number of diversionary branches off the main cholesterogenic route. These branch points, yielding polyisoprenyl side chains, have been found to covalently modify an assortment of proteins involved in signaling cell proliferation. Among the most influential of these mevalonate-generated isoprenyl intermediates are the farnesyl- (C_{15}) and geranylgeranly- (C_{20}) moieties (Casey, 1992, 1995; Sebti, 2005; Wang and Casey, 2016), catalyzed by farnesyltransferase (or geranylgeranyltransferase) enzymes. These enzymes effect covalent modification of the Ras superfamily of plasma membrane-associated G-proteins, as well as various cytoskeletal Rho and nuclear lamin proteins, along with other potential cell cycle signaling species which influence the activity of the cyclin family of proteins that regulates passage through the cell cycle (Rahman and Kipreos, 2010). Considerable attention continues to be focused on elucidating potential roles of prenylated proteins as signaling elements in cell proliferation because, among other observations, specific inhibition of the farnesyl protein transferase enzyme elicits upregulation of a protein ($p21^{Waf1/Cip1}$) involved in cyclin control of cell cycle progression (Sepp-Lorenzino et al., 1991; Sepp-Lorenzino and Rosen, 1998; Tamanoi et al., 2001).

Such mevalonate pathway details, although vitally important, distract scrutiny of the accelerated, continuous, citrate-supplied, carbon flux through cholesterognesis, and the resulting membrane cholesterol enrichment that helps define the Warburg effect phenotype of tumors. Meaningful to the theme of this review was a study that demonstrated the tight coupling between the rate of mevalonate availability and the rate of protein prenylation in cultured murine erythroleukemia cells (Repko and Maltese, 1989). A principal result of these experiments showed that inhibition of protein synthesis with cycloheximide almost immediately abolished [^{3}H]-mevalonate incorporation into prenylated proteins. But inhibition of HMGR by a statin diminished [^{3}H]-mevalonate incorporation into susceptible proteins over a slower time-course, suggesting two correlated events: (1) protein prenylation from the available pool of mevalonate occurs very rapidly upon synthesis of susceptible proteins (including, of course, the responsible prenyltransferase enzymes); (2) the rate of mevalonate manufacture—i.e., the carbon flux through cholesterogensis—determines the pool size, and thus, the availability of isoprenyl intermediates for covalent protein modification. This conclusion reminds us that in synchronized cell cultures, the inhibition of HMGR during early G_1 obliterates manufacture of not only mevalonate, and therefore of cholesterol (whose synthesis peaks in mid-G_1 and declines at the G_1/S boundary) but prevents DNA synthesis

and cell division. To restart cell growth at this synchronized stage, both mevalonate and cholesterol are required. Yet, if HMGR is inhibited after the G_1-peak cholesterol synthesis occurs, DNA synthesis is restored merely by mevalonate addition (Sinensky and Logel, 1985; Langan and Volpe, 1987). This result is consonant with the findings of Repko and Maltese (1989), and implies the cholesterol-independent requirement of mevalonate-derived prenylated proteins as feasible signaling triggers for DNA replication.

BTC Inhibition of CTP Arrests (Reversibly) Cholesterol Synthesis and DNA Replication in Synchronized Tumor Cells

After cholesterol synthesis has peaked in mid-G_1, the synthesis of new DNA in preparation for cell division requires a constantly re-supplied pool of mevalonate. How might the effects on DNA synthesis be explored if the supply of mevalonate substrate precursors, such as acetyl-CoA (or *its* cytosolic precursor, citrate), were limited? As described previously in this review, our studies with *ex vivo* liver and hepatoma incubations and isolated liver and hepatoma mitochondria, utilized the CTP inhibitor BTC to encourage and reinforce the proposal of a truncated Krebs/TCA cycle (**Figure 7**), a paradigm for the Warburg effect in cholesterol-enriched tumor mitochondrial membranes.

As detailed, BTC inhibition of the CTP, in both hepatoma and exogenously cholesterol-enriched normal liver mitochondria, re-established the participation of mitochondrial citrate as substrate for oxidative phosphorylation (**Figure 5**). Simultaneously, BTC blockage of CTP eliminates the continual cytosolic citrate re-supply via mitochondrial exchange export for malate, and thus would starve the cell of mevalonate carbons required for cholesterogenesis and ensuing DNA replication.

Our observations (Rao and Coleman, 1989) with both G_0/G_1-synchronized, as well as unsynchronized, proliferating murine lymphoma (70Z/3) cultures ($\leq 10^6$ cells/ml), demonstrated that BTC (between 1 and 10 mM) not only inhibited [^{14}C]-pyruvate incorporation into cholesterol, but concomitantly inhibited [^{3}H]-thymidine incorporation into DNA, thereby arresting cell proliferation (**Figure 8**). We were impressed that BTC, despite its aromaticity and sparing solubility in the pH 7 environment of cellular homeostasis, very rapidly transited the plasma membrane, dispersed within the cell, and, within 1 min, manifested its metabolic effects on carbon flux and DNA synthesis (**Figure 9**). Furthermore (and surprisingly), these BTC-induced metabolic inhibitions proved completely reversible upon washing the cells free of BTC, without exhibiting deleterious effects on cell viability. BTC, thus, appeared non-cytotoxic, at least with this tumor cell system.

We confirmed that citrate's well-known metal chelating ability (Mg^{2+}, Ca^{2+}) is shared by BTC. Attempts to even partially overcome the BTC inhibition of DNA replication by the addition of 0.5 mM mevalonate to the culture required inclusion of the plasma membrane cation ionophore A23187 to the incubation. This permitted cytosolic Ca^{2+}/Mg^{2+} to become replenished from the culture medium (~0.5 mM), compensating, partially, for the chelating effects of BTC, and illuminating

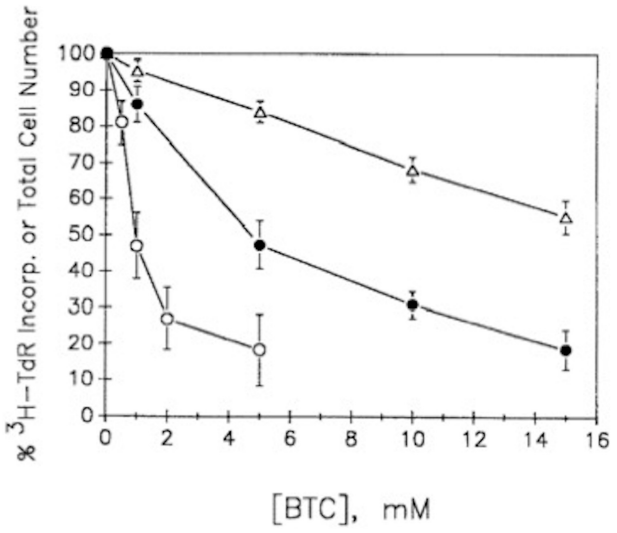

FIGURE 8 | BTC inhibits cell growth and [^{3}H]TdR incorporation into DNA. Exponentially growing unsynchronized or double-thymidine-block-generated G_1/S synchronized 70Z/3 murine lymphoma cultures were incubated with [^{3}H]TdR together with the BTC concentrations indicated (see Rao and Coleman, 1989, for experimental details). Synchronized cultures were found to incorporate maximal [^{3}H]TdR about 3 h after release from the thymidine blockade. Data show means ± SEM for three experiments (12 replicate samples/experiment). △, % of total number of unsynchronized cells; ●, % of [^{3}H]TdR incorporation into unsynchronized cells; ○, % of [^{3}H]TdR incorporation into G_1/S synchronized cells (adapted with permission, Rao and Coleman, 1989).

the mevalonate pathway's well-established promotion of DNA replication (Rao and Coleman, 1989).

The BTC-implemented metabolic shift of pyruvate-supplied carbons, and its effect on DNA synthesis, proved to unconditionally require the cellular cytosolic environment (mitochondria, ER, etc.). Experiments with isolated nuclear preparations from the 70Z/3 murine lymphoma affirmed that DNA synthesis was not significantly inhibited in BTC-treated, mevalonate-supplied incubations, but could be completely restored merely by addition of 5 mM Mg^{2+}. In these studies adequate levels of serum cholesterol were available to the cultures, signifying that the documented BTC effects on DNA synthesis were not due to cholesterol or fatty acid starvation.

Analysis of further experimental permutations with this tumor system (Rao and Coleman, 1989) gave authority to the following conclusions: (1) Inhibition of both pyruvate-fueled cholesterol and DNA syntheses are direct intracellular metabolic responses to BTC, not inhibitor uptake issues; (2) BTC inhibition proved non-toxic, allowing complete recovery of DNA replication and cell viability after removal; (3) Blocking the mitochondrial CTP at the end of G_1, limiting the supply of cytosolic citrate and thus acetyl-CoA, and thereby ultimately mevalonate, arrests further progression through S-phase, abruptly halting cell proliferation.

In terms of the generally protracted time-line of tumor cell growth, therefore, accumulated data accentuate these

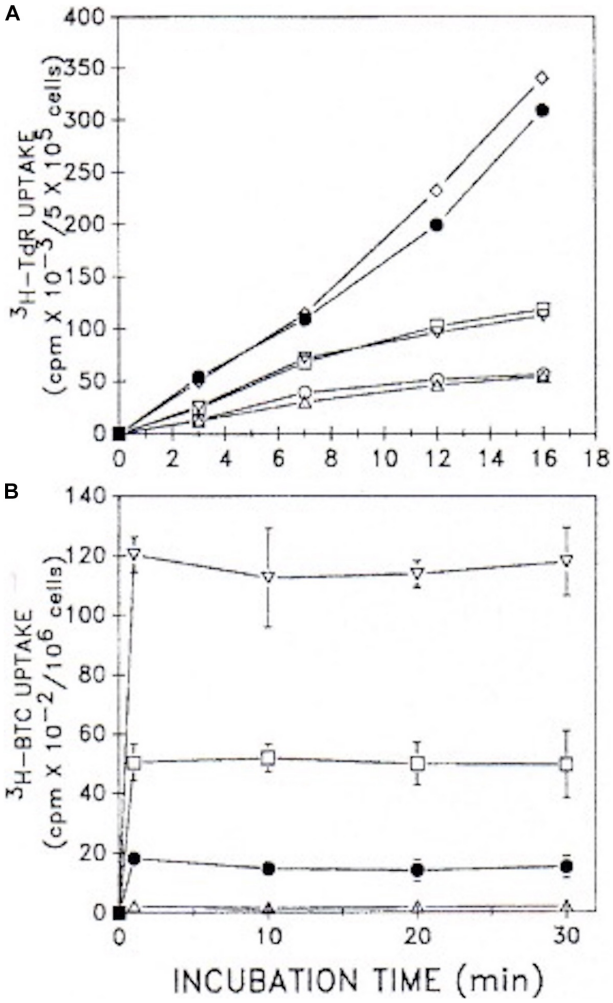

FIGURE 9 | Uptake kinetics of [^{3}H]TdR and [^{3}H]BTC into cells. **(A)** [^{3}H]TdR uptake kinetics were assessed in unsynchronized 70Z/3 murine lymphoma cultures (5 × 10^5 cells/ml) *plus* and *minus* 10 mM BTC. Cells were incubated for the times indicated with varying [^{3}H]TdR concentrations. Mean values of two experiments performed in duplicate are shown. △, □, ●, minus BTC; and ○, ▽, ◇, plus 10 mM BTC, with 1, 3, or 6 μCi [^{3}H]TdR under both conditions, respectively. **(B)** [5-^{3}H]BTC uptake kinetics were assessed in unsynchronized cultures (10^6 cells/ml) over the time course shown. Increasing concentrations of BTC (0.1–10 mM) together with [5-^{3}H]BTC were employed under a constant specific activity of 1 μCi/0.1 mM. Two experiments performed in duplicate (±SD) are given. △, with 0.1 mM BTC; ●, with 1 mM BTC; □ with 5 mM BTC; ▽, with 10 mM BTC (adapted with permission, Rao and Coleman, 1989).

tightly linked metabolic hallmarks of uncontrolled cell proliferation: deregulation of cholesterogenesis at the HMGR metabolic locus; mitochondrial membrane enrichment with cholesterol; preferential export of pyruvate-generated (glycolysis-generated) citrate from cholesterol-enriched mitochondria; and the requirement of a continual supply of mevalonate for ensuing DNA synthesis and cell replication. Collectively, these metabolomic profiles coincide to help endorse our proposed "truncated Krebs/TCA cycle" model (**Figure 7**).

Deregulated Cholesterogenesis Promotes Vesicle Exfoliation From Cholesterol-Rich Plasma Membrane Lipid Raft Domains

Nearly a decade before the introduction of the collective term "exosomes" to characterize exfoliated vesicles from normal and tumor cells (Trams et al., 1981), research demonstrated the shedding of vesicular plasma membrane fragments into the cell-free ascites fluid from various murine leukemias and lymphomas, as well as in the sera and pleural effusions of leukemia patients (Grohsman and Nowotny, 1972; Raz et al., 1978; van Blitterswijk et al., 1979). Further investigations restricted the exosome nomenclature to vesicles of endosomal derivation based on the protein components within their membranes, or by the cargo enclosed within them, compared with extracellular microvesicles (sometimes called "ectosomes") shed from the plasma membranes of healthy, growing cells, whether of normal or pathological origin (Raposo and Stoorvogel, 2013). There remains nomenclature confusion over the biogenesis of shed membrane vesicles, which are referred to merely as extracellular vesicles (EV) (Kato et al., 2020).

Despite recent decades employing sophisticated membrane cholesterol imaging and other analytical techniques that have elucidated the roles and evolution of shed vesicles (whether exosomes or ectosomes) in intercellular trafficking, and their potential involvement in immune surveillance (Raposo and Stoorvogel, 2013; Record et al., 2014; Litvinov et al., 2018; Kato et al., 2020), cholesterol's organization in the cholesterol-rich lipid raft microdomains of the plasma membrane remains poorly understood (Schroeder et al., 2010). Evidence shows the distribution of cholesterol between lipid bilayer leaflets in plasma membranes is not equal, with the cytosol-facing leaflet cholesterol-enriched by as much as 40 mol% of the lipids in that leaflet (Mondal et al., 2009). The greater lateral "rigidity" of this inner-facing vs. the exterior-facing bilayer leaflet has biologic (Pike, 2003) as well as physical manifestations (Vámosi et al., 2006). An early theoretical model, potentially applicable to membrane vesicle exfoliation, was based on free-energy calculations of the plasma membrane's inner leaflet surface area expansion, due to asymmetric (enhanced) cholesterol incorporation (Luke and Kaplan, 1979). Mathematical modeling predicts an outwardly growing spherical distortion of the bilayer, developing into a dumbbell-shaped, narrow-necked structure that eventually pinches off, releasing the cholesterol-rich lipid spheroid to the exterior milieu in an attempt to re-establish the pre-enrichment bilayer lipid composition and surface area. Other models have been proposed (Khatibzadeh et al., 2013). Whether or not such modeling for microvesicle formation is applicable to the shedding of cholesterol-rich vesicles from tumors, convincing evidence exists that cholesterol-rich lipid raft domains play unambiguous, although incompletely understood, roles in the variety of modes that characterize cancer's accelerated pathological and immunosurveillance situations (Pfrieger and Vitale, 2018; Vu et al., 2019).

Mitochondrial membrane cholesterol enrichment in the graded growth series of Morris hepatomas 16 and 3924A (Parlo and Coleman, 1984, 1986) prompted initiation of further study of possible correlations between enhanced, deregulated cholesterol synthesis and the augmentation in membrane cholesterol content of tumor plasma membranes, as well as that of exfoliated microvesicles isolated from the cell-free ascites fluid (CFAF) of a chemically induced murine hepatoma (MH-129) carried in C3H mice. The results revealed both far-reaching and corroborative data germane to the theme of this review, linking the Warburg effect, the proposed truncated Krebs/TCA cycle, and the continuing carbon flux from tumor mitochondria to newly synthesized cholesterol (Puma, 1982).

Although no longer the case (Fonsato et al., 2012), at the time these studies were undertaken (Puma, 1982) little information existed about vesicle exfoliation from hepatomas. The MH129 ascites hepatoma used in these early investigations was readily grown in culture, C3H mouse liver served as the normal (control) membrane source, and, most importantly, MH129 was known to have no viral etiology to complicate the biologic derivation of the vesicles shed into the CFAF. The latter fact was confirmed via transmission electron microscopy of the isolated membrane fraction, which revealed no evidence of ER contamination in the CFAF, and disclosed dimensional aspects of the vesicles consistent with contemporary (van Blitterswijk et al., 1979) or current (Raposo and Stoorvogel, 2013) isolated membrane microvesicle preparations. Multiple marker enzyme assays confirmed the identity of the isolated plasma and shed microvesicle membranes.

These studies (Puma, 1982) showed that the MH129 tumor cell homogenate contained nearly 30% more cholesterol compared with that of normal C3H mouse liver. Microvesicles shed from these cholesterol-enriched hepatoma cells, recovered from the CFAF, demonstrated a 77% greater cholesterol content than the plasma membranes isolated from the MH129 tumor itself, and possessed very substantial increases in the activities of the plasma membrane marker enzymes 5′-nucleotidase and Na^+/K^+-ATPase. Significantly, when the ascites culture was fed 54 μg mevalonate/10^6 cells for 3 h, the microvesicles exfoliated into the CFAF were cholesterol enriched 81% more than the shed vesicles from cultures *minus* added mevalonate. The data emphasize three important features that uphold the preferential carbon-flow concept of mitochondrially exported citrate that feeds deregulated, enhanced cholesterogenesis in tumors: (1) exfoliated vesicles contain higher amounts of cholesterol than the tumor plasma membranes from which they were shed; (2) supplying mevalonate to ascites tumor cultures dramatically yields an even further increase in the amount of cholesterol in the exfoliated microvesicles; and (3) the process of cholesterol-enriched microvesicle shedding in these tumors not only occurs both *in vivo* and *in vitro*, but is continuous and, *in vitro*, rapid (within 3 h), highlighting the tumor's accelerated carbon flux through cholesterol synthesis anabolism.

Contemplating Coordinated Operation Between CTP/ *SLC25A1* and PMCT/*SLC13A5* for Citrate-Sustained Control of Glycolysis and Cholesterogenesis in Tumors

Management of the supply chain of such a critical anabolic fuel as cytosolic citrate must be flexible enough to compensate for its deficit, if biosynthetic demand for citrate's carbons outstrips availability. Due to a cancer cell's heterogenous stromal tissue environment *in vivo* [prostate cancer is a prime example—(Tolkach and Kristiansen, 2018)] and the fact that tumors derived from different tissues present varying metabolomic profiles, including highly varying glycolytic and mitochondrial respiratory rates, the cytosolic demand for biosynthetically employed citrate would be expected to vary.

The two well-known means of conveying citrate into the cytosolic pool are the mitochondrial citrate transporter CTP/*SLC25A1* and the more recently established plasma membrane Na^+-dependent citrate transporter PMCT/*SLC13A5*. Both membrane transporters are considered prime focal points for the development of cancer chemotherapeutic drug development (Catalina-Rodriguez et al., 2012; Huard et al., 2015; Mycielska et al., 2019). It is of significant interest to consider if and how both transporters might coordinate the steady-state level of cytosolic citrate, and thereby serve as cooperative means of adjusting the tumor's carbon flux through our proposed truncated Krebs/TCA cycle, accelerated cholesterogenesis, and the resulting enhanced glycolysis that together help characterize the Warburg effect profile.

Of the more than 50 mitochondrial membrane substrate/ion transporters of the SLC25 superfamily that have been identified and characterized to date (for reviews see: Kaplan, 2001; Palmieri and Monné, 2016), Kaplan's laboratory (Remani et al., 2008; Aluvila et al., 2010; Sun et al., 2010; Nie, 2017) has provided significantly detailed information on the structure, substrate transport mechanism and analysis of inhibition by BTC and other potential inhibitors of the citrate-malate CTP carrier, as well as on the PMCT membrane transporter. PMCT is the more recently characterized plasma membrane citrate transporter variant in humans and has garnered considerable attention since it serves as an additional (and, so far only) channel for the influx of citrate into the cytosol from the extracellular space (Mycielska et al., 2009). A potent synthetic dicarboxylate inhibitor of the PMCT has been described (Huard et al., 2015; Pajor et al., 2016), and surprisingly, gluconate, an abundant natural oxidation product of glucose, is a competitive irreversible inhibitor of the PMCT (Mycielska et al., 2019). The inhibition of both plasma membrane and mitochondrial citrate transporters in experimental hepatomas (by moieties the authors merely designated CTP_i and $PMCT_i$) was reported to dramatically inhibit lipogenesis, enhance apoptosis and induce cell cycle arrest (Poolsri et al., 2018). In studies comparing malignant (PC-3M) and benign epithelial prostate cells, as well as other tumor and normal cells, the proliferating cancers were consistently found to take up greater amounts of citrate than their normal counterparts via the PMCT (Mycielska et al., 2018). Significantly,

prostate tumor cells have been shown to possess enriched levels of cholesterol (Murtola et al., 2012).

CTP/*SLC25A1* and PMCT/*SLC13A5* comprise the only known membrane-partitioned, compartmentally separated supply routes for adjusting homeostatic levels of cytosolic citrate in humans. Despite obvious reprogramming of metabolism that establishes the tumor's deregulated cholesterogenesis which encourages its cell proliferation phenotype, and unlike the case with the CTP of hepatoma mitochondria documented previously in this review, we are not aware of studies that focus on correlating effects between the specific cholesterol level of tumor plasma membranes and the activity of the PMCT. Yet, sophisticated techniques are now available (Liu et al., 2017; Hu et al., 2019) that allow the positional sensing of cholesterol within micro domains of the plasma, or the exfoliated vesicle, membrane bilayer. Given a particular tumor's transformable metabolic adaptability, the cholesterol content of lipid rafts in the lateral bilayer membrane environment of the PMCT might modulate the passage of citrate into or extrusion from the tumor cell, and thereby exert a pleiotropic influence on the manner in which citrate is employed catabolically and anabolically in cancer.

SUMMARY

This review, a reminder of the prescience of the Warburg effect and its influence on half a century of molecular-level cancer research, has been designed to reignite awareness of the dominant and continuous metabolic carbon flux in tumors whose uncontrolled growth fundamentally depends upon two linearly linked metabolic patterns: (1) the ubiquitously observed loss-of-control of HMGR activity promoting an elevated cholesterol biosynthesis rate, the operation of which is mandatory for DNA synthesis and cell division, and fueled by cytosolic citrate; (2) preferential metabolic routes, involving critical participation of the mitochondrial CTP and, potentially, the plasma membrane PMCT, through which an augmented supply of cytosolic citrate is sustained. Herein, we have enlarged the scope of tumor cell metabolomics by considering not only the mitochondrial bioenergetic carbon flux patterns in tumors and their adherence to the Warburg effect, but by emphasizing the paramount role assumed by cytoplasmic citrate, we have delineated consequences for tumor cell proliferation when accelerated cholesterogenesis prevails. Thus:

1. The molecular basis for the absence or reduced control of citrate-fueled cholesterogenesis in tumors has been traced to a combination of defective feedback control elements and/or proteolytic degradation failures at the rate-controlling HMGR step of the synthetic pathway, in concert with a constitutively elevated expression of the HMGR enzyme. Our own research documented a 10-fold increase in the HMGR protein/cell in a rapidly proliferating heptoma, and a corresponding 9-fold increase in the rate of citrate-fueled cholesterol synthesis, compared with the normal liver system. Notwithstanding the cause, continuously escalated tumor cholesterogenesis requires a commensurately elevated and continuous supply of citrate as its fundamental biosynthetic substrate.
2. Membranes of tumor cell mitochondria, as well as their plasma membranes, have been long known to possess more cholesterol than those of their normal tissue counterparts. *In situ*, the extent of such cholesterol enrichment appears to correlate with the proliferative rate of the particular tumor and the heterogeneity of its tissue environment.
3. Mitochondria from an increasingly graded growth series of rat hepatomas display corresponding enrichment with cholesterol, with directly correlating increased rates of citrate export, and proportionate curtailment of pyruvate- or citrate-fueled O_2 consumption. Exogenous enrichment of normal liver mitochondria with titratable increased levels of cholesterol mimics this abnormal curtailment of early substrate Krebs/TCA cycle respiration in tumor mitochondria, proportional to the level of cholesterol enrichment. By blocking citrate export, the specific CTP inhibitor BTC completely reverses the decrease in pyruvate- and citrate-fueled respiration associated with aberrant membrane cholesterol enrichment. Yet, under either tumor or exogenously cholesterol-enriched-normal mitochondrial experimental conditions, fueling mitochondrial respiration-linked oxidative phosphorylation with substrates that enter the Krebs/TCA cycle beyond the aconitate hydratase step yields normal rates of O_2 consumption. Thus, mitochondrial membrane cholesterol enrichment occurring during the progression from normal-homeostatic to tumorigenic-cell proliferative states directly effects increased CTP activity and drives accelerated export of mitochondrial citrate into the cytosol (Section "Mitochondrial Metabolism Is Anomalous in Tumors," subsection "Cholesterol-Enriched, Isolated Hepatoma Mitochondria Preferentially Export Citrate").
4. These aberrant tumor respiratory patterns with isolated hepatoma mitochondria are replicated in *ex vivo* hepatoma tissue slice incubations fueled with pyruvate or citrate. Furthermore, following the preferential utilization of either substrate enabled the tracking of the carbon flow either through the tumor's deregulated cholesterogenesis pathway to cholesterol, or into the CO_2 end-product of normal tissue respiration. As with the isolated mitochondrial experiments, BTC reverses the pattern by preventing export of mitochondrially generated citrate to the cytosol, thus depriving the cholesterogenesis pathway of its precursor source of cytosolic acetyl-CoA (section "Mitochondrial Metabolism Is Anomalous in Tumors," subsection "Tracking Carbon Flux With Liver vs. Hepatoma Tissue *ex vivo*: What Happens to Pyruvate-Derived Citrate?"). Considered together, these results are congruent with our proposed "truncated" Krebs/TCA cycle (**Figure 7**) portraying an altered metabolomic carbon flux that, in concert with an enhanced glycolytic rate, and regardless of the tumor environment's O_2 level, satisfies the deduced mitochondrial dysfunction originally proposed by the Warburg effect.

5. The critical importance of supplying cytoplasmic citrate from mitochondria as prerequisite for cell cycle progression is well documented. We demonstrated that BTC, the classic CTP inhibitor, rapidly enters exponentially growing ascites lymphoma cell cultures and arrests DNA synthesis (**Figures 8**, **9**). BTC can transit the tumor cell's plasma membrane (apparently in both directions) with ease, and its inhibitory effect on CTP is both sensitively expressed and appears non-toxic, since the arrest of DNA synthesis and termination of cell replication is reversible upon BTC's removal from the culture. Addition of BTC starved the cytosol of mitochondrially exported citrate and inhibited DNA replication. However, without the presence of cytosolic components, isolated cell nuclei displayed unimpeded DNA replication even in the presence of BTC.
6. Together with the continuous accelerated citrate export from the hepatoma's cholesterol-enriched mitochondria, the loss of regulatory control at the HMGR locus of the cholesterogenesis pathway forecasts a potential accumulation of cholesterol, with consequential cholesterol enrichment of plasma membrane lipid rafts. Our exploratory studies with murine ascites hepatomas, *in vivo* and *in vitro*, revealed the rapid and continuous exfoliation of microvesicles, heavily enriched with cholesterol, from the tumor's plasma membranes into the cell-free ascites fluid. Addition of mevalonate to the ascites culture medium dramatically increased the cholesterol content of the already-cholesterol-enriched exfoliated microvesicles. It is clearly recognized that microvesicle shedding from tumor plasma membranes commensurate with deregulated cholesterogenesis has provocative implications regarding the role of these processes in cancer immunosurveillance.
7. Finally, speculations are raised about potential regulated coordination between the CTP and PMCT in tumors.

AUTHOR CONTRIBUTIONS

All original research documented in this review was performed in the laboratory of PSC by research associates accredited in the references herein, in the Laboratory of Biochemistry, Department of Biology, New York University. RAP and many others performed the research. PSC and RAP contributed equally to the writing of this review, and both approved the submitted version.

FUNDING

Research from the laboratory of PSC referred to in this review was supported by USPHS grant CA28677.

ACKNOWLEDGMENTS

The authors regret that, inadvertently, they have no doubt omitted reference to many outstanding research studies concerning the Warburg effect and the metabolism of tumors relevant to the theme of this review, and would be grateful if such omissions would be brought to their attention. The authros are indebted to their cherished colleagues and longtime friends who, with them, participated in various aspects of the research presented in this review, including (but not limited to): Ronald Kaplan, Arnold Weg, Beverly Lavietes, Neal Azrolan, Alan Posner, Patricia Puma, Laura Sepp-Lorenzino, and Srinivasa Rao.

REFERENCES

Abdel-Haleem, A. M., Lewis, N. E., Jamshidi, N., Mineta, K., Gao, X., and Gojobori, T. (2017). The emerging facets of non-cancerous warburg effect. *Front. Endocrinol.* 8:279. doi: 10.3389/fendo.2017.00279

Aisenberg, A. C. (1961). Studies on normal and neoplastic mitochondria. *I. Respirat. Cancer Res.* 21, 295–303.

Aluvila, S., Kotaria, R., Sun, J., Mayor, J. A., Walters, D. E., Harrison, D. H., et al. (2010). The yeast mitochondrial citrate transport protein: molecular determinants of its substrate specificity. *JBC* 285, 27314–27326 doi: 10.1074/jbc.M110.137364

Azrolan, N. I., and Coleman, P. S. (1989). A discoordinate increase in the cellular amount of 3-hydroxy-3-methylglutaryl-CoA reductase results in the loss of rate-limiting control over cholesterogenesis in a tumour cell- free system. *Biochem. J.* 258, 421–425. doi: 10.1042/bj2580421

Bao, J., Zhu, L., Zhu, Q., Su, J., Liu, M., and Huang, W. (2016). SREBP-1 is an independent prognostic marker and promotes invasion and migration in breast cancer. *Oncol. Lett.* 12, 2409–2416. doi: 10.3892/ol.2016.4988

Baulies, A., Montero, J., Matías, N., Insausti, N., Terrones, O., Basañez, G., et al. (2018). The 2-oxoglutarate carrier promotes liver cancer by sustaining mitochondrial GSH despite cholesterol loading. *Redox Biol.* 14, 164–177. doi: 10.1016/j.redox.2017.08.022

Bender, T., and Martinou, J. C. (2016). The mitochondrial pyruvate carrier in health and disease: to carry or not to carry? *Biochimica et Biophysica Acta* 1863, 2436–2442. doi: 10.1016/j.bbamcr.2016.01.017

Bloch, K. (1965). The biological synthesis of cholesterol. *Science* 150(3692), 19–28. doi: 10.1126/science.150.3692.19

Brown, M. S., and Goldstein, J. L. (1980). Multivalent feedback regulation of HMG CoA reductase, a control mechanism coordinating isoprenoid synthesis and cell growth. *J. Lipid Res.* 21, 505–517.

Cairns, R. A., Harris, I. S., and Mak, T. W. (2011). Regulation of cancer cell metabolism. *Nat. Rev. Cancer* 11, 85–95. doi: 10.1038/nrc2981

Camara, A., Zhou, Y., Wen, P. C., Tajkhorshid, E., and Kwok, W. M. (2017). Mitochondrial VDAC1: a key gatekeeper as potential therapeutic target. *Front. Physiol.* 8:460. doi: 10.3389/fphys.2017.00460

Campbell, A. M., and Chan, S. H. (2008). Mitochondrial membrane cholesterol, the voltage dependent anion channel (VDAC), and the warburg effect. *J. Bioenerget. Biomembranes* 40, 193–197. doi: 10.1007/s10863-008-9138-x

Carter, H., Chen, S., Isik, L., Tyekucheva, S., Velculescu, V. E., Kinzler, K. W., et al. (2009). Cancer-specific high- throughput annotation of somatic mutations: computational prediction of driver missense mutations. *Cancer Res.* 69, 6660–6667. doi: 10.1158/0008-5472.CAN-09-1133

Casey, P. J. (1992). Biochemistry of protein prenylation. *J. Lipid. Res.* 33, 1731–1740.

Casey, P. J. (1995). Protein lipidation in cell signaling. *Science* 268, 221–225. doi: 10.1126/science.7716512

Cassim, S., Vučetić, M., Ždralević, M., and Pouyssegur, J. (2020). Warburg and beyond: the power of mitochondrial metabolism to collaborate or replace fermentative glycolysis in cancer. *Cancers* 12, 1119–1140. doi: 10.3390/cancers12051119

Catalina-Rodriguez, O., Kolukula, V. K., Tomita, Y., Preet, A., Palmieri, F., Wellstein, A., et al. (2012). The mitochondrial citrate transporter, CIC, is essential for mitochondrial homeostasis. *Oncotarget* 3, 1220–1235. doi: 10.18632/oncotarget.714

Chan, S. H., and Barbour, R. L. (1983). Adenine nucleotide transport in hepatoma mitochondria. characterization of factors influencing the kinetics of ADP and ATP uptake. *Biochim. et Biophys. Acta* 723, 104–113

Chaouch, A., Porcelli, V., Cox, D., Edvardson, S., Scarcia, P., De Grassi, A., et al. (2014). Mutations in the mitochondrial citrate carrier SLC25A1 are associated with impaired neuromuscular transmission. *J. Neuromuscular Dis.* 1, 75–90. doi: 10.3233/JND-140021

Chen, H. W., Kandutsch, A. A., and Heiniger, H. J. (1978). "The role of cholesterol in malignancy," in *Membrane Anomalies of Tumor Cells. Prog Tumor Res*. ed. D. F. Wallach (Boston, MA: Basel, Karger Press), 22, 275–316. doi: 10.1159/000401203

Chen, H. W., Heiniger, H. J., and Kandutsch, A. A. (1975). Relationship between sterol synthesis and DNA synthesis in phytohemagglutinin- stimulated mouse lymphocytes. *PNAS (USA)* 72, 1950–1954. doi: 10.1073/pnas.72.5.1950

Cluntun, A. A., Lukey, M. J., Cerione, R. A., and Locasale, J. W. (2017). Glutamine metabolism in cancer: understanding the heterogeneity. *Trends Cancer* 3, 169–180. doi: 10.1016/j.trecan.2017.01.005

Colell, A., García-Ruiz, C., Lluis, J. M., Coll, O., Mari, M., and Fernández- Checa, J. C. (2003). Cholesterol impairs the adenine nucleotide translocator-mediated mitochondrial permeability transition through altered membrane fluidity. *JBC* 2278, 33928–33935. doi: 10.1016/j.redox.2019.101214

Coleman, P. S., Chen, L. C., and Sepp-Lorenzino, L. (1997). Cholesterol metabolism and tumor cell proliferation. *Subcell. Biochem.* 28, 363–435. doi: 10.1007/978-1-4615-5901-6_13

Coleman, P. S., Ewell, A. J., and Good, R. A. (1978a). Retention of susceptibility to mitogens after direct dansylation of viable human lymphocytes. *PNAS (USA)* 75, 3766–3770. doi: 10.1073/pnas.75.8.3766

Coleman, P. S., Lavietes B., Born, R., and Weg, A. (1978b). Cholesterol enrichment of normal mitochondria *in vitro*: – A model system with properties of hepatoma mitochondria. *BBRC* 84, 202–207. doi: 10.1016/0006-291X90282-6

Coleman, P. S., and Lavietes, B. B. (1981). Membrane cholesterol, tumorigenesis, and the biochemical phenotype of neoplasia. *CRC Crit. Rev. Biochem.* 11, 341–393. doi: 10.1080/10409238109104421

Coleman, P. S., and Sepp-Lorenzino, L., (1990). "The role of the cholesterol synthesis pathway during tumor cell proliferation," in *Adv. Cholesterol Res*. eds M. Esfahani and J. Swaney (New Jersey, NJ: Telford Press), 201–270.

Colombini, M. (2004). VDAC: the channel at the interface between mitochondria and the cytosol. *Mol. Cell Biochem.* 256-257, 107–115. doi: 10.1023/b:mcbi.0000009862.17396.8d

Cox, D. L., and Nelson, M. M. (2005). *Lehninger Principles of Biochemistry*. New York, NY: W.H. Freeman

Crabtree, H. G. (1929). Observations on the carbohydrate metabolism of tumors. *Biochem. J.* 23, 536–545. doi: 10.1042/bj0230536

Crain, R. C., Clark, R. W., and Harvey, B. E. (1983). Role of lipid transfer proteins in the abnormal lipid content of Morris hepatoma mitochondria and microsomes. *Cancer Res.* 43, 3197–3202.

Cui, J., Shi, M., Xie, D., Wei, D., Jia, Z., Zheng, S., et al. (2014). FOXM1 promotes the warburg effect and pancreatic cancer progression via transactivation of LDHA expression. *Clin. Cancer Res.* 20, 2595–2606. doi: 10.1158/1078-0432.CCR-13-2407

DeBerardinis, R. J., and Chandel, N. S. (2016). Fundamentals of cancer metabolism. *Sci. Adv.* 2, 1–18. doi: 10.1126/sciadv.1600200

DeBerardinis, R. J., Mancuso, A., Daikhin, E., Nissim, I., Yudkoff, M., Wehrli, S., et al. (2007). Beyond aerobic glycolysis: transformed cells can engage in glutamine metabolism that exceeds the requirement for protein and nucleotide synthesis. *PNAS (USA)* 104, 19345–19350. doi: 10.1073/pnas.0709747104

Demel, R. A., and De Kruyff, B. (1976). The function of sterols in membranes. *Biochim. Biophys. Acta* 457, 109–132. doi: 10.1016/0304-4157900 8-3

Dietzen, D. J., and Davis, E. J. (1993). Oxidation of pyruvate, malate, citrate, and cytosolic reducing equivalents by AS-30D hepatoma mitochondria. *Arch. Biochem. Biophys.* 305, 91–102. doi: 10.1006/abbi.1993.1397

Dietzen, D. J., and Davis, E. J. (1994). Excess membrane cholesterol is not responsible for metabolic and bioenergetic changes in AS-30D hepatoma mitochondria. *Arch. Biochem. Biophys.* 309, 341–347. doi: 10.1006/abbi.1994.1122

Doyle, J. W., and Kandutsch, A. A. (1988). Requirement for mevalonate in cycling cells: quantitative and temporal aspects. *J. Cell. Physiol.* 137, 133–140. doi: 10.1002/jcp.1041370116

Elstrom, R. L., Bauer, D. E., Buzzai, M., Karnauskas, R., Harris, M. H., Plas, D. R., et al. (2004). Akt stimulates aerobic glycolysis in cancer cells. *Cancer Res.* 64, 3892–3899. doi: 10.1158/0008-5472.CAN-03-2904

Elustondo, P., Martin, L. A., and Kaarten, B. (2017). Mitochondrial cholesterol import. *Biochim. Biophys. Acta. Mol. Cell Biol. Lipids* 1862, 90–101 doi: 10.1016/j.bbalip.2016.08.012

Epand, R. M. (2006). Cholesterol and the interaction of proteins with membrane domains. *Prog. Lipid Res.* 45, 279–294. doi: 10.1016/j.plipres.2006.02.001

Erickson, J. W., and Cerione, R. A. (2010). Glutaminase: a hot spot for regulation of cancer cell metabolism? *Oncotarget* 1, 734–740. doi: 10.18632/oncotarget.208

Erickson, S. K., Cooper, A. D., Barnard, G. F., Havel, C. M., Watson, J. A., Feingold, K. R. Moser, M. H. F., et al. (1988). Regulation of cholesterol metabolism in a slow-growing hepatoma *in vivo*. *Biochim. et Biophys. Acta.* 960, 131–138. doi: 10.1016/0005-276090058-6

Fairbanks, K. P., Witte, L. D., and Goodman, D. S. (1984). Relationship between mevalonate and mitogenesis in human fibroblasts stimulated with platelet-derived growth factor. *JBC* 259, 1546–1551.

Faubert, B., Solmonson, A., and DeBerardinis, R. J. (2020). Metabolic reprogramming and cancer progression. *Science* 368, 1–22. doi: 10.1126/science.aaw5473

Feo, F., Canuto, R. A., Garcea, R., and Gabriel, L. (1975). Effect of cholesterol content on some physical and functional properties of mitochondria isolated from adult rat liver, fetal liver, cholesterol- enriched liver and hepatomas AH-130, 3924A and 5123. *Biochimica et Biophysica Acta* 413, 116–134. doi: 10.1016/0005-273690063-2

Flis, V. V., and Daum, G. (2013). Lipid transport between the endoplasmic reticulum and mitochondria. *Cold Spring Harb. Perspect. Biol.* 5:a013235. doi: 10.1101/cshperspect.a013235

Fonsato, V., Collino, F., Herrera, M. B., Cavallari, C., Deregibus, M. C., Cisterna, B., et al. (2012). Human liver stem cell-derived microvesicles inhibit hepatoma growth in SCID mice by delivering antitumor microRNAs. *Stem Cells* 30, 1985–1998. doi: 10.1002/stem.1161

Frigerio, F., Casimir, M., Carobbio, S., and Maechler, P. (2008). Tissue specificity of mitochondrial glutamate pathways and the control of metabolic homeostasis. *Biochim. Biophys. Acta* 1777, 965–972. doi: 10.1016/j.bbabio.2008.04.031

Fruman, D. A., and Rommel, C. (2014). PI3K and cancer: lessons, challenges and opportunities. *Nat. Rev. Drug Discov.* 13, 140–156. doi: 10.1038/nrd4204

Gnoni, G. V., Priore, P., Geelen, M. J., and Siculella, L. (2009). The mitochondrial citrate carrier: metabolic role and regulation of its activity and expression. *IUBMB Life* 61, 987–994. doi: 10.1002/iub.249

Goldstein, J. L., and Brown, M. S. (1990). Regulation of the mevalonate pathway. *Nature* 343, 425–430. doi: 10.1038/343425a0

Goldstein, J. L., DeBose-Boyd, R. A., and Brown M. S. (2006). Protein sensors for membrane sterols. *Cell* 124, 35–46. doi: 10.1016/j.cell.2005.12.022

Grohsman, J., and Nowotny, A. (1972). The immune recognition of TA3 tumors, its facilitation by endotoxin, and abrogation by ascites fluid. *J. Immunol.* 109, 1090–1095.

Hanahan, D., and Weinberg, R. A. (2011). Hallmarks of cancer: the next generation. *Cell* 144, 646–674. doi: 10.1016/j.cell.2011.02.013

Hanse, E. A., Ruan, C., Kachman, M., Wang, D., Lowman, X. H., and Kelekar, A. (2017). Cytosolic malate dehydrogenase activity helps support glycolysis in actively proliferating cells and cancer. *Oncogene* 36, 3915–3924. doi: 10.1038/onc.2017.36

Heiniger, H. J. (1981). Cholesterol and its biosynthesis in normal and malignant. *Cancer Res.* 41(9 Pt 2), 3792–3794.

Hensley, C. T., Wasti, A. T., and DeBerardinis, R. J. (2013). Glutamine and cancer: cell biology, physiology, and clinical opportunities. The Journal of Clinical Investigation 123, 3678–3684.

Hiller, S., Abramson, J., Mannella, C., Wagner, G., and Zeth, K. (2010). The 3D structures of VDAC represent a native conformation. *Trends Biochem. Sci.* 35, 514–521. doi: 10.1016/j.tibs.2010.03.005

Holleran, A. L., Fiskum, G., and Kelleher, J. K. (1997). Quantitative analysis of acetoacetate metabolism in AS-30D hepatoma cells with 13C and 14C isotopic techniques. *Am. J. Physiol.* 272(6 Pt 1), E945-E951. doi: 10.1152/ajpendo.1997.272.6.E945

Horvath, S. E., and Daum, G. (2013). Lipids of mitochondria. *Prog. Lipid Res.* 52, 590–614. doi: 10.1016/j.plipres.2013.07.002

Hu, F., Shi, L., and Min, W. (2019). Biological imaging of chemical bonds by stimulated raman scattering microscopy. *Nat. Methods* 16, 830–842. doi: 10.1038/s41592-019-0538-0

Huard, K., Brown, J., Jones, J. C., Cabral, S., Futatsugi, K., Gorgoglione, M., et al. (2015). Discovery and characterization of novel inhibitors of the sodium-coupled citrate transporter (NaCT or SLC13A5). *Sci. Rep.* 5:17391. doi: 10.1038/srep17391

Hulce, J. J., Cognetta, A. B., Niphakis, M. J., Tully, S. E., and Cravatt, B. F. (2013). Proteome-wide mapping of cholesterol-interacting proteins in mammalian cells. *Nat. Methods* 10, 259–264 .doi: 10.1038/nmeth.2368

Iacobazzi, V., and Infantino, V. (2014). Citrate–new functions for an old metabolite. *Biol. Chem.* 395, 387–399. doi: 10.1515/hsz-2013-0271

Icard, P., Poulain, L., and Lincet, H. (2012). Understanding the central role of citrate in the metabolism of cancer cells. *Biochimica et Biophysica Acta* 1825, 111–116. doi: 10.1016/j.bbcan.2011.10.007

Jiang, L., Boufersaoui, A., Yang, C., Ko, B., Rakheja, D., Guevara, G., et al. (2017). Quantitative metabolic flux analysis reveals an unconventional pathway of fatty acid synthesis in cancer cells deficient for the mitochondrial citrate transport protein. *Metab. Eng.* 43(Pt B), 198–207. doi: 10.1016/j.ymben.2016.11.004

Johnson, B. M., and DeBose-Boyd, R. A. (2018). Underlying mechanisms for sterol-induced ubiquitination and ER-associated degradation of HMG CoA reductase. *Sem. Cell Dev. Biol.* 81, 121–128. doi: 10.1016/j.semcdb.2017.10.019

Kaplan, R. S., Morris, H. P., and Coleman, P. S. (1982). Kinetic characteristics of citrate influx and efflux with mitochondria from morris hepatomas 3924A and 16. *Cancer Res.* 42, 4399–4407.

Kaplan, R. S., Parlo, R. A., and Coleman, P. S. (1986). Measurement of citrate transport in tumor mitochondria. *Methods Enzymol.* 125, 671–691. doi: 10.1016/s0076-687925055-7

Kaplan R. S. (2001). Structure and function of mitochondrial anion transport proteins. *J. Membr. Biol.* 179, 165–183. doi: 10.1007/s002320010046

Kato, T., Fahrmann, J. F., Hanash, S. M., and Vykoukal, J. (2020). Extracellular vesicles mediate B cell immune response and are a potential target for cancer therapy. *Cells* 9:1518. doi: 10.3390/cells9061518

Kennedy, B. E., Madreiter, C. T., Vishnu, N., Malli, R., Graier, W. F., and Karten, B. (2014). Adaptations of energy metabolism associated with increased levels of mitochondrial cholesterol in Niemann-Pick type C1- deficient cells. *J. Biol. Chem.* 289, 16278–16289. doi: 10.1074/jbc.M114.559914

Khatibzadeh, N., Spector, A. A., Brownell, W. E., and Anvari, B. (2013).] Effects of plasma membrane cholesterol level and cytoskeleton F-actin on cell protrusion mechanics. *PLoS ONE* 8:e57147. doi: 10.1371/journal.pone.0057147

Kolukula, V. K., Sahu, G., Wellstein, A., Rodriguez, O. C., Preet, A., Iacobazzi, V., et al. (2014). SLC25A1, or CIC, is a novel transcriptional target of mutant p53 and a negative tumor prognostic marker. *Oncotarget* 5, 1212–1225. doi: 10.18632/oncotarget.1831

Koppenol, W. H., Bounds, P. L., and Dang, C. V. (2011). Otto Warburg's contributions to current concepts of cancer metabolism. *Nat. Rev. Cancer* 11, 325–337. doi: 10.1038/nrc3038

Langan, T. J., and Volpe, J. J. (1987). Cell cycle-specific requirement for mevalonate, but not for cholesterol, for DNA synthesis in glial primary cultures. *J. Neurochem.* 49, 513–521. doi: 10.1111/j.1471-4159.1987.tb02894.x

LaNoue, K. F., and Schoolwerth, A. C. (1979). Metabolite transport in mitochondria. *Annu. Rev. Biochem.* 48, 871–922. doi: 10.1146/annurev.bi.48.070179.004255

Litvinov, D. Y., Savushkin, E. V., and Dergunov, A. D. (2018). Intracellular and plasma membrane events in cholesterol transport and homeostasis. *J. Lipids* 2018:3965054. doi: 10.1155/2018/3965054

Liu, J., Rone, M. B., and Papadopoulos, V. (2006). Protein-protein interactions mediate mitochondrial cholesterol transport and steroid biosynthesis. *JBC* 281, 38879–38893.

Liu, S. L., Sheng, R., Jung, J. H., Wang, L., Stec, E., O'Connor, M. J., et al. (2017). Orthogonal lipid sensors identify transbilayer asymmetry of plasma membrane cholesterol. *Nat. Chem. Biol.* 13, 268–274. doi: 10.1038/nchembio.2268

Lu, J., Tan, M., and Cai, Q. (2015). The Warburg effect in tumor progression: mitochondrial oxidative metabolism as an anti-metastasis mechanism. *Cancer Lett.* 356(2 Pt A), 156–164. doi: 10.1016/j.canlet.2014.04.001

Luke, J. C., and Kaplan, J. I. (1979). Theoretical shapes of bilipid vesicles under conditions of increasing membrane area. *Biophys. J.* 25, 107–111. doi: 10.1016/s0006-349585280-7

Maltese, W. A., and Sheridan, K. M. (1985). Differentiation of neuroblastoma cells induced by an inhibitor of mevalonate synthesis: relation of neurite outgrowth and acetylcholinesterase activity to changes in cell proliferation and blocked isoprenoid synthesis. *J. Cell. Physiol.* 125, 540–558. doi: 10.1002/jcp.1041250326

Manna, P. R., Ahmed, A. U., Vartak, D., Molehin, D., and Pruitt, K. (2019). Overexpression of the steroidogenic acute regulatory protein in breast cancer: regulation by histone deacetylase inhibition. *Biochem. Biophys. Res. Commun.* 509, 476–482. doi: 10.1016/j.bbrc.2018.12.145

Marquardt, D., Kučerka, N., Wassall, S. R., Harroun, T. A., and Katsaras, J. (2016). Cholesterol's location in lipid bilayers. *Chem. Phys. Lipids* 199, 17–25. doi: 10.1016/j.chemphyslip.2016.04.001

Martin, L. A., Kennedy, B. E., and Karten, B. (2016). Mitochondrial cholesterol: mechanisms of import and effects on mitochondrial function. *J. Bioenerget. Biomembranes* 48, 137–151. doi: 10.1007/s10863-014-9592-6

Matés, J. M., Campos-Sandoval, J. A., Santos-Jiménez, J. L., and Márquez, J. (2019). Dysregulation of glutaminase and glutamine synthetase in cancer. *Cancer Lett.* 467, 29–39. doi: 10.1016/j.canlet.2019.09.011

Mishra, D., and Banerjee, D. (2019). Lactate dehydrogenases as metabolic links between tumor and stroma in the tumor microenvironment. *Cancers* 11:750. doi: 10.3390/cancers11060750

Mollinedo, F., Fernández, M., Hornillos, V., Delgado, J., Amat-Guerri, F., Acuña, A. U., et al. (2011). Involvement of lipid rafts in the localization and dysfunction effect of the antitumor ether phospholipid edelfosine in mitochondria. *Cell Death Dis.* 2, 1–9. doi: 10.1038/cddis.2011.41

Mondal, M., Mesmin, B., Mukherjee, S., and Maxfield, F. R. (2009). Sterols are mainly in the cytoplasmic leaflet of the plasma membrane and the endocytic recycling compartment in CHO cells. *Mol. Biol. Cell* 20, 581–588. doi: 10.1091/mbc.e08-07-0785

Mountford, C. E., Wright, L. C., Holmes, K. T., Mackinnon, W. B., Gregory, P., and Fox, R. M. (1984). High-resolution proton nuclear magnetic resonance analysis of metastatic cancer cells. *Science* 226, 1415–1418. doi: 10.1126/science.6505699

Mullen, A. R., Hu, Z., Shi, X., Jiang, L., Boroughs, L. K., Kovacs, Z., et al. (2014). Oxidation of alpha-ketoglutarate is required for reductive carboxylation in cancer cells with mitochondrial defects. *Cell Rep.* 7, 1679–1690. doi: 10.1016/j.celrep.2014.04.037

Murtola, T. J., Syvälä, H., Pennanen, P., Bläuer, M., Solakivi, T., Ylikomi, T., et al. (2012). The importance of LDL and cholesterol metabolism for prostate epithelial cell growth. *PLoS ONE* 7:e39445. doi: 10.1371/journal.pone.0039445

Mycielska, M. E., Mohr, M., Schmidt, K., Drexler, K., Rümmele, P., Haferkamp, S., et al. (2019). Potential use of gluconate in cancer therapy. *Front. Oncol.* 9:522. doi: 10.3389/fonc.2019.00522

Mycielska, M. E., Patel, A., Rizaner, N., Mazurek, M. P., Keun, H., Patel, A., et al. (2009). Citrate transport and metabolism in mammalian cells: prostate epithelial cells and prostate cancer. *BioEssays* 31, 10–20. doi: 10.1002/bies.080137

Mycielska, M. E., Dettmer, K., Rümmele, P., Schmidt, K., Prehn, C., Milenkovic, V. M., et al. (2018).Extracellular citrate affects critical elements of cancer cell metabolism and supports cancer development *in vivo*. *Cancer Res.* 78, 2513–2523. doi: 10.1158/0008-5472.CAN-17-2959

Nie, R., Stark, S., Symersky, J., Kaplan, R. S., and Lu, M. (2017). Structure and function of the divalent anion/Na^+ symporter from *Vibrio cholerae* and a humanized variant. *Nat. Commun.* 8:15009. doi: 10.1038/ncomms15009

Otto, A. M. (2016). Warburg effect(s)-A biographical sketch of Otto Warburg and his impacts on tumor metabolism. *Cancer Metab.* 4:5. doi: 10.1186/s40170-016-0145-9

Pajor, A. M., de Oliveira, C. A., Song, K., Huard, K., Shanmugasundaram, V., and Erion, D. M. (2016). Molecular basis for inhibition of the Na+/Citrate

transporter NaCT (SLC13A5) by Dicarboxylate inhibitors. *Mol. Pharmacol.* 90, 755–765. doi: 10.1124/mol.116.105049

Palmieiri, F., Stipani, I., Quagliariello, E., and Klingenberg, M. (1972). Kinetic study of the tricarboxylate carrier in rat liver mitochondria. *Eur. J. Biochem.* 26, 587–594. doi: 10.1111/j.1432-1033.1972.tb01801.x

Palmieri, F., and Monné, M. (2016). Discoveries, metabolic roles and diseases of mitochondrial carriers: a review. *Biochimica et Biophysica Acta* 1863, 2362–2378. doi: 10.1016/j.bbamcr.2016.03.007

Palmieri, F. (2013). The mitochondrial transporter family SLC25: identification, properties and physiopathology. *Mol. Asp. Med.* 34, 465–484. doi: 10.1016/j.mam.2012.05.005

Parlo, R. A., and Coleman, P. S. (1986). Continuous pyruvate carbon flux to newly synthesized cholesterol and the suppressed evolution of pyruvate-generated CO2 in tumors: further evidence for a persistent truncated Krebs cycle in hepatomas. *Biochim. et Biophys. Acta* 886, 169–176. doi: 10.1016/0167-488990134-5

Parlo, R. A., and Coleman, PS. (1984). Enhanced rate of citrate export from cholesterol-rich hepatoma mitochondria. the truncated Krebs cycle and other metabolic ramifications of mitochondrial membrane cholesterol. *J. Biol. Chem.* 259, 9997–10003.

Pascale, R. M., Calvisi, D. F., Simile, M. M., Feo, C. F., and Feo, F. (2020). The Warburg effect 97 years after its discovery. *Cancers* 12, 2819–2851. doi: 10.3390/cancers12102819

Pfrieger, F. W., and Vitale, N. (2018). Cholesterol and the journey of extracellular vesicles. *J. Lipid Res.* 59, 2255–2261. doi: 10.1194/jlr.R084210

Pike, L. J. (2003). Lipid rafts: bringing order to chaos. *J. Lipid Res.* 44, 655–667. doi: 10.1194/jlr.R200021-JLR200

Poolsri, W. A., Phokrai, P., Suwankulanan, S., Phakdeeto, N., Phunsomboon, P., Pekthong, D., et al. (2018). Combination of mitochondrial and plasma membrane citrate transporter inhibitors inhibits *de novo* lipogenesis pathway and triggers apoptosis in hepatocellular carcinoma cells. *BioMed. Res. Int.* 2018:3683026. doi: 10.1155/2018/3683026

Porstmann, T., Griffiths, B., Chung, Y. L., Delpuech, O., Griffiths, J. R., Downward, J., et al. (2005). PKB/Akt induces transcription of enzymes involved in cholesterol and fatty acid biosynthesis via activation of SREBP. *Oncogene* 24, 6465–6481. doi: 10.1038/sj.onc.1208802

Potter, M., Newport, E., and Morten, K. J. (2016). The Warburg effect: 80 years on. *Biochem. Soc. Trans.* 44, 1499–1505. doi: 10.1042/BST20160094

Puma, P. (1982). *Vesicle Exfoliation from the Plasma Membrane of an Ascites Hepatoma*. thesis, Ph.D. dissertation/doctoral. New York University: New York, NY.

Quesney-Huneeus, V., Galick, H. A. Siperstein, M. D., Erickson, S. K., Spencer, T. A., and Nelson, J. A. (1983). The dual role of mevalonate in the cell cycle. *JBC* 258, 378–385.

Rahman, M. M., and Kipreos, E. T. (2010). The specific roles of mitotic cyclins revealed. *Cell Cycle* 9, 22–23. doi: 10.4161/cc.9.1.10577

Rao, S., and Coleman, P. S. (1989). Control of DNA replication and cell growth by inhibiting the export of mitochondrially derived citrate. *Exp. Cell. Res.* 180, 341–352. doi: 10.1016/0014-482790062-1

Raposo, G., and Stoorvogel, W. (2013). Extracellular vesicles: exosomes, microvesicles, and friends. *J. Cell Biol.* 200, 373–383. doi: 10.1083/jcb.201211138

Rauckhorst, A. J., and Taylor, E. B. (2016). Mitochondrial pyruvate carrier function and cancer metabolism. *Curr. Opin. Genet. Dev.* 38, 102–109. doi: 10.1016/j.gde.2016.05.003

Raz, A., Goldman, R., Yuli, I., and Inbar, M. (1978). Isolation of plasma membrane fragments and vesicles from ascites fluid of lymphoma- bearing mice and their possible role in the escape mechanism of tumors from host immune rejection. *Cancer Immunol. Immunother* 4, 53–59. doi: 10.1007/BF00205571

Record, M., Carayon, K., Poirot, M., and Silvente-Poirot, S. (2014). Exosomes as new vesicular lipid transporters involved in cell-cell communication and various pathophysiologies. *Biochim. Biophys. Acta* 1841, 108–120. doi: 10.1016/j.bbalip.2013.10.004

Reitzer, L. J., Wice, B. M., and Kennell, D. (1979). Evidence that glutamine, not sugar, is the major energy source for cultured HeLa cells. *J. Biol. Chem.* 254, 2669–2676.

Remani, S., Sun, J., Kotaria, R., Mayor, J. A., Brownlee, J. M., Harrison, D. H., et al. (2008). The yeast mitochondrial citrate transport protein: identification of the Lysine residues responsible for inhibition mediated by Pyridoxal 5'- phosphate. *J. Bioenerg. Biomembr.* 40, 577–585. doi: 10.1007/s10863-008-9187-1w

Repko, E. M., and Maltese, W. A. (1989). Post-translational isoprenylation of cellular proteins is altered in response to mevalonate availability. *JBC* 264, 9945–9952.

Ribas, V., García-Ruiz, C., and Fernández-Checa, J. C. (2016). Mitochondria, cholesterol and cancer cell metabolism. *Clin. Transl. Med.* 5:22. doi: 10.1186/s40169-016-0106-5

Rostovtseva, T. K., and Bezrukov, S. M. (2008). VDAC regulation: role of cytosolic proteins and mitochondrial lipids. *J. Bioenerget. Biomembr.* 40, 163–170. doi: 10.1007/s10863-008-9145-y

Sánchez-Martín, C. C., Dávalos, A., Martín-Sánchez, C., de la Peña, G., Fernández-Hernando, C., and Lasunción, M. A. (2007). Cholesterol starvation induces differentiation of human leukemia HL-60 cells. *Cancer Res.* 67, 3379–3386. doi: 10.1158/0008-5472.CAN-06-4093?

Schneider, H., Höchli, M., and Hackenbrock, C. R. (1982). Relationship between the density distribution of intramembrane particles and electron transfer in the mitochondrial inner membrane as revealed by cholesterol incorporation. *J. Cell Biol.* 94, 387–393. doi: 10.1083/jcb.94.2.387

Schroeder, F., Huang, H., McIntosh, A. L., Atshaves, B. P., Martin, G. G., and Kier, A. B. (2010). Caveolin, sterol carrier protein-2, membrane cholesterol-rich microdomains and intracellular cholesterol trafficking. *Sub-Cellular Biochem.* 51, 279–318. doi: 10.1007/978-90-481-8622-8_10

Sebti, S. M. (2005). Protein farnesylation: implications for normal physiology, malignant transformation, and cancer therapy. *Cancer Cell* 7, 297–300. doi: 10.1016/j.ccr.2005.04.005

Senyilmaz, D., and Teleman, A. A. (2015). Chicken or the egg: warburg effect and mitochondrial dysfunction. *F1000Prime Reports* 7:41. doi: 10.12703/P7-41

Sepp-Lorenzino, L., Rao, S., and Coleman, P. S. (1991). Cell-cycle dependent, differential prenylation of proteins. *Eur. J. Biochem.* 200, 579–590. doi: 10.1111/j.1432-1033.1991.tb16221.x

Sepp-Lorenzino, L., and Rosen, N. (1998). A farnesyl-protein transferase inhibitor induces p21 expression and G1 block in p53 wild type tumor cells. *JBC* 273, 20243–20251. doi: 10.1074/jbc.273.32.20243

Seyfried, T. N. (2015). Cancer as a mitochondrial metabolic disease. *Front. Cell Dev. Biol.* 3:43. doi: 10.3389/fcell.2015.00043

Shoshan-Barmatz, V., Ben-Hail, D., Admoni, L., Krelin, Y., and Tripathi, S. S. (2015). The mitochondrial voltage-dependent anion channel 1 in tumor cells. *Biochim. Biophys. Acta* 1848(10 Pt B), 2547–2575. doi: 10.3389/fonc.2017.00060

Sinensky, M., and Logel, J. (1985). Defective macromolecule biosynthesis and cell-cycle progression in a mammalian cell starved for mevalonate. *PNAS (USA)* 82, 3257–3261. doi: 10.1073/pnas.82.10.3257

Singh, P., Saxena, R., Srinivas, G., Pande, G., and Chattopadhyay, A. (2013). Cholesterol biosynthesis and homeostasis in regulation of the cell cycle. *PLoS One* 8:e58833. doi: 10.1371/journal.pone.0058833

Siperstein, M. D., and Fagan, V. M. (1964). Deletion of the cholesterol- negative feedback system in liver tumors. *Cancer Res.* 24, 1108–1115.

Siperstein, M. D. (1984). Role of cholesterogenesis and isoprenoid synthesis in DNA replication and cell growth. *J. Lipid Res.* 25, 1462–1468.

Sola, M. M., Oliver, F. J., Salto, R., Gutiérrez, M., and Vargas, A. (1994). Citrate inhibition of rat-kidney cortex phosphofructokinase. *Mol. Cell. Biochem.* 135, 123–128. doi: 10.1007/BF00926514

Solsona-Vilarrasa, E., Fucho, R., Torres, S., Nuñez, S., Nuño-Lámbarri, N., Enrich, C., et al. (2019). Cholesterol enrichment in liver mitochondria impairs oxidative phosphorylation and disrupts the assembly of respiratory supercomplexes. *Redox Biol.* 24, 1–13. doi: 10.1016/j.redox.2019.101214

Sun, J., Aluvila, S., Kotaria, R., Mayor, J. A., Walters, D. E., and Kaplan, R. S. (2010). Mitochondrial and plasma membrane citrate transporters: discovery of selective inhibitors and application to structure/function analysis. *Mol. Cell. Pharmacol.* 2, 101–110.

Tait, S. W., and Green, D. R. (2012). Mitochondria and cell signalling. *J. Cell Sci.* 125(Pt 4), 807–815. doi: 10.1242/jcs.099234

Tamanoi, F., Kato-Stankiewicz, J., Jiang, C., Machado, I., and Thapar, N. (2001). Farnesylated proteins and cell cycle progression. *J. Cell. Biochem. Suppl.* 37, 64–70. doi: 10.1002/jcb.10067

Tolkach, Y., and Kristiansen, G. (2018). The heterogeneity of prostate cancer: a practical approach. *Pathobiology* 85, 108–116. doi: 10.1159/000477852

Trams, E. G., Lauter, C. J., Salem, N. Jr., and Heine, U. (1981). Exfoliation of membrane ecto-enzymes in the form of micro-vesicles. *Biochim. Biophys. Acta* 645, 63–70. doi: 10.1016/0005-273690512-5

Usenik, A., and Legiša, M. (2010). Evolution of allosteric citrate binding sites on 6-phosphofructo-1-kinase. *PLoS One* 5:e15447. doi: 10.1371/journal.pone.0015447

Vacanti, N. M., Divakaruni, A. S., Green, C. R., Parker, S. J., Henry, R. R., Ciaraldi, T. P., et al. (2014). Regulation of substrate utilization by the mitochondrial pyruvate carrier. *Mol. Cell* 56, 425–435.

Vámosi, G., Bodnár, A., Vereb, G., Szöllösi, J., and Damjanovich, S. (2006). Role of lipid microdomains in the formation of supramolecular protein complexes and transmembrane signaling. *Lipid Rafts and Caveolae* (C J. Fielding, ed) Wiley-Vch Verlag GmbH & Co: Hoboken, NJ. doi: 10.1002/3527608079.ch7

van Blitterswijk, W. J., Emmelot, P., Hilkmann, H. A., Hilgers, J., and Feltkamp, C. A. (1979). Rigid plasma-membrane-derived vesicles, enriched in tumour-associated surface antigens (MLr), occurring in the ascites fluid of a murine leukaemia (GRSL). *Int. J. Cancer* 23, 62–70. doi: 10.1002/ijc.2910230112

van Hoeven, R. P., and Emmelot, P. (1972). Studies on plasma membranes : XVIII. lipid class composition of plasma membranes isolated from rat and mouse liver and hepatomas. *J. Membr. Biol.* 9, 105–126. doi: 10.1007/BF01868047

Vander Heiden, M. G., Cantley, L. C., and Thompson, C. B. (2010). Understanding the Warburg effect: the metabolic requirements of cell proliferation. *Science* 324(5930), 1029–1033. doi: 10.1126/science.1160809

Voet, D., and Voet, J. G. (2011). *Biochemistry* 4th ed. New York, NY: John Wiley and Sons.

Vogelstein, B., Papadopoulos, N., Velculescu, V. E., Zhou, S., Diaz, L. A. Jr., and Kinzler, K. W. (2013). Cancer genome landscapes. *Science* 339, 1546–1558. doi: 10.1126/science.1235122

Vu, L. T., Peng, B., Zhang, D. X., Ma, V., Mathey-Andrews, C. A., Lam, C. K., et al. (2019). Tumor-secreted extracellular vesicles promote the activation of cancer-associated fibroblasts via the transfer of microRNA-125b. *J. Extracell. Vesicles* 8:1599680. doi: 10.1080/20013078.2019.1599680

Wang, D., Yin, L., Wei, J., Yang, Z., and Jiang, G. (2017). ATP citrate lyase is increased in human breast cancer, depletion of which promotes apoptosis. *Tumour Biol.* 39:1010428317698338. doi: 10.1177/1010428317698338

Wang, M., and Casey, P. J. (2016). Protein prenylation: unique fats make their mark on biology. *Nat. Rev. Mol. Cell Biol.* 17, 110–122. doi: 10.1038/nrm.2015.11

Warburg, O. (1925). The metabolism of carcinoma cells. *J. Cancer Res.* 9, 148–163. doi: 10.1158/jcr.1925.148

Warburg, O. (1956). On the origin of cancer cells. *Science* 123, 309–314. doi: 10.1126/science.123.3191.309

Weiser, B. P., Salari, R., Eckenhoff, R. G., and Brannigan, G. (2014). Computational investigation of cholesterol binding sites on mitochondrial VDAC. *J. Phys. Chem. B* 118, 9852–9860. doi: 10.1021/jp504516a

Wise, D. R., Ward, P. S., Shay, J. E., Cross, J. R., Gruber, J. J., Sachdeva, U. M., et al. (2011). Hypoxia promotes isocitrate dehydrogenase-dependent carboxylation of α-ketoglutarate to citrate to support cell growth and viability. *PNAS (USA)* 108, 19611–19616. doi: 10.1073/pnas.1117773108

Yang, C., Ko, B., Hensley, C. T., Jiang, L., Wasti, A. T., Kim, J., et al. (2014). Glutamine oxidation maintains the TCA cycle and cell survival during impaired mitochondrial pyruvate transport. *Mol. Cell.* 56, 414–424. doi: 10.1016/j.molcel.2014.09.025

Zaidi, N., Swinnen, J. V., and Smans, K. (2012). ATP-citrate lyase: a key player in cancer metabolism. *Cancer Res.* 72, 3709–3714. doi: 10.1158/0008-5472.CAN-11-4112

Conflict of Interest: The authors declare that the research was conducted in the absence of any commercial or financial relationships that could be construed as a potential conflict of interest.

frontiers in Cell and Developmental Biology

ORIGINAL RESEARCH
published: 08 July 2021
doi: 10.3389/fcell.2021.695540

Identification of Novel Serum Metabolic Biomarkers as Indicators in the Progression of Intravenous Leiomyomatosis: A High Performance Liquid Chromatography-Tandem Mass Spectrometry-Based Study

Zhitong Ge[1†], Penghui Feng[2†], Zijuan Zhang[3], Jianchu Li[1] and Qi Yu[2]**

[1] Department of Ultrasound, State Key Laboratory of Complex Severe and Rare Diseases, Peking Union Medical College Hospital, Chinese Academy of Medical Science and Peking Union Medical College, Beijing, China, [2] Department of Obstetrics and Gynecology, Peking Union Medical College Hospital, Chinese Academy of Medical Sciences, Peking Union Medical College, Beijing, China, [3] Department of Pathology, Molecular Pathology Research Center, Peking Union Medical College Hospital, Chinese Academy of Medical Sciences, Peking Union Medical College, Beijing, China

Background: Intravenous leiomyomatosis (IVL) is a rare estrogen-dependent neoplasm. However, identifiable and reliable biomarkers are still not available for clinical application, especially for the diagnosis and prognosis of the disease.

Methods: In the present study, 30 patients with IVL and 30 healthy controls were recruited. Serum samples were isolated from these participants for further high performance liquid chromatography-tandem mass spectrometry (HPLC-MS/MS) analysis to study metabolomics alterations and identify differentially expressed metabolites based on orthogonal partial least-squares discriminant analysis (OPLS-DA). Subsequently, lasso regression analysis and a generalized linear regression model were applied to screen out hub metabolites associated with the progression of IVL.

Results: First, 16 metabolites in the positive ion mode were determined from the 240 identifiable metabolites at the superclass level, with ten metabolites upregulated in the IVL group and the remaining six metabolites downregulated. Our data further proved that four metabolites [hypoxanthine, acetylcarnitine, glycerophosphocholine, and hydrocortisone (cortisol)] were closely related to the oncogenesis of IVL. Hypoxanthine and glycerophosphocholine might function as protective factors in the development of IVL (OR = 0.19 or 0.02, respectively). Nevertheless, acetylcarnitine and hydrocortisone (cortisol), especially the former, might serve as risk indicators for the disease to promote the development or recurrence of IVL (OR = 18.16 or 2.10, respectively). The predictive

OPEN ACCESS

Edited by:
Sebastian Haferkamp, University of Regensburg, Germany

Reviewed by:
Marco Sciacovelli, University of Cambridge, United Kingdom
Mingxing Xie, Huazhong University of Science and Technology, China

***Correspondence:**
Jianchu Li
jianchu.li@163.com
Qi Yu
yuqi2008001@sina.com

[†] These authors have contributed equally to this work

Specialty section:
This article was submitted to Molecular and Cellular Oncology, a section of the journal Frontiers in Cell and Developmental Biology

Received: *15 April 2021*
Accepted: *18 June 2021*
Published: *08 July 2021*

Citation:
Ge Z, Feng P, Zhang Z, Li J and Yu Q (2021) Identification of Novel Serum Metabolic Biomarkers as Indicators in the Progression of Intravenous Leiomyomatosis: A High Performance Liquid Chromatography-Tandem Mass Spectrometry-Based Study. Front. Cell Dev. Biol. 9:695540. doi: 10.3389/fcell.2021.695540

accuracy of these hub metabolites was further validated by the multi-class receiver operator characteristic curve analysis (ROC) with the Scikit-learn algorithms.

Conclusion: Four hub metabolites were finally determined via comprehensive bioinformatics analysis, and these substances could potentially serve as novel biomarkers in predicting the prognosis or progression of IVL.

Keywords: metabolomics, biomarkers, intravenous leiomyomatosis, progression, HPLC-MS/MS

INTRODUCTION

Intravenous leiomyomatosis (IVL) is a rare estrogen-dependent neoplastic disease (Low et al., 2012; Price et al., 2017), that was first described in 1896 (Marshall and Morris, 1959; Zhang Y. et al., 2016). In 1907, Durck documented and reported the first case of IVL involving the heart (Gui et al., 2016). It is characterized by invasive growth even though IVL appears to be benign histologically. The tumor originates from the venous wall of the uterus or the pelvic cavity outside the uterus, protrudes into the venous passage of the uterus or pelvis, invades through the iliac vein or ovarian vein, and extends to the inferior vena cava (Spanuchart et al., 2012). It can cause severe circulatory disturbance and syncope or sudden death once the tumor enters the right atrium or the right ventricle as well as the pulmonary artery through the tricuspid valve (Shi and Shkrum, 2018). If part of the tumor in the heart dislodges, this can lead to pulmonary embolism or cerebral infarction, which is life-threatening (Zhang et al., 2012; Knight et al., 2017; Kong et al., 2020). According to a single-center study of 30,757 Chinese patients who received treatment for hysteromyoma, the incidence of IVL disease among patients with uterine leiomyoma was 0.25% (Ma et al., 2016). Nevertheless, the rate of misdiagnosis and missed diagnosis of IVL before the operation is relatively high as the clinical symptoms and imaging findings are not specific. When IVL lesions are confined to the pelvic cavity without vascular invasion in the early stage, they may behave similarly to uterine leiomyoma (Yu et al., 2021). If the tumor invades into the inferior vena cava or heart in the later stage, it tends to be misdiagnosed as a primary cardiac tumor or venous thrombosis (Ribeiro et al., 2013; Kuklik et al., 2020). In clinical practice, surgical resection of the primary tumor, vena cava and right cardiac system tumor is the best choice (Deng et al., 2020). Studies have shown that the risk of postoperative recurrence of IVL is as high as 30% (Virzi et al., 2007), and the risk of postoperative recurrence in patients with large vein involvement is significantly higher than that in patients without it (Yu et al., 2016).

Abbreviations: IVL, intravenous leiomyomatosis; HPLC-MS/MS, high performance liquid chromatography-tandem mass spectrometry; OPLS-DA, orthogonal partial least-squares discriminant analysis; Co-no, control group without uterine myoma; Co-um, control group with uterine myoma; IVL-no, IVL group without recurrence; IVL-re, IVL group with recurrence; ISVF, ion spray voltage floating; IDA, information dependent acquisition; CAMERA, collection of algorithms of metabolite profile annotation; VIP, variable importance in the projection; IVC, inferior vena cava; DEMs, differentially expressed metabolites; TIC, comparisons of total ion chromatogram; QC, quality control; PCA, principal component analysis; HCA, hierarchical clustering analysis; DA, differential abundance; GLM, generalized linear regression model; AMH, anti-Mullerian hormone.

At present, an increasing number of studies have begun to focus on finding potential regulatory factors and biomarkers that affect the occurrence and progression of the disease, which are of great significance for the diagnosis, treatment and prognosis of IVL. Based on RNA sequencing analysis and reverse transcription-quantitative PCR, Wang W. et al. (2020) verified that IVL tended to be a solid tumor differing from uterine leiomyoma and found that *CDKN2A*, *BCL2A1*, and angiogenesis-related gene *CXCL8* might be new specific biomarkers of IVL. However, these findings remained to be further confirmed by larger samples (Wang W. et al., 2020). In another study, molecular analysis of 17 cases of IVL revealed that *MED12* mutations, *MSI* and *LOH* were inconsistent among patients with either uterine or extrauterine IVL. These findings suggested that IVL disease had a different molecular pathogenesis pattern from typical uterine leiomyoma (Lu et al., 2020). Other studies have detected 22q repeat deletions (66%) and complex copy number variants using array comparative genomic hybridization (Buza et al., 2014). Zhang et al. (2019) found that *HOXA13* was significantly downregulated in IVL when compared with myometrial tissue via RNA sequencing. Besides, the *Rb* pathway was proved to be involved in the pathogenesis of IVL disease (Ordulu et al., 2020). The above studies have initiated meaningful exploration of the mechanism of the occurrence and development of IVL, which are of great importance for deepening our understanding of the disease. However, most studies only explored the potential regulatory genes that affected the pathogenesis and prognosis of IVL and did not pay attention to the changes in a series of metabolites in patients. Thus, there have been no specific biochemical indicators for the diagnosis and prognosis of IVL.

Therefore, in the present study, we analyzed the difference in serum metabolomics between IVL patients and healthy controls based on high performance liquid chromatography-tandem mass spectrometry (HPLC-MS/MS). The core metabolic indicators affecting disease progression and recurrence were screened and identified, which provided a valuable theoretical basis for the development of new non-invasive methods for the diagnosis and prognostic intervention of IVL based on these biomarkers.

MATERIALS AND METHODS

Experimental Design and Sample Collection

This study adhered to the Helsinki Declaration and the guidelines of the Clinical Practice Coordination Conference and was

approved by the Ethics Committee of Peking Union Medical College Hospital (Ethics: JS-2654). All participants in the study signed informed consent forms. The disease group in this study included patients with IVL who underwent surgery at Peking Union Medical College Hospital from December 2011 to May 2020 and were followed up regularly. The study population was divided into groups: 30 healthy controls as a Co group, with half of them without uterine myoma (Co-no) and the rest with uterine myoma (Co-um); 30 patients with IVL were further classified into a non-recurrence group (IVL-no) or recurrence group (IVL-re) according to postoperative recurrence. There were 15 individuals in each of the above four subgroups.

In the Co-no group, the myometrium echo of these healthy women was uniform, there were no uterine myomas or pelvic space-occupying lesions, and the abdominal pelvic vein was confirmed by ultrasound examination. The Co-um group was characterized by a hypoechoic mass found in the mesometrium by ultrasound (maximum diameter $\geq$2 cm), the ultrasound pattern of which showed a typical vortex-like structure, and the abdominal and pelvic veins were confirmed by ultrasound. In the IVL-re group, a space-occupying lesion ($\geq$1 cm) was found in the pelvic or abdominal veins (inferior vena cava and iliac veins) or the residual lesion was larger than the previous size on by at least two consecutive ultrasound examinations. If there were no space-occupying lesions in the pelvic cavity or blood vessels, patients were categorized into IVL-no group.

The admission criteria of the disease group were as follows: (1) abdominal and pelvic veins (parauterine reproductive vein, iliac vein, and inferior vena cava) or right atrium-occupying lesions observed in preoperative imaging or during surgery; (2) patients who received surgical treatment at Peking Union Medical College Hospital; (3) postoperative pathological diagnosis of IVL with vascular invasion; and (4) age $\geq$18 years. The exclusion criteria of the disease group were as follows: (1) incomplete clinical data; (2) pregnant and lactating women; (3) people with intellectual disability or an inability to take care of themselves; (4) patients who were not willing to participate in this study; and (5) patients with other malignant tumors. At the same time, we recruited women to the healthy control group. The criteria for the healthy control group were as follows: (1) age $\geq$18 years old; (2) no history of other malignant tumors; (3) non-pregnant and lactating women; and (4) no previous history of hysteromyomectomy or hysterectomy-related gynecological surgery.

First, ultrasound examinations were performed on all subjects by senior doctors, results were read independently, and inconsistent results were resolved after discussion. All participants' abdominal and pelvic blood vessels were examined on an empty stomach, and they were advised to retain their urine properly so that their uterine and double appendices could be properly evaluated. For the patients in the IVL group, the first step was to check the patency of the large abdominal vessels, including the inferior vena cava and bilateral iliac veins, followed by observing whether there was a space-occupying lesion within the pelvic cavity. In the Co group, inferior vena cava, iliac vein and gynecological ultrasonography were performed to confirm that there was no space-occupying lesion in the abdominal and pelvic blood vessels and whether there was myoma in the uterus. The location and size of the largest leiomyoma were recorded simultaneously if uterine myoma was present. After each patient finished the ultrasound examination, the venous blood was collected from the cubital vein for further metabolomics tests.

Sample Preparation and LC-MS/MS Analysis

Serum was isolated from fasting blood samples after centrifugation for 15 min at 2,000 $\times$ *g*. Each aliquot (150 μL) of the serum samples was maintained at -80°C until UPLC-Q-TOF/MS analysis. After thawing, the serum aliquots were mixed with 400 μL of precooled methanol/acetonitrile (1:1, v/v) to remove the protein, followed by centrifugation for 15 min at 14,000 $\times$ *g*. The supernatant was further dried through vacuum centrifugation and redissolved in 100 μL acetonitrile/water liquor (1:1, v/v) for LC-MS analysis, which was carried out with an UHPLC (1290 Infinity LC, Agilent Technologies) coupled to a quadrupole time-of-flight (AB SCIEX TripleTOF 6600). For HILIC separation, samples were detected using an ACQUITY UPLC BEH column (Waters, Ireland). In ESI either positive or negative modes, the mobile phase included solution A (25 mM ammonium acetate and 25 mM ammonium hydroxide in water) and solution B (acetonitrile). The gradient condition was as follows: 85% solution B for 1 min, linearly reduced to 65% in 11 min, and then reduced to 40% in 0.1 min and sustained for 4 min, followed by elevation to 85% in 0.1 min, with a 5 min reequilibration period employed. The ESI source conditions were executed as follows: ion source gas1 (Gas1) of 60, ion source gas2 (Gas2) of 60, curtain gas (CUR) of 30, source temperature of 600°C, and ion spray voltage floating (ISVF) $\pm$ 5,500 V. The product ion scan was finally obtained based on information-dependent acquisition (IDA) with the high sensitivity mode selected.

The raw MS data (wiff.scan files) were transformed into MzXML files with ProteoWizard MSConvert before being imported into XCMS software. Collection of algorithms of the metabolite profile annotation (CAMERA) was applied to annotate the isotopes and adducts. For the extracted ion features, only the variables with no less than 50% of the non-zero measurement values in at least one group were screened out. Compound identification of metabolites was carried out in comparisons of accuracy m/z value ($<$25 ppm), and MS/MS spectra.

Statistical Analysis

For baseline information, data were expressed as numbers (percentages) for categorical variables or medians (upper quartile and lower quartile) for continuous variables based on the normality test of data distribution. The Kruskal–Wallis non-parametric test was performed for comparisons among different specialties. For LC-MS/MS data, after normalization to the total peak intensity, the processed data were analyzed by R package (ropls), where it was subjected to orthogonal partial least-squares discriminant analysis (OPLS-DA). The cross-validation and response permutation testing were used to evaluate the

robustness of the model. The variable importance in the projection (VIP) value of each variable in the OPLS-DA model was calculated to represent its contribution to the classification. Metabolites with a VIP value >1 were further subjected to Student's *t*-test or Mann-Whitney *U* test at the univariate level to measure the significance of each metabolite, and *P*-values less than 0.05 were considered statistically significant.

RESULTS

Baseline Characteristics of the Subjects

This study involved 30 IVL patients and 30 healthy controls, whose median age was 49.0 and 49.5 years, respectively ($P = 0.25$). Additionally, the age at menarche did not differ between groups. The symptoms of the IVL patients were atypical, mainly including lower limb edema ($n = 4$), flustered shortness of breath ($n = 8$), and lumbago or back pain ($n = 4$). Some of the patients were asymptomatic, and only a few people complained about abdominal masses, hypermenorrhagia, a ventral belly, or even syncope. In most cases, the average diameter of the pelvic mass varied by approximately 8.3 cm. All IVL patients in this study had a history of uterine fibroids. Likewise, more than two-thirds of these patients have undergone uterine surgeries. It is worth noting that the extension route of IVL was concentrated in the left or right iliac veins and right gonadal vein. Furthermore, the extensions of involvement chiefly consisted of the right ventricle ($n = 4$), right atrium ($n = 14$), and infrarenal inferior vena cava (IVC) ($n = 4$), with shapes categorized as either cast or luminal. Regarding the IVL staging operation, 23 patients underwent a surgery with stage I disease, and the remaining patients underwent a surgery with stage II disease. In addition, most of these patients received complete resection except for four patients who had an intravascular residue and 1 patient who had a pelvic residue. More importantly, half of the patients experienced recurrence after surgery, with the lesions primarily presenting within the blood vessel, pelvis, or both locations. The detailed information was presented in **Table 1**.

TABLE 1 | Baseline characteristics of the involved patients.

Characteristic	Groups		*P*-value
	IVL patients ($n = 30$)	Normal controls ($n = 30$)	
Age (years)	49.0 (45.0∼53.5)	49.5 (43.0∼52.0)	0.25
Age of menarche (years)	14.0 (13.0∼15.0)	15.0 (13.0∼16.0)	0.07
Symptoms			–
Lower limb edma	4 (13.3)	–	
Flustered shortness of breath	8 (26.7)	–	
Abdominal mass	1 (3.3)	–	
Lumbago and back pain	4 (13.3)	–	
Hypermenorrhagia	2 (6.7)	–	
Ventral belly	2 (6.7)	–	
Syncope	2 (6.7)	–	
Asymptomatic	7 (23.3)	–	
Pelvic mass (cm)	8.3 (0.0∼12.2)	–	–
History of uterine fibroids	30 (100)	–	–
Uterine surgery history	22 (73.3)	–	–
Route of extension			–
Left iliac vein	4 (13.3)	–	
Right iliac vein	24 (80.0)	–	
Left gonadal vein	1 (3.3)	–	
Right gonadal vein	4 (13.3)	–	
Left parauterine vein	1 (3.3)	–	
Right parauterine vein	1 (3.3)	–	
Extent of involvement			–
Right ventricle	4 (13.3)	–	
Right atrium	14 (46.7)	–	
Retrohepatic IVC	3 (10.0)	–	
Infrarenal IVC	4 (13.3)	–	
Distal IVC	1 (3.3)	–	
Left iliac vein	1 (3.3)	–	
Right iliac vein	3 (10.0)	–	
Shape of IVL			–
Cast	27 (90.0)	–	
Luminal	3 (10.0)	–	
Thread-like	0 (10.0)	–	
Mixed	0 (10.0)	–	
Staging surgery			–
I	23 (76.7)	–	
II	7 (23.3)	–	
Postoperative residual lesions			–
No	25 (83.3)	–	
Intravascular residue	4 (13.3)	–	
Pelvic residue	1 (3.3)	–	
Site of recurrence			
Intravascular	4 (13.3)		
Pelvic	9 (30.0)		
Both	2 (6.7)		

IVL, intravenous leiomyomatosis; IVC, inferior vena cava. Data were expressed as number (percentage) for categorical variables or median (upper quartile and lower quartile) for continuous ones. Kruskal–Wallis non-parametric test was performed for comparisons among different specialties.

Differential Metabolites Between IVL Patients and Healthy Controls

As exhibited in **Figure 1A**, a total of 240 kinds of metabolites at the superclass level (above level two, including undefined metabolites) were finally identified in this project and detected in the positive and negative ion modes. These metabolites were classified according to their chemical compound attributes. Our results demonstrated that most of these identifiable metabolites were lipids or lipid-like molecules (17.92%), organic acids or derivatives (16.25%) and organoheterocyclic compounds (9.167%). Besides, some organic oxygen compounds, nucleosides, nucleotides, or analogs, benzenoids, organic nitrogen compounds, and phenylpropanoids or polyketides were detected in the serum specimens as well. To analyze the differences between the IVL and healthy control groups in the positive ion mode, we used univariate statistical analysis methods, including fold change (FC) analysis and Student's *t*-test or the Mann-Whitney *U* test. Among these metabolites, the

differentially expressed metabolites (DEMs) were filtered out and displayed as the volcano plot in **Figure 1B**, with FC > 1.5 and *P*-value < 0.05. In the volcano plot, the upregulated and downregulated metabolites were marked in red or blue, respectively. Our data indicated that these DEMs were classified into lipids or lipid-like molecules, nucleosides, nucleotides or analogs, and organoheterocyclic compounds.

In order to screen out the metabolites correlated with the oncogenesis of IVL, OPLS-DA, a supervised discriminant analysis method, was applied to distinguish the two groups of samples by establishing the discriminant model according to the metabolites. As shown in **Figure 1C**, the two groups were well separated from each other in positive ion mode based on the scores. So as to avoid overfitting of the supervised model in the modeling process, the permutation test was adopted to ensure the efficacy of the model. **Figure 1D** demonstrated that the R^2 and Q^2 values of the random model gradually decreased as the permutation retention lessened, which implied that the robustness of the model was acceptable and that the model established in this study had a favorable degree of fitting and predictability with $R^2Y = 0.95$ and $Q^2 = 0.66$ of the original model. Based on the analysis, 16 metabolites in the positive ion mode were ultimately identified when meeting the screening criteria in this experiment: VIP > 1 and *P*-value < 0.05, as displayed in **Figure 1E**. Among these metabolites, 10 of them were upregulated in the IVL group, including adenosine, decanoyl-L-carnitine, bilirubin, hydrocortisone (cortisol), and biliverdin, etc. Conversely, 1-palmitoyl-sn-glycero-3-phosphocholine, 1-oleoyl-sn-glycero-3-phosphocholine, glycerophosphocholine, phe-phe, 2-amino-1-phenylethanol, and hypoxanthine were downregulated when compared with the Co group.

Comparisons of the total ion chromatograms (TICs) of quality control (QC) samples in both the positive and negative ion modes were performed. Our results manifested that the response intensity and retention time of each chromatographic peak basically overlapped, indicating that the variation caused by the error of the instrument was negligible throughout the whole experiment (**Supplementary Figures 1A,B**). Additionally, the comprehensive evaluation results of the total sample by principal component analysis (PCA) were expressed in **Supplementary Figures 1C,D**, and signified that, in this experiment, the stability and repeatability of the investigation, and the reliability of the data quality were sufficient for further analysis.

Hierarchical Cluster Analysis and KEGG Pathway Enrichment

To fully and intuitively reveal the relationships and differences between different samples, hierarchical clustering analysis (HCA) was conducted. Metabolites clustered in the same cluster were characterized by similar expression patterns and might have similar functions or participate in the same metabolic processes or cellular pathways. The HCA results included the above 16 significant DEMs (VIP > 1, $P < 0.05$), as shown in **Figure 2A**. It was noticed that the two groups shared completely different metabolic patterns with six upregulated metabolites chiefly enriched in the Co group, including glycerophosphocholine, 1-palmitoyl-sn-glycero-3-phosphocholine, 1-oleoyl-sn-glycero-3-phosphocholine, hypoxanthine, phe-phe, and 2-amino-1-phenylethanol. In contrast, the remaining ten metabolites were abundant in the IVL group. Subsequently, in order to capture the average and overall variation of the above 16 DEMs in specific pathways, the analysis of the metabolic changes based on differential abundance (DA) score was introduced into this study. As shown in **Figure 2B**, these metabolites were mainly involved in the cGMP-PKG signaling pathway, neuroactive ligand-receptor interaction, GABAergic synapse, glutamatergic synapse, D-glutamine or D-glutamate metabolism, purine metabolism, and cortisol synthesis or secretion, as well as choline metabolism in cancer. All differential metabolic pathways were further classified and assigned according to their previous pathway hierarchy, and these metabolites were principally engaged in cancer, endocrine or metabolic disease, metabolism of other amino acids or nucleotides, signaling molecule interaction or transduction, and lipid metabolism, along with membrane transport.

Screening of Metabolites Based on Lasso Regression Analysis

Among the metabolites screened above, lasso regression analysis was carried out and five metabolites were determined, which were further validated based on the cross-validation, including hypoxanthine, glycerophosphocholine, hydrocortisone (cortisol), decanoyl-L-carnitine, and acetylcarnitine (**Figures 3A,B**). To interpret the metabolic correlation among all DEMs, correlation analysis was performed, which was meaningful for further understanding the mutual regulation of metabolites. Metabolites with expression correlations might jointly participate in the biological processes, namely, functional correlations. On the basis of this analysis, we found that hypoxanthine exhibited a positive relationship with glycerophosphocholine (Cor = 0.31), and decanoyl-L-carnitine also shared a positive correlation with either hydrocortisone (cortisol) or acetylcarnitine (Cor = 0.42, 0.58, respectively). Instead, acetylcarnitine presented a negative trend with the abundance of both hypoxanthine and glycerophosphocholine (**Figure 3C**). According to the expression levels of these five metabolites between the IVL and Co groups, we discovered that hypoxanthine and glycerophosphocholine were significantly downregulated in the IVL group, while hydrocortisone (cortisol), decanoyl-L-carnitine, and acetylcarnitine were upregulated in the IVL group (**Figures 4A–E**). To investigate the roles of these metabolites in the progression of IVL, all samples were further classified into four groups as mentioned above in accordance with the presence of uterine leiomyoma and recurrence. It appeared that the relative content of hypoxanthine in the Co-no and Co-um groups significantly differed from that in the IVL-no and IVL-re groups ($P < 0.01$) (**Figure 4F**). Regarding acetylcarnitine and decanoyl-L-carnitine in **Figures 4G,H**, they were elevated in the IVL-no group when compared with the healthy controls. Besides, the levels of these metabolites were significantly different in the IVL-re group in comparison with the Co-no

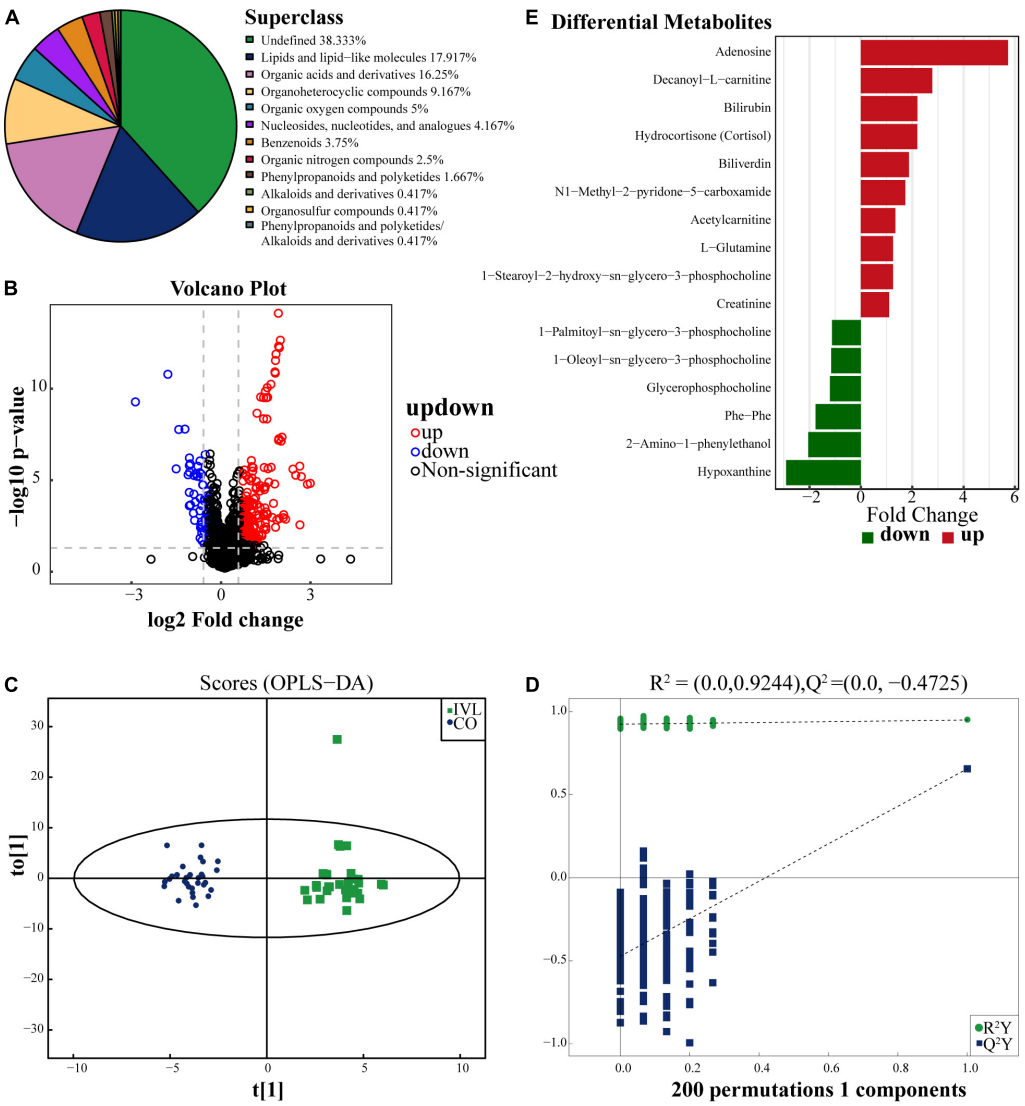

FIGURE 1 | Identification of differentially expressed metabolites. **(A)** The pie chart displayed all the metabolites identified in this project in either positive or negative ion modes, and their chemical attribution. **(B)** Volcano diagram revealed the changes between the IVL group and the healthy subjects. The red dots on the right side of the figure represented the upregulated metabolites, the blue dots on the left side meant the downregulated metabolite, and the black dots referred to non-significant difference. *X*-axis corresponded to log2 fold change and *y*-axis corresponded to –log10 *P*-value. **(C)** Score plot of OPLS-DA for IVL and control groups, indicating the separation degree between the two groups. **(D)** A permutation test conducted with 200 randomly initiated permutations in an OPLS-DA model by cross-validation. T[1] referred to principal component 1, to[1] represented principal component 2, and the ellipse was 95% confidence interval. The dots in the same color meant each biological repetition within the group, and the distribution state of the dots reflected the degree of difference between groups and within groups. **(E)** The bar chart displayed 16 significant metabolites between IVL patients and control group (VIP > 1, $P < 0.05$). The *x*-axis represented the fold change of differential expression of these metabolites.

group. Glycerophosphocholine showed a tendency of declining consistency as the disease progressed even though we only observed a noticeable difference in the IVL-no and IVL-re groups when compared with the Co-no group but not when compared with the Co-um group (relative content = 1.00 ± 0.10, 0.95 ± 0.19, 0.82 ± 0.11, 0.80 ± 0.24 for each group, respectively) (**Figure 4I**). Conversely, a gradual upward trend was observed in hydrocortisone (cortisol) except that there seemed to be no statistical significance regarding the comparison between the IVL-no and Co-um groups, as suggested in **Figure 4J** (relative content = 1.00 ± 0.75, 1.08 ± 0.62, 1.99 ± 0.96, 2.58 ± 2.54 for each group, respectively).

Determination of Hub Metabolites Associated With the Progression of IVL

Given the mutual interaction of the metabolites, we further used a generalized linear regression model (GLM) to find the hub metabolites that were associated with the progression of IVL with the relative content of the five metabolites. Our

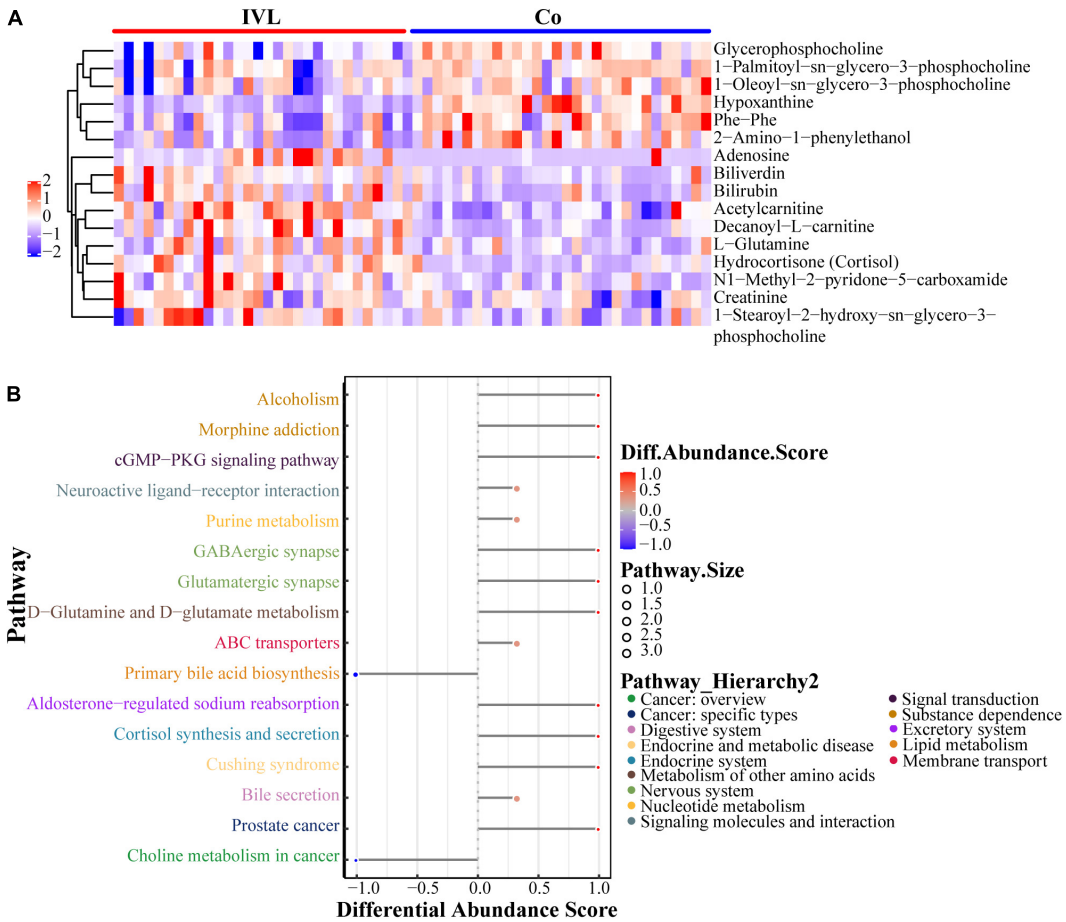

FIGURE 2 | Characteristics of 16 identified metabolites. **(A)** Heatmap visualization of metabolomics data with hierarchical clustering analysis in the positive ion mode. Colors reflected the relative content of metabolites in serum. The more similar the colors were, the more similar the expression pattern. The panel on the right indicated the different metabolites. Each blockage meant a sample of either the IVL or Co groups. **(B)** The differential abundance (DA) score of differential metabolic pathways. *Y*-axis represented the name of the differential pathways, and *X*-axis coordinates meant the DA score. DA score was defined as the total change of all metabolites in the metabolic pathway. A score of 1 indicated an upregulated expression trend for all identified metabolites in the pathway, while −1 was exactly the opposite. The length of the line segment represented the absolute value of DA score; the size of the dot at the end of the line segment referred to the number of metabolites in the pathway; the larger the dot was, the greater the number of metabolites. The color depth of the line segment and dot was proportional to DA score.

data proved that four metabolites [hypoxanthine, acetylcarnitine, glycerophosphocholine, and hydrocortisone (cortisol)] were closely related to the progression of IVL, as displayed in **Figure 5**. Hypoxanthine and glycerophosphocholine might function as independent protective factors in the progression of the disease (OR = 0.19 or 0.02, respectively); nevertheless, acetylcarnitine and hydrocortisone (cortisol), especially the former, might act as hazardous indicators or risk factors for the disease to promote the progression of IVL (OR = 18.16 or 2.10, respectively). These results implied that these four metabolites were promising factors for future prediction of the prognosis and progression of IVL.

Validation of the Prediction of the Hub Metabolites by ROC Analysis

To confirm the prediction accuracy of the four hub metabolites mentioned above, we further performed the receiver operator characteristic curve analysis using a Python module, Scikit-learn[1]. Two comprehensive state-of-the-art machine-learning algorithms were introduced in the present study, including micro-average ROC (calculating metrics globally by considering each element of the label indicator matrix as a label) and macro-average ROC (calculating metrics for each label, and finding their unweighted mean). Our results indicated that these four metabolites functioned well in distinguishing cases from distinct pathological statuses with the area under the curve (AUC) to be 0.72 or even 0.81 for the results of micro or macro-average ROC analyses, respectively (**Figure 6**). Additionally, it was worth noting that the four hub metabolites exhibited a reliable discrimination to recognize patients with uterine leiomyoma or intravenous leiomyomatosis from normal controls (AUC value = 0.88). These findings signified

[1]https://scikit-learn.org/

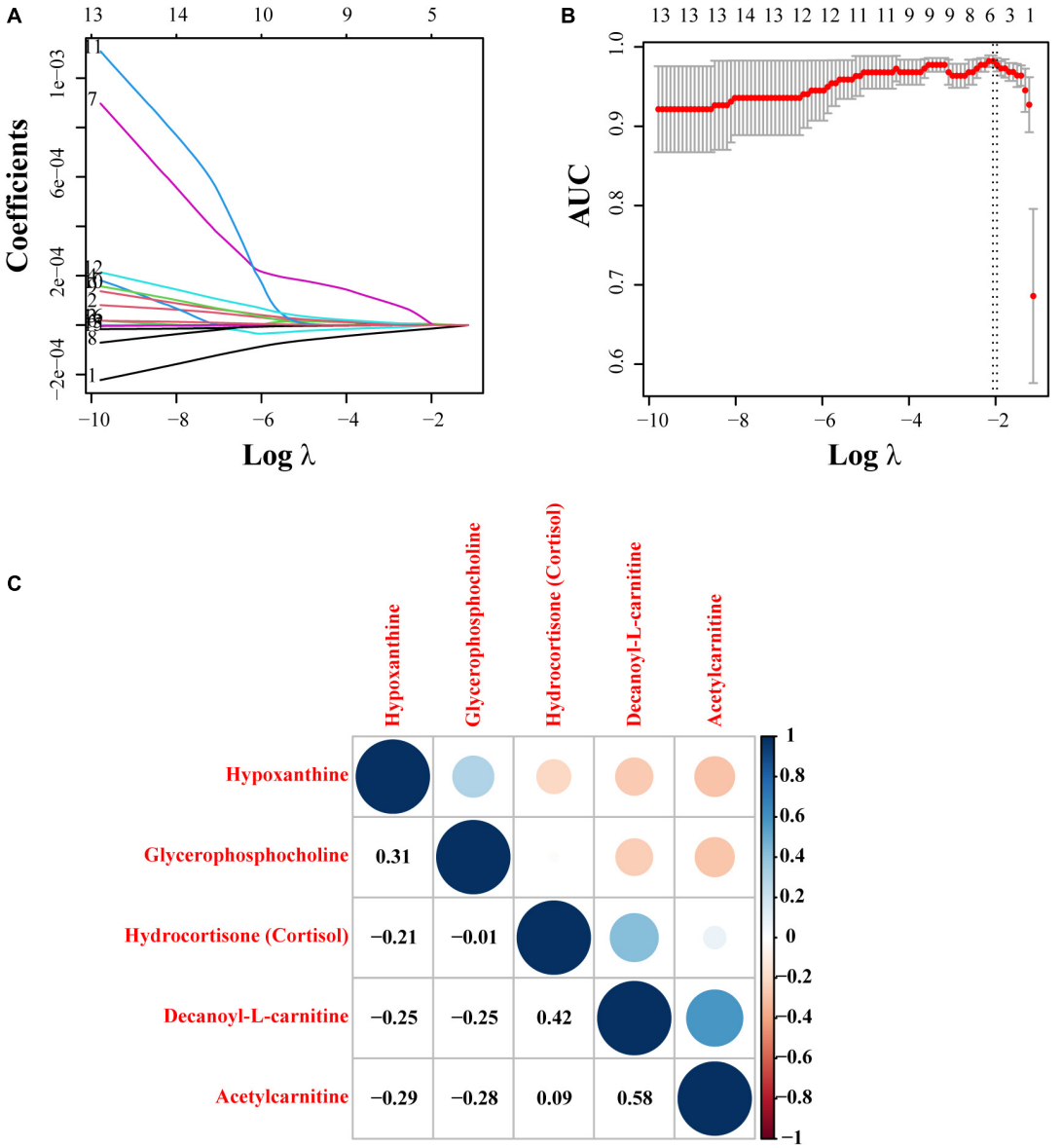

FIGURE 3 | Lasso regression model construction and correlation analysis. **(A)** The process of fitting the lasso regression model. Each curve represented a metabolite. **(B)** Partial likelihood deviance was calculated by the cross-validation for the best λ to determine the minimum mean cross-validated error. Red dots and solid vertical lines referred to partial likelihood deviance and corresponding 95% CI, respectively. In addition, the left and right dotted vertical lines represented the λ value with minimum cvm (namely, lambda.min) and the largest value, whose error was within one standard error of the minimum (lambda.1se). **(C)** The correlation figure revealed the correlation of expression pattern of five selected metabolites. Red represented a positive correlation, and blue showed a negative correlation. The size of the point was proportional to the correlation coefficient.

the predictive value of the model established by the four hub metabolites.

DISCUSSION

With the rapid development of modern biological analysis technology, metabolomics has been successfully applied in many fields, such as cancer research (Tayanloo-Beik et al., 2020). Metabolomics is one of the "omics" techniques, and is complementary to genomics, transcriptomics, and proteomics (Xuan et al., 2020). Metabolites are defined as small organic and low-molecular-weight compounds (<1,500 Dalton), which are the final products during the metabolic process (Alonso et al., 2015). The study of metabolites helps to identify metabolic pathways that are activated or dysfunctional in patients (Christodoulou et al., 2020). At the molecular level, metabolomics adopts novel biomarkers to explore the underlying mechanisms of disease development (Wang et al., 2011). A recent study discovered that histidinyl-lysine, docosahexaenoic acid

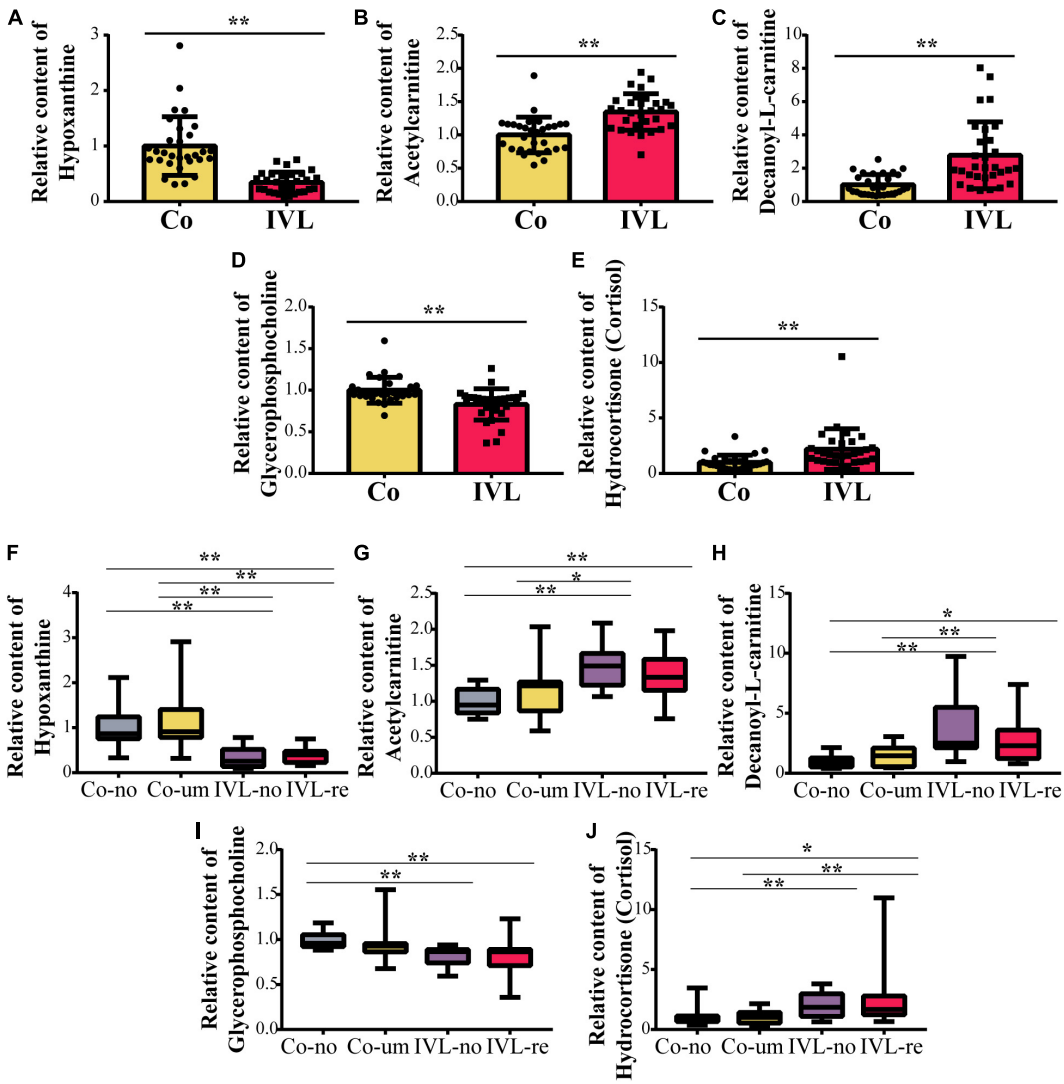

FIGURE 4 | The relative content of metabolites among groups. **(A–E)** Boxplots of the differentially expressed metabolites between the IVL and control groups (**$P < 0.01$), including hypoxanthine, glycerophosphocholine, hydrocortisone (cortisol), decanoyl-L-carnitine, and acetylcarnitine. **(F–J)** Comparisons of the expression of five metabolites as mentioned above among the Co-no, Co-um, IVL-no, and IVL-re groups (*$P < 0.05$, **$P < 0.01$).

Variable	Co_no	Co_um	IVL_no	IVL_re	*P* value
Hypoxanthine	1.00±0.47	1.07±0.63	0.34±0.22	0.38±0.17	0.013
Acetylcarnitine	1.00±0.18	1.15±0.36	1.50±0.27	1.40±0.32	0.004
Decanoyl−L−carnitine	1.00±0.55	1.43±0.88	4.05±2.81	2.69±1.84	0.403
Glycerophosphocholine	1.00±0.10	0.95±0.19	0.82±0.11	0.80±0.24	0.031
Hydrocortisone (Cortisol)	1.00±0.75	1.08±0.62	1.99±0.96	2.58±2.54	0.007

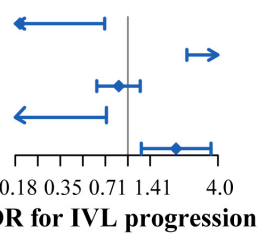

FIGURE 5 | Identification of hub metabolites based on generalized linear regression model. Forest plot displayed the odds ratio of five metabolites in the progression of IVL. *P*-value was calculated by generalized linear regression model, adjusted for the relative content of these metabolites.

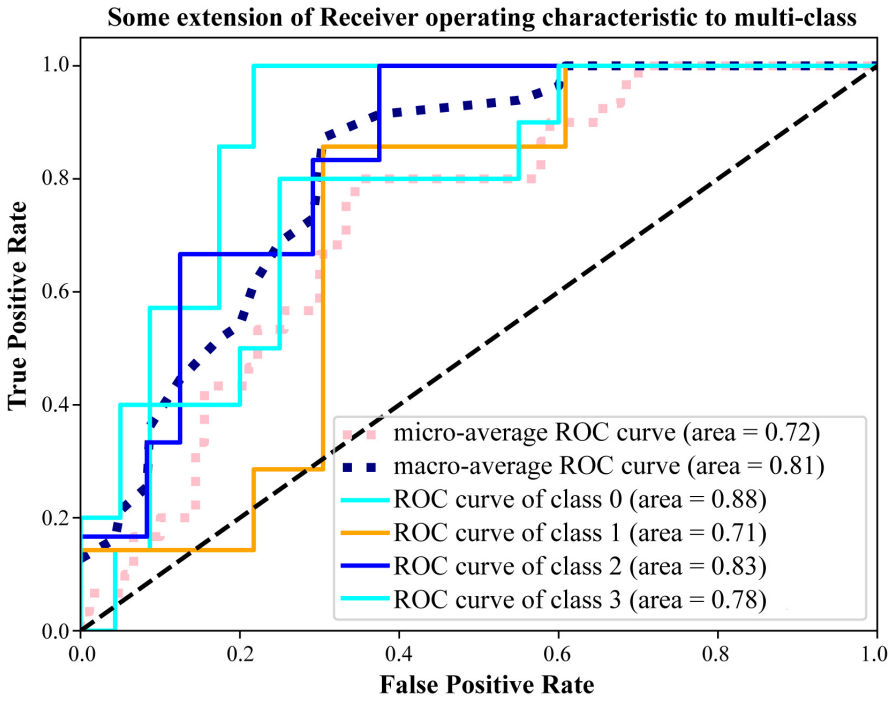

FIGURE 6 | Validation the prediction accuracy of the model. ROC analysis of the four hub metabolites by micro and macro-average ROC machine-learning algorithms for multi-class variables. Class 0 ∼ 3 represented the Co-no, Co-um, IVL-no, and IVL-re groups, respectively. AUC value was applied to characterize the model performance.

and lysoPC combined with CA199, based on metabolomics analysis, showed high sensitivity and specificity in detecting patients with pancreatic ductal adenocarcinoma, indicating that these metabolites could be used as potential indicators to distinguish pancreatic ductal adenocarcinoma disease from normal controls (Zhang et al., 2020). Additionally, another team also proved that increased levels of circulating anti-Mullerian hormone (AMH) in premenopausal women were associated with elevated risks of breast cancer (Eliassen et al., 2016). A study involving 101 unstable angina pectoris patients screened out a series of DEMs, as new biomarkers in the identification of the illness (Yao et al., 2017). Similarly, Farshidfar et al. (2016) also tested some biomarkers that could achieve early detection or even preliminary staging information for colorectal cancer. The above studies demonstrated that metabolomics plays a vital role in the diagnosis and prognosis of diseases. However, there have been no relevant studies focusing on metabolic differences in patients with IVL.

In this study, 30 IVL patients and 30 healthy controls were recruited, and the program yielded a total of 240 significantly different metabolites at the superclass level, which were prevailingly characterized as lipids or lipid-like molecules, organic acids or derivatives, organoheterocyclic compounds, and organic oxygen compounds. Subsequently, we identified several metabolites associated with IVL based on OPLS-DA and univariate analysis. Further identification via GLM was performed, and four hub metabolic markers were finally screened out, namely, hypoxanthine, acetylcarnitine, glycerophosphocholine, and hydrocortisone (cortisol), which could distinguish IVL patients from healthy subjects. These metabolites were involved in purine metabolism, cortisol synthesis or secretion, and choline metabolite in cancer on the basis of enrichment analysis. Subsequently, the micro and macro-average ROC machine-learning algorithms were applied in this study to validate the prognostic reliability of the hub metabolite. What made sense was that the ROC analysis confirmed the discrimination of the model to recognize the corresponding disease conditions of these included cases. Particular, it performed well to distinguish patients with uterine leiomyoma or intravenous leiomyomatosis from healthy subjects.

Hypoxanthine is a purine, engaged in the metabolism of adenine and guanine, and therefore, in the synthesis of the corresponding nucleosides (Barberini et al., 2019). Hypoxanthine is known to be related to various cancers. A targeted study constructed by Yoo et al. (2010) revealed that the downstream metabolites, hypoxanthine and xanthine, were reduced in non-Hodgkin's lymphoma, which were likely to be defined as suitable markers for non-Hodgkin's lymphoma, with AUROC values of 0.85 and 0.83, respectively. Another study also elucidated the underlying mechanisms of the low content of hypoxanthine in urine samples of patients with hepatocellular carcinoma (Wu et al., 2009). Likewise, a research focusing on cerebrospinal fluid-based metabolomics, suggested that it was downregulated in patients with lung adenocarcinoma with brain metastasis compared with controls (Wang F.X. et al., 2020). In previous reports, the potential correlation between

the reduced hypoxanthine levels and cancers such as colorectal cancer (Long et al., 2017), non-Hodgkin lymphoma (Yoo et al., 2010), and gastric cancer (Jung et al., 2014) has already been explained; in other words, increased synthesis of DNA (adenine utilization) in hyperproliferative tissues might be responsible for the decreased level of hypoxanthine. Consistent with previous studies, in the present research, the level of hypoxanthine was significantly lower in the IVL groups than in the control group (P-value = 0.013). As a substrate and nitrogen source, the alteration in hypoxanthine levels shown in our study was possibly associated with the higher invasive probability of the tumor cells.

Acetylcarnitine is an acetylated form of L-carnitine, mainly used for energy production by transporting activated long-chain fatty acids from the cytosol into mitochondria (Lee et al., 2020). Long-chain acetylcarnitine was reported to be an essential source of energy production in cancer cells (Linher-Melville et al., 2011). In recent years, acetylcarnitine has attracted much attention in tumor research (Fong et al., 2011). Several studies have carried out metabolomics analysis to compare patients with hepatocellular carcinoma and healthy individuals. The findings revealed that it was increased in serum of patients with hepatocellular cancer (Ladep et al., 2014; Li et al., 2017; Lee et al., 2020). Lu et al. (2016) also suggested that serum acetylcholine could be regarded as a new indicator of hepatocellular carcinoma. In addition, differences in acetylcarnitine levels were observed among different breast cancer subtypes (Fan et al., 2016). Conversely, given that advanced stages of hepatocellular carcinoma usually impelled patients to be prone to cachexia, serum acetylcarnitine levels declined accordingly for reduced carnitine synthesis in hepatocellular carcinoma patients (Lee et al., 2020), which was commonly seen in the terminal phase of patients with digestive system neoplasms (Malaguarnera et al., 2006). Acetylcarnitine in our study was higher in the IVL group than in the control group, and it functioned as a hazardous factor in the progression of IVL. Based on these theories, it was reasonable to believe that acetylcarnitine became elevated as the disease progressed by promoting energy production in the lesions.

Glycerophosphocholine is one of the intermediates of choline metabolism (Kinross et al., 2009). Abnormal choline phospholipid metabolism has been verified to be associated with carcinogenesis and tumor progression (Zhang X. et al., 2016). Besides, variations have been found in choline phospholipid metabolism, which could be observed among several types of cancers (Glunde et al., 2011). Similar to previous studies, our data showed that IVL patients had lower levels of glycerophosphocholine, a metabolite of choline, than the healthy controls, suggesting that abnormal choline and carbon metabolism might contribute to oncogenesis. As reported, when choline is oxidized to betaine (trimethylglycine), it participates in methylation, which is not only necessary for the methionine/homocysteine cycle but also plays a central role in choline-mediated carbon metabolism (it donates a methyl group for methionine and dimethylglycine remethylation of homocysteine) (Zhang X. et al., 2016). Choline can also be metabolized by intestinal bacteria to produce trimethylamine, which is then further transformed into trimethyl-amine N-oxide (Glunde et al., 2006). Compared with normal tissues, tumor tissues tended to present an abnormal choline phospholipid metabolic spectrum, characterized by abnormally high levels of choline-containing compounds. This eventually led to a decrease in these compounds in blood.

Regarding hydrocortisone (cortisol), it is the major endogenous glucocorticoid secreted by the adrenal cortex (Marik, 2009). As a glucocorticoid receptor agonist, hydrocortisone is involved in protein catabolism, gluconeogenesis, capillary wall stability, renal excretion of calcium, and suppression of immune or inflammatory responses. Furthermore, studies have validated that cortisol also exhibits special significance in some tumors; that is, as cancer progresses, cortisol secretion increases abnormally in cancers such as breast cancer, lung cancer and oral squamous cell carcinoma, which is not relative to the tumor tissue type (Lichter and Sirett, 1975; van der Pompe et al., 1996; McEwen et al., 1997; Lissoni et al., 2007; Sharma et al., 2018). In our experiment, cortisol levels could distinguish the IVL group from the control group, and the cortisol concentration in the IVL-re group was significantly higher than that in the IVL-no group, which revealed that cortisol might be associated with the recurrence of IVL.

Here, metabolomics and comprehensive bioinformatics analyses were combined to distinguish metabolites between patients with IVL and healthy controls. The aim was to determine the metabolic characteristics of IVL and improve the understanding of IVL development and the related prognosis. However, the limitations of the current study need to be pointed out either, that more cases of IVL patients should be recruited from multiple clinical centers to validate the reliability and feasibility of the model in the future application. Besides, it really makes much sense to distinguish the potential alteration or similarity in the metabolic hallmarks between solid tissues and serum samples from IVL patients given that tumors are characterized by peculiar internal environment and metabolic patterns.

CONCLUSION

We found that metabolomics based on HPLC-MS/MS could efficaciously differentiate IVL patients from healthy subjects. This study characterized the serum metabolomics pattern of IVL. Ultimately, we developed a four-metabolite-based panel that was closely correlated with the progression of IVL. Among them, hypoxanthine, and glycerophosphocholine performed as underlying protective indicators, which decreased as the disease progressed. Conversely, acetylcarnitine and hydrocortisone (cortisol) were proved to be risk factors, augmenting with the oncogenesis and recurrence of IVL, further confirmed based on the multi-class ROC analysis. Thus, the abnormal metabolism and relevant metabolite differences in this study provided valuable evidence for developing novel non-invasive methods concerning the diagnosis and prognosis of IVL based on these potential biomarkers.

DATA AVAILABILITY STATEMENT

The datasets presented in this study can be found in online repositories. The names of the repository/repositories and accession number(s) can be found below: MetaboLights (https://www.ebi.ac.uk/metabolights/). The identifier of this study is MTBLS2714.

ETHICS STATEMENT

The studies involving human participants were reviewed and approved by the Ethics Committee of Peking Union Medical College Hospital (Ethics: JS-2654). The patients/participants provided their written informed consent to participate in this study.

AUTHOR CONTRIBUTIONS

ZG and PF: software, data curation, formal analysis, and visualization. ZG, PF, and ZZ: writing-original draft preparation and writing-review and editing. JL and QY: conceptualization and design, and administration and funding acquisition. All authors contributed to the article and approved the submitted version.

FUNDING

This work was supported by grants from the National Natural Science Foundation of China (grant number 61971448) and the Non-profit Central Research Institute Fund of Chinese Academy of Medical Sciences (grant number 2020-PT320-003).

ACKNOWLEDGMENTS

The authors would like to thank AJE (https://www.aje.cn/) for English language editing.

SUPPLEMENTARY MATERIAL

The Supplementary Material for this article can be found online at: https://www.frontiersin.org/articles/10.3389/fcell.2021.695540/full#supplementary-material

Supplementary Figure 1 | Quality control analysis of the project. **(A,B)** Total ion chromatogram of all samples along with quality controls in positive and negative modes, respectively. The abscissa represented the retention time of each chromatographic peak, and the ordinate represented the peak intensity. **(C,D)** Principal component analysis of all samples PCA in the positive and negative modes, respectively.

REFERENCES

Alonso, A., Marsal, S., and Julia, A. (2015). Analytical methods in untargeted metabolomics: state of the art in 2015. *Front. Bioeng. Biotechnol.* 3:23. doi: 10.3389/fbioe.2015.00023

Barberini, L., Noto, A., Fattuoni, C., Satta, G., Zucca, M., Cabras, M. G., et al. (2019). The Metabolomic Profile of Lymphoma Subtypes: A Pilot Study. *Molecules* 24:2367.

Buza, N., Xu, F., Wu, W., Carr, R. J., Li, P., and Hui, P. (2014). Recurrent chromosomal aberrations in intravenous leiomyomatosis of the uterus: high-resolution array comparative genomic hybridization study. *Hum. Pathol.* 45, 1885–1892. doi: 10.1016/j.humpath.2014.05.010

Christodoulou, C. C., Zachariou, M., Tomazou, M., Karatzas, E., Demetriou, C. A., Zamba-Papanicolaou, E., et al. (2020). Investigating the Transition of Pre-Symptomatic to Symptomatic Huntington's Disease Status Based on Omics Data. *Int. J. Mol. Sci.* 21:7414. doi: 10.3390/ijms21197414

Deng, Y., Dong, S., and Song, B. (2020). Surgical Strategy for Intravenous Cardiac Leiomyomatosis. *Heart Lung Circ.* 30, 240–246. doi: 10.1016/j.hlc.2020.07.006

Eliassen, A. H., Zeleniuch-Jacquotte, A., Rosner, B., and Hankinson, S. E. (2016). Plasma Anti-Müllerian Hormone Concentrations and Risk of Breast Cancer among Premenopausal Women in the Nurses' Health Studies. *Cancer Epidemiol. Biomarkers Prev.* 25, 854–860. doi: 10.1158/1055-9965.epi-15-1240

Fan, Y., Zhou, X., Xia, T. S., Chen, Z., Li, J., Liu, Q., et al. (2016). Human plasma metabolomics for identifying differential metabolites and predicting molecular subtypes of breast cancer. *Oncotarget* 7, 9925–9938. doi: 10.18632/oncotarget.7155

Farshidfar, F., Weljie, A. M., Kopciuk, K. A., Hilsden, R., McGregor, S. E., Buie, W. D., et al. (2016). A validated metabolomic signature for colorectal cancer: exploration of the clinical value of metabolomics. *Br. J. Cancer* 115, 848–857. doi: 10.1038/bjc.2016.243

Fong, M. Y., McDunn, J., and Kakar, S. S. (2011). Identification of metabolites in the normal ovary and their transformation in primary and metastatic ovarian cancer. *PLoS One* 6:e19963. doi: 10.1371/journal.pone.0019963

Glunde, K., Bhujwalla, Z. M., and Ronen, S. M. (2011). Choline metabolism in malignant transformation. *Nat. Rev. Cancer* 11, 835–848. doi: 10.1038/nrc3162

Glunde, K., Jacobs, M. A., and Bhujwalla, Z. M. (2006). Choline metabolism in cancer: implications for diagnosis and therapy. *Expert Rev. Mol. Diagn.* 6, 821–829. doi: 10.1586/14737159.6.6.821

Gui, T., Qian, Q., Cao, D., Yang, J., Peng, P., and Shen, K. (2016). Computerized tomography angiography in preoperative assessment of intravenous leiomyomatosis extending to inferior vena cava and heart. *BMC Cancer* 16:73. doi: 10.1186/s12885-016-2112-9

Jung, J., Jung, Y., Bang, E. J., Cho, S. I, Jang, Y. J., Kwak, J. M., et al. (2014). Noninvasive diagnosis and evaluation of curative surgery for gastric cancer by using NMR-based metabolomic profiling. *Ann. Surg. Oncol.* 21, S736–S742.

Kinross, J., Warren, O., Basson, S., Holmes, E., Silk, D., Darzi, A., et al. (2009). Intestinal ischemia/reperfusion injury: defining the role of the gut microbiome. *Biomark. Med.* 3, 175–192. doi: 10.2217/bmm.09.11

Knight, J., Phillips, D. P., Esper, S. A., Zeh, H. J., Badhwar, V., and Subramaniam, K. (2017). Paradoxical Tumor Embolism and Recurrent Intracardiac Mass From Uterine Intravenous Leiomyomatosis. *J. Cardiothorac. Vasc. Anesth.* 31, 642–645. doi: 10.1053/j.jvca.2016.05.013

Kong, L. Y., Chen, L. L., Xiang, W., and Liu, F. (2020). Intravenous Leiomyomatosis With Paradoxical Embolism: Unusual Presentation of Uterine Leiomyoma. *Circ. Cardiovasc. Imaging* 13:e009930.

Kuklik, E., Drelich-Zbroja, A., Kuczynska, M., Szmygin, M., Grzycka, L., and Jargiello, T. (2020). Intravenous leiomyomatosis as an unusual cause of misdiagnosis of deep vein thrombosis. *Pol. Arch. Intern. Med.* 131, 75–77. doi: 10.1016/j.ejvsextra.2007.02.006

Ladep, N. G., Dona, A. C., Lewis, M. R., Crossey, M. M., Lemoine, M., Okeke, E., et al. (2014). Discovery and validation of urinary metabotypes for the diagnosis of hepatocellular carcinoma in West Africans. *Hepatology* 60, 1291–1301. doi: 10.1002/hep.27264

Lee, C. W., Yu, M. C., Lin, G., Chiu, J. C., Chiang, M. H., Sung, C. M., et al. (2020). Serum metabolites may be useful markers to assess vascular invasion and identify normal alpha-fetoprotein in hepatocellular carcinoma undergoing liver resection: a pilot study. *World J. Surg. Oncol.* 18:121.

Li, H., Fan, S. F., Wang, Y., Shen, S. G., and Sun, D. X. (2017). Rapid Detection of Small Molecule Metabolites in Serum of Hepatocellular Carcinoma Patients Using Ultrafast Liquid Chromatography-Ion Trap-Time of Flight Tandem Mass Spectrometry. *Anal. Sci.* 33, 573–578. doi: 10.2116/analsci.33.573

Lichter, I., and Sirett, N. E. (1975). Serial measurement of plasma cortisol in lung cancer. *Thorax* 30, 91–94. doi: 10.1136/thx.30.1.91

Linher-Melville, K., Zantinge, S., Sanli, T., Gerstein, H., Tsakiridis, T., and Singh, G. (2011). Establishing a relationship between prolactin and altered fatty acid beta-oxidation via carnitine palmitoyl transferase 1 in breast cancer cells. *BMC Cancer* 11:56. doi: 10.1186/1471-2407-11-56

Lissoni, P., Brivio, F., Fumagalli, L., Messina, G., Secreto, G., Romelli, B., et al. (2007). Immune and endocrine mechanisms of advanced cancer-related hypercortisolemia. *In Vivo* 21, 647–650.

Long, Y., Sanchez-Espiridion, B., Lin, M., White, L., Mishra, L., Raju, G. S., et al. (2017). Global and targeted serum metabolic profiling of colorectal cancer progression. *Cancer* 123, 4066–4074. doi: 10.1002/cncr.30829

Low, G., Rouget, A. C., and Crawley, C. (2012). Case 188: Intravenous leiomyomatosis with intracaval and intracardiac involvement. *Radiology* 265, 971–975. doi: 10.1148/radiol.12111246

Lu, B., Liu, Q., Tang, L., Ma, Y., and Shi, H. (2020). Intravenous leiomyomatosis: molecular analysis of 17 cases. *Pathology* 52, 213–217. doi: 10.1016/j.pathol.2019.10.009

Lu, Y., Li, N., Gao, L., Xu, Y. J., Huang, C., Yu, K., et al. (2016). Acetylcarnitine Is a Candidate Diagnostic and Prognostic Biomarker of Hepatocellular Carcinoma. *Cancer Res.* 76, 2912–2920. doi: 10.1158/0008-5472.can-15-3199

Ma, G., Miao, Q., Liu, X., Zhang, C., Liu, J., Zheng, Y., et al. (2016). Different surgical strategies of patients with intravenous leiomyomatosis. *Medicine* 95:e4902. doi: 10.1097/md.0000000000004902

Malaguarnera, M., Risino, C., Gargante, M. P., Oreste, G., Barone, G., Tomasello, A. V., et al. (2006). Decrease of serum carnitine levels in patients with or without gastrointestinal cancer cachexia. *World J. Gastroenterol.* 12, 4541–4545. doi: 10.3748/wjg.v12.i28.4541

Marik, P. E. (2009). Critical illness-related corticosteroid insufficiency. *Chest* 135, 181–193. doi: 10.1378/chest.08-1149

Marshall, J. F., and Morris, D. S. (1959). Intravenous leiomyomatosis of the uterus and pelvis: case report. *Ann. Surg.* 149, 126–134. doi: 10.1097/00000658-195901000-00017

McEwen, B. S., Biron, C. A., Brunson, K. W., Bulloch, K., Chambers, W. H., Dhabhar, F. S., et al. (1997). The role of adrenocorticoids as modulators of immune function in health and disease: neural, endocrine and immune interactions. *Brain Res. Brain Res. Rev.* 23, 79–133. doi: 10.1016/s0165-0173(96)00012-4

Ordulu, Z., Chai, H., Peng, G., McDonald, A. G., De Nictolis, M., Garcia-Fernandez, E., et al. (2020). Molecular and clinicopathologic characterization of intravenous leiomyomatosis. *Mod. Pathol.* 33, 1844–1860. doi: 10.1038/s41379-020-0546-8

Price, J. D., Anagnostopoulos, C., Benvenisty, A., Kothuru, R. K., and Balaram, S. K. (2017). Intracardiac Extension of Intravenous Leiomyomatosis. *Ann. Thorac. Surg.* 103, e145–e147.

Ribeiro, V., Almeida, J., Madureira, A. J., Lopez, E., Machado, L., Albuquerque, R., et al. (2013). Intracardiac leiomyomatosis complicated by pulmonary embolism: a multimodality imaging case of a rare entity. *Can. J. Cardiol.* 29, e1–e3.

Sharma, P., Sandhu, S. V., Bhandari, R., Verma, I., Bhullar, R. K., and Khangura, R. K. (2018). Estimation of cortisol levels in patients with premalignant disorders and oral squamous cell carcinoma. *J. Oral. Maxillofac. Pathol.* 22, 27–34.

Shi, T., and Shkrum, M. J. (2018). A Case Report of Sudden Death From Intracardiac Leiomyomatosis. *Am. J. Forensic Med. Pathol.* 39, 119–122. doi: 10.1097/paf.0000000000000377

Spanuchart, I., Satitthummanid, S., Cheanvechai, C., Chantranuwatana, P., Trivijitsilp, P., Chattranukulchai, P., et al. (2012). Intracardiac and intravenous leiomyomatosis. *J. Am. Coll. Cardiol.* 60:e27.

Tayanloo-Beik, A., Sarvari, M., Payab, M., Gilany, K., Alavi-Moghadam, S., Gholami, M., et al. (2020). OMICS insights into cancer histology; Metabolomics and proteomics approach. *Clin. Biochem.* 84, 13–20. doi: 10.1016/j.clinbiochem.2020.06.008

van der Pompe, G., Antoni, M. H., and Heijnen, C. J. (1996). Elevated basal cortisol levels and attenuated ACTH and cortisol responses to a behavioral challenge in women with metastatic breast cancer. *Psychoneuroendocrinology* 21, 361–374. doi: 10.1016/0306-4530(96)00009-1

Virzi, G., Ragazzi, S., Bussichella, F., D'Agati, P., Caputo, S., Scaravilli, F., et al. (2007). Intravenous leiomyomatosis extending from the inferior caval vein to the pulmonary artery. *J. Thorac. Cardiovasc. Surg.* 133, 831–832. doi: 10.1016/j.jtcvs.2006.10.050

Wang, F. X., Chen, K., Huang, F. Q., Alolga, R. N., Ma, J., Wu, Z. X., et al. (2020). Cerebrospinal fluid-based metabolomics to characterize different types of brain tumors. *J. Neurol.* 267, 984–993. doi: 10.1007/s00415-019-09665-7

Wang, T. J., Larson, M. G., Vasan, R. S., Cheng, S., Rhee, E. P., McCabe, E., et al. (2011). Metabolite profiles and the risk of developing diabetes. *Nat. Med.* 17, 448–453.

Wang, W., Wang, Y., Chen, F., Zhang, M., Jia, R., Liu, X., et al. (2020). Intravenous leiomyomatosis is inclined to a solid entity different from uterine leiomyoma based on RNA-seq analysis with RT-qPCR validation. *Cancer Med.* 9, 4581–4592. doi: 10.1002/cam4.3098

Wu, H., Xue, R., Dong, L., Liu, T., Deng, C., Zeng, H., et al. (2009). Metabolomic profiling of human urine in hepatocellular carcinoma patients using gas chromatography/mass spectrometry. *Anal. Chim. Acta.* 648, 98–104. doi: 10.1016/j.aca.2009.06.033

Xuan, Q., Ouyang, Y., Wang, Y., Wu, L., Li, H., Luo, Y., et al. (2020). Multiplatform Metabolomics Reveals Novel Serum Metabolite Biomarkers in Diabetic Retinopathy Subjects. *Adv. Sci.* 7:2001714. doi: 10.1002/advs.202001714

Yao, W., Gao, Y., and Wan, Z. (2017). Serum Metabolomics Profiling to Identify Biomarkers for Unstable Angina. *Biomed. Res. Int.* 2017:7657306.

Yoo, B. C., Kong, S. Y., Jang, S. G., Kim, K. H., Ahn, S. A., Park, W. S., et al. (2010). Identification of hypoxanthine as a urine marker for non-Hodgkin lymphoma by low-mass-ion profiling. *BMC Cancer* 10:55. doi: 10.1186/1471-2407-10-55

Yu, X., Fu, J., Cao, T., Huang, L., Qie, M., and Ouyang, Y. (2021). Clinicopathologic features and clinical outcomes of intravenous leiomyomatosis of the uterus. *Medicine* 100:e24228. doi: 10.1097/md.0000000000024228

Yu, X., Zhang, G., Lang, J., Liu, B., and Zhao, D. (2016). Factors Associated With Recurrence After Surgical Resection in Women With Intravenous Leiomyomatosis. *Obstet. Gynecol.* 128, 1018–1024. doi: 10.1097/aog.0000000000001718

Zhang, C., Liu, X., Ma, G., Zhang, H., Wang, C., Liu, J., et al. (2012). Pulmonary embolization as the primary clinical manifestation of intravenous leiomyomatosis with intracardiac extension. *Ann. Thorac. Surg.* 94:1012. doi: 10.1016/j.athoracsur.2012.02.019

Zhang, X., Shi, X., Lu, X., Li, Y., Zhan, C., Akhtar, M. L., et al. (2020). Novel Metabolomics Serum Biomarkers for Pancreatic Ductal Adenocarcinoma by the Comparison of Pre-, Postoperative and Normal Samples. *J. Cancer* 11, 4641–4651. doi: 10.7150/jca.41250

Zhang, X., Wu, L., Xu, R., Zhu, C., Ma, G., Zhang, C., et al. (2019). Identification of the molecular relationship between intravenous leiomyomatosis and uterine myoma using RNA sequencing. *Sci. Rep.* 9:1442.

Zhang, X., Zhu, X., Wang, C., Zhang, H., and Cai, Z. (2016). Non-targeted and targeted metabolomics approaches to diagnosing lung cancer and predicting patient prognosis. *Oncotarget* 7, 63437–63448. doi: 10.18632/oncotarget.11521

Zhang, Y., Clark, L. H., Sheng, X., and Zhou, C. (2016). Successful en bloc venous resection with reconstruction and subsequent radiotherapy for 2 consecutive recurrences of intravenous leiomyoma–a case report. *BMC Cancer* 16:6. doi: 10.1186/s12885-015-2045-8

Conflict of Interest: The authors declare that the research was conducted in the absence of any commercial or financial relationships that could be construed as a potential conflict of interest.

frontiers in Cell and Developmental Biology

ORIGINAL RESEARCH
published: 11 August 2021
doi: 10.3389/fcell.2021.722412

Cysteine Boosts Fitness Under Hypoxia-Mimicked Conditions in Ovarian Cancer by Metabolic Reprogramming

*Sofia C. Nunes[1,2], Cristiano Ramos[1,2], Inês Santos[1,2], Cindy Mendes[1,2], Fernanda Silva[1,2], João B. Vicente[3], Sofia A. Pereira[1], Ana Félix[1,2], Luís G. Gonçalves[3] and Jacinta Serpa[1,2]**

[1] Centro de Estudos de Doenças Crónicas, NOVA Medical School/Faculdade de Ciências Médicas, Universidade Nova de Lisboa, Lisbon, Portugal, [2] Instituto Português de Oncologia de Lisboa Francisco Gentil, Lisbon, Portugal, [3] Instituto de Tecnologia Química e Biológica António Xavier, Universidade Nova de Lisboa, Oeiras, Portugal

OPEN ACCESS

Edited by:
Maria E. Mycielska, University Medical Center Regensburg, Germany

Reviewed by:
Isabel Soto-Cruz, Universidad Nacional Autónoma de México, Mexico
Marie-Pierre Golinelli, UPR 2301 Institut de Chimie des Substances Naturelles (ICSN CNRS), France

***Correspondence:**
Jacinta Serpa
jacinta.serpa@nms.unl.pt

Specialty section:
This article was submitted to Molecular and Cellular Oncology, a section of the journal Frontiers in Cell and Developmental Biology

Received: *08 June 2021*
Accepted: *13 July 2021*
Published: *11 August 2021*

Citation:
Nunes SC, Ramos C, Santos I, Mendes C, Silva F, Vicente JB, Pereira SA, Félix A, Gonçalves LG and Serpa J (2021) Cysteine Boosts Fitness Under Hypoxia-Mimicked Conditions in Ovarian Cancer by Metabolic Reprogramming. Front. Cell Dev. Biol. 9:722412. doi: 10.3389/fcell.2021.722412

Among gynecologic malignancies, ovarian cancer is the third most prevalent and the most common cause of death, especially due to diagnosis at an advanced stage together with resistance to therapy. As a solid tumor grows, cancer cells in the microenvironment are exposed to regions of hypoxia, a selective pressure prompting tumor progression and chemoresistance. We have previously shown that cysteine contributes to the adaptation to this hypoxic microenvironment, but the mechanisms by which cysteine protects ovarian cancer cells from hypoxia-induced death are still to be unveiled. Herein, we hypothesized that cysteine contribution relies on cellular metabolism reprogramming and energy production, being cysteine itself a metabolic source. Our results strongly supported a role of xCT symporter in energy production that requires cysteine metabolism instead of hydrogen sulfide (H_2S) *per se*. Cysteine degradation depends on the action of the H_2S-synthesizing enzymes cystathionine β-synthase (CBS), cystathionine γ-lyase (CSE), and/or 3-mercaptopyruvate sulfurtransferase (MpST; together with cysteine aminotransferase, CAT). In normoxia, CBS and CSE inhibition had a mild impact on cysteine-sustained ATP production, pointing out the relevance of CAT + MpST pathway. However, in hypoxia, the concomitant inhibition of CBS and CSE had a stronger impact on ATP synthesis, thus also supporting a role of their hydrogen sulfide and/or cysteine persulfide-synthesizing activity in this stressful condition. However, the relative contributions of each of these enzymes (CBS/CSE/MpST) on cysteine-derived ATP synthesis under hypoxia remains unclear, due to the lack of specific inhibitors. Strikingly, NMR analysis strongly supported a role of cysteine in the whole cellular metabolism rewiring under hypoxia. Additionally, the use of cysteine to supply biosynthesis and bioenergetics was reinforced, bringing cysteine to the plateau of a main carbon sources in cancer. Collectively, this work supports that sulfur and carbon metabolism reprogramming underlies the adaptation to hypoxic microenvironment promoted by cysteine in ovarian cancer.

Keywords: carbon source, cysteine, hypoxia, ovarian cancer, hydrogen sulfide, cystine, bioenergetics, microenvironment

INTRODUCTION

Despite all the progresses developed in prevention and new treatment approaches, cancer corresponds to the second leading cause of death worldwide (Fitzmaurice et al., 2015). Ovarian cancer is not an exception to this scenario, being expected, in 2020, 0.28 million new cases and 0.18 million ovarian cancer deaths worldwide (Ferlay et al., 2013). The late diagnosis together with resistance to conventional therapy represent the major causes for the poor prognosis of this disease (Jayson et al., 2014).

Epithelial ovarian cancer (EOC) includes most (90%) ovarian malignancies (Bast et al., 2009; Desai et al., 2014) that can be classified based on histopathology and molecular/genetic features, being mainly classified as serous low-grade (LG-OSC, <5%) and high-grade (HG-OSC, 70%), endometrioid (OEC, 10%), clear cell (OCCC, 10%) and mucinous (OMC, 3%) (Prat, 2012; Reid et al., 2017).

As a solid tumor grows, cancer cells are exposed to varying oxygen tensions and to different degrees of hypoxia, being these oxygen fluctuations strongly linked to oxidative stress (Fruehauf and Meyskens, 2007; Saed et al., 2017) and known to be responsible for tumor progression and resistance to therapy (Vaupel and Mayer, 2007; Semenza, 2012). In ovarian cancer, oxidative stress was already associated with the pathogenesis of the disease (Senthil et al., 2004; Saed et al., 2017), indicating that ovarian cancer cells present mechanisms that allow them to cope with the harmful oxidative conditions. We disclosed that cysteine facilitates the adaptation of ovarian cancer cells to hypoxic environments and to carboplatin-induced death (Nunes et al., 2018a,b). Moreover, the relevance of cysteine in the clinical context of ovarian cancer was also corroborated, since ascitic fluid from ovarian cancer patients – an important compartment of tumor microenvironment – showed cysteine as the prevalent thiol and because cysteine levels were also altered in serum from patients with ovarian tumors (Nunes et al., 2018b). Cysteine role in cancer cells survival was already associated with its role as a precursor of the antioxidant glutathione (GSH) (Schnelldorfer et al., 2000; Balendiran et al., 2004; Lopes-Coelho et al., 2016) and due to hydrogen sulfide (H_2S) generation (Bhattacharyya et al., 2013; Szabo et al., 2013; Pan et al., 2015; Panza et al., 2015; Sen et al., 2015; Gai et al., 2016; Szczesny et al., 2016) by cysteine catabolism through the activity of the enzymes cystathionine β-synthase (CBS), cystathionine γ-lyase (CSE), and/or 3-mercapto-pyruvate sulfurtransferase (MpST) together with cysteine aminotransferase (CAT) (Wang, 2012; Kabil and Banerjee, 2014; Giuffrè and Vicente, 2018; Hipólito et al., 2020). CBS, CSE, and MpST also catalyze the cyst(e)ine-dependent production of cysteine persulfide (CysSSH), which in several (patho)physiological contexts affords protection from damaging cysteine oxidation (e.g., Filipovic et al., 2018; Zivanovic et al., 2019; Zuhra et al., 2021). Another recently proposed pathway linking cysteine catabolism with mitochondrial bioenergetics concerns the mitochondrial isoform of cysteinyl-tRNA synthase (CARS2), which converts cysteine into CysSSH and also incorporates persulfidated cysteine into nascent polypeptides (Akaike et al., 2017; Bianco et al., 2019). The uptake of cysteine by cells seems to be preferentially mediated by xCT, a member of the cystine-glutamate transporter xc- system, known to mediate the uptake of cystine, the oxidized form of cysteine (Sato et al., 2000). Interestingly, it was reported that xCT was associated with intracellular GSH level and with cisplatin resistance in human ovarian cancer cell lines (Okuno et al., 2003). More recently, xCT has been implicated as part of highly favorable metabolic cancer phenotype, presenting increased capacity of ATP generation amongst other features pivotal for cancer cells survival and chemoresistance (Polewski et al., 2016; Jourdain et al., 2021).

Here, we aimed to address the mechanism by which cysteine protects ovarian cancer cells from hypoxia-induced death, hypothesizing that in addition to its role as GSH precursor, cysteine contributes to cell bioenergetics and biosynthesis under hypoxic conditions, as both a donor of H_2S and as a carbon source. To test this hypothesis, we used two different ovarian cancer cell lines derived from two different histological types. ES2 cells correspond to an ovarian clear cell carcinoma (OCCC), an uncommon but highly chemoresistant histotype, and OVCAR3 cells correspond to a high-grade ovarian serous carcinoma (HG-OSC, the most frequent histotype), which usually acquires resistance during chemotherapy (Goff et al., 1996; Sugiyama et al., 2000; Cooke et al., 2011; Beaufort et al., 2014).

MATERIALS AND METHODS

Cell Culture

Cell lines from OCCC (ES2; CRL-1978) and HG-OSC (OVCAR-3; HTB-161) were obtained from American Type Culture Collection (ATCC). Cells were maintained at 37°C in a humidified 5% CO_2 atmosphere, and cultured in Dulbecco's Modified Eagle medium (DMEM, 41965-039, Gibco, Life Technologies), containing 4.5 g/L of D-glucose and 0.58 g/L of L-glutamine, 1% FBS (S 0615, Merck), 1% antibiotic-antimycotic (P06-07300, PAN Biotech) and 0.1% gentamicin (15750-060, Gibco, Life Technologies). Cells were exposed either to 0.402 mM L-cysteine (102839, Merck) and/or to hypoxia induced with 0.1 mM cobalt chloride ($CoCl_2$) (C8661, Sigma-Aldrich) as previously (Nunes et al., 2018a,b).

Prior to any experiment, cells were synchronized under starvation (culture medium without FBS) for 8 h at 37°C and 5% CO_2.

ATP Quantification

To test the effect of xCT inhibition on ATP levels, cells (5×10^5 or 2.5×10^5 cells/well) were seeded in 6-well white plates in hypoxia-mimic conditions induced with 0.1 mM $CoCl_2$ and challenged with 0.25 mM sulfasalazine (S0883, Sigma), an xCT inhibitor (Gout et al., 2001). After 24 h, the medium was replaced and the challenging/stimulatory conditions reset. Cells were collected at 48 h after stimulation.

To test the effect of the enzymes involved in cysteine metabolism on ATP synthesis, cells (5×10^5 or 2.5×10^5 cells/well) were seeded in 6-well plates and cultured in control condition and exposed to 0.402 mM L-cysteine and/or 0.100 mM

$CoCl_2$. The previous conditions were combined with 1 mM O-(carboxymethyl)hydroxylamine hemihydrochloride (AOAA, C13408, Sigma) and 3 mM DL-propargylglycine (PAG, P7888, Sigma). AOAA is an inhibitor of both CBS and CSE, whereas PAG is selective toward CSE. After 24 h, the medium was replaced and the challenging/stimulatory conditions reset. Cells were collected at 16 and 48 h after stimulation. This assay was also performed with cell collection after 2 h of experimental conditions. In this case, 5×10^5 cells were seeded in 6-well white plates for both ES2 and OVCAR3 cells.

To investigate the effect of cyst(e)ine and NaHS (H_2S donor) on ATP synthesis upon xCT inhibition, cells (5×10^5 or 2.5×10^5 cells/well) were seeded in 6-well plates and exposed to hypoxia induced with 0.1 mM $CoCl_2$ with and without 0.402 mM L-cysteine combined with 0.25 mM sulfasalazine, 30 μM NaHS (161527 Sigma-Aldrich) or both. After 24 h, the medium was replaced and the challenging/stimulatory conditions reset. Cells were collected at 48 h after stimulation. This assay was also performed with cell collection after 1 h of experimental conditions. In this case, 5×10^5 cells were seeded in 6-well white plates for both ES2 and OVCAR3 cells.

Cells were scraped with cold PBS containing 2 mM EDTA and homogenized in 1% Non-idet P-40 (NP-40) lysis buffer (1% NP40 N-6507 Sigma, and 1× protease inhibitor, SIGMAFAST™ Protease inhibitor cocktail tablets S8830, Sigma) on ice for 30 min and centrifuged at 20,000 × *g* for 5 min at 4°C. Protein was quantified and the same amount of total protein was used within each assay, in a range between 2.5 and 10 μg. ATP determination kit (A22066, Molecular probes) was used in accordance with the manufacturer's instructions. The measurements were performed using the Luciferase protocol in a VIKTOR3 plate reader (PerkinElmer), using the Wallac 1420 software, version 3.0 (Luminometry, Luciferase FIR protocol). ATP concentration was determined against an ATP calibration curve, within the range between 0 and 30 μM.

Immunofluorescence Analysis

Cells (1×10^5 cells/well) were seeded in 24-well plates and cultured either in control or stimulated/challenged conditions. After 16 h of experimental conditions, cells were fixed with 4% paraformaldehyde for 15 min at 4°C and permeabilized with saponin 0.1% in PBS-BSA (PBS buffer containing 0.5%, w/v, bovine serum albumin) for 15 min at room temperature. Cells were then incubated with anti-xCT (ab175186, abcam) for 30 min (diluted 1:100 in PBS-BSA) and incubated with secondary antibody for 2 h at room temperature (Alexa Fluor® 488 anti-rabbit, A-11034, Invitrogen) (1:1000 in PBS-BSA). The protocol was repeated for anti-TOMM20 (1:100 in PBS PBS-BSA; ab186734 from abcam) for 2 h at room temperature and incubated with secondary antibody for 2 h at room temperature (Alexa Fluor®594 anti-rabbit, A-11037, Invitrogen) (1:1000 in PBS-BSA).

The slides were mounted in VECTASHIELD media with 4′-6-diamidino-2-phenylindole (DAPI) (Vector Labs) and examined by standard fluorescence microscopy (Zeiss Imajer.Z1 AX10 microscope). Images were acquired and processed with CytoVision software.

Western Blotting Analysis of Mitochondria Extracts

Cells (7×10^6 cells/flask) were cultured in 150 cm^2 culture flasks and submitted to control condition and to 0.402 mM L-cysteine and/or 0.1 mM $CoCl_2$. Cells were collected after 16 h of experimental conditions, and mitochondria were isolated with the Mitochondria Isolation Kit for profiling cultured cells (MITOISO2, Sigma). Briefly, cells were scraped, centrifuged for 5 min at 600 × *g* and washed in ice cold PBS. The cell pellet was resuspended in 650 μL of Lysis Buffer, according to the manufacturer's instructions.

The mitochondrial lysates were centrifuged at 20,817 × *g* for 5 min at 4°C and total protein concentration was determined based on the Bradford method (500-0006, Bio Rad). Western blotting for xCT and TOMM20 detection was performed with 15 μg of total protein, whereas for MpST, 20 μg of total protein were used. TOMM20 was used as a mitochondrial endogenous control.

Total protein in SDS-PAGE gels was transferred to PVDF membranes by semi-dry transfer. Membranes were blocked with PBS-milk (PBS containing 5% non-fat skimmed powdered milk) incubated with anti-xCT (1:1000 in PBS-milk; ab175186 from abcam) or anti-MpST (1:250 in PBS-milk; HPA001240 from Sigma) at 4°C with stirring, overnight. The membranes were then washed three times, for 5 min, with PBS 1 × 0.1% (v/v) Tween 20, and further incubated with secondary antibody (anti-rabbit 1:5,000 in PBS-milk; 31460 from Thermo Scientific) for 2 h at room temperature. For the membrane that was previously incubated with xCT, the protocol was repeated for anti-TOMM20 (1:1000 in PBS 1x-Milk 5%; ab186734 from abcam).

Cell Death Analysis

To test whether the protective effect of cysteine under hypoxia was dependent on H_2S production, cells (1×10^5 cells/well) were seeded in 24-well plates. Cells were cultured in control condition and exposed to 0.402 mM L-cysteine and/or hypoxia induced with 0.1 mM $CoCl_2$, combined to 1 mM O-(carboxymethyl)hydroxylamine hemihydrochloride (AOAA, C13408, Sigma), to 3 mM of DL-propargylglycine (PAG, P7888, Sigma), or the combination of both. Cells were collected 16 h after stimulation.

Cells were harvested by centrifugation at 153 × *g* for 3 min, cells were incubated with 0.5 μL FITC-Annexin V (640906, BioLegend) in 100 μL annexin V binding buffer 1 × 10 mM HEPES (pH 7.4), 0.14 M sodium chloride (NaCl), 2.5 mM calcium chloride ($CaCl_2$) and incubated at room temperature and in the dark for 15 min. After incubation, samples were rinsed with 0.2% (w/v) BSA (A9647, Sigma) in PBS and centrifuged at 153 × *g* for 3 min. Cells were suspended in 200 μL of annexin V binding buffer 1× and 2.5 μL propidium iodide (50 μg/mL) were added. Acquisition was performed in a FACScalibur (Becton Dickinson). Data were analyzed with FlowJo software.

Nuclear Magnetic Resonance (NMR) Analysis

To address the metabolic effects of cysteine under normoxia and hypoxia in ES2 and OVCAR3 cells, the levels of several metabolites were measured by ^{1}H-NMR. Cells (6.5×10^6 cells) were seeded in 175 cm^2 culture flasks and cultured in control condition and exposed to 0.402 mM L-cysteine and/or hypoxia-mimicked conditions induced with 0.1 mM $CoCl_2$. Cells and supernatants were collected at 48 h after stimulation and stored at −20°C.

To follow all the metabolites directly derived from cysteine, cells (6.5×10^6 cells) were seeded in 175 cm^2 culture flasks and cultured in control condition and exposed to 0.402 mM L-cysteine and/or hypoxia induced with 0.1 mM $CoCl_2$. In this assay, a fully U-^{13}C-labeled L-cysteine (CLM-1868-PK, Cambridge Isotopes Laboratories, Inc.) was used. Cells were collected at 48 h after stimulation and supernatants were collected at 12, 24, 36, and 48 h of incubation and stored at −20°C.

Cell extracts were performed with methanol and chloroform to separate organic and aqueous phases. After cold methanol mixture (4 mL methanol/1 g weight pellet), two volumes (vol) of water were added, mixed, and incubated for 5 min on ice. Chloroform (1 vol) was then added to the sample and mixed. Finally, 1 vol of water was added and samples were incubated for 10 min on ice, following centrifugation at 1,699 × *g* for 15 min at 4°C. Aqueous (upper) and organic (lower) phases were collected. After extraction of solvents by evaporation, using a Speed Vac Plus Scllon, the samples were suspended on KPi buffer (50 mM, pH 7.4) in deuterated water (D_2O) with 4% (v/v) sodium azide (NaN_3) and 0.097 mM of 3-(trimethylsilyl)propionic-2,2,3,3-d4 (TSP). Culture supernatants were also diluted in this solution at 1:10 ratio. The 1H-NMR (noesypr1d), 13C-NMR (zgdc) and 13C-1H-HSQC (hsqcetgpsisp2) was obtained at 25°C in an Avance 500 II+ (Bruker) spectrometer operating at 500.133 MHz, equipped with a 5 mm TCI(F)-z H-C/N Prodigy cryo-probe. The chemical shifts in aqueous sample were referred to the TSP. Topspin 4.0.7 (Bruker) was used for acquisition and spectra analysis. Compound identification was performed by resorting to the Human Metabolome database (HMDB)[1] and Chenomx NMR suite software version 8.1 (Chenomx Inc.). Metabolites concentration was determined using Chenomx NMR suite software version 8.1 for 1H-NMR spectra (Chenomx Inc.). Quantification of the resonances in 13C-1H-HSQC spectra was done by calculate the 1D projections and integrate the resonances areas in Topspin 4.0.7, using the TSP resonance was reference.

Statistical Analysis

All data are presented as the mean ± SD with the exception of ^{1}H-NMR data, which are presented as the median with 25th to 75th percentiles. All the graphics were done using the PRISM software package (PRISM 6.0 for Mac OS X; GraphPad software, United States, 2013) and Microsoft Excel. Assays were performed with at least three biological replicates per treatment, with the exception of NMR assay with ^{13}C-labeled L-cysteine for which only two biological replicates were performed for the majority of treatments, and hence no statistical analysis was conducted. For comparisons of two groups, a two-tailed independent-samples *t*-test was used. For comparison of more than two groups, one-way analysis of variance (ANOVA) with Tukey's multiple-comparisons *post hoc* test was used. Statistical significance was established as $p < 0.05$. All statistical analyses were performed using the IBM Corp. Released 2013. IBM SPSS Statistics for Macintosh, Version 22.0. Armonk, NY: IBM Corp. software, with the exception of metabolic pathway analysis that was performed with MetaboAnalyst 4.0[2].

RESULTS

xCT Transporter Localizes in Ovarian Cancer Cells' Mitochondria and Its Inhibition Impairs ATP Production Under Hypoxia, Which Is Further Rescued by Cysteine Supplementation

We have previously reported that cysteine supplementation was able to protect ovarian cancer cells from hypoxia-induced death (Nunes et al., 2018a,b). Herein, we hypothesized that an increase in intracellular cysteine facilitates this adaptation to hypoxia by an increase in ATP production.

Results show that after 16 h of experimental conditions, for ES2 cells, ATP levels did not differ among hypoxia with and without cysteine supplementation, and were higher under hypoxia without cysteine compared to normoxia with cysteine ($p = 0.017$) (**Figure 1A**). With 48 h of experimental conditions, ATP levels were increased under hypoxia without cysteine compared both to hypoxia ($p = 0.018$) and normoxia ($p = 0.033$) with cysteine (**Figure 1A**).

In OVCAR3 cells, after 16 h of experimental conditions, no differences were observed among treatments (**Figure 1B**). However, with 48 h of experimental conditions, the results were identical to ES2 cells, where cells cultured under hypoxia without cysteine presented higher ATP levels compared both to normoxia ($p = 0.008$) and hypoxia ($p < 0.001$) with cysteine (**Figure 1B**).

Therefore, after 48 h of experimental conditions, we observed increased ATP levels in hypoxia-mimicked conditions, which were prevented by cysteine administration in both ES2 and OVCAR3 (**Figures 1A,B**). These results support that ovarian cancer cells exhibit alternative ways that allow sustaining energy production under hypoxic environments. Since cells cultured under hypoxia without cysteine supplementation also present cysteine in the medium (yet in lower concentrations), and also because cells cultured under hypoxia with cysteine reach higher cellular confluence levels compared to hypoxia without cysteine, we cannot, nevertheless, rule out a role of cysteine in ATP production. Therefore, we further explored the role of xCT, a member of the cystine-glutamate transporter xc^- system, known to mediate the uptake of cystine (Sato et al., 2000)

[1] http://www.hmdb.ca/

[2] https://www.metaboanalyst.ca/faces/home.xhtml

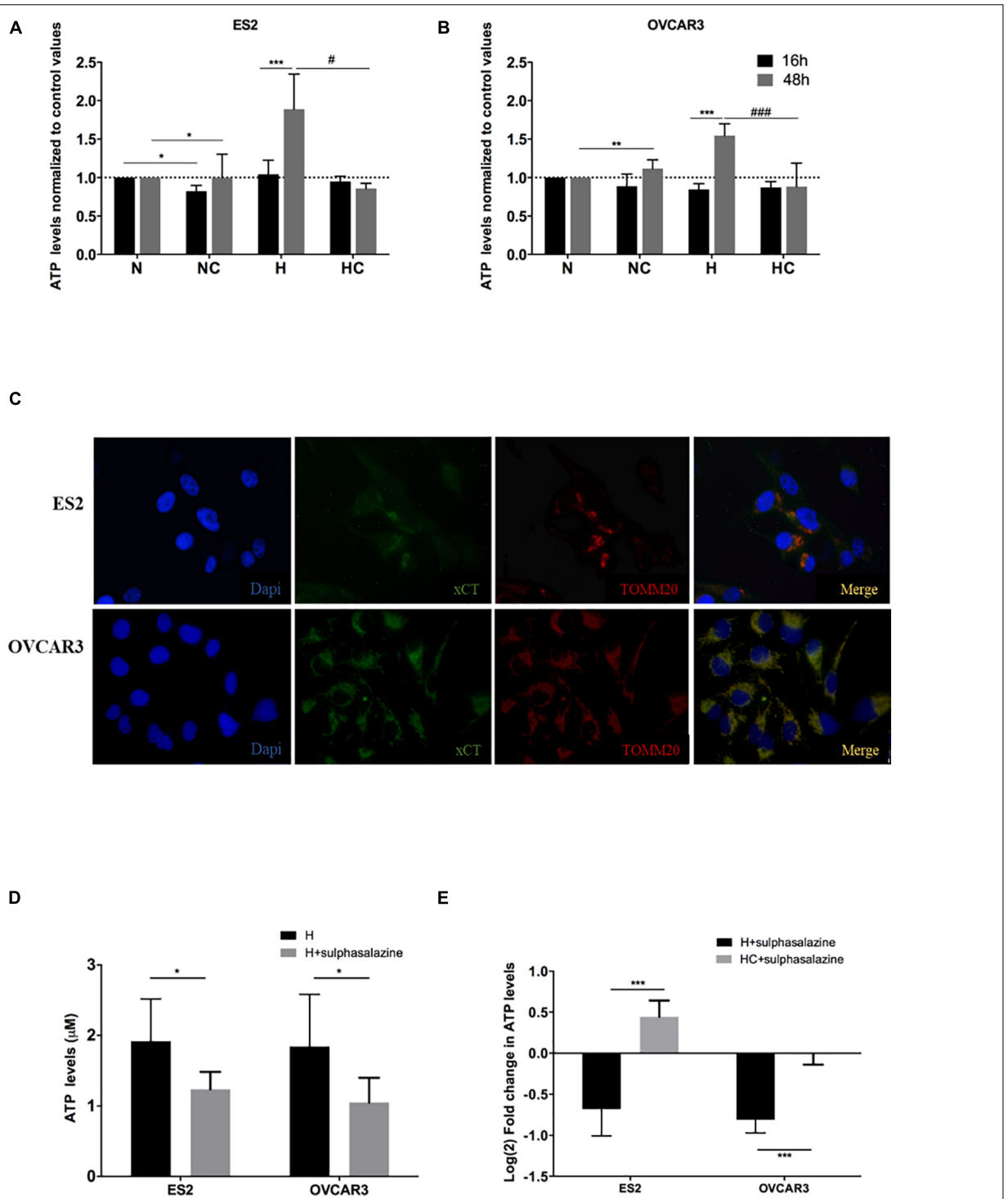

FIGURE 1 | xCT transporter localizes in ovarian cancer cells' mitochondria and its inhibition impairs ATP production under hypoxia, which is further rescued by cysteine. ATP levels normalized to control values (normoxia without cysteine supplementation) for 16 h and 48 h of experimental conditions for **(A)** ES2 cells and **(B)** OVCAR3 cells. The differences among treatments are pointed in the figure (one-way ANOVA with *post hoc* Tukey tests. For ES2, $n = 6$ for all treatments for 16 h of experimental conditions and $n = 3$ for 48 h of experimental conditions. For OVCAR3, $n = 6$ for all experimental conditions). **(C)** Immunofluorescence analysis for the xCT transporter and TOMM20 under control conditions (normoxia) for ES2 and OVCAR3 cells ($n = 3$). **(D)** ATP levels for 48 h of experimental conditions for ES2 and OVCAR3 cells under hypoxia and in the presence of the xCT inhibitor, sulfasalazine. **(E)** ATP levels for 48 h of experimental conditions for ES2 and OVCAR3 cells under hypoxia and in the presence of sulfasalazine and cysteine. The values were normalized to the respective control and $\log_2$ fold change was calculated. The differences among treatments are pointed in panels **(D,E)** (independent-samples *t*-test; $n = 6$ for all experimental conditions and for both cell lines). N, normoxia; NC, normoxia with cysteine; H, hypoxia; HC, hypoxia with cysteine. Results are shown as mean ± SD. $^{*/\#}p < 0.05$, $^{**/\#\#}p < 0.01$, $^{***/\#\#\#}p < 0.001$.

(the oxidized form of cysteine that is the predominant status of cysteine extracellularly), on ATP production under hypoxic environments. Thus, we started by addressing if this transporter could localize in ovarian cancer cells' mitochondria thus suggesting a role of cysteine metabolism in ATP production via xc^- system. Immunofluorescence analysis suggested a mitochondrial localization of xCT in both ES2 and OVCAR3 cells (**Figure 1C**) that was further confirmed by western blotting analysis mitochondrial extracts (**Supplementary Figure 1A**). Interestingly, by western blotting with anti-TOMM20 (a mitochondrial marker) results show that ES2 cells present higher levels of TOMM20 under hypoxia compared to the other experimental conditions, whereas OVCAR3 cells seem to present the opposite tendency. As a consequence, the ratio xCT/TOMM20 was decreased under hypoxia-mimicked conditions in ES2 cells and increased in OVCAR3 cells (**Supplementary Figure 1A**).

We then explored the effect of xCT inhibition (with sulfasalazine) in the ability of ovarian cancer cells to produce ATP under hypoxia. Strikingly, xCT inhibition led to impaired ATP production in both cell lines ($p = 0.038$ for ES2 and $p = 0.010$ for OVCAR3) (**Figure 1D**). Importantly, cysteine was able to rescue this impaired ATP production upon xCT inhibition. Hence, we observed a significant increase in ATP levels upon cysteine supplementation ($p < 0.001$) (**Figure 1E**).

CBS and CSE Inhibition Does Not Impair ATP Synthesis but Induces Cell Death in ES2 Cells

Since results suggested that cysteine has a role in ATP synthesis mediated by the xCT transporter, we next measured ATP levels upon CBS and CSE inhibition. Results have shown that after 16 h of experimental conditions, no differences were found in ATP levels with or without CSE (PAG) and CBS/CSE inhibitors (AOAA) for both ES2 and OVCAR3 cells in any culture condition (**Figures 2A–D**). As in **Figure 1**, prolonged (48 h) exposure to hypoxia of both ES2 and OVCAR3 cells resulted in increased ATP production. However, under the same conditions, cysteine decreased ATP levels in both cell lines. Given the dual nature of H_2S as an electron supply for the mitochondrial ETC at low concentrations, or as an inhibitor of Complex IV at higher levels, this observation further suggests that exogenous cysteine affects ATP production via CBS/CSE-catalyzed H_2S production.

Strikingly, upon exposure to CBS/CSE inhibitors for 48 h, increased ATP levels were observed in all experimental conditions for both ES2 (N $p = 0.002$, NC $p = 0.001$, H $p = 0.004$, HC $p = 0.001$) and OVCAR3 cells (N, NC and HC $p < 0.0001$ and H $p = 0.003$) with respect to their respective controls (48 h, no inhibitors; **Figures 2A–D**). In both cell lines exposed for 48 h to CBS/CSE inhibitors, hypoxia decreased significantly ATP production as compared to normoxia, but cysteine rescued this phenomenon (**Figures 2B,D**). These observations support the relevance of cysteine degradation on ATP production under hypoxia and put forward the possibility of a compensatory mechanism, e.g., via CAT/MpST or CARS2 to sustain H_2S/CysSSH production under hypoxic conditions.

As ATP levels may increase under stressful conditions (e.g., Zhou et al., 2012) we investigate if there was an increase of cell death in the presence of CSE (PAG) and CBS + CSE (AOAA) inhibitors. We found that for ES2 cells, under normoxia both with and without cysteine supplementation (N and NC), CSE inhibition induced more cell death compared to joint CSE/CBS inhibition ($p = 0.017$) (**Figure 2E**). Under hypoxia (H), the combination of both inhibitors induced more cell death compared to their separate administration ($p < 0.001$). Interestingly, under hypoxia with cysteine, PAG alone resulted in increased cell death ($p = 0.038$ compared to the control) as well as in combination with AOAA ($p = 0.002$ compared to the control and $p = 0.01$ compared to AOAA alone) (**Figure 2E**). Regarding OVCAR3 cells, no differences were observed among treatments, with or without the inhibitors and/or cysteine (**Figure 2F**).

Together, results indicate that CBS and CSE inhibition, at least at the used doses, is not sufficient to impair ATP production but the inhibition of both enzymes affected ATP synthesis mainly under hypoxia for both cell lines. The role of MpST could not be addressed as no specific inhibitor is available.

Moreover, ES2 cells showed reduced viability upon the inhibition of both CBS and CSE under hypoxia-mimicked conditions, showing that ES2 cells are especially sensitive to the inhibition of these enzymes in this experimental condition, highlighting their role in hypoxia adaptation and the contribution of cysteine non-oxidative catabolism for cell survival in conditions of hypoxic stress.

Cysteine Degradation Is Necessary to Rescue ATP Production Triggered by xCT Inhibition

Since results have suggested that cysteine has a role in ATP production under hypoxia-mimicked conditions that can be in part related to H_2S synthesis, we investigated if the impact of cysteine on ATP production rely on CBS/CSE-catalyzed H_2S production. For that we ascertained if cysteine metabolism was necessary or if a bolus addition of an H_2S donor, as NaHS, would be sufficient to counteract the ATP impairment triggered by xCT inhibition, both at short (1 h) and long (48 h) exposure times.

Due to the unstable nature of NaHS that was reported in culture medium (Sun et al., 2017) leading to an instant release of H_2S that decays rapidly (Hu et al., 2011), we evaluated ATP levels upon NaHS exposure for 1 h in the experimental conditions tested before. Fu et al. (2012) have reported that in vascular smooth-muscle cells, 1 h of NaHS exposure was sufficient to alter mitochondrial ATP production under hypoxia in a concentration-dependent manner, consistently with the dual stimulatory/inhibitory nature of H_2S for mitochondrial bioenergetics.

In hypoxic ES2 cells, within 1 h of conditions, while sulfasalazine alone tended to promote a slight increase in ATP (**Figure 3A**), 30 μM NaHS alone led to decreased ATP levels ($p = 0.047$) (**Figure 3C**), even upon xCT inhibition (H NaHS vs. H sulfasalazine $p < 0.001$; H NaHS + sulfasalazine vs. H sulfasalazine $p < 0.001$; HC NaHS vs. HC sulfasalazine $p = 0.002$; HC NaHS + sulfasalazine vs. HC sulfasalazine

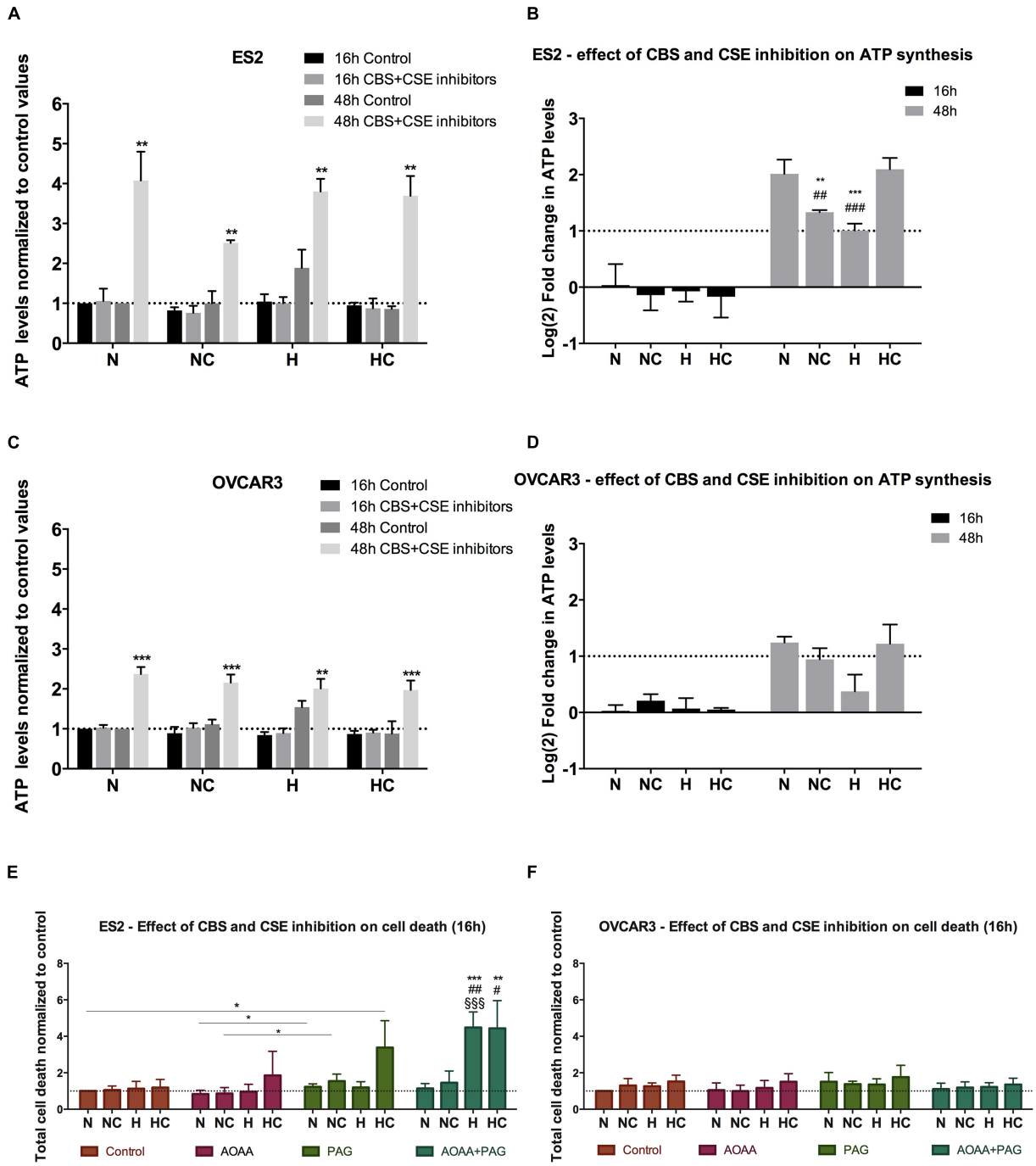

FIGURE 2 | CBS and CSE inhibition does not impair ATP synthesis in ovarian cancer cells but affect ES2 cells survival, mainly in hypoxia-mimicked conditions. **(A–D)** ATP levels in the presence of 1 mM AOOA and 3 mM PAG for 16 h and 48 h of experimental conditions for ES2 [**A** – values normalized to control (normoxia without cysteine and without inhibitors) and **(B)** – values normalized to the respective control and $\log_2$ fold change calculation] and OVCAR3 [**C** – values normalized to control (normoxia without cysteine and without inhibitors) and **(D)** – values normalized to the respective control and $\log_2$ fold change calculation] cells. **(A,C)** The asterisks (*) represent the statistical significance compared to the respective control. **(B,D)** The asterisks (*) represent the statistical significance compared to N, the section symbols (§) represents the statistical significance compared to NC and the cardinals (#) represent statistical significance compared to HC. For ES2, $n = 6$ for all treatments for 16 h of experimental conditions and $n = 3$ for 48 h of experimental conditions. For OVCAR3, $n = 6$ for all experimental conditions. **(E,F)** Cell death levels in the control condition, in the presence of CBS/CSE inhibitor (1 mM AOAA), CSE inhibitor (3 mM PAG) or both inhibitors for ES2 **(E)** and OVCAR3 **(F)** cells. The asterisks (*) represent statistical significance between the respective treatments or between AOAA + PAG and its control, the cardinals (#) represent statistical significance between AOAA + PAG and AOAA alone and the section symbols (§) represent statistical significance between AOAA + PAG and PAG alone. For both cell lines, at least $n = 6$ were performed for all experimental conditions. N, normoxia; NC, normoxia with cysteine; H, hypoxia; HC, hypoxia with cysteine. Results are shown as mean ± SD. *$p < 0.05$, **$p < 0.01$, ***$p < 0.001$ [**(A,C)** independent-samples *t*-test; **(B,D–F)** one-way ANOVA with *post hoc* Tukey tests].

$p < 0.001$) **(Figure 3A)**. In addition, under hypoxia with cysteine supplementation, NaHS did not affect ATP production **(Figure 3C)**. For OVCAR3 cells, NaHS led to decreased ATP levels both under hypoxia with ($p = 0.002$) and without cysteine ($p = 0.003$) **(Figure 3C)**, but no further differences were observed among treatments **(Figure 3B)**. Furthermore, while 1 h of sulfasalazine was not sufficient to inhibit ATP levels in ES2 cells, there was a tendency for lower ATP levels in OVCAR3 cells **(Figures 3A,B)**, suggesting that ES2 present higher basal levels of the xCT transporter or that these cells activate xCT (or other cysteine transporter) transcription in a more efficient way compared to OVCAR3 cells. In fact, in basal conditions, ES2 cells express higher xCT levels compared to OVCAR3 cells **(Supplementary Figure 1B)**, hence supporting that a more prolonged exposure to sulfasalazine is necessary for the effective blocking of xCT in ES2 cells.

While the 1 h of experimental conditions is suitable to study NaSH effects, may not allow enough cysteine metabolism to permit relevant H_2S production. In fact, with 48 h of experimental conditions, results have shown that whereas cysteine was able to revert the ATP impairment upon xCT inhibition in both ES2 and OVCAR3 cells ($p < 0.001$), NaHS alone (H_2S donor) was not, as no differences were found with sulfasalazine with or without NaHS, for both cell lines ($p > 0.05$). These results might indicate that H_2S by itself does not rescue ATP production, being cysteine degradation a requirement **(Figures 3D,E)**.

Cysteine Rescues Cellular Metabolism of Hypoxic ES2 Cells

In order to address the metabolic effects of cysteine supplementation under normoxia and hypoxia in ES2 and OVCAR3 cells, we measured the levels of several metabolites by ^{1}H-NMR (**Figures 4**, **5** and **Supplementary Figure 2**).

The intracellular metabolites were analyzed comparing the effect of cysteine in the metabolic profile of cells cultured in hypoxia with cells cultured in normoxia, in order to determine the variations in organic compounds driven by the presence of cysteine in both environments.

Regarding hypoxic ES2 cells, cysteine increased the intracellular levels of the amino acids alanine ($p = 0.009$), glutamate ($p = 0.012$), glycine ($p = 0.008$) and threonine ($p = 0.016$) **(Figure 4A)**. Cysteine also led to increased intracellular levels of lactate ($p = 0.021$) **(Figure 5B)**, choline ($p = 0.005$) and creatine ($p = 0.005$) **(Figure 4C)**. In the extracellular media (supernatants), Co^{2+} employed to elicit hypoxia reacted as expected with histidine and therefore precluded any conclusion regarding histidine uptake **(Supplementary Figure 2C)**. Cysteine decreased the release of fumarate under hypoxia ($p = 0.046$) **(Figure 4E)**.

Through metabolic pathway analysis, results predicted that nine metabolic pathways are significantly and differently altered in ES2 cells by cysteine and hypoxia. The analysis showed alteration in the biosynthetic pathways of: (1) glycine, serine and/threonine; (2) alanine, aspartate and glutamate; (3) glutamine and glutamate; (4) arginine and proline; (5) GSH; (6) primary bile acid; (7) glycerophospholipid; (8) aminoacyl-tRNA; and (9) purine nitrogen bases **(Figure 4G)**.

Regarding OVCAR3 cells, the only significant difference found on the effect of cysteine and hypoxia on intracellular metabolites concentration was on glucose levels, where there was a decrease in the intracellular levels of glucose ($p = 0.021$) **(Figure 5)**. However, cysteine and hypoxia also provided a general tendency for increased intracellular amino acids such as alanine, glutamate, tyrosine and valine **(Figure 5A)**. The measurement of the levels of these amino acids in the cell culture media showed that OVCAR3 cells uptake lower levels of alanine ($p = 0.023$) and proline ($p = 0.008$) and higher levels of glycine ($p = 0.013$) and phenylalanine ($p = 0.049$) due to the exposure to cysteine and hypoxia **(Figure 5D)**. Cysteine and hypoxia also decreased the release of 2-hydroxybutyrate ($p < 0.001$), formate ($p = 0.002$) and isobutyrate ($p < 0.001$) **(Figure 5E)**. As observed in ES2 cells, cysteine seemed to induce the release of glutamine, especially under normoxia **(Supplementary Figure 2C)**.

The metabolite pathway analysis was not performed for OVCAR3 cells because cysteine and hypoxia only altered significantly one metabolite (glucose), thus making this analysis inaccurate.

Importantly, in the absence of cysteine, hypoxia did not alter the intracellular and extracellular levels of glucose and lactate in both cell lines, whereas it led to a decreased uptake of glutamine ($p = 0.032$) and to an increased release of fumarate ($p = 0.041$) in OVCAR3 cells **(Supplementary Figure 2D)**.

Cysteine Supplies Crucial Metabolic Pathways in ES2 Cells, Under Normoxia and Hypoxia

To clarify the role of cysteine as a carbon source, we followed the metabolites directly derived from cysteine, by using ^{13}C-L-cysteine. Our results supported that ES2 cells convert cysteine into lactate **(Figures 6A,B)**. Whereas we observed the presence of satellite resonances indicating double ^{13}C-labeled lactate ($^{13}CH_3{}^{13}CH(OH)COOH$) in ES2 spectra, these were not observed in OVCAR3 **(Figure 6A)**. The presence of ^{13}C satellite resonances in the lactate is a direct result of ^{13}C-L-cysteine conversion into lactate. Furthermore, total (single and double-labeled) ^{13}C-lactate and the percentage of double-labeled ^{13}C-lactate tended to be higher under normoxia (NC ^{13}C and NC double ^{13}C, respectively) compared to hypoxia (HC ^{13}C and HC double ^{13}C, respectively) **(Figure 6B)**. We also observed that ES2 cells tended to consume glucose faster than OVCAR3 cells both under normoxia and hypoxia in the presence of cysteine **(Figure 6C)**.

Furthermore, our results indicated that ES2 cells convert cysteine mainly in GSH (GSH-CYS), lactate (Lac-3) and acetyl-CoA (A-CoA). Small amounts of alanine (Ala3) and glutamate (Glu4) and of other two unidentified compounds (Unk1 and Unk2) were also detected **(Figure 6D)**.

Finally, under normoxia, ES2 cells (ES2 NC) presented cysteine in solution instead of cystine, and produced different unknown compounds, while under hypoxia (ES2 HC) the main compound presented was cystine. In the case of OVCAR3

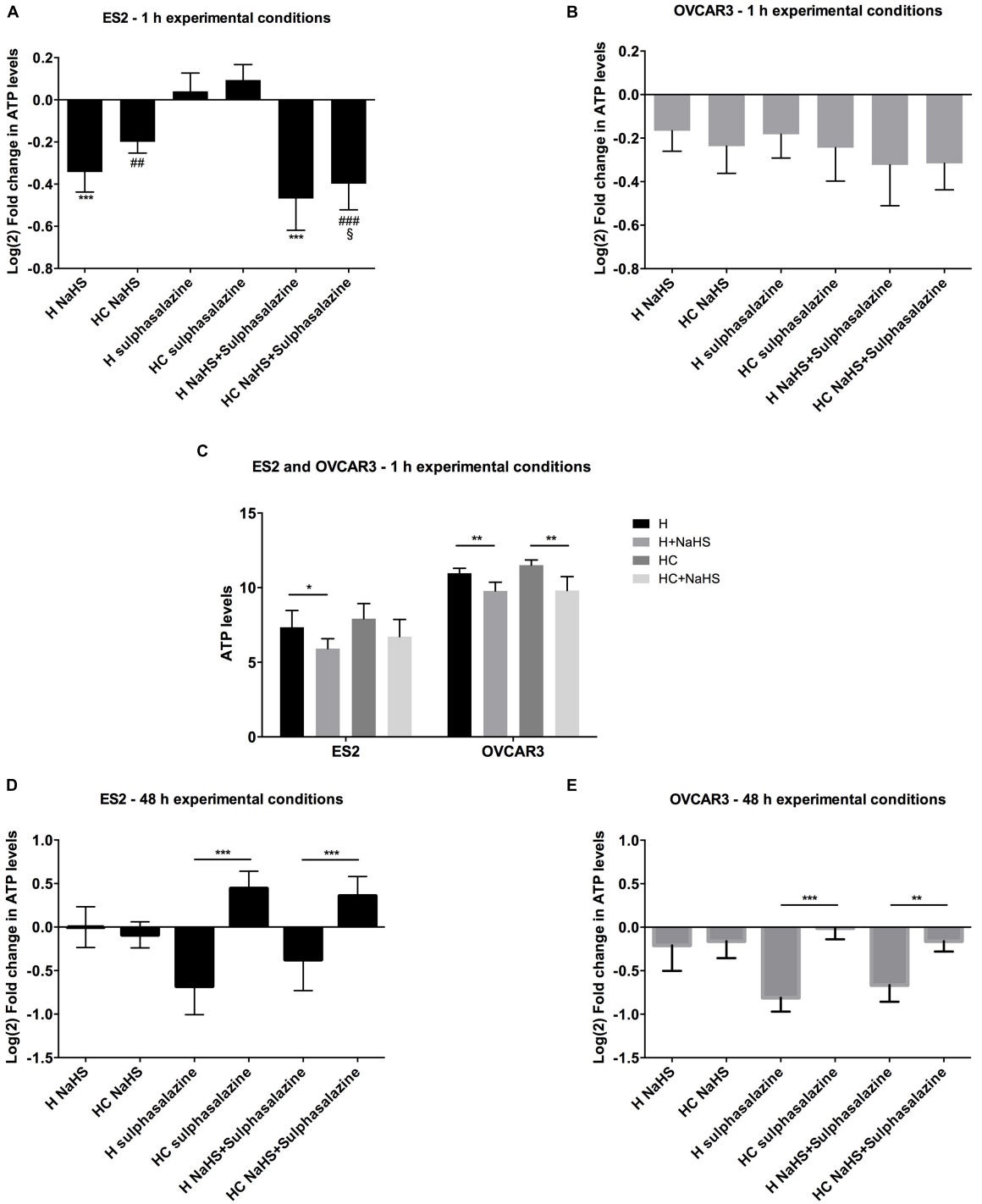

FIGURE 3 | Cysteine, but not NaHS, is able to rescue the ATP synthesis impairment, after 48 h under hypoxia triggered by xCT inhibition. **(A–C)** ATP levels for 1 h of experimental conditions for **(C)**. ES2 and OVCAR3 cells under hypoxia with and without cysteine and in the presence of the H2S donor, NaHS sulfasalazine in which $n = 5$ for ES2; and H sulfasalazine and H NaHS C sulfasalazine, in which $n = 5$ for OVCAR3. **(D,E)** ATP levels for 48 h of experimental (un-normalized data), and **(D)** ES2 and **(E)** OVCAR3 cells under hypoxia with and without cysteine supplementation and in the presence of the xCT inhibitor, conditions for **(A)** ES2 and **(B)** OVCAR3 cells under hypoxia with and without cysteine and in the presence of the xCT inhibitor, sulfasalazine and the H2S donor, NaHS. Data were normalized to the respective control condition (the same environmental condition H/HC without NaHS or sulfasalazine). Data are presented as log2 fold change ($n = 6$ for both cell lines). H, hypoxia; HC, hypoxia with cysteine. Results are shown as mean ± SD. $^{*/\#}p < 0.05$, $^{**/\#\#}p < 0.01$, and $^{***/\#\#\#}p < 0.001$ [one-way ANOVA with *post hoc* Tukey tests for **(A,B,D,E)** and independent-samples *t*-test for **(C)**].

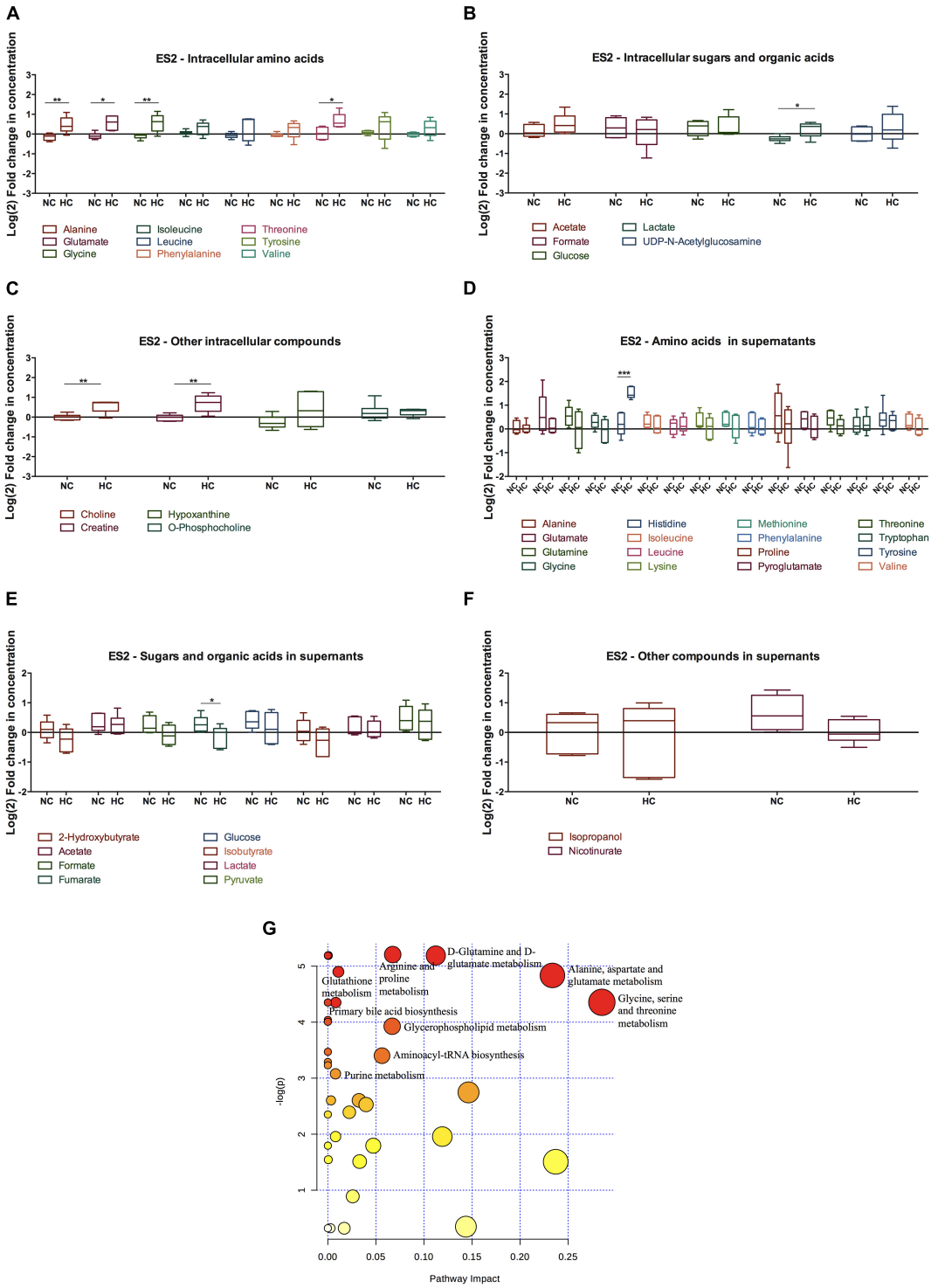

FIGURE 4 | Cysteine rescues ES2 cellular metabolism and impacts several metabolic pathways under hypoxia. **(A–F)** Metabolites levels for 48 h of experimental conditions for ES2 cells. **(A)** Intracellular amino acids; **(B)** intracellular sugars and organic acids; **(C)** other intracellular metabolites; **(D)** amino acids in supernatants; **(E)** sugars and organic acids in supernatants; **(F)** other metabolites in supernatants. Data were normalized to the respective control condition (the same environmental condition NC/N and HC/H). NC, normoxia with cysteine; HC, hypoxia with cysteine. Results are shown as median with 25th to 75th percentiles. $^{*}p < 0.05$, $^{**}p < 0.01$, $^{***}p < 0.001$ (independent-samples *t*-test: NC, $n = 6$; HC, $n = 5$). **(G)** Metabolic pathway analysis for the effect of cysteine under normoxia and hypoxia in intracellular ES2 metabolites. All the matched pathways are displayed as circles. The color and size of each circle are based on *p*-value and pathway impact value, respectively. The most impacted pathways having statistical significance ($p < 0.05$) are indicated. Source: https://www.metaboanalyst.ca/MetaboAnalyst/faces/home.xhtml.

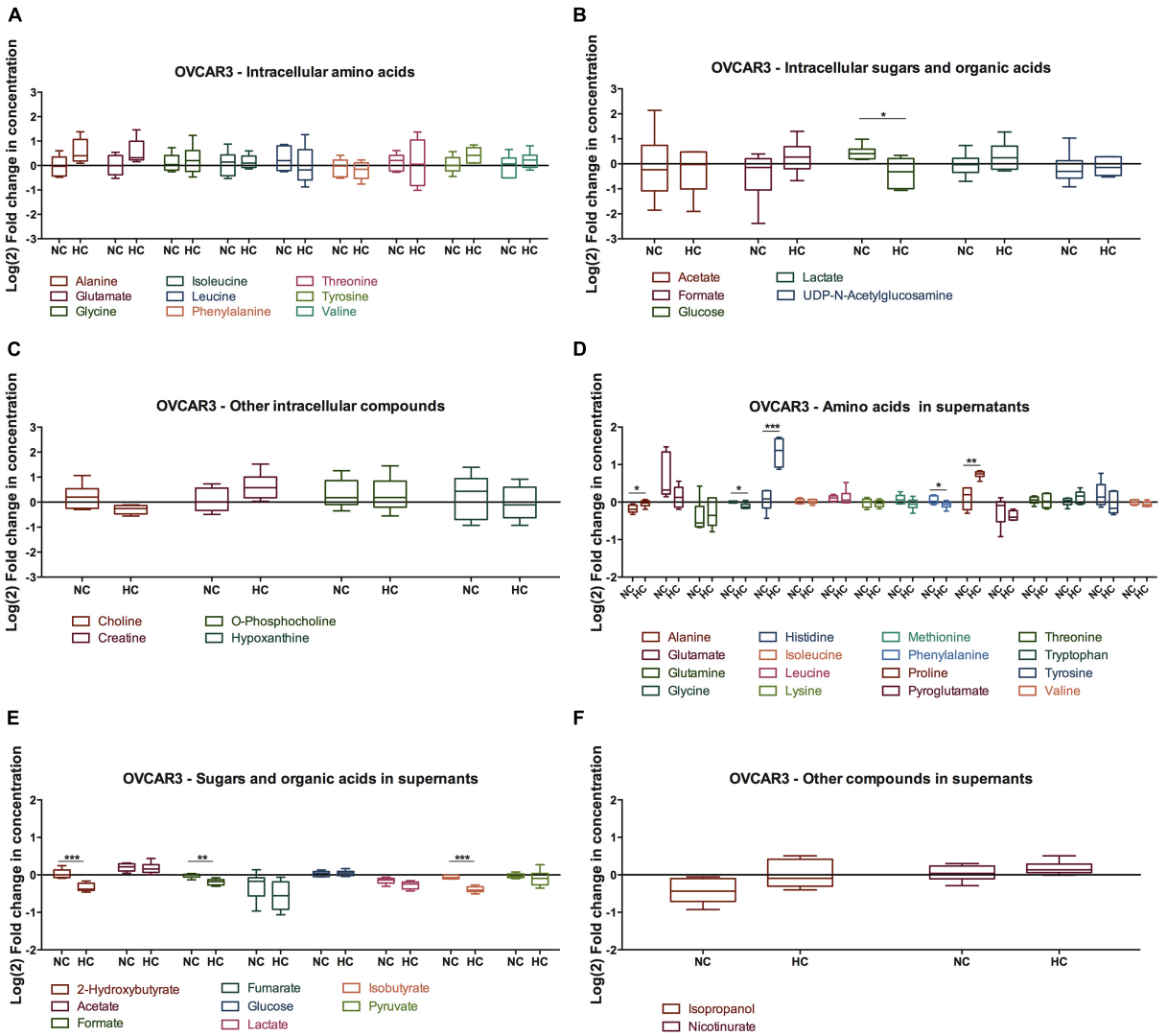

FIGURE 5 | Effect of cysteine in OVCAR3 metabolites under normoxia and hypoxia. Metabolites levels for 48 h of experimental conditions for OVCAR3 cells. **(A)** Intracellular amino acids; **(B)** intracellular sugars and organic acids; **(C)** other intracellular metabolites; **(D)** amino acids in supernatants; **(E)** sugars and organic acids in supernatants; **(F)** other metabolites in supernatants. Data were normalized to the respective control condition (the same environmental condition NC/N and HC/H). NC, normoxia with cysteine; HC, hypoxia with cysteine. Results are shown as median with 25th to 75th percentiles. $^{*}p < 0.05$, $^{**}p < 0.01$, $^{***}p < 0.001$ (independent-samples *t*-test: NC, $n = 6$; HC, $n = 6$).

cells the profile was similar both under normoxia (OVCAR3 NC) and hypoxia (OVCAR3 HC), with cystine being the most representative compound (**Figure 6E**).

DISCUSSION

In this work, we provide novel data supporting that cysteine promotes sulfur and carbon metabolism reprogramming, underlying the adaptation to hypoxic microenvironment in ovarian cancer cells.

As a solid tumor grows, cancer cells are exposed to regions of hypoxia, long established as a stimulus for tumor progression and resistance to therapy (Vaupel and Mayer, 2007; Semenza, 2012). We have recently proposed that cysteine allows adaptation to hypoxic environments and also contributes to escape from carboplatin-induced death in ovarian cancer cells (Nunes et al., 2018a,b). In here, we aimed to investigate the mechanisms by which cysteine protects ovarian cancer cells under hypoxia, by addressing its role in cellular metabolism, namely through energy production.

Uptake of cystine, the oxidized form of cysteine, is mediated by xCT (solute carrier family 7 member 11 – SLC7A11), a member of the cystine-glutamate transporter xc^- system (Sato et al., 2000). Intracellularly, cystine is reduced to cysteine, which is the rate-limiting substrate for GSH synthesis, making xCT pivotal in the cellular redox balance maintenance (reviewed in Conrad and Sato, 2012). Herein, we have shown mitochondrial localization of

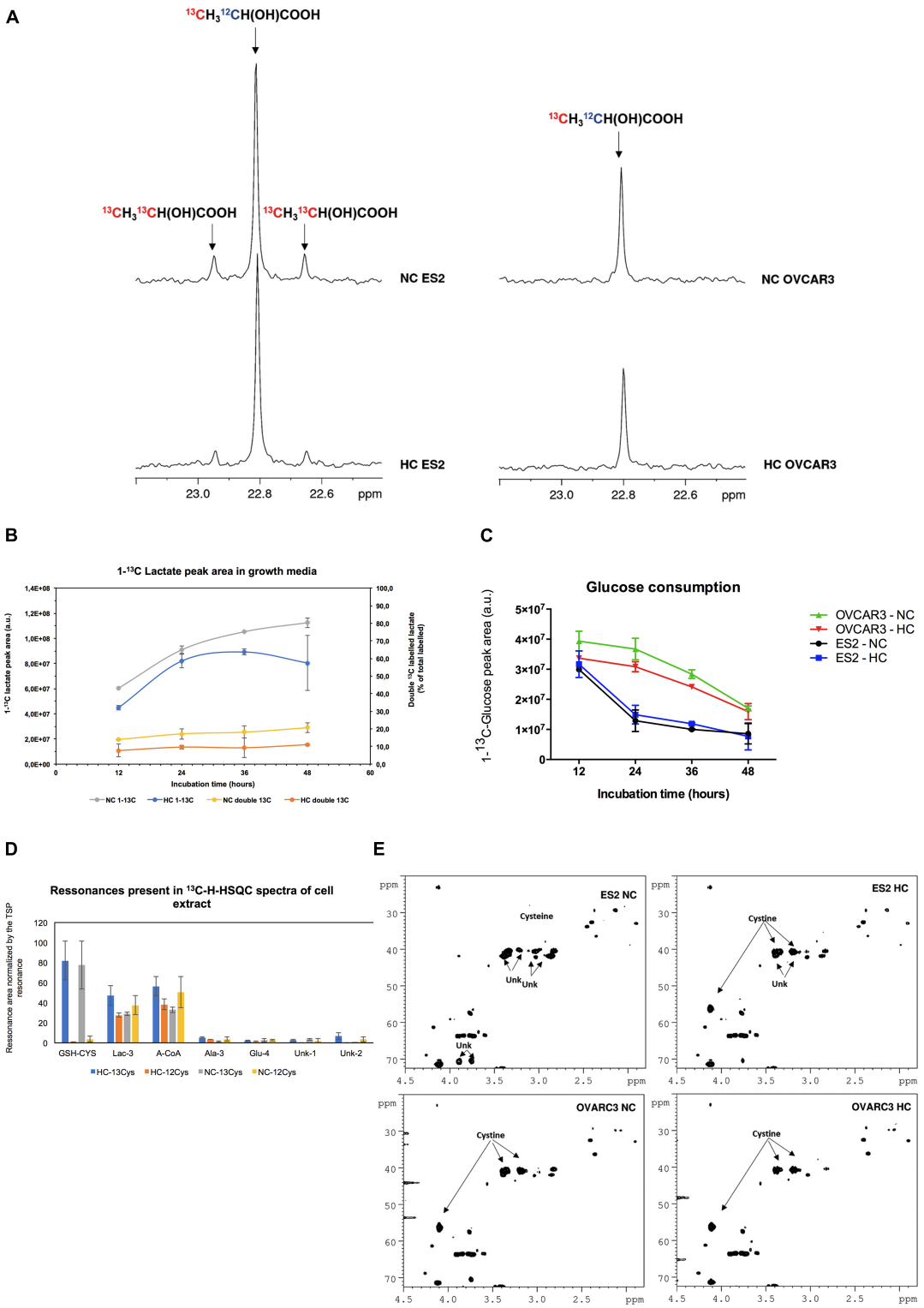

FIGURE 6 | Cysteine is directly used by ES2 cells in the main metabolic pathways. **(A)** Highlight of the lactate methyl group resonance on the ^{13}C-NMR spectra of 48 h culture media incubated with U-^{13}C-cysteine. On the left panel, ES2 cells under normoxia (upper spectra) and under hypoxia (lower spectra); on the right panel, OVCAR3 cells under normoxia (upper spectra) and under hypoxia (lower spectra). **(B)** Production of lactate by ES2 cells in culture media at different time points (12, 24, 36, and 48 h). **(C)** Glucose consumption in ES2 and OVCAR3 cells. **(D)** Resonances areas of the ^{13}C-1H-HSQC projection on ^{13}C spectra normalized by TSP area in the cell extracts. **(E)** Highlight of ^{13}C-1H-HSQC spectra of the growth media at 48 h incubation in the presence of U-^{13}C-cysteine under normoxia and hypoxia conditions. NC, normoxia with cysteine; HC, hypoxia with cysteine. **(B–D)** Results are shown as mean ± SD. Assays were performed in biological triplicates.

the xCT transporter concomitant with impaired ATP production triggered by its pharmacological inhibition under hypoxia, thus indicating a role of the xc^- system via cystine uptake also in energy production. These data are in accordance with recent findings supporting a role of Nrf2 in the regulation of mitochondrial ATP synthesis (reviewed in Vomund et al., 2017). As a transcription factor, Nrf2 was already reported to regulate the expression of xCT and the activity of the xc^- system in response to oxidative stress in human breast cancer cells (Habib et al., 2015).

Cysteine's role in mitochondrial ATP synthesis might be associated to its non-oxidative metabolism resulting in H_2S (via CBS, CSE or MpST) and/or CysSSH (via CARS2) release. H_2S is the only inorganic compound presenting a bioenergetic role in mammalian cells' mitochondria (Goubern et al., 2007), that was already reported to contribute to mitochondrial ATP production through the activity of the enzymes involved in cysteine metabolism: MpST in conjunction with CAT (Módis et al., 2013a,b; Abdollahi Govar et al., 2020; Augsburger et al., 2020), CSE (Fu et al., 2012), and CBS (Bhattacharyya et al., 2013; Szabo et al., 2013). At low concentrations (nM), H_2S is known to stimulate mitochondrial bioenergetics by way of different mechanisms: through donation of electron equivalents to the quinol pool via sulfide:quinone oxidoreductase (SQR); by the glycolytic enzyme glyceraldehyde 3-phosphate dehydrogenase activation, and by persulfidation of ATP synthase (reviewed in Giuffrè and Vicente, 2018). In addition, Li and Yang (2015) reported a role of CSE/H_2S system in enhancing mtDNA replication and cellular bioenergetics both in smooth muscle cells and mouse aorta tissues. In fact, this can be an explanation for the increased number of mitochondria in ES2 cells under hypoxia, as the mitochondrial marker/endogenous control TOMM20 is overexpressed. More recently, Chakraborty et al. (2018) reported a new role of CBS in the regulation of mitochondria morphogenesis, promoting tumor progression in ovarian cancer. Specifically under hypoxia conditions, H_2S was reported to decrease reactive oxygen species (ROS), mediated by CBS mitochondrial accumulation (Teng et al., 2013) and induce ATP production, mediated by CSE translocation into the mitochondria (Fu et al., 2012). A different adaptive strategy to hypoxia has been reported by Malagrinò et al. (2019) for the colorectal cancer cell line SW480, which exhibited a lower mitochondrial mass in response to hypoxia, although the mitochondria were enriched in H_2S-disposal capacity via increased mitochondrial SQR expression. This increased mitochondrial SQR renders hypoxic SW480 cells more equipped to inject H_2S-derived electron equivalents into the mitochondrial electron transfer chain and sustain mitochondrial bioenergetics.

In our study, short (2–16 h) exposure to CBS and CSE inhibitors did not afford significant differences in ATP levels in both cell lines, with the exception of OVCAR3 cells at 2 h under hypoxia with cysteine supplementation in which the inhibitors led to decreased ATP levels (**Supplementary Figure 3A**). Hence, OVCAR3 cells, under hypoxia, may channel the extra cysteine to degradation, thereby producing H_2S and/or CysSSH, and enhancing ATP production. Despite the absent effects at shorter times, the observed increased ATP levels at prolonged (48 h) exposure to CBS and CSE inhibitors indicates that the inhibition of both enzymes allows for compensatory or alternative mechanisms of energy production, probably including CAT/MpST and/or CARS2 activity. Given the fact that both CBS and CSE have been reported to partially relocate to mitochondria in hypoxia (Fu et al., 2012; Teng et al., 2013), available cysteine may be converted in the mitochondria to H_2S by CBS, CSE and MpST, or to CysSSH by CARS2. Additionally, cystine can be converted to CysSSH and pyruvate by CBS and CSE. Therefore, whereas excess cysteine may trigger over-production of H_2S and/or CysSSH via CBS and CSE to the point they inhibit the mitochondrial electron transfer chain and thereby impair ATP production, in the presence of their inhibitors AOAA and PAG, this inhibitory effect is likely released and 'safer' cysteine-degradation mechanisms can be deployed, linked to stimulation of ATP production.

Under hypoxia we did not observe differences in MpST protein levels in both cell lines (**Supplementary Figure 3B**), although we observed a mitochondrial MpST enrichment compared to the cytosolic content (**Supplementary Figure 3C**). Given that cysteine is a poor co-substrate for MpST as sulfane sulfur acceptor to generate CysSSH with respect to other possible co-substrates such as thioredoxin, the excess cysteine load imposed on hypoxic cells may push the CAT/MpST system into higher – yet controlled – CysSSH/H_2S production. Interestingly, enzymatic studies performed in *E. coli* showed that a bacterial MpST homolog abrogates oxidative stress via L-cysteine (Mironov et al., 2017). Another hypothesis is that diversion of cysteine for CARS2-mediated generation of CysSSH affords a protective role from cysteine oxidation in oxidative stress triggered by hypoxic conditions, as recently shown by Zivanovic et al. (2019) regarding the cysteine persulfidation prevention of protein cysteine oxidative damage.

Considering the relevance of cysteine in ATP production, our results showed that cysteine metabolism may operate in a more intricate manner than simply increased H_2S production and concurrent ATP production. Although some studies showed that NaHS, an exogenous H_2S source, was sufficient to increase mitochondrial ATP production under hypoxia (Fu et al., 2012), our results showed that H_2S *per se* was not sufficient to counteract the impaired ATP production driven by sulfasalazine (xCT inhibitor), under hypoxia in both ES2 and OVCAR3 cells. Therefore, our experiments support that cysteine metabolism, dependent on xCT transporter, provides alternative sources for energy production in ovarian cancer cells (**Figure 7A**).

The synthesis of GSH is another way of cysteine contributing for ATP production. The incorporation of extra cysteine in GSH allows cells to escape from oxidative stress and enables increased cell viability and proliferation, therefore leading to increased ATP synthesis. In fact, our previous data have supported a role of a higher thiols turnover in hypoxia adaptation, especially in ES2 cells (Nunes et al., 2018b). Interestingly, H_2S was also reported to increase the production of GSH by inducing the expression of cystine/cysteine transporters and by redistributing GSH to mitochondria in mouse neuronal cell models (Kimura et al., 2010).

Despite the fact that in addition to H_2S and CysSSH production, cysteine and cystine catabolism generate pyruvate

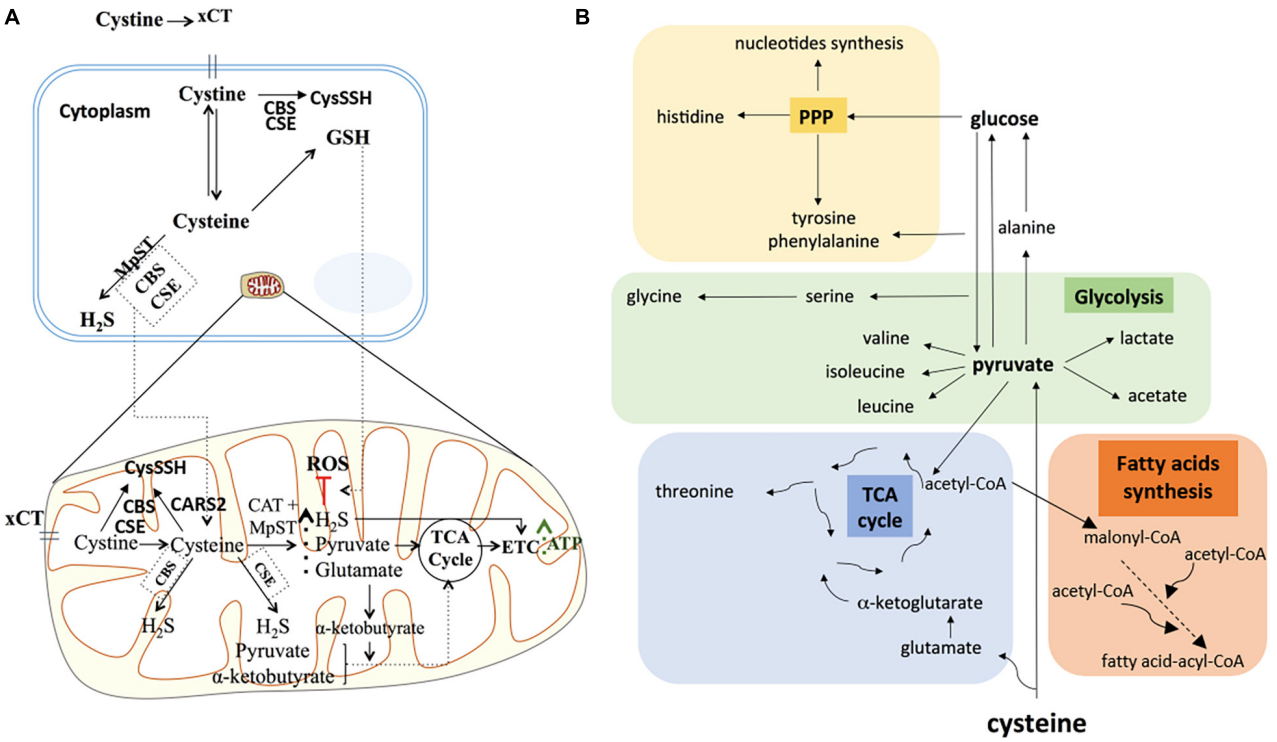

FIGURE 7 | Cysteine possible direct and indirect roles in ATP synthesis and in carbon metabolism reprogramming under hypoxia in ovarian cancer cells. **(A)** Under hypoxia, cysteine degradation could contribute directly to ATP production via not only H_2S generation, but also via pyruvate and α-ketobutyrate that could further supply the TCA cycle, leading to increased ATP synthesis. Cysteine could also present an indirect role in ATP synthesis mediated by increasing GSH content under hypoxia, hence counteracting oxidative stress and thereby increasing cellular metabolism. Cystine can also be converted into cysteine persulfide (CysSSH) by CSE and CBS in the cytoplasm or by CSE, CBS and CARS2 in the mitochondria. **(B)** The axis cysteine-pyruvate-glucose is central in whole metabolic network of carbon. Cysteine degradation can originate pyruvate and glutamate. Pyruvate besides being a major supplier of tricarboxylic acids (TCA) cycle, it can be converted into valine, isoleucine, leucine, alanine, lactate, and acetate. Alanine can be a source of glucose through gluconeogenesis. Glycolysis produce intermediates to supply the TCA cycle (a hub for many precursors of organic compounds, such as threonine) and the pentose phosphate pathway (PPP). PPP intermediates can be converted into amino acids such as histidine and can be conjugated with glycolysis intermediates, originating tyrosine, phenylalanine and serine, which can be converted into glycine. PPP is also crucial in the nucleotide's synthesis. Acetyl-CoA is a central organic compound in metabolism, when cysteine-derived it proves that cysteine is a valuable supplier of TCA cycle and amino acids and fatty acids syntheses. The increased concentration of these compounds under hypoxia, suggests that cysteine is pushing the metabolic flow in order to supply the main carbon metabolic pathways. The direct incorporation of cysteine into these compounds is possible, however, further studies are needed to clarify this. Based on information from www.bioinfo.org.cn.

as well (Wang, 2012; Bonifácio et al., 2020), cysteine is not commonly considered as a carbon source. Herein, we showed that cysteine gives rise to lactate by being firstly converted into pyruvate and alanine, indicating that cysteine could also be used in gluconeogenesis (**Figure 7B**). Most importantly, cysteine also originates acetyl-CoA, which is a central metabolite, supplying the TCA cycle, fatty acids synthesis and amino acids synthesis. Our study reinforces that cysteine can account for biosynthesis and bioenergetics not only as a sulfur source but also as a carbon donor.

Importantly, Beaufort et al. (2014) characterized 39 ovarian cancer cell lines in order to correlate the cellular and molecular features with their tumorigenic phenotype. In that study, ES2, but not OVCAR3, was included in the most aggressive subset of ovarian cancer cells (Beaufort et al., 2014). In here, our data supported that cysteine orchestration in metabolic remodeling and plasticity can be a crucial phenomenon for more aggressive cancer cells phenotype. Strikingly, ^{1}H-NMR results showed that the metabolic impact of cysteine under hypoxia was much more pronounced in ES2 cells than in OVCAR3 cells, translated by the remarkable number of metabolic pathways that were significantly altered. Therefore, taken together, our results reinforced the role of cysteine as a valuable carbon source, from which cancer cells take advantage on the course of the metabolic rewiring they undergo under hypoxia. In particular, cysteine is a central carbon source for ES2 cells, supporting their redox capacity by supplying GSH synthesis and allowing the maintenance of pivotal biosynthetic and bioenergetic pathways dependent on acetyl-CoA. Furthermore, results suggested that under hypoxia, cysteine allowed to increase the rate of some metabolic pathways in ES2 cells, as increased intracellular levels of several amino acids and other compounds were observed. Regarding OVCAR3 cells, results supported that cysteine impacts differently the

cellular needs of amino acids under normoxia and hypoxia. Moreover, when comparing to OVCAR3, results suggest that ES2 cells are better adapted to hypoxia and to the use of cysteine to overcome the hypoxic stress, as seen by the higher number of metabolic pathways that were significantly altered by cysteine under hypoxia.

Interestingly, while cysteine was able to rescue the impaired ATP synthesis triggered by xCT inhibition, it was not able to increase ATP synthesis upon β-oxidation and glycolysis inhibition (**Supplementary Figure 3D**), indicating that cysteine is not enough to replace the contribution of these pathways for ATP production.

Together, the results support that ES2 and OVCAR3 cells use cysteine differently in order to cope with hypoxia, where cysteine especially impacts hypoxic ES2 cells metabolic features, enhancing the metabolic reprogramming. In **Figure 7**, we present the possible direct and indirect pathways in which cysteine can be a metabolic coin, promoting ATP production in hypoxic ovarian cancer cells. The profound metabolic impact that cysteine showed under hypoxia in ES2 cells suggests a strong remodeling of the carbon metabolism.

This work lights again that disturbing cysteine metabolic network can be a promising tool not only in ovarian cancer but also in all cancer models that rely their survival on cysteine bioavailability and metabolic versatility.

DATA AVAILABILITY STATEMENT

The original contributions presented in the study are included in the article/**Supplementary Material**, further inquiries can be directed to the corresponding author.

AUTHOR CONTRIBUTIONS

SN planned and performed most experiments. CR, IS, and FS performed experimental assays. JV coordinated H2S experiments. SP coordinated the pharmacological assays. AF participated in the pathophysiological contextualization of the study. LG coordinated NMR spectroscopy analyses. JS coordinated the whole research project and ensured the funding. CM performed the experiments and contributed for the revised version of the manuscript, which ended up being accepted for publication. All the authors read, discussed, and approved the final version of the manuscript.

FUNDING

This research was supported by Fundação para a Ciência e Tecnologia (FCT) (Ph.D. ProRegeM program, Ref: PD/BD/105893/2014; FCT individual Ph.D. fellowship Ref: 2020.06956.BD) and iNOVA4 Health (Project 4 and Project 21). iNOVA4Health-UID/Multi/04462/2013 is a program financially supported by Fundação para a Ciência e Tecnologia/ Ministério da Educação e Ciência, through national funds. The authors would like to acknowledge the Instituto Português de Oncologia de Lisboa Francisco Gentil (IPOLFG) for partially funding the project.

SUPPLEMENTARY MATERIAL

The Supplementary Material for this article can be found online at: https://www.frontiersin.org/articles/10.3389/fcell.2021.722412/full#supplementary-material

REFERENCES

Abdollahi Govar, A., Törő, G., Szaniszlo, P., Pavlidou, A., Bibli, S.-I., Thanki, K., et al. (2020). 3-Mercaptopyruvate sulfurtransferase supports endothelial cell angiogenesis and bioenergetics. *Br. J. Pharmacol.* 177, 866–883. doi: 10.1111/bph.14574

Akaike, T., Ida, T., Wei, F. Y., Nishida, M., Kumagai, Y., Alam, M. M., et al. (2017). Cysteinyl-tRNA synthetase governs cysteine polysulfidation and mitochondrial bioenergetics. *Nat. Commun.* 8:1177. doi: 10.1038/s41467-017-01311-y

Augsburger, F., Randi, E. B., Jendly, M., Ascencao, K., Dilek, N., and Szabo, C. (2020). Role of 3-mercaptopyruvate sulfurtransferase in the regulation of proliferation, migration, and bioenergetics in murine colon cancer cells. *Biomolecules* 10:447. doi: 10.3390/biom10030447

Balendiran, G. K., Dabur, R., and Fraser, D. (2004). The role of glutathione in cancer. *Cell Biochem. Funct.* 22, 343–352. doi: 10.1002/cbf.1149

Bast, R. C. Jr., Hennessy, B., and Mills, G. B. (2009). The biology of ovarian cancer: new opportunities for translation. *Nat. Rev. Cancer* 9, 415–428. doi: 10.1038/nrc2644

Beaufort, C. M., Helmijr, J. C. A., Piskorz, A. M., Hoogstraat, M., Ruigrok-Ritstier, K., Besselink, N., et al. (2014). Ovarian cancer cell line panel (OCCP): clinical importance of in vitro morphological subtypes. *PLoS One* 9:e103988. doi: 10.1371/journal.pone.0103988

Bhattacharyya, S., Saha, S., Giri, K. I, Lanza, R., Nair, K. S., Jennings, N. B., et al. (2013). Cystathionine beta-synthase (CBS) contributes to advanced ovarian cancer progression and drug resistance. *PLoS One* 8:e79167. doi: 10.1371/journal.pone.0079167

Bianco, C. L., Akaike, T., Ida, T., Nagy, P., Bogdandi, V., Toscano, J. P., et al. (2019). The reaction of hydrogen sulfide with disulfides: formation of a stable trisulfide and implications for biological systems. *Br. J. Pharmacol.* 176, 671–683. doi: 10.1111/bph.14372

Bonifácio, V. D. B., Pereira, S. A., Serpa, J., and Vicente, J. B. (2020). Cysteine metabolic circuitries: druggable targets in cancer. *Br. J. Cancer* 124, 862–879. doi: 10.1038/s41416-020-01156-1

Chakraborty, P. K., Murphy, B., Mustafi, S. B., Dey, A., Xiong, X., Rao, G., et al. (2018). Cystathionine β-synthase regulates mitochondrial morphogenesis in ovarian cancer. *FASEB J.* 32, 4145–4157. doi: 10.1096/fj.201701095R

Conrad, M., and Sato, H. (2012). The oxidative stress-inducible cystine/glutamate antiporter, system xc-: cystine supplier and beyond. *Amino Acids* 42, 231–246. doi: 10.1007/s00726-011-0867-5

Cooke, S. L., Brenton, J. D., and Way, R. (2011). Evolution of platinum resistance in high-grade serous ovarian cancer. *Lancet Oncol.* 12, 1169–1174. doi: 10.1016/S1470-2045(11)70123-1

Desai, A., Xu, J., Aysola, K., Qin, Y., Okoli, C., Hariprasad, R., et al. (2014). Epithelial ovarian cancer: an overview. *World J. Transl. Med.* 3, 10–29. doi: 10.5528/wjtm.v3.i1.1.Epithelial

Ferlay, J., Soerjomataram, I., Ervik, M., Dikshit, R., Eser, S., Mathers, C., et al. (2013). GLOBOCAN 2012 v1.0, cancer incidence and mortality worldwide: IARC cancerbase no. 11. *Lyon. Int J Cancer* 144, 1941–1953. doi: 10.1002/ijc.31937

Filipovic, M. R., Zivanovic, J., Alvarez, B., and Banerjee, R. (2018). Chemical biology of H(2)S signaling through persulfidation. *Chem. Rev.* 118, 1253–1337. doi: 10.1021/acs.chemrev.7b00205

Fitzmaurice, C., Dicker, D., Pain, A., Hamavid, H., Moradi-Lakeh, M., MacIntyre, M. F., et al. (2015). The global burden of cancer 2013. *JAMA Oncol.* 1, 505–527. doi: 10.1001/jamaoncol.2015.0735

Fruehauf, J. P., and Meyskens, F. L. (2007). Reactive oxygen species: a breath of life or death? *Clin. Cancer Res.* 13, 789–794. doi: 10.1158/1078-0432.CCR-06-2082

Fu, M., Zhang, W., Wu, L., Yang, G., Li, H., and Wang, R. (2012). Hydrogen sulfide (H2S) metabolism in mitochondria and its regulatory role in energy production. *Proc. Natl. Acad. Sci. U.S.A.* 109, 2943–2948. doi: 10.1073/pnas.1115634109

Gai, J. W., Qin, W., Liu, M., Wang, H. F., Zhang, M., Li, M., et al. (2016). Expression profile of hydrogen sulfide and its synthases correlates with tumor stage and grade in urothelial cell carcinoma of bladder. *Urol. Oncol. Semin. Orig. Investig.* 34, e15–e20. doi: 10.1016/j.urolonc.2015.06.020

Giuffrè, A., and Vicente, J. B. (2018). Hydrogen sulfide biochemistry and interplay with other gaseous. *Oxid. Med. Cell. Longev.* 2018:6290931. doi: 10.1155/2018/6290931

Goff, B. A., de la Cuesta, R. S., Muntz, H. G., Fleischhacker, D., Ek, M., Rice, L. W., et al. (1996). Clear cell carcinoma of the ovary: a distinct histologic type with poor prognosis and resistance to platinum-based chemotherapy in stage III disease. *Gynecol. Oncol.* 60, 412–417. doi: 10.1006/gyno.1996.0065

Goubern, M., Andriamihaja, M., Nubel, T., Blachier, F., and Bouillaud, F. (2007). Sulfide, the first inorganic substrate for human cells. *FASEB J.* 21, 1699–1706. doi: 10.1096/fj.06-7407com

Gout, P. W., Buckley, A. R., Simms, C. R., and Bruchovsky, N. (2001). Sulfasalazine, a potent suppressor of lymphoma growth by inhibition of the x(c)- cystine transporter: a new action for an old drug. *Leukemia* 15, 1633–1640. doi: 10.1038/sj.leu.2402238

Habib, E., Linher-Melville, K., Lin, H. X., and Singh, G. (2015). Expression of xCT and activity of system xc-are regulated by NRF2 in human breast cancer cells in response to oxidative stress. *Redox Biol.* 5, 33–42. doi: 10.1016/j.redox.2015.03.003

Hipólito, A., Nunes, S. C., Vicente, J. B., and Serpa, J. (2020). Cysteine aminotransferase (CAT): a pivotal sponsor in metabolic remodeling and an ally of 3-mercaptopyruvate sulfurtransferase (MST) in cancer. *Molecules* 25:3984. doi: 10.3390/molecules25173984

Hu, L.-F., Lu, M., Hon Wong, P. T., and Bian, J.-S. (2011). Hydrogen sulfide: neurophysiology and neuropathology. *Antioxid. Redox Signal.* 15, 405–419. doi: 10.1089/ars.2010.3517

Jayson, G. C., Kohn, E. C., Kitchener, H. C., and Ledermann, J. A. (2014). Ovarian cancer. *Lancet* 384, 1376–1388. doi: 10.1016/S0140-6736(13)62146-7

Jourdain, A. A., Begg, B. E., Mick, E., Shah, H., Calvo, S. E., Skinner, O. S., et al. (2021). Loss of LUC7L2 and U1 snRNP subunits shifts energy metabolism from glycolysis to OXPHOS. *Mol. Cell* 81, 1905–1919. doi: 10.1016/j.molcel.2021.02.033

Kabil, O., and Banerjee, R. (2014). Enzymology of H $_2$ S biogenesis, decay and signaling. *Antioxid. Redox Signal.* 20, 770–782. doi: 10.1089/ars.2013.5339

Kimura, Y., Goto, Y.-I., and Kimura, H. (2010). Hydrogen sulfide increases glutathione production and suppresses oxidative stress in mitochondria. *Antioxid. Redox Signal.* 12, 1–13. doi: 10.1089/ars.2008.2282

Li, S., and Yang, G. (2015). Hydrogen sulfide maintains mitochondrial DNA replication via demethylation of TFAM. *Antioxid. Redox Signal.* 23, 630–642. doi: 10.1089/ars.2014.6186

Lopes-Coelho, F., Gouveia-Fernandes, S., Gonçalves, L. G., Nunes, C., Faustino, I., Silva, F., et al. (2016). HNF1B drives glutathione (GSH) synthesis underlying intrinsic carboplatin resistance of ovarian clear cell carcinoma (OCCC). *Tumor Biol.* 37, 4813–4829. doi: 10.1007/s13277-015-4290-5

Malagrinò, F., Zuhra, K., Mascolo, L., Mastronicola, D., Vicente, J. B., Forte, E., et al. (2019). Hydrogen sulfide oxidation: adaptive changes in mitochondria of sw480 colorectal cancer cells upon exposure to hypoxia. *Oxid. Med. Cell. Longev.* 2019:8102936. doi: 10.1155/2019/8102936

Mironov, A., Seregina, T., Nagornykh, M., Luhachack, L. G., Korolkova, N., Lopes, L. E., et al. (2017). Mechanism of H 2 S-mediated protection against oxidative stress in *Escherichia coli*. *Proc. Natl. Acad. Sci. U.S.A.* 114, 6022–6027. doi: 10.1073/pnas.1703576114

Módis, K., Coletta, C., Erdélyi, K., Papapetropoulos, A., and Szabo, C. (2013a). Intramitochondrial hydrogen sulfide production by 3-mercaptopyruvate sulfurtransferase maintains mitochondrial electron flow and supports cellular bioenergetics. *FASEB J.* 27, 601–611. doi: 10.1096/fj.12-216507

Módis, K., Panopoulos, P., Coletta, C., Papapetropoulos, A., and Szabo, C. (2013b). Hydrogen sulfide-mediated stimulation of mitochondrial electron transport involves inhibition of the mitochondrial phosphodiesterase 2A, elevation of cAMP and activation of protein kinase A. *Biochem. Pharmacol.* 86, 1311–1319. doi: 10.1016/j.bcp.2013.08.064

Nunes, S. C., Lopes-Coelho, F., Gouveia-Fernandes, S., Ramos, C., Pereira, S. A., and Serpa, J. (2018a). Cysteine boosters the evolutionary adaptation to CoCl2 mimicked hypoxia conditions, favouring carboplatin resistance in ovarian cancer. *BMC Evol. Biol.* 18:97. doi: 10.1186/s12862-018-1214-1

Nunes, S. C., Ramos, C., Lopes-Coelho, F., Sequeira, C. O., Silva, F., Gouveia-Fernandes, S., et al. (2018b). Cysteine allows ovarian cancer cells to adapt to hypoxia and to escape from carboplatin cytotoxicity. *Sci. Rep.* 8:9513. doi: 10.1038/s41598-018-27753-y

Okuno, S., Sato, H., Tamba, M., Wang, H., Sohda, S., Hamada, H., et al. (2003). Role of cystine transport in intracellular glutathione level and cisplatin resistance in human ovarian cancer cell lines. *Br. J. Cancer* 88, 951–956. doi: 10.1038/sj.bjc.6600786

Pan, Y., Zhou, C., Yuan, D., Zhang, J., and Shao, C. (2015). Radiation exposure promotes hepatocarcinoma cell invasion through epithelial mesenchymal transition mediated by H2S/CSE pathway. *Radiat. Res.* 185, 96–105. doi: 10.1667/RR14177.1

Panza, E., De Cicco, P., Armogida, C., Scognamiglio, G., Gigantino, V., Botti, G., et al. (2015). Role of the cystathionine γ lyase/hydrogen sulfide pathway in human melanoma progression. *Pigment Cell Melanoma Res.* 28, 61–72. doi: 10.1111/pcmr.12312

Polewski, M. D., Reveron-Thornton, R. F., Cherryholmes, G. A., Marinov, G. K., Cassady, K., and Aboody, K. S. (2016). Increased expression of system xc- in glioblastoma confers an altered metabolic state and temozolomide resistance. *Mol. Cancer Res.* 14, 1229–1242. doi: 10.1158/1541-7786.MCR-16-0028

Prat, J. (2012). Ovarian carcinomas: five distinct diseases with different origins, genetic alterations, and clinicopathological features. *Virchows Arch* 460, 237–249. doi: 10.1007/s00428-012-1203-5

Reid, B. M., Permuth, J. B., and Sellers, T. A. (2017). Epidemiology of ovarian cancer: a review. *Cancer Biol. Med.* 14, 9–32. doi: 10.20892/j.issn.2095-3941.2016.0084

Saed, G. M., Diamond, M. P., and Fletcher, N. M. (2017). Updates of the role of oxidative stress in the pathogenesis of ovarian cancer. *Gynecol. Oncol.* 145, 595–602. doi: 10.1016/j.ygyno.2017.02.033

Sato, H., Tamba, M., Kuriyama-Matsumura, K., Okuno, S., and Bannai, S. (2000). Molecular cloning and expression of human xCT, the light chain of amino acid transport system xc-. *Antioxid. Redox Signal.* 2, 665–671. doi: 10.1089/ars.2000.2.4-665

Schnelldorfer, T., Gansauge, S., Gansauge, F., Schlosser, S., Beger, H. G., and Nussler, A. K. (2000). Glutathione depletion causes cell growth inhibition and enhanced apoptosis in pancreatic cancer cells. *Cancer* 89, 1440–1447. doi: 10.1002/1097-0142(20001001)89:7<1440::AID-CNCR5<3.0.CO;2-0

Semenza, G. L. (2012). Hypoxia-inducible factors: mediators of cancer progression and targets for cancer therapy. *Trends Pharmacol. Sci.* 33, 207–214. doi: 10.1016/j.tips.2012.01.005

Sen, S., Kawahara, B., Gupta, D., Tsai, R., Khachatryan, M., Farias-eisner, R., et al. (2015). Role of cystathionine β -synthase in human breast Cancer. *Free Radic. Biol. Med.* 86, 228–238. doi: 10.1016/j.freeradbiomed.2015.05.024

Senthil, K., Aranganathan, S., and Nalini, N. (2004). Evidence of oxidative stress in the circulation of ovarian cancer patients. *Clin. Chim. Acta* 339, 27–32. doi: 10.1016/j.cccn.2003.08.017

Sugiyama, T., Kamura, T., Kigawa, J., Terakawa, N., Kikuchi, Y., Kita, T., et al. (2000). Clinical characteristics of clear cell carcinoma of the ovary : a distinct histologic type with poor prognosis and resistance to platinum-based chemotherapy. *Cancer* 88, 2584–2589. doi: 10.1002/1097-0142(20000601)88:11<2584::aid-cncr22>3.0.co;2-5

Sun, X., Wang, W., Dai, J., Jin, S., Huang, J., Guo, C., et al. (2017). A long-term and slow-releasing hydrogen sulfide donor protects against myocardial ischemia/reperfusion injury. *Sci. Rep.* 7:3541. doi: 10.1038/s41598-017-03941-0

Szabo, C., Coletta, C., Chao, C., Módis, K., Szczesny, B., and Papapetropoulos, A. (2013). Tumor-derived hydrogen sulfide, produced by cystathionine-β -synthase, stimulates bioenergetics, cell proliferation, and angiogenesis in colon cancer. *PNAS Pharmacol.* 110, 12474–12479. doi: 10.1073/pnas.1306241110

Szczesny, B., Marcatti, M., Zatarain, J. R., Druzhyna, N., Wiktorowicz, J. E., Nagy, P., et al. (2016). Inhibition of hydrogen sulfide biosynthesis sensitizes lung adenocarcinoma to chemotherapeutic drugs by inhibiting mitochondrial DNA repair and suppressing cellular bioenergetics. *Sci. Rep.* 6:36125. doi: 10.1038/srep36125

Teng, H., Wu, B., Zhao, K., Yang, G., Wu, L., and Wang, R. (2013). Oxygen-sensitive mitochondrial accumulation of cystathionine -synthase mediated by Lon protease. *Proc. Natl. Acad. Sci. U.S.A.* 110, 12679–12684. doi: 10.1073/pnas.1308487110

Vaupel, P., and Mayer, A. (2007). Hypoxia in cancer: significance and impact on clinical outcome. *Cancer Metastasis Rev.* 26, 225–239. doi: 10.1007/s10555-007-9055-1

Vomund, S., Schäfer, A., Parnham, M. J., Brüne, B., and Von Knethen, A. (2017). Nrf2, the master regulator of anti-oxidative responses. *Int. J. Mol. Sci.* 18:2772. doi: 10.3390/ijms18122772

Wang, R. (2012). Physiological implications of hydrogen sulfide: a whiff exploration that blossomed. *Physiol. Rev.* 92, 791–896. doi: 10.1152/physrev.00017.2011

Zhou, Y., Tozzi, F., Chen, J., Fan, F., Xia, L., Wang, J., et al. (2012). Intracellular ATP levels are a pivotal determinant of chemoresistance in colon cancer cells. *Cancer Res.* 72, 304–314. doi: 10.1158/0008-5472.CAN-11-1674

Zivanovic, J., Kouroussis, E., Kohl, J. B., Adhikari, B., Bursac, B., Schott-Roux, S., et al. (2019). Selective persulfide detection reveals evolutionarily conserved antiaging effects of S-sulfhydration. *Cell Metab.* 30, 1152–1170. doi: 10.1016/j.cmet.2019.10.007

Zuhra, K., Tomé, C. S., Forte, E., Vicente, J. B., and Giuffrè, A. (2021). The multifaceted roles of sulfane sulfur species in cancer-associated processes. *Biochim. Biophys. Acta Bioenerg.* 1862:148338. doi: 10.1016/j.bbabio.2020.148338

Conflict of Interest: The authors declare that the research was conducted in the absence of any commercial or financial relationships that could be construed as a potential conflict of interest.

Publisher's Note: All claims expressed in this article are solely those of the authors and do not necessarily represent those of their affiliated organizations, or those of the publisher, the editors and the reviewers. Any product that may be evaluated in this article, or claim that may be made by its manufacturer, is not guaranteed or endorsed by the publisher.

frontiers in Cell and Developmental Biology

REVIEW
published: 06 September 2021
doi: 10.3389/fcell.2021.728759

Glucose Metabolism and Glucose Transporters in Breast Cancer

*Eunah Shin and Ja Seung Koo**

Department of Pathology, Yonsei University College of Medicine, Seoul, South Korea

Breast cancer is the most common malignancy in women worldwide and is associated with high mortality rates despite the continuously advancing treatment strategies. Glucose is essential for cancer cell metabolism owing to the Warburg effect. During the process of glucose metabolism, various glycolytic metabolites, such as serine and glycine metabolites, are produced and other metabolic pathways, such as the pentose phosphate pathway (PPP), are associated with the process. Glucose is transported into the cell by glucose transporters, such as GLUT. Breast cancer shows high expressions of glucose metabolism-related enzymes and GLUT, which are also related to breast cancer prognosis. Triple negative breast cancer (TNBC), which is a high-grade breast cancer, is especially dependent on glucose metabolism. Breast cancer also harbors various stromal cells such as cancer-associated fibroblasts and immune cells as tumor microenvironment, and there exists a metabolic interaction between these stromal cells and breast cancer cells as explained by the reverse Warburg effect. Breast cancer is heterogeneous, and, consequently, its metabolic status is also diverse, which is especially affected by the molecular subtype, progression stage, and metastatic site. In this review, we will focus on glucose metabolism and glucose transporters in breast cancer, and we will additionally discuss their potential applications as cancer imaging tracers and treatment targets.

Keywords: breast cancer, glucose metabolism, glucose transporter, pentose phosphate pathway, serine/glycine pathway

OPEN ACCESS

Edited by:
Maria E. Mycielska, University Medical Center Regensburg, Germany

Reviewed by:
Fátima Martel, Universidade do Porto, Portugal
Pedro Gonzalez-Menendez, UMR 5535 Institut de Génétique Moléculaire de Montpellier (IGMM), France

***Correspondence:**
Ja Seung Koo
kjs1976@yuhs.ac

Specialty section:
This article was submitted to Molecular and Cellular Oncology, a section of the journal Frontiers in Cell and Developmental Biology

Received: *22 June 2021*
Accepted: *10 August 2021*
Published: *06 September 2021*

Citation:
Shin E and Koo JS (2021) Glucose Metabolism and Glucose Transporters in Breast Cancer. Front. Cell Dev. Biol. 9:728759. doi: 10.3389/fcell.2021.728759

INTRODUCTION

Breast cancer is the most common malignancy in women worldwide, and ranks top in the cause of death in female cancers worldwide (Bray et al., 2018). A total of 2.1 million women were newly diagnosed with breast cancer in 2018, and 627,000 women died of breast cancer (Bray et al., 2018). Breast cancer is increasing in underdeveloped and developing countries, and it is

Abbreviations: HK2, hexokinase II; PFK, phosphofructokinase; PKM2, pyruvate kinase isozymes M2; LDHA, lactate dehydrogenase A; G6PD, glucose 6-phosphate dehydrogenase; 6PGD, 6-phosphogluconate dehydrogenase; RPE, ribulose-5-phosphate epimerase; RPI, ribose 5-phosphate isomerase; TKT, transketolase; TALDO, transaldolase; PHGDH, phosphoglycerate dehydrogenase; PSAT1, phosphohydroxythreonine aminotransferase; PSPH, phosphoserine phosphatase; SHMT, serine hydroxymethyltransferase; GLDC, glycine decarboxylase; CAF, cancer-associated fibroblast; HIF, hypoxia-inducible factor; MCT, Monocarboxylate transporter; OXPHOS, oxidative phosphorylation; TAM, tumor-associated macrophage; PPP, pentose phosphate pathway; DHEA, dehydroepiandrosterone; PHGDH, phosphoglycerate dehydrogenase; ROS, reactive oxygen species; EMT, epithelial-mesenchymal transition; CSC, cancer stem cell; NADPH, nicotinamide adenine dinucleotide phosphate; 6PGDH, 6-phosphogluconate dehydrogenase; PI3K, phosphoinositide 3-kinase; mTOR, mammalian target of rapamycin; AMPK, AMP-activated protein kinase; VEGF, vascular endothelial growth factor; BMI, body mass index; E2, 17 beta-estradiol; IGF, insulin-like growth factor.

decreasing in developed countries since the early 2000s (Rossouw et al., 2002; Bray et al., 2004; DeSantis et al., 2015). Breast cancer presents with diverse characteristics. To categorize such diverse features of breast cancer, molecular subtypes have been developed: luminal A, luminal B, HER-2, and basal-like type. Moreover, estrogen receptor (ER), progesterone receptor (PR), and HER-2 are the main targets for targeted therapy in breast cancer, and samples/cases that are negative for these three receptors are defined as triple negative breast cancer (TNBC), which comprises about 15% of breast cancer cases. Each of the molecular subtypes of breast cancer and TNBC shows distinct clinical and molecular features in treatment response. Generally, breast cancer is treated with surgery, chemo-radiotherapy, and targeted therapy for biomarkers. Breast cancer showing hormone receptor expressions is treated with hormonal therapy such as tamoxifen, and breast cancer showing HER-2 amplification is treated with targeted therapy such as trastuzumab. Those that do not have any treatment targets are treated with a non-specific chemotherapy.

One of the fundamental characteristics of cancer cells that differs from normal cells is metabolic reprogramming—producing energy through glycolysis rather than mitochondrial oxidative phosphorylation, which is known as the Warburg effect after the German scientist Otto Warburg who first described it in the 1950s. The Warburg effect was first described in the 1950s by Otto Warburg, a German scientist, who stated that cancer cells secrete high levels of lactate because of an increase in glycolysis (Warburg, 1956). In the process of glycolysis, which is one of the main processes of glucose metabolism, glucose can enter cancer cells by glucose transporters. As a result, various glucose metabolites are produced that are related to diverse metabolic pathways, such as the serine/glycine metabolic pathway and pentose phosphate pathway (PPP). These glucose metabolic pathways and glucose transporters have pivotal roles in cancer metabolism as well as in cancer progression and metastasis, and such metabolic characteristics can be used in imaging diagnosis and targeted therapies. This review will focus on the glucose metabolic pathways, such as glycolysis, serine/glycine pathway, and PPP, in breast cancer and glucose transporters used in glycolysis and their potential implications in clinical practice.

GENERAL ASPECTS OF GLUCOSE METABOLISM AND RELATED METABOLIC PATHWAYS IN CANCER

Glucose metabolism consists of glycolysis and PPP, and glycolysis-related metabolic pathways consist of serine and glycine metabolism (**Figure 1**). A major pathway in the glucose metabolism of cancer cells is aerobic glycolysis, in the process of which glucose is first transported into the cancer cells by glucose transporters and then metabolized to pyruvate by various enzymes. Many enzymes are involved in this process, of which, the key enzymes are hexokinase II (HKII), phosphofructokinase (PFK), and pyruvate kinase (PK) (Li et al., 2015). Pyruvates produced in glycolysis are then moved into the mitochondria by mitochondrial pyruvate carriers 1 and 2, where they are turned into acetyl-CoA and oxaloacetate by pyruvate dehydrogenase and pyruvate carboxylase, respectively, to enter the TCA cycle for oxidative phosphorylation (OXPHOS) (Corbet and Feron, 2017). With one of the intermediate metabolites produced during the process of glycolysis, 3-phosphoglycerate (3PG), starts the serine pathway, in which 3-phosphoglycerate (3PG) is oxidized to 3-phosphohydroxypyruvate (pPYR) by phosphoglycerate dehydrogenase (PHGDH) and pPYR is transaminated to phosphoserine (pSER) by phosphoserine aminotransferase (PSAT). pSER is dephosphorylated to serine by phosphoserine phosphatase. In glycine metabolism, glycine is metabolized to H-protein-*S*-aminomethyldihydrolipoyllysine by glycine decarboxylase (GLDC), an important component of the glycine cleavage system. This serine metabolism and glycine metabolism are linked by serine hydroxymethyltransferse (SHMT), which causes a reversible conversion of serine and glycine (Locasale, 2013). Lastly, PPP is a metabolic pathway that occurs with glycolysis (Ramos-Martinez, 2017), playing a pivotal role in cell survival and growth by providing pentose phosphate for nucleic acid synthesis and also nicotinamide adenine dinucleotide phosphate (NADPH) for fatty acid synthesis and cell survival (Patra and Hay, 2014). PPP is comprised of two branches, the oxidative branch and non-oxidative branch. The oxidative branch converts glucose 6-phosphate (G6P) to ribulose-5-phosphate, CO_2, and NADPH (Kruger and von Schaewen, 2003), and the non-oxidative branch produces glycolytic intermediates, such as fructose 6-phosphate (F6P), glyceraldehyde 3-phosphate (G3P), and sedoheptulose. These glycolytic intermediates are important for amino acid synthesis and produce ribose-5-phosphate (R5P) that is also important for nucleic acid synthesis (Stincone et al., 2015). Enzymes that are involved in the oxidative branch are 6-phosphogluconate dehydrogenase (6PGD) and glucose 6-phosphate dehydrogenase (G6PD), and those that are involved in the non-oxidative branch are ribulose-5-phosphate epimerase (RPE), ribose 5-phosphate isomerase (RPI), transaldolase (TALDO), and transketolase (TKT).

Cancer cells produce a high level of reactive oxygen species (ROS) compared to normal cells due to the increased activation of various metabolic pathways (Ahmad et al., 2005). Cancer cell metabolism is closely related to ROS homeostasis; they cause ROS detoxifications by using various substrates and metabolic intermediates in metabolic pathways, the most representative of which are glycolysis by the Warburg effect and PPP (Aykin-Burns et al., 2009). Glycolysis by the Warburg effect maintains redox homeostasis by being independent of mitochondrial OXPHOS that produces a large amount of ROS (Lee and Yoon, 2015), and PPP by producing ROS-detoxifying molecule, NADPH, by G6PD and 6-Phosphogluconate dehydrogenase (6PGDH) (Salazar, 2018).

Molecules involved in the regulation of glucose metabolism in cancer in general are oncogenes such as Ras, Src, and MYC, transcription factors such as hypoxia-inducible factor-1 (HIF-1), signaling pathway such as phosphoinositide 3-kinase (PI3K)/Akt/mammalian target of rapamycin (mTOR), and tumor suppressor such as p53. Oncogenes such as Ras, Src, and MYC increase the expression of HIF-1 that increases the expression of various glycolytic enzymes, and HIF-1, MYC, and KRAS increase

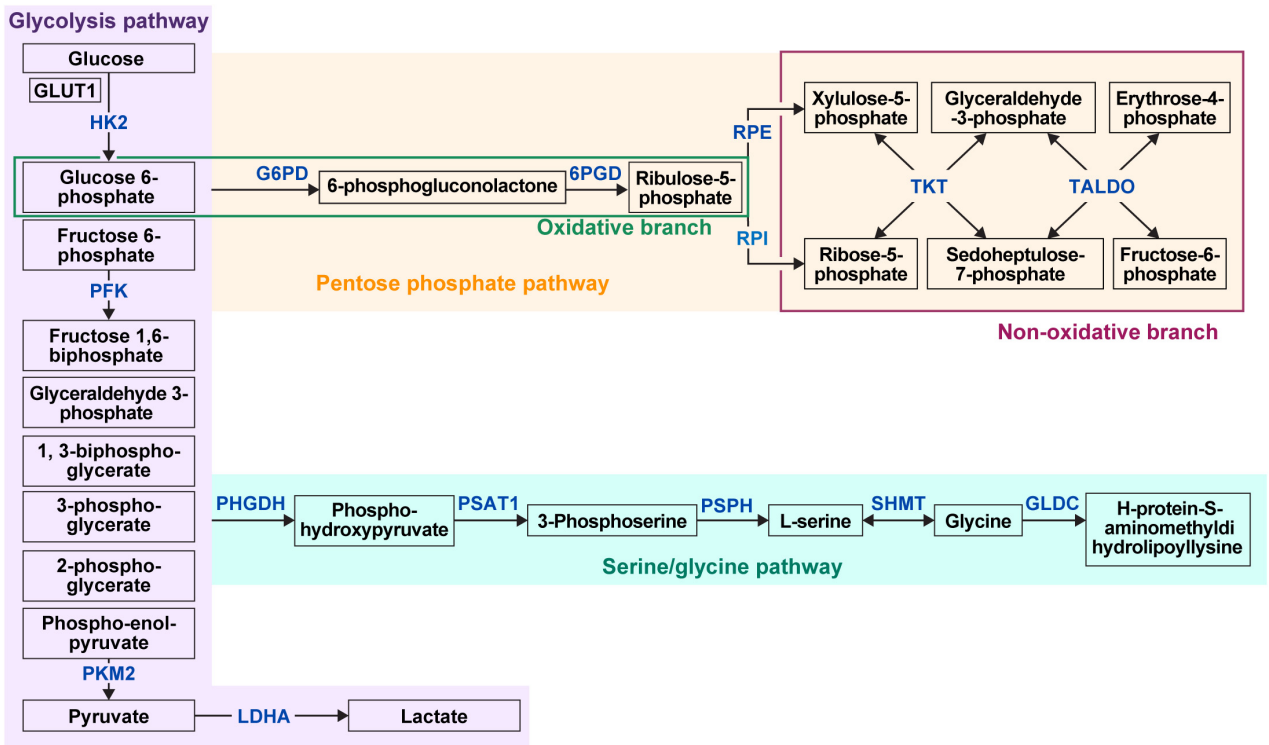

FIGURE 1 | Overview of glucose metabolism in cancer cells. Glucose metabolism in tumor cells consists of three main types: glycolysis, the pentose phosphate pathway (PPP), and the serine/glycine pathway. First, in glycolysis, glucose influx occurs in the cell by glucose transporter GLUT1. Using HK2, PFK, and PKM2, glucose becomes pyruvate and is eventually converted to lactate by LDHA. PPP comprises an oxidative branch and a non-oxidative branch, where glucose 6-phosphate is converted to 6-phosphogluconolactone and then ribulose-5-phosphate by 6PGD and G6PD. The non-oxidative branch produces xylulose-5-phosphate by RPE and ribose-5-phosphate by RPI, and then produces fructose 6-phosphate, glyceraldehyde 3-phosphate, sedoheptulose-7-phosphate, and erythrose-4-phosphate by TKT and TALDO through complex interchangeable reactions. The serine pathway starts with 3-phosphoglycerate, which is converted to phosphohydroxypyruvate by PHGDH, which is converted to 3-phosphoserine by PSAT1, and 3-phosphoserine is converted to serine by PSPH. In addition, glycine is converted by GLDC to H-protein-*S*-aminomethyldihydrolipoyllysine in glycine metabolism, which is linked to serine metabolism by SHMT in the form of reversible conversion. HK2, hexokinase II; PFK, phosphofructokinase; PKM2, pyruvate kinase isozymes M2; LDHA, lactate dehydrogenase A; G6PD, glucose 6-phosphate dehydrogenase; 6PGD, 6-phosphogluconate dehydrogenase; RPE, ribulose-5-phosphate epimerase; RPI, ribose 5-phosphate isomerase; TKT, transketolase; TALDO, transaldolase; PHGDH, phosphoglycerate dehydrogenase; PSAT1, phosphohydroxythreonine aminotransferase; PSPH, phosphoserine phosphatase; SHMT, serine hydroxymethyltransferase; GLDC, glycine decarboxylase.

glucose uptake by inducing GLUT expression. In addition, the PI3K/Akt/mTOR pathway induces glycolytic enzymes and GLUT expression, and p53 regulates glycolysis and GLUT through mTOR and AMP-activated protein kinase (AMPK) (Abdel-Wahab et al., 2019; Ghanavat et al., 2021).

GLUCOSE TRANSPORTERS IN GLYCOLYSIS

There are two families of glucose transporters: facilitative sugar transporters (GLUT, gene family name *SLC2A*) and Na^+/glucose co-transporters (SGLT, gene family name solute carrier *SLC5A*). Additionally found families of glucose transporters are the Sugars Will Eventually be Exported Transporters (SWEET; SLC50) family and the Spinter protein (SLC63) family. SLC50 is a Na (+)/substrate co-transporter involved in the transport of glucose, myoinositol, and anions and located in the plasma membrane. SGLT1 (SLC5A1) and SGLT2 (SLC5A2) are important in glucose uptake with the former expressed mainly in the intestine and the latter in the kidney (Wright, 2013). GLUT has 14 isoforms that share structural features, such as 12 transmembrane domains, amino terminus, carboxy-terminus, and an *N*-glycosylation site. GLUTs can be subgrouped into three classes: class I (GLUT1–4 and GLUT14), class II (GLUT5, 7, 9, and 11), and class III (GLUT6, 8, 10, 12, and 13). Class I and class II GLUTs are called odd transporters, whereas class III GLUTs are called even transporters (Mueckler and Thorens, 2013). Except for GLUT13, which is a proton-driven myoinositol transporter, all GLUTs are facilitative transporters. These GLUT isoforms differ in the tissue type in which they are present, their location within the cells, cohesiveness with substrates, and control mechanism (Mueckler and Thorens, 2013). For instance, GLUT1 and GLUT3 are found in the brain, where they function mainly in glucose transport (Leino et al., 1997; Yeh et al., 2008), whereas GLUT3–5 and GLUT10–11 are found in the muscle (Bilan et al., 1992; McVie-Wylie et al., 2001; Rogers et al., 2002; Douard and Ferraris, 2008). Glucose is an important substrate for GLUT,

but GLUT can also transport other substrates such as galactose, mannose, glucosamine, dehydroacetic acid, fructose, urate, and myo-inositol (Barron et al., 2016; Holman, 2020).

GLUCOSE METABOLISM AND GLYCOLYSIS-RELATED METABOLIC PATHWAYS IN BREAST CANCER

Cancer cells harbor a metabolic shift to aerobic glycolysis that plays an important role in tumor growth, progression, and metastasis; therefore, glucose metabolism and glycolysis-related metabolic pathways can have a diverse impact on cancer cells in breast cancer.

Expression of Glycolysis-Related Enzymes and GLUTs in Breast Cancer

Breast cancer shows an increased expression of glycolysis-related enzymes, namely, HKII (Brown et al., 2002; Yang T. et al., 2018), 6-phosphofructo-2-kinase/fructose-2, 6-biphosphatase 3 (PFKFB3) (O'Neal et al., 2016), and pyruvate kinase M2 (PKM2) (Lin et al., 2015). In primary breast cancer, HKII is overexpressed in about 79% of tumors (Brown et al., 2002), which has been correlated with an increased histologic grade and proliferative activity (Sato-Tadano et al., 2013). The expression of 6-phosphofructo-2-kinase/fructose-2, 6-biphosphatase 3 activates PFK-1, a key enzyme in glycolysis (Okar et al., 2001), and is correlated with HER-2 expression and poor prognosis (O'Neal et al., 2016; Peng et al., 2018). Additionally, 6-phosphofructo-2-kinase/fructose-2, 6-biphosphatase 3 expression is related to the expression of vascular endothelial growth factor (VEGF)-α in breast cancer, which contributes to angiogenesis and distant metastasis (Peng et al., 2018). PFK-2 is a muscle isoform M2 of PK, a key enzyme in glycolysis, and its expression is correlated with a poor prognosis in breast cancer (Lin et al., 2015). Lactates produced by glycolysis are transported in and out of cells by monocarboxylate transporter (MCT) (Wilde et al., 2017). MCT1 overexpression in breast cancer is correlated with ER negativity, PR negativity, high Ki-67 labeling index (Li et al., 2018), basal-like type (Pinheiro et al., 2010), high grade, high stage, increased recurrence, and poor prognosis (Johnson et al., 2017). As for MCT4, tumoral MCT4 expression (Li et al., 2018) and stromal MCT4 expression (Baenke et al., 2015) are associated with poor prognosis.

Breast cancer has been reported to have an increased expression of GLUT1–6 and 12 (**Table 1**; Barron et al., 2016), and the most important glucose transporter for glucose uptake in breast cancer is GLUT1 (Grover-McKay et al., 1998; López-Lázaro, 2008; Furuta et al., 2010; Wuest et al., 2018). Glucose uptake by GLUT1 is important in the carcinomatous transformation and carcinogenesis of breast cancer, and it plays an important role in the early phase of breast cancer development (Young et al., 2011; Wellberg et al., 2016). GLUT1 overexpression in breast cancer is correlated with high histologic grade, high proliferative activity, poor differentiation, and poor prognosis (Pinheiro et al., 2011; Krzeslak et al., 2012). GLUT4 is an insulin-stimulated glucose transporter (Vargas et al., 2021), and glucose uptake is dependent on insulin stimulation in cancer cell lines (Harmon and Patel, 2004; Moreira et al., 2013; Guedes et al., 2016). It has also been reported that hyperinsulinemia increases the risk of breast cancer irrespective of the body mass index (BMI) (Lawlor et al., 2004; Kabat et al., 2009; Gunter et al., 2015), and so it can be postulated that insulin is associated with breast cancer. Cross-talks between signaling pathways regulated by 17 beta-estradiol (E2) and insulin-like growth factor (IGF) (Bruning et al., 1992; Conover et al., 1992), strong mitogen for cancer cells (Beckwith and Yee, 2014), and actions through ER-signaling (Katzenellenbogen and Norman, 1990) are some possible mechanisms associated with the insulin effect on breast cancer.

Overexpression of glycolysis-related enzymes and GLUTs in breast cancer is due to the activation of the signaling pathways controlling the enzyme expression in breast cancer (**Figure 2**). The main molecular pathways involved in the control of aerobic glycolysis are the PI3K/AKT, AMP-activated protein kinase (AMPK), mitogen-activated protein kinase, Wnt, and mTOR pathways (Engelman et al., 2006; Han et al., 2015; Cai et al., 2018; Hibdon et al., 2019; Irey et al., 2019). Among these, the PI3K/AKT, AMPK, and mTOR pathways are activated in breast cancer. PI3K/AKT activates phosphofructokinase-2 (PFK-2) by phosphorylation (Novellasdemunt et al., 2013; Lee et al., 2018). PI3K/AKT pathway activation leads to GLUT1 overexpression, which is then translocated from the cytoplasm to the plasma membrane (Samih et al., 2000). AKT is activated by E2, thus increasing the glucose uptake in MCF-7 breast cancer cell line through translocation of GLUT4 to the plasma membrane (Garrido et al., 2013). PIK3CA and AKT1 gene mutations are common in breast cancer (Castaneda et al., 2010; Koboldt et al., 2012), and PIK3CA mutation is usually found in ER-positive and HER-2 positive breast cancer. AMPK translocates GLUT4 to the cytoplasmic membrane by activating PFK-2 (Marsin et al., 2000) and increases GLUT1 expression (Barnes et al., 2002). AMPK is highly expressed in TNBC and known to be associated with poor prognosis (Huang et al., 2016). mTOR is a downstream effector of AKT, comprising mTOR complex 1 (mTORC1) and mTOR complex 2 (mTORC2) (Hara et al., 2002; Vivanco and Sawyers, 2002; Baretić and Williams, 2014). mTORC1 promotes the transition from OXPHOS to glycolysis and increases the expression of HIF-1α, which in turn increases the expression of glycolysis-related enzymes such as PFK (Düvel et al., 2010). mTORC2 promotes glycolysis by activating AKT (García-Martínez and Alessi, 2008; Ikenoue et al., 2008; Cybulski and Hall, 2009) and GLUT1-related glucose uptake (Beg et al., 2017). mTOR is activated in breast cancer through HER-2 overexpression, PI3K pathway alteration, and mTOR mutation (Hare and Harvey, 2017). Second, the increased expression of glycolysis-related enzymes in breast cancer is because of the activation of transcription factors (**Figure 2**). The transcription factors associated with glycolysis are c-myc, p53, and HIF-1. c-myc is responsible for increasing the gene expression of glycolysis-related genes and, consequently, glycolysis-related enzymes, such as GLUT, HK, and PFK (Hsieh et al., 2015). Moreover, estrogen is responsible for the increased expression

TABLE 1 | GLUT expressed in breast cancer.

GLUT type	Patient number and diagnosis	Material and method	GLUT status	Related factors	References
GLUT1 GLUT2 GLUT3 GLUT4 GLUT5 GLUT6	33, IDC	IHC, FFPE	90.9% + + / + + + 90.9% + / + + 9.1% + 6.1% + 84.8% + / + + 50.0% +	n/a	Godoy et al., 2006
GLUT1	118, IBC	IHC, FFPE	42% positive	High Ki-67 High HG bcl-2 negative	Younes et al., 1995
GLUT1	124, IBC	IHC, FFPE	46% positive	High HG basal-like type PR negative High Ki-67	Pinheiro et al., 2011
GLUT1	100, IBC	IHC, FFPE	47% positive	High nuclear grade ER negative PR negative Shorter DFS, OS	Kang et al., 2002
GLUT1	78, IDC, No LN mets	IHC, FFPE	28.0% + in HG 1 63.8% + in HG 2 58.7% + in HG 3	n/a	Ravazoula et al., 2003
GLUT1	61, BC	IHC, FFPE	86.9% +	High HG	Alò et al., 2001
GLUT1	523, IBC −55 BLBC −231 non-BLBC	IHC, FFPE	76.4% + in BLBC 23.8% + in non-BLBC	High HG ER negative PR negative basal-marker + p53 expression	Hussein et al., 2011
GLUT1	132, TNBC	IHC, FFPE	65.2% + in tumor 5.3% + in stroma	n/a	Kim et al., 2013
GLUT1	276, IBC	IHC, FFPE	88.4% low 11.4% high	High HG ER negative PR negative No LN mets	Choi et al., 2013
GLUT1	809, IBC −692 IDC −114 ILC	IHC, FFPE	32.9% positive −37.3% + in IDC −6.1% + in ILC	High HG in ILC Shorter OS in ILC	Kim Y. H. et al., 2014
GLUT1 GLUT2	12, BC, 5, LN mets	IHC, FFPE	100% positive 100% positive	n/a	Brown and Wahl, 1993
GLUT1 GLUT3	70, BC	PCR, Western blotting	48.7% positive 21.0% positive	Higher HG	Krzeslak et al., 2012
GLUT1 GLUT4	30, BC	ICC	57% positive 43% positive	n/a	Binder et al., 1997
GLUT5	20, BC	IHC, FFPE	100% positive	n/a	Zamora-León et al., 1996
GLUT12	10, IBC	IHC, FFPE	80% positive	n/a	Rogers et al., 2003

IDC, invasive ductal carcinoma; IHC, immunohistochemistry; ICC, immunocytochemistry; FFPE, formalin-fixed paraffin-embedded; IBC, invasive breast cancer; HG, histologic grade; ER, estrogen receptor; PR, progesterone receptor; LN, lymph node; BLBC, basal-like breast cancer; TNBC, triple negative breast cancer; ILC, invasive lobular carcinoma; PCR, polymerase chain reaction.

of c-myc, and about 80% of breast cancers are ER-positive (Butt et al., 2008). p53 is a well-known tumor suppressor, gene mutations of which are found in most cancers including breast cancer. p53 mutation is found in about 20%–30% of breast cancers and more often in ER-negative breast cancer. p53 suppresses phosphoglycerate mutase (PGM), GLUT1, GLUT3, and GLUT4 expression (Kawauchi et al., 2008; Vousden and Ryan, 2009); hence, p53 mutation leads to an increased glycolysis in breast cancer. Lastly, the transcription factor HIF-1α, which is activated by hypoxia, is an important regulator in glycolysis and increases the expression of glycolysis-related molecules, such as HKII, PFK-1, lactate dehydrogenase (LDH) A, GLUT-1, and GLUT-3. HIF-1α promotes the metabolic shift to glycolysis by suppressing the mitochondrial function through the activation of pyruvate dehydrogenase kinase 1 (PKD1) and MAX interactor 1 (MXI1) (Denko, 2008). HIF-1α overexpression

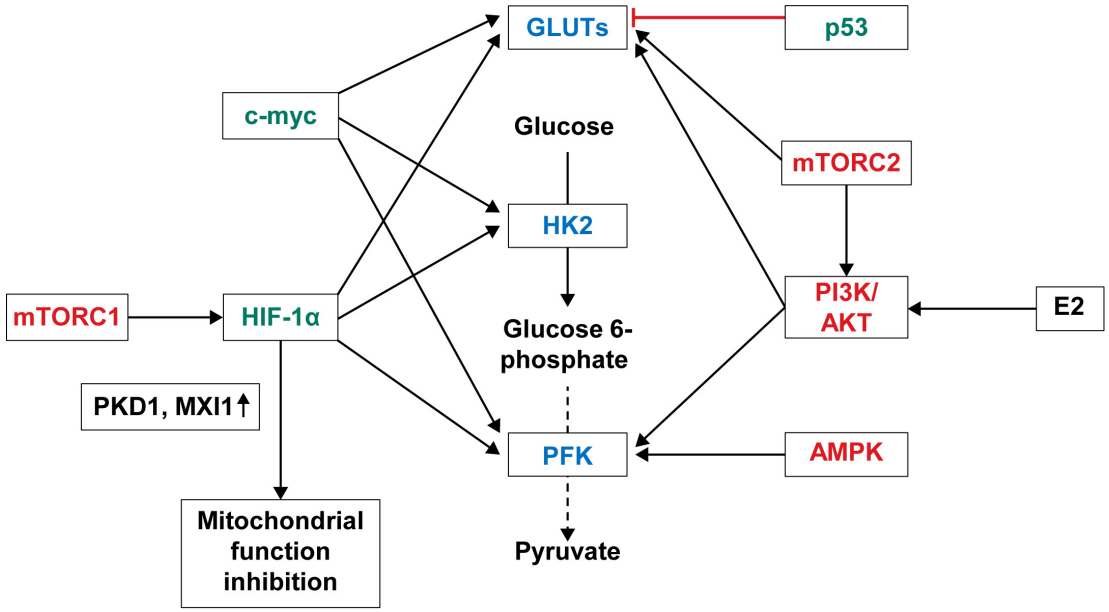

FIGURE 2 | Regulation of glycolysis and glucose transporters in breast cancer. Important signaling pathways regulating glycolysis and glucose transporters in breast cancer are the PI3K/AKT, AMPK, and mTOR pathways. PI3K/AKT pathway activated by 17-estradiol (E2) or genetic mutations increases expression of PFK2 and GLUT. AMPK pathway activated in breast cancer transports GLUT4 to cell membrane through activation of PFK-2 and increases GLUT expression. mTORC1 among the mTOR complex increases the expression of PFK by activating HIF-1α. mTORC2 either activates AKT or increases GLUT1 expression. Transcription factors regulating glucose metabolism in breast cancer are c-myc, p53, and HIF-1α. As such, breast cancer with p53 mutation shows increased expression of GLUT because c-myc induces increased expression of GLUT, HK, and PFK, and p53 suppresses expression of GLUT. Lastly, activated HIF-1α increases expressions of HK, PFK, LDHA, and GLUT, and suppresses mitochondrial function by activating PKD1 and MXII. PI3K, phosphoinositide 3-kinase; AKT, Ak strain transforming protein kinase B; AMPK, AMP-activated protein kinase; mTOR, mechanistic target of rapamycins; PFK, phosphofructokinase; HIF, hypoxia-inducible factor; HK, hexokinase; LDHA, lactate dehydrogenase A; PKD1, pyruvate dehydrogenase kinase 1; MXI1, MAX interactor 1.

has been reported in breast cancer (Zhong et al., 1999), and it is attributed to the increased expression of glycolysis-related proteins in breast cancer because HIF-1α overexpression is related to HER-2 positivity (Giatromanolaki et al., 2004) and TNBC (Jin et al., 2016).

Breast cancer is susceptible to sex hormones such as estrogen, which may have an effect on the regulation of glucose metabolism. E2 and ERα stimulation activates the MAPK pathway (Ronda et al., 2010a,b), regulates expression of GLUT4 (Barros et al., 2006, 2008), and increases glucose uptake (Niu et al., 2003; Gorres et al., 2011). Furthermore, E2 activates the PI3K pathway that is involved in glucose metabolism in breast cancer cells (Simoncini et al., 2000; Lee et al., 2005), and suppresses phosphatase and tensin homolog (PTEN), a phosphatidylinositol-3 kinase inhibitory protein (Noh et al., 2011).

Expression of Glycolysis-Related Enzymes and GLUTs in TNBC

Triple negative breast cancer is defined as breast cancer that is negative for ER, PR, and HER-2 and accounts for about 15% of breast cancer cases. Basal-like breast cancer (BLBC) is defined as those that have high expressions of basal genes in gene expression studies such as DNA microarray. Therefore, TNBC and BLBC are not the same in the strict sense of definitions (Carey et al., 2010), although they can overlap in many instances. TNBC is a heterogeneous group, and many researches have focused on the subgrouping of TNBC. Lehmann et al. (2011) have grouped TNBC further into basal-like1, basal-like2, mesenchymal, and luminal androgen receptor, and Burstein et al. (2015) have grouped TNBC further into basal-like immune-activated, basal-like immune suppressed, mesenchymal, and luminal androgen receptor. The general characteristics of TNBC include the histological characteristics of high grade, high proposition index, and tumor necrosis, and clinical characteristics of higher rate of metastasis and poor prognosis (Kumar and Aggarwal, 2016; Borri and Granaglia, 2020). With these histological and clinical features, TNBC can be postulated to be of high metabolic status. One of the important metabolic features of TNBC is high glucose uptake, and GLUT1 overexpression is seen in TNBC (Hussein et al., 2011; Oh et al., 2017). High expression of glycolysis-related enzymes, such as HK2 (Jiang S. et al., 2012), PKM2 (Christofk et al., 2008; Ma et al., 2019), and LDH (McCleland et al., 2012; Huang et al., 2016; Dong et al., 2017), and that of lactate transporters MCT1 and MCT4 have also been reported in TNBC (Pinheiro et al., 2010; McCleland et al., 2012; Doyen et al., 2014). The high expression of glycolysis-related proteins in TNBC is owing to the fact that the glycolysis regulatory factors, such as HIF-1 (Lin et al., 2016; De Blasio et al., 2020), c-myc (Palaskas et al., 2011; Shen et al., 2015), and EGF signaling (Avanzato et al., 2018), are promoted in TNBC. Therefore, TNBC cells are much more dependent on glucose metabolism than non-TNBC cells

(MCF-7) (Robey et al., 2005), and GLUT1 inhibition shows a more anti-proliferative effect for TNBC cells than non-TNBC cells (MCF-7) (Yang et al., 2021).

Non-glycolysis Glucose Metabolism Pathway in Breast Cancer

In glucose metabolism, non-glycolysis metabolic pathways, such as the serine/glycine metabolic pathway and PPP, play important roles in breast cancer. The expression of serine/glycine metabolic pathway-related proteins in breast cancer differs depending on the breast cancer molecular subtype. Serine metabolic pathway-related proteins were highly expressed in TNBC (Labuschagne et al., 2014), and glycine metabolic pathway-related proteins were highly expressed in HER-2 type breast cancer (Kim S. K. et al., 2014). The basal-like type also showed a higher expression of serine/glycine metabolic pathway-related proteins among the TNBC subtypes (Noh et al., 2014). Analysis using the cBioPortal TCGA Pan-Cancer Atlas shows PHGDH amplification in approximately 2.2% of breast cancers (Geeraerts et al., 2021a). PHGDH expression is observed frequently in ER-negative breast cancer (Possemato et al., 2011), and increased PHGDH expression in breast cancer is associated with poor prognosis (Locasale et al., 2011; Possemato et al., 2011). Similarly, phosphoserine aminotransferase 1 (PSAT1) is more frequently expressed in ER-negative breast cancer and is associated with poor prognosis (Gao et al., 2017). Serine hydroxymethyltransferase 2 expression level is associated with the histologic grade of breast cancer (Yin, 2015).

High expression of PPP-related enzymes, such as 6PGD (Yang X. et al., 2018) and TKT (Benito et al., 2017; Yang X. et al., 2018), is reported in breast cancer. G6PD, one of the PPP-related enzymes, is associated with the molecular subtype of breast cancer, and G6PD overexpression is associated with poor prognosis of breast cancer (Pu et al., 2015; Dong et al., 2016). 6PGDH expression is high in TNBC, and the expression of G6PDH and 6PGL are high in HER-2 type (Choi et al., 2018b). The expression of G6PDH is also the highest in brain metastasis among metastatic breast cancers (Cha et al., 2017). The expression of TKT is associated with tumor size and high TKT expression is associated with poor prognosis in a mouse model of breast cancer (Tseng et al., 2018). Increased PPP flux by G6PD and HK2 enhancement induces tamoxifen resistance in breast cancer (Wang et al., 2016). An increase in HK2 transcription by the yes-associated protein (YAP) axis also promotes the migration of breast cancer cells (Tseng et al., 2018).

Glucose Metabolism in the Tumor Microenvironment of Breast Cancer

Breast cancer is one of those tumors that harbors tumor stroma, the main cell components of which include cancer-associated fibroblasts (CAFs), cancer-associated adipocytes (CAAs), and immune cells. These stromal cells affect the development, progression, and metastasis of breast cancer through various interactions with breast cancer cells (Mao et al., 2013; Soysal et al., 2015; Choi et al., 2018a; Mittal et al., 2018; Wu et al., 2019b). Thus, metabolic interactions are present between breast cancer cells and stromal cells (**Figure 3**), and glucose metabolism in tumor stromal cells is suggested in the reverse Warburg effect. According to the reverse Warburg effect, aerobic glycolysis occurs in CAFs that are present in the breast cancer stroma. In brief, the reverse Warburg theory describes the glycolysis that occurs in CAFs by ROS, HIF1A, and nuclear factor-κB

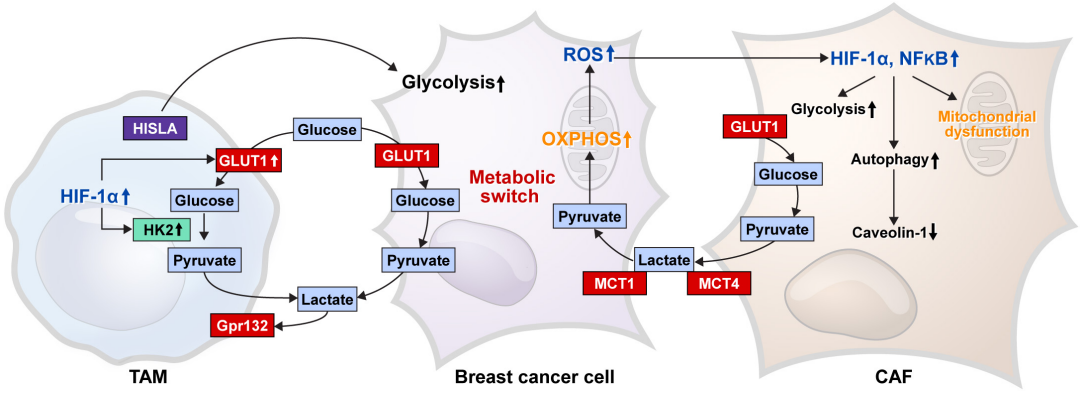

FIGURE 3 | Glucose metabolic interaction between breast cancer cells and stromal cells. The glucose metabolic interaction between the breast cancer cell and CAF is presented as the reverse Warburg effect, where mitochondrial dysfunction results in a decrease in caveolin-1 levels because of increased autophagy, and an increase in glycolysis occurs by enhanced HIF-1α and NF-κB in CAF. Lactate produced by glycolysis is transferred to cancer cells by MCT4 in CAF and MCT1 in cancer cells, which is converted to pyruvate and used as a material for mitochondrial OXPHOS. ROS produced by the OXPHOS process cause an increase in HIF-1α and NF-κB in CAF. TAM, one of the immune cells of breast cancer stroma, shows increased glycolysis because of the increased GLUT1 and HK2 activity by enhanced HIF-1α expression; therefore, TAM can compete with cancer cells for glucose. G protein-coupled receptor 132 (Gpr132) senses the lactate produced by glycolysis to convert the macrophage to an M2-like phenotype, which promotes cancer cell adaptation, migration, and invasion. HIF-1α-stabilizing long non-coding RNA (HISLA) is transferred from TAM to breast cancer cells through extracellular vesicle transmission, and then, HISLA promotes glycolysis in breast cancer cells. Breast cancer cells have a metabolic switch that controls glycolysis and OXPHOS depending on the circumstances. CAF, cancer-associated fibroblast; HIF, hypoxia-inducible factor; MCT, monocarboxylate transporter; OXPHOS, oxidative phosphorylation; HK, hexokinase; ROS, reactive oxygen species; TAM, tumor-associated macrophage.

(NF-κB), resulting in lactate being released from CAFs by MCT4, which is then transported into the tumor cells by MCT1 in breast cancer, creating energy by mitochondrial OXPHOS (Pavlides et al., 2009; Fu et al., 2017; Wilde et al., 2017). Lactate produced by CAFs is transported into the tumor cells as potent nutrients for the TCA cycle, and this lactate can be an important source of energy for cancer cells because lactate is the primary source of carbon for the TCA cycle among circulating metabolites (Hui et al., 2017; Martínez-Reyes and Chandel, 2017). In co-cultural studies of breast cancer cell lines and fibroblasts and studies of human breast cancer tissue, MCT4 was expressed in CAFs, whereas MCT1 was expressed in tumor cells (Whitaker-Menezes et al., 2011; Witkiewicz et al., 2012; Johnson et al., 2017). In a co-cultural study of MCF7 breast cancer cells and normal fibroblasts, culture of MCF7 breast cancer cells alone or fibroblasts alone did not exhibit MCT4 expression, whereas co-culture of MCF7 breast cancer cells and fibroblasts showed MCT4 expression in CAFs. The co-culture with fibroblasts showed MCT1 upregulation in MCF7 breast cancer cells (Whitaker-Menezes et al., 2011). Breast CAFs showed higher expressions of GLUT1 and PDK1 than normal fibroblasts (Pasanen et al., 2016), and the co-cultural study of breast cancer cells and fibroblasts showed an increase in glycolysis and glucose transporter-related genes in CAFs (Ueno et al., 2015). The reverse Warburg effect is not only observed between cancer cells and CAFs but also between hypoxic and oxygenated cancer cells (Sonveaux et al., 2008; Doherty and Cleveland, 2013).

One type of immune cells in the tumor stroma is tumor-associated macrophages (TAMs) that inhibit antitumor immunity in breast cancer, resulting in tumor progression. In general, TAMs exhibit properties of M2 macrophages (Mantovani et al., 2002; Hollmén et al., 2015), and TAMs in hypoxic tumor regions express HIF-1 (Burke et al., 2003), which controls the expression of glycolysis-related genes, including *GLUT1*, *HK2*, *PFFB3*, and *PGK1* (Semenza et al., 1994). Therefore, TAMs in hypoxic tumor environments may utilize glycolysis. In addition, lactate generated in the glycolysis process is an important metabolite, which activates M2 macrophages (Colegio et al., 2014; Chen P. et al., 2017; Mu et al., 2018). In a co-culture study of breast cancer cells and macrophages, G protein-coupled receptor 132 (Gpr132) senses lactate in the tumor environment to transform macrophages into M2-like phenotypes to promote cancer cell adherence, migration, and invasion (Chen P. et al., 2017). In addition, HIF-1α-stabilizing long non-coding RNA (HISLA) is transferred from TAMs to breast cancer cells *via* extracurricular vessel transmission, which increases glycolysis in breast cancer cells (Chen et al., 2019).

IMPACT OF GLUCOSE METABOLISM AND GLUCOSE TRANSPORTERS ON BREAST CANCER BIOLOGY AND THE RESPONSE TO TREATMENT

First, the proliferation of tumor cells requires a lot of energy and a variety of materials are needed to create new tumor cells, which is also true for breast cancer cells. Therefore, glucose metabolism and glucose transporters, which provide energy sources for breast cancer, and PPP, which provides the materials needed for the synthesis of nucleotides, lipids, and non-essential amino acids, play important roles in breast cancer proliferation. Second, glucose metabolism affects the maintenance of epithelial-mesenchymal transition (EMT) and cancer stem cell (CSC) phenotype in breast cancer. Increased glycolysis and PPP by epigenetic silencing of fructose-1,6-biphosphatase can increase NADPH and reduce ROS levels, which enhance EMT and CSC phenotype in basal-like breast cancer (Dong et al., 2013; Schieber and Chandel, 2013). In a breast cancer cell line study, high glucose levels increased glycolytic enzyme, motor protein, and NF-κB levels and glucose uptake, and reduced actin, resulting in EMT phenotype activation (Santos and Hussain, 2020). In addition, HIF-1 activation by hypoxia maintains ROS homeostasis through the glycolytic pathway and serine synthesis pathway, which is important for breast CSC induction (Semenza, 2017). Moreover, glucose metabolism is associated with treatment resistance in breast cancer, where induced glycolysis is observed by AKT/mTOR/HIF-1α axis activation in tamoxifen resistant breast cancer cells, and when HKII is inhibited, tamoxifen sensitivity is recovered (Woo et al., 2015). Increased glycolysis is observed in trastuzumab resistant breast cancer cells, and glycolytic inhibition reduces trastuzumab resistance (Zhao et al., 2011). The expression of PFK-2 is linked to the responsiveness of anticancer drugs such as epirubicin and 5-fluorouacil in breast cancer cells (Benesch et al., 2010; Lin et al., 2015). Chemoresistant TNBC cells exhibit increased glycolysis and lactate permutation (Zhou et al., 2010), and PHGDH expression correlates with the responsiveness of chemotherapy in TNBC cells (Samanta et al., 2016). GLUT is associated with breast cancer metastasis; a proteomic analysis of MDA-MB-231 (metastatic breast cancer cell line) and MCF-10A (normal breast epithelial cell line) showed that one of the three strongest breast cancer-related proteins was GLUT1 (Risha et al., 2020). The GLUT expression showed a difference according to the metastatic sites, and the expression of GLUT1 was the highest in brain metastasis (Kim H. M. et al., 2014). Additionally, GLUT12 plays an important role in tumor growth and metastasis through aerobic glycolysis in TNBC (Shi et al., 2020).

CLINICAL APPLICATION OF GLUCOSE TRANSPORTERS AND GLUCOSE METABOLISM IN BREAST CANCER

As we have seen earlier, glucose transporter expression is high in breast cancer, and glucose metabolism is carried through the glycolytic, serine/glycine, and PPPs that play important roles in tumor growth and progression. Therefore, they may have a variety of clinical applications, especially in imaging diagnosis and targeted therapy.

Imaging Diagnosis

Positron emission tomography (PET) using ^{18}F-fluorodeoxy glucose (FDG), a radioactive analog of glucose, is the

representative functional imaging technique based on the principle that tumor cells uptake large amounts of glucose by GLUT *via* the Warburg effect. These PETs are used for tumor staging and treatment response monitoring (Bohndiek and Brindle, 2010). These FDG-PET/CTs are also useful for diagnosis, staging, and treatment evaluation in breast cancer (Groheux et al., 2016; Caresia Aroztegui et al., 2017; Paydary et al., 2019). In addition to FDG-PET/CT, functional imaging based on glucose metabolism can be performed using magnetic resistance spectroscopy (MRS). Multiple metabolites can be simultaneously identified in tumor tissues using MRS, which can analyze labeling patterns using stable isotopic traces, and glucose metabolites can be analyzed using ^{13}C-MRS and [^{13}C]-labeled glucose to image the glycolysis status. MRS can perform effective metabolic monitoring in breast cancer (Rivenzon-Segal et al., 2002). Breast cancer with different ^{13}C-MRS expression patterns show a different glucose metabolism (Grinde et al., 2011). A high-resolution magic angle spinning MRS analysis of metabolites in breast cancer, such as β-glucose, lactate, and glycine, shows good prognosis with reduced concentrations of glycine. The concentration of β-glucose shows a negative correlation with proliferation index (MIB-1), indicating that MR metabolite analysis is valuable in breast cancer prognostication (Sitter et al., 2010).

Therapeutic Target of Glucose Metabolism and Glucose Transporters

The expression of glucose transporters and glucose metabolic enzymes in breast cancer is high; thus, their inhibition can serve as an effective treatment strategy against breast cancer (**Figure 4**). Various preclinical and clinical studies have been conducted to investigate this implication.

GLUT1 Inhibitors

GLUT1 inhibitors—WZB117 and SFT-31—inhibit cell proliferation and promote apoptosis in breast cancer cell lines (Xintaropoulou et al., 2015). WZB117 increases the effectiveness of radiation (Zhao et al., 2016) and anticancer drugs in breast cancer cell lines (Liu et al., 2012; Chen Q. et al., 2017). BAY-876, a selective GLUT1 inhibitor, decreases glucose uptake in TNBC cell lines (Wu et al., 2019a) and 2-deoxy-D-glucose (2-DG), a synthetic non-metabolizable glucose analog, competes with glucose for binding GLUT, which reduces glucose uptake in the MDA-MB-231 TNBC cell line (Amaral et al., 2018). As for 2-DG, there are two different phenomena resulting from the suppression of glycolysis: first, glucose can be deviated to PPP because 2-DG is not metabolized any further after phosphorylation into 2-deoxy-D-glucose-6-phosphate (2-DG-6-P) by HKII (Ralser et al., 2008); and second, 2-DG induces autophagy due to endoplasmic reticulum (ER) stress. Suppression of glycolysis leads to a decreased ATP, by which *N*-linked glycosylation is suppressed and AMPK is activated. AMPK activation and *N*-linked glycosylation lead to ER stress (Xi et al., 2011, 2013). Autophagy promotes tumor growth in the early stage of cancer (Cheong, 2015), maintains tumor survival, and increases metastasis in the advanced stage (Yang et al., 2011). Anti-GLUT1 monoclonal antibody decreases glucose uptake in the MDA-MB-231 TNBC cell line, and decreases cancer cell proliferation and promotes apoptosis in MCF-1 and T47D breast cancer cell lines (Rastogi et al., 2007). Polyphenols, a huge family of natural compounds found in plants or food, is one category of the GLUT1 inhibitors (Williamson, 2017) that shows an anti-tumoral effect against various cancers including breast cancer. The anti-tumoral mechanism of polyphenols against breast cancer includes increased apoptosis, cell cycle arrest, enhanced autophagy, decreased angiogenesis, anti-inflammatory effect, blockade for estrogen, aromatase modulation, altered redox balance, and inhibition of the HER-2 pathway (Mocanu et al., 2015; Losada-Echeberría et al., 2017). Polyphenols inhibiting GLUT1 in breast cancer are as follows: Resveratol suppresses glucose uptake in T-47D cell line by reducing GLUT1 protein level (Jung et al., 2013), and hesperetin suppresses glucose uptake by decreasing GLUT 1 mRNA and protein levels (Yang et al., 2013). Quercetin decreases the glucose uptake in MCF-7 and MDA-MB-231 by reducing GLUT1 protein level (Jia L. et al., 2018), as does glabridin in MDA-MB-231 (Li et al., 2019). Epigallocatechin-3-gallate (EGCG) decreases the glucose and lactate levels in cancer cells by reducing GLUT1 mRNA levels in 4T1 cell line (Wei et al., 2018), and cantharidin suppresses metastasis by inhibiting glucose uptake and lactate production through decreasing GLUT1 protein level in MCF-7 and MDA-MB-231 (Pan et al., 2019). Kudingcha, one of the Ligustrum robustum species, inhibit cancer proliferation through decreasing GLUT1 protein level in MDA-MB-231 and HCC1806 (Zhu et al., 2020). Vitamin D_3 decreases glucose uptake by decreasing GLUT1 mRNA and protein levels in MCF-7 and MDA-MB-231 (Santos et al., 2018).

Glucose Metabolic Enzyme Inhibitors

First, 3-bromopyruvate (3-BrPA), an inhibitor of hexokinase, causes apoptosis in MDA-MB-231 breast cancer cell line (Liu et al., 2014; Chen et al., 2018) and increases the response to daunorubicin (Liu et al., 2015) and tamoxifen (Attia et al., 2015) in breast cancer. Methyl jasmonate, another hexokinase inhibitor, caused a decrease in tumor volume in mice bearing 4T1 breast cancer cell line (Yousefi et al., 2020). Resveratrol, an inhibitor of PFK, decreases the cell viability and glucose consumption in MCF-7 breast cancer cell line (Gomez et al., 2013). Cyclosporin A, an immunosuppressive agent, inhibits the expression and activity of PKM2 in breast cancer cell lines (MCF-7, MDA-MB-435, and MDA-MB-231) and causes tumor cell death by reducing cell viability (Jiang K. et al., 2012). Cyclosporin A also maintains mitochondrial function by suppressing mitochondrial permeability transition pore (Halestrap et al., 1997; Mishra et al., 2019). When oxamate, an LDH inhibitor, is administered in conjunction with doxorubicin and metformin, it causes a rapid tumor growth inhibition in the xenograft model using human MDA-MB-231 TNBC cell line (García-Castillo et al., 2017). When paclitaxel and oxamate are administered together, they induce an effective killing of paclitaxel-resident TNBC cells (Zhou et al., 2010). Gossypol, a lipid soluble polyphenolic compound, exhibits antitumor effects by inhibiting glycolysis through LDH isoenzyme type 5 inhibition (Coyle et al., 1994). Gossypol causes anti-proliferative

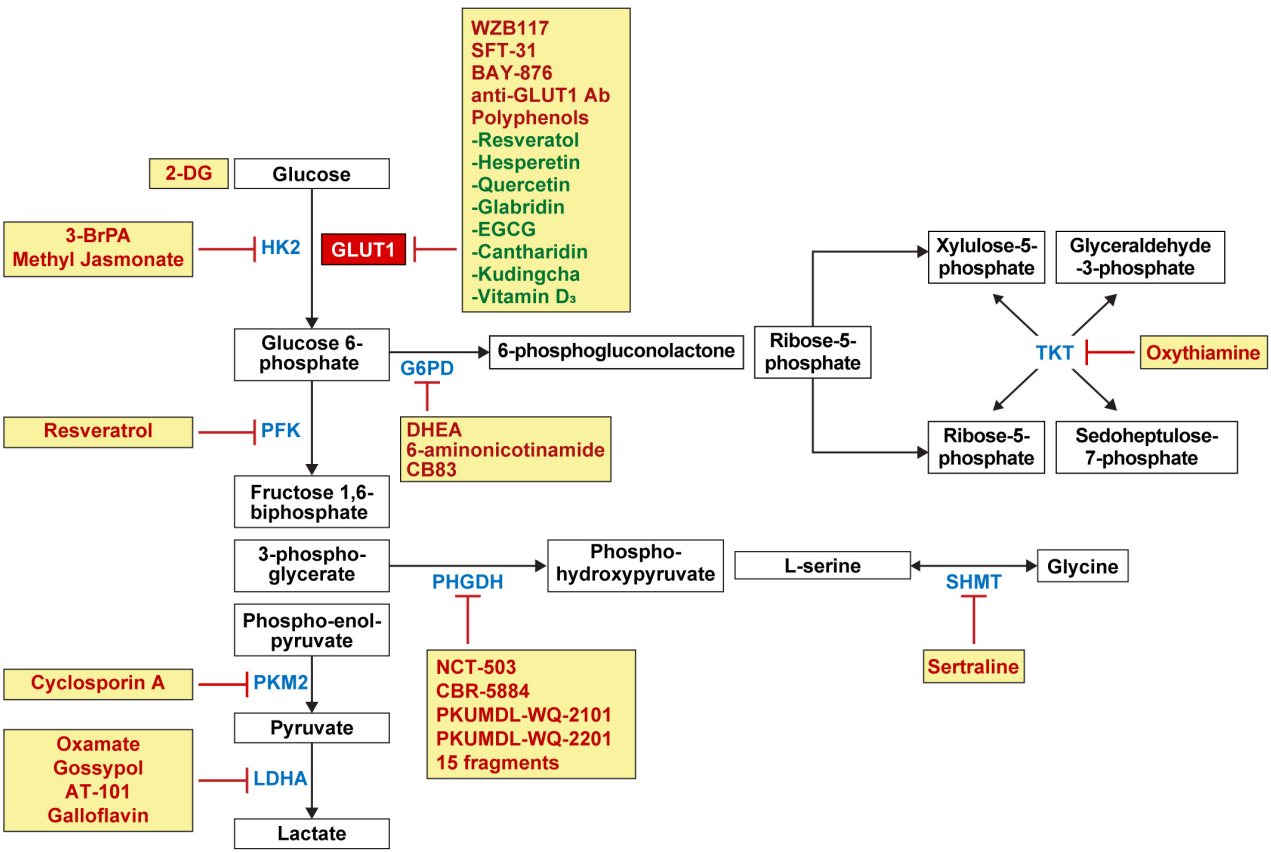

FIGURE 4 | Candidate drugs for the inhibition of glucose metabolism and glucose transporters in breast cancer. Inhibitors for GLUT1 involved in glucose influx in glycolysis include WZB117, SFT-31, BAY-876, anti-GLUT1 antibody, and polyphenols such as resveratrol, hesperetin, quercetin, glabridin, EGCG, cantharidin, kudingcha, and vitamin D_3. 2-DG competes with glucose for binding GLUT1. Enzyme inhibitors for HK2 involved in glycolysis include 3-BrPA and methyl jasmonate, and resveratrol as PKF inhibitors; cyclosporine A as PKM2 inhibitor; and oxamate, gossypol, AT-101, and galloflavin as LDHA inhibitors. Enzyme inhibitors for G6PD involved in PPP include DHEA, 6-aminonicotinamide, and CB83 and oxythiamine as TKT inhibitor. In the serine and glycine pathway, PHGDH inhibitors include NCT-503, CBR-5884, PKUMDL-WQ-2101, PKUMDL-WQ-2201, and 15 fragments, and sertraline as SHMT inhibitors. HK, hexokinase; PKF, phosphofructokinase; PKM2, pyruvate kinase isozymes M2; LDHA, lactate dehydrogenase A; G6PD, glucose 6-phosphate dehydrogenase; PPP, pentose phosphate pathway; DHEA, dehydroepiandrosterone; TKT, transketolase; PHGDH, phosphoglycerate dehydrogenase; SHMT, serine hydroxymethyltransferase.

activity and apoptosis in breast cancer cells (Gilbert et al., 1995; Ye et al., 2010; Messeha et al., 2019), and when R-(-)-gossypol (AT-101) is administered in conjunction with trastuzumab in HER-2 positive breast cancer cell line, it causes synergistic cytotoxicity and apoptosis (Bulut et al., 2020). Galloflavin, an LDHA inhibitor, induces cell death in MDA-MB-231 cell lines and acquired tamoxifen resistance MCF-7 breast cancer cell lines (Farabegoli et al., 2012).

Serine and glycine pathway inhibitors can be used for the management of tumors that use serine and glycine metabolism and for treatment of tumors showing recurrence and treatment resistance. PHGDH inhibitors—NCT-503 and CBR-5884—are both allosteric PHGDH inhibitors; NCT-503 binds to the near substrate-binding pockets; and CBR-5884 hinders PHGD holigomerization (Mullarky et al., 2016; Pacold et al., 2016). NCT-503 inhibits tumor growth in PHGDH-amplified breast cancer xenografts (Pacold et al., 2016), and CBR-5884 inhibits tumor cell proliferation in high PHGDH-expressing breast cancer cell lines (MDA-MB-468, MDA-MB-436, HCC70, and Hs578T) (Mullarky et al., 2016). PKUMDL-WQ-2101 and PKUMDL-WQ-2201, which are allosteric PHGDH inhibitors, show an antitumor activity in PHGDH-amplified breast cancer cell lines (MDA-MB-468 and HCC70) (Wang et al., 2017). An NAD-competitive PHGDH inhibitor, 15 fragments, reduces cell proliferation in *PHGDH*-amplified breast cancer cell line (MDA-MB-468) (Unterlass et al., 2018). Sertraline, an antidepressant, is a selective serotonin reuptake inhibitor (SSRI) class (MacQueen et al., 2001), but it also works as a competitive dual SHMT1/2 inhibitor, reducing the cell growth in serine/glycine synthesis-addicted breast cancer cell line (MDA-MB-468) and decreasing the tumor growth in a mouse xenograft study (Geeraerts et al., 2021b).

G6PD, one of the important enzymes in PPP, has a potent non-competitive inhibitor, dehydroepiandrosterone (DHEA), which is an adrenal cortical steroid. DHEA inhibits the growth and migration of breast cancer cell lines (MCF-7, MDA-MB-231, and Hs578T) (López-Marure et al., 2011). DHEA can bind estrogen or androgen receptors because it is metabolized

to estrogen or androgen (Labrie et al., 2001), however, the suppression of MCT-7 cell line growth by DHEA is reported to be independent of estrogen or androgen receptors (Gayosso et al., 2006). 6-aminonicotinamide, a G6PD inhibitor, can decrease mammosphere formation and aldehyde dehydrogenase (ALDH) activity when given with DHEA in breast cancer stem-like cells that show high PPP activity (Debeb et al., 2016). CB83, another G6PD inhibitor, can inhibit growth of MCF10-AT1 breast cancer cell line (Preuss et al., 2013). Oxythiamine, an inhibitor of TKT, also increases the response of breast cancer cells to doxorubicin or docetaxel (Tseng et al., 2018).

CONCLUSION

Because of the high expressions of GLUT-1 and the enzymes involved in glucose metabolism, tumor cells in breast cancer, as in other tumors, are provided with energy through glucose metabolism. There are several characteristic factors to consider in the glucose metabolism of breast cancer. Because breast cancer is heterogeneous, inter- and intratumoral heterogeneity is also seen in glucose metabolism. First, glucose metabolic activity is different among the molecular subtypes, especially in TNBC, which shows an increased glycolytic phenotype (Wang et al., 2020). According to the traditional Warburg theory, tumors showing aerobic glycolysis are suggested to exhibit a decreased mitochondrial OXPHOS; however, TNBC with a high metabolic activity shows both enhanced glycolysis and sustained mitochondrial OXPHOS (Park et al., 2016; Lanning et al., 2017; Luo et al., 2018; Jia et al., 2019). Luminal type breast cancer rely more on OXPHOS than glycolysis compared to TNBC (Pelicano et al., 2014). It also presents metabolic switches between glycolysis and OXPHOS during cancer progression (Levine and Puzio-Kuter, 2010; Jia D. et al., 2018; Lai et al., 2020; Moldogazieva et al., 2020). Therefore, metabolic intratumoral heterogeneity is exhibited in breast cancer, showing different glycolytic activities depending on the tumor cell type. Second, there is a metabolic interaction between tumor cells and the surrounding stromal cells in breast cancer. Breast cancer is a typical tumor that contains various stromal cells, the main components of which are CAFs, CAAs, and immune cells. Metabolic interactions exist between breast cancer cells and stromal cells; especially according to the reverse Warburg theory, lactates produced by glycolysis in CAFs enter tumor cells and produce energy through OXPHOS. Among the immune cells, B-cells and NK cells use glycolysis, and tumor-associated neutrophils use glycolysis and PPP, allowing a metabolic competition with the tumor cells. Third, unlike in other tumors, CAAs are stromal cells that are specifically present in breast cancer, and previous studies suggest that β-oxidation in tumor cells is primarily studied through the lipid transfer between CAAs and tumor cells. As the glucose metabolic interaction between CAAs and tumor cells is rarely studied in breast cancer, it requires further study. Metabolic interactions between tumor cells and stromal cells in these breast cancer cases are also reported to be affected by cancer phenotypes (Brauer et al., 2013), which may require further research on the metabolic cross-talk between the cancer cells and stromal cells according to the molecular subtype of breast cancer. Fourth, breast cancer shows differential metabolic features depending on the stage and metastatic site. In order for the tumor to progress into distant metastasis, multiple and complex processes, such as intravasation, survival in blood stream, and extravasation, must be accomplished during this process, and the hurdles, such as anchorage independent survival and tumor cell proliferation in foreign microenvironment, should be overcome. One way to overcome this challenge is metabolic reprogramming. Breast cancer shows metabolic differences between the primary and metastatic tumors (Chen et al., 2007; LeBleu et al., 2014; Dupuy et al., 2015; Simões et al., 2015; Andrzejewski et al., 2017), and breast cancer does not rely on a single metabolic pathway, but uses multiple metabolic pathways. Highly metastatic 4T1 cells show increased glycolysis and OXPHOS compared to non-metastatic 67NR breast cancer cells (Simões et al., 2015). The most common metastatic sites are the brain, bone, lung, and liver, which exhibit differential metabolic features owing to different microenvironments. Liver metastatic breast cancer demonstrates increased glycolytic pathways compared to bone and lung metastatic breast cancer (Dupuy et al., 2015), whereas brain metastatic breast cancer shows increased glycolysis and PPP compared to bone metastatic breast cancer (Chen et al., 2007). As a result of the above characteristics of glucose metabolism in breast cancer, further studies are needed to consider tumor imaging using glucose metabolism and glucose metabolic markers as treatment targets. In addition, because glucose metabolism is associated with resistance to anticancer drugs or targeted treatments in breast cancer, glucose metabolic inhibitors can also be considered for a combined therapy with conventional treatments.

AUTHOR CONTRIBUTIONS

ES and JK: writing—original draft, investigation, and writing—review and editing. Both authors contributed to the article and approved the submitted version.

ACKNOWLEDGMENTS

The authors would like to thank Dong-Su Jang, MFA (Medical Illustrator), for his help with the illustrations.

REFERENCES

Abdel-Wahab, A. F., Mahmoud, W., and Al-Harizy, R. M. (2019). Targeting glucose metabolism to suppress cancer progression: prospective of anti-glycolytic cancer therapy. *Pharmacol. Res.* 150:104511.

Ahmad, I. M., Aykin-Burns, N., Sim, J. E., Walsh, S. A., Higashikubo, R., Buettner, G. R., et al. (2005). Mitochondrial O2*- and H2O2 mediate glucose deprivation-induced stress in human cancer cells. *J. Biol. Chem.* 280, 4254–4263.

Alò, P. L., Visca, P., Botti, C., Galati, G. M., Sebastiani, V., Andreano, T., et al. (2001). Immunohistochemical expression of human erythrocyte glucose

transporter and fatty acid synthase in infiltrating breast carcinomas and adjacent typical/atypical hyperplastic or normal breast tissue. *Am. J. Clin. Pathol.* 116, 129–134. doi: 10.1309/5y2l-cdck-yb55-kdk6

Amaral, I., Silva, C., Correia-Branco, A., and Martel, F. (2018). Effect of metformin on estrogen and progesterone receptor-positive (MCF-7) and triple-negative (MDA-MB-231) breast cancer cells. *Biomed. Pharmacother.* 102, 94–101. doi: 10.1016/j.biopha.2018.03.008

Andrzejewski, S., Klimcakova, E., Johnson, R. M., Tabariès, S., Annis, M. G., McGuirk, S., et al. (2017). PGC-1α Promotes Breast Cancer Metastasis and Confers Bioenergetic Flexibility against Metabolic Drugs. *Cell Metab.* 26, 778–787.e5. doi: 10.1016/j.cmet.2017.09.006

Attia, Y. M., El-Abhar, H. S., Al Marzabani, M. M., and Shouman, S. A. (2015). Targeting glycolysis by 3-bromopyruvate improves tamoxifen cytotoxicity of breast cancer cell lines. *BMC Cancer* 15:838. doi: 10.1186/s12885-015-1850-4

Avanzato, D., Pupo, E., Ducano, N., Isella, C., Bertalot, G., Luise, C., et al. (2018). High USP6NL Levels in Breast Cancer Sustain Chronic AKT Phosphorylation and GLUT1 Stability Fueling Aerobic Glycolysis. *Cancer Res.* 78, 3432–3444. doi: 10.1158/0008-5472.Can-17-3018

Aykin-Burns, N., Ahmad, I. M., Zhu, Y., Oberley, L. W., and Spitz, D. R. (2009). Increased levels of superoxide and H2O2 mediate the differential susceptibility of cancer cells versus normal cells to glucose deprivation. *Biochem. J.* 418, 29–37. doi: 10.1042/bj20081258

Baenke, F., Dubuis, S., Brault, C., Weigelt, B., Dankworth, B., Griffiths, B., et al. (2015). Functional screening identifies MCT4 as a key regulator of breast cancer cell metabolism and survival. *J. Pathol.* 237, 152–165. doi: 10.1002/path.4562

Baretić, D., and Williams, R. L. (2014). The structural basis for mTOR function. *Semin. Cell Dev. Biol.* 36, 91–101. doi: 10.1016/j.semcdb.2014.09.024

Barnes, K., Ingram, J. C., Porras, O. H., Barros, L. F., Hudson, E. R., Fryer, L. G., et al. (2002). Activation of GLUT1 by metabolic and osmotic stress: potential involvement of AMP-activated protein kinase (AMPK). *J. Cell Sci.* 115, 2433–2442. doi: 10.1242/jcs.115.11.2433

Barron, C. C., Bilan, P. J., Tsakiridis, T., and Tsiani, E. (2016). Facilitative glucose transporters: implications for cancer detection, prognosis and treatment. *Metabolism* 65, 124–139. doi: 10.1016/j.metabol.2015.10.007

Barros, R. P., Machado, U. F., Warner, M., and Gustafsson, J. A. (2006). Muscle GLUT4 regulation by estrogen receptors ERbeta and ERalpha. *Proc. Natl. Acad. Sci. U. S. A.* 103, 1605–1608. doi: 10.1073/pnas.0510391103

Barros, R. P., Morani, A., Moriscot, A., and Machado, U. F. (2008). Insulin resistance of pregnancy involves estrogen-induced repression of muscle GLUT4. *Mol. Cell Endocrinol.* 295, 24–31. doi: 10.1016/j.mce.2008.07.008

Beckwith, H., and Yee, D. (2014). Insulin-like growth factors, insulin, and growth hormone signaling in breast cancer: implications for targeted therapy. *Endocr. Pract.* 20, 1214–1221. doi: 10.4158/ep14208.Ra

Beg, M., Abdullah, N., Thowfeik, F. S., Altorki, N. K., and McGraw, T. E. (2017). Distinct Akt phosphorylation states are required for insulin regulated Glut4 and Glut1-mediated glucose uptake. *Elife* 6:e26896. doi: 10.7554/eLife.26896

Benesch, C., Schneider, C., Voelker, H. U., Kapp, M., Caffier, H., Krockenberger, M., et al. (2010). The clinicopathological and prognostic relevance of pyruvate kinase M2 and pAkt expression in breast cancer. *Anticancer Res.* 30, 1689–1694.

Benito, A., Polat, I. H., Noé, V., Ciudad, C. J., Marin, S., and Cascante, M. (2017). Glucose-6-phosphate dehydrogenase and transketolase modulate breast cancer cell metabolic reprogramming and correlate with poor patient outcome. *Oncotarget* 8, 106693–106706. doi: 10.18632/oncotarget.21601

Bilan, P. J., Mitsumoto, Y., Maher, F., Simpson, I. A., and Klip, A. (1992). Detection of the GLUT3 facilitative glucose transporter in rat L6 muscle cells: regulation by cellular differentiation, insulin and insulin-like growth factor-I. *Biochem. Biophys. Res. Commun.* 186, 1129–1137. doi: 10.1016/0006-291x(92)90864-h

Binder, C., Binder, L., Marx, D., Schauer, A., and Hiddemann, W. (1997). Deregulated simultaneous expression of multiple glucose transporter isoforms in malignant cells and tissues. *Anticancer Res.* 17, 4299–4304.

Bohndiek, S. E., and Brindle, K. M. (2010). Imaging and 'omic' methods for the molecular diagnosis of cancer. *Expert. Rev. Mol. Diagn.* 10, 417–434. doi: 10.1586/erm.10.20

Borri, F., and Granaglia, A. (2020). Pathology of triple negative breast cancer. *Semin. Cancer Biol.* 72, 136–145. doi: 10.1016/j.semcancer.2020.06.005

Brauer, H. A., Makowski, L., Hoadley, K. A., Casbas-Hernandez, P., Lang, L. J., Romàn-Pèrez, E., et al. (2013). Impact of tumor microenvironment and epithelial phenotypes on metabolism in breast cancer. *Clin. Cancer Res.* 19, 571–585. doi: 10.1158/1078-0432.Ccr-12-2123

Bray, F., Ferlay, J., Soerjomataram, I., Siegel, R. L., Torre, L. A., and Jemal, A. (2018). Global cancer statistics 2018: GLOBOCAN estimates of incidence and mortality worldwide for 36 cancers in 185 countries. *CA Cancer J. Clin.* 68, 394–424. doi: 10.3322/caac.21492

Bray, F., McCarron, P., and Parkin, D. M. (2004). The changing global patterns of female breast cancer incidence and mortality. *Breast Cancer Res.* 6, 229–239. doi: 10.1186/bcr932

Brown, R. S., Goodman, T. M., Zasadny, K. R., Greenson, J. K., and Wahl, R. L. (2002). Expression of hexokinase II and Glut-1 in untreated human breast cancer. *Nucl. Med. Biol.* 29, 443–453. doi: 10.1016/s0969-8051(02)00288-3

Brown, R. S., and Wahl, R. L. (1993). Overexpression of Glut-1 glucose transporter in human breast cancer. An immunohistochemical study. *Cancer* 72, 2979–2985. doi: 10.1002/1097-0142(19931115)72:10<2979::aid-cncr2820721020<3.0.co;2-x

Bruning, P. F., Bonfrèr, J. M., van Noord, P. A., Hart, A. A., de Jong-Bakker, M., and Nooijen, W. J. (1992). Insulin resistance and breast-cancer risk. *Int. J. Cancer* 52, 511–516. doi: 10.1002/ijc.2910520402

Bulut, G., Atmaca, H., and Karaca, B. (2020). Trastuzumab in combination with AT-101 induces cytotoxicity and apoptosis in Her2 positive breast cancer cells. *Future Oncol.* 16, 4485–4495. doi: 10.2217/fon-2019-0521

Burke, B., Giannoudis, A., Corke, K. P., Gill, D., Wells, M., Ziegler-Heitbrock, L., et al. (2003). Hypoxia-induced gene expression in human macrophages: implications for ischemic tissues and hypoxia-regulated gene therapy. *Am. J. Pathol.* 163, 1233–1243. doi: 10.1016/s0002-9440(10)63483-9

Burstein, M. D., Tsimelzon, A., Poage, G. M., Covington, K. R., Contreras, A., Fuqua, S. A., et al. (2015). Comprehensive genomic analysis identifies novel subtypes and targets of triple-negative breast cancer. *Clin. Cancer Res.* 21, 1688–1698. doi: 10.1158/1078-0432.Ccr-14-0432

Butt, A. J., Sergio, C. M., Inman, C. K., Anderson, L. R., McNeil, C. M., Russell, A. J., et al. (2008). The estrogen and c-Myc target gene HSPC111 is over-expressed in breast cancer and associated with poor patient outcome. *Breast Cancer Res.* 10:R28. doi: 10.1186/bcr1985

Cai, C. F., Ye, G. D., Shen, D. Y., Zhang, W., Chen, M. L., Chen, X. X., et al. (2018). Chibby suppresses aerobic glycolysis and proliferation of nasopharyngeal carcinoma via the Wnt/β-catenin-Lin28/let7-PDK1 cascade. *J. Exp. Clin. Cancer Res.* 37:104. doi: 10.1186/s13046-018-0769-4

Caresia Aroztegui, A. P., García Vicente, A. M., Alvarez Ruiz, S., Delgado Bolton, R. C., Orcajo Rincon, J., Garcia Garzon, J. R., et al. (2017). 18F-FDG PET/CT in breast cancer: evidence-based recommendations in initial staging. *Tumour Biol.* 39:1010428317728285. doi: 10.1177/1010428317728285

Carey, L., Winer, E., Viale, G., Cameron, D., and Gianni, L. (2010). Triple-negative breast cancer: disease entity or title of convenience? *Nat. Rev. Clin. Oncol.* 7, 683–692. doi: 10.1038/nrclinonc.2010.154

Castaneda, C. A., Cortes-Funes, H., Gomez, H. L., and Ciruelos, E. M. (2010). The phosphatidyl inositol 3-kinase/AKT signaling pathway in breast cancer. *Cancer Metastasis Rev.* 29, 751–759. doi: 10.1007/s10555-010-9261-0

Cha, Y. J., Jung, W. H., and Koo, J. S. (2017). Differential Site-Based Expression of Pentose Phosphate Pathway-Related Proteins among Breast Cancer Metastases. *Dis. Markers* 2017:7062517. doi: 10.1155/2017/7062517

Chen, E. I., Hewel, J., Krueger, J. S., Tiraby, C., Weber, M. R., Kralli, A., et al. (2007). Adaptation of energy metabolism in breast cancer brain metastases. *Cancer Res.* 67, 1472–1486. doi: 10.1158/0008-5472.Can-06-3137

Chen, F., Chen, J., Yang, L., Liu, J., Zhang, X., Zhang, Y., et al. (2019). Extracellular vesicle-packaged HIF-1α-stabilizing lncRNA from tumour-associated macrophages regulates aerobic glycolysis of breast cancer cells. *Nat. Cell Biol.* 21, 498–510. doi: 10.1038/s41556-019-0299-0

Chen, P., Zuo, H., Xiong, H., Kolar, M. J., Chu, Q., Saghatelian, A., et al. (2017). Gpr132 sensing of lactate mediates tumor-macrophage interplay to promote breast cancer metastasis. *Proc. Natl. Acad. Sci. U. S. A.* 114, 580–585. doi: 10.1073/pnas.1614035114

Chen, Q., Meng, Y. Q., Xu, X. F., and Gu, J. (2017). Blockade of GLUT1 by WZB117 resensitizes breast cancer cells to adriamycin. *Anticancer Drugs* 28, 880–887. doi: 10.1097/cad.0000000000000529

Chen, Y., Wei, L., Zhang, X., Liu, X., Chen, Y., Zhang, S., et al. (2018). 3-Bromopyruvate sensitizes human breast cancer cells to TRAIL-induced

apoptosis via the phosphorylated AMPK-mediated upregulation of DR5. *Oncol. Rep.* 40, 2435–2444. doi: 10.3892/or.2018.6644

Cheong, H. (2015). Integrating autophagy and metabolism in cancer. *Arch. Pharm. Res.* 38, 358–371. doi: 10.1007/s12272-015-0562-2

Choi, J., Gyamfi, J., Jang, H., and Koo, J. S. (2018a). The role of tumor-associated macrophage in breast cancer biology. *Histol. Histopathol.* 33, 133–145. doi: 10.14670/hh-11-916

Choi, J., Kim, E. S., and Koo, J. S. (2018b). Expression of Pentose Phosphate Pathway-Related Proteins in Breast Cancer. *Dis. Markers* 2018:9369358. doi: 10.1155/2018/9369358

Choi, J., Jung, W. H., and Koo, J. S. (2013). Metabolism-related proteins are differentially expressed according to the molecular subtype of invasive breast cancer defined by surrogate immunohistochemistry. *Pathobiology* 80, 41–52. doi: 10.1159/000339513

Christofk, H. R., Vander Heiden, M. G., Harris, M. H., Ramanathan, A., Gerszten, R. E., Wei, R., et al. (2008). The M2 splice isoform of pyruvate kinase is important for cancer metabolism and tumour growth. *Nature* 452, 230–233. doi: 10.1038/nature06734

Colegio, O. R., Chu, N. Q., Szabo, A. L., Chu, T., Rhebergen, A. M., Jairam, V., et al. (2014). Functional polarization of tumour-associated macrophages by tumour-derived lactic acid. *Nature* 513, 559–563. doi: 10.1038/nature13490

Conover, C. A., Lee, P. D., Kanaley, J. A., Clarkson, J. T., and Jensen, M. D. (1992). Insulin regulation of insulin-like growth factor binding protein-1 in obese and nonobese humans. *J. Clin. Endocrinol. Metab.* 74, 1355–1360. doi: 10.1210/jcem.74.6.1375600

Corbet, C., and Feron, O. (2017). Cancer cell metabolism and mitochondria: nutrient plasticity for TCA cycle fueling. *Biochim. Biophys. Acta Rev. Cancer* 1868, 7–15. doi: 10.1016/j.bbcan.2017.01.002

Coyle, T., Levante, S., Shetler, M., and Winfield, J. (1994). In vitro and in vivo cytotoxicity of gossypol against central nervous system tumor cell lines. *J. Neurooncol.* 19, 25–35. doi: 10.1007/bf01051046

Cybulski, N., and Hall, M. N. (2009). TOR complex 2: a signaling pathway of its own. *Trends Biochem. Sci.* 34, 620–627. doi: 10.1016/j.tibs.2009.09.004

De Blasio, A., Di Fiore, R., Pratelli, G., Drago-Ferrante, R., Saliba, C., Baldacchino, S., et al. (2020). A loop involving NRF2, miR-29b-1-5p and AKT, regulates cell fate of MDA-MB-231 triple-negative breast cancer cells. *J. Cell Physiol.* 235, 629–637. doi: 10.1002/jcp.29062

Debeb, B. G., Lacerda, L., Larson, R., Wolfe, A. R., Krishnamurthy, S., Reuben, J. M., et al. (2016). Histone deacetylase inhibitor-induced cancer stem cells exhibit high pentose phosphate pathway metabolism. *Oncotarget* 7, 28329–28339. doi: 10.18632/oncotarget.8631

Denko, N. C. (2008). Hypoxia, HIF1 and glucose metabolism in the solid tumour. *Nat. Rev. Cancer* 8, 705–713. doi: 10.1038/nrc2468

DeSantis, C. E., Bray, F., Ferlay, J., Lortet-Tieulent, J., Anderson, B. O., and Jemal, A. (2015). International Variation in Female Breast Cancer Incidence and Mortality Rates. *Cancer Epidemiol. Biomarkers Prev.* 24, 1495–1506. doi: 10.1158/1055-9965.Epi-15-0535

Doherty, J. R., and Cleveland, J. L. (2013). Targeting lactate metabolism for cancer therapeutics. *J. Clin. Invest.* 123, 3685–3692. doi: 10.1172/jci69741

Dong, C., Yuan, T., Wu, Y., Wang, Y., Fan, T. W., Miriyala, S., et al. (2013). Loss of FBP1 by Snail-mediated repression provides metabolic advantages in basal-like breast cancer. *Cancer Cell* 23, 316–331. doi: 10.1016/j.ccr.2013.01.022

Dong, T., Kang, X., Liu, Z., Zhao, S., Ma, W., Xuan, Q., et al. (2016). Altered glycometabolism affects both clinical features and prognosis of triple-negative and neoadjuvant chemotherapy-treated breast cancer. *Tumour Biol.* 37, 8159–8168. doi: 10.1007/s13277-015-4729-8

Dong, T., Liu, Z., Xuan, Q., Wang, Z., Ma, W., and Zhang, Q. (2017). Tumor LDH-A expression and serum LDH status are two metabolic predictors for triple negative breast cancer brain metastasis. *Sci. Rep.* 7:6069. doi: 10.1038/s41598-017-06378-7

Douard, V., and Ferraris, R. P. (2008). Regulation of the fructose transporter GLUT5 in health and disease. *Am. J. Physiol. Endocrinol. Metab.* 295, E227–E237. doi: 10.1152/ajpendo.90245.2008

Doyen, J., Trastour, C., Ettore, F., Peyrottes, I., Toussant, N., Gal, J., et al. (2014). Expression of the hypoxia-inducible monocarboxylate transporter MCT4 is increased in triple negative breast cancer and correlates independently with clinical outcome. *Biochem. Biophys. Res. Commun.* 451, 54–61. doi: 10.1016/j.bbrc.2014.07.050

Dupuy, F., Tabariès, S., Andrzejewski, S., Dong, Z., Blagih, J., Annis, M. G., et al. (2015). PDK1-Dependent Metabolic Reprogramming Dictates Metastatic Potential in Breast Cancer. *Cell Metab.* 22, 577–589. doi: 10.1016/j.cmet.2015.08.007

Düvel, K., Yecies, J. L., Menon, S., Raman, P., Lipovsky, A. I., Souza, A. L., et al. (2010). Activation of a metabolic gene regulatory network downstream of mTOR complex 1. *Mol. Cell* 39, 171–183. doi: 10.1016/j.molcel.2010.06.022

Engelman, J. A., Luo, J., and Cantley, L. C. (2006). The evolution of phosphatidylinositol 3-kinases as regulators of growth and metabolism. *Nat. Rev. Genet.* 7, 606–619. doi: 10.1038/nrg1879

Farabegoli, F., Vettraino, M., Manerba, M., Fiume, L., Roberti, M., and Di Stefano, G. (2012). Galloflavin, a new lactate dehydrogenase inhibitor, induces the death of human breast cancer cells with different glycolytic attitude by affecting distinct signaling pathways. *Eur. J. Pharm. Sci.* 47, 729–738. doi: 10.1016/j.ejps.2012.08.012

Fu, Y., Liu, S., Yin, S., Niu, W., Xiong, W., Tan, M., et al. (2017). The reverse Warburg effect is likely to be an Achilles' heel of cancer that can be exploited for cancer therapy. *Oncotarget* 8, 57813–57825. doi: 10.18632/oncotarget.18175

Furuta, E., Okuda, H., Kobayashi, A., and Watabe, K. (2010). Metabolic genes in cancer: their roles in tumor progression and clinical implications. *Biochim. Biophys. Acta* 1805, 141–152. doi: 10.1016/j.bbcan.2010.01.005

Gao, S., Ge, A., Xu, S., You, Z., Ning, S., Zhao, Y., et al. (2017). PSAT1 is regulated by ATF4 and enhances cell proliferation via the GSK3β/β-catenin/cyclin D1 signaling pathway in ER-negative breast cancer. *J. Exp. Clin. Cancer Res.* 36:179. doi: 10.1186/s13046-017-0648-4

García-Castillo, V., López-Urrutia, E., Villanueva-Sánchez, O., Ávila-Rodríguez, M., Zentella-Dehesa, A., Cortés-González, C., et al. (2017). Targeting Metabolic Remodeling in Triple Negative Breast Cancer in a Murine Model. *J. Cancer* 8, 178–189. doi: 10.7150/jca.16387

García-Martínez, J. M., and Alessi, D. R. (2008). mTOR complex 2 (mTORC2) controls hydrophobic motif phosphorylation and activation of serum- and glucocorticoid-induced protein kinase 1 (SGK1). *Biochem. J.* 416, 375–385. doi: 10.1042/bj20081668

Garrido, P., Morán, J., Alonso, A., González, S., and González, C. (2013). 17β-estradiol activates glucose uptake via GLUT4 translocation and PI3K/Akt signaling pathway in MCF-7 cells. *Endocrinology* 154, 1979–1989. doi: 10.1210/en.2012-1558

Gayosso, V., Montano, L. F., and López-Marure, R. (2006). DHEA-induced antiproliferative effect in MCF-7 cells is androgen- and estrogen receptor-independent. *Cancer J.* 12, 160–165.

Geeraerts, S. L., Heylen, E., De Keersmaecker, K., and Kampen, K. R. (2021a). The ins and outs of serine and glycine metabolism in cancer. *Nat. Metab.* 3, 131–141. doi: 10.1038/s42255-020-00329-9

Geeraerts, S. L., Kampen, K. R., Rinaldi, G., Gupta, P., Planque, M., Louros, N., et al. (2021b). Repurposing the Antidepressant Sertraline as SHMT Inhibitor to Suppress Serine/Glycine Synthesis-Addicted Breast Tumor Growth. *Mol. Cancer Ther.* 20, 50–63. doi: 10.1158/1535-7163.Mct-20-0480

Ghanavat, M., Shahrouzian, M., Deris Zayeri, Z., Banihashemi, S., Kazemi, S. M., and Saki, N. (2021). Digging deeper through glucose metabolism and its regulators in cancer and metastasis. *Life Sci.* 264:118603. doi: 10.1016/j.lfs.2020.118603

Giatromanolaki, A., Koukourakis, M. I., Simopoulos, C., Polychronidis, A., Gatter, K. C., Harris, A. L., et al. (2004). c-erbB-2 related aggressiveness in breast cancer is hypoxia inducible factor-1alpha dependent. *Clin. Cancer Res.* 10, 7972–7977. doi: 10.1158/1078-0432.Ccr-04-1068

Gilbert, N. E., O'Reilly, J. E., Chang, C. J., Lin, Y. C., and Brueggemeier, R. W. (1995). Antiproliferative activity of gossypol and gossypolone on human breast cancer cells. *Life Sci.* 57, 61–67. doi: 10.1016/0024-3205(95)00243-y

Godoy, A., Ulloa, V., Rodríguez, F., Reinicke, K., Yañez, A. J., García Mde, L., et al. (2006). Differential subcellular distribution of glucose transporters GLUT1-6 and GLUT9 in human cancer: ultrastructural localization of GLUT1 and GLUT5 in breast tumor tissues. *J. Cell Physiol.* 207, 614–627. doi: 10.1002/jcp.20606

Gomez, L. S., Zancan, P., Marcondes, M. C., Ramos-Santos, L., Meyer-Fernandes, J. R., Sola-Penna, M., et al. (2013). Resveratrol decreases breast cancer cell viability and glucose metabolism by inhibiting 6-phosphofructo-1-kinase. *Biochimie* 95, 1336–1343. doi: 10.1016/j.biochi.2013.02.013

Gorres, B. K., Bomhoff, G. L., Morris, J. K., and Geiger, P. C. (2011). In vivo stimulation of oestrogen receptor α increases insulin-stimulated skeletal muscle glucose uptake. *J. Physiol.* 589, 2041–2054. doi: 10.1113/jphysiol.2010.199018

Grinde, M. T., Moestue, S. A., Borgan, E., Risa, Ø, Engebraaten, O., and Gribbestad, I. S. (2011). 13C high-resolution-magic angle spinning MRS reveals differences in glucose metabolism between two breast cancer xenograft models with different gene expression patterns. *NMR Biomed.* 24, 1243–1252. doi: 10.1002/nbm.1683

Groheux, D., Cochet, A., Humbert, O., Alberini, J. L., Hindié, E., and Mankoff, D. (2016). ^{18}F-FDG PET/CT for Staging and Restaging of Breast Cancer. *J. Nucl. Med.* 57, 17s–26s. doi: 10.2967/jnumed.115.157859

Grover-McKay, M., Walsh, S. A., Seftor, E. A., Thomas, P. A., and Hendrix, M. J. (1998). Role for glucose transporter 1 protein in human breast cancer. *Pathol. Oncol. Res.* 4, 115–120. doi: 10.1007/bf02904704

Guedes, M., Araújo, J. R., Correia-Branco, A., Gregório, I., Martel, F., and Keating, E. (2016). Modulation of the uptake of critical nutrients by breast cancer cells by lactate: impact on cell survival, proliferation and migration. *Exp. Cell Res.* 341, 111–122. doi: 10.1016/j.yexcr.2016.01.008

Gunter, M. J., Xie, X., Xue, X., Kabat, G. C., Rohan, T. E., Wassertheil-Smoller, S., et al. (2015). Breast cancer risk in metabolically healthy but overweight postmenopausal women. *Cancer Res.* 75, 270–274. doi: 10.1158/0008-5472.Can-14-2317

Halestrap, A. P., Connern, C. P., Griffiths, E. J., and Kerr, P. M. (1997). Cyclosporin A binding to mitochondrial cyclophilin inhibits the permeability transition pore and protects hearts from ischaemia/reperfusion injury. *Mol. Cell Biochem.* 174, 167–172. doi: 10.1007/978-1-4615-6111-8_25

Han, J., Zhang, L., Guo, H., Wysham, W. Z., Roque, D. R., Willson, A. K., et al. (2015). Glucose promotes cell proliferation, glucose uptake and invasion in endometrial cancer cells via AMPK/mTOR/S6 and MAPK signaling. *Gynecol. Oncol.* 138, 668–675. doi: 10.1016/j.ygyno.2015.06.036

Hara, K., Maruki, Y., Long, X., Yoshino, K., Oshiro, N., Hidayat, S., et al. (2002). Raptor, a binding partner of target of rapamycin (TOR), mediates TOR action. *Cell* 110, 177–189. doi: 10.1016/s0092-8674(02)00833-4

Hare, S. H., and Harvey, A. J. (2017). mTOR function and therapeutic targeting in breast cancer. *Am. J. Cancer Res.* 7, 383–404.

Harmon, A. W., and Patel, Y. M. (2004). Naringenin inhibits glucose uptake in MCF-7 breast cancer cells: a mechanism for impaired cellular proliferation. *Breast Cancer Res. Treat* 85, 103–110. doi: 10.1023/B:BREA.0000025397.56192.e2

Hibdon, E. S., Razumilava, N., Keeley, T. M., Wong, G., Solanki, S., Shah, Y. M., et al. (2019). Notch and mTOR Signaling Pathways Promote Human Gastric Cancer Cell Proliferation. *Neoplasia* 21, 702–712. doi: 10.1016/j.neo.2019.05.002

Hollmén, M., Roudnicky, F., Karaman, S., and Detmar, M. (2015). Characterization of macrophage–cancer cell crosstalk in estrogen receptor positive and triple-negative breast cancer. *Sci. Rep.* 5:9188. doi: 10.1038/srep09188

Holman, G. D. (2020). Structure, function and regulation of mammalian glucose transporters of the SLC2 family. *Pflugers Arch.* 472, 1155–1175. doi: 10.1007/s00424-020-02411-3

Hsieh, A. L., Walton, Z. E., Altman, B. J., Stine, Z. E., and Dang, C. V. (2015). MYC and metabolism on the path to cancer. *Semin. Cell Dev. Biol.* 43, 11–21. doi: 10.1016/j.semcdb.2015.08.003

Huang, X., Li, X., Xie, X., Ye, F., Chen, B., Song, C., et al. (2016). High expressions of LDHA and AMPK as prognostic biomarkers for breast cancer. *Breast* 30, 39–46. doi: 10.1016/j.breast.2016.08.014

Hui, S., Ghergurovich, J. M., Morscher, R. J., Jang, C., Teng, X., Lu, W., et al. (2017). Glucose feeds the TCA cycle via circulating lactate. *Nature* 551, 115–118. doi: 10.1038/nature24057

Hussein, Y. R., Bandyopadhyay, S., Semaan, A., Ahmed, Q., Albashiti, B., Jazaerly, T., et al. (2011). Glut-1 Expression Correlates with Basal-like Breast Cancer. *Transl. Oncol.* 4, 321–327. doi: 10.1593/tlo.11256

Ikenoue, T., Inoki, K., Yang, Q., Zhou, X., and Guan, K. L. (2008). Essential function of TORC2 in PKC and Akt turn motif phosphorylation, maturation and signalling. *EMBO J.* 27, 1919–1931. doi: 10.1038/emboj.2008.119

Irey, E. A., Lassiter, C. M., Brady, N. J., Chuntova, P., Wang, Y., Knutson, T. P., et al. (2019). JAK/STAT inhibition in macrophages promotes therapeutic resistance by inducing expression of protumorigenic factors. *Proc. Natl. Acad. Sci. U. S. A.* 116, 12442–12451. doi: 10.1073/pnas.1816410116

Jia, D., Lu, M., Jung, K. H., Park, J. H., Yu, L., Onuchic, J. N., et al. (2019). Elucidating cancer metabolic plasticity by coupling gene regulation with metabolic pathways. *Proc. Natl. Acad. Sci. U. S. A.* 116, 3909–3918. doi: 10.1073/pnas.1816391116

Jia, D., Park, J. H., Jung, K. H., Levine, H., and Kaipparettu, B. A. (2018). Elucidating the Metabolic Plasticity of Cancer: mitochondrial Reprogramming and Hybrid Metabolic States. *Cells* 7:21. doi: 10.3390/cells7030021

Jia, L., Huang, S., Yin, X., Zan, Y., Guo, Y., and Han, L. (2018). Quercetin suppresses the mobility of breast cancer by suppressing glycolysis through Akt-mTOR pathway mediated autophagy induction. *Life Sci.* 208, 123–130. doi: 10.1016/j.lfs.2018.07.027

Jiang, K., He, B., Lai, L., Chen, Q., Liu, Y., Guo, Q., et al. (2012). Cyclosporine A inhibits breast cancer cell growth by downregulating the expression of pyruvate kinase subtype M2. *Int. J. Mol. Med.* 30, 302–308. doi: 10.3892/ijmm.2012.989

Jiang, S., Zhang, L. F., Zhang, H. W., Hu, S., Lu, M. H., Liang, S., et al. (2012). A novel miR-155/miR-143 cascade controls glycolysis by regulating hexokinase 2 in breast cancer cells. *EMBO J.* 31, 1985–1998. doi: 10.1038/emboj.2012.45

Jin, M. S., Lee, H., Park, I. A., Chung, Y. R., Im, S. A., Lee, K. H., et al. (2016). Overexpression of HIF1α and CAXI predicts poor outcome in early-stage triple negative breast cancer. *Virchows Arch.* 469, 183–190. doi: 10.1007/s00428-016-1953-6

Johnson, J. M., Cotzia, P., Fratamico, R., Mikkilineni, L., Chen, J., Colombo, D., et al. (2017). MCT1 in Invasive Ductal Carcinoma: monocarboxylate Metabolism and Aggressive Breast Cancer. *Front. Cell Dev. Biol.* 5:27. doi: 10.3389/fcell.2017.00027

Jung, K. H., Lee, J. H., Thien Quach, C. H., Paik, J. Y., Oh, H., Park, J. W., et al. (2013). Resveratrol suppresses cancer cell glucose uptake by targeting reactive oxygen species-mediated hypoxia-inducible factor-1α activation. *J. Nucl. Med.* 54, 2161–2167. doi: 10.2967/jnumed.112.115436

Kabat, G. C., Kim, M., Caan, B. J., Chlebowski, R. T., Gunter, M. J., Ho, G. Y., et al. (2009). Repeated measures of serum glucose and insulin in relation to postmenopausal breast cancer. *Int. J. Cancer* 125, 2704–2710. doi: 10.1002/ijc.24609

Kang, S. S., Chun, Y. K., Hur, M. H., Lee, H. K., Kim, Y. J., Hong, S. R., et al. (2002). Clinical significance of glucose transporter 1 (GLUT1) expression in human breast carcinoma. *Jpn J. Cancer Res.* 93, 1123–1128. doi: 10.1111/j.1349-7006.2002.tb01214.x

Katzenellenbogen, B. S., and Norman, M. J. (1990). Multihormonal regulation of the progesterone receptor in MCF-7 human breast cancer cells: interrelationships among insulin/insulin-like growth factor-I, serum, and estrogen. *Endocrinology* 126, 891–898. doi: 10.1210/endo-126-2-891

Kawauchi, K., Araki, K., Tobiume, K., and Tanaka, N. (2008). p53 regulates glucose metabolism through an IKK-NF-kappaB pathway and inhibits cell transformation. *Nat. Cell Biol.* 10, 611–618. doi: 10.1038/ncb1724

Kim, H. M., Jung, W. H., and Koo, J. S. (2014). Site-specific metabolic phenotypes in metastatic breast cancer. *J. Transl. Med.* 12:354. doi: 10.1186/s12967-014-0354-3

Kim, S. K., Jung, W. H., and Koo, J. S. (2014). Differential expression of enzymes associated with serine/glycine metabolism in different breast cancer subtypes. *PLoS One* 9:e101004. doi: 10.1371/journal.pone.0101004

Kim, Y. H., Jung, W. H., and Koo, J. S. (2014). Expression of metabolism-related proteins in invasive lobular carcinoma: comparison to invasive ductal carcinoma. *Tumour Biol.* 35, 10381–10393. doi: 10.1007/s13277-014-2345-7

Kim, S., Kim, D. H., Jung, W. H., and Koo, J. S. (2013). Metabolic phenotypes in triple-negative breast cancer. *Tumour Biol.* 34, 1699–1712. doi: 10.1007/s13277-013-0707-1

Koboldt, D. C., Fulton, R. S., McLellan, M. D., Schmidt, H., Kalicki-Veizer, J., McMichael, J. F., et al. (2012). Comprehensive molecular portraits of human breast tumours. *Nature* 490, 61–70. doi: 10.1038/nature11412

Kruger, N. J., and von Schaewen, A. (2003). The oxidative pentose phosphate pathway: structure and organisation. *Curr. Opin. Plant Biol.* 6, 236–246. doi: 10.1016/s1369-5266(03)00039-6

Krzeslak, A., Wojcik-Krowiranda, K., Forma, E., Jozwiak, P., Romanowicz, H., Bienkiewicz, A., et al. (2012). Expression of GLUT1 and GLUT3 glucose transporters in endometrial and breast cancers. *Pathol. Oncol. Res.* 18, 721–728. doi: 10.1007/s12253-012-9500-5

Kumar, P., and Aggarwal, R. (2016). An overview of triple-negative breast cancer. *Arch. Gynecol. Obstet.* 293, 247–269. doi: 10.1007/s00404-015-3859-y

Labrie, F., Luu-The, V., Labrie, C., and Simard, J. (2001). DHEA and its transformation into androgens and estrogens in peripheral target tissues: intracrinology. *Front. Neuroendocrinol.* 22, 185–212. doi: 10.1006/frne.2001.0216

Labuschagne, C. F., van den Broek, N. J., Mackay, G. M., Vousden, K. H., and Maddocks, O. D. (2014). Serine, but not glycine, supports one-carbon metabolism and proliferation of cancer cells. *Cell Rep.* 7, 1248–1258. doi: 10.1016/j.celrep.2014.04.045

Lai, X., Li, Q., Wu, F., Lin, J., Chen, J., Zheng, H., et al. (2020). Epithelial-Mesenchymal Transition and Metabolic Switching in Cancer: lessons From Somatic Cell Reprogramming. *Front. Cell Dev. Biol.* 8:760. doi: 10.3389/fcell.2020.00760

Lanning, N. J., Castle, J. P., Singh, S. J., Leon, A. N., Tovar, E. A., Sanghera, A., et al. (2017). Metabolic profiling of triple-negative breast cancer cells reveals metabolic vulnerabilities. *Cancer Metab.* 5:6. doi: 10.1186/s40170-017-0168-x

Lawlor, D. A., Smith, G. D., and Ebrahim, S. (2004). Hyperinsulinaemia and increased risk of breast cancer: findings from the British Women's Heart and Health Study. *Cancer Causes Control* 15, 267–275. doi: 10.1023/B:CACO.0000024225.14618.a8

LeBleu, V. S., O'Connell, J. T., Gonzalez Herrera, K. N., Wikman, H., Pantel, K., Haigis, M. C., et al. (2014). PGC-1α mediates mitochondrial biogenesis and oxidative phosphorylation in cancer cells to promote metastasis. *Nat. Cell Biol.* 16, 992–1003. doi: 10.1038/ncb3039

Lee, J. H., Liu, R., Li, J., Wang, Y., Tan, L., Li, X. J., et al. (2018). EGFR-Phosphorylated Platelet Isoform of Phosphofructokinase 1 Promotes PI3K Activation. *Mol. Cell* 70, 197–210.e7. doi: 10.1016/j.molcel.2018.03.018

Lee, M., and Yoon, J. H. (2015). Metabolic interplay between glycolysis and mitochondrial oxidation: the reverse Warburg effect and its therapeutic implication. *World J. Biol. Chem.* 6, 148–161. doi: 10.4331/wjbc.v6.i3.148

Lee, Y. R., Park, J., Yu, H. N., Kim, J. S., Youn, H. J., and Jung, S. H. (2005). Up-regulation of PI3K/Akt signaling by 17beta-estradiol through activation of estrogen receptor-alpha, but not estrogen receptor-beta, and stimulates cell growth in breast cancer cells. *Biochem. Biophys. Res. Commun.* 336, 1221–1226. doi: 10.1016/j.bbrc.2005.08.256

Lehmann, B. D., Bauer, J. A., Chen, X., Sanders, M. E., Chakravarthy, A. B., Shyr, Y., et al. (2011). Identification of human triple-negative breast cancer subtypes and preclinical models for selection of targeted therapies. *J. Clin. Invest.* 121, 2750–2767. doi: 10.1172/jci45014

Leino, R. L., Gerhart, D. Z., van Bueren, A. M., McCall, A. L., and Drewes, L. R. (1997). Ultrastructural localization of GLUT 1 and GLUT 3 glucose transporters in rat brain. *J. Neurosci. Res.* 49, 617–626. doi: 10.1002/(sici)1097-4547(19970901)49:5<617::Aid-jnr12<3.0.Co;2-s

Levine, A. J., and Puzio-Kuter, A. M. (2010). The control of the metabolic switch in cancers by oncogenes and tumor suppressor genes. *Science* 330, 1340–1344. doi: 10.1126/science.1193494

Li, L. J., Li, G. W., and Xie, Y. (2019). [Regulatory effects of glabridin and quercetin on energy metabolism of breast cancer cells]. *Zhongguo Zhong Yao Za Zhi* 44, 3786–3791. doi: 10.19540/j.cnki.cjcmm.20190505.401

Li, X. B., Gu, J. D., and Zhou, Q. H. (2015). Review of aerobic glycolysis and its key enzymes - new targets for lung cancer therapy. *Thorac Cancer* 6, 17–24. doi: 10.1111/1759-7714.12148

Li, Z., Wu, Q., Sun, S., Wu, J., Li, J., Zhang, Y., et al. (2018). Monocarboxylate transporters in breast cancer and adipose tissue are novel biomarkers and potential therapeutic targets. *Biochem. Biophys. Res. Commun.* 501, 962–967. doi: 10.1016/j.bbrc.2018.05.091

Lin, A., Li, C., Xing, Z., Hu, Q., Liang, K., Han, L., et al. (2016). The LINK-A lncRNA activates normoxic HIF1α signalling in triple-negative breast cancer. *Nat. Cell Biol.* 18, 213–224. doi: 10.1038/ncb3295

Lin, Y., Lv, F., Liu, F., Guo, X., Fan, Y., Gu, F., et al. (2015). High Expression of Pyruvate Kinase M2 is Associated with Chemosensitivity to Epirubicin and 5-Fluorouracil in Breast Cancer. *J. Cancer* 6, 1130–1139. doi: 10.7150/jca.12719

Liu, Y., Cao, Y., Zhang, W., Bergmeier, S., Qian, Y., Akbar, H., et al. (2012). A small-molecule inhibitor of glucose transporter 1 downregulates glycolysis, induces cell-cycle arrest, and inhibits cancer cell growth in vitro and in vivo. *Mol. Cancer Ther.* 11, 1672–1682. doi: 10.1158/1535-7163.Mct-12-0131

Liu, Z., Sun, Y., Hong, H., Zhao, S., Zou, X., Ma, R., et al. (2015). 3-bromopyruvate enhanced daunorubicin-induced cytotoxicity involved in monocarboxylate transporter 1 in breast cancer cells. *Am. J. Cancer Res.* 5, 2673–2685.

Liu, Z., Zhang, Y. Y., Zhang, Q. W., Zhao, S. R., Wu, C. Z., Cheng, X., et al. (2014). 3-Bromopyruvate induces apoptosis in breast cancer cells by downregulating Mcl-1 through the PI3K/Akt signaling pathway. *Anticancer Drugs* 25, 447–455. doi: 10.1097/cad.0000000000000081

Locasale, J. W. (2013). Serine, glycine and one-carbon units: cancer metabolism in full circle. *Nat. Rev. Cancer* 13, 572–583. doi: 10.1038/nrc3557

Locasale, J. W., Grassian, A. R., Melman, T., Lyssiotis, C. A., Mattaini, K. R., Bass, A. J., et al. (2011). Phosphoglycerate dehydrogenase diverts glycolytic flux and contributes to oncogenesis. *Nat. Genet.* 43, 869–874. doi: 10.1038/ng.890

López-Lázaro, M. (2008). The warburg effect: why and how do cancer cells activate glycolysis in the presence of oxygen? *Anticancer Agents Med. Chem.* 8, 305–312. doi: 10.2174/187152008783961932

López-Marure, R., Contreras, P. G., and Dillon, J. S. (2011). Effects of dehydroepiandrosterone on proliferation, migration, and death of breast cancer cells. *Eur. J. Pharmacol.* 660, 268–274. doi: 10.1016/j.ejphar.2011.03.040

Losada-Echeberría, M., Herranz-López, M., Micol, V., and Barrajón-Catalán, E. (2017). Polyphenols as Promising Drugs against Main Breast Cancer Signatures. *Antioxidants (Basel)* 6:88. doi: 10.3390/antiox6040088

Luo, M., Shang, L., Brooks, M. D., Jiagge, E., Zhu, Y., Buschhaus, J. M., et al. (2018). Targeting Breast Cancer Stem Cell State Equilibrium through Modulation of Redox Signaling. *Cell Metab.* 28, 69–86.e6. doi: 10.1016/j.cmet.2018.06.006

Ma, C., Zu, X., Liu, K., Bode, A. M., Dong, Z., Liu, Z., et al. (2019). Knockdown of Pyruvate Kinase M Inhibits Cell Growth and Migration by Reducing NF-kB Activity in Triple-Negative Breast Cancer Cells. *Mol. Cells* 42, 628–636. doi: 10.14348/molcells.2019.0038

MacQueen, G., Born, L., and Steiner, M. (2001). The selective serotonin reuptake inhibitor sertraline: its profile and use in psychiatric disorders. *CNS Drug Rev.* 7, 1–24. doi: 10.1111/j.1527-3458.2001.tb00188.x

Mantovani, A., Sozzani, S., Locati, M., Allavena, P., and Sica, A. (2002). Macrophage polarization: tumor-associated macrophages as a paradigm for polarized M2 mononuclear phagocytes. *Trends Immunol.* 23, 549–555. doi: 10.1016/s1471-4906(02)02302-5

Mao, Y., Keller, E. T., Garfield, D. H., Shen, K., and Wang, J. (2013). Stromal cells in tumor microenvironment and breast cancer. *Cancer Metastasis Rev.* 32, 303–315. doi: 10.1007/s10555-012-9415-3

Marsin, A. S., Bertrand, L., Rider, M. H., Deprez, J., Beauloye, C., Vincent, M. F., et al. (2000). Phosphorylation and activation of heart PFK-2 by AMPK has a role in the stimulation of glycolysis during ischaemia. *Curr. Biol.* 10, 1247–1255. doi: 10.1016/s0960-9822(00)00742-9

Martínez-Reyes, I., and Chandel, N. S. (2017). Waste Not, Want Not: lactate Oxidation Fuels the TCA Cycle. *Cell Metab.* 26, 803–804. doi: 10.1016/j.cmet.2017.11.005

McCleland, M. L., Adler, A. S., Shang, Y., Hunsaker, T., Truong, T., Peterson, D., et al. (2012). An integrated genomic screen identifies LDHB as an essential gene for triple-negative breast cancer. *Cancer Res.* 72, 5812–5823. doi: 10.1158/0008-5472.Can-12-1098

McVie-Wylie, A. J., Lamson, D. R., and Chen, Y. T. (2001). Molecular cloning of a novel member of the GLUT family of transporters, SLC2a10 (GLUT10), localized on chromosome 20q13.1: a candidate gene for NIDDM susceptibility. *Genomics* 72, 113–117. doi: 10.1006/geno.2000.6457

Messeha, S. S., Zarmouh, N. O., Mendonca, P., Alwagdani, H., Cotton, C., and Soliman, K. F. A. (2019). Effects of gossypol on apoptosis-related gene expression in racially distinct triple-negative breast cancer cells. *Oncol. Rep.* 42, 467–478. doi: 10.3892/or.2019.7179

Mishra, J., Davani, A. J., Natarajan, G. K., Kwok, W. M., Stowe, D. F., and Camara, A. K. S. (2019). Cyclosporin A Increases Mitochondrial Buffering of Calcium: an Additional Mechanism in Delaying Mitochondrial Permeability Transition Pore Opening. *Cells* 8:1052. doi: 10.3390/cells8091052

Mittal, S., Brown, N. J., and Holen, I. (2018). The breast tumor microenvironment: role in cancer development, progression and response to therapy. *Expert. Rev. Mol. Diagn.* 18, 227–243. doi: 10.1080/14737159.2018.1439382

Mocanu, M. M., Nagy, P., and Szöllősi, J. (2015). Chemoprevention of Breast Cancer by Dietary Polyphenols. *Molecules* 20, 22578–22620. doi: 10.3390/molecules201219864

Moldogazieva, N. T., Mokhosoev, I. M., and Terentiev, A. A. (2020). Metabolic Heterogeneity of Cancer Cells: an Interplay between HIF-1, GLUTs, and AMPK. *Cancers (Basel)* 12:862. doi: 10.3390/cancers12040862

Moreira, L., Araújo, I., Costa, T., Correia-Branco, A., Faria, A., Martel, F., et al. (2013). Quercetin and epigallocatechin gallate inhibit glucose uptake and metabolism by breast cancer cells by an estrogen receptor-independent mechanism. *Exp. Cell Res.* 319, 1784–1795. doi: 10.1016/j.yexcr.2013.05.001

Mu, X., Shi, W., Xu, Y., Xu, C., Zhao, T., Geng, B., et al. (2018). Tumor-derived lactate induces M2 macrophage polarization via the activation of the ERK/STAT3 signaling pathway in breast cancer. *Cell Cycle* 17, 428–438. doi: 10.1080/15384101.2018.1444305

Mueckler, M., and Thorens, B. (2013). The SLC2 (GLUT) family of membrane transporters. *Mol. Aspects Med.* 34, 121–138. doi: 10.1016/j.mam.2012.07.001

Mullarky, E., Lucki, N. C., Beheshti Zavareh, R., Anglin, J. L., Gomes, A. P., Nicolay, B. N., et al. (2016). Identification of a small molecule inhibitor of 3-phosphoglycerate dehydrogenase to target serine biosynthesis in cancers. *Proc. Natl. Acad. Sci. U. S. A.* 113, 1778–1783. doi: 10.1073/pnas.1521548113

Niu, W., Huang, C., Nawaz, Z., Levy, M., Somwar, R., Li, D., et al. (2003). Maturation of the regulation of GLUT4 activity by p38 MAPK during L6 cell myogenesis. *J. Biol. Chem.* 278, 17953–17962. doi: 10.1074/jbc.M211136200

Noh, E. M., Lee, Y. R., Chay, K. O., Chung, E. Y., Jung, S. H., Kim, J. S., et al. (2011). Estrogen receptor α induces down-regulation of PTEN through PI3-kinase activation in breast cancer cells. *Mol. Med Rep.* 4, 215–219. doi: 10.3892/mmr.2011.412

Noh, S., Kim, D. H., Jung, W. H., and Koo, J. S. (2014). Expression levels of serine/glycine metabolism-related proteins in triple negative breast cancer tissues. *Tumour Biol.* 35, 4457–4468. doi: 10.1007/s13277-013-1588-z

Novellasdemunt, L., Tato, I., Navarro-Sabate, A., Ruiz-Meana, M., Méndez-Lucas, A., Perales, J. C., et al. (2013). Akt-dependent activation of the heart 6-phosphofructo-2-kinase/fructose-2,6-bisphosphatase (PFKFB2) isoenzyme by amino acids. *J. Biol. Chem.* 288, 10640–10651. doi: 10.1074/jbc.M113.455998

Oh, S., Kim, H., Nam, K., and Shin, I. (2017). Glut1 promotes cell proliferation, migration and invasion by regulating epidermal growth factor receptor and integrin signaling in triple-negative breast cancer cells. *BMB Rep.* 50, 132–137. doi: 10.5483/bmbrep.2017.50.3.189

Okar, D. A., Manzano, A., Navarro-Sabatè, A., Riera, L., Bartrons, R., and Lange, A. J. (2001). PFK-2/FBPase-2: maker and breaker of the essential biofactor fructose-2,6-bisphosphate. *Trends Biochem. Sci.* 26, 30–35. doi: 10.1016/s0968-0004(00)01699-6

O'Neal, J., Clem, A., Reynolds, L., Dougherty, S., Imbert-Fernandez, Y., Telang, S., et al. (2016). Inhibition of 6-phosphofructo-2-kinase (PFKFB3) suppresses glucose metabolism and the growth of HER2+ breast cancer. *Breast Cancer Res. Treat.* 160, 29–40. doi: 10.1007/s10549-016-3968-8

Pacold, M. E., Brimacombe, K. R., Chan, S. H., Rohde, J. M., Lewis, C. A., Swier, L. J., et al. (2016). A PHGDH inhibitor reveals coordination of serine synthesis and one-carbon unit fate. *Nat. Chem. Biol.* 12, 452–458. doi: 10.1038/nchembio.2070

Palaskas, N., Larson, S. M., Schultz, N., Komisopoulou, E., Wong, J., Rohle, D., et al. (2011). 18F-fluorodeoxy-glucose positron emission tomography marks MYC-overexpressing human basal-like breast cancers. *Cancer Res.* 71, 5164–5174. doi: 10.1158/0008-5472.Can-10-4633

Pan, Y., Zheng, Q., Ni, W., Wei, Z., Yu, S., Jia, Q., et al. (2019). Breaking Glucose Transporter 1/Pyruvate Kinase M2 Glycolytic Loop Is Required for Cantharidin Inhibition of Metastasis in Highly Metastatic Breast Cancer. *Front. Pharmacol.* 10:590. doi: 10.3389/fphar.2019.00590

Park, J. H., Vithayathil, S., Kumar, S., Sung, P. L., Dobrolecki, L. E., Putluri, V., et al. (2016). Fatty Acid Oxidation-Driven Src Links Mitochondrial Energy Reprogramming and Oncogenic Properties in Triple-Negative Breast Cancer. *Cell Rep.* 14, 2154–2165. doi: 10.1016/j.celrep.2016.02.004

Pasanen, I., Lehtonen, S., Sormunen, R., Skarp, S., Lehtilahti, E., Pietilä, M., et al. (2016). Breast cancer carcinoma-associated fibroblasts differ from breast fibroblasts in immunological and extracellular matrix regulating pathways. *Exp. Cell Res.* 344, 53–66. doi: 10.1016/j.yexcr.2016.04.016

Patra, K. C., and Hay, N. (2014). The pentose phosphate pathway and cancer. *Trends Biochem. Sci.* 39, 347–354. doi: 10.1016/j.tibs.2014.06.005

Pavlides, S., Whitaker-Menezes, D., Castello-Cros, R., Flomenberg, N., Witkiewicz, A. K., Frank, P. G., et al. (2009). The reverse Warburg effect: aerobic glycolysis in cancer associated fibroblasts and the tumor stroma. *Cell Cycle* 8, 3984–4001. doi: 10.4161/cc.8.23.10238

Paydary, K., Seraj, S. M., Zadeh, M. Z., Emamzadehfard, S., Shamchi, S. P., Gholami, S., et al. (2019). The Evolving Role of FDG-PET/CT in the Diagnosis, Staging, and Treatment of Breast Cancer. *Mol. Imaging Biol.* 21, 1–10. doi: 10.1007/s11307-018-1181-3

Pelicano, H., Zhang, W., Liu, J., Hammoudi, N., Dai, J., Xu, R. H., et al. (2014). Mitochondrial dysfunction in some triple-negative breast cancer cell lines: role of mTOR pathway and therapeutic potential. *Breast Cancer Res.* 16:434. doi: 10.1186/s13058-014-0434-6

Peng, F., Li, Q., Sun, J. Y., Luo, Y., Chen, M., and Bao, Y. (2018). PFKFB3 is involved in breast cancer proliferation, migration, invasion and angiogenesis. *Int. J. Oncol.* 52, 945–954. doi: 10.3892/ijo.2018.4257

Pinheiro, C., Albergaria, A., Paredes, J., Sousa, B., Dufloth, R., Vieira, D., et al. (2010). Monocarboxylate transporter 1 is up-regulated in basal-like breast carcinoma. *Histopathology* 56, 860–867. doi: 10.1111/j.1365-2559.2010.03560.x

Pinheiro, C., Sousa, B., Albergaria, A., Paredes, J., Dufloth, R., Vieira, D., et al. (2011). GLUT1 and CAIX expression profiles in breast cancer correlate with adverse prognostic factors and MCT1 overexpression. *Histol. Histopathol.* 26, 1279–1286. doi: 10.14670/hh-26.1279

Possemato, R., Marks, K. M., Shaul, Y. D., Pacold, M. E., Kim, D., Birsoy, K., et al. (2011). Functional genomics reveal that the serine synthesis pathway is essential in breast cancer. *Nature* 476, 346–350. doi: 10.1038/nature10350

Preuss, J., Richardson, A. D., Pinkerton, A., Hedrick, M., Sergienko, E., Rahlfs, S., et al. (2013). Identification and characterization of novel human glucose-6-phosphate dehydrogenase inhibitors. *J. Biomol. Screen* 18, 286–297. doi: 10.1177/1087057112462131

Pu, H., Zhang, Q., Zhao, C., Shi, L., Wang, Y., Wang, J., et al. (2015). Overexpression of G6PD is associated with high risks of recurrent metastasis and poor progression-free survival in primary breast carcinoma. *World J. Surg. Oncol.* 13:323. doi: 10.1186/s12957-015-0733-0

Ralser, M., Wamelink, M. M., Struys, E. A., Joppich, C., Krobitsch, S., Jakobs, C., et al. (2008). A catabolic block does not sufficiently explain how 2-deoxy-D-glucose inhibits cell growth. *Proc. Natl. Acad. Sci. U. S. A.* 105, 17807–17811. doi: 10.1073/pnas.0803090105

Ramos-Martinez, J. I. (2017). The regulation of the pentose phosphate pathway: remember Krebs. *Arch. Biochem. Biophys.* 614, 50–52. doi: 10.1016/j.abb.2016.12.012

Rastogi, S., Banerjee, S., Chellappan, S., and Simon, G. R. (2007). Glut-1 antibodies induce growth arrest and apoptosis in human cancer cell lines. *Cancer Lett.* 257, 244–251. doi: 10.1016/j.canlet.2007.07.021

Ravazoula, P., Batistatou, A., Aletra, C., Ladopoulos, J., Kourounis, G., and Tzigounis, B. (2003). Immunohistochemical expression of glucose transporter Glut1 and cyclin D1 in breast carcinomas with negative lymph nodes. *Eur. J. Gynaecol. Oncol.* 24, 544–546.

Risha, Y., Minic, Z., Ghobadloo, S. M., and Berezovski, M. V. (2020). The proteomic analysis of breast cell line exosomes reveals disease patterns and potential biomarkers. *Sci. Rep.* 10:13572. doi: 10.1038/s41598-020-70393-4

Rivenzon-Segal, D., Margalit, R., and Degani, H. (2002). Glycolysis as a metabolic marker in orthotopic breast cancer, monitored by in vivo (13)C MRS. *Am. J. Physiol. Endocrinol. Metab.* 283, E623–E630. doi: 10.1152/ajpendo.00050.2002

Robey, I. F., Lien, A. D., Welsh, S. J., Baggett, B. K., and Gillies, R. J. (2005). Hypoxia-inducible factor-1alpha and the glycolytic phenotype in tumors. *Neoplasia* 7, 324–330. doi: 10.1593/neo.04430

Rogers, S., Docherty, S. E., Slavin, J. L., Henderson, M. A., and Best, J. D. (2003). Differential expression of GLUT12 in breast cancer and normal breast tissue. *Cancer Lett.* 193, 225–233. doi: 10.1016/s0304-3835(03)00010-7

Rogers, S., Macheda, M. L., Docherty, S. E., Carty, M. D., Henderson, M. A., Soeller, W. C., et al. (2002). Identification of a novel glucose transporter-like protein-GLUT-12. *Am. J. Physiol. Endocrinol. Metab.* 282, E733–E738. doi: 10.1152/ajpendo.2002.282.3.E733

Ronda, A. C., Buitrago, C., and Boland, R. (2010a). Role of estrogen receptors, PKC and Src in ERK2 and p38 MAPK signaling triggered by 17β-estradiol in skeletal muscle cells. *J. Steroid Biochem. Mol. Biol.* 122, 287–294. doi: 10.1016/j.jsbmb.2010.05.002

Ronda, A. C., Vasconsuelo, A., and Boland, R. (2010b). Extracellular-regulated kinase and p38 mitogen-activated protein kinases are involved in the antiapoptotic action of 17beta-estradiol in skeletal muscle cells. *J. Endocrinol.* 206, 235–246. doi: 10.1677/joe-09-0429

Rossouw, J. E., Anderson, G. L., Prentice, R. L., LaCroix, A. Z., Kooperberg, C., Stefanick, M. L., et al. (2002). Risks and benefits of estrogen plus progestin in healthy postmenopausal women: principal results From the Women's Health

Initiative randomized controlled trial. *JAMA* 288, 321–333. doi: 10.1001/jama.288.3.321

Salazar, G. (2018). NADPH Oxidases and Mitochondria in Vascular Senescence. *Int. J. Mol. Sci.* 19:1327. doi: 10.3390/ijms19051327

Samanta, D., Park, Y., Andrabi, S. A., Shelton, L. M., Gilkes, D. M., and Semenza, G. L. (2016). PHGDH Expression Is Required for Mitochondrial Redox Homeostasis, Breast Cancer Stem Cell Maintenance, and Lung Metastasis. *Cancer Res.* 76, 4430–4442. doi: 10.1158/0008-5472.Can-16-0530

Samih, N., Hovsepian, S., Aouani, A., Lombardo, D., and Fayet, G. (2000). Glut-1 translocation in FRTL-5 thyroid cells: role of phosphatidylinositol 3-kinase and N-glycosylation. *Endocrinology* 141, 4146–4155. doi: 10.1210/endo.141.11.7793

Santos, J. M., and Hussain, F. (2020). Higher Glucose Enhances Breast Cancer Cell Aggressiveness. *Nutr. Cancer* 72, 734–746. doi: 10.1080/01635581.2019.1654527

Santos, J. M., Khan, Z. S., Munir, M. T., Tarafdar, K., Rahman, S. M., and Hussain, F. (2018). Vitamin D(3) decreases glycolysis and invasiveness, and increases cellular stiffness in breast cancer cells. *J. Nutr. Biochem.* 53, 111–120. doi: 10.1016/j.jnutbio.2017.10.013

Sato-Tadano, A., Suzuki, T., Amari, M., Takagi, K., Miki, Y., Tamaki, K., et al. (2013). Hexokinase II in breast carcinoma: a potent prognostic factor associated with hypoxia-inducible factor-1α and Ki-67. *Cancer Sci.* 104, 1380–1388. doi: 10.1111/cas.12238

Schieber, M. S., and Chandel, N. S. (2013). ROS links glucose metabolism to breast cancer stem cell and EMT phenotype. *Cancer Cell* 23, 265–267. doi: 10.1016/j.ccr.2013.02.021

Semenza, G. L. (2017). Hypoxia-inducible factors: coupling glucose metabolism and redox regulation with induction of the breast cancer stem cell phenotype. *EMBO J.* 36, 252–259. doi: 10.15252/embj.201695204

Semenza, G. L., Roth, P. H., Fang, H. M., and Wang, G. L. (1994). Transcriptional regulation of genes encoding glycolytic enzymes by hypoxia-inducible factor 1. *J. Biol. Chem.* 269, 23757–23763. doi: 10.1016/s0021-9258(17)31580-6

Shen, L., O'Shea, J. M., Kaadige, M. R., Cunha, S., Wilde, B. R., Cohen, A. L., et al. (2015). Metabolic reprogramming in triple-negative breast cancer through Myc suppression of TXNIP. *Proc. Natl. Acad. Sci. U. S. A.* 112, 5425–5430. doi: 10.1073/pnas.1501555112

Shi, Y., Zhang, Y., Ran, F., Liu, J., Lin, J., Hao, X., et al. (2020). Let-7a-5p inhibits triple-negative breast tumor growth and metastasis through GLUT12-mediated warburg effect. *Cancer Lett.* 495, 53–65. doi: 10.1016/j.canlet.2020.09.012

Simões, R. V., Serganova, I. S., Kruchevsky, N., Leftin, A., Shestov, A. A., Thaler, H. T., et al. (2015). Metabolic plasticity of metastatic breast cancer cells: adaptation to changes in the microenvironment. *Neoplasia* 17, 671–684. doi: 10.1016/j.neo.2015.08.005

Simoncini, T., Hafezi-Moghadam, A., Brazil, D. P., Ley, K., Chin, W. W., and Liao, J. K. (2000). Interaction of oestrogen receptor with the regulatory subunit of phosphatidylinositol-3-OH kinase. *Nature* 407, 538–541. doi: 10.1038/35035131

Sitter, B., Bathen, T. F., Singstad, T. E., Fjøsne, H. E., Lundgren, S., Halgunset, J., et al. (2010). Quantification of metabolites in breast cancer patients with different clinical prognosis using HR MAS MR spectroscopy. *NMR Biomed.* 23, 424–431. doi: 10.1002/nbm.1478

Sonveaux, P., Végran, F., Schroeder, T., Wergin, M. C., Verrax, J., Rabbani, Z. N., et al. (2008). Targeting lactate-fueled respiration selectively kills hypoxic tumor cells in mice. *J. Clin. Invest.* 118, 3930–3942. doi: 10.1172/jci36843

Soysal, S. D., Tzankov, A., and Muenst, S. E. (2015). Role of the Tumor Microenvironment in Breast Cancer. *Pathobiology* 82, 142–152. doi: 10.1159/000430499

Stincone, A., Prigione, A., Cramer, T., Wamelink, M. M., Campbell, K., Cheung, E., et al. (2015). The return of metabolism: biochemistry and physiology of the pentose phosphate pathway. *Biol. Rev. Camb. Philos. Soc.* 90, 927–963. doi: 10.1111/brv.12140

Tseng, C. W., Kuo, W. H., Chan, S. H., Chan, H. L., Chang, K. J., and Wang, L. H. (2018). Transketolase Regulates the Metabolic Switch to Control Breast Cancer Cell Metastasis via the α-Ketoglutarate Signaling Pathway. *Cancer Res.* 78, 2799–2812. doi: 10.1158/0008-5472.Can-17-2906

Ueno, T., Utsumi, J., Toi, M., and Shimizu, K. (2015). Characteristic Gene Expression Profiles of Human Fibroblasts and Breast Cancer Cells in a Newly Developed Bilateral Coculture System. *Biomed. Res. Int.* 2015:960840. doi: 10.1155/2015/960840

Unterlass, J. E., Baslé, A., Blackburn, T. J., Tucker, J., Cano, C., Noble, M. E. M., et al. (2018). Validating and enabling phosphoglycerate dehydrogenase (PHGDH) as a target for fragment-based drug discovery in PHGDH-amplified breast cancer. *Oncotarget* 9, 13139–13153. doi: 10.18632/oncotarget.11487

Vargas, E., Podder, V., and Carrillo Sepulveda, M. A. (2021). *Physiology, Glucose Transporter Type 4*. Treasure Island: StatPearls Publishing.

Vivanco, I., and Sawyers, C. L. (2002). The phosphatidylinositol 3-Kinase AKT pathway in human cancer. *Nat. Rev. Cancer* 2, 489–501. doi: 10.1038/nrc839

Vousden, K. H., and Ryan, K. M. (2009). p53 and metabolism. *Nat. Rev. Cancer* 9, 691–700. doi: 10.1038/nrc2715

Wang, J., Duan, Z., Nugent, Z., Zou, J. X., Borowsky, A. D., Zhang, Y., et al. (2016). Reprogramming metabolism by histone methyltransferase NSD2 drives endocrine resistance via coordinated activation of pentose phosphate pathway enzymes. *Cancer Lett.* 378, 69–79. doi: 10.1016/j.canlet.2016.05.004

Wang, Q., Liberti, M. V., Liu, P., Deng, X., Liu, Y., Locasale, J. W., et al. (2017). Rational Design of Selective Allosteric Inhibitors of PHGDH and Serine Synthesis with Anti-tumor Activity. *Cell Chem. Biol.* 24, 55–65. doi: 10.1016/j.chembiol.2016.11.013

Wang, Z., Jiang, Q., and Dong, C. (2020). Metabolic reprogramming in triple-negative breast cancer. *Cancer Biol. Med.* 17, 44–59. doi: 10.20892/j.issn.2095-3941.2019.0210

Warburg, O. (1956). On the origin of cancer cells. *Science* 123, 309–314. doi: 10.1126/science.123.3191.309

Wei, R., Mao, L., Xu, P., Zheng, X., Hackman, R. M., Mackenzie, G. G., et al. (2018). Suppressing glucose metabolism with epigallocatechin-3-gallate (EGCG) reduces breast cancer cell growth in preclinical models. *Food Funct.* 9, 5682–5696. doi: 10.1039/c8fo01397g

Wellberg, E. A., Johnson, S., Finlay-Schultz, J., Lewis, A. S., Terrell, K. L., Sartorius, C. A., et al. (2016). The glucose transporter GLUT1 is required for ErbB2-induced mammary tumorigenesis. *Breast Cancer Res.* 18:131. doi: 10.1186/s13058-016-0795-0

Whitaker-Menezes, D., Martinez-Outschoorn, U. E., Lin, Z., Ertel, A., Flomenberg, N., Witkiewicz, A. K., et al. (2011). Evidence for a stromal-epithelial "lactate shuttle" in human tumors: MCT4 is a marker of oxidative stress in cancer-associated fibroblasts. *Cell Cycle* 10, 1772–1783. doi: 10.4161/cc.10.11.15659

Wilde, L., Roche, M., Domingo-Vidal, M., Tanson, K., Philp, N., Curry, J., et al. (2017). Metabolic coupling and the Reverse Warburg Effect in cancer: implications for novel biomarker and anticancer agent development. *Semin. Oncol.* 44, 198–203. doi: 10.1053/j.seminoncol.2017.10.004

Williamson, G. (2017). The role of polyphenols in modern nutrition. *Nutr. Bull.* 42, 226–235. doi: 10.1111/nbu.12278

Witkiewicz, A. K., Whitaker-Menezes, D., Dasgupta, A., Philp, N. J., Lin, Z., Gandara, R., et al. (2012). Using the "reverse Warburg effect" to identify high-risk breast cancer patients: stromal MCT4 predicts poor clinical outcome in triple-negative breast cancers. *Cell Cycle* 11, 1108–1117. doi: 10.4161/cc.11.6.19530

Woo, Y. M., Shin, Y., Lee, E. J., Lee, S., Jeong, S. H., Kong, H. K., et al. (2015). Inhibition of Aerobic Glycolysis Represses Akt/mTOR/HIF-1α Axis and Restores Tamoxifen Sensitivity in Antiestrogen-Resistant Breast Cancer Cells. *PLoS One* 10:e0132285. doi: 10.1371/journal.pone.0132285

Wright, E. M. (2013). Glucose transport families SLC5 and SLC50. *Mol Aspects Med.* 34, 183–196. doi: 10.1016/j.mam.2012.11.002

Wu, Q., Heidenreich, D., Zhou, S., Ackloo, S., Krämer, A., Nakka, K., et al. (2019a). A chemical toolbox for the study of bromodomains and epigenetic signaling. *Nat. Commun.* 10:1915. doi: 10.1038/s41467-019-09672-2

Wu, Q., Li, B., Li, Z., Li, J., Sun, S., and Sun, S. (2019b). Cancer-associated adipocytes: key players in breast cancer progression. *J. Hematol. Oncol.* 12:95. doi: 10.1186/s13045-019-0778-6

Wuest, M., Hamann, I., Bouvet, V., Glubrecht, D., Marshall, A., Trayner, B., et al. (2018). Molecular Imaging of GLUT1 and GLUT5 in Breast Cancer: a Multitracer Positron Emission Tomography Imaging Study in Mice. *Mol. Pharmacol.* 93, 79–89. doi: 10.1124/mol.117.110007

Xi, H., Barredo, J. C., Merchan, J. R., and Lampidis, T. J. (2013). Endoplasmic reticulum stress induced by 2-deoxyglucose but not glucose starvation activates AMPK through CaMKKβ leading to autophagy. *Biochem. Pharmacol.* 85, 1463–1477. doi: 10.1016/j.bcp.2013.02.037

Xi, H., Kurtoglu, M., Liu, H., Wangpaichitr, M., You, M., Liu, X., et al. (2011). 2-Deoxy-D-glucose activates autophagy via endoplasmic reticulum stress rather

than ATP depletion. *Cancer Chemother. Pharmacol.* 67, 899–910. doi: 10.1007/s00280-010-1391-0

Xintaropoulou, C., Ward, C., Wise, A., Marston, H., Turnbull, A., and Langdon, S. P. (2015). A comparative analysis of inhibitors of the glycolysis pathway in breast and ovarian cancer cell line models. *Oncotarget* 6, 25677–25695. doi: 10.18632/oncotarget.4499

Yang, L., Li, J., Li, Y., Zhou, Y., Wang, Z., Zhang, D., et al. (2021). Diclofenac impairs the proliferation and glucose metabolism of triple-negative breast cancer cells by targeting the c-Myc pathway. *Exp. Ther. Med.* 21:584. doi: 10.3892/etm.2021.10016

Yang, T., Ren, C., Qiao, P., Han, X., Wang, L., Lv, S., et al. (2018). PIM2-mediated phosphorylation of hexokinase 2 is critical for tumor growth and paclitaxel resistance in breast cancer. *Oncogene* 37, 5997–6009. doi: 10.1038/s41388-018-0386-x

Yang, X., Peng, X., and Huang, J. (2018). Inhibiting 6-phosphogluconate dehydrogenase selectively targets breast cancer through AMPK activation. *Clin. Transl. Oncol.* 20, 1145–1152. doi: 10.1007/s12094-018-1833-4

Yang, Y., Wolfram, J., Boom, K., Fang, X., Shen, H., and Ferrari, M. (2013). Hesperetin impairs glucose uptake and inhibits proliferation of breast cancer cells. *Cell Biochem. Funct.* 31, 374–379. doi: 10.1002/cbf.2905

Yang, Z. J., Chee, C. E., Huang, S., and Sinicrope, F. A. (2011). The role of autophagy in cancer: therapeutic implications. *Mol. Cancer Ther.* 10, 1533–1541. doi: 10.1158/1535-7163.Mct-11-0047

Ye, W., Chang, H. L., Wang, L. S., Huang, Y. W., Shu, S., Sugimoto, Y., et al. (2010). Induction of apoptosis by (-)-gossypol-enriched cottonseed oil in human breast cancer cells. *Int. J. Mol. Med.* 26, 113–119.

Yeh, W. L., Lin, C. J., and Fu, W. M. (2008). Enhancement of glucose transporter expression of brain endothelial cells by vascular endothelial growth factor derived from glioma exposed to hypoxia. *Mol. Pharmacol.* 73, 170–177. doi: 10.1124/mol.107.038851

Yin, K. (2015). Positive correlation between expression level of mitochondrial serine hydroxymethyltransferase and breast cancer grade. *Onco. Targets Ther.* 8, 1069–1074. doi: 10.2147/ott.S82433

Younes, M., Brown, R. W., Mody, D. R., Fernandez, L., and Laucirica, R. (1995). GLUT1 expression in human breast carcinoma: correlation with known prognostic markers. *Anticancer Res.* 15, 2895–2898.

Young, C. D., Lewis, A. S., Rudolph, M. C., Ruehle, M. D., Jackman, M. R., Yun, U. J., et al. (2011). Modulation of glucose transporter 1 (GLUT1) expression levels alters mouse mammary tumor cell growth in vitro and in vivo. *PLoS One* 6:e23205. doi: 10.1371/journal.pone.0023205

Yousefi, S., Darvishi, P., Yousefi, Z., and Pourfathollah, A. A. (2020). Effect of methyl jasmonate and 3-bromopyruvate combination therapy on mice bearing the 4 T1 breast cancer cell line. *J. Bioenerg. Biomembr.* 52, 103–111. doi: 10.1007/s10863-019-09811-w

Zamora-León, S. P., Golde, D. W., Concha, I. I., Rivas, C. I., Delgado-López, F., Baselga, J., et al. (1996). Expression of the fructose transporter GLUT5 in human breast cancer. *Proc. Natl. Acad. Sci. U. S. A.* 93, 1847–1852. doi: 10.1073/pnas.93.5.1847

Zhao, F., Ming, J., Zhou, Y., and Fan, L. (2016). Inhibition of Glut1 by WZB117 sensitizes radioresistant breast cancer cells to irradiation. *Cancer Chemother. Pharmacol.* 77, 963–972. doi: 10.1007/s00280-016-3007-9

Zhao, Y., Liu, H., Liu, Z., Ding, Y., Ledoux, S. P., Wilson, G. L., et al. (2011). Overcoming trastuzumab resistance in breast cancer by targeting dysregulated glucose metabolism. *Cancer Res.* 71, 4585–4597. doi: 10.1158/0008-5472.Can-11-0127

Zhong, H., De Marzo, A. M., Laughner, E., Lim, M., Hilton, D. A., Zagzag, D., et al. (1999). Overexpression of hypoxia-inducible factor 1alpha in common human cancers and their metastases. *Cancer Res.* 59, 5830–5835.

Zhou, M., Zhao, Y., Ding, Y., Liu, H., Liu, Z., Fodstad, O., et al. (2010). Warburg effect in chemosensitivity: targeting lactate dehydrogenase-A re-sensitizes taxol-resistant cancer cells to taxol. *Mol. Cancer* 9:33. doi: 10.1186/1476-4598-9-33

Zhu, S., Wei, L., Lin, G., Tong, Y., Zhang, J., Jiang, X., et al. (2020). Metabolic Alterations Induced by Kudingcha Lead to Cancer Cell Apoptosis and Metastasis Inhibition. *Nutr. Cancer* 72, 696–707. doi: 10.1080/01635581.2019.1645865

Conflict of Interest: The authors declare that the research was conducted in the absence of any commercial or financial relationships that could be construed as a potential conflict of interest.

Publisher's Note: All claims expressed in this article are solely those of the authors and do not necessarily represent those of their affiliated organizations, or those of the publisher, the editors and the reviewers. Any product that may be evaluated in this article, or claim that may be made by its manufacturer, is not guaranteed or endorsed by the publisher.

Advantages of publishing in Frontiers

OPEN ACCESS
Articles are free to read for greatest visibility and readership

FAST PUBLICATION
Around 90 days from submission to decision

HIGH QUALITY PEER-REVIEW
Rigorous, collaborative, and constructive peer-review

TRANSPARENT PEER-REVIEW
Editors and reviewers acknowledged by name on published articles

Frontiers
Avenue du Tribunal-Fédéral 34
1005 Lausanne | Switzerland

Visit us: www.frontiersin.org
Contact us: frontiersin.org/about/contact

REPRODUCIBILITY OF RESEARCH
Support open data and methods to enhance research reproducibility

DIGITAL PUBLISHING
Articles designed for optimal readership across devices

FOLLOW US
@frontiersin

IMPACT METRICS
Advanced article metrics track visibility across digital media

EXTENSIVE PROMOTION
Marketing and promotion of impactful research

LOOP RESEARCH NETWORK
Our network increases your article's readership